



Environmental Engineering and Management Journal

Founding Editor: Matei Macoveanu

Editor-in-Chief: Maria Gavrilescu

Guest Editors: Irina Volf

Dan Cascaval

Innovative Materials and Processes



"Gheorghe Asachi" Technical University of Iasi



Environmental Engineering and Management Journal

An International Journal

Founding Editor: Matei Macoveanu

Editor-in-Chief: Maria Gavrilescu

Guest Editors: Irina Volf

Dan Cașcaval

Innovative Materials and Processes



“Gheorghe Asachi” Technical University of Iasi

Environmental Engineering and Management Journal

Environmental Engineering and Management Journal encourages initiatives and actions concerning the improvement of education, research, marketing and management, in order to achieve sustainable development. This journal brings valuable opportunities for those offering products, technologies, services, educational programs or other related activities, creating thus a closer relation with the request of the market in the fields of environmental engineering, management and education. This journal address researchers, designers, academic staff, specialists with responsibilities in the field of environmental protection and management from government organizations (central and local administrations, environmental protection agencies) or from the private or public companies. Also, graduates of specialization courses or of the Environmental Engineering and Management profile, as well as other specialists may find in this journal a direct linkage between the offer and request of the market concerned with the protection of the environment and the administration of natural resources in the national and international context.

The journal was conceived as a means to develop scientific and technical relationships between people who offer and request solutions for environmental protection and conservation of natural resources, creating thus the premises to enhance the transfer of technology and know-how, the confirmation and implementation of ecological products and services.

Taking into consideration these aspects, we gladly welcome any persons or companies which correspond to the above-mentioned purposes and objectives to use our journal to identify potential collaborators.

For subscriptions and orders please contact us at:
OAIMDD (Academic Organization for Environmental Engineering and Sustainable Development),
73 Mangeron Blvd., PO 10, Box 2111, 700050 Iasi, Romania, CIF: 10150285

Phone/Fax: 0040-232-271759
E-mail: brindusa.sluser.at@gmail.com, mgav_eemj.at.yahoo.com

In LEI:

ALPHA BANK ROMANIA (ABR)
SWIFT Code: BUCUROBU
IBAN: RO87BUCU1032235333663RON
Beneficiary: OAIMDD-EEMJ
Address: PO 10, Box 2111, 700050 Iasi, Romania

In EURO:

ALPHA BANK ROMANIA (ABR)
SWIFT Code: BUCUROBU
IBAN: RO79BUCU1031215940036EUR
Beneficiary: OAIMDD-EEMJ
Address: PO 10, Box 2111, 700050 Iasi, Romania

**Department of Environmental Engineering and Management and
EcoZone Publishing House - O.A.I.M.D.D.**
73 Prof.Dr.Docent Dimitrie Mangeron Street, 700050-Iasi, Romania
Phone/Fax: 0040-232-271759

EDITORIAL BOARD

Founding Editor:

Matei Macoveanu, *Gheorghe Asachi* Technical University of Iasi, Romania

Editor-in-Chief:

Maria Gavrilescu, *Gheorghe Asachi* Technical University of Iasi, Romania

SCIENTIFIC ADVISORY BOARD

Maria Madalena dos Santos Alves
University of Minho, Braga
Portugal

Abdeltif Amrane
University of Rennes, ENSCR
France

Ecaterina Andronescu
University *Polytechnica* of Bucharest
Romania

Robert Armon
Technion-Israel Institute of Technology, Haifa
Israel

Adisa Azapagic
The University of Manchester
United Kingdom

Hamidi Abdul Aziz
Universiti Sains Malaysia, Penang
Malaysia

Pranas Baltrenas
Vilnius *Gediminas* Technical University
Lithuania

Hans Bressers
University of Twente, Enschede
The Netherlands

Han Brezet
Delft University of Technology
The Netherlands

Dan Cascaval
Gheorghe Asachi Technical University of Iasi
Romania

Aleg Cherp
Central European University, Budapest
Hungary

Yusuf Chisti
Massey University, Palmerston North
New Zealand

Philippe Corvini
University of Applied Sciences Northwestern
Switzerland, Muttentz, Switzerland

Igor Cretescu
Gheorghe Asachi Technical University of Iasi
Romania

Silvia Curteanu
Gheorghe Asachi Technical University of Iasi
Romania

Andrew J. Daugulis
Queen's University Kingston
Canada

Valeriu David
Gheorghe Asachi Technical University of Iasi
Romania

Katerina Demnerova
University of Prague
Czech Republic

Gheorghe Duca
State University of Moldavia, Kishinev
Republic of Moldavia

Emil Dumitriu
Gheorghe Asachi Technical University of Iasi
Romania

Jurek Duszczyk
Delft University of Technology
The Netherlands

Anca Duta Capra
Transilvania University of Brasov
Romania

Fabio Fava
Alma Mater Studiorum University of Bologna
Italy

Eugenio Campos Ferreira
University of Minho, Braga,
Portugal

Cristian Fosalau
Gheorghe Asachi Technical University of Iasi
Romania

Anton Friedl
Vienna University of Technology
Austria

Anne Giroir Fendler
University *Claude Bernard* Lyon 1
France

Silvia Fiore
Polytechnic University of Turin,
Italy

Ion Giurma
Gheorghe Asachi Technical University of Iasi
Romania

Yuh-Shan Ho
Peking University
People's Republic of China

Arjen Y. Hoekstra
University of Twente, Enschede
The Netherlands

Nicolae Hurduc
Gheorghe Asachi Technical University of Iasi
Romania

Ralf Isenmann
Munich University of Applied Sciences
Germany

Marcel Istrate
Gheorghe Asachi Technical University of Iasi
Romania

Ravi Jain
University of Pacific, Baun Hall Stockton
United States of America

Michael Sogaard Jørgensen
Aalborg University
Denmark

Nicolas Kalogerakis
Technical University of Crete, Chania
Greece

Gheorghe Lazaroiu
University *Polytechnica* of Bucharest
Romania

Thomas Lindqvist
International Institute for Industrial Environmental
Economics, Lund University, Sweden

Andreas Paul Loibner
University of Natural Resources and Life Sciences,
Vienna, Austria

Tudor Lupascu
Academy of Sciences, Institute of Chemistry,
Kishinev, Republic of Moldavia

Antonio Marzocchella
University of Naples *Federico II*,
Naples, Italy

José Mondéjar Jiménez
University Castilla-La Mancha, Cuenca
Spain

Shin'ichi Nakatsuji
University of Hyogo
Japan

Valentin Nedeff
Vasile Alecsandri University of Bacau
Romania

Alexandru Ozunu
Babes-Bolyai University of Cluj-Napoca
Romania

Yannis A. Phillis
Technical University of Crete, Chania
Greece

Marcel Ionel Popa
Gheorghe Asachi Technical University of Iasi
Romania

Marcel Popa
Gheorghe Asachi Technical University of Iasi
Romania

Valentin I. Popa
Gheorghe Asachi Technical University of Iasi
Romania

Tudor Prisecaru
University *Polytechnica* of Bucharest
Romania

Gabriel-Lucian Radu
Polytechnica University of Bucharest
Romania

Ákos Rédey
Pannon University, Veszprém
Hungary

Joop Schoonman
Delft University of Technology
The Netherlands

Dan Scutaru
Gheorghe Asachi Technical University of Iasi
Romania

Bogdan C. Simionescu
Gheorghe Asachi Technical University of Iasi
Romania

Florian Stacuseu
Gheorghe Asachi Technical University of Iasi
Romania

Carmen Teodosiu
Gheorghe Asachi Technical University of Iasi
Romania

Saulius Vasarevicius
Vilnius *Gediminas* Technical University
Lithuania

Angheluta Vadineanu
The University of Bucharest
Romania

Colin Webb
The University of Manchester
United Kingdom

Peter Wilderer
Technical University Munich
Germany

Petra Winzer
Bergische University Wuppertal
Germany

Environmental Engineering and Management Journal

Environmental Engineering and Management Journal is included and indexed in:

CABI
Chemical Abstracts Service/SciFinder (ACS) (since 2002)
EBSCO Database (since 2002)
EVISA
ICAAP (International Consortium for Advancement of Academic Publications)
Index Copernicus Journal Master List (**ICV/2015=156.46**)
Journal Citation Reports® 2016 Edition (**IF=1.096**), (*Environmental Sciences*, Ranked **179 out of 229**; 5-Year Impact Factor: 0.849
Article Influence® Score: 0.073; Immediacy Index: 0.057)

MedSci
ProQuest (since 2002)
The National University Research Council (RO)
Science Citation Index Expanded™ (Thomson ISI)
SJR (SCImago Journal & Country Rank) (*Environmental Sciences*, **SJR index/2016= 0.341**; **SNIP index/2016 = 0.481**;
CiteScore/2016=0.72; Ranked **682 out of 1356, H=27**)

SCOPUS (since 2008)
Thomson ISI Master Journal List
Web of Science® (Thomson ISI) (**H=27**)

Home page: <http://www.eemj.icpm.tuiasi.ro>; <http://www.eemj.eu>

Full text: <http://www.ecozone.ro>, <http://www.eemj.eu>

Founding Editor: Matei Macoveanu, Iasi (RO)

Editor-in-Chief: Maria Gavrilăscu, Iasi (RO)

Environmental Engineering and Management Journal is edited by
Gheorghe Asachi Technical University of Iasi and EcoZone Publishing House of the Academic Organization for Environmental Engineering and Sustainable Development (O.A.I.M.D.D.)

Editorial and Production Office:

Department of Environmental Engineering and Management - Faculty of Chemical Engineering and Environmental Protection and EcoZone-O.A.I.M.D.D., 73 Prof.Dr.Docent Dimitrie Mangeron Street, 700050 Iasi, Romania
Phone: +40-232-278680, ext. 2259, 2137
Fax: +40-232-271759
e-mail: eemjournal.at.yahoo.com, eem_journal.at.yahoo.com, eemjeditor.at.yahoo.com, eemj_editor.at.yahoo.com, eemjournal.at.gmail.com, eemj.editor.at.gmail.com, eemj.office.at.gmail.com

Editorial production assistants and secretariat:

Raluca-Maria Hlihor
Laura Bulgariu
Elena-Diana Comăniță
Petronela Cozma
Mihaela Roșca
Isabela Maria Simion
Camelia Smaranda
Sebastian Ionuț Vasilică

Administrative and financial management:

O.A.I.M.D.D. President, Brîndușa Mihaela Slușer

Published 12 issues per year, under the aegis of the "Gheorghe Asachi" Technical University of Iasi, Romania
by EcoZone Publishing House of the Academic Organization for Environmental Engineering and Sustainable Development (O.A.I.M.D.D.), <http://www.ecozone.ro>

Annual subscription rate 2018 (12 issues)

Print:	Electronic:	Print+Electronic:
EURO 500 per volume	400 per volume	800 per volume

Individual costs

EURO 50 per issue	40 per issue
-------------------	--------------

Order directly to the Editorial Office

73 Prof.Dr.docent Dimitrie Mangeron Street, 700050 Iasi, Romania
Phone/Fax: Fax: +40-232-271759, e-mail: brindusa.sluser.at.gmail.com, eemj.office.at.gmail.com

Electronic, full text: Order or purchase on-line at: www.ecozone.ro

Bank account (EURO):

ALPHA BANK ROMANIA (ABR)

SWIFT Code: BUCUROBU,

IBAN: RO79BUCU1031215940036EUR

Beneficiary: OAIMDD-EEMJ, Address: PO 10, Box 2111, 700050 Iasi, Romania

Bank account (LEI):

ALPHA BANK ROMANIA (ABR), IBAN: RO87BUCU1032235333663RON,

Beneficiary: OAIMDD-EEMJ

All rights reserved, including those of translation into foreign languages. No part of each issue may be reproduced in any form (photoprint, microfilm, or any other means) nor transmitted or translated without written permission from the publishers. Only single copies of contributions, or parts thereof, may be made for personal use. This journal was carefully produced in all its parts. Even so, authors, editors and publisher do not guarantee the information contained there to be free of errors. Registered names, trademarks etc. used in this journal, even when not marked as such, are not considered unprotected by law.



“Gheorghe Asachi” Technical University of Iasi, Romania



CONTENTS

New complex compounds with β -aminoisobutyric acid bidentate ligand for potential application in sustainable agriculture <i>Doina Sibiescu, Carmen Mita, Mihaela Vizitiu.....</i>	755
Promoting effect of ceria on the catalytic activity of CeO ₂ -ZnO polycrystalline materials <i>Nicolae Apostolescu, Corina Cernatescu, Ramona-Elena Tataru Farmus, Claudia Cobzaru, Gabriela Antoaneta Apostolescu.....</i>	765
Mathematical modelling for phenolation of spent sulfite liquor <i>Andrei Ionut Simion, Cristina-Gabriela Grigoras, Alexandru Chiriac, Catalin Nicolae Tampu, Lucian Gavrila.....</i>	771
Kinetics and equilibrium studies of 4-chlorophenol adsorption onto magnetic activated carbon composites <i>Marius Sebastian Secula, Etelka David, Benoit Cagnon, Andreea Vajda, Corneliu Stan, Ioan Mamaliga.....</i>	783
Evaluation of phenolic compounds content in grape seeds <i>Valeriu V. Cotea, Camelia Luchian, Marius Niculaua, Catalin Ioan Zamfir, Ioan Moraru, Bogdan Constantin Nechita, Cintia Colibaba.....</i>	795
Effect of metal tolerant plant growth promoting rhizobacteria on bean growth, cadmium and zinc uptake and stress responses <i>Eva Boglarka Vincze, Rozalia Veronika Salamon, Erika Kovacs, Gyongyver Mara.....</i>	803

Effectiveness factor approach for chemical absorption process <i>Maria Harja, Gabriela Ciobanu, Lacramioara Rusu, Liliana Lazar</i>	813
Multiple Linear Regression (MLR) models used to predict the thermal stability of some polyimides <i>Catalin Lisa, Corneliu Hamciuc, Elena Hamciuc, Gabriela Lisa</i>	821
Mass transfer in solid-liquid extraction at high solute concentrations <i>Marcela Popa, Eugenia Teodora Iacob Tudose, Ioan Mamaliga</i>	827
Valorization of microalgal biomass <i>Alexandra Cristina Blaga, Dan Cascaval, Lenuta Kloetzer, Alexandra Tucaliuc, Anca Irina Galaction</i>	841
Study of different encapsulating agents for the microencapsulation of vitamin B12 <i>Ioana C. Carlan, Berta N. Estevinho, Fernando Rocha</i>	855
Passenger car dependency and consequent air pollutants emissions in Iasi metropolitan area (Romania) <i>Lucian Rosu, Marinela Istrate, Alexandru Banica</i>	865
Antibacterial activities of beech bark (<i>Fagus sylvatica</i> L.) polyphenolic extract <i>Corneliu Tanase, Sanda Cosarca, Felicia Toma, Anca Mare, Adrian Man, Amalia Miklos, Silvia Imre, Irina Boz</i>	877
Influence of husk on the contamination of grain by <i>Fusarium spp.</i> and <i>Alternaria spp.</i> in hulled spelt (<i>Triticum spelta</i> L.) <i>Karel Suchy, Petr Konvalina, Ivana Capouchova, Dagmar Janovska, Leona Leisova-Svobodova, Zdenek Sterba, Jan Moudry jr., Daniel Bucur, Jaroslav Bernas, Marek Kopecky, Dang Khoa Tran</i>	885
Chemical oxidation integrated into bioleaching of pyrite and chalcopyrite using immobilized biomass <i>Arevik Vardanyan, Narine Vardanyan, Anna Khachatryan, Zaruhi Melkonyan</i>	897
Influence of farming system on greenhouse gas emissions within cereal cultivation <i>Jan Moudry jr., Jaroslav Bernas, Marek Kopecky, Petr Konvalina, Daniel Bucur, Jan Moudry, Ladislav Kolar, Zdenek Sterba, Zuzana Jelinkova</i>	905
Application of <i>Sphagnum</i> moss peat in ecological remediation of oxyanions contaminated aqueous solutions <i>Gabriela Ungureanu, Catalin D. Balan, Irina Volf</i>	915

Preparation and characterization of nanocomposite material based on TiO ₂ -Ag for environmental applications <i>Catalina Nutescu Duduman, Jose Maria Gómez de Salazar y Caso de Los Cobos, Maria Harja, Maria I. Barrena Pérez, Consuelo Gómez de Castro, Doina Lutic, Olga Kotova, Igor Cretescu.....</i>	925
Indicators system for assessing the organizational knowledge acquisition process <i>Daniela Geanina Luca Cososchi, Alina Luca, Luminita Mihaela Lupu, Ionut Viorel Herghiligiu.....</i>	937
Dielectric properties of some bent core liquid crystals <i>Irina Carlescu, Aurel Simion, Adrian Bele, Petru Marian Carlescu, Cristina Maria Herghiligiu, Dan Scutaru.....</i>	951
Soil seed bank and its relationship to the above-ground vegetation in grazed and ungrazed oxbow wetlands of the Yangtze River, China <i>Dong Yang, Wenzhi Liu, Hui Liu, Wei Li.....</i>	959
Analysis of the material composition of mixed municipal solid waste in the Kosice region of the Slovak Republic <i>Takacova Zita, Vindt Tomas, Havlik Tomas, Kvokacka Jozef.....</i>	969
Fate and biodegradation of estrogens in the environment and engineering systems – A review <i>Hai-Liang Song, Shi-Bei Huang, Xiao-Li Yang.....</i>	977
Cost-effectiveness of optimizing concentrated feed blends to decrease greenhouse gas emissions <i>Ricardo F.M. Teixeira.....</i>	999
An enhanced environmental multimedia modelling system (FEMMS): Part II – User interface and field validation <i>Zhi Chen, Rong-Rong Zhang, Zong-Ping Wang.....</i>	1009



"Gheorghe Asachi" Technical University of Iasi, Romania



NEW COMPLEX COMPOUNDS WITH β -AMINOISOBUTYRIC ACID BIDENTATE LIGAND FOR POTENTIAL APPLICATION IN SUSTAINABLE AGRICULTURE

Doina Sibiescu¹, Carmen Mita^{2*}, Mihaela Vizitiu^{1*}

¹"Gheorghe Asachi" Technical University of Iasi, Faculty of Chemical Engineering and Environmental Protection,
73 Prof. Dr. doc. D. Mangeron Street, 700050 Iasi, Romania

²"Alexandru Ioan Cuza" University of Iasi, Faculty of Chemistry, 11 Carol I Blvd, 700506 Iasi, Romania

Abstract

The synthesis and the study of the complexes obtained in this paper represent the beginning of our research for applied coordinative compounds of this type in agriculture. The analysis and the study of Mn(II) complexes with DL- β -Aminoisobutyric acid as ligand were accomplished in aqueous and alcoholic solution and also in solid state. The composition ratios and the stability of the synthesised compounds were analysed with specific methods: conductance, pH measurements, spectrophotometry and thermogravimetry. There were obtained two complexes, at the metal:ligand molar ratio 1:1 and 1:2. In order to determine the structures of the new compounds, the following methods were applied: chemical analysis, IR, UV-VIS and XRD spectroscopy. The $[\text{MnLCl}]_2 \cdot 2/5\text{H}_2\text{O}$ and $[\text{MnL}_2] \cdot 1/2\text{H}_2\text{O}$ presented a triclinic and respectively, monoclinic crystalline structure. From the thermal decomposition data, the kinetic parameters of the studied compounds were calculated observing that both new complex compounds have a higher thermal stability than the ligand. The experimental data confirmed that ligand DL- β -Aminoisobutyric acid presented a bi-dentate behavior towards Mn(II) ions in solution.

Key words: DL- β -aminoisobutyric acid, complex compounds, manganese (II)

Received: May, 2017; *Revised final:* January, 2018; *Accepted:* March, 2018; *Published in final edited form:* April 2018

1. Introduction

The interest for amino acids is very well known from different fields of research presenting a lot of application areas as: food industries for their bacteriostatic and antioxidant properties, enhancement of aliment flavours (alanine, arginine, aspartate); as supplement feed in livestock breeding in order to increase nutritional value; in agriculture for growth and plants protection (Wang et al., 2016). In the last decade, this class of compounds is extensively used in pharmaceutical industries for many organ dysfunction treatment (Hwang et al., 1997; Marcucci et al., 2010) and more recent in textile industry as new

compounds for ecological leather tanning (Crudu, 2008; Crudu et al., 2009).

The aminobutyric acids are safe enough to use in food industry inducing resistance against a broad organisms as: bacteria (Cohen, 1994; Cohen et al., 1994; Cohen, 2000), viruses (Cohen, 2002; Cohen et al., 2011), fungi (Tamm et al., 2011), nematode and aphids and reduce plant diseases from tomatoes (Cohen et al., 1994), potatoes, cucumbers (Sahebani et al., 2011), grapevines (Barillia et al., 2012; Cohen et al., 1999). The aminobutyric acids are known to induce resistance to microbial pathogens, nematodes and insects in several host plant/pest systems (Tiwari et al., 2013), improving early growth (Li et al., 2016)

*Author to whom all correspondence should be addressed: e-mail: cmita@uaic.ro; Phone: +40-232-201288; Fax: +40-232-201313, e-mail: mvizitiu@ch.tuiasi.ro; Phone: +40746225713; Fax: +40-232-2721311

and protection from salts stress injury by improving photosynthesis processes (Wang et al., 2017). Also, it play an important role in degradation and interorganellar transport of lipids in plant (Mitrofanova et al., 2018) or animal cells (Kammoun et al., 2014, Molfino et al., 2017) acting as O_2^- , H_2O_2 and HO-scavenger (Signorelli et al., 2015).

Regarding the main interest for amino acids used in various fields of research, mentioned above, we selected DL- β -aminoisobutyric acid (BAIBA). Our intention was to test the behavior of this acid along with its new coordination compounds with Mn(II) chloride compared to DL- β -Amino-n-butyric acid (BABA) found in literature as an important biological reagent against soybean aphid, for example *Aphis glycines* increasing the activity of some defense enzymes (Yunpeng et al., 2014). Supplemental Mn(II) reduce uptake of some heavy metal cations (Cd, Cu, Pb) from soil (Iordache et al., 2016) and their toxic effects (Cd, Pb) on plant physiology (Rahman et al., 2016; Secu, 2016). We have chosen Mn(II) for coordination with the BAIBA as ligand, due to its $3d^5$ electronic configuration (Chandra et al., 2005; Tutulea et al., 2011) with high tendency of accomplishing coordinative bonds, especially with oxygen and nitrogen donor-ligands (Crudu et al., 2009; Gerey et al., 2016; Mei et al., 2017) and greater their antibacterial activity (Kim and Park, 2017; Maurya et al., 2016).

This research represents a preliminary stage for studying the effects of different concentrations of BAIBA treatment on the growth of soybean seedlings compared to the biological activity of the new synthesized compounds.

2. Experimental

All the reagents used were of analytical grade, Fluka, 99% - 99.9% purity. The concentrations of the solutions in double distilled water were 10^{-2} M for $MnCl_2 \cdot 6H_2O$ and DL- β -aminoisobutyric acid (BAIBA), respectively. The Mn(II): BAIBA molar ratios were determined in aqueous solution by pH-metric and conductometric methods at room temperature and the values of stability constants were calculated using the Harvey-Manning method (Foca et al., 2006; Sibiescu, 2012).

The compounds were synthesized in aqueous medium by mixing the isomolar 10^{-2} M solutions in molar ratio of 1:1 and 1:2. Then the solutions were submitted to a refluxing process for three hours at $30^\circ C$ temperature. The solid compounds were obtained by the solvent evaporation at room temperature. The recrystallization process of complexes was applied both in aqueous and 80% ethylic alcohol solutions at low ($8^\circ C$) temperature (Spătărescu et al., 2010). The final products are presented as slightly pink microcrystalline powders, very soluble in water and alcohol. Chemical elemental analysis was performed on Thermo Fisher Scientific Flash EA-10 1112 CHNS/O equipment provided with Eager 300 software. Chemical elemental analysis was

accomplished for the synthesized complex compounds, in order to determine the content of carbon, hydrogen, nitrogen and manganese and to compare the results with the theoretical one.

The IR absorption spectra of crystalline complexes were recorded in $4000-200\text{ cm}^{-1}$ domain, using a Jasco FTIR 660 Plus Spectrometer, in order to determine changes of specific chemical bonds frequencies of ligand induced by the presence of manganese (II) cations. The UV-VIS absorption spectra of aqueous solution samples and study of substitution of manganese ions in solution were performed spectrophotometrically with CAMSPEC 501M single beam spectrophotometer (equipped with kinetic motorization software) using $5 \cdot 10^{-2}$ M and 10^{-3} M solution of BAIBA (HL), $[MnLCl]_2$, $[MnL_2]$, $FeSO_4 \cdot 7H_2O$, $Co(NO_3)_2 \cdot 6H_2O$ and $Cd(NO_3)_2$, at ionic strength, $I=5 \cdot 10^{-2}$ M (NaCl), pH = 6.7 (HCl - NaOH balance), at $25 \pm 0.2^\circ C$ solution temperature (HAAKE thermo-stating system), in 0.2 and 0.5 cm quartz cell, in the 190 - 800 nm range at specific wavelength of every system (Fe(II)-301 nm, Co(II)-293 nm and Cd(II)-217 nm). Each set of kinetic determination run was repeated at least twice.

XRD patterns were recorded in the $10 - 90$ degree 2θ range on a PanalyticalX'Pert Pro diffractometer, provided with a Cu $K\alpha$ radiation ($k = 1.5418740 \text{ \AA}$), Step size: 0.0131303, 45 kV - 40 mA. Unit cell parameters of the investigated complexes were further refined with PanalyticalX'Pert High Score Plus and Celref software.

The thermogravimetric study was conducted using a Mettler Toledo SDTA 851 $^\circ$ derivatograph. Thermogravimetric curves (TG) and derivative thermogravimetric curves (DTG) were recorded in the nitrogen atmosphere, in the temperature range $25-700^\circ C$, at $10^\circ C/min$ heating rate. The sample subjected to analysis weighted between 3 and 5 mg. The data used to obtain the main thermogravimetric and kinetic characteristics were processed with STAR software, using the "Kinetics nth order" module from Mettler Toledo.

3. Results and discussion

3.1. Combination molar ratio and stability constants

From the conductivity and pH versus molar ratio L/M graphs, (Figs.1a and 1b) it is observed, for each experiment, a curve that changes the slope in the points corresponding to the 1:1 and 2:1 for DL- β -aminoisobutyric acid / Mn^{2+} ratio values, indicating that two complex compounds are formed in solution. The stability constants values of the two compounds are $\beta_1=2.617 \cdot 10^6 \text{ L} \cdot \text{M}^{-1}$ and $\beta_2=1.728 \cdot 10^{12} \text{ L}^2 \cdot \text{M}^{-2}$. The highest stability is presented by the complex with maximum combination ratio, L/Mn=1/2 at pH= 3.7.

3.2. Chemical-elemental analysis

The experimental and theoretical results are presented in Table 1.

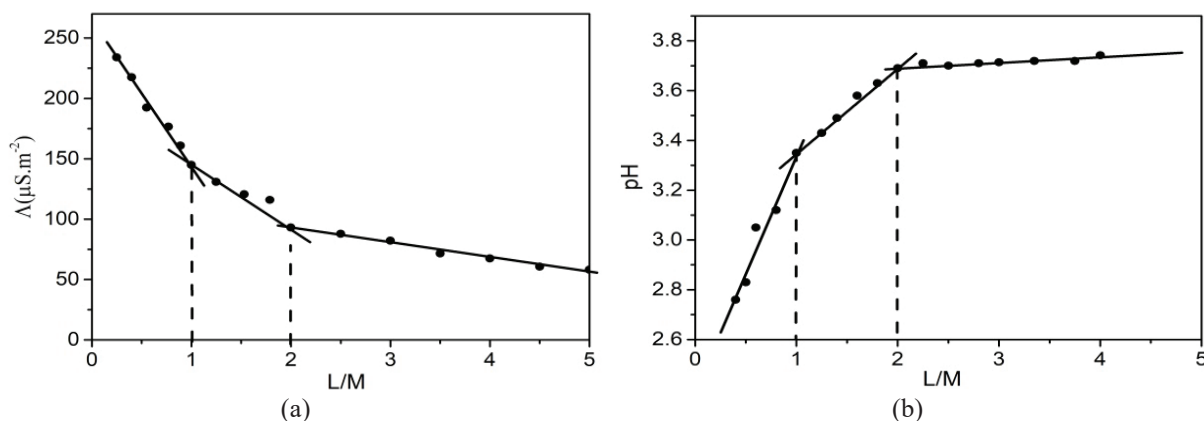


Fig. 1. The conductivity (a) and pH (b) values of $Mn(II)_{aq}$ - $BAIBA_{aq}$ solutions at different L/M molar ratio

Table 1. Content of carbon, hydrogen, nitrogen, oxygen, chlorine and manganese for the obtained complex compounds

Comp.	C%		H%		N%		O%		Cl%		Mn%	
	Exp.	Calc.	Exp.	Calc.	Exp.	Cal.	Exp.	Calc.	Exp.	Calc.	Exp.	Calc.
L:M 1:1	24.111	24.462	4.812	4.280	7.010	7.134	117.471	17.939	18.131	18.091	28.421	28.029
L:M 2:1	35.411	35.788	6.109	6.337	10.191	10.438	26.141	26.841	-	-	20.101	20.504

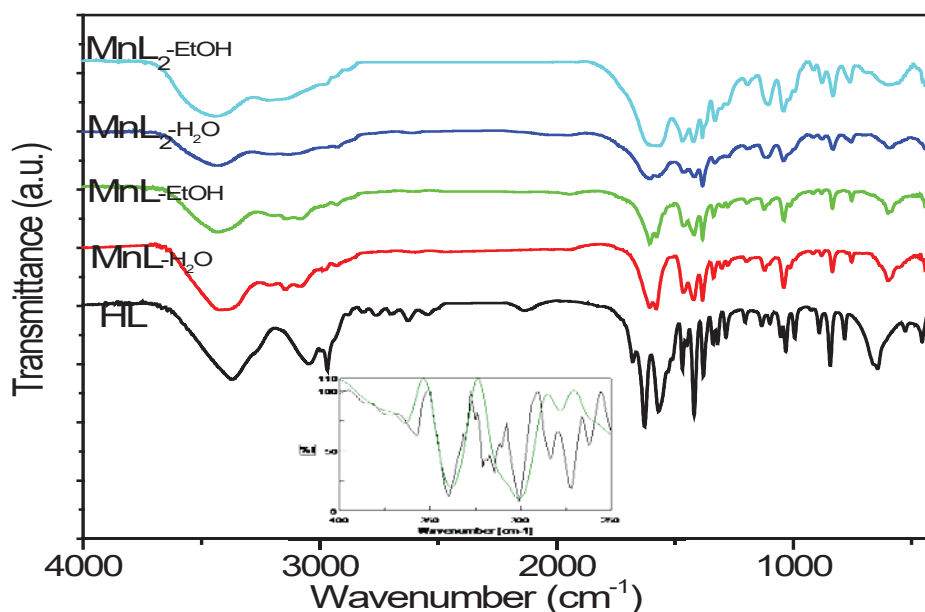
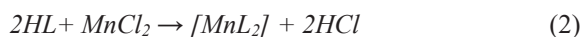
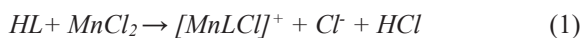


Fig. 2. IR spectra of HL, $[MnLCl]_2 \cdot 2/5H_2O$ (MnL) and $[MnL_2] \cdot 1/2H_2O$ (MnL_2) crystallized from water and ethylic alcohol and inset IR spectra of $[MnL]$ and $[MnL_2]$ in 400-250 cm^{-1} range

The experimental data were in accordance with calculated values with errors included 0.3-0.69 %. From the L:Mn(II) molar ratio and elemental chemical analysis of the obtained compounds, resulted the (1) and (2) chemical preparing reactions, in solution:



The process was followed by the separation of $[MnLCl]_2 \cdot 2/5H_2O$ (ML) and $[MnL_2] \cdot 1/2H_2O$ (ML_2) crystallized complexes.

3.3. FTIR spectra

The FTIR spectra of solid HL and Mn(II)-L coordinative compounds are shown in Fig. 2. The significant IR frequency bands values of the complexes $[ML]$ and $[ML_2]$ do not depend on the obtaining method. Among the various vibrational modes of the BAIBA, the study of the NH_2 and $COOH$ group vibrations are useful for establishment of the mode of coordination of amino acid ligand toward to manganese cation. The IR spectra of BAIBA shown a broad band centred at 3370 cm^{-1} assignable to $\nu(OH)$

vibration of carboxylic group and two other bands at 3046 cm^{-1} and 2969 cm^{-1} due to the symmetric (ν_s) and asymmetric (ν_{as}) vibration modes of NH_2 group. Lower value of $\nu(\text{OH})$ can be explained by the involving of O-H group in a hydrogen bond. The $\nu(\text{C}=\text{O})$ and $\nu(\text{C}-\text{O})$ vibration modes of carboxylic group are observed at 1628 cm^{-1} and, respectively, 1418 cm^{-1} . In [ML] and [ML₂] complexes the $\nu(\text{OH})$ and vibration band is shifted to higher frequency (3433 cm^{-1} and 3439 cm^{-1}) and overlap with $\nu(\text{NH})$ modes. These can be related with the coordinated or lattice water molecules. Also, the bands observed at 3146 , 3083 (for [ML]), 3213 and 3131 cm^{-1} (for [ML₂]), assigned to $\nu(\text{NH})$ vibration modes, have higher values compared to uncoordinated ligand.

The disappearance of $\nu(\text{OH})$ carboxylate and shift of $\nu(\text{NH})$ modes clearly suggest the deprotonization of $-\text{COOH}$ and involving of $-\text{COO}^-$ and $-\text{NH}_2$ groups in the coordination process. These are confirmed by the shifting of $\nu(\text{C}=\text{O})$ vibration mode to lower wave numbers from 1628 cm^{-1} (for HL) to 1607 cm^{-1} ([ML]) and 1605 cm^{-1} ([ML₂]), until $\nu(\text{C}-\text{O})$ vibration mode values are very close (1421 cm^{-1} and 1417 cm^{-1}) to the free HL. The $\Delta\nu(\text{COO}^-)$ values for ligand and complexes are 210, 190 and 185 cm^{-1} , fact that suggest a mono-dentate interaction of $-\text{C}-\text{O}^-$ carboxylate group with Mn(II) ion and involvement of sp^2 oxygen atom ($-\text{C}=\text{O}$) of the same group in a bridged bond with manganese cation of neighbouring complex molecule (Nakamoto, 1997). The phenomenon is more evident for ML₂. In the $700-400\text{ cm}^{-1}$ domain, the IR spectra show new bands assigned to $\nu(\text{Mn}-\text{N})$ and $\nu(\text{Mn}-\text{O})$, respectively: 599 , 442 cm^{-1} ([ML]) and 596 , 430 cm^{-1} ([ML₂]). The electronic and thermal analyses suggest a possible Mn-Cl bond in [ML]. Literature data located $\nu(\text{Mn}-\text{Cl})$ vibration mode from $[\text{MnL}_4\text{Cl}_2]$ coordinative compounds below 300 cm^{-1} (Nakamoto, 1997; Boucher et al., 2013). The IR spectra of [ML] show a new bands at 283 and 263 cm^{-1} which may be ascribed to $\nu(\text{Mn}-\text{Cl})$ stretching vibrations.

3.4. Electronic spectra

The electronic spectrum of HL (Fig. 3) exhibits an asymmetric absorption band which is centered below 190 nm . The Gaussian deconvolution of BAIBA spectrum, revealed three absorption bands at 199 , 209 and 212 nm assigned to $\pi-\pi^*$ (50251 cm^{-1}), $n_{\text{O}}-\pi^*$ (47846 cm^{-1}), and $n_{\text{N}}-\pi^*$ (47170 cm^{-1}), respectively.

The spectra of aqueous solution of [ML] and [ML₂] complexes are similar, with an intense and asymmetric absorption band in $190-250\text{ nm}$ range and a number of weak bands in visible domain, more evident for [ML₂] compound, assigned to d-d transition of Mn(II)- d^5 . After the deconvolution of spectra, the bands of coordinated ligand shifted to the lower energy values in case of [ML₂] due to electronic effect determined by the second L- ion from coordination sphere of manganese cation: 191 nm

(52356 cm^{-1}), 197 nm (50761 cm^{-1}), 204 nm (49019 cm^{-1}) for [ML] and 197 nm (50761 cm^{-1}), 212 nm (47170 cm^{-1}), 217 nm (46083 cm^{-1}) for [ML₂].

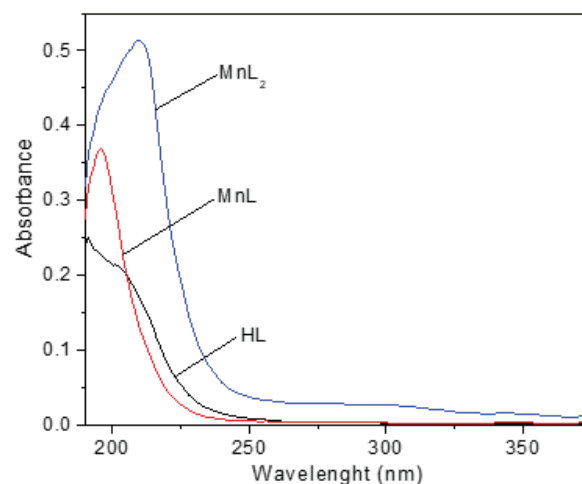
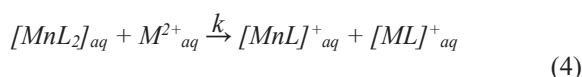
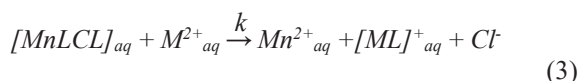


Fig. 3. Electronic spectra of HL, [MnL] and [MnL₂] in aqueous solution: $C_{\text{HL}} = C_{\text{compl}} = 10^{-3}\text{ M}$, $l = 0.2\text{ cm}$

Additional bands assigned to ligand – metal charge transfer, LMCT, overlapped with ligand absorption bands, centred at 220 nm (45454 cm^{-1} , [ML]) and 283 nm (35336 cm^{-1} , [ML₂]), respectively, were identified. The [ML₂] complex displays the d-d absorption bands at 462 nm (21645 cm^{-1}) and 343 nm (29154 cm^{-1}) attributed to ${}^6\text{A}_{1g} - {}^4\text{T}_{1g}(\text{G})$ and ${}^6\text{A}_{1g} - {}^4\text{T}_{2g}(\text{G})$ forbidden electronic transitions which are characteristic for octahedral Mn(II)-high spin coordinative compound (Boucher, 2013; Mei et al., 2017).

3.5. Substitution reactions of Mn(II) in aqueous solution

Mixing $1\text{ mL } 5 \cdot 10^{-2}\text{ M } [\text{MnLCl}]_2 \cdot 2/5\text{H}_2\text{O}$ complex solution and $[\text{MnL}_2] \cdot 1/2\text{H}_2\text{O}$, respectively, with 1 mL solution $10^{-3}\text{ M } \text{Fe}^{2+}_{\text{aq}}$, $\text{Co}^{2+}_{\text{aq}}$ and $\text{Cd}^{2+}_{\text{aq}}$ respectively, the substitution of Mn^{2+} ions from complexes takes place. The monitored absorbance, at specific wavelengths, change in time for each reaction systems (Astilean, 2002). In Fig. 4 is presented the concentration traces of $[\text{FeL}]^+_{\text{aq}}$, $[\text{CoL}]^+_{\text{aq}}$ and $[\text{CdL}]^+_{\text{aq}}$ in time for all studied systems. The formation of [ML] species and the movement of equilibrium to the direct reactions 1 is presented below (Eqs. 3, 4):



It is evidenced by the evolution of [ML] concentration complexes determined at the wavelengths corresponding to the coordination compounds of L (BAIBA) with M^{2+} from mixed solutions. The most pronounced increase of concentration is recorded for [MnL] – Fe^{2+} and [MnL₂] – Fe^{2+} systems.

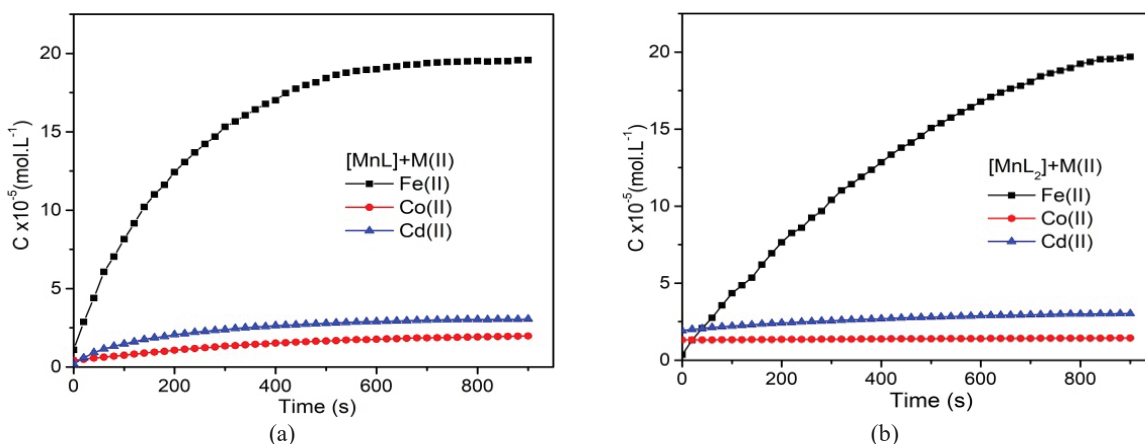


Fig. 4. Concentration evolution of new [ML] (M= Fe, Co and Cd) complexes during the Mn(II) substitution from $[MnL]aq$ (a) and $[MnL_2]aq$ (b) in aqueous solution at pH=6.7, T= 298 K and scan time of every 20 s

Table 2. Values of observable rate constant, k_{obs} , for $n=1$ and $n=2$ kinetic models, for the reversible first step of reactions (1) and (2)

Reaction system		$n=1$		$n=2$	
Complex	Metal cation	k_{obs}, s^{-1}	r	$k_{obs} mol \cdot L^{-1}$	r
[MnL]	Fe ²⁺	1.250·10 ⁻²	0.9927	8.630·10 ⁻²	0.8433
	Co ²⁺	3.777·10 ⁻³	0.9928	1.116·10 ⁻²	0.8802
	Cd ²⁺	8.597·10 ⁻⁴	0.9989	8.093·10 ⁻³	0.9339
[MnL ₂]	Fe ²⁺	6.556·10 ⁻³	0.9836	7.039·10 ⁻³	0.861
	Co ²⁺	4.993·10 ⁻⁴	0.9855	5.539·10 ⁻²	0.9066
	Cd ²⁺	6.469·10 ⁻⁴	0.9927	1.063·10 ⁻²	0.9090

r - correlation coefficient

Based on the obtained data, the rate constants were calculated (Table 2) for the determining step of reaction rate (the slowest step). The observable rate constants, k_{obs} , were determined graphically by applying the pseudo-first and second order kinetic models (Eqs. 5, 6) (Bugarcic et al, 2015; Topolski et al., 2017).

$$n=1 \\ \ln(C_1 - C_0) = \ln(C_0) - k_{obs} \cdot t \quad (5)$$

$$n=2 \\ 1/(C_1 - C_0) = 1/C_0 + k_{obs} \cdot t \quad (6)$$

The correlation coefficients presented in Table 2 show the higher values for first order rate constant ($n=1$) which correspond to a linear dependence of ligands interchange (BAIBA – H₂O). The comparison of the first order rate constants k_1 of all reaction systems shows that the compatibility between Lewis hardness of M²⁺ and O-, N-donor ligand plays an important role, more evident in case of [MnL] – Co²⁺ system ($k_1 = 3.777 \cdot 10^{-3} s^{-1}$). Also, the presence of supplementary Cl⁻ ions (Eq. 3) has a direct consequence on the increasing of products solvation process and of k_{obs} values, respectively.

Extension of Mn²⁺ coordination sphere in [MnL₂] increases the influence of elemental solvation process of the reactants and reaction intermediates. In

this case, the proton donor species can interfere in elementary first step of mechanism, favouring a certain type of movement – associative (nucleophile substitution SN_2 by A -associative or I_a - associative interchange mechanism) or dissociative (nucleophile substitution SN_1 by D - dissociative or I_d - dissociative interchange mechanism). In hydrogen bond formation the water molecules, supplementary polarized by coordination at M²⁺ cations, participate with higher probability. The rate of proton transfer depends on electronegativity and polarizability of metal cation. This stage could be the determining rate step which corresponds of I_d mechanism. The cumulative influence of all mentioned factors can explain the k_{obs} lower values for [ML₂] – M²⁺ systems and the small difference between them.

3.5. X-ray diffraction analysis

The possible crystal structures of $[MnLCl]_2 \cdot 2/5H_2O$ and $[MnL_2] \cdot 1/2H_2O$ complexes have been determined on the X-ray powder diffraction analysis. The X-ray data were refined with Celref program at maximum deviation of $2\theta=0.07^\circ$ and h, k, l Miller indices were assigned (Fig. 5).

The final results show that $[MnLCl]_2 \cdot 2/5H_2O$ belongs to triclinic crystal system ($P(-1)$ space group) with unit cell parameters: $a=5.4286 \text{ \AA}$, $b=7.2745 \text{ \AA}$, $c=15.0061 \text{ \AA}$, $\alpha=50.43(4)^\circ$, $\beta=97.95(3)^\circ$, $\gamma=87.54(2)^\circ$

and $V=445,707 \text{ \AA}^3$ (Giacovazzo et al., 2008; Vainstein, 1989).

The $[\text{MnL}_2] \cdot 1/2\text{H}_2\text{O}$ solid compound crystallized in monoclinic system, $C2/c$ space group with $a=22.3911 \text{ \AA}$, $b=13.6913 \text{ \AA}$, $c=19.6709 \text{ \AA}$, $\beta=114.54(4)^\circ$ and $V=5489.446 \text{ \AA}^3$.

3.7. Thermal-gravimetric analysis and the kinetics of the decomposition reactions

Studying the TG curves for both ligand and complexes (Fig. 6) reveals that the thermal destruction takes place in four steps with the emission of gaseous compounds resulted from the organic part of the ligand. The final solid products of the thermal decomposition corresponds to MnO and some carbon

compounds residue (Freeman and Carroll, 1958; Segal and Fatu, 1983). Also, it is observed that the thermal stability of the compounds increases in order: $\text{HL} < \text{MnL}_2 < \text{MnL}$ as it is shown in the Fig. 6 and Table 3. The transport phenomena of the gaseous products through the solid compound, the interphase interactions and also the vaporization of the volatile products are related to the fraction reaction order values. The reaction order value increases with the dispersion degree of the resulted products (Table 4).

3.8. The proposed structure of the new synthesized complex compounds

Based on the above observation we proposed the possible structures of Mn(II) –BAIBA complexes, in aqueous solutions and solid state (Fig. 7).

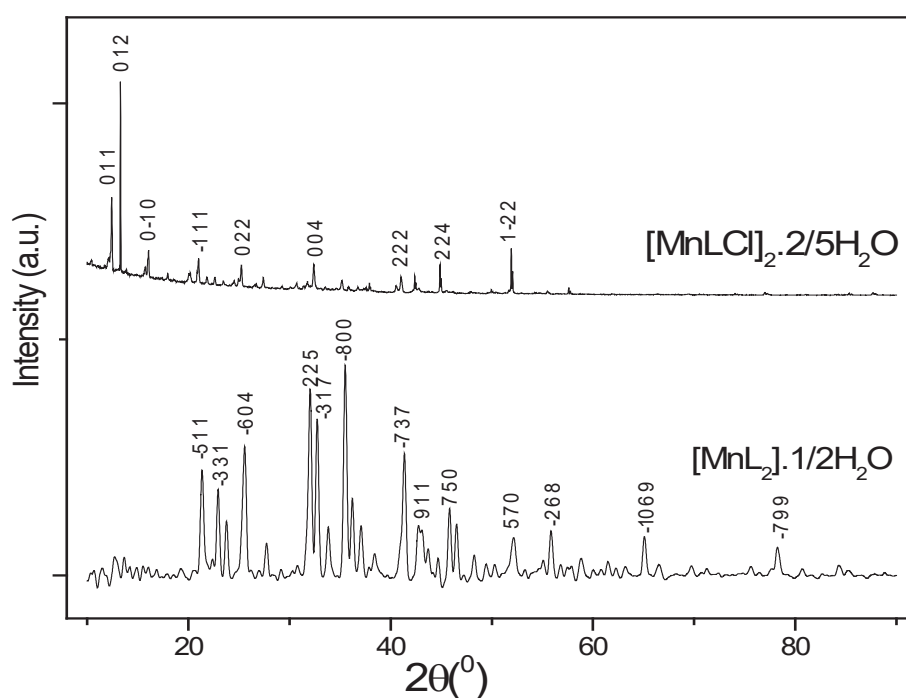


Fig. 5. Diffractograms of $[\text{MnLCl}_2]_2 \cdot 2/5\text{H}_2\text{O}$ and $[\text{MnL}_2] \cdot 1/2\text{H}_2\text{O}$

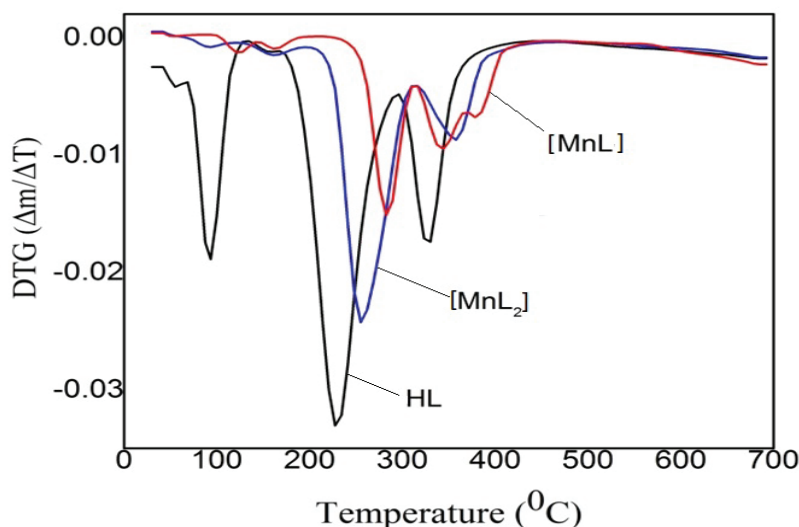


Fig. 6. The DTG curves of the ligand and the synthesized compounds

Table 3. Thermal characteristics of the degradation process of the ligand and synthesized manganese complexes

Sample	Step	T_{onset} , °C	T_{peak} , °C	T_{endset} , °C	Weight loss, %	Residue, %
HL	I	47.8	50	62.5	2.67	0
	II	84.4	92.1	102.1	15.67	
	III	198.7	229.2	259.2	53.28	
	IV	314.7	327.1	352.1	28.31	
[MnLCl] ₂ ·2/5H ₂ O	I	115.4	123.0	129.9	0.94	57.18
	II	154.1	162.3	175.8	0.80	
	III	270.8	283.0	300.2	15.78	
	IV	328.9	381.4	395.7	25.30	
[MnL ₂]·1/2H ₂ O	I	81.6	89.2	109.0	0.96	38.66
	II	143.7	160.2	189.2	2.42	
	III	240.0	253.7	292.0	37.81	
	IV	330.2	358.7	372.2	20.15	

Table 4. The kinetic parameters (activation energy, E_a ; reaction order, n ; pre-exponential factor, $\ln k_0$) of the decomposition reactions of the ligand and the synthesized Mn(II) complexes

Sample	Step	E_a , kJ/mol	n	$\ln k_0$
HL	I	137.63±2.77	0.82	46.69±1.03
	II	111.14±0.53	0.50	32.39±0.18
	III	157.82±0.47	1.56	33.31±0.12
	IV	288.59±3.53	0.95	53.69±0.71
[MnLCl] ₂ ·2/5H ₂ O	I	129.10±8.48	0.47	35.18±2.61
	II	132.50±11.00	0.59	32.34±3.06
	III	270.70±13.97	1.04	54.68±3.06
	IV	111.05±2.48	0.90	13.17±2.68
[MnL ₂]·1/2H ₂ O	I	133.78±18.18	0.74	40.45±6.06
	II	148.54±7.63	0.62	37.60±2.18
	III	282.03±11.81	1.34	60.69±2.76
	IV	111.90±6.22	0.14	16.44±1.20

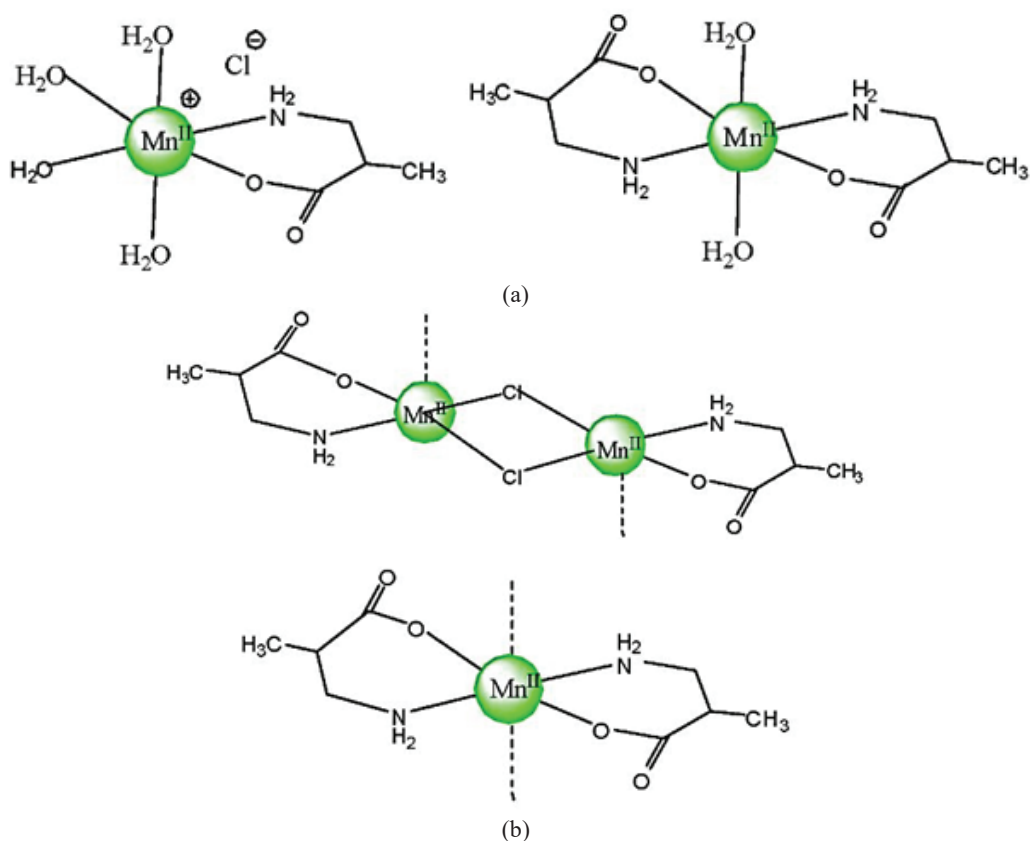


Fig. 7. Proposed structure of [ML] and [ML₂] coordination units in aqueous solution (a) and solid state (b)

4. Conclusions

We have synthesized two new complexes of Mn (II) with DL- β -Aminoisobutyric acid in 1:1 and 1:2 molar ratio in aqueous solution. They were characterized by physical-chemical methods in order to determine their structures and properties: pH-metry, conductometry, chemical analysis, IR-absorption spectra, XRD and the thermal analysis. Both 1:1 and 1:2 molar ratio compounds are slightly pink crystalline solids.

Thermal decomposition begins at 100°C for both complexes and at above 50°C for the ligand, showing the increased thermal stability of the coordinative compounds due to the coordination process.

The experimental data were in agreement with the literature indications and we proposed the structures of the new complex compounds with Mn(II), revealing the bi-dentate properties of the ligand.

In further studies, this research will be continued for testing the biological properties of the ligand BAIBA and its coordinative compounds in agriculture.

References

- Astilean S., (2002), *Methods and Modern Techniques of Optical Spectroscopy* (in Romanian), Book Publishing House of Science, Cluj-Napoca, Romania.
- Barillia E., Rubialesa D., Castillejo M.Á., (2012), Comparative proteomic analysis of BTH and BABA - induced resistance in pea (*Pisum sativum*) toward infection with pea rust (*Uromyces pisi*), *Journal of Proteomics*, **75**, 5189-5205.
- Bugaric Z.D., Bogojeskia J., van Eldik R., (2015), Kinetics, mechanism and equilibrium studies on the substitution reactions of Pd(II) in reference to Pt(II) complexes with bio-molecules, *Coordination Chemistry Reviews*, **292**, 91-106.
- Boucher L.J., Kotowski M., Koeber K., Tille D., (2013), *Mn Manganese: Coordination Compounds 7, Handbook of Inorganic and Organometallic Chemistry - 8th Edition*, Springer Science & Business Media.
- Chandra S., Kumar U., (2005), Spectral and magnetic studies on manganese(II), cobalt(II) and nickel(II) complexes with Schiff bases, *Spectrochimica Acta Part A*, **61**, 219-224.
- Cohen Y., (1994), 3-Aminobutyric acid induces systemic resistance against *Peronospora tabacina*, *Physiological and Molecular Plant Pathology*, **44**, 273-288.
- Cohen Y., Niderman T., Möisinger E., Fluhr R., (1994), β -Aminobutyric acid induces the accumulation of pathogenesis - related proteins in tomato (*Lycopersicon esculentum* L.) plants and resistance to late blight infection caused by *Phytophthora infestans*, *Plant Physiology*, **104**, 59-66.
- Cohen Y., Reuveni M., Baider A., (1999), Local and systemic activity of BABA (DL-3-aminobutyric acid) against *Plasmopara viticola* grapevines, *European Journal of Plant Pathology*, **105**, 351-361.
- Cohen Y., (2000), Method for protecting plants from fungal infection, USA Patent, No. 6075051.
- Cohen Y., (2002), β -Aminobutyric acid - induced resistance against plant pathogens, *Plant Disease*, **86**, 448-457.
- Cohen Y., Rubin A.E., Vakinin M., (2011), Post infection application of DL- β -aminobutyric acid (BABA) induces multiple forms of resistance against *Bremialactuceae*, *European Journal of Plant Pathology*, **130**, 13-27.
- Crudu M., (2008), *Study on the use of inorganic processing of natural leather concerning the prevention of environmental pollution* (in Romanian), PhD Thesis, "Gheorghe Asachi" Technical University of Iasi, Romania.
- Crudu M., Sibiescu D., Rosca I., Sutiman D., Vizitiu M., Apostolescu G., (2009), New coordination compounds of Cr(III) used in leather tanning, *Proceedings of SPIE*, The International Society for Optical Engineering, 7297, DOI: 10.1117/12.823638.
- Crudu M., Sibiescu D., Rosca I., Sutiman D., Vizitiu M., (2009), Studies of obtaining and stability in aqueous medium of new complex compounds of Ti(IV) and Zr(IV) used in ecological leather tanning, *Proceedings of SPIE*, The International Society for Optical Engineering, 7297.
- Foca N., Sibiescu D., Oancea S., (2006), *Physico-Chemical Methods Applied in the Complex Combination Studies*, Tehnopress, Iasi, Romania, 58-97.
- Freeman S.E., Carroll B., (1958), The application of thermoanalytical techniques to reaction kinetics. The thermogravimetric evaluation of the kinetics of the decomposition of calcium oxalate monohydrate, *The Journal of Physical Chemistry*, **62**, 394-397.
- Gerey B., Goure E., Fortage J., Pecaut J., Collomb M.N., (2016), Manganese-calcium/strontium heterometallic compounds and their relevance for the oxygen-evolving center of photosystem II, *Coordination Chemistry Reviews*, **319**, 1-24.
- Hwang B.K., Sunwoo J.Y., Kim Y.J., Kim B.S., (1997), Accumulation of β -1,3-glucanase and chitinase isoforms, and salicylic acid in the DL- β -amino-n-butyric acid induced resistance response of pepper stems to *Phytophthora capsici*, *Physiological and Molecular Plant Pathology*, **51**, 305-322.
- Kammoun H.L., Mark A., Febbraio M.A., (2014), Come on BAIBA Light My Fire, *Cell Metabolism*, **19**, 1-2, <http://dx.doi.org/10.1016/j.cmet.2013.12.007>.
- Kim J.W., Park J.K., (2017), Synergistic antimicrobial properties of active molecular chitosan with EDTA-divalent metal ion compounds, *Journal of Phytopathology*, **165**, 641-651, DOI: 10.1111/jph.12603.
- Iordache M., Branzoi I.V., Popescu L.R., Iordache I., (2016), Evaluation of heavy metal pollution into a complex industrial area from Romania, *Environmental Engineering and Management Journal*, **15**, 389-394.
- Li W., Liu J., Ashraf U., Li G., Li Y., Lu W., Gao L., Han F., Hu J., (2016), Exogenous α -aminobutyric acid (GABA) application improved early growth, net photosynthesis, and associated physio-biochemical events in maize, *Frontiers in Plant Science*, **7**, doi: 10.3389/fpls.2016.00919.
- Giacovazzo C., Monaco H.L., Artioli G., Viterbo D., Ferraris G., Gilli G., Zanotti G., Catii M., (2008), *Fundamentals of Crystallography*, 2nd Edition, reprinted, Oxford University Press, Oxford.
- Maurya R.C., Bohre P., Sahu S., Martin M.H., Sharma A.K., (2016), Manganese(II) chelates of bioinorganic and medicinal relevance: Synthesis, characterization, antibacterial activity and 3D-molecular modelling of

- some penta-coordinated manganese(II) chelates in O,N-donor coordination matrix of b-diketoenolates and picolinate, *Arabian Journal of Chemistry*, **9**, S54-S63.
- Marcucci E., Aleandri M.P., Chilosi G., Magro P., (2010), Induced resistance by β -aminobutyric acid in artichoke against white mould caused by *Sclerotinia clerotiorum*, *Journal of Phytopathology*, **158**, 659-667.
- Mei Y.X., Hui Yu H., Wei E.H., Mei G.Q., Cai H., (2017), Two coordinated geometries of Mn^{2+} ions in one single molecule: organic-inorganic hybrids constructed with tris(2-aminoethyl)amine and manganese halide and fluorescent properties, *Polyhedron*, **127**, 458-463.
- Molfino A., Amabile M.I., Ammann T., Alessio Farcomeni A., Lionetto L., Simmaco M., Lai S., Laviano A., Rossi Fanelli F., Chiappini M.G., Muscaritoli M., (2017), The metabolite beta-aminoisobutyric acid and physical inactivity among hemodialysis patients, *Nutrition*, **34**, 101-107.
- Nakamoto K., (1997), *Infrared and Raman Spectra of Inorganic and Coordination Compounds*, John Wiley and Sons, New-York.
- Rahman A., Nahar K., Hasanuzzaman M., Masayuki Fujita M., (2016), Manganese-induced cadmium stress tolerance in rice seedlings: Coordinated action of antioxidant defense, glyoxalase system and nutrient homeostasis, *Comptes Rendus Biologies*, **339**, 462-474.
- Sahebani N., Hadavi N.S, Zade F.O., (2011), The effects of β -aminobutyric acid on resistance of cucumber against rootknot nematode *Meloidogyne javanica*, *Acta Physiologiae Plantarum*, **33**, 443-450.
- Segal E., Fatu D., (1983), *Introduction to Kinetic Non-Isotherm Reactions*, Romanian Academy Publishing House, Bucharest, Romania.
- Sibiescu D., (2012), *Chemistry of Coordination Compounds*, (in Romanian), Pim Publishing House, Iasi, Romania.
- Signorelli S., Dans P.D., Coitino E.L., Borsani O., Monza J., (2015), Connecting proline and γ -aminobutyric acid in stressed plants through non-enzymatic reactions, *PLoS ONE*, **10**, e0115349, doi:10.1371/journal.pone.0115349.
- Tiwari S., Meyer W.L., Stelinski L., (2013), Induced resistance against the Asian *Citrus psyllid*, *Diaphorina citri*, by β -aminobutyric acid in citrus, *Bulletin of Entomological Research*, **103**, 592-600.
- Topolski A., Rozmarynowska P., Maj M., Czajkowski R., (2017), Kinetics and mechanism of chloride substitution by thiourea, L-methionine and glutathione in bimetallic $[Pt_2(6NNqui)Cl_4]$ complex in water-DMF medium. Unusually slow reaction with thiourea, *Inorganica Chimica Acta*, **462**, 10-15.
- Secu C.V., (2016), Potentially toxic elements in urban soils of Iasi (Romania), *Environmental Engineering and Management Journal*, **15**, 687-698.
- Spătărescu I., Sibiescu D., Roșca I., (2010), The characterization and the synthesis of a new coordination compound for removal of Cr(III) from wastewaters, *Environmental and Engineering and Management Journal*, **9**, 443-447.
- Tamm L., Thürig B., Fließbach A., Goltlieb A.E., Karavani S., Cohen Y., (2011), Elicitors and soil management to induce resistance against fungal plant diseases, *Journal of Life Sciences*, **58**, 131-137.
- Tutulea M.D., Rosca I., Cretescu I., Cailean A., Bistricianu I.L., (2011), New coordinative compounds of Mn(II) and Cu(II) using as ligand N-hydroxy-succinimide, *Revista de Chimie*, **62**, 293-298.
- Vainstein K.B., (1989), *Modern Crystallography*, (in Romanian), vol. 1, Scientific and Encyclopaedic Publishing House, Bucharest, Romania.
- Yunpeng Z., Biao W., Junhui Y., Linjing C., Luming Y., Liang X., Tianlong W., (2014), DL- β -Aminobutyric Acid induced resistance in soybean against *Aphis glycines* Matsumura (Hemiptera: Aphididae), *PLoS ONE*, **9**, e85142, <https://doi.org/10.1371/journal.pone.0085142>.
- Wang Y., Gu W., Meng Y., Xie T., Li L., Li J., Wei S., (2017), γ -Aminobutyric acid imparts partial protection from salt stress injury to maize seedlings by improving photosynthesis and upregulating osmoprotectants and antioxidants, *Scientific Reports*, **7**, Article number:43609, DOI: 10.1038/srep43609.
- Wang L., Zhang H., Jin P., Guo X., Li Y., Fan C., Wang J., Zheng Y., (2016), Enhancement of storage quality and antioxidant capacity of harvested sweet cherry fruit by immersion with β -aminobutyric acid, *Postharvest Biology and Technology*, **118**, 71-78



“Gheorghe Asachi” Technical University of Iasi, Romania



PROMOTING EFFECT OF CERIA ON THE CATALYTIC ACTIVITY OF CeO₂-ZnO POLYCRYSTALLINE MATERIALS

Nicolae Apostolescu, Corina Cernătescu, Ramona-Elena Tătaru Fărnuș,
Claudia Cobzaru, Gabriela Antoaneta Apostolescu*

“Gheorghe Asachi” Technical University of Iasi, Faculty of Chemical Engineering and Environmental Protection,
73 Prof. Dr. docent Dimitrie Mangeron Str., 700050 Iasi, Romania

Abstract

A polycrystalline CeO₂-ZnO catalyst was prepared by using a hydrothermal procedure in order to improve the structural properties. This polycrystalline material was then used to remove organic pollutants from aqueous solutions by the means of photocatalysis. The structural, morphological and optical properties of as-prepared materials were characterized by several techniques, such as UV-visible spectroscopy, SEM, FTIR, XRD. The SEM analysis shows that the crystallite size sample varies in the range of 0.3-2 μm. The photocatalytic activity under UV irradiation was estimated by measuring the degradation rate of aqueous solutions of methylene blue (MB, 0.01mM/L) and 4'-(1-methyl-benzimidazolyl-2)-phenylazo-2''-(8''-amino-1''-hydroxy-3'', 6''-disulphonic)-naphthalene acid (PMBH, 0.05mM/L). The effect of catalyst content on the photocatalytic activity was also studied. The results confirm that this material can be potentially applied for the treatment of water contaminated by organic pollutants.

Key words: band gap energy, CeO₂-ZnO nanoparticles, photocatalytic degradation

Received: May, 2017; *Revised final:* February, 2018; *Accepted:* March, 2018; *Published in final edited form:* April 2018

1. Introduction

Recently, the need to keep the environment clean and safe has led to looking for efficient, and economically convenient solutions, such as semiconductor materials. Semiconductor materials have become particularly attractive to the scientific community, and are used in various fields, such as electronics, environmental remediation techniques (*i.e.* catalysts or photocatalysts (Favier et al., 2016; Fujishima and Zhang, 2006; Jesudoss et al., 2016; Nascimento et al., 2014; Paz, 2006; Reddy et al., 2015) or for conversion of solar energy (Bhosale et al., 2016; Fujishima and Honda, 1972; Lira-Cantu and Krebs, 2006).

Thus, when a semiconductor is irradiated with energy close to, or greater than the band gap energy (E_g), electrons are generated in the conduction band

(e^-) and holes in the valence band (h^+). These electric charges are mobile and are able to initiate various redox reactions on the surface of the catalyst, but they have the tendency to recombine quickly, thus dissipating the absorbed energy. Therefore, a semiconductor photocatalytic activity is dependent on the competition between the transfer of electric charge on its surface and recombination of electron-hole pairs (Faisal et al., 2013; Kaviyarasu et al., 2017). For many materials with the same chemical composition, the structural, catalytic and electronic properties may be completely different, depending on how these are processed (Jafari et al., 2016).

Zinc oxide and cerium (IV) oxide have been and still are intensively studied due to their versatility and multiple applications (Faisal et al., 2013; Nascimento et al., 2014). ZnO crystallizes in a hexagonal or cubic system, but the hexagonal form is

* Author to whom all correspondence should be addressed: e-mail: ganto@ch.tuiasi.ro

more stable. It is a semiconductor compound with the ionicity on the border between the ionic and covalent semiconductor. The chemical bond becomes partially ionic due to electronic charge transfer from Zn to O. In this way, the Coulomb interaction between the ions increases, hence the width of the band gap material also increases. One of its most important features is the polar surface that causes a series of specific properties, such as spontaneous polarization and piezoelectricity, leading to many applications in electronics, gas sensors or photocatalysis (Amira et al., 2017). ZnO is cheap, it can be recovered from waste products (Jule et al., 2016; Lopez et al., 2017) and has a low toxicity (Xia et al., 2008) being used as an ingredient in numerous products such as: drugs, cosmetics, photocatalyst, additive for textiles and paper (Atchudan et al., 2017; Faisal et al., 2013; Mirzaei and Darroudi, 2017). The properties of zinc oxide can be considerably improved by doping it with the various components such as transitional metal ions or oxides (Choi et al., 1994; Kannadasan et al., 2014; Lira-Cantu and Krebs, 2006; Mogensen et al., 2000). In the present paper, we focused on the study of a CeO₂-ZnO polycrystalline mixture.

2. Experimental

2.1. Material and methods

The chemicals used in this study were Zn(CH₃COO)₂ x2H₂O, Ce(NO₃)₃ x6H₂O, citric acid (all 99.99% purity, supplied from Sigma-Aldrich). The reagents were first dissolved in distilled water, and then mixed under vigorous stirring with the appropriate amounts of citric acid, at 333 K, for two hours, the obtained yellow precipitate was separated by decantation, then was washed and transferred into a furnace for 3 hours at 773 K, to remove the organic phase (Apostolescu et al., 2015). Other researchers have observed that Ce³⁺, heated over 773 K passes in Ce⁴⁺ (Nagy and Dekany, 2009). The yellow-white powders were used to establish the photocatalytic activity, without other treatments. Two samples were prepared, first named a1, starting from 1 mmol Ce(NO₃)₃ x6H₂O and 9 mmol Zn(CH₃COO)₂ x2H₂O and the second sample, named a2 starting from 3

mmol Ce(NO₃)₃ x6H₂O and 7 mmol Zn(CH₃COO)₂ x2H₂O.

The organic dyes tested were methylene blue-MB (Chemical Company) and 4'-(1-methylbenzimidazol-2''-phenylazo-2''-(8''-amino-1''-hydroxy-3'',6''-disulphonic)-naphthalene acid abbreviated PMBH (synthesized in our laboratories) (Cernatescu et al., 2015) and are presented in Table 1.

2.2. Characterization methods

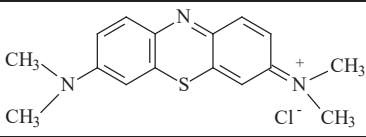
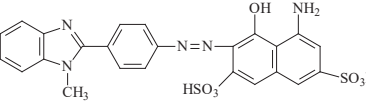
The phase composition of all powders and obtained samples were identified by the X-ray diffraction method (Philips PW 1840 diffractometer) under the following conditions: 40 kV, 30 mA, monochromatic CuK α radiation ($\lambda = 0.15418$ nm) over a 2θ range from 10 to 70°. The FTIR spectra were recorded on a Perkin Elmer Spectrum 100, resolution 2 cm⁻¹ using 32 scans in the range 4000 - 400 cm⁻¹; all samples were prepared as KBr pellets (ratio 5 / 95 wt.%). The morphology of prepared samples was observed by scanning electron microscope (Vega Tescan 30 kV). The ultraviolet-visible spectra were carried out using a spectrophotometer (UV-Vis SPECORD 200 Analytik Jena) for solid sample and SP 870plus METERTech for dyes residual concentration.

2.3. Photocatalysis experiments

Photocatalysis experiments were performed using an 18W Hg UV B lamp. The incident radiation intensity was measured as being 0.105 mW/cm², and was determined by a Hamamatsu C9536-01 meter with H9958 detector for 310 - 380 nm, scaled between 1 μ W/cm² and 100 mW/cm².

Samples containing the dyes (MB, 10⁻⁵ M, or PMBH, 5·10⁻⁵M, at natural pH), and 0.2 - 0.3 g/L photocatalytic materials were UV irradiated, and the concentration of the dye was monitored by UV-vis measurements (at 664 nm for MB and 540 nm for PMBH). Before recording the spectrum, the samples were centrifuged (5000 rotation/min) to separate the solid content. The dye-photocatalyst system was initially left for 30 minutes stirring in the dark, until adsorption equilibrium was reached.

Table 1. Characteristics of organic dye

Dye	Chemical structure	Molecular formula	λ_{max}	Molar mass
Methylene blue (MB)		C ₁₆ H ₁₈ ClN ₃ S	664 nm	319.85 g/mol
4'-(1-methylbenzimidazol-2''-phenylazo-2''-(8''-amino-1''-hydroxy-3'',6''-disulphonic)-naphthalene acid (PMBH)		C ₂₄ H ₁₉ N ₅ O ₇ S ₂	540 nm	553 g/mol

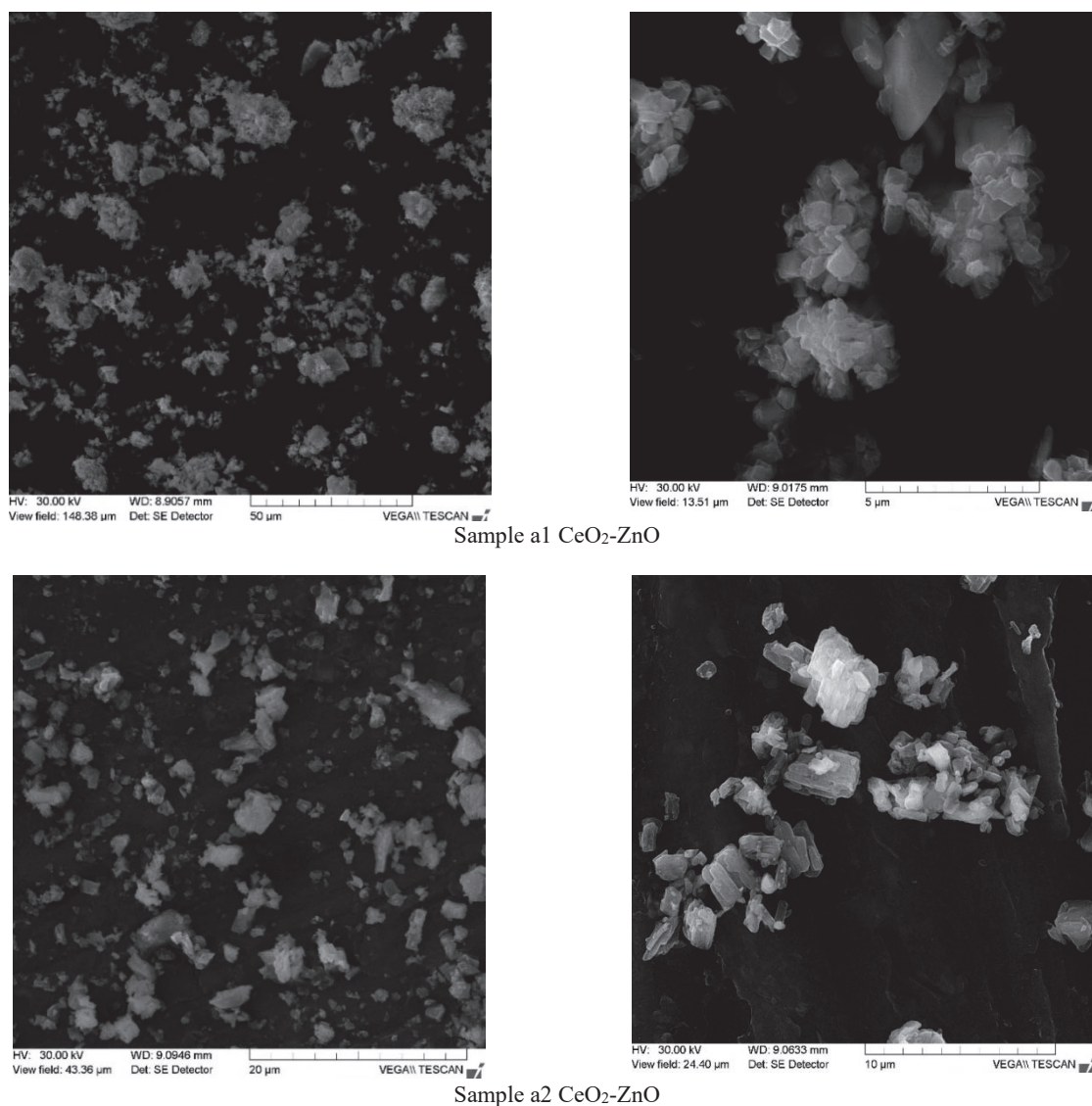


Fig. 1. SEM micrographs of a1 and a2 samples at different magnification

Degradation efficiency $D(\%)$, was calculated with Eq. (1):

$$D(\%) = \left[\frac{A(dye)_i - A(dye)_t}{A(dye)_i} \right] \cdot 100 \quad (1)$$

where $A(dye)_i$ and $A(dye)_t$ are the absorbance of MB at 664 nm and PMBH at 540 nm, in the dark and under UV irradiation (at t minutes).

3. Results and discussion

3.1. Morphology and structure of CeO₂-ZnO photocatalysts

SEM micrograph of the surface morphology of CeO₂-ZnO prepared samples are shown in Fig. 1. Sample 1 with a low-CeO₂ content presents tabular aggregates, with size $0.3 \times 0.6 \mu\text{m}$ and $0.4 \times 0.7 \mu\text{m}$. The second sample shows prismatic aggregates ranging in size from $1 \times 0.5 \times 0.25 \mu\text{m}$ up to $2.5 \times 0.8 \times 0.3 \mu\text{m}$. The large aggregates are actually composed of small CeO₂-ZnO

particles leading to a relatively rough surface. Microcrystals agglomeration is a common phenomenon, which tends to reach a state of minimum energy, by reducing the contact with the outside environment (Chen and Chang, 2006). The small size of crystallites reported is in accordance with determined photocatalytic activity.

UV-vis absorption spectra of the two samples is presented in Fig. 2, (inset), and were used to calculate the band gap energy, using the Tauc plot. According to the photocatalytic mechanism, the band gap of the semiconductor plays a major role in the photocatalytic activity of as-prepared materials. Band gap of the photocatalysts was determined through Eq. (2):

$$(ah\nu)^2 = k \cdot (h\nu - E_g) \quad (2)$$

where: $h\nu$ is the photon energy (eV), a is the absorption coefficient, k is a constant and E_g (eV) is the band gap energy. By extrapolating the linear region in a plot of $(ah\nu)^2$ versus photon energy, the

band gap can be estimated from graph, using Eq.(2). The band gap values are presented in Fig. 2 and have been found to be different than the value reported for bulk ZnO (3.3 eV) and CeO₂ (3.2 eV) due to quantum confinement, according to literature (Jha et al., 2013; Sabari Arul et al., 2015), the estimated band gap values for CeO₂-ZnO are 2.45eV and 2.7 eV.

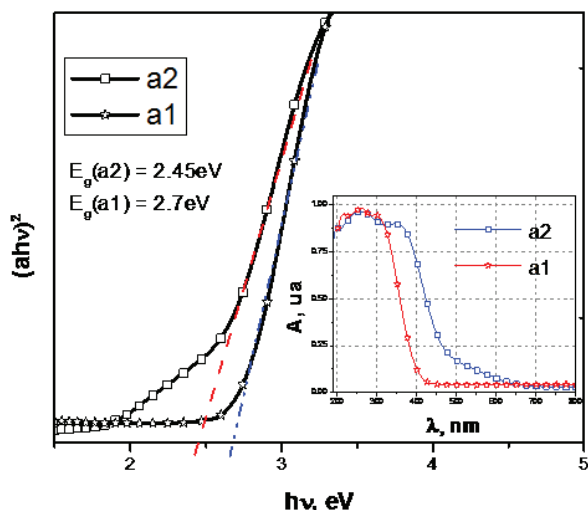


Fig. 2. The optical absorption energy band gap estimated for CeO₂-ZnO samples. Inset: the corresponding UV-vis absorption spectrum

FTIR analysis presented in Fig. 3 was performed in order to verify if during calcination, the organic phase left the system. It is observed that the characteristic peaks of the organic phase (1629-1590 cm⁻¹ corresponding to the carboxylic salt, 1310 cm⁻¹ alkyl bond and 796 cm⁻¹ C-H bonds) present in uncalcined samples are not found in the calcined samples. The Zn-O vibration is around 550 cm⁻¹, the large band located at 3400 - 3450 cm⁻¹ is attributed to the stretching vibration of O-H in the adsorbed water molecules (Khataee et al., 2015) and the Ce-O symmetric stretching vibration is around 520cm⁻¹ (Tambat et al., 2016).

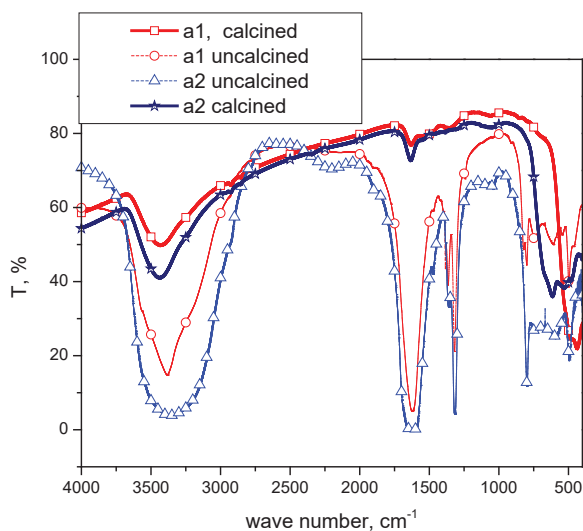


Fig. 3. FTIR analysis for sample a1 and a2 calcinated and uncalcinated

XRD patterns of CeO₂-ZnO composites are shown in Fig 4 and exhibits various peaks which could be indexed according to ZnO diffraction peaks (JCPDS card no. 36-1451) and CeO₂ diffraction peaks (JCPDS card no 34-0394): for CeO₂, the peaks presented at 2θ 28.5, 33.09, 47.49 and 56.4 can be indexed as (111), (200), (220) and (311) planes, and for ZnO the peaks presented at 2θ 31.9, 34.6, 36.4, 47.8 and 56.8 can be indexed as (100), (002), (101), (102), (110) (Jule et al., 2016; Sabari Arul et al., 2015). For the XRD pattern of the CeO₂-ZnO clearly matches with the polycrystalline structures of CeO₂ and ZnO, indicating the formation of composite CeO₂-ZnO without any other impurity.

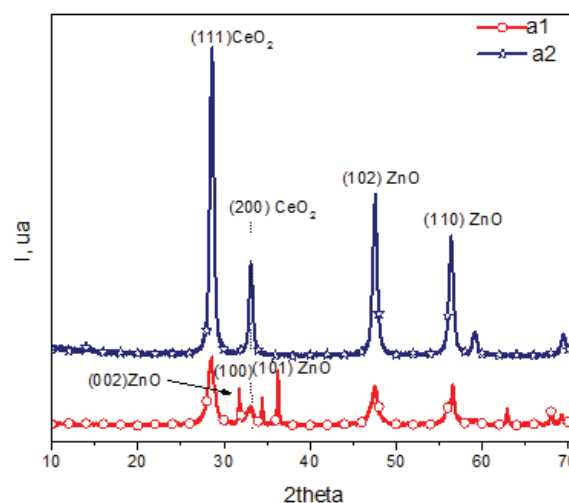


Fig. 4. The XRD patterns of CeO₂-ZnO composites

3.2. Photocatalytic activity

Photocatalytic activity of synthesized samples was evaluated by studying the behavior at UV irradiation of a cationic dye MB, and a diazoderivate, PMBH and are presented in Fig. 5 and Fig. 6. Blank experiments show that the two materials are stable at UV radiation.

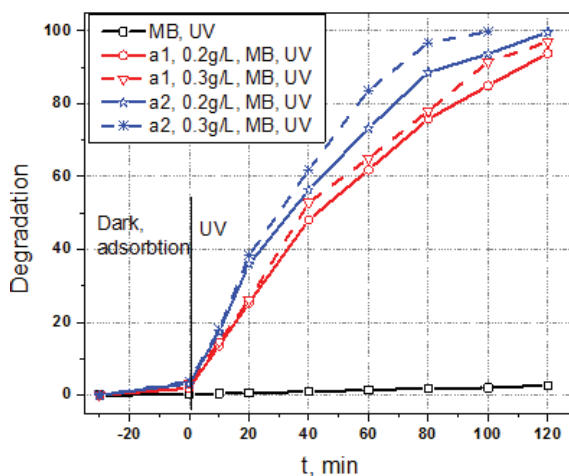


Fig. 5. Photocatalytic degradation rate of MB dye with CeO₂-ZnO prepared sample at different catalyst dose and under various UV-vis light irradiation times

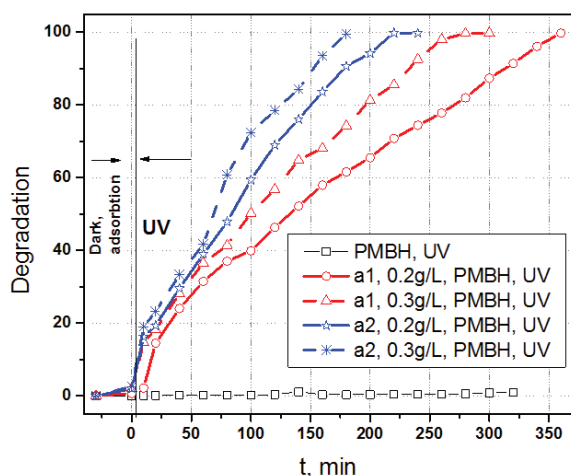
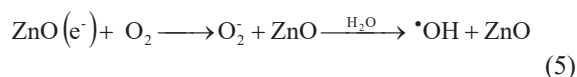
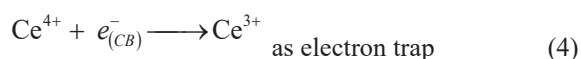
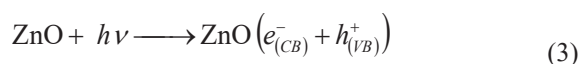


Fig. 6. Photocatalytic degradation rate of PMBH dye with CeO₂-ZnO prepared sample at different catalyst doses and under various UV-vis light irradiation times

After an hour of irradiation of the system (MB + sample a1), using 0.2 g/L catalyst concentration was achieved 60.5% as degree of discoloration and 63% for 0.3 g/L catalyst concentration. For sample a2 and after one hour of irradiation, the amount of discoloration varies from 73.4% for the dose of 0.2 g/L to 83.5% for 0.3 g/L catalyst. MB was discolored in a percentage of 97.6% after 80 minutes in the sample a2, 0.3 g/L.

When PMBH was used, the time was greater, compared with MB, so after 100 minutes for sample a1 was obtained a value of 39.8% for the dose of 0.2 g/L and 50% for the dose of 0.3 g/L and sample a2, 59.4% to 0.2 g/L and 72% to 0.3 g/L. A degree of discoloration by 99% was achieved after 180 minutes for sample a2, 0.3 g/L. Sample a1 (0.2 g/L) was completely degraded only after 360 minutes.

For the two dyes similar behavior was observed, such as increasing catalyst dose has resulted in a higher rate of degradation. The photocatalytic reactions describing the mechanism are shown in Eqs. (3 – 7), in agreement with the literature (Atchudan et al., 2017):



Also, the higher percentage of CeO₂ in the synthesized materials has led to higher rate of degradation, Ce⁴⁺ ions act as a trap to prevent recombination of electron-hole pairs created by

irradiation with ultraviolet radiation with $E > E_g$ (Lv et al., 2016), thus accelerating the photocatalytic process.

4. Conclusion

In this paper the synthesis, characterization and photocatalytic activity of two oxide materials based on CeO₂-ZnO are presented. The structure of materials synthesized by the hydrothermal process were investigated by SEM, FTIR, XRD, UV-vis and the band gap energy values were calculated.

The two catalytic materials are sensitive to low radiation doses, compared to those reported in the literature. Both samples show good photocatalytic activity measured for the degradation of PMBH and MB and the degree of discoloration of organic materials increased with the increasing percentage of CeO₂.

References

- Amira G., Chaker B., Habib E., (2017), Spectroscopic properties of Dy³⁺ doped ZnO for white luminescence applications, *Spectrochimica Acta Part A: Molecular and Biomolecular Spectroscopy*, **177**, 164-169.
- Apostolescu G.A., Cernatescu C., Cobzaru C., Tataru-Farmus R.E., Apostolescu N., (2015), Studies on the photocatalytic degradation of organic dyes using CeO₂ - ZnO mixed oxides, *Environmental Engineering and Management Journal*, **14**, 415-420.
- Atchudan R., Edison T.N.J.I., Perumal S., Shanmugam M., Lee Y.R., (2017), Direct solvothermal synthesis of zinc oxide nanoparticle decorated graphene oxide nanocomposite for efficient photodegradation of azo-dyes, *Journal of Photochemistry and Photobiology A: Chemistry*, **337**, 100-111.
- Bhosale R.R., Pujari S.R., Muley G.G., Patil S.H., Patil K.R., Shaikh M.F., Gambhire A.B., (2016), Solar photocatalytic degradation of methylene blue using doped TiO₂ nanoparticles, *Ceramics International*, **42**, 6728-6737.
- Cernatescu C., Apostolescu G.A., Cobzaru C., Tătaru-Fărmus R.E., Apostolescu N., Marinioiu A., (2015), Synthesis and physico-chemical behaviour studies for a new benzimidazole azodye, *Revue Roumaine de Chimie*, **60**, 837-844.
- Chen H.-I., Chang H.-Y., (2005), Synthesis of nanocrystalline cerium oxide particles by the precipitation method, *Ceramics International*, **31**, 795-802.
- Choi W., Termin A., Hoffmann M.R., (1994), The role of metal ion dopants in quantum-sized TiO₂: Correlation between photoreactivity and charge carrier recombination dynamics, *The Journal of Physical Chemistry*, **98**, 13669-13679.
- Faisal M., Ismail A.A., Ibrahim A., Bouzid H., Al-Sayari S.A., (2013), Highly efficient photocatalyst based on Ce doped ZnO nanorods: Controllable synthesis and enhanced photocatalytic activity, *Chemical Engineering Journal*, **229**, 225-233.
- Favier L., Simion A.I., Matei E., Grigoras C.G., Kadmi Y., Bouzaza A., (2016), Photocatalytic oxidation of a hazardous phenolic compound over TiO₂ in a batch system, *Environmental Engineering and Management Journal*, **15**, 1059-1067.

- Fujishima A., Honda K., (1972), Electrochemical photolysis of water at a semiconductor electrode, *Nature*, **238**, 37-38.
- Fujishima A., Zhang X., (2006), Titanium dioxide photocatalysis: present situation and future approaches, *Comptes Rendus Chimie*, **9**, 750-760.
- Jafari A.J., Dehghanifard E., Kalantary R.R., Gholami M., Esrafil A., Yari A.R., Baneshi M.M., (2016), Photocatalytic degradation of aniline in aqueous solution using ZnO nanoparticles, *Environmental Engineering and Management Journal*, **15**, 53-60.
- Jesudoss S.K., Judith Vijaya J., John Kennedy L., Iyyappa Rajan P., Al-Lohedan H.A., Jothi Ramalingam R., Kaviyarasu K., Bououdina M., (2016), Studies on the efficient dual performance of Mn_{1-x}Ni_xFe₂O₄ spinel nanoparticles in photodegradation and antibacterial activity, *Journal of Photochemistry and Photobiology B: Biology*, **165**, 121-132.
- Jha P.K., Gupta S.K., Lukacevic I., (2013), Electronic structure, photocatalytic properties and phonon dispersions of X-doped (X ¼ N, B and Pt) rutile TiO₂ from density functional theory, *Solid State Sciences*, **22**, 8-15.
- Jule L.T., Dejene F.B., Roro K.T., Urgessa Z.N., Both J.R., (2016), Rapid synthesis of blue emitting ZnO nanoparticles for fluorescent applications, *Physica B*, **497**, 71-77.
- Kannadasan N., Shanmugam N., Cholan S., Sathishkumar K., Viruthagiri G., Poonguzhali R., (2014), The effect of Ce⁴⁺ incorporation on structural, morphological and photocatalytic characters of ZnO nanoparticles, *Materials Characterization*, **97**, 37-46.
- Kaviyarasu K., Maria Magdalane C., Kanimozhi K., Kennedy J., Siddhardha B., Subba Reddy E., Rotte N.K., Sharma C.S., Thema F.T., Letsholathebe D., Mola G.T., Maaza M., (2017), Elucidation of photocatalysis, photoluminescence and antibacterial studies of ZnO thin films by spin coating method, *Journal of Photochemistry and Photobiology B: Biology*, **173**, 466-475.
- Khataee A., Karimi A., Arefi-Oskoui S., Soltani R.D.C., Hanifehpour Y., Soltani B., Joo S.W., (2015), Sonochemical synthesis of Pr-doped ZnO nanoparticles for sonocatalytic degradation of Acid Red 17, *Ultrasonics Sonochemistry*, **22**, 371-381.
- Lira-Cantu M., Krebs F.C., (2006), Hybrid solar cells based on MEH-PPV and thin film semiconductor oxides (TiO₂, Nb₂O₅, ZnO, CeO₂ and CeO₂-TiO₂): Performance improvement during long-time irradiation C.F., *Solar Energy Materials and Solar Cells*, **90**, 2076-2086.
- Lopez F.A., Cebriano T., García-Díaz I., Fernandez P., Rodríguez O., Lopez Fernandez A., (2017), Synthesis and microstructural properties of zinc oxide nanoparticles prepared by selective leaching of zinc from spent alkaline batteries using ammoniacal ammonium carbonate, *Journal of Cleaner Production*, **148**, 795-803.
- Lv Z., Zhong Q., Ou M., (2016), Utilizing peroxide as precursor for the synthesis of CeO₂/ZnO composite oxide with enhanced photocatalytic activity, *Applied Surface Science*, **376**, 91-96.
- Mirzaei H., Darroudi M., (2017), Zinc oxide nanoparticles: Biological synthesis and biomedical applications, *Ceramics International*, **43**, 907-914.
- Mogensen M., Sammes N.M., Tompsett G.A., (2000), Physical, chemical and electrochemical properties of pure and doped ceria, *Solid State Ionics*, **129**, 63-94.
- Nagy K., Dekany I., (2009), Preparation of nanosize cerium oxide particles in W/O microemulsions, *Colloids and Surfaces A: Physicochemical and Engineering Aspects*, **345**, 31-40.
- Nascimento L.F., Martins R.F., Silva R.F., Serra O.A., (2014), Catalytic combustion of soot over ceria-zinc mixed oxides catalysts supported onto cordierite, *Journal of Environmental Sciences*, **26**, 694-701.
- Paz Y., (2006), Preferential photodegradation - why and how?, *Comptes Rendus Chimie*, **9**, 774-787.
- Reddy D.A., Ma R., Kim T.K., (2015), Efficient photocatalytic degradation of methylene blue by heterostructured ZnO-RGO/RuO₂ nanocomposite under the simulated sunlight irradiation, *Ceramics International*, **4**, 6999-7009.
- Sabari Arul N., Mangalaraj D., Han I.J., (2015), Facile hydrothermal synthesis of CeO₂ nanopebbles, *Bulletin of Materials Science*, **38**, 1135-1139.
- Tambat S., Umale S., Sontakke S., (2016) Photocatalytic degradation of Milling Yellow dye using sol-gel synthesized CeO₂, *Materials Research Bulletin*, **76**, 466-472.
- Xia T., Kovochich M., Liang M., Madler L., Gilbert B., Shi H., Yeh J.I., Zink J.I., Nel A.E., (2008), Comparison of the mechanism of toxicity of zinc oxide and cerium oxide nanoparticles based on dissolution and oxidative stress properties, *American Chemical Society Nano*, **2**, 2121-2134.



“Gheorghe Asachi” Technical University of Iasi, Romania



MATHEMATICAL MODELLING FOR PHENOLATION OF SPENT SULFITE LIQUOR

Andrei Ionuț Simion¹, Cristina-Gabriela Grigoraș¹, Alexandru Chiriac²,
Cătălin Nicolae Tâmpu³, Lucian Gavrilă^{1*}

¹“Vasile Alecsandri” University of Bacău, Faculty of Engineering, Department of Chemical and Food Engineering,
157 Calea Mărășești, 600115 Bacău, Romania

²“Gheorghe Asachi” Technical University of Iasi, Faculty of Chemical Engineering and Environmental Protection, Department
of Environmental Engineering and Management, 73 Mangeron Blvd, 700050 Iasi, Romania

³“Vasile Alecsandri” University of Bacău, Faculty of Engineering, Department of Engineering and Management, Mechatronics,
157 Calea Mărășești, 600115 Bacău, Romania

Abstract

In this study major factors affecting the phenolation process of lignosulfonate (LS) waste liquor (recovered from pulp and paper industry) were optimized in order to improve LS substitution for replacing petroleum-based phenols during phenolic resin manufacturing. Four different parameters, namely phenol/lignosulfonate ratio, time, temperature and lignosulfonate waste liquor concentration, were varied in an experimental program having as response function the reaction yield. Response Surface Methodology (based on central composite or Box-Behnken designs) and Artificial Neuronal Network were applied for establishing the process parameters impact on phenolation yield.

The developed mathematical models presented a high accuracy being able to adequately estimate the phenol conversion and adduct formation. Yields over 80 % were obtained when lignosulfonate waste liquor with a concentration in lignosulfonate between 35 % and 45 % was used in a ratio of 1:1 with phenol and the reaction was conducted at temperatures in a range of 100 °C – 110 °C for a period of time of 3.0 – 3.5 hours.

Key words: Artificial Neural Network, lignosulfonate, mathematical optimization, resin, Response Surface Methodology

Received: May, 2017; Revised final: January, 2018; Accepted: March, 2018; Published in final edited form: April 2018

1. Introduction

Phenolic resins, known as the first polymer synthesized at industrial level, are thermosetting resins that form a three-dimensional network structure through covalent bonds (Shudo et al., 2017). Characterized as possessing high aromatic density, very good thermal, chemical and mechanical stability and strength, high thermal insulating properties (Martin et al., 2006), and solvent resistance (Foyer et al., 2016), they are widely used in the aerospace, automotive, construction, and semiconductor

industries (Shudo et al., 2016). These types of resins are successfully employed to fabricate a large variety of products from electric laminates to carbon foams (Zhao et al., 2009), adhesives (Roslan et al., 2014; Yang and Frazier, 2016), molding compounds (Hirano and Asami, 2013), acid-resistant coatings (Biedermann and Grob, 2006a, 2006b), fiber-reinforced composites (Bu et al., 2014; Li et al., 2016; Wu et al., 2017) and binders (Wang et al., 2017).

There are two types of phenolic resins commonly resulting from a synthesis process using two reagents: phenol and formaldehyde. When an

* Author to whom all correspondence should be addressed: e-mail: lgavrila@ub.ro; Phone: +40 234 524 411 ext. 145; Fax: +40 234 580 170

excess of formaldehyde and an alkaline catalyst are used *resol phenolic resin* is obtained while an excess of phenol and acidic pH conditions lead to *novolac phenolic resin* (Foyer et al., 2016; Noparvar-Qarebagh, 2016). In the last period, the rising cost and the predictable upcoming insufficiency of petrochemicals have stimulated the necessity to evaluate the possibility of replacing the phenol with other products (Greco et al., 2016). Dedicated researches conducted to the conclusion that lignosulfonates (compounds from pulp and paper wastewaters known as chemically stable, resistant to biological degradation, and difficult to separate by conventional wastewater treatment methods (Zulfikar et al., 2012)) constitute one of the best alternatives (Hu et al., 2012; Perez et al., 2007). Even though good results were reported when non-modified lignosulfonates were incorporated in phenolic resin, their reactivity is improved if the chemical structure is modified (Alonso et al., 2001), one way to accomplish this structure change being represented by the phenolation reaction. According to data reported by Alonso et al. (2005) and by Hu et al. (2011), the mentioned method involves: benzyl-hydroxyl group protonation; dehydration at the α -carbon in order to give a carbonium ion; electrophilic attack by carbonium ion of the phenol molecule leading to a phenol condensation product; incorporation of *ortho* or *para*-phenyl substituent to the α -hydroxyl groups of the propane side chains and adduct fragmentation and insures, in the same time, a decrease of molecular weight supporting a more appropriate incorporation of phenolation products to phenolic resins.

Considering the information previously presented, this paper is focused on the optimization of the main factors affecting the lignosulfonate phenolation process. To this purpose, lignosulphonate (LS) from spent sulphite liquor resulting from pulp and paper industry and phenol (P) were used and four different parameters: P/LS ratio, time, temperature and LS concentration were varied in an experimental program having as response function the reaction yield. In order to obtain the optimal values for the above-mentioned parameters two different methodologies were employed: Response Surface Methodology (RSM) and Artificial Neural Network (ANN).

RSM is a widely used collection of mathematical and statistical techniques which gives, among others, a second order polynomial equation able to accurately describe the experimental data behavior (Xiang et al., 2015). It applies for response functions influenced by different variables (Koricic et al., 2016) and has as main aim to simultaneously optimize the levels of these variables in order to achieve the best results (Almeida Bezerra et al., 2008; Shirneshan et al., 2016). In the present study, two second-order symmetrical RSM designs were developed: central composite design (CCD) and Box-Behnken design (BBD) the difference between them being given by the selection of experimental points

and the number of runs. ANN is an assembly of simple computational units interlinked by a system of connections (Cheng and Titterington, 1994) which implement algorithms that attempt to achieve a neurological related performance including learning and making generalization from similar situations (Cemek et al., 2013; Meireles et al., 2003; Rajakovic-Ognjanovic et al., 2014).

The simplest ANN requires three layers (input, hidden and output), activation function, learning technique and weights. In terms of layers, the input one receives information and passes it for processing; the hidden layer processes the information offered by the input layer while the output layer receives processed information from hidden layers and give the results. The activation function affects the neural network behavior and scales the output into an adequate range. The learning system adapts itself to various changes insuring that during the training phase weights can be modified in response to input/output chances (Dharwal and Kaur, 2016). For this paper, the experimental acquired data were used to build and train an artificial neural network in order to decide if it is more appropriate than RSM for establishing the optimal values for the parameters affecting the LS phenolation reaction.

The accuracy of the resulted mathematical models was investigated by applying several different tests: sequential model sum of squares, lack of fit test and Analysis of Variance (ANOVA) test.

2. Material and methods

2.1. Reagents

Phenol used for the experiments was of analytical purity and was purchased from Sigma Aldrich (Redox Lab Supplies Bucharest, Romania). Lignosulfonate waste liquor (with 50 wt % LS) was obtained from a local pulp and paper industry. All the solutions were prepared only with demineralized water.

2.2. Phenolation reaction

Following the experimental setup detailed in Table 1, Table 2 and in Table 3 from the section dedicated to RSM modelling, different proportions of lignosulfonate waste liquor of different concentrations and 50 g of pure phenol were solubilized in 500 mL of demineralized water and introduced in a 1 L glass laboratory reactor equipped with a thermometer and a reflux condenser. Sulphuric acid (0.5 wt % reported at the phenol quantity) was added in order to insure an acidic media.

The resulted mixtures were heated under stirring on a Nahita Blue 692 magnetic heating plate (Auxilab, Spain) to various temperatures for different periods of time according to the established exploratory plan. At the end, the remaining water was removed by atmospheric pressure distillation.

Table 1. Independent variable and levels used for CCD and BBD

Parameter	Levels of variation	
	CCD	BBD
A (P/LS ratio)	0.5; 1; 1.5; 2; 2.5	1; 1.5; 2
B (time, hours)	2; 2.5; 3; 3.5; 4	2.5; 3; 3.5
C (Temperature, °C)	80; 90; 100; 110; 120	90; 100; 110
D (LS concentration, %)	35; 40; 45; 50	35; 40; 45

Table 2. CCD exploratory plan for LS phenolation reaction

Run	A P/LS ratio	B Time, t [hours]	C Temperature, T [°C]	D Concentration, LS [%]	Yield, η [%]		
					1 st trial	2 nd trial	3 rd trial
1	1	2.5	90	35	68.80	67.29	67.63
2	2	2.5	90	35	22.11	21.42	22.49
3	1	3.5	90	35	69.03	71.17	67.93
4	2	3.5	90	35	38.33	41.05	37.87
5	1	2.5	110	35	83.71	82.71	82.20
6	2	2.5	110	35	42.15	43.67	41.01
7	1	3.5	110	35	86.02	86.88	85.85
8	2	3.5	110	35	44.32	46.71	44.19
9	1	2.5	90	45	67.60	67.40	66.79
10	2	2.5	90	45	21.22	20.99	21.45
11	1	3.5	90	45	68.87	68.04	70.04
12	2	3.5	90	45	31.30	31.99	31.27
13	1	2.5	110	45	78.89	76.44	80.63
14	2	2.5	110	45	45.70	45.20	44.92
15	1	3.5	110	45	86.10	82.48	86.87
16	2	3.5	110	45	47.50	46.55	46.98
17	0.5	3	100	40	85.52	86.97	84.92
18	2.5	3	100	40	26.53	26.98	26.34
19	1.5	2	100	40	43.21	43.51	43.12
20	1.5	4	100	40	52.30	51.10	52.09
21	1.5	3	80	40	40.87	40.01	40.34
22	1.5	3	120	40	59.11	57.45	59.88
23	1.5	3	100	30	58.25	56.85	58.54
24	1.5	3	100	50	60.65	58.77	60.95
25	1.5	3	100	40	54.30	54.73	54.46
26	1.5	3	100	40	55.44	55.83	55.50
27	1.5	3	100	40	54.20	53.66	54.04
28	1.5	3	100	40	52.98	54.20	52.77
29	1.5	3	100	40	53.93	53.66	53.66
30	1.5	3	100	40	56.10	56.44	56.83
31	1.5	3	100	40	53.77	54.09	54.36

2.3. Free phenol determination

A Varian 3400 gas chromatograph (Varian, Inc. USA) with flame ionization detector and helium as carrier gas and equipped with an HP-INNOWax capillary column (0.2 μm thickness, 50 m length, 0.2 mm internal diameter) was used for free phenol determination from every reaction. The method described by Alonso et al. (2005) was followed.

2.4. Reaction yield calculation

The phenolation reaction yield was established as ratio between the amount of phenol registered at the end of reaction and that introduced in the reactor and the results were expressed as percentages.

2.5. RSM modelling

Two different RSM designs (central composite design (CCD) and Box-Behnken design (BBD)), chosen due to the fact that they require a reduced number of experiments, were evaluated with Design-Expert 7.0 software in order to describe linear, quadratic, and interactions occurring in the mathematical model developed on an exploratory plan including various levels of variation for four different parameters considered as affecting the liginosulfonate phenolation reaction. The variation of these factors is given in Table 1.

The quadratic model for predicting the optimal values for the studied parameters is shown by the Eq. (1):

$$Y = A_0 + \sum_{i=1}^4 A_i X_i + \sum_{i=1}^4 A_{ii} X_i^2 + \sum_{i=1}^3 \sum_{j=i+1}^4 A_{ij} X_i X_j \tag{1}$$

where Y is the response function (phenolation reaction yield), A_i , A_{ii} and A_{ij} ($i \neq j$) are the regression coefficients of variables for the linear, quadratic and interaction terms, X_i is a code for the four parameters (A, B, C, D) and X_j is a code for the combinations of the parameters (AB, AC, AD, BC, BD, CD).

2.6. ANN modelling

Data used for RSM development were considered as input and output data for a three-layered

feed forward momentum ANN. A varying number of neurons (2 – 8) in the hidden layer was tested with NeuroSolutions 6.0 software. Four input nodes, 2 – 8 hidden neurons, one output node, 3000 epochs, and momentum learning rule were employed for ANN training.

3. Results and discussion

3.1. RSM modelling

Table 2 and Table 3 show the runs for CCD and BDD respectively along with reaction yields registered for each of them. All the experiments were conducted in triplicate

Table 3. BBD exploratory plan for LS phenolation reaction

Run	A P/LS ratio	B Time, τ [hours]	C Temperature, t [°C]	D Concentration, LS [%]	Yield, η [%]		
					1 st trial	2 nd trial	3 rd trial
1	2	2.5	100	40	38.50	38.73	38.92
2	2	3	90	40	31.29	30.95	30.88
3	1	3	100	35	81.60	80.46	82.17
4	1	3	90	40	66.12	64.33	65.72
5	2	3	100	35	41.56	41.73	41.77
6	1.5	3.5	100	35	57.67	56.57	58.59
7	1	2.5	100	40	78.33	80.05	78.02
8	1	3	110	40	86.09	87.55	85.92
9	1.5	3.5	110	40	61.33	62.13	61.23
10	1.5	3	110	45	60.11	61.01	59.99
11	1.5	3.5	90	40	47.53	48.05	47.01
12	1	3.5	100	40	83.12	82.46	82.46
13	1.5	3	90	35	44.12	44.83	43.72
14	1.5	2.5	100	45	53.53	54.39	53.16
15	1.5	2.5	110	40	61.02	62.00	61.08
16	1	3	100	45	81.81	82.71	80.42
17	1.5	3	100	40	55.70	55.64	55.09
18	1.5	3	100	40	56.10	55.71	55.09
19	1.5	2.5	100	35	53.40	53.13	52.65
20	1.5	3	110	35	58.21	58.44	57.69
21	1.5	3.5	100	45	57.78	57.95	57.90
22	1.5	2.5	90	40	28.11	27.52	27.60
23	2	3	110	40	33.96	33.38	33.59
24	2	3	100	45	27.33	26.81	27.25
25	2	3.5	100	40	30.14	29.84	30.05
26	1.5	3	100	40	55.44	54.89	55.38
27	1.5	3	100	40	52.98	52.56	52.93
28	1.5	3	90	45	26.18	26.22	25.84
29	1.5	3	100	40	53.77	53.55	52.86

The CCD and BBD developed mathematical models are expressed by Eqs. (2) and (3) given below:

$$Y_{CCD} = 54.49 - 18.10 \cdot A + 2.48 \cdot B + 7.65 \cdot C - 0.10 \cdot D + 1.20 \cdot A \cdot B + 0.39 \cdot A \cdot C + 0.31 \cdot A \cdot D - 0.89 \cdot B \cdot C - 0.04 \cdot B \cdot D + 0.70 \cdot C \cdot D + 0.68 \cdot A^2 - 1.38 \cdot B^2 + 0.42 \cdot C^2 + 1.54 \cdot D^2 \tag{2}$$

$$Y_{BBD} = 54.49 + 54.60 \cdot A - 22.86 \cdot B + 2.06 \cdot C + 9.78 \cdot D - 2.48 \cdot A \cdot B - 3.29 \cdot A \cdot C - 4.32 \cdot A \cdot D - 3.61 \cdot B \cdot C - 4.78 \cdot B \cdot D - 0.005 \cdot C \cdot D + 4.96 \cdot A^2 + 3.98 \cdot B^2 + 0.31 \cdot C^2 - 5.49 \cdot D^2 \tag{3}$$

The adequacy of the second order polynomial equations obtained by RSM modelling was tested by the mean of various tests: standard deviation (SD) which quantifies data dispersion; sum of squares (SS) and mean of square (MS) which measures the deviation from the mean value; correlation coefficient (R^2) which considers in the same time linear, quadratic and interaction effects; the adjusted coefficient of determination (adj. R^2) which estimates only square and interaction effects between two input variables; the predicted coefficient of determination (pred. R^2) which studies the effects for software generated values; the predicted residual sum of squares (PRESS) which measures the fit of a model to observations samples not involved in model assessment; degrees of freedom (df) which reveals the number of values that may vary independently; F value and p value which show the probabilities of predicting results similar to the experimental data when the null hypothesis is true; lack of fit test and pure error which illustrate the differences between the mathematical model and the experimental data.

The analysis of these tests results (Table 4 and Table 5) reveals that the mathematical models developed by RSM describe accurately the behavior of data recorded for LS phenolation reaction yield. For both of them, R^2 , adj. R^2 , Pred. R^2 presented values higher than 0.97, 0.94 and 0.84 respectively.

The significance of coefficients found for the two RSM established second order polynomial equations indicate that the more important parameters affecting the LS phenolation process are represented by the P/LS ratio and temperature (p value < 0.0001) and that the time and LS concentration have a lower influence. The interactions between the factors do not affect the reaction yield in a considerable manner.

The “Lack of Fit” results sustain also the RSM models accuracy since the chances that the large values registered for this test could occur due to noise are under 1 %.

Fig. 1 and Fig. 2 depict the response surfaces for reaction yield of the first CCD and of the first BBD sets of runs. Since, according to data given in Table 3 and in Table 4, values recorded for the second and the third set of runs both for CCD and BBD present a high similarity, they were not pictured here.

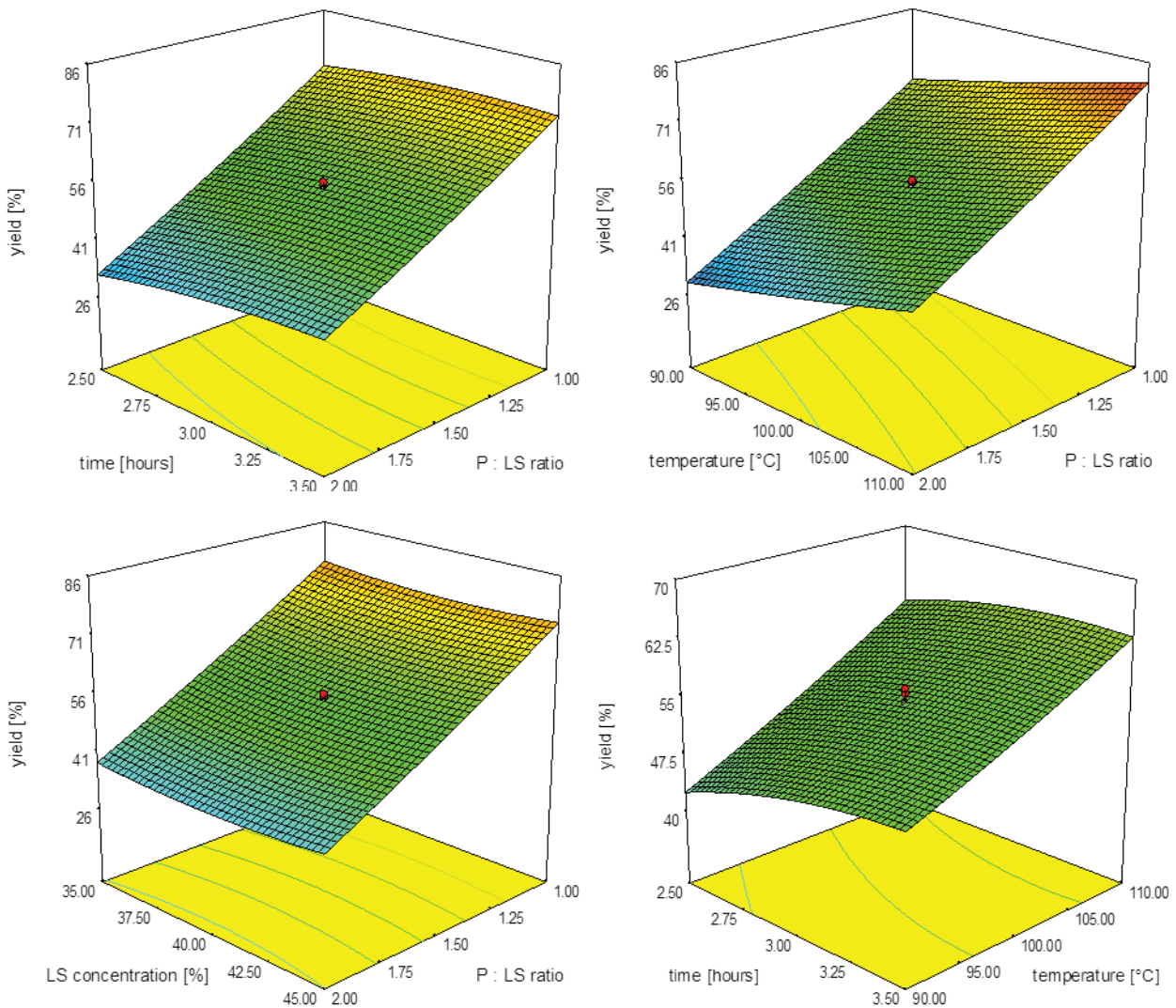
Fig. 3 and Fig. 4 indicate that LS phenolation yields predicted by CCD and BBD mathematical models are greater than 80 % for a P/LS ratio set at 1. In the case of CCD, the reaction yield reached 82 % when the used LS has a concentration of 45 %, and the reaction is conducted at a temperature of 110 °C for 3 hours. For BBD, the reaction yield raised at 86 % when LS concentration was of 35 %, and the reaction took place at 100 °C for 3.5 hours. In other words, the analysis of these data shows that a reaction with a more important concentration of LS requires a higher temperature and a shorter period of time. On the contrary, a greater reaction yield can be reached when a lower concentration of LS is involved and the reaction is conducted at a lower temperature for a longer time. These results are similar with that reported by Alonso et al. (2005) and sustained by the fact that the supplementary experiments carried out in the optimal conditions released by both RSM designs the reaction yields were between 82 % and 85 %. The observed differences between CCD and BBD results can be explained by the ability of BBD to ignore the extreme values chosen for the tested variables presenting, in the same time, the possibility to obtain a reliable mathematical model from fewer experiments.

Table 4. CCD mathematical model accuracy tests results

Source	-	SD	-	R^2	Adj. R^2	Pred. R^2	PRESS
Quadratic Model	-	4.18	-	0.9734	0.9486	0.8497	1484.92
Source	Coefficient Estimate	-	SS	df	MS	F value	p-value Prob > F
Model	-	-	9614.512	14	686.7508	39.2496	< 0.0001
Intercept	54.49	1.71	-	-	-	-	-
A-P : LS ratio	-18.10	0.85	9614.51	14	686.75	39.25	< 0.0001
B-time	2.48	0.85	7861.55	1	7861.55	449.31	< 0.0001
C-temperature	7.65	0.85	147.36	1	147.36	8.42	0.0109
D-LS concentration	-0.10	0.85	1404.69	1	1404.69	80.28	< 0.0001
AB	1.20	1.05	0.26	1	0.26	0.01	0.9049
AC	0.39	1.05	23.16	1	23.16	1.32	0.2679
AD	0.31	1.05	2.47	1	2.47	0.14	0.7122
BC	-0.89	1.05	1.51	1	1.51	0.09	0.7732
BD	-0.04	1.05	12.80	1	12.80	0.73	0.4059
CD	0.70	1.05	0.02	1	0.02	1.16E-003	0.9733
A ²	0.68	0.80	7.94	1	7.94	0.45	0.5108
B ²	-1.38	0.80	12.80	1	12.80	0.73	0.4059
C ²	0.42	0.80	52.57	1	52.57	3.00	0.1035
D ²	1.54	0.80	4.94	1	4.94	0.28	0.6031
Residual	-	-	64.99	1	64.99	3.71	0.0731
Lack of Fit	-	-	262.46	15	17.50	-	-
Pure Error	-	-	256.25	10	25.62	20.64	0.0019
Cor Total	-	-	6.21	5	1.24	-	-

Table 5. BBD mathematical model accuracy tests results

Source	-	SD	-	R ²	Adj. R ²	Pred. R ²	PRESS
Quadratic Model	-	4.231647	-	0.970581	0.941161	0.833244	1421.01
Source	Coefficient Estimate	-	SS	df	MS	F value	p-value Prob > F
Model	-	-	8270.775	14	590.7696	32.99129	< 0.0001
Intercept	54.4917	1.7077	-	-	-	-	-
A-P : LS ratio	54.6	1.89	6269.5840	1	6269.5840	350.1223	< 0.0001
B-time	-22.86	1.22	50.7585	1	50.7585	2.8346	0.1144
C-temperature	2.06	1.22	1147.9760	1	1147.9760	64.1083	< 0.0001
D-LS concentration	9.78	1.22	74.1027	1	74.1027	4.1382	0.0613
AB	-2.48	1.22	43.2306	1	43.2306	2.4142	0.1425
AC	-3.29	2.12	74.8225	1	74.8225	4.1784	0.0602
AD	-4.32	2.12	52.1284	1	52.1284	2.9111	0.11
BC	-3.61	2.12	91.2980	1	91.2980	5.0985	0.0404
BD	-4.78	2.12	0.0001	1	0.0001	0.0000	0.9981
CD	-5.00E-03	2.12	98.4064	1	98.4064	5.4955	0.0343
A ²	4.96	2.12	102.7787	1	102.7787	5.7396	0.0311
B ²	3.98	1.66	0.6107	1	0.6107	0.0341	0.8561
C ²	0.31	1.66	195.6399	1	195.6399	10.9254	0.0052
D ²	-5.49	1.66	2.2439	1	2.2439	0.1253	0.7286
Residual	-	-	250.6957	14	17.9068	-	-
Lack of Fit	-	-	245.2168	10	24.5217	17.9027	0.0068
Pure Error	-	-	5.4789	4	1.3697	-	-
Cor Total	-	-	8521.4700	28	-	-	-



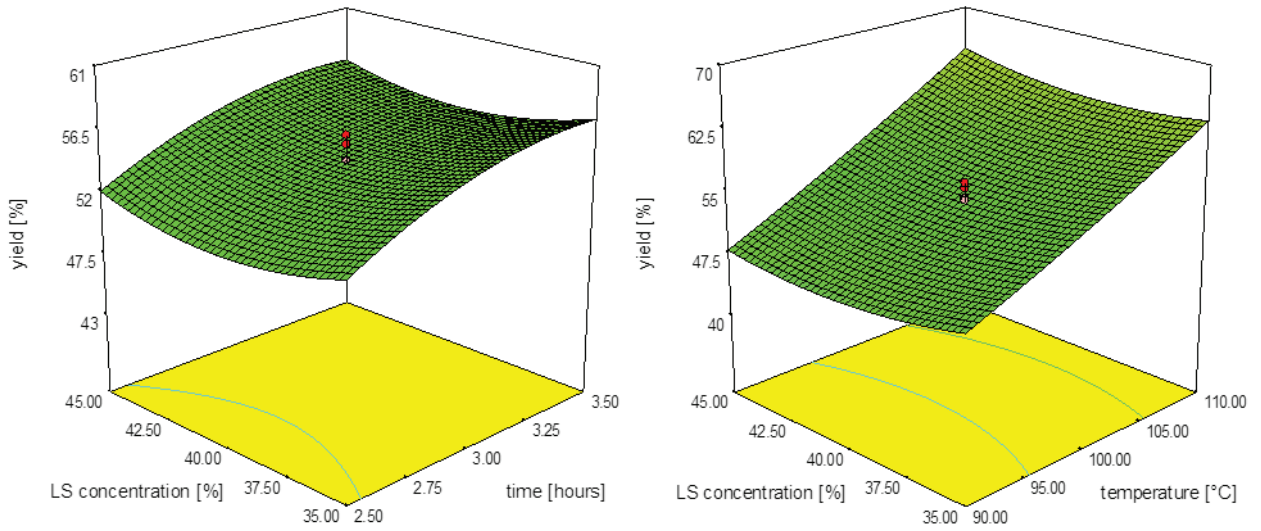
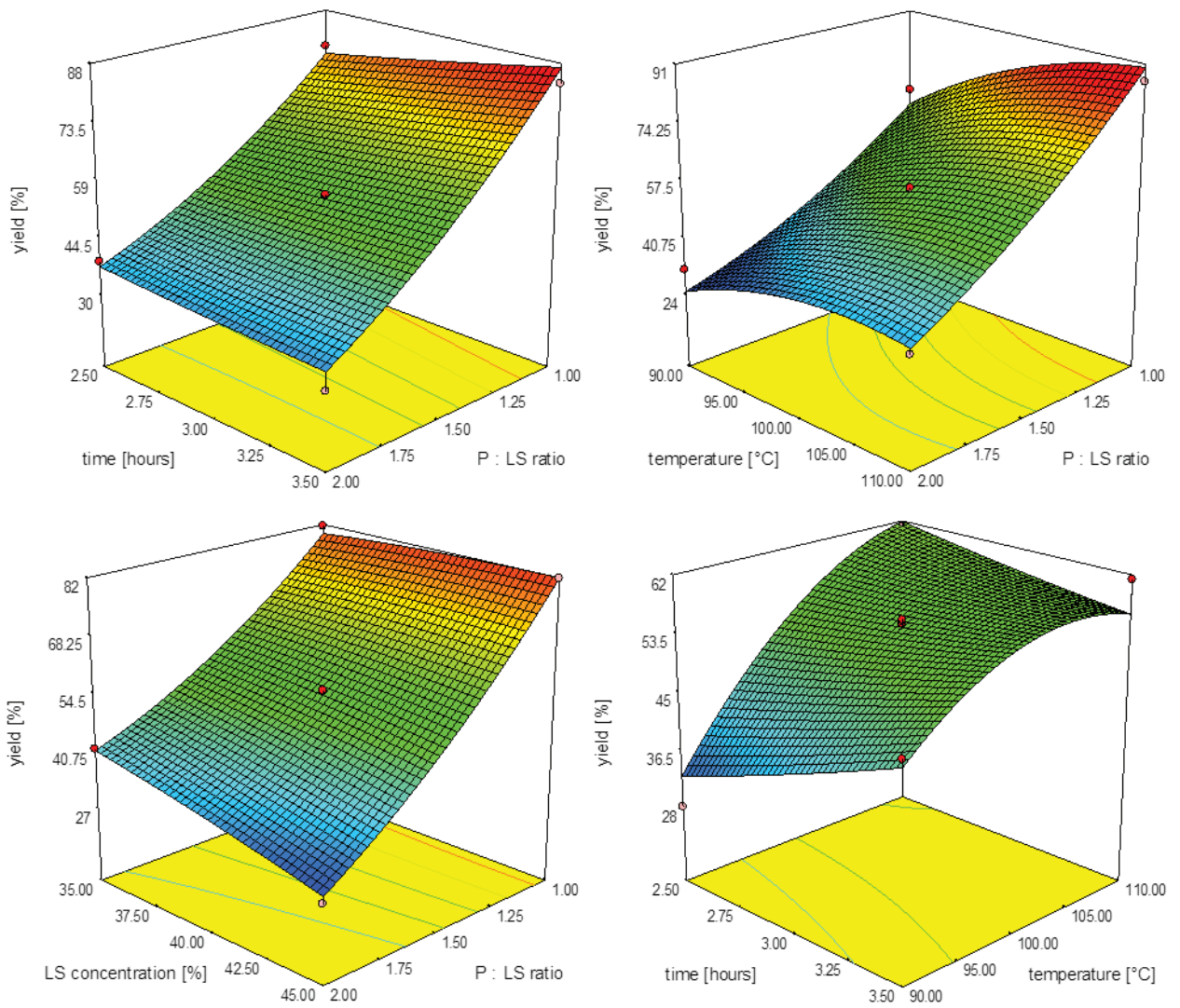


Fig. 1. 3D response surfaces for CCD phenolation reaction yield



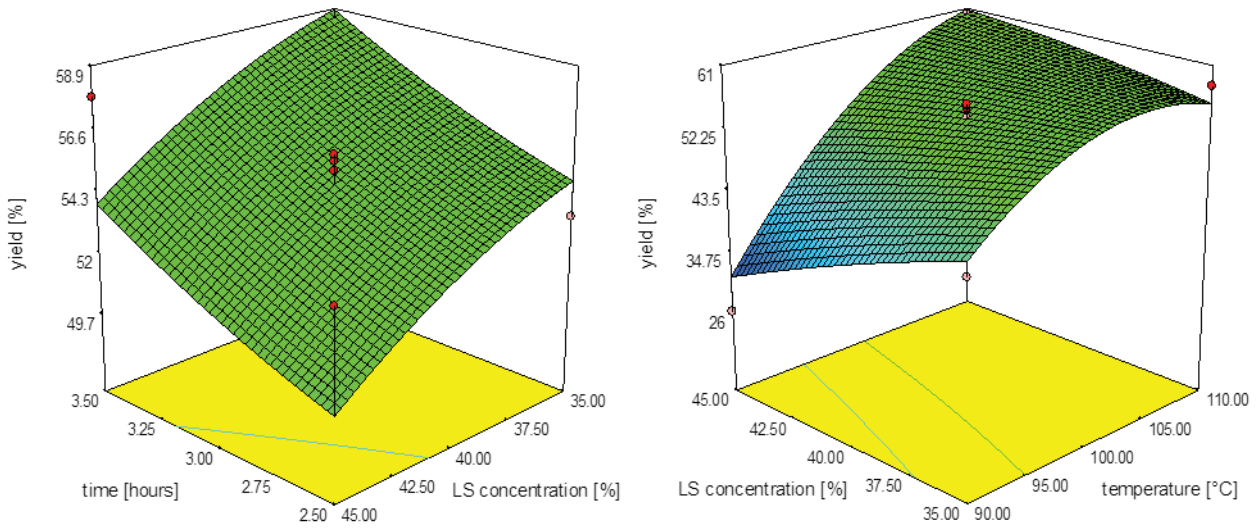


Fig. 2. 3D response surfaces for BBD phenolation reaction yield

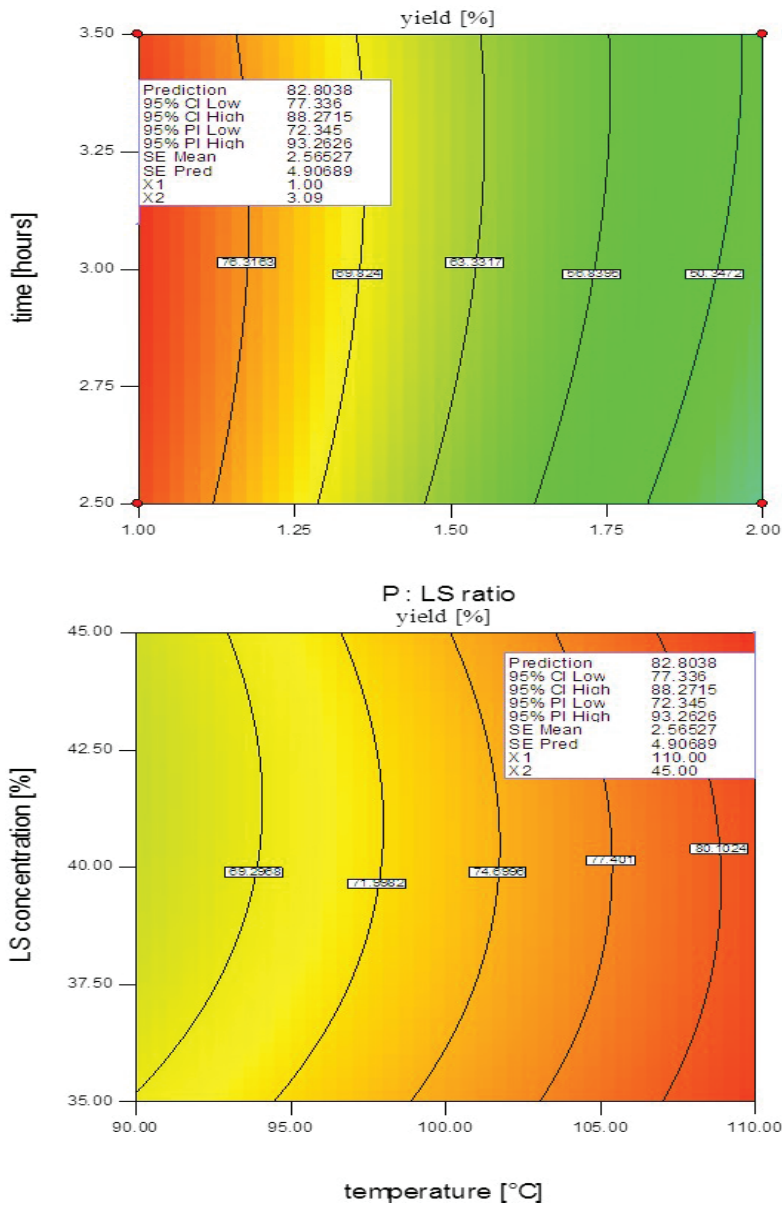


Fig. 3. LS phenolation yield predicted by CCD mathematical model

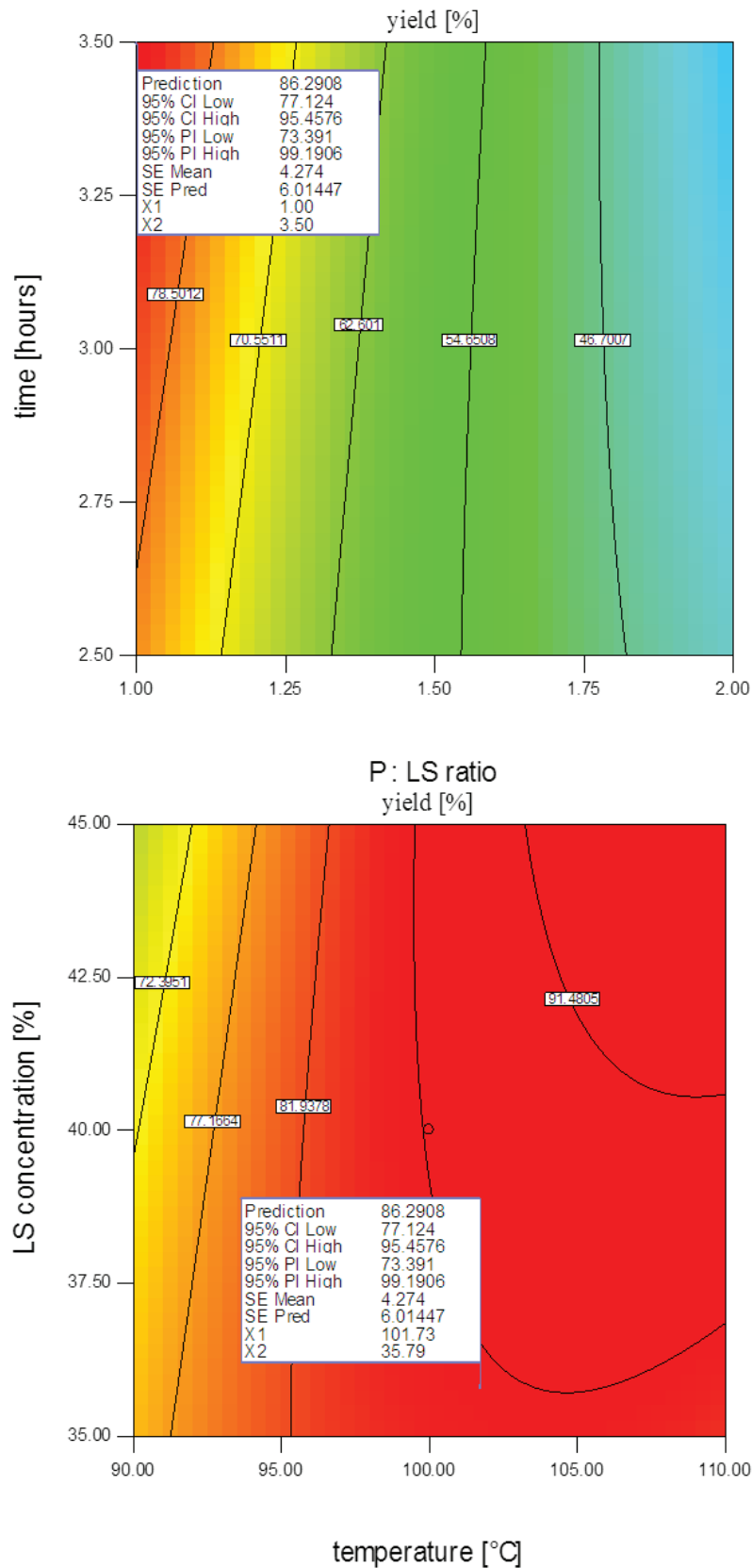


Fig. 4. LS phenolation yield predicted by BBD mathematical model

3.2. ANN modelling

A feed forward multilayer perceptron's ANN based on data included in Table 2 and in Table 3 was

established using as input the values of the four parameters influencing the LS phenolation reaction (P/LS ratio, time, temperature and LS concentration) and as output the reaction yields registered in triplicate

for CCD and BBD. This network was chosen due to the fact that it is easy to use, and it is recognized as being able to approximate any input/output map. 70 % of the input data were utilized for network training while the remaining 30 % were equally divided between the cross validation and testing steps. Tests conducted with different number of hidden neurons revealed that when a large number of neurons are considered, the ANN requires a more important period of time to train itself while too few neurons are not sufficient for an appropriate training process. The best results were attained with a hidden layer of 3 neurons: the first one with ten, the second one with five and the third one with four process elements. The developed ANN is given in Fig. 5.

As it can be remarked from Fig. 6, the mean squared error follows a similar path both for training stage and for cross validation at 3000 epochs reaching minimum final values of 0.0283 and of 0.0388 respectively.

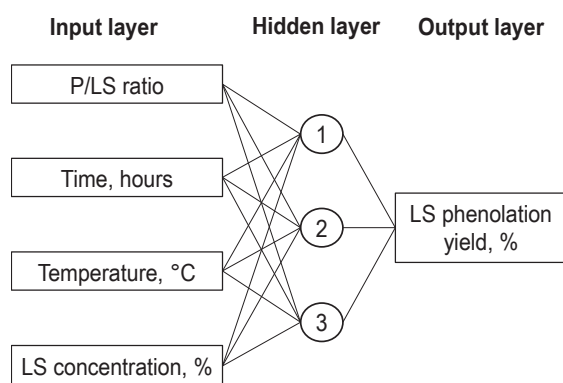


Fig. 5. Schematic representation of the (4 – 3 – 1) neural network (with four neurons in the input layer, three in the hidden layer, and one in the output layer)

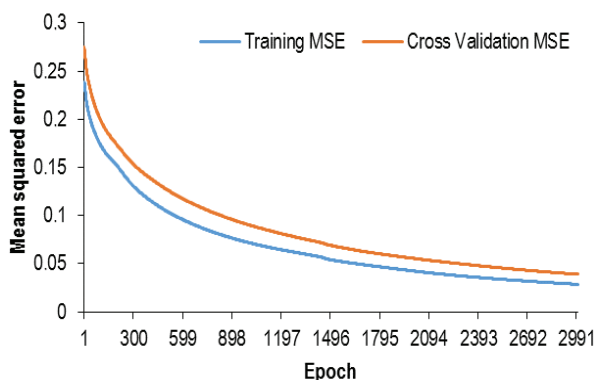


Fig. 6. Comparison between mean squared error (MSE) obtained in training and in cross validation ANN processes

The analysis of experimental recorded LS phenolation yields and of those predicted by ANN (Fig. 7) reveals no significant differences. The selected ANN helps to conclude that the use of all RSM data can provide an accurate model characterized by a MSE of only 5.573, a minimum and a maximum absolute error of 0.0222 and of 7.9258 and by a very high correlation coefficient with a value of

0.9912 suggesting a very good fit with the experimental data.

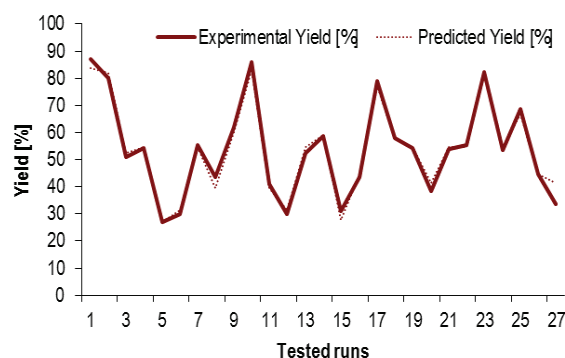


Fig. 7. Evolution of experimental and ANN predicted yield LS phenolation

4. Conclusions

This study was dedicated to the optimization process of the main parameters (phenol – lignosulfonate ratio, time, temperature, lignosulfonate concentration) recognized as affecting the phenolation reaction yield conducted between lignosulfonate waste liquor and phenol.

Two powerful techniques (Response Surface Methodology with Central Composite Design and Box-Behnken Design and Artificial Neural Network) were employed in order to establish the experimental program and to analyze the obtained data. Yields higher than 80 % were recorded when the phenolation was conducted with equal amounts of phenol and lignosulfonate, the lignosulfonate had a concentration varying from 35 % to 45 % and a temperature between 100 °C and 110 °C was insured for more than 3 hours.

Mathematical models generated by RSM (CCD and BBD) were able to accurately estimate the phenol conversion and adduct formation and their adequacy was confirmed by the high similarity existing between the experimental and model predicted data revealed by ANN.

References

Almeida Bezerra M., Santelli R.E., Padua Oliveira E., Silveira Villar L., Escalera L.A., (2008), Response surface methodology (RSM) as a tool for optimization in analytical chemistry, *Talanta*, **76**, 965-977.

Alonso M.V., Rodriguez J.J., Oliet M., Rodriguez F., Garcia J., Gilarranz M.A., (2001), Characterization and structural modification of ammoniac lignosulfonate by methylation, *Journal of Applied Polymer Science*, **82**, 2661-2668.

Alonso M.V., Oliet M., Rodriguez F., Garcia J., Gilarranz M.A., Rodriguez J.J., (2005), Modification of ammonium lignosulfonate by phenolation for use in phenolic resins, *Bioresource Technology*, **96**, 1013-1018.

Biedermann M., Grob K., (2006a), Phenolic resins for can coatings: I. Phenol-based resol analysed by GC-MS, GC x GC, NPLC-GC and SEC, *LWT – Food Science and Technology*, **39**, 633-646.

- Biedermann M., Grob K., (2006b), Phenolic resins for can coatings: II. Resoles based on cresol/phenol mixtures or tert. butyl phenol, *LWT – Food Science and Technology*, **39**, 647-659.
- Bu Z., Hu J., Li, B., (2014), Novel silicon-modified phenolic novolac resins: Non-isothermal curing kinetics, and mechanical and thermal properties of their biofiber-reinforced composites, *Thermochimica Acta*, **575**, 244-253.
- Cemek B., Rahman S., Rahman A., (2013), Artificial Neural Network for predicting nutrients concentration in runoff from beef cattle feedlot, *Environmental Engineering and Management Journal*, **12**, 2385-2396.
- Cheng B., Titterton D.M., (1994), Neural networks: A review from a statistical perspective, *Statistical Science*, **9**, 2-54.
- Dharwal R., Kaur L., (2016), Application of artificial neural network: A review, *Indian Journal of Science and Technology*, **9**, 1-8.
- Foyer G., Chafi B.-H., Boutevin B., Caillol S., David G., (2016), New method for the synthesis of formaldehyde-free phenolic resins from lignin-based aldehyde precursors, *European Polymer Journal*, **74**, 296-309.
- Greco A., Ferrari F., Maffezzoli A., Delogu P., Velardi R., Timo A., Tarzia A., Marseglia A., Calo M., (2016), Solubility and durability of cardanol derived plasticizers for soft PVC, *Environmental Engineering and Management Journal*, **15**, 1989-1995.
- Hirano K., Asami M., (2013), Phenolic resins – 100 years of progress and their future, *Reactive & Functional Polymers*, **73**, 256-269.
- Hu L., Pan H., Zhou Y., Zhang M., (2011), Methods to improve lignin's reactivity as a phenol substitute and as replacement for other phenolic compounds: A brief review, *BioResources*, **6**, 3515-3525.
- Hu L., Zhou Y., Zhang M., Liu R., (2012), Characterization and properties of a lignosulfonate-based phenolic foam, *BioResources*, **7**, 554-564.
- Koricic K., Kusic H., Koprivanac N., Papic S., (2016), Mineralization of salicylic acid in water by catalytic ozonation, *Environmental Engineering and Management Journal*, **15**, 151-166.
- Li W., Jing S., Wang S., Wang C., Xie X., (2016), Experimental investigation of expanded graphite/phenolic resin composite bipolar plate, *International Journal of Hydrogen Energy*, **41**, 16240-16246.
- Martin C., Ronda J.C., Cadiz V., (2006), Boron-containing novolac resins as flame retardant materials, *Polymer Degradation and Stability*, **91**, 747-754.
- Meireles M.R.G., Almeida P.E.M., Godoy Simoes M., (2003), A comprehensive review for industrial applicability of artificial neural networks, *IEEE Transactions on Industrial Electronics*, **50**, 585-601.
- Noparvar-Qarebagh A., Roghani-Mamaqani H., Salami-Kalajahi M., (2016), Novolac phenolic resin and graphene aerogel organic-inorganic nanohybrids: High carbon yields by resin modification and its incorporation into aerogel network, *Polymer Degradation and Stability*, **124**, 1-14.
- Perez J.M., Rodriguez F., Alonso M.V., Oliet M., Echeverria J.M., (2007), Characterization of a novolac resin substituting phenol by ammonium lignosulfonate as filler or extender, *BioResources*, **2**, 270-283.
- Rajakovic-Ognjanovic V.N., Jovanovic B.M., Zijonovic D.Z., Rajakovic L.V., (2014), Challenging analytical task: Analysis and monitoring of arsenic species in water, *Environmental Engineering and Management Journal*, **13**, 2275-2282.
- Roslan R., Zakaria S., Chia C.H., Boehm R., Laborie M.-P., (2014), Physico-mechanical properties of resol phenolic adhesives derived from liquefaction of oil palm empty fruit bunch fibres, *Industrial Crops and Products*, **62**, 119-124.
- Shirmeshan A., Almassi M., Ghobadian B., Borghei A.M., Najafi G., (2016), Response Surface Methodology (RSM) based optimization of biodiesel-diesel blends and investigation of their effects on diesel engine operating conditions and emission characteristics, *Environmental Engineering and Management Journal*, **15**, 2771-2780.
- Shudo Y., Izumi A., Hagita K., Nakao T., Shibayama M., (2016), Large-scale molecular dynamics simulation of crosslinked phenolic resins using pseudo-reaction model, *Polymer*, **103**, 261-276.
- Shudo Y., Izumi A., Hagita K., Nakao T., Shibayama M., (2017), Structure-mechanical property relationships in crosslinked phenolic resin investigated by molecular dynamics simulation, *Polymer*, **116**, 506-517.
- Wang J., Deng X., Zhang H., Zhang D., Duan H., Lu L., Song J., Tian L., Song S., Zhang S., (2017), Synthesis of carbon nanotubes via Fe-catalyzed pyrolysis of phenolic resin, *Physica E*, **86**, 24-35.
- Wu H., Yin R., Qian L., Zhang Z., (2017), Three-dimensional graphene network/phenolic resin composites towards tunable and weakly negative permittivity, *Materials and Design*, **117**, 18-23.
- Xiang Y., Wang L., Xiang Y., (2015), Optimization of ultrasonic extraction conditions for excess sludge protein using Response Surface Methodology, *Environmental Engineering and Management Journal*, **14**, 1151-1159.
- Yang X., Frazier C.E., (2016), Influence of organic fillers on rheological behavior in phenol-formaldehyde adhesives, *International Journal of Adhesion & Adhesives*, **66**, 93-98.
- Zhao X., Lai S., Liu H., Gao L., (2009), Preparation and characterization of activated carbon foam from phenolic resin, *Journal of Environmental Sciences Supplement*, S121-S123.
- Zulfikar M.A., Mariske E.D., Djajanti S.D., (2012), Adsorption of lignosulfonate compounds using powdered eggshell, *Songklanakarinn Journal of Science and Technology*, **34**, 309-316.



“Gheorghe Asachi” Technical University of Iasi, Romania



KINETICS AND EQUILIBRIUM STUDIES OF 4-CHLOROPHENOL ADSORPTION ONTO MAGNETIC ACTIVATED CARBON COMPOSITES

Marius Sebastian Secula^{1*}, Etelka Dávid¹, Benoît Cagnon², Andreea Vajda¹,
Corneliu Stan¹, Ioan Mămăligă¹

¹“Gheorghe Asachi” Technical University of Iasi, Faculty of Chemical Engineering and Environmental Protection,
73 Prof.dr.doc. D. Mangeron, 700050 Iasi, Romania

²ICMN (UMR 7374 CNRS), Université d'Orléans, 1B, Rue de la Ferrollerie, 45071 Orleans, France

Abstract

Among the organic pollutants, the chlorinated phenols represent an important class of compounds having a stable world market of ca. 100 kt per year. Due to their aryl structure and presence of the chlorine atom, chlorinated phenols are exceptionally recalcitrant toward chemical reactions aimed at their reduction. Adsorption from liquid phase has received special interest due to its flexibility and simplicity in operation. Especially adsorption using activated carbon (AC) has been recognized by the US Environmental Protection Agency as one of the best available control technologies due to the high surface area, large adsorption capacities and porous structure of AC.

The purpose of this study was to investigate the adsorption mechanisms of 4-chlorophenol (4-CP) from aqueous solutions on AC-based magnetic composites. Three different granular activated carbon materials (GAC), L27, S21 and X17, were selected based on their chemical surface properties to prepare magnetic composites through the co-precipitation method. Two kinds of composites, magnetic composites (M-L27, M-S21 and M-X17), and pre-oxidized magnetic composites (M-L27/HNO₃, M-S21/HNO₃ and M-X17/HNO₃) were tested. Significant lower values of surface area were obtained in case of pre-oxidized magnetic composites due to their higher hydrophilicity. L27-based adsorbents lead to the fastest kinetics of 4-CP adsorption, whereas S21-based adsorbents have the highest values of adsorption capacity. The highest Fe content of 4.41% was achieved in case of M-L27 composite.

Key words: adsorption, equilibrium, kinetics, magnetic activated carbon, micropollutant

Received: May, 2017; *Revised final:* February, 2018; *Accepted:* March, 2018; *Published in final edited form:* April 2018

1. Introduction

Chlorophenols (CPs) are among the most persistent and hazardous organic compounds. Given their strong toxicity and resistance to biodegradation, they have been listed as persistent organic pollutants (POP) by the Clean Water Act of the US Environment Protection Authority and European Decision 2455/2001/EC (Ajeel et al., 2015; Allaboun and Abu Al-Rub, 2016; Hwang et al., 2015; Nourmoradi et al., 2015). The major source of chlorophenol pollution is represented by the industrial discharges from

petrochemical and pesticide industries and their hospital and domestic use. Chlorophenols are also generated *in-situ* during the chlorination process applied for the elimination of microbes from water (Duan et al., 2014; Lavand and Malghe, 2015). For human consumption, the limiting levels of various chlorophenols in water are below 0.1 mg/L (Aslam et al., 2015). Compared to meta- and para-chlorophenols, the ortho- substituted congeners are known to be of lower toxicity. The former substituted chlorines apparently shield the HO- group, thus having the property to interact with the available

* Author to whom all correspondence should be addressed: e-mail: mariussecula@ch.tuiasi.ro, Phone: +40 - 232 278683 / int. 2135; Fax: +40 - 232 271311

active sites from the aquatic media (Markovic et al., 2015). In particular, *p*-chlorophenol is directly relevant for water remediation due to its solubility and the severity of its threat to terrestrial and aquatic life (Nguyen and Juang, 2015).

Adsorption and advanced oxidation processes are known as highly efficient treatment methods for the removal of organic pollutants from water environments. Various adsorbents have been designed and tested for the removal of organics (Aghdam et al., 2015; Fard et al., 2017; Fard and Barkdoll, 2018). Although the adsorption process is relatively simple and involves mild operational conditions, its performance towards the removal of organic compounds is lower than that of other techniques (Irani et al., 2015). Advanced oxidation processes (AOPs) are based on the generation of highly reactive species, mainly hydroxyl radicals (HO·), which have the strongest oxidation potential, excepting fluorine (in acidic media), and are able to mineralize almost all organic compounds to carbon dioxide and water (Liu et al., 2015; Nourmoradi et al., 2015). Among AOPs, the Fenton process using a mixture of hydrogen peroxide (H₂O₂) as oxidant and ferrous iron (Fe²⁺) as catalyst (to accelerate the degradation rate of organic compounds) has been intensively studied for environmental remediation (Chen et al., 2015; Messele et al., 2015; Yao et al., 2013). It has many advantages, such as high performance and simplicity for the oxidation of organics, mild reaction conditions (operated at room temperature and atmospheric pressure), non-toxicity (H₂O₂ can break down into environmentally safe species like H₂O and O₂) and the materials required are inexpensive (Wang M. et al., 2016; Wang N. et al., 2016).

The Fenton process consists in a transfer of electrons from a strong oxidizing agent (hydrogen peroxide) towards a transitive metal in the bulk solution, generally iron (II) (Fe²⁺), resulting in the formation of hydroxyl radicals that attack further the organic matter (Martin del Campo et al., 2014). The chemical reaction is described by Eq. (1):



AOPs can be also used in combinations termed *hybrid methods* such as ultrasound assisted Fenton, sonophotocatalysis, photo-Fenton, and ozone/hydrogen peroxide, in order to enhance the oxidation efficiency and overcome the limitations of individual AOPs toward some specific pollutants (Saharan et al., 2014). The combined system of UV irradiation and Fenton process, namely the photo-Fenton process, has been developed (Fard et al., 2013). This process results in a higher degree of mineralization due to the enhanced production of •OH radicals. In this case, hydroxyl radicals are generated due to both the photo-decomposition of hydrogen peroxide and iron catalyzed decomposition (Eq. 2) (Bel Hadjltaief et al., 2014).



In particular, iron oxide nanoparticles represent a promising adsorbent due to their high reactivity; moreover, elemental iron is non-toxic and ubiquitous on Earth (accounting for 6% wt. of the Earth's crust) (Xu et al., 2013).

Considering the excellent adsorption capacity of activated carbon, many studies have been focusing on the development of novel adsorbents that combine the adsorption capacity of carbon materials with the magnetic properties of iron oxides (Istratie et al., 2016).

In the present study, a combined adsorption and Fenton oxidation method is proposed using granular activated carbons as starting materials. The ACs were modified by chemical treatment in order to obtain supports with different surface chemistry. The co-precipitation method was employed to prepare iron-impregnated catalysts on different activated carbon supports, and applied in the photo-Fenton-like degradation process of *4-CP*.

The adsorption step of the treatment process allows *4-CP* to be immobilized and concentrated on the activated carbon surface and when Fenton oxidation is carried out the degradation of the adsorbate is much more efficient and effective compared to chemical oxidative processes carried out in the dilute solution (Kim et al., 2015).

The main objective of this study was to develop and compare the performance of raw activated carbons having different surface properties, magnetic and pre-oxidized magnetic activated carbons applied further for the removal method of *4-CP* from water by adsorption and photo-Fenton processes.

The physical and chemical properties of GAC composites were analyzed and the catalytic performances were assessed according to the effects of some key parameters, such as initial value of solution pH, phenol initial concentration, and contact time. The reaction kinetics, isotherms, material stability and degradation mechanism were evaluated.

Experimental data on the desorption of *4-CP* from GAC by NaOH and Et-OH solutions are also presented and discussed.

2. Material and methods

2.1. Material

Activated carbon materials were acquired from PICA-Jacobi (France). Three types of ACs, L27, S21 and X17, were employed in this study in order to establish the influence of surface pH_{PZC} on the performance of the achieved Fenton-like catalysts. Before use, the ACs were washed for 24 h with bidistilled water to eliminate the residual acidity or basicity, and then dried at 75°C for 24 h. The *4-CP* (>99.5%), HNO₃ (65%), ferrous sulfate heptahydrate (>99%), iron(III) nitrate nonahydrate (≥98%), ammonium hydroxide, ethanol (97%) and hydrogen peroxide were purchased from Sigma Aldrich and used without further purification. All solutions were prepared using bidistilled water.

2.2. Preparation of acid treated Fe-amended activated carbon

The ACs were used either as such (to prepare magnetic GACs) or each of the adsorbents was oxidized with concentrated HNO₃ (pre-oxidized GACs) in an ultrasonic bath (GFL 1092) for 60 min, washed with bidistilled water and dried. The active metal was supported on activated carbons by co-precipitation of FeSO₄·7H₂O and Fe(NO₃)₃·9H₂O. The magnetic composites were prepared by contacting 3 g of raw and oxidized ACs respectively with the solution of precursors with a calculated concentration. The resulting mixture was sonicated for 15 min at room temperature. 8 M ammonium hydroxide solution was added dropwise to adjust the pH to 12 in order to precipitate Fe₃O₄. This reaction was conducted for 1 h at 50°C under mechanical stirring. After impregnation, the samples were rinsed and dried at 55°C in an oven. Two types of composites were obtained: magnetic composites and pre-oxidized magnetic composites denoted here in further as M-L27, M-S21, M-X17 and M-L27/HNO₃, M-S21/HNO₃, M-X17/HNO₃ respectively.

2.3. Characterization methods

Textural characterization of the supports and catalysts was performed by means of the N₂ adsorption-desorption isotherms, recorded at 77 K using an ASAP 2020 (Micromeritics Inc., USA). The pore size distribution was determined by the Density Functional Theory (DFT) method (function provided by Micromeritics software). Thermogravimetric analyses (TG/DTG) were recorded on Thermogravimetric analysis (TGA 92 Setaram) in the temperature range of 21 - 1000°C. Fourier transform infrared (FTIR) spectra of the complexes were recorded using a Perkin Elmer Spectrum 100 spectrometer over a wavenumber range of 4000–400 cm⁻¹ and the conventional KBr pellet method. Total iron content in the obtained composites and iron leakage were determined by spectrophotometry using phenantroline method (Clesceri et al., 1989). The concentration of 4-CP was determined using a UV-Vis Hitachi 5100 spectrophotometer at the maximum specific wavelength of 223 nm.

2.4. Adsorption-desorption experiments

The adsorption experiments were performed in batch mode with the aid of an orbital shaker. The initial concentration was varied between 20-250 mg/L. An adsorbent mass of 0.1 g was added to 250 mL glass flasks filled with 250 mL of adsorbate solution of known initial concentration and shaken for 24h. In the kinetics tests, samples of 4 mL were systematically taken at appropriate time intervals using a syringe. Then, they were separated by centrifugation and then 1mL was diluted and analyzed spectrophotometrically. The desorption runs were carried out also in batch mode. Certain weights of

spent adsorbents were added to 50 mL bidistilled water and samples were taken after the equilibrium has been established.

The performance of the synthesized catalysts was evaluated in Fenton and photo-Fenton processes of 4-CP degradation. Catalytic degradation experiments were carried out for 2h in conical flasks, on a magnetic stirrer using a catalyst dosage of 0.1 g/250 mL 4-CP solution, pH of 3, H₂O₂ concentration of 100 mg/L. Photo-catalytic oxidation was conducted under the irradiation of a Pen-Ray-Power Supply lamp (UVP Products, TQ 718, and 700 W) at 312 nm and at room temperature. 4 mL of reaction mixture were systematically sampled, separated by centrifugation and then 1mL was diluted and analyzed by means of a UV-Vis spectrophotometer following absorbance at the maximum wavelength of 4-CP, 280 nm. After analysis, the undiluted solution was added back into the photocatalytic reactor to minimize the loss in total volume and maintain the solid/liquid ratio.

The amount of solute adsorbed at time t , q_t (mg/g) and at equilibrium state, q_e (mg/g) were calculated according to the following equations (Eqs. 3-4):

$$q_t = (C_0 - C_t) \frac{V}{m} \quad (3)$$

$$q_e = (C_0 - C_e) \frac{V}{m} \quad (4)$$

where: C_0 is the initial concentration of the adsorbate (mg/L); C_t and C_e are the concentration of 4-CP in solution at equilibrium and at time t (mg/L); V is the volume of the aqueous solution (L); m is the mass of adsorbent (g).

2.5. Kinetic models

The 4-CP adsorption kinetics data were fitted with the linearized form of the following three adsorption models:

- pseudo-first-order kinetic model (Lagergren and Svenska, 1898) (Eq. 5):

$$\log(q_e - q_t) = \log q_e - k_1 t \quad (5)$$

- pseudo-second-order kinetic model (Ho and McKay, 1998) (Eq. 6):

$$\frac{t}{q_t} = \frac{1}{k_2 q_e^2} + \frac{t}{q_e} \quad (6)$$

where: q_e and q_t are the adsorption capacities at equilibrium and at time t , respectively (mg g⁻¹); k_1 is the rate constant of pseudo-first-order adsorption (L min⁻¹); k_2 is the rate constant of pseudo-second-order adsorption (g (mg·min)⁻¹).

- intraparticle diffusion model (Weber and Morris, 1963) (Eq. 7):

$$q_t = K_{dif} \cdot t^{0.5} + I \quad (7)$$

where: K_{dif} is the intraparticle diffusion rate constant ($\text{mg (g h}^{0.5}\text{)}^{-1}$); I indicates the thickness of the boundary layer diffusion (mg g^{-1}).

2.6. Adsorption isotherms

The experimental data on adsorption were analyzed using Langmuir, Freundlich, and Dubinin Radushkevich (DR) isotherm models. The theoretical form of the Langmuir isotherm is given by the following equation (Langmuir, 1916) (Eq. 8):

$$q_e = \frac{Q_{max}K_L C_e}{1+K_L C_e} \quad (8)$$

where: Q_{max} is the maximum adsorption capacity (mg g^{-1}); K_L is a constant related to the adsorption free energy (L mg^{-1}).

The essential characteristics of the Langmuir isotherm can be expressed by the separation factor (a dimensionless constant), R_L , which is expressed as (Eq. 9):

$$R_L = \frac{1}{1+K_L C_0} \quad (9)$$

When the R_L value is zero the adsorption process is irreversible, if it one, the adsorption is linear, and if R_L takes values between zero and one, the adsorption is favorable.

The Freundlich isotherm is given by Eq. (10) (Freundlich, 1906):

$$q_e = K_F C_e^{1/n} \quad (10)$$

where: K_F (L mg^{-1}) is Freundlich constant related to the adsorption capacity; n is a constant related to the adsorption intensity. When $n > 1$, it means the adsorption conditions for are favorable.

The third isotherm investigated within this study was the Dubinin–Raduchkevitch (DR) isotherm which is used to estimate the nature of the adsorption process (physical or chemical). It is described by the following relation (Dubinin et al., 1947) (Eq. 11):

$$\ln q_e = \ln q_m - K_{ads} \varepsilon^2 \quad (11)$$

where: q_e is the uptake at equilibrium (mg g^{-1}); K_{ads} is the adsorption energy constant ($\text{J}^2 \text{mol}^{-2}$); ε is the Polanyi potential defined by (Eq. 12):

$$\varepsilon = RT \ln \left(1 + \frac{1}{C_e} \right) \quad (12)$$

where: R is the gas constant (8.314 J/(mol K)) and T is the absolute temperature.

Describing the nature of the adsorption, the value of the adsorption energy (E), which indicates the, was determined through Eq. (13) (Barkat et al., 2015):

$$E = \frac{1}{\sqrt{2K_{ads}}} \quad (13)$$

A value of E less than 8 kJ/mol points out a physical adsorption, an E value between 8 and 25 kJ/mol shows a chemical ion exchange process, and if it is higher than 25 kJ/mol it involves chemical adsorption.

3. Results and discussion

3.1. Characterization of adsorbents

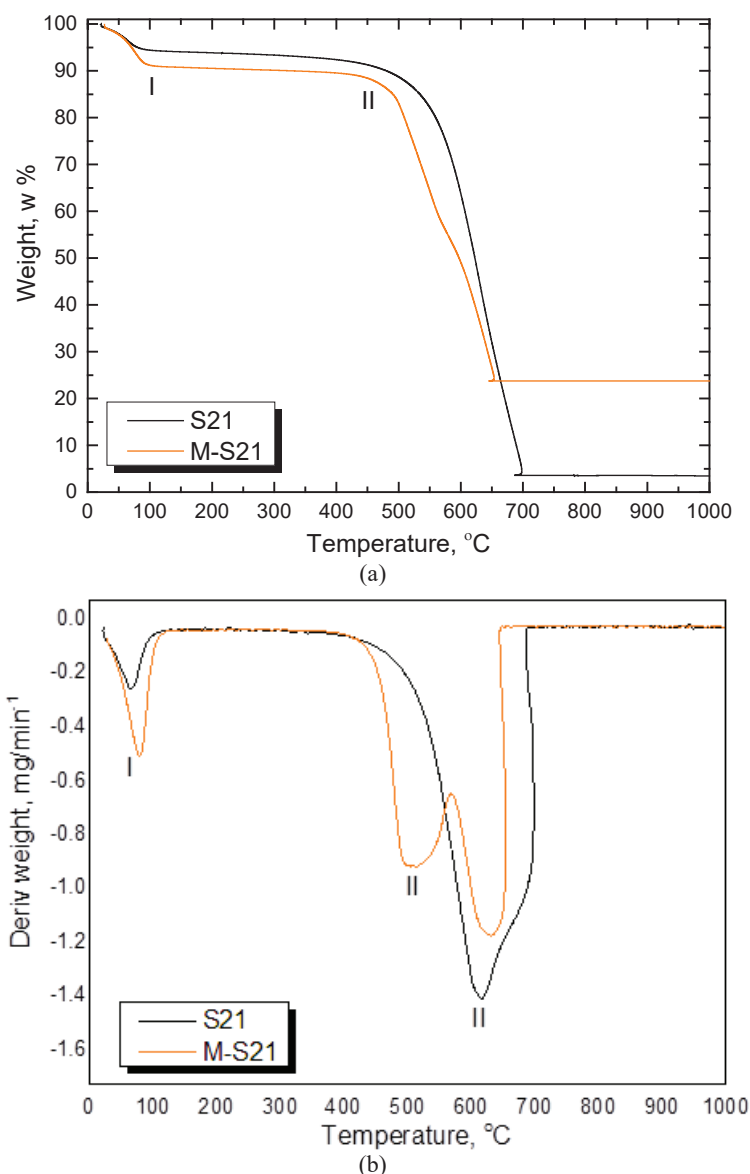
The raw ACs (L27, S21 and X17) have different porous properties. The N_2 adsorption-desorption isotherms showed that L27 and X17 were microporous but also contained some mesopores while S21 was microporous only, which was confirmed by the values of its S_{micro} and S_{ext} . L27 AC is acidic, S21, neutral and X17, basic. Table 1 summarizes the textural properties of the ACs based on N_2 isotherms. The N_2 adsorption-desorption isotherms recorded for M-L27 (figure not shown) showed an enlarged hysteresis loop compared to raw L27, indicating an increased mesopore volume, confirmed by the increased mean pore size. For the oxidized M-L27 the adsorbed volume decreased even more pronounced. Before each N_2 isotherm, a degassing step was conducted for 24 h at 250°C and $4 \mu\text{m Hg}$, and the mass loss corresponds to water evaporation. The determined values of water loss are shown in Table 2.

Table 1. Textural properties of the raw and magnetic GACs

AC	$V_{micro}(\text{cm}^3 \text{g}^{-1})$	$L_0(\text{Å})$	$S_{ext}(\text{m}^2 \text{g}^{-1})$	$S_{micro}(\text{m}^2 \text{g}^{-1})$	$S_{total}(\text{m}^2 \text{g}^{-1})$
L27	0.57	18.5	444	616	1060
M-L27	0.46	25.4	644	362	1006
M-L27/ HNO_3	0.38	17.2	492	442	934
S21	0.47	9.7	18	969	987
M-S21	0.06	19.5	12	62	74
M-S21/ HNO_3	0.30	8.3	23	723	746
X17	0.29	15.1	130	382	514
M-X17	0.28	15.0	145	373	518
M-X17/ HNO_3	0.26	13.7	155	380	535

Table 2. Water loss of magnetic GACs

GAC	M-L27	M-L27/HNO ₃	M-S21	M-S21/HNO ₃	M-X17	M-X17/HNO ₃
Water loss (%)	5.6	11.4	4.0	6.8	4.2	8.2

**Fig. 1.** TG and DTG curves of S21 (a) and M-S21 (b)

In case of the magnetic composites prepared on the support S21, characterized by microporosity, a strong decrease in the microporous volume was observed, caused by pore-clogging due to the impregnation with iron oxides, resulting in a decrease of the total surface area. For X17 and M-X17 it was observed a significant increase in the pores similar in size to the 4-CP molecule ($6.47 \times 4.17 \text{ \AA}$). However, the change in porous structure appears to be less important in case of X17 in comparison with those noticed in case of L27 and S21.

The decreased surface area of the pre-oxidized magnetic composites may be due to the high amount of oxygen-containing groups introduced on the AC surface with HNO₃ treatment, which may block the

entry of N₂ molecules inside the small pores (Chen et al., 2015).

Thermogravimetric analysis was employed in order to determine the main decomposition stages of raw and composite GACs. Since all the ACs showed similar behavior, Fig. 1 presents the TG of S21 and M-S21 only. The shape of the thermal curves is similar for the two types of adsorbents, which exhibit only two decomposition stages: one up to 100°C, which corresponds to the dry AC, while stage II, in the range 500-600°C, corresponds to a carbonized material showing a slower deconstruction of the magnetic composite compared to that of raw AC. The residual weight of S21 and M-S21 points out the presence of iron oxides in the magnetic composites.

Total iron content was determined by using phenanthroline spectrophotometric method. The results showed that the iron content in the Fe-GAC magnetic composites decreased in the following order: magnetic L27>S21>X17 (Fig. 2). Thus M-L27 has the highest total iron content (4.41%) while X17 is expected to be less suitable as a catalyst support for Fe₃O₄ (Bayazit and Kerkez, 2014) as it has the lowest total iron content. However, M-GACs have proven to have a higher total iron content than those activated with HNO₃.

Fig. 3 exemplifies the case for S21. This AC has no surface oxygen groups. HNO₃ activation increases the hydrophilicity of magnetic GACs as emphasized by the peaks at 3423 and 3491 cm⁻¹. The spectrum of M-S21/HNO₃ shows peaks at 1510, 1710 which are characteristics of carboxylic groups.

Both the FTIR spectra and the water loss data (after drying the GACs) point out that the pre-oxidized carbons are more hydrophilic, suggesting that HNO₃ activation increases the hydrophilicity of magnetic

GACs. Therefore, it is expected a relatively lower adsorption capacity of these adsorbents.

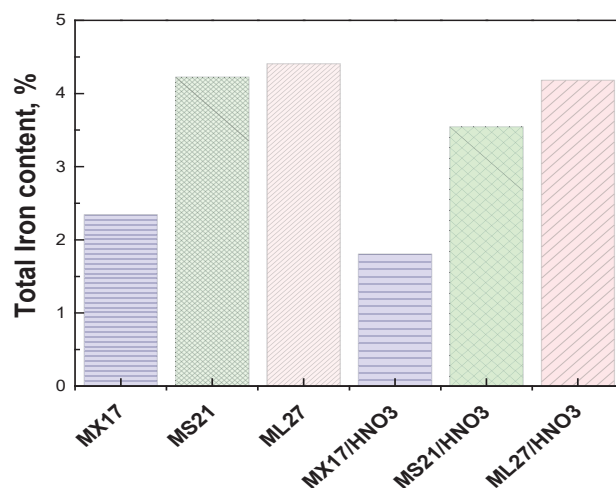


Fig. 2. Total Iron content in synthesized Magnetic GACs

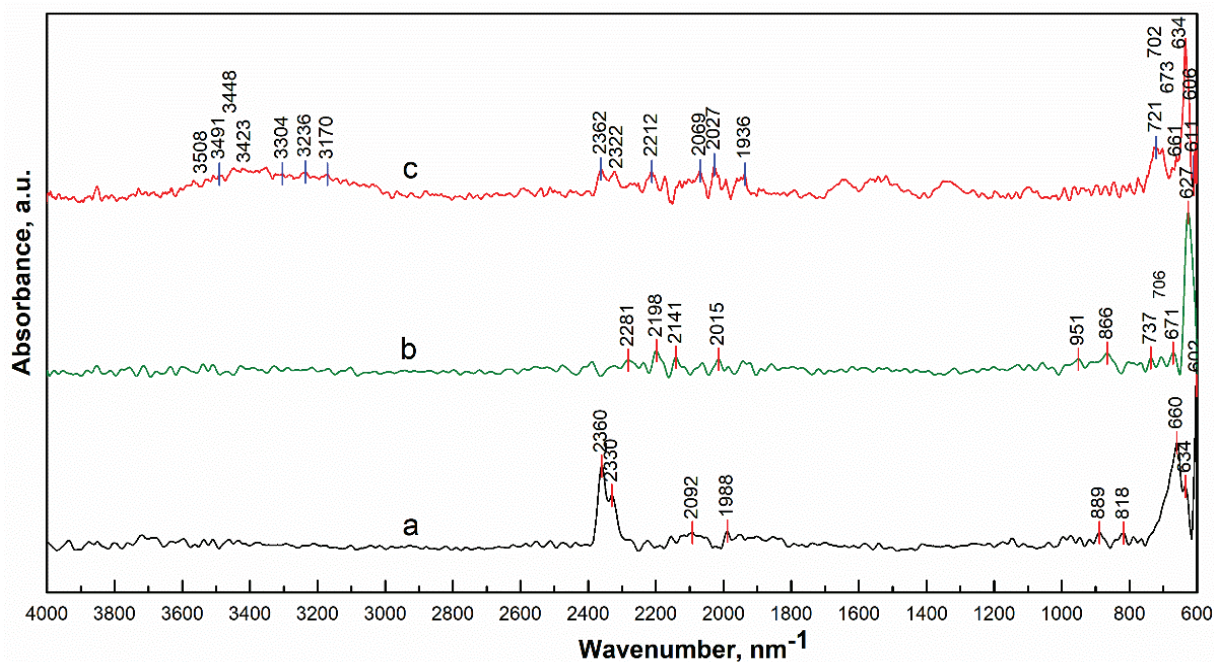
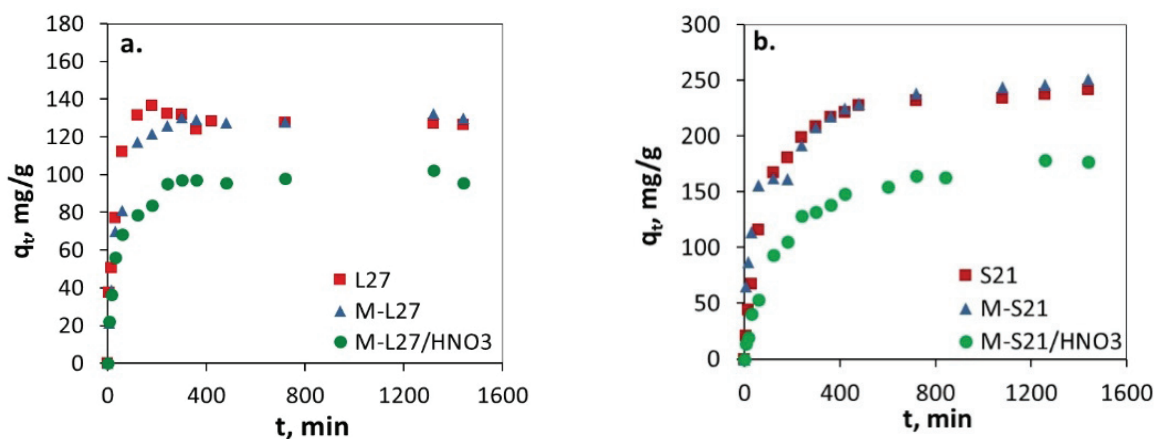


Fig. 3. FTIR spectra of raw and magnetic S21: a. S21, b. M-S21, c. M-S21/HNO₃



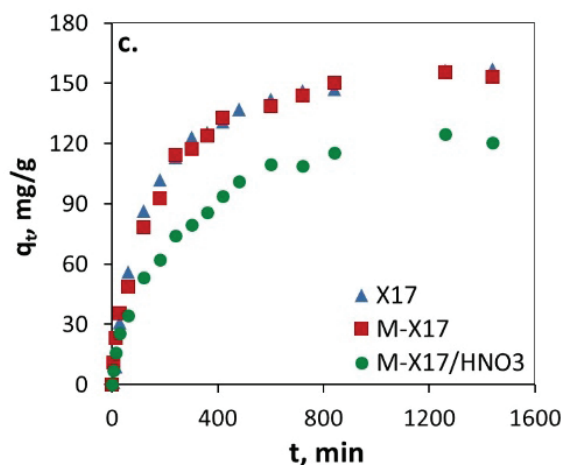


Fig. 4. Amount of 4-CP adsorbed as a function of contact time ($C_0 = 100$ mg/L, 0.1 g CA)

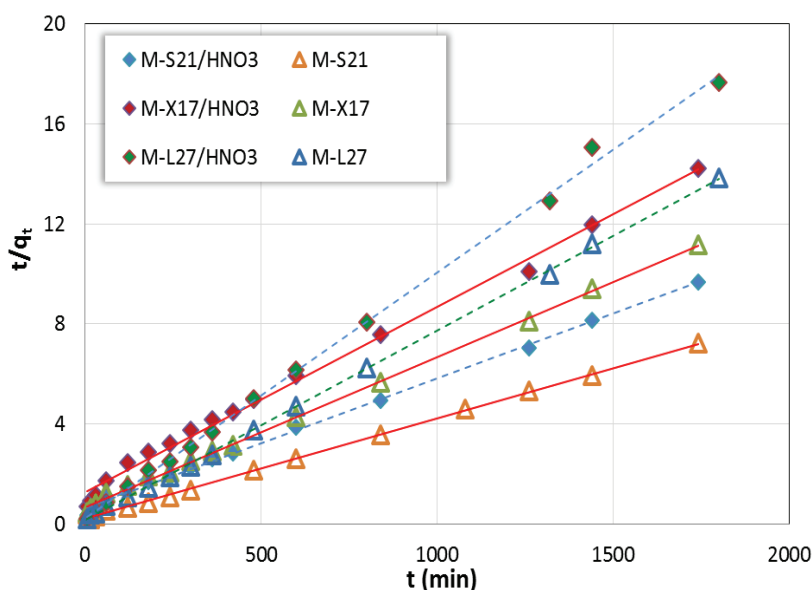


Fig. 5. Pseudo-second-order kinetic plots for adsorption of 4-CP onto magnetic AC

3.2. Effect of contact time

The time dependence for 4-CP adsorption onto the activated carbons modified with HNO_3 and iron salts was investigated to determine the time needed to reach the equilibrium. The experimental data are plotted as adsorbed amounts versus contact time (Fig. 4).

As shown in Fig. 4, 4-CP adsorption was quite fast in the first 2h, then gradually increased with the extended contact time. After 12h of contact time, no obvious variation in the amounts of 4-CP adsorbed was noted. The raw and magnetic carbons had a similar adsorption behavior toward 4-CP, the main difference being the adsorption capacity of M-X17 which decreased slightly due to alteration of the microporous matrix after impregnation with iron. As regards the pre-oxidized magnetic composites, the figures show a significant decrease in adsorption capacity. This phenomenon was already reported by Messele et al. (2015) who suggested that water forms hydrogen bonds with the hydrophilic oxygenated groups present on the carbon surface, resulting in

clusters that can block the passage of phenolic molecules to the surface. It is worth mentioning also that the solubility of 4-CP (26 g/L) is significantly lower than that of phenol (76 g/L) so there is a competition between water and 4-CP.

3.3. Kinetic models and adsorption mechanism

Generally, kinetic models are employed to determine the rate of the adsorption process (Ahmed and Theydan, 2013). Three kinetic models - pseudo-first order, pseudo-second order and intraparticle diffusion- were used to correlate the experimental kinetic data.

Table 3 shows the values of kinetic parameters for 4-CP adsorption onto the considered adsorbents. There is a high deviation between the experimental and calculated adsorption capacity for the pseudo-first order model, which reflects the poor fitting of this model to the experimental data. Moreover, the pseudo-first order had low R^2 values, whereas for the pseudo-second order equation the correlation of the linear plot between t/qt and t (Fig. 5) has high R^2 values (Table 3).

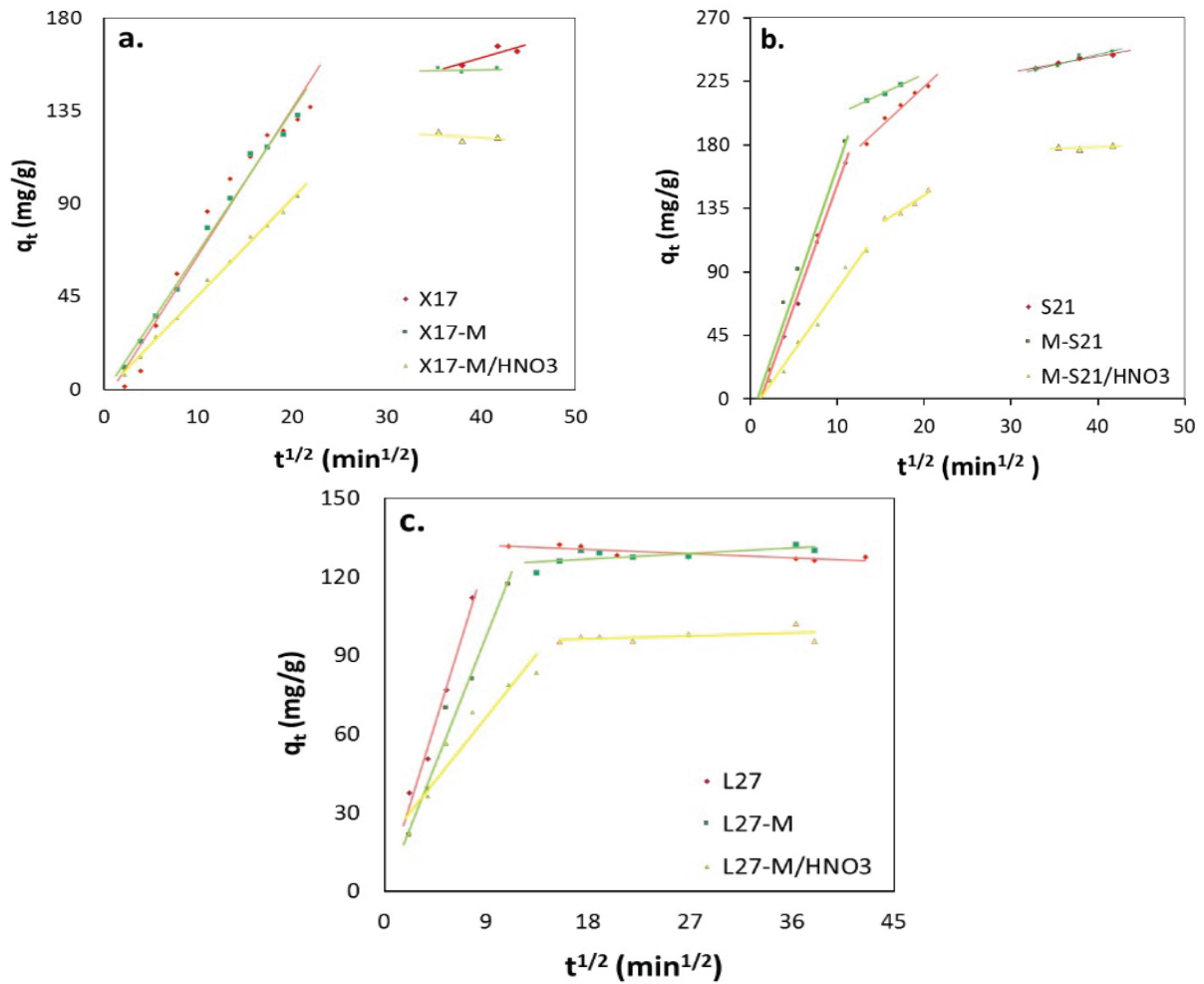


Fig. 6. Adsorption of 100 mg/L 4-CP onto raw and magnetic AC

Table 3. Kinetic parameters for 4-CP adsorption onto raw and magnetic activated carbons

AC	q_{exp} (mg/g)	Pseudo-first-order			Pseudo-second-order			Intraparticle diffusion		
		q_{calc} (mg/g)	k_1 (h ⁻¹)	R ²	q_{calc} (mg/g)	k_2 (g/(mg h))	R ²	K_{dif} (mg/(g h ^{1/2}))	I (mg/g)	R ²
L27	127.60	123.18	0.027	0.998	127.62	0.0016	0.999	13.851	2.388	0.983
								-0.18	133.78	0.770
M-L27	129.99	71.08	0.008	0.816	132.16	0.0004	0.999	10.108	3.161	0.965
								0.209	123.09	0.383
M-L27/HNO ₃	101.99	54.05	0.006	0.838	101.82	0.0004	0.998	5.416	-18.099	0.909
								0.122	94.184	0.217
								17.224	-21.388	0.996
S21	246.54	114.69	0.002	0.906	252.45	6.103·10 ⁻⁵	0.999	5.730	107.33	0.965
								0.962	512.173	0.989
								17.896	-15.472	0.962
M-S21	242.96	104.67	0.002	0.813	249.08	7.533·10 ⁻⁵	0.998	1.427	194.416	0.799
								1.392	188.229	0.916
								8.754	-9.651	0.983
M-S21/HNO ₃	179.51	138.86	0.003	0.956	193.03	4.089·10 ⁻⁵	0.998	3.954	65.209	0.942
								0.225	169.60	0.272
								10.197	-25.024	0.990
X17	201.72	131.25	0.001	0.798	205.76	1.074·10 ⁻⁵	0.967	3.923	51.543	0.973
								0.870	128.222	0.977
								7.571	-6.517	0.994
M-X17	155.76	137.57	0.004	0.988	166.57	5.206·10 ⁻⁵	0.999	5.133	28.253	0.926
								0.088	151.48	0.041
								4.715	-1.966	0.998
M-X17/HNO ₃	122.37	111.48	0.003	0.993	134.95	4.414·10 ⁻⁵	0.995	4.715	-1.966	0.998

Table 4. Isotherm constants and correlation coefficients for adsorption of 4-CP onto AC

AC	Langmuir				Freundlich			Dubinin-Radushkevich			
	K_L (L/mg)	b (mg/g)	R_L	R^2	K_F	n	R^2	$K_{ads} \times 10^{-9}$	q_m (mg/g)	E (kJ/mol)	R^2
L27	0.028	236.71	0.320	0.981	23.920	2.360	0.943	4.810	793.27	10.190	0.960
M-L27	0.028	261.98	0.319	0.914	32.633	2.647	0.982	3.510	550.84	11.942	0.988
M-L27/HNO ₃	0.064	115.53	0.120	0.954	30.623	3.928	0.974	2.765	238.03	13.448	0.983
S21	1.276	295.09	0.009	0.912	154.83	6.026	0.957	1.533	551.56	18.061	0.990
M-S21	0.112	292.00	0.118	0.965	111.27	5.263	0.847	2.890	681.40	13.162	0.869
M-S21/HNO ₃	0.157	214.06	0.089	0.996	80.46	4.964	0.917	2.530	463.82	14.058	0.894
X17	0.209	194.97	0.069	0.995	81.933	5.486	0.901	2.500	439.56	14.146	0.938
M-X17	0.139	190.15	0.107	0.968	53.278	3.380	0.992	2.712	467.75	13.578	0.994
M-X17/HNO ₃	0.057	128.42	0.218	0.969	29.867	3.579	0.989	3.094	278.51	12.713	0.995

The results listed in Table 3 show that the adsorption kinetic data are better represented by the pseudo-second order model and the calculated values (q_{calc}) agree well with the experimental ones (q_{exp}). This indicates the second-order kinetics for 4-CP adsorption on the studied carbons, suggesting that adsorption depends on the adsorbate as well as the adsorbent and involves chemical reaction as a rate controlling parameter, in addition to physisorption (Goscianska et al., 2015; Mohd et al., 2009).

The curve-fitting plots of the intraparticle diffusion model are presented in Fig. 6 at 25°C. In case of raw and magnetic X17 and L27 the adsorption process can be divided in two regions: the first one, sharper portion is attributed to the external surface adsorption and the second plateau portion corresponds to the final equilibrium process when intraparticle diffusion starts to slow down due to extremely low solute concentrations in the solution.

The existence of an external layer diffusion process can be inferred because these plots do not pass through the origin (Liu et al., 2010). Between the sharp rise and the plateau portion, a less steep stage is observed for the composite adsorbents based on S21. The second region corresponds, in this case, to the gradual adsorption stage when diffusion is restricted mainly by the microporous structure of the ACs. The third portion is the final equilibrium stage where diffusion is retarded by the formerly adsorbed molecules. The I values for all the ACs indicate that intraparticle diffusion is not the only rate-limiting step in the sorption process.

3.4. Equilibrium models

An adsorption isotherm is commonly depicted by expressing graphically the unit mass of solid-phase against the solute equilibrium concentration. Three widely used models, Langmuir, Freundlich and Dubinin-Radushkevich, were applied for the fitting of the experimental data. Table 4 indicates the sorption isotherms parameters. The adsorption of 4-CP on magnetic L27 and X17 composites is best described by the Dubinin-Radushkevich model, whereas that based on S21 fits the Langmuir model better in terms of determination coefficients. The n value obtained

from the Freundlich isotherm was more than one, suggesting that the uptake of 4-CP was suitably accomplished by all the adsorbents. The adsorption energy, E , calculated from the adsorption energy constant, ranged between 10.19 and 18.06 kJ/mol, clearly indicating a chemical ion exchange mechanism.

3.5. Fenton and photo-Fenton degradation of 4-CP

Several batch experiments were performed to assess the catalytic ability of magnetic GACs toward 4-CP degradation in presence of H₂O₂. Among the different catalysts used in heterogeneous Fenton-like reactions, Fe containing carbons have shown high catalytic activities in the oxidation of organic compounds, with minimal iron leaching and easy recovery. The studies showed that M-L27, beside its highest Fe content, has the fastest adsorption kinetics in relation to 4-CP among all the synthesized composites.

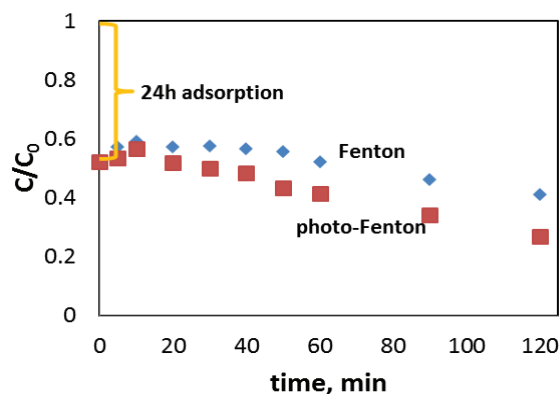


Fig. 7. Degradation and photo-degradation of 4-CP by heterogeneous Fenton, (100 mg/L 4-CP, 0.4 g/L M-L27, 100 mg/L H₂O₂)

Therefore, before the AOP tests, M-L27 previously saturated with 4-CP was subjected to the oxidation process. Fig. 7 shows the measured 4-CP degradation performance by Fenton and photo-Fenton oxidation as a function of reaction time. The results show an increase in 4-CP concentration in the first hour of the Fenton reaction which can be explained by

4-CP desorption from the M-L27 surface. However, the degradation process starts as the catalyst surface is unloaded. UV irradiation also seems to be an important feature for achieving higher 4-CP removal efficiencies.

3.6. Desorption studies

The feasibility of regenerating the spent activated carbon saturated with 4-CP was evaluated. The effect of ultrasound and agitation on the desorption of 4-CP from the spent magnetic ACs using solutions of NaOH and Et-OH (ethyl alcohol) were evaluated and compared. For this purpose, a volume of 50 mL of ethyl alcohol or 20% NaOH solution, respectively were added to the desorption system in the presence of sonication for 2h, or agitation for 24h, at room temperature.

The results presented in Fig. 8 emphasize that 4-CP desorption significantly increased in the presence of ultrasound and ethanol solution. According to iron leakage studies, sonication and NaOH solutions are detrimental to magnetic composites. Therefore, ethanol and agitation are recommended for the desorption of 4-CP in order to minimize the leakage of iron from the magnetic composites.

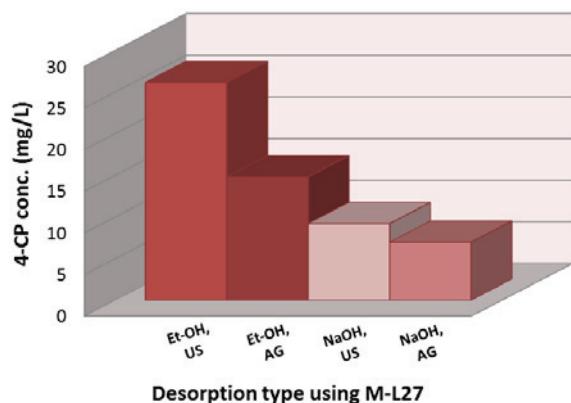


Fig. 8. Effect of agitation and stripping solution type on the desorption of 4-CP

4. Conclusions

The adsorption mechanisms and Fenton oxidation of 4-CP from aqueous solutions on magnetic composites were studied. Total iron content in M-GAC was higher than in the pre-oxidized magnetic composites. M-L27 had the highest iron content.

Adsorption experimental data showed a better fit with the pseudo-second-order kinetic model as indicated by higher values of the correlation coefficient. The incorporation of iron decreased the sorption capacity of X17 and S21 for 4-CP due to alteration of the porous structure.

HNO₃ preactivation resulted in an increase in hydrophilicity and consequently in a significant decrease in the sorption capacity.

Adsorption of 4-CP on the Magnetic X17 composite was best described by the Dubinin-Radushkevich model, magnetic L27 by the Freundlich model whereas that obtained on S21 composites was best described by the Langmuir model.

Among all the synthesized adsorbents, only M-L27 and M-L27/HNO₃ were suitable for Fenton and photo-Fenton reactions. The optimal desorption of 4-CP was obtained under agitation in ethanol solutions.

Acknowledgements

This work was supported by a grant from the Romanian National Authority for Scientific Research and Innovation, CNCS - UEFISCDI, project number PN-II-RU-TE-2014-4-0405.

References

- Aghdam E., Aminzadeh B., Baghdadi M., Fard M.A., (2015), Removal of BTEX from aqueous solutions by paper mill sludge-based activated carbon, *Journal of Advances in Chemistry*, **11**, 3416-3432.
- Ahmed M.J., Theydan S.K., (2013), Adsorption of p-chlorophenol onto microporous activated carbon from Albizialebbeck seed pods by one-step microwave assisted activation, *Journal of Analytical and Applied Pyrolysis*, **100**, 253-260.
- Ajeel M.A., Aroua M.K., Wan Daud W.M.A., (2015), Anodic degradation of 2-chlorophenol by carbon black diamond and activated carbon composite electrodes, *Electrochimica Acta*, **180**, 22-28.
- Allaboun H., Abu Al-Rub F.A., (2016), Removal of 4-chlorophenol from contaminated water using activated carbon from dried date pits: equilibrium, kinetics, and thermodynamics analyses, *Materials*, **9**, 1-15.
- Aslam M., Soomro M.T., Ismail I.M.I., Salah N., Gondal M.A., Hameed A., (2015), Sunlight mediated removal of chlorophenols over tungsten supported ZnO: Electrochemical and photocatalytic studies, *Journal of Environmental Chemical Engineering*, **3**, 1901-1911.
- Barkat M., Nibou D., Amokrane S., Chegrouche S., Mellah A., (2015), Uranium (VI) adsorption on synthesized 4A and P1 zeolites: Equilibrium, kinetic, and thermodynamic studies, *Comptes Rendus Chimie*, **18**, 261-269.
- Bayazit Ş.S., Kerkez Ö., (2014), Hexavalent chromium adsorption on superparamagnetic multi-wall carbon nanotubes and activated carbon composites, *Chemical Engineering Research and Design*, **92**, 20725-2733.
- Bel Hadjltaief H., Da Costa P., Beaunier P., Gálvez M.E., Ben Zina M., (2014), Fe-clay-plate as a heterogeneous catalyst in photo-Fenton oxidation of phenol as probe molecule for water treatment, *Applied Clay Science*, **91-92**, 46-54.
- Chen H., Zhang L., Zeng H., Yin D., Zhai Q., Zhao X., Li J., (2015), Highly active iron-containing silicotungstate catalyst for heterogeneous Fenton oxidation of 4-chlorophenol, *Journal of Molecular Catalysis A: Chemical*, **406**, 72-77.
- Clesceri L.S., Greenberg A.E., Trussell R.R., (1989), *WEF Standard Methods for the Examination of Water and Wastewater*, Method 3500-Fe D, Phenanthroline Method, 17th Edition, APHA, AWWA.
- Duan F., Yang Y., Li Y., Hongbin C., Yi W., Yi Z., (2014), Heterogeneous Fenton-like degradation of 4-chlorophenol using iron/ordered mesoporous carbon

- catalyst, *Journal of Environmental Sciences*, **26**, 1171-1179.
- Dubinin M.M., Zaverina E.D., Radushkevich L.V., (1947), Sorption and structure of active carbon I. Adsorption of organic vapors, *Journal of Physical Chemistry A*, **21**, 1351-1362.
- Fard M.A., Torabian A., Bidhendi G.R.N., Aminzadeh B., (2013), Fenton and photo-Fenton oxidation of petroleum aromatic hydrocarbons using nanoscale zero-valent iron, *Journal of Environmental Engineering*, **139**, 966-974.
- Fard M.A., Vosoogh A., Barkdoll B., Aminzadeh B., (2017), Using polymer coated nanoparticles for adsorption of micropollutants from water, *Colloids and Surfaces A: Physicochemical and Engineering Aspects*, **531**, 189-97.
- Fard M.A., Barkdoll B., (2018), Using recyclable magnetic carbon nanotube to remove micropollutants from aqueous solutions, *Journal of Molecular Liquids*, **249**(Supplement C), 193-202.
- Freundlich H.M.F., (1906), About the adsorption in liquids (in German), *Zeitschrift für Physikalische Chemie*, **57**, 385-470.
- Goscianska J., Ptaszowska M., Pietrzak R., (2015), Equilibrium and kinetic studies of chromotrope 2R adsorption onto ordered mesoporous carbons modified with lanthanum, *Chemical Engineering Journal*, **270**, 140-149.
- Ho Y.S., McKay G., (1998), A comparison of chemisorption kinetic models applied to pollutant removal on various sorbents, *Process Safety and Environmental Protection*, **76**, 332-340.
- Hwang Y., Mines P.D., Jakobsen M.H., Andersen H.R., (2015), Simple colorimetric assay for dehalogenation reactivity of nanoscale zero-valent iron using 4-chlorophenol, *Applied Catalysis B: Environmental*, **166-167**, 18-24.
- Irani M., Roshanfekr Rad L., Pourahmad H., Haririan I., (2015), Optimization of the combined adsorption/photo-Fenton method for the simultaneous removal of phenol and paracetamol in a binary system, *Microporous and Mesoporous Materials*, **206**, 1-7.
- Istratie R., Stoia M., Pacurariu C., Locovei C., (2016), Single and simultaneous adsorption of methyl orange and phenol onto magnetic iron oxide/carbon Nanocomposites, *Arabian Journal of Chemistry*, In press, Doi.org/10.1016/j.arabjc.2015.12.012.
- Kim J.R., Huling S.G., Kan E., (2015), Effects of temperature on adsorption and oxidative degradation of bisphenol A in an acid-treated iron-amended granular activated carbon, *Chemical Engineering Journal*, **262**, 1260-1267.
- Lagergren S., Svenska B.K., (1898), Theory of the so-called adsorption solutes (in German), *Vetenskapsakademiens Handlingar*, **24**, 1-39.
- Langmuir I., (1916), The constitution and fundamental properties of solids and liquids, *Journal of the American Chemical Society*, **38**, 2221-2295.
- Lavand A.B., Malghe Y.S., (2015), Visible light photocatalytic degradation of 4-chlorophenol using C/ZnO/CdS nanocomposite, *Journal of Saudi Chemical Society*, **19**, 471-478.
- Liu J., Zhao Z., Shao P., Cui F., (2015), Activation of peroxymonosulfate with magnetic Fe₃O₄-MnO₂ core-shell nanocomposites for 4-chlorophenol degradation, *Chemical Engineering Journal*, **262**, 854-861.
- Liu Q.-S., Zheng T., Wang P., Jiang J.-P., Li N., (2010), Adsorption isotherm, kinetic and mechanism studies of some substituted phenols on activated carbon fibres, *Chemical Engineering Journal*, **157**, 348-356.
- Markovic M.D., Dojcinovic B.P., Obradovic B.M., Nešic J., Natic M.M., Tosti T.B., Kuraica M.M., Manojlovic D.D., (2015), Degradation and detoxification of the 4-chlorophenol by non-thermal plasma-influence of homogeneous catalysts, *Separation and Purification Technology*, **154**, 246-254.
- Martin del Campo E., Romero R., Roa G., Peralta-Reyes E., Espino-Valencia J., Natividad R., (2014), Photo-Fenton oxidation of phenolic compounds catalyzed by iron-PILC, *Fuel*, **138**, 149-155.
- Messele S.A., Soares O.S.G.P., Órfão J.J.M., Bengoa C., Stüber F., Fortuny A., Fabregat A., Font J., (2015), Effect of activated carbon surface chemistry on the activity of ZVI/AC catalysts for Fenton-like oxidation of phenol, *Catalysis Today*, **240**, 73-79.
- Mohd Din A.T., Hameed B.H., Ahmad A.L., (2009), Batch adsorption of phenol onto physiochemical-activated coconut shell, *Journal of Hazardous Materials*, **161**, 1522-1529.
- Nguyen A.T., Juang R.-S., (2015), Photocatalytic degradation of p-chlorophenol by hybrid H₂O₂ and TiO₂ in aqueous suspensions under UV irradiation, *Journal of Environmental Management*, **147**, 271-277.
- Nourmoradi H., Avazpour M., Ghasemian N., Heidari M., Moradnejadi K., Khodarahmi F., Javaheri M., Moghadam F.M., (2015), Surfactant modified montmorillonite as a low cost adsorbent for 4-chlorophenol: Equilibrium, kinetic and thermodynamic study, *Journal of the Taiwan Institute of Chemical Engineers*, **59**, 244-251.
- Saharan V.K., Pinjari D.V., Gogate P.R., Pandit A.B., (2014), *Advanced Oxidation Technologies for Wastewater Treatment: An Overview*, In: *Industrial Wastewater Treatment, Recycling and Reuse*, Ranade V.V., Bhandari V.M. (Eds.), Elsevier, 141-191.
- Wang M., Fang G., Liua P., Zhou D., Ma C., Zhang D., Zhan J., (2016), Fe₃O₄@β-CD nanocomposite as heterogeneous Fenton-like catalyst for enhanced degradation of 4-chlorophenol (4-CP), *Applied Catalysis B: Environmental*, **188**, 113-122.
- Wang N., Zheng T., Zhang G., Wang P., (2016), A review on Fenton-like processes for organic wastewater treatment, *Journal of Environmental Chemical Engineering*, **4**, 762-787.
- Weber W.J., Morris J.C., (1963), Kinetics of adsorption on carbon from solution, *Journal of the Sanitary Engineering Division*, **89**, 31-59.
- Xu J.-H., Gao N.-Y., Deng Y., Xia S.-Q., (2013), Nanoscale iron hydroxide-doped granular activated carbon (Fe-GAC) as a sorbent for perchlorate in water, *Chemical Engineering Journal*, **222**, 520-526.
- Yao Y., Wang L., Sun L., Zhu S., Huang Z., Mao Y., Lu W., Chen W., (2013), Efficient removal of dyes using heterogeneous Fenton catalysts based on activated carbon fibers with enhanced activity, *Chemical Engineering Science*, **101**, 424-431.



“Gheorghe Asachi” Technical University of Iasi, Romania



EVALUATION OF PHENOLIC COMPOUNDS CONTENT IN GRAPE SEEDS

Valeriu V. Cotea², Camelia Luchian^{1*}, Marius Niculau², Cătălin Ioan Zamfir²,
Ioan Moraru¹, Bogdan Constantin Nechita², Cintia Colibaba¹

¹The University of Agricultural Sciences and Veterinary Medicine "Ion Ionescu de la Brad", Faculty of Horticulture, 3 Mihail Sadoveanu Alley, 700490 Iasi, Romania

²Research Centre for Oenology - Romanian Academy - Iasi Branch, 9 Mihail Sadoveanu Alley, 700505 Romania

Abstract

There is an increasing interest in the food industry and in protective health care for the expansion of natural antioxidants from plant materials. The solid wastes generated by the winemaking industry represent about 30% of the material used and it consists mainly of grape pomace (containing seeds, pulp, stem and skin). It is well known that high quantities of valuable compounds like dietary fibre, oils from the seeds, anthocyanins and phenolic compounds still remain within the grape marc. The phenolic compounds have great potential due to their antioxidant capacity and health benefits to prevent coronary problems and other chronic diseases: cancer, diabetes or neurodegenerative issues. Based on this evidence the evaluation of the polyphenols concentration of grape pomace, a by-product of winemaking, might be of great importance. The aim of this work was to determine by using a HPLC method, the amounts of phenolic compounds in six experimental and unconventional aqueous and ethanolic extracts, from grape marc and its components, and to evaluate the ability to obtain extracts for pharmaceutical uses. The results showed that all the grape marc extracts showed remarkable amounts of polyphenols and that supercritical fluid extraction method was the most efficient.

Key words: antioxidants, extraction methods, grape pomace, phenolic compounds

Received: May, 2017; *Revised final:* January, 2018; *Accepted:* March, 2018; *Published in final edited form:* April 2018

1. Introduction

Grapes are among the most cultivated fruits around the world, therefore the composition and properties have been extensively investigated, with significant results that confirm the presence of large amounts of phenolic compounds with beneficial effects on consumer health. Most of the phenolic compounds found in wine are able to act as antioxidants. In addition, the wine industry by-products are also characterized by a high content of phenolic compounds due to their incomplete extraction during winemaking (Ky et al., 2014; Maier et al., 2009; Teixeira et al., 2014). Solid waste originated from the wine industry represents 25% -

30% of raw matter used and consists mainly of grape pomace (containing seeds, pulp, stem and skin) (Dwyer et al., 2014). These by-products constitute a cheap source for the extraction of compounds with antioxidant effect, which can have a significant benefit for the pharmaceutical industry and the overall economy (González-Centeno et al., 2013).

The amount of soluble phenolic compounds found in grapes is unevenly distributed, as follows: 60-70% of total soluble phenolic compounds are present in seeds, 28-35% in skins and the rest of about 10% are found in pulp. The grape skins are rich in flavonols; the proanthocyanidins and the flavan-3-ols are the most predominant phenolics in grape seeds (Godevac et al., 2010). Also, red grape skins are

* Author to whom all correspondence should be addressed: e-mail: kamelia_luchian@yahoo.com; Phone: 0232407519

characterized by a high amount of anthocyanins, which is greatly influenced by the plant variety and other factors like *terroir* or viticultural practice (Rodríguez-Montealegre et al., 2006). Grape seeds, as other authors have previously reported, have the following general composition, expressed in g constituent/g seeds: 40% fiber, 16% volatile oil, 11% protein, 7% phenolic compounds and other substances (sugars, minerals etc.) (Campos et al., 2008).

The main scope of this study was to determine and quantify the amount of phenolic compounds found in six experimental aqueous and ethanolic extracts; these were obtained from grape seeds and their composition was analysed using a HPLC method, in order to evaluate the possibility of obtaining extracts with bioactive properties for pharmaceutical uses.

One of the methods used, the supercritical fluid extraction (SFE), is a well-known technique applied in the separation of bioactive compounds found in fruits and other plants. This method is valued because it uses a very high solvent power and, also, for the distinctive physicochemical properties of supercritical fluids. Due to relatively low viscosity and the high diffusivity of the fluids, these can be easily inserted into solid materials more efficiently than other liquid solvents, thus reducing the overall analysis time and increasing the method's efficiency (Qingyong and Wai, 2001).

Previous published work has shown that SFE technique is highly selective for phenolic compounds, such as gallic acid, epicatechin, catechin and quercetin, thus high amounts of polyphenols from grape marc were retained. This method cannot be applied for the extraction of polyphenols with larger molecule, such as proanthocyanidins (Massias et al., 2015; Pinelo et al., 2007). Therefore, the aim of this study is to investigate, using a chromatographic method, the phenolic content of the obtained extracts by different methods and to correlate the results with the possibility of using them for pharmaceutical purposes.

2. Material and methods

2.1. Extract preparation

Plant material used in the experiments is Fetească neagră grape seeds from 2014 harvest at 195 g/L total sugars from the Iași region Adamachi vineyard.

After 5 days of controlled maceration-fermentation at 18°C the seeds were collected from the bottom of the fermentation tank. Immediately afterwards using type 1 water (with resistivity 18.2 MΩ×cm) the seeds were washed by hand three times. The wet seeds were dried overnight at room temperature. The next day using an Ika M20 universal mill the dry material was ground at less than 500 μm particles (the product was sieved with Bolin stainless steel wire mesh sieve). The powder material was dried out for 60 minutes in a vacuum oven (JP Selecta Vaciotem-T) at 50 °C and 100 mbar. The material was

cooled and stored in a vacuum dessicator until extractions were performed.

Lipids were removed in five steps with 100 mL ethyl ether each time at room temperature using a magnetic stirrer Falc F30 at 300 rpm. For phenolic compounds analysis, a 5 g powdered material was introduced in a 250 mL Soxhlet apparatus. Extraction was carried out continuously with 130 mL of 96% ethanol at 80°C using a Falc F60 heating block.

2.2. Supercritical fluid carbon dioxide extraction (SFE)

In the case of supercritical extraction (SFE), the equipment used is manufactured by Jasco (Japan). The device has a 10 mL extraction cell (EV-2) for solid samples in a CO-2060 extraction oven. The chemical modifier is added in the mixing chamber with a PU-2089 quaternary gradient pump with a build-in degasser and is combined with the flow of CO₂ liquid from a PU-2080-CO₂ pump with cooled piston heads. The system is pressurised at 10 MPa by the back pressure regulator BP-2080 in order to maintain the liquid state in the system. All the modules are coordinated by a LC-NetII/ADC unit which can manage physical parameters of the system (Colibaba et al., 2015). Five extractions were performed from 5 g of plant material (*Fetească neagră* grape seeds from 2014 harvest) each time, using liquid CO₂ at a rate of 1 mL/min and ethanol at a rate of 0.5 mL/min. The extraction lasted 60 min. each time and, in the end, 142 mL of liquid were collected.

2.3. Subcritical water extraction (SWE)

Subcritical water extraction was made at 3 bar (SWE 3 bar) and 15 bar (SWE 15 bar) using two commercial espresso machines. Two samples were made by using water and a 75% ethanol solution for each two pressure equipment's (SWE 15 bar 75% EtOH and also SWE 3 bar 75% EtOH). The amount of 7 g of grounded material was used in extractions and the collected volume of 200 mL was obtained at the end of each extraction.

All the extracts were concentrated to dryness using a rotary evaporator (Heidolph Laborota 4003) at 40 mbar, constant 40°C bath temperature and a rotational speed of 80 rpm. During the distillation, the system was stopped in order to remove the different solvents whenever the process is not progressing.

All extraction was done in triplicate so it can evaluate the influence of the methodology upon the complexity of bio-organic phenolic compounds.

2.4. Phenolic compounds analysis

The flask was washed five times with 2 mL of water. The samples were filtered through 0.45 μm nylon 25 mm syringe filters prior to LC analysis in order to remove colloids. The LC analysis was performed using a monolithic column (Castellari et al., 2002). For the analysis of phenolic acids, samples

were processed on a Shimadzu HPLC (LC-DAD) consisting of: quaternary pump Shimadzu Prominence series LC-20AD with five-channel degasser DGU-20A5 Shimadzu Prominence series, autoinjector SIL-20AC Shimadzu Prominence series (injection volume: 10 μ L, sample temperature 20°C), column oven CTO-20AC Shimadzu Prominence series, diode array detector SPD-M20A Shimadzu Prominence series (200-440 nm), fluorescence detector (Shimadzu FLD RF-10Ax1) in order to achieve a double spectral certification for substances, chromatographic system controller CBM-20A Shimadzu Prominence series PC connectivity via LAN.

The gradient was optimized using trifluoroacetic acid (TFA) as an eluent for 1% methanol MeOH (A channel) and 50% MeOH (B channel). The column system is composed of a pre-column Chromolith Guard Cartridge 5 \times 4.6 mm and two Chromolith Performance RP-18 endcapped 100 \times 4.6 mm columns manufactured by Merck.

Phenolic compounds were characterized by their UV spectra which were recorded at 256, 280, 324, and 365nm. The different chemical compounds were identified according to their order of elution and retention times of pure standard compounds.

The chromatogram represented in Fig. 2 it was plotted after HPLC system calibration using the method published by Castellari (Castellari et al., 2002), in order to analyze the obtained samples.

2.5. Statistical analyses

Statistical analyses were performed using Statgraphics Centurion XVI[®] software, (StatPoint

Technologies, Inc, U.S.A.). In this study, we applied a one-way ANOVA procedure that was designed to construct a statistical model describing the impact of one categorical factors X_j (different variants of extraction method) on a dependent variable Y (some phenolic compounds from Fetească neagră grape seeds). The statistic displayed Fisher's LSD (Least Significant Difference) it is the way that we can select a single pair of samples and declare their means to be significantly different. While the chance of incorrectly declaring two samples to be different with this method is fixed at 5%, making comparisons amongst many pairs of means may result in an error on at least one pair with a considerably higher probability (Zamfir et al., 2014).

3. Results and discussion

The first set of phenolic acids that have eluted for the LC analysis, usually are benzoic acids and in the Fig. 2 the results were presented for a group of compounds with medium concentration. Vanillic acid is well known for its "sweet mouthfeel" characteristics and has a very high extraction rate in polar type environments like alcohols. By comparing with static Soxhlet extraction, in the case of SFE method, the amount extracted was doubled and, by applying high pressure, an improvement in the extraction process can be observed.

CO₂ exerts a small influence on *p*-hydroxybenzoic acids, mainly due to the solubility of these compounds in lipid-like substances (logP=1.58) and also, these acids are marginally influenced by the techniques applied.

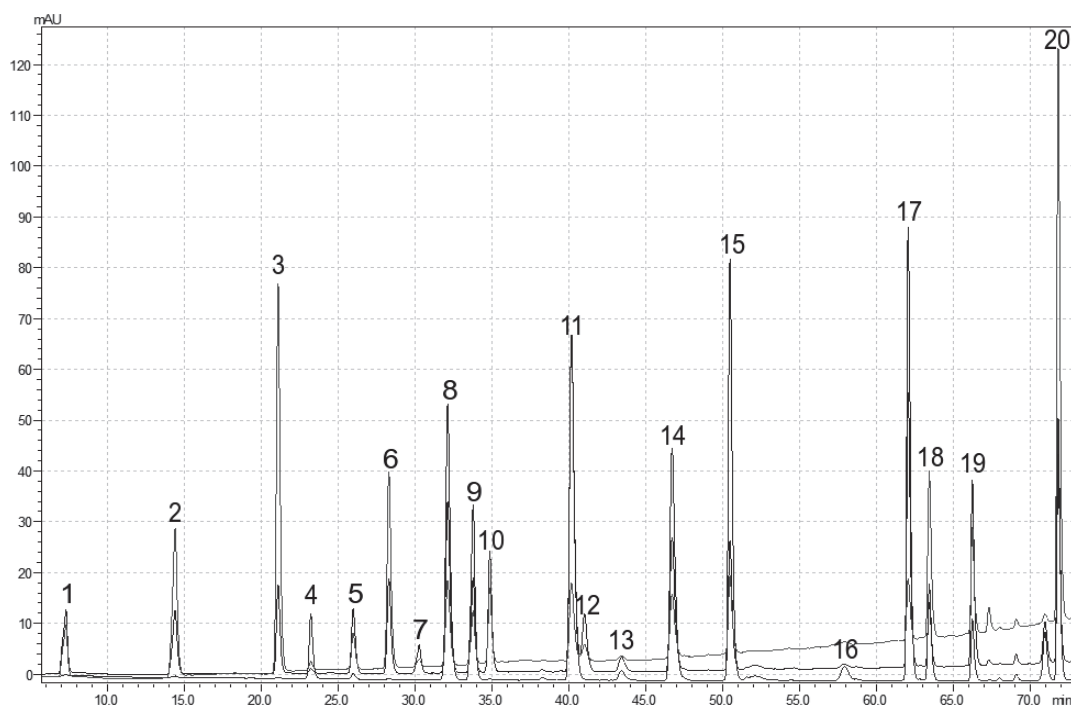


Fig. 1. Chromatogram of standards separated by LC-DAD (1 – gallic acid; 2 – protocatechuic acid; 3 – *p*-hydroxybenzoic acid; 4 – gentisic acid; 5 – catechin; 6 – *m*-hydroxybenzoic acid; 7 – vanillic acid; 8 – caffeic acid; 9 – chlorogenic acid; 10 – syringic acid; 11 – epicatechin; 12 – *p*-coumaric acid; 13 – ferulic acid; 14 – salicylic acid; 15 – sinapinic acid; 16 – ellagic acid; 17 – trans-resveratrol; 18 – rutin; 19 – cis-resveratrol; 20 – quercetin)

The amount of syringic acid, a minor compound, is not influenced by the experimental protocol, because its concentration in wines is usually below 30 mg/L.

Salicylic acid is considered to have great value in the pharmaceutical applied field as a painkiller and it was found in high concentrations in berry like fruits, including grapes. The increased pressure effect from the force applied in the experiment and also some solvent interactions double the efficiency (2.06 logP), but marginally due to the techniques applied at normal atmospheric pressure.

The second most important benzoic acid concerning its concentration in wine, the protocatechuic acid (5-100 mg/L), is highly soluble in water, ethanol and also ether. It was adequately extracted by adding some ethanol to the water and also by SFE method, as shown in Fig. 3. In the case of the SFE method, a rather low concentration of *m*-hydroxybenzoic acid can be observed, when using an ethanol solution at low pressure, although other proposed techniques did not extract *m*-hydroxybenzoic acid. This was possibly due to the fact that some other substances might have been transformed into this compound during the extraction process.

According to Yilmaz and Toledo, the gallic acid has the highest concentration among all benzoic acids (around 15-100 mg/g dry matter) (Yilmaz and Toledo, 2004) and it is considered to be a “backbone” for tannins (as monomeric structure) in the majority of the Romanian grape varieties’ seeds. The results show a great improvement in all extraction techniques in

comparison with the classical Soxhlet solvent reflux method. The solvent and the pressure applied are important to overall process yield, therefore, and by combining the two factors, the entire extraction process can be improved.

The lack of influence on ellagic acid content, which has the same concentration for all tested extraction protocols, is presented in Table 1. A small amount of catechin was detected in the extract obtained by using supercritical carbon dioxide, but epicatechin was not present. These monomeric procyanidins are found in large amounts in grape seeds, but their low water solubility explains the small extracted quantity. In the cases of Soxhlet, SFE and ethanol assisted extraction methods, one can expect to obtain higher concentrations (Nechita et al., 2015). *Trans*-resveratrol, has been extracted using the SFE method and also with subcritical water, in the presence of ethanol at both high and low pressure. This molecule have certified biological activity and increasing interest in the pharmaceutical industry.

B1 and B2 procyanidins are dimeric tannins that have been extracted using all proposed methods, except the classical Soxhlet method (Fig. 4). As in wines, the amounts of sinapic acid found in grape seed extracts has low values because it is transformed into hydroxycinnamic acids, like ferulic acid, which has a good solubility and extractability in aquatic medium. The largest quantity of ferulic acid is present in the sample obtained using the SFE method, but also in the ones obtained under high pressure by using water and ethanol; these methods showed a higher extractability than the Soxhlet technique.

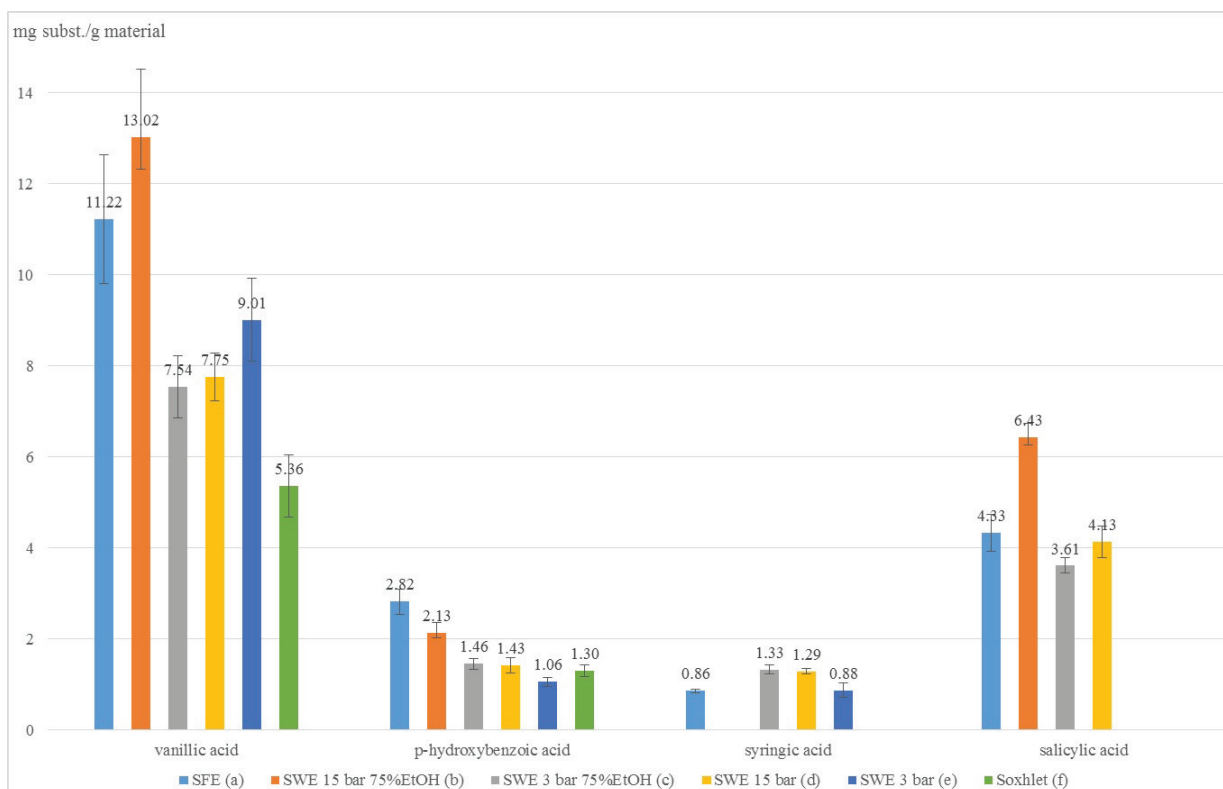


Fig. 2. Effect of separation techniques upon some minor benzoic acids

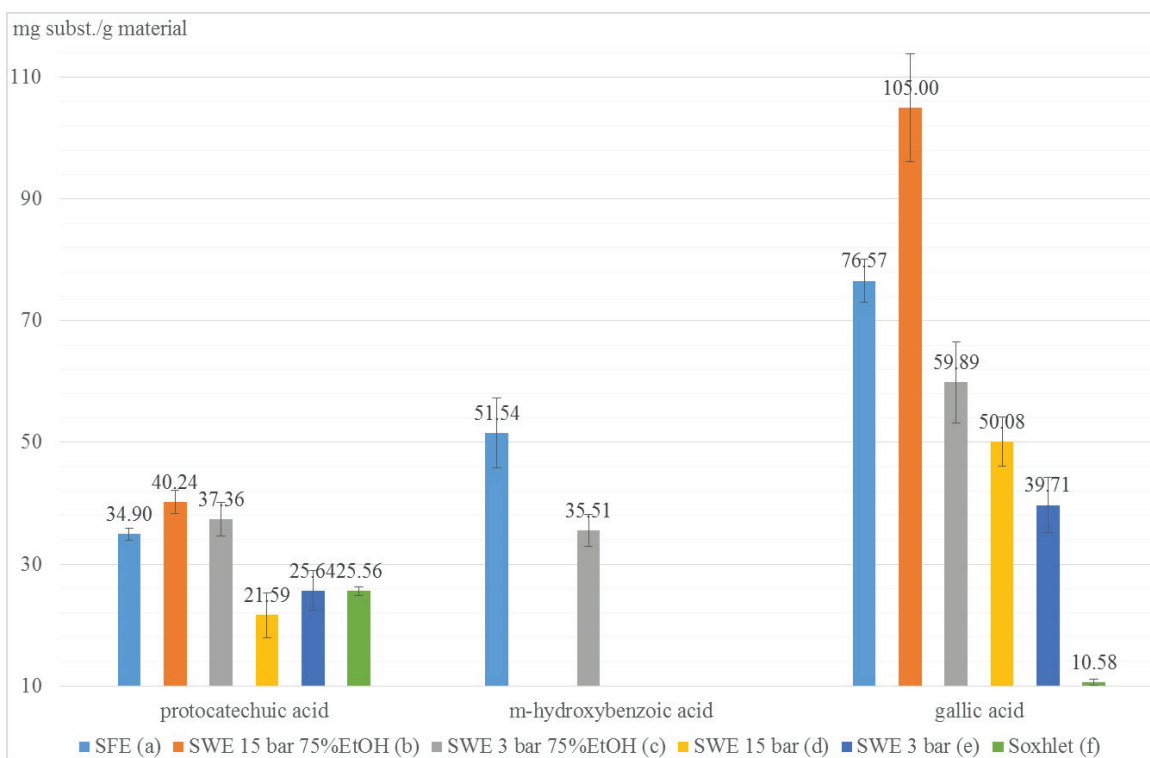


Fig. 3. Effect of separation techniques upon some major benzoic acids

Table 1. Other minor phenolic compounds extracted

mg substance / g grape seed	SFE(a)		SWE 15 bar 75%EtOH (b)		SWE 3 bar 75%EtOH (c)		SWE 15 bar (d)		SWE 3 bar (e)		Soxhlet (f)	
	mg/g	±SD	mg/g	±SD	mg/g	±SD	mg/g	±SD	mg/g	±SD	mg/g	±SD
ellagic acid	0.19	0.01	0.18	0.01	0.18	0.02	0.16	0.02	nd	nd	0.12	0.01
catechin	0.82	0.14	nd	nd	nd	nd	nd	nd	nd	nd	nd	nd
trans-resveratrol	4.99	0.23	4.37	0.44	4.1	0.35	3.94	0.50	nd	nd	nd	nd

*nd - not detected

The results obtained from the statistical analysis are presented in Table 2. These information present the estimated difference between each pair of means. A superscript letter has been placed next to the means pairs, indicating that these pairs show statistically significant differences at the 95.0% confidence level. We used Fisher's least significant difference (LSD) procedure for discriminate among the means that represent different kind of extraction method of these compounds. With this method, there is a 5.0% risk of calling each pair of means significantly different when the actual difference equals 0. In Table 3 are displayed the samples arranged into homogeneous groups, shown as columns of X's. A homogeneous group is a group within which there are no significant differences. For understanding in the protocatechuic acid case, sample comes from SFE method is in a group with samples from SWE 3 bar 75%EtOH method. Samples from SWE 15 bar 75%EtOH method are in a group with samples from

SWE 3 bar 75%EtOH method that is mean need more data to distinguish which group sample SWE 3 bar 75%EtOH actually belongs to.

For protocatechuic acid, m-hydroxybenzoic acid, vanillic acid, syringic acid and trans-resveratrol, 3 homogenous groups are identified. Within each column, the levels containing X or Y's form a group of means within which there are no statistically significant differences, which means that the extraction methods can provide similar results.

It can be observed that the SFE method has generated the highest values in eight of of the studied compounds. In the case of vanillic acid, ellagic acid and ferrulic acid, homogenous groups were formed, from a statistic point of view, for a significance level of 95%. The method SWE 15 bar 75%tOH generated the highest values in the case of five compounds. protocathechuic acid, vanillic acid and ellagic acid generate homogenous groups from a statistical point of view.

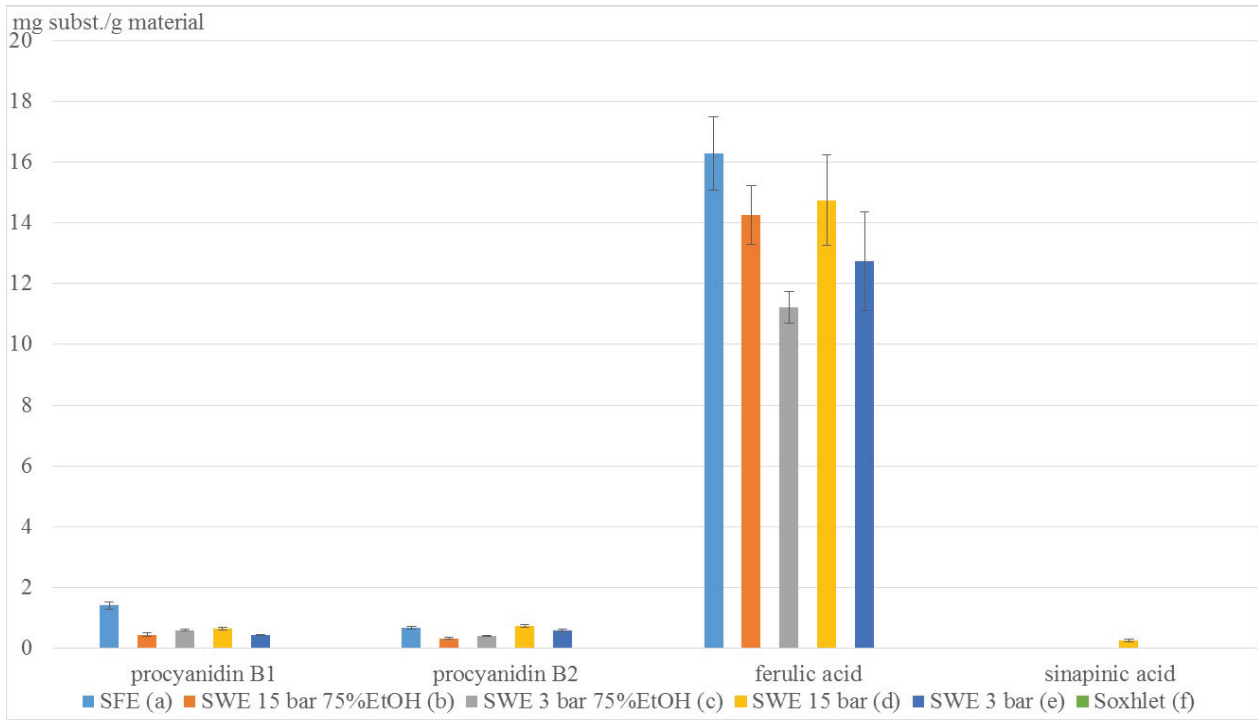


Fig. 4. Effect of separation techniques upon some other phenolic compounds identified

Table 2. The mean values and standard deviations of the analysed phenolic compound and the significant statistical differences

Extraction Method	SFE (a)	SWE 15 bar 75%EtOH (b)	SWE 3 bar 75%EtOH (c)	SWE 15 bar (d)	SWE 3 bar (e)	Soxhlet (f)
protocatechuic acid	34.90 ± 0.97 _{b,d,e,f}	40.24 ± 1.91 _{a,d,e,f}	37.36 ± 2.77 _{d,e,f}	21.59 ± 3.72 _{a,b,c}	25.63 ± 3.25 _{a,b,c}	25.56 ± 0.71 _{a,b,c}
<i>m</i> -hydroxybenzoic acid	51.54 ± 5.71 ^c	nd	35.50 ± 2.63 ^a	nd	nd	nd
gallic acid	76.57 ± 3.58 _{b,c,d,e,f}	105 ± 8.91 _{a,c,d,e,f}	59.88 ± 6.63 _{a,b,d,e,f}	50.07 ± 4.04 _{a,b,c,e,f}	39.70 ± 4.56 _{a,b,c,d,f}	10.58 ± 0.49 _{a,b,c,d,e}
vanillic acid	11.22 ± 1.42 _{c,d,e,f}	13.02 ± 1.49 _{c,d,e,f}	7.53 ± 0.69 _{a,b,f}	7.75 ± 0.52 _{a,b,f}	9.00 ± 0.90 _{a,b,f}	5.36 ± 0.68 _{a,b,c,d,e}
<i>p</i> -hydroxybenzoic acid	2.82 ± 0.28 _{b,c,d,e,f}	2.13 ± 0.23 _{a,c,e,f}	1.45 ± 0.11 _{a,b,e}	1.42 ± 0.16 _{a,b,e}	1.06 ± 0.09 _{a,b,c,d}	1.30 ± 0.13 _{a,b}
syringic acid	0.86 ± 0.04 _{c,d}	nd	1.33 ± 0.09 _{a,e}	1.29 ± 0.06 _{a,e}	0.87 ± 0.15 _{c,d}	nd
salicylic acid	4.33 ± 0.40 _{b,c}	6.42 ± 0.30 _{a,c,d}	3.60 ± 0.16 _{a,b,d}	4.13 ± 0.35 _{b,c}	nd	nd
<i>trans</i> -resveratrol	4.99 ± 0.23 _{b,c,d}	4.37 ± 0.44 ^a	4.10 ± 0.34 ^a	3.94 ± 0.50 ^a	nd	nd
ellagic acid	0.19 ± 0.01 _{d,f}	0.18 ± 0.01 _{d,f}	0.17 ± 0.02 _{d,f}	0.15 ± 0.02 _{a,b,c,f}	nd	0.12 ± 0.01 _{a,b,c,d}
catechin	0.82 ± 0.14 _{b,c,d,e,f}	nd	nd	nd	nd	nd
procyanidin B1	1.41 ± 0.12 _{b,c,d,e}	0.44 ± 0.05 _{a,c,d}	0.59 ± 0.02 _{a,b,e}	0.64 ± 0.04 _{a,b,e}	0.42 ± 0.02 _{a,c,d}	nd
Procyanidin B2	0.67 ± 0.05 _{b,c,d,e}	0.31 ± 0.02 _{a,c,d,e}	0.39 ± 0.01 _{a,b,d,e}	0.73 ± 0.03 _{a,b,c,e}	0.58 ± 0.04 _{a,b,c,d}	nd
Ferulic Acid	16.29 ± 1.21 _{b,c,e}	14.26 ± 0.96 _{a,c}	11.21 ± 0.52 _{a,b,d}	14.74 ± 1.48 _{c,e}	12.73 ± 1.61 _{a,d}	nd
Sinapinic Acid	nd	nd	nd	0.25 ± 0.04 _{a,b,c,e,f}	nd	nd

The superscript letter (^{a,b,c,d,e,f}) indicates that these pairs show statistically significant differences at the 95.0% confidence level between each pair of means

Table 3. Distribution of samples obtained from different kind of extraction methods on statistically homogeneous groups

Extraction method	SFE	SWE 15 bar 75%EtOH	SWE 3 bar 75%EtOH	SWE 15 bar	SWE 3 bar	Soxhlet
protocatechuic acid	X	Y	XY	X	X	X
m-hydroxy benzoic acid	Y	X	X	X	X	X
gallic acid	X	Y	X	X	X	X
vanillic acid	Y	Y	X	X	X	X
p-hydroxybenzoic acid	Y	X	X	X	X	XX
syringic acid	X	X	Y	Y	X	X
salicylic acid	X	Y	X	X	X	X
trans-resveratrol	Y	X	X	X	X	X
ellagic acid	Y	Y	Y	X	X	X
catechin	Y	X	X	X	X	X
procyanidin B1	Y	X	X	X	X	X
procyanidin B2	X	X	X	Y	X	X
ferulic acid	Y	XX	X	XY	XX	X
sinapinic acid	X	X	X	Y	X	X

Y - homogeneous means groups that exhibit the highest extraction values
X - homogeneous means groups exhibiting lower extraction values

4. Conclusions

By using a HPLC method to obtain the polyphenolic profile of grape seed extracts, can be concluded that the recommended extraction technique, which employs supercritical fluids (SFE), is an alternative for the classical Soxhlet procedure.

A superior extraction of the phenolic acids, non-hydrolysed tannins, stilbenes and flavones, can be obtained by using ethanol solutions as solvents. These extracts can be converted into different physiological formulations, thus making it possible to be used in the pharmaceutical field.

Acknowledgments

This research was carried out by the Partnership in priority areas - PN II, developed with the support of MEN - UEFISCDI, project no. 183/2014 (PN-II-PT-PCCA-2013-4-0333) "Technology of capitalization of the bioactive elements from the grape seed waste with usefulness in the food and pharmaceutical industry, plant and environmental protection" (Acronym: PROVITIS).

References

- Campos L.M.A.S., Leimann F.V., Pedrosa R.C., Ferreira S.R.S., (2008), Free radical scavenging of grape pomace extracts from Cabernet Sauvignon (*Vitis vinifera*), *Bioresource Technology*, **99**, 8413-84.
- Castellari M., Sartini E., Fabiani A., Arfelli G., Amati A., (2002), Analysis of wine phenolics by high-performance liquid chromatography using a monolithic type column, *Journal of Chromatography A*, **973**, 221-227.
- Colibaba L.C., Cotea V.V., Rotaru L., Nechita B., Niculaua M., Tudose-Sandu-Ville S., Luchian C., (2015), Volatiles in *Tămâioasă Românească* via supercritical fluid extraction (SFE) analysis, *Environmental Engineering and Management Journal*, **14**, 297-302.
- Dwyer K., Hosseinian F., Rod M., (2014), The market potential of grape waste alternatives, *Journal of Food Research*, **3**, 91-106.
- Godevac D., Těsević V., Veličković M., Vujisić Lj., Vajs V., Milosavljević S., (2010), Polyphenolic compounds in seeds from some grape cultivars grown in Serbia, *Journal of the Serbian Chemical Society*, **75**, 1641-1652.
- González-Centeno M.R., Jourdes M., Femenia A., Simal S., Rosselló C., Teissedre P.L., (2013), Characterization of polyphenols and antioxidant potential of white grape pomace by-products (*Vitis vinifera* L.), *Journal of Agricultural and Food Chemistry*, **61**, 11579-11587.
- Ky I., Lorrain B., Kolbas N., Crozier A., Teissedre P.L., (2014), Wine by-products: Phenolic characterization and antioxidant activity evaluation of grapes and grape pomaces from six different French grape varieties, *Molecules*, **19**, 482-506.
- Maier T., Schieber A., Kammerer D.R., Carle R., (2009), Residues of grape (*Vitis vinifera* L.) seed oil production as a valuable source of phenolic antioxidants, *Food Chemistry*, **112**, 551-559.
- Massias A., Boisard S., Baccaudaud M., Leal Calderon F., Subra-Paternault P., (2015), Recovery of phenolics from apple peels using CO₂ ethanol extraction: kinetics and antioxidant activity of extracts, *The Journal of Supercritical Fluids*, **98**, 172-182.
- Nechita B.C., Niculaua M., Cotea V.V., (2015), Assessment and adaptation of methods of extraction of grape seed polyphenol compounds, *Scientific Papers Journal, Horticulture Series*, **58**, 195-200.
- Pinelo M., Ruiz-Rodríguez A., Sineiro J., Señorans F.J., Reglero G., Núñez M.J., (2007), Supercritical fluid and solid-liquid extraction of phenolic antioxidants from grape pomace: A comparative study, *European Food Research and Technology*, **226**, 199-205.
- Qingyong L., Wai C.M., (2001), Supercritical fluid extraction in herbal and natural product studies- A practical review, *Talanta*, **53**, 771-782.
- Rodríguez-Montealegre R., Romero-Peces R., Chacón-Vozmediano J.L., Martínez-Gascuña J., García-Romero E., (2006), Phenolic compounds in skins and seeds of ten grape *Vitis vinifera* varieties grown in a warm climate, *Journal of Food Composition and Analysis*, **19**, 687-693.

- Teixeira A., Baenas N., Dominguez-Perles R., Barros A., Rosa E., Moreno D.A., Garcia-Viguera C., (2014), Natural bioactive compounds from winery by-products as health promoters: A Review, *International Journal of Molecular Sciences*, **15**, 15638-15678.
- Yilmaz Y., Toledo R.T., (2004), Major flavonoids in grape seeds and skins: antioxidant capacity of catechol, epicatechin and gallic acid, *Journal of Agricultural and food Chemistry*, **52**, 255-260.
- Zamfir C.I., Cotea V.V., Luchian C.E., Nicolaua M., Odăgeriu G., (2014), The influence of different prefermentative maceration processes and tartaric stabilization treatments on the color, cation content and other physico-chemical parameters of 'Băbească neagră' rosé wines, *Vitis*, **53**, 45-52.



“Gheorghe Asachi” Technical University of Iasi, Romania



EFFECT OF METAL TOLERANT PLANT GROWTH PROMOTING RHIZOBACTERIA ON BEAN GROWTH, CADMIUM AND ZINC UPTAKE AND STRESS RESPONSES

Éva Boglárka Vincze¹, Rozália Veronika Salamon², Erika Kovács¹, Gyöngyvér Mara^{1*}

¹Sapientia Hungarian University of Transylvania, Faculty of Economics, Socio-Human Sciences and Engineering, Department of Bioengineering, Miercurea Ciuc, RO-530104 Libertății sq., No.1, Romania

²Sapientia Hungarian University of Transylvania, Faculty of Economics, Socio-Human Sciences and Engineering, Department of Food Science, Miercurea Ciuc, RO-530104 Libertății sq., no. 1, Romania

Abstract

Plant growth promoting rhizobacteria (PGPR) serve as an alternative tool in sustainable agriculture. PGPR influence the heavy metal accumulation of crops in contaminated soils, either by decreasing or increasing the accumulation. This study focuses on the effect of plant growth-promoting rhizobacteria on the heavy metal uptake, plant growth and stress response of bean plants. The simultaneous treatment of Cd²⁺ and *Mitsuaria chitosanitabida* T₃10⁻²/4 (PGPR strain) as well as Zn²⁺ and bacteria resulted in the inhibition of root elongation in bean plants, but no differences were recorded in root biomass. A higher accumulation of the phytotoxic Cd²⁺ in the root compared to the shoot was observed in bean plants due to the limited translocation (varying between 7.95-23%). In the case of Zn²⁺ treatment the translocation from root to shoot was not limited. In the case of Cd²⁺ treatment the *Mitsuaria chitosanitabida* T₃10⁻²/4 decreased the accumulation of Cd²⁺ in bean plants. Differences in polyphenol oxidase (POD) and peroxidase activity (GPOX) were observed among metal stressed and control plants. *Mitsuaria chitosanitabida* T₃10⁻²/4 strain diminished the oxidative stress in the case of toxic metal (Cd²⁺) treated bean plants most probably due to the inhibited metal uptake.

Key words: antioxidant enzymes, bean, heavy metal, plant growth promoting rhizobacteria, *Mitsuaria chitosanitabida*

Received: May, 2017; Revised final: January, 2018; Accepted: March, 2018; Published in final edited form: April 2018

1. Introduction

The heavy metal pollution of the soil is a major environmental problem due to the rapid development of the industry. Heavy metals are non-biodegradable and persist prolonged in environment, affecting the soil microbial composition (Khan et al., 2009). Plants are sensitive to essential heavy metal deficiency (Cu, Zn, Fe, Mn, Mo, Ni, Co), and to excess of non-essential heavy metals (Cd, As, Hg, Pb) (Nagajyoti et al., 2010). Due to the plant metal uptake and transport, heavy metals are accumulated and affect the yield of the crops (Khan et al., 2009), caused by the alteration

of metabolic processes, inhibited growth and injuries (chlorosis, browning) (Nagajyoti et al., 2010). Each plant has a different molecular mechanism to deal with the metal stress. The metal toxicity has three mechanisms: a). metals interacting directly with proteins due to their affinity for thioyl-, histidyl- and carboxyl-groups; b). metals modifying the antioxidant defense and generate oxidative stress, stimulating the production of reactive oxygen species (ROS); and c). metals displacing essential cations from specific binding sites inhibiting protein function (Sharma and Dietz, 2006). Plant responses to heavy metals are regulated biochemically by the homeostatic processes,

* Author to whom all correspondence should be addressed: e-mail: maragyongyver@cs.sapientia.ro; Phone: +40 266 314657; Fax: +40 266 372099

which include the regulation of the metal-induced reactive oxygen species (ROS) signaling pathway. ROS generation and signaling plays an important role in heavy metal detoxification and tolerance (Lin and Aarts, 2012).

Plant growth-promoting rhizobacteria (PGPR) are found in association with a large range of host plants. Plant growth-promoting (PGP) mechanisms can be categorized as 1). phytostimulating rhizobacteria, that enhance plant growth directly by providing nutrients and/or phytohormones; 2). mycorrhiza and root nodule symbiosis helper rhizobacteria; and 3). biocontrol rhizobacteria that protect plants from pathogens through the production of antimicrobial compounds, nutrient competence with the pathogen, or by stimulating plant resistance (Drogue et al., 2012). The PGPR in a heavy metal polluted environment need to deal with their toxic effect, evolving different mechanisms as: a). pumping the metal ions out of the cell; b.) accumulation and sequestration inside the cell; c). biosorption and metal transformation from a toxic to a less toxic metal (Khan et al., 2009). Due to the microbial effect, the plant bioavailability of trace elements can be either increased in the rhizosphere (Sessitsch et al., 2013) or decreased locally (Karthik et al., 2016). The bioavailability of heavy metals depends on their chemical properties, climate, soil conditions and its biological attributions (Miransari, 2011). Additionally, the plant associated bacteria, due to their effect on plant growth - increasing the root surface, length but also the number of root hairs - can influence the absorption, root-shoot translocation and complexation of trace elements (Sessitsch et al., 2013). The PGPR can also increase the metal accumulation due to the production of biosurfactants, siderophores and organic acids (Ullah et al., 2015). Some of the PGPR have mechanisms to diminish the heavy metal stress decreasing the metal concentration either in the soil or in the plant (Miransari, 2011). The PGPR bacteria can act as metal sink reducing the local concentration in soil by immobilization, chelation, exclusion, active removal, biosorption and bioaccumulation of heavy metal (Karthik et al., 2016). Some important genera of PGPR include *Serratia*, *Bacillus*, *Pseudomonas*, *Burkholderia*, *Enterobacter*, *Erwinia* and *Klebsiella* (Ullah et al., 2015). For example *Pseudomonas sp.* produced siderophores that form high solubility complexes and improved the metal uptake of plants (Ullah et al., 2015). *Pseudomonas putida* increased the Cd (Kamran et al., 2015), Ni (Kamran et al., 2016) and Cr uptake and enhanced the growth of *Eruca sativa* plants (Kamran et al., 2017). Other strains from *Bacillus* and *Serratia* genera were reported as biosorbents of Cd, Cu and Zn (Khan et al., 2009). *Ensifer adherens* bacterial strain isolated by Oves et al. (2017) from chickpea root surface showed accumulation and biosorption potential of Cd, Cr, Cu, Zn and Ni, whereas *Rhizobium sp.* strain obtained from root nodules of *Phaseolus vulgaris* was able of Cr removal (Karthik et al., 2017b). Other PGPR have the ability to decrease the

level of ethylene (stress hormone) in plants, due to the ACC deaminase (1-aminocyclopropane-1-carboxylate) production, that catalyzes the ACC (precursor of ethylene) transformation into ammonium and α -ketobutyric acid (Miransari, 2011; Ullah et al., 2015). Increased growth and plant protecting effect against heavy metal toxicity was reported in Pb and Zn resistant *Bacillus* strains on *Brassica juncea*, Cd resistant *Xanthomonas*, *Azomonas*, *Pseudomonas* and *Bacillus* strains on canola, and Cd resistant *Variovorax*, *Rhodococcus* and *Flavobacter* strains on Indian mustard (Khan et al., 2009).

The aim of our research was to select PGPR bacterial strains based on metal tolerance, and to determine the effect of a PGPR strain on bean heavy metal accumulation (Cd^{2+} , Zn^{2+}) and stress response. In the present research the plant growth (length, weight), heavy metal accumulation and the stress protein amount (GPOX, POD) were determined from plants treated with different heavy metal concentrations in the presence or lack of the PGPR strain *Mitsuaria chitosanitabida* $T_310^{-2}/4$ respectively.

2. Material and methods

2.1. PGPR strains

Three bacterial strains: *Serratia proteomaculans* ($T_110^{-2}/2$), *Serratia sp.* ($T_310^{-1}/2$) and *Mitsuaria chitosanitabida* ($T_310^{-2}/4$) were isolated from wild leguminous plant rhizosphere from Ciuc Mountains. *Serratia proteomaculans* ($T_110^{-2}/2$) showed the following PGP characteristics: nitrogen fixation, siderophore production, organic phosphate mobilization and indole acetic acid production. The *Serratia sp.* ($T_310^{-1}/2$) bacterial strain has PGP traits both as organic and inorganic phosphate mobilization, indole acetic acid production and nitrogen fixation. *Mitsuaria chitosanitabida* ($T_310^{-2}/4$) showed positive values for all five plant growth promoting characteristics listed above.

2.2. Heavy metal tolerance of PGPR

The ability of the strains to grow under increasing concentrations of Cd^{2+} and Zn^{2+} was tested using plate assay. Nutrient agar media (0.5% peptone, 0.3% yeast extract, 1.5% agar and 0.5% NaCl, pH adjusted to 7.4) was supplemented independently either with $\text{ZnSO}_4 \cdot 7\text{H}_2\text{O}$ salt from 0.5 mM to 25 mM or with $\text{CdSO}_4 \cdot 8\text{H}_2\text{O}$ salt from 0.5 mM to 6 mM. 10 μl bacterial suspension ($\text{OD}_{600}=0.3$) was inoculated on agar plates, and incubated at 28°C for 5 days. The experiments were carried out in triplicate. The inhibitory effect of the heavy metals was determined using colony diameter measurement. Agar plates without metals were used as controls (Sun et al., 2010).

2.3. Plant experiments

Based on the bacterial metal tolerance the *M. chitosanitabida* ($T_310^{-2}/4$) strain was selected for plant experiments.

Table 1. Controls and samples used in the experiments

<i>Controls</i>	<i>Mitsuaria chitosanitabida T₃10⁻²/4</i>	<i>Heavy metals</i>	<i>Heavy metal concentration (mM)</i>
K1	-	-	-
K2	+	-	-
K3	-	Cd ²⁺	0.1
K4	-	Cd ²⁺	0.5
K5	-	Zn ²⁺	0.5
K6	-	Zn ²⁺	3
Cd0.1	+	Cd ²⁺	0.1
Cd0.5	+	Cd ²⁺	0.5
Zn0.5	+	Zn ²⁺	0.5
Zn3	+	Zn ²⁺	3

Legend: (-) absence / (+) presence

The bean seeds (*Phaseolus vulgaris*) were surface disinfected, following the above described protocol. Seeds were soaked in 70% ethanol for 10 seconds followed by a 2% sodium hypochlorite treatment for 10 minutes, then rinsed in sterile distilled water five times. The seeds were germinated in dark, on wet filter paper in Petri dishes at 28°C for 7 days in Memmert Incubator.

The soil samples were treated with different concentrations of heavy metals and PGPR suspension (Table 1). Each seedling was inoculated with 1 mL of bacterial suspension (*M. chitosanitabida*, OD₆₀₀=1.5). In order to detect the effect of bacteria and heavy metals, 6 control samples were used (K1-K6, Table 1).

Eight equally developed bean seedlings were sown in plastic pots (top diameter 17.5 cm, bottom diameter 11.5 cm, height 13.5 cm) filled with approximately 1L sterilized soil (autoclaved for 30 min at 105°C), that contained macronutrients (mg L⁻¹) N, 50-400; available P₂O₅, 50-300; K₂O, 80-400; pH 5.5-6.5; salt content, 1-2 g KCl L⁻¹. The plants were grown under controlled conditions in a plant growth chamber (Sanyo MLR-351, Versatile Environmental Test Chamber), maintained at 22±1°C, 70% relative humidity with a 12/12h dark/light cycle 2500 lx illumination for 30 days. The pots were irrigated with 100 mL distilled water every second day. After 10, 20 and 30 days one whole plant from each treatment was removed for enzyme activity determination. At the end of the experiment plants were harvested, the soil was carefully removed from the roots and further analyzed for plant growth parameters, accumulation and enzyme activity.

2.4. Plant growth parameter measurements

Shoot and root length, fresh and dry weight were measured (n=5). The length of shoot and root of the treated plants were measured using a digital caliper whereas for the biomass measurement a technical scale (KERN EMB 200-2) was used. The obtained results were compared to controls. In order to determine the moisture content, the plants were dried 48 h at 105°C in a G-Therm 115 (F-lli Galli) thermostatic oven to constant weight. The tolerance

index (TI) was calculated for both shoot and root elongation and biomass using Eq. (1):

$$TI = V_m/V_c * 100 \quad (1)$$

where V_m is the measured value (shoot and root length or weight) in the presence of metal, and V_c is the measured value for the control (Wilkins, 1978).

2.5. Heavy metal accumulation

The concentrations of Cd²⁺ and Zn²⁺ were determined by atomic absorption spectrophotometry (AAS). Five replicates of each treatment were oven dried at 105°C to constant weight. Plant sample preparation was carried out using cremation in Gefran 1001 incinerator. The samples were placed in porcelain jars, followed by incineration. The temperature was gradually increased from 250°C with 100°C/h to 450°C and then was kept at 450°C for 4 h. The ash obtained was dissolved in 5 mL of 25% HNO₃ premixed solution and then filtered on filter paper. The volume was completed to 10 mL with distilled water.

The prepared samples were atomized in the atomic absorption spectrophotometer (Varian Spektra AA 110) and the absorbance values were read. In order to determine the concentration of the unknown solution, calibration curves were determined. Metal concentration in tissues will be expressed as µg g⁻¹ dry matter.

2.6. Antioxidant enzyme activity and protein content determination

An amount of 0.2 g of plant tissue (shoot), three repetition per treatment was measured in Eppendorf tubes, porcelain beads were added with 1 mL QB buffer (100 mM KPO₄ (pH 7.8), 1 mM EDTA, 1% Triton X-100, 10% glycerol, and 1 mM DTT added before use). The cells were disrupted in FastPrep-24 mill two times (30 seconds) with 5 m/s speed.

The samples were centrifuged at 4°C and 10000g for 30 min, and the supernatants were removed in new Eppendorf tubes and stored at -20°C until use. The amount of total protein was determined

based on the Bradford method using a BSA calibration curve (Elavarthi and Martin, 2010).

The activity of polyphenol oxidase (POD) was determined by adding 50 µL crude protein extract to 950 µL of a solution containing 0.2 mM phosphate buffer (pH 7.5) and 50 mM 3-methyl-catechol (substrate). The absorbance was measured every 30 seconds for 10 minutes at 400 nm until the end of reaction (Cheema and Sommerhalter, 2015).

The activity of guaiacol peroxidase (GPOX) was determined by adding 25 µL crude protein extract to 975 µL of a solution containing 0.2 mM phosphate buffer (pH 7.5), 20 mM H₂O₂ and 20 mM guaiacol. The absorbance was measured every minute for 5 minutes at 480 nm until the end of reaction. One enzymatic unit was defined as the change of 1.0 absorbance unit per mL enzymatic extract, and expressed as units of enzyme activity per g fresh matter (U/g) (Cavalcanti et al., 2004).

2.7. Statistical analysis

Microsoft Office Excel Worksheet 2007 and Past.exe 2.17c statistical program were used for statistical analysis. Analysis of variance (ANOVA) was used to compare datasets.

3. Results and discussion

3.1. Heavy metal tolerance of PGPR

The growth of the selected PGPR strains in the presence of heavy metals is presented in Table 2. The average diameter of bacterial colonies and the standard deviation values are listed only for the strains and concentrations where growth was observed. *Mitsuaria chitosanitabida* T₃10⁻²/4 and *S. proteomaculans* T₁10⁻²/2 strains were able to tolerate up to 1 mM Zn²⁺ and 0.5 mM Cd²⁺ concentrations, showing growth on agar medium. The growth of *Serratia sp.* T₅10⁻¹/2 bacterial strain was inhibited by the higher concentrations of both metals.

Based on our results the *M. chitosanitabida* T₃10⁻²/4 bacterial strain showing higher heavy metal tolerance was selected for further experiments.

3.2. Plant growth in the presence of heavy metals

The effect of different Cd²⁺ and Zn²⁺ concentration on plant growth was examined under controlled conditions. The length and weight of the root and shoot of bean plants were measured. Table 3 presents the obtained values and the standard deviations.

Table 2. Growth of PGPR colonies Nutrient agar media, supplemented with ZnSO₄*7H₂O and CdSO₄*8H₂O

Heavy metal	Concentration	Bacterial strain	The average diameter of the colonies (mm)
Zn ²⁺	0.5 mM	<i>Mitsuaria chitosanitabida</i> T ₃ 10 ⁻² /4	12.94 ± 2.49
		<i>Serratia sp.</i> T ₅ 10 ⁻¹ /2	9.86 ± 2.10
		<i>Serratia proteomaculans</i> T ₁ 10 ⁻² /2	10.97 ± 2.22
	1 mM	<i>Mitsuaria chitosanitabida</i> T ₃ 10 ⁻² /4	10.04 ± 0.59*
		<i>Serratia sp.</i> T ₅ 10 ⁻¹ /2	8.70 ± 0.64*
		<i>Serratia proteomaculans</i> T ₁ 10 ⁻² /2	9.67 ± 0.55*
	5 mM	<i>Mitsuaria chitosanitabida</i> T ₃ 10 ⁻² /4	6.45 ± 1.12*
		<i>Serratia sp.</i> T ₅ 10 ⁻¹ /2	0.00 ± 0.00
		<i>Serratia proteomaculans</i> T ₁ 10 ⁻² /2	6.51 ± 1.36*
Cd ²⁺	0.5 mM	<i>Mitsuaria chitosanitabida</i> T ₃ 10 ⁻² /4	11.21 ± 1.75*
		<i>Serratia sp.</i> T ₅ 10 ⁻¹ /2	9.09 ± 0.55*
		<i>Serratia proteomaculans</i> T ₁ 10 ⁻² /2	9.84 ± 1.03*
	1 mM	<i>Mitsuaria chitosanitabida</i> T ₃ 10 ⁻² /4	7.22 ± 1.63*
		<i>Serratia sp.</i> T ₅ 10 ⁻¹ /2	0.00 ± 0.00
		<i>Serratia proteomaculans</i> T ₁ 10 ⁻² /2	6.93 ± 2.04*
Control		<i>Mitsuaria chitosanitabida</i> T ₃ 10 ⁻² /4	15.48 ± 0.82
		<i>Serratia sp.</i> T ₅ 10 ⁻¹ /2	12.88 ± 0.30
		<i>Serratia proteomaculans</i> T ₁ 10 ⁻² /2	11.73 ± 0.62

(* - significantly different from control at p<0.05 level)

Table 3. Length and biomass of the root and shoot (n=5) recorded in bean plants

			Cd ²⁺		Zn ²⁺		Control
			0.1 mM	0.5 mM	0.5 mM	3 mM	
Without bacteria	Shoot	Length (cm)	31.3±1.85	32.6±1.67	32.2±0.00	30.0±1.94	30.7±3.78
		Biomass (g)	4.9±0.72	5.6±0.48	5.2±0.00	4.4±0.51	4.3±1.68
	Root	Length (cm)	13.3±4.66	11.7±5.23	8.5±0.00*	7.1±2.52*	17.2±4.43
		Biomass (g)	0.4±0.09	0.6±0.24	0.5±0.00	0.7±0.30	0.7±0.45
<i>Mitsuaria chitosanitabida</i> T ₃ 10 ⁻² /4	Shoot	Length (cm)	33.7±6.49	30.2±7.93	33.6±1.53	31.6±4.26	33.3±3.67
		Biomass (g)	4.5±1.17	4.1±1.31	4.6±0.80	4.0±0.42	4.4±0.40
	Root	Length (cm)	10.1±3.56*	10.3±3.49	9.2±5.74*	9.0±1.51*	18.±3.21
		Biomass (g)	0.46±0.12*	0.5±0.16	0.42±0.16	0.51±0.16	0.69±0.21

(* - significantly different from control at p<0.05 level)

The presence of Cd^{2+} (0.1 and 0.5 mM), with or without bacterization with *M. chitosanitabida* T₃10²/4, had no significant effect on the shoot elongation. The root elongation in bean plants was inhibited by the simultaneous presence of Cd^{2+} and bacteria, statistically significant differences were observed (ANOVA, $p=0.038$ in the case of Cd0.1 and $p=0.045$ in the case of Cd0.5). No statistically significant differences were recorded in the case of the shoot and root biomass in the presence of Cd^{2+} with or without bacterial inoculation (Fig. 1). In a similar study, the effect of cadmium in the presence or absence of *Pseudomonas putida* was studied on growth and biomass of *Eruca sativa* by Kamran et al. (2015). Cadmium treatment caused decreased growth and biomass, whereas the inoculation with *P. putida* increased both parameters (Kamran et al., 2015). Our results are different from those presented by Kamran et al. (2015), which can be explained by the contrasting effect of bacterization on Cd uptake, being increased in *E. sativa* and decreased in *P. vulgaris* plants. Karthik et al. (2016) observed enhanced growth (shoot and root length and biomass) and limited Cr accumulation in PGPR inoculated *Phaseolus vulgaris*. An increased root length was reported by Karthik et al. (2017a) in *Zea mays*, *Vigna mungo*, *V. radiata*, *P. vulgaris* and *Sesbiana aculeata* plants when inoculated with *Cellulosimicrobium funkei*-like bacteria.

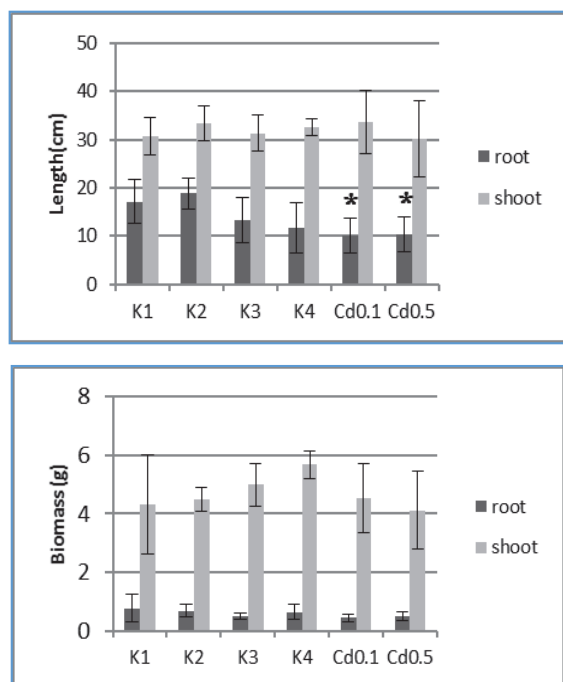


Fig. 1. Bean plant growth parameters in the presence of Cd^{2+} (* - significantly different from control at $p < 0.05$ level), treatments: K1 (absolute control), K2 (bacterized control), K3 (0.1 mM Cd), K4 (0.5 mM Cd), Cd0.1 (0.1 mM Cd and bacteria), Cd0.5 (0.5 mM Cd and bacteria)

The presence of Zn^{2+} in the used concentrations (0.5 and 3 mM), with or without bacterization, had no

significant effect on shoot elongation (Fig. 2). The root elongation was inhibited by the presence of Zn^{2+} with or without bacterial inoculation. The differences between control (K1) and samples were statistically significant (ANOVA, $p=0.01$ in case of K5, $p=0.004$ in case of K6, $p=0.009$ in case of Zn0.5 and $p=0.02$ in case of Zn3), but also between control with inoculation and samples (ANOVA, $p=0.003$ in case of K5, $p=0.0008$ in case of K6, $p=0.002$ in case of Zn0.5 and $p=0.006$ in case of Zn3). No statistically significant differences were recorded in the case of the shoot and root biomass in the presence of Zn^{2+} with or without bacterial inoculation (Fig. 2).

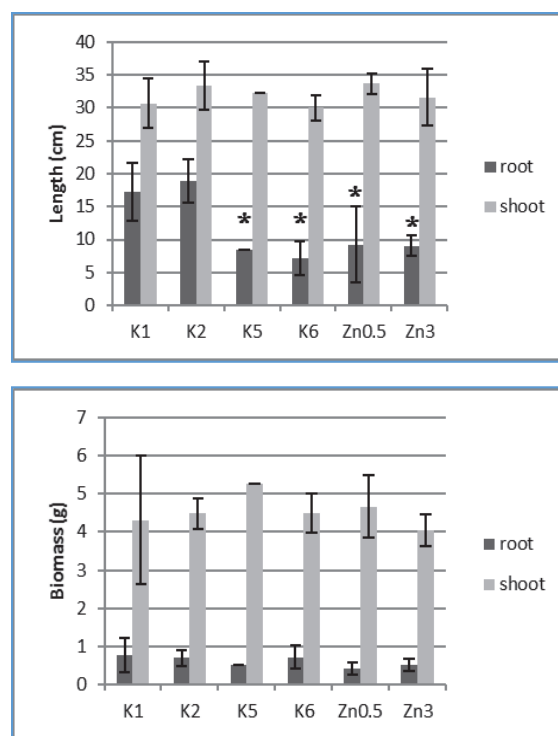


Fig. 2. Bean plant growth parameters in the presence of Zn^{2+} (* - significantly different from control at $p < 0.05$ level), treatments: K1 (absolute control), K2 (bacterized control), K5 (0.5 mM Zn), K6 (3 mM Zn), Zn0.5 (0.5 mM Zn and bacteria), Zn3 (3 mM Zn and bacteria)

The lowest TI was observed in the bean root biomass and elongation (Fig. 3). The observed tolerance index for shoot length and biomass in the case of the bean plants was higher. The shoot growth was less inhibited by Cd^{2+} , with or without PGPR, than the root growth. The observed TI for the length and biomass of the root showed lower values whereas in the case of the shoot the tolerance index showed higher values (except the sample treated with 3 mM Zn^{2+} concentration and PGPR).

The decrease of the tolerance index of shoot length and biomass was observed in the case of the combined treatment with Zn^{2+} and PGPR (Fig. 3). The limited growth in root length and biomass can be attributed to its increased exposition to heavy metal treated soil as well as higher accumulation and metal stress.

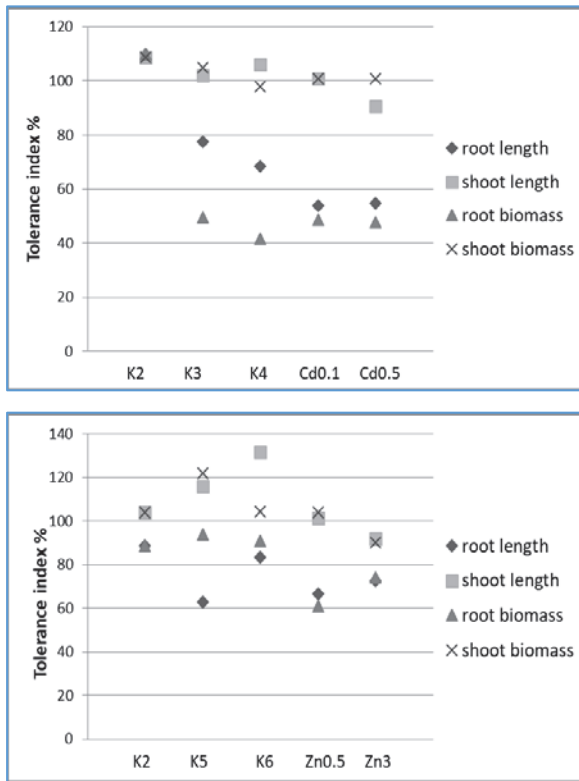


Fig. 3. Tolerance index of bean plants in the presence of heavy metal, treatments: K2 (bacterized control), K3 (0.1 mM Cd), K4 (0.5 mM Cd), Cd0.1 (0.1 mM Cd and bacteria), Cd0.5 (0.5 mM Cd and bacteria), K5 (0.5 mM Zn), K6 (3 mM Zn), Zn0.5 (0.5 mM Zn and bacteria), Zn3 (3 mM Zn and bacteria)

3.3. Heavy metal accumulation

The uptake of Cd²⁺ and Zn²⁺ by the bean root and shoot, under inoculated and uninoculated conditions, were determined by AAS. We observed that higher amounts of Cd²⁺ were accumulated in the root than in the shoot of the bean plants (Fig. 4). The heavy metal accumulation was decreased, in both shoot and root, by the bacterial inoculation. The use of *M. chitosanitabida* T310^{-2/4} decreased the Cd uptake of bean root with 68% and 41%, and shoot with 23% and 46% in Cd0.1 and Cd0.5 samples. The difference was statistically significant (ANOVA, p=0.008) only in case of root accumulation for the higher Cd²⁺ concentration (K4 to K1 absolute control). In case of Cd²⁺ resistant PGP rhizobacterial strains (*Pseudomonas sp.* and *Mycobacterium sp.*) the protection of *Brassica napus* plants against the toxic effect of the heavy metal was already reported (Dell’Amico et al., 2008). In contrast, the improved accumulation of Cd²⁺, Pb²⁺, Zn²⁺ and growth enhancement by *Enterobacter sp.* and *Klebsiella sp.* bacterial strains on the same plant (*Brassica napus*) were reported by Jing et al. (2014). Enhanced Cd²⁺ plant uptake by PGPR was reported by several authors in the case of *Solanum nigrum* by *Pseudomonas sp.* (Chen et al., 2014), *Lycopersicon esculentum* and *Zea mays* by *Burkholderia sp.* (Jiang et al., 2008), *Eruca sativa* by *Pseudomonas putida* (Kamran et al., 2015).

Variations in cadmium and zinc uptake among plant species exist due to their individual response (Kamran et al., 2014), which can be modified by PGPR and plant association.

The Zn²⁺ accumulation in the shoot and root was determined with or without PGPR inoculation (Fig. 4). The heavy metal accumulation was slightly decreased by bacterial inoculation both in the case of the shoot and root. The differences were statistically significant in the case of root accumulation for the higher Zn²⁺ concentration in both treatments: without bacterization (K6, ANOVA, p=0.0006 and p=0.0004 compared to K1 and K2 control) and with bacterization (Zn3, ANOVA, p=0.002, p=0.001 and p=0.004 compared to K1, K2 and K6 control). Statistically significant differences of shoot accumulation were observed among control, inoculated control and Zn²⁺ amended plants, but no differences were observed between PGPR inoculated and uninoculated plants. The effect of inoculation was reported in the case of *Brassica napus*, where the inoculation with *Rahnella sp.* caused an increase in Zn²⁺ accumulation (He et al., 2013). Tiwari et al. (2012) also reported an enhanced Zn²⁺ accumulation in *Brassica juncea* inoculated with *Paenibacillus sp.* and *Bacillus sp.* strains.

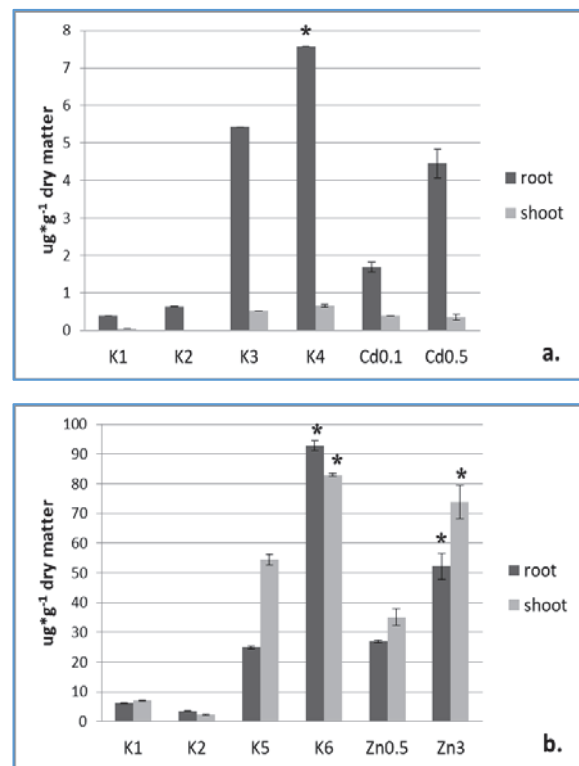


Fig. 4. Accumulation of Cd²⁺ (a) and Zn²⁺ (b) in shoot and root (* - significantly different from control at p<0.05 level), treatments: K1 (absolute control), K2 (bacterized control), K3 (0.1 mM Cd), K4 (0.5 mM Cd), Cd0.1 (0.1 mM Cd and bacteria), Cd0.5 (0.5 mM Cd and bacteria), K6 (0.5 mM Zn), K5 (3 mM Zn), Zn0.5 (0.5 mM Zn and bacteria), Zn3 (3 mM Zn and bacteria)

Due to the differences recorded in the case of the accumulation values for shoot and root, the

shoot/root accumulation ratio was calculated for Cd²⁺ and Zn²⁺ treated plants. The shoot/root ratio was lower in the case of Cd²⁺ and higher in the case of Zn²⁺ treated plants (Fig. 5). Our results show that there is a limited translocation between bean root and shoot in the case of the Cd²⁺ being a toxic metal, both in inoculated (23% and 7.95% in Cd0.1 and Cd0.5 treatments) and uninoculated (9.5% and 8.7% in K3 and K4 treatments) plants. Due to the fact that Zn²⁺ is an essential micronutrient, an allowed translocation was observed, the accumulation in the shoot being more accentuated. Low translocation was observed for Pb, Cr, Cd, Co, Cu, Zn and Ni in *Populus nigra* (Barbeş and Bărbulescu, 2017).

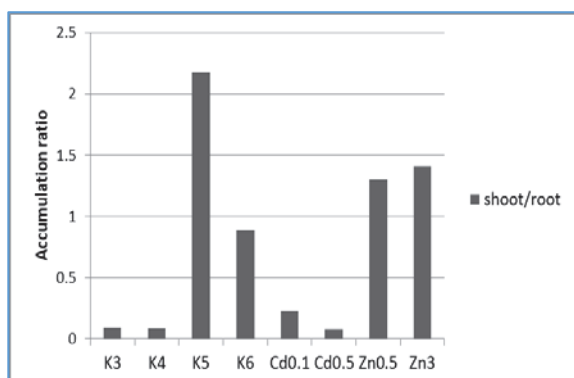


Fig. 5. Accumulation ratio in the case of Cd²⁺ and Zn²⁺ treatment in inoculated and uninoculated bean samples, treatments: K3(0.1 mM Cd), K4 (0.5 mM Cd), Cd0.1 (0.1 mM Cd and bacteria), K5 (0.5 mM Zn), K6 (3 mM Zn), Cd0.5 (0.5 mM Cd and bacteria), Zn0.5 (0.5 mM Zn and bacteria), Zn3 (3 mM Zn and bacteria)

3.4. Enzyme activity

The enzyme activity for POD was higher in the case of plants treated only with Cd²⁺ than in the plants treated with Cd²⁺ and PGPR. *Mitsuraria*

chitosanitabida T₃10⁻²/4 decreased the oxidative stress caused by toxic metals (Fig. 6). Similar data are presented in Karthik et al. (2016) study, when chromium treated *P. vulgaris* plants were inoculated with rhizosphere bacteria that reduced the toxic effect and lowered the polyphenol oxidase activity. In the case of Zn²⁺ treatment, the POD enzyme activity increased together with the used concentration, and the PGPR strain accentuated both the accumulation and the oxidative stress.

Increase in antioxidant enzyme activity was reported previously by Zhang et al. (2012) in inoculated *Elymus dahuricus* under cadmium stress. Very strong (r=0.82, for cadmium treatment) and moderate (r=0.54, for zinc treatment) positive correlations were observed between the mean POD enzyme activity and metal accumulation. This strengthens the presumption that the PGPR inoculation diminished the oxidative stress due to the limited accumulation. The values of POD enzyme activity vary among sampling.

In case of GPOX no significant differences were detected (Fig. 7). The values of GPOX decreased while the accumulated Cd²⁺ and Zn²⁺ in plants increased. Moderate (r=-0.5, for cadmium treatment) and weak (r=-0.3, for zinc treatment) negative correlations were observed between the mean GPOX enzyme activity and metal accumulation. The values of GPOX enzyme activity varied among sampling.

4. Conclusions

In this work we investigated the effect of inoculation with the Cd²⁺ and Zn²⁺ tolerant PGP bacterial strain *M. chitosanitabida T₃10⁻²/4* on the growth, accumulation and stress of bean plants supplemented with Cd²⁺ and Zn²⁺. We observed that the root elongation of bean plants was inhibited by the simultaneous treatment of Cd²⁺ and PGPR, as well as Zn²⁺ and PGPR.

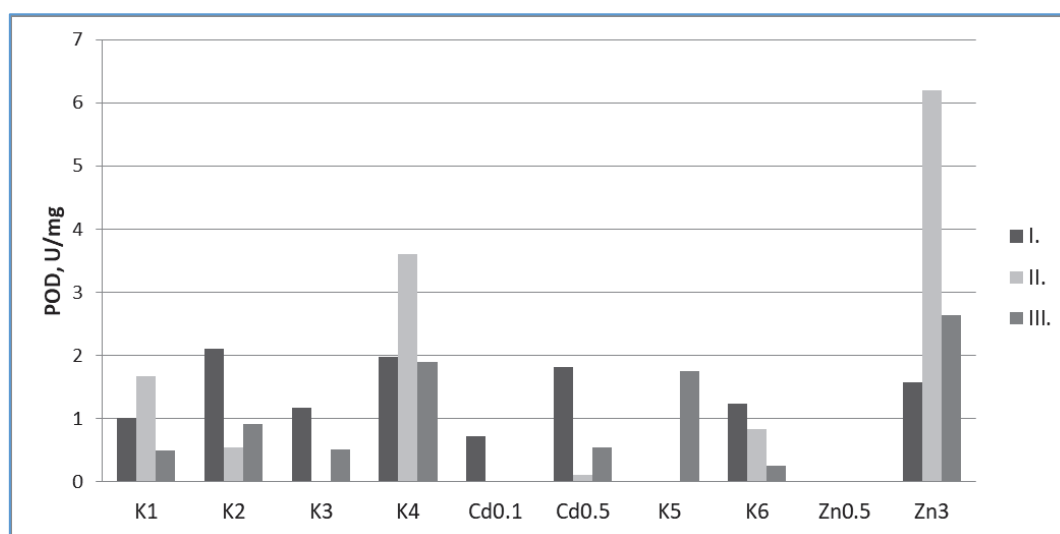


Fig. 6. POD activity (I-first sampling after 10 days, II- second sampling after 20 days, III.-sampling after 30 days), treatments: K1 (absolute control), K2 (bacterized control), K3(0.1 mM Cd), K4 (0.5 mM Cd), Cd0.1 (0.1 mM Cd and bacteria), K5 (0.5 mM Zn), K6 (3 mM Zn), Cd0.5 (0.5 mM Cd and bacteria), Zn0.5 (0.5 mM Zn and bacteria), Zn3 (3 mM Zn and bacteria)

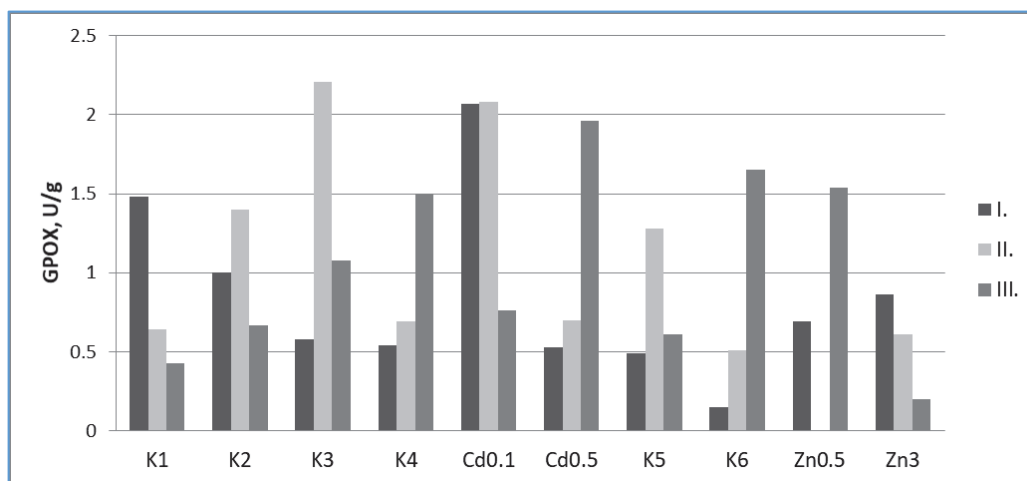


Fig. 7. GPOX activity (I-first sampling after 10 days, II- second sampling after 20 days, III.-sampling after 30 days), treatments: K1 (absolute control), K2 (bacterized control), K3 (0.1 mM Cd), K4 (0.5 mM Cd), Cd0.1 (0.1 mM Cd and bacteria), K5 (0.5 mM Zn), K6 (3 mM Zn), Cd0.5 (0.5 mM Cd and bacteria), Zn0.5 (0.5 mM Zn and bacteria), Zn3 (3 mM Zn and bacteria)

No significant effect of heavy metal treatment with or without PGPR was observed in the case of shoot development, root biomass and shoot biomass. A higher accumulation in the root, with respect to shoot, was observed in bean plants treated with the phytotoxic Cd^{2+} , due to a limited translocation. The inoculation with *M. chitosanitabida* $T_310^{-2}/4$ lowered the amount of accumulated Cd^{2+} . The higher accumulation in shoot, with respect to root, was observed in plants treated with Zn^{2+} , and the amount accumulated Zn^{2+} , was increased with *M. chitosanitabida* $T_310^{-2}/4$ inoculation. The POD enzyme activity increased with the used heavy metal concentration, and the inoculation with PGPR diminished the oxidative stress in case of Cd^{2+} . *Mitsuaria chitosanitabida* $T_310^{-2}/4$ reduced the accumulation of Cd^{2+} and the antioxidant enzyme (POD) activity in the bean plants compared with the control.

References

- Barbeş L., Bărbulescu A., (2017), Monitoring and statistical assessment of heavy metals in soil and leaves of *Populus nigra* L., *Environmental Engineering and Management Journal*, **16**, 187-196.
- Cavalcanti F.R., Oliveira J.T.A., Martins-Miranda A.S., Viegas R.A., Silveira J.A.G., (2004), Superoxide dismutase, catalase and peroxidase activities do not confer protection against oxidative damage in salt-stressed cowpea leaves, *New Phytologist*, **163**, 563-571.
- Cheema S., Sommerhalter M., (2015), Characterization of polyphenol oxidase activity in *Ataulfo mango*, *Food Chemistry*, **171**, 382-387.
- Chen L., Luo S., Li X., Wan Y., Chen J., Liu C., (2014), Interaction of Cd hyperaccumulator *Solanum nigrum* L. and functional endophyte *Pseudomonas* sp. Lk9 on soil heavy metals uptake, *Soil Biology and Biochemistry*, **68**, 300-308.
- Dell'Amico E., Cavalcanti L., Andreoni V., (2008), Improvement of *Brassica napus* growth under cadmium stress by cadmium-resistant rhizobacteria, *Soil Biology and Biochemistry*, **40**, 74-84.
- Droque B., Doré H., Borland S., Wisniewski-Dyé F., Prigent-Combaret C., (2012), Which specificity in cooperation between phyto-stimulating rhizobacteria and plants?, *Research in Microbiology*, **163**, 500-510.
- He H., Ye Z., Yang D., Yan J., Xiao L., Zhong T., Yuan M., Cai X., Fang Z., Jing Y., (2013), Characterization of endophytic *Rahnella* sp. JN6 from *Polygonum pubescens* and its potential in promoting growth and Cd Pb, Zn uptake by *Brassica napus*, *Chemosphere*, **90**, 1960-1965.
- Jiang C., Sheng X., Qian M., Wang Q., (2008), Isolation and characterization of a heavy metal-resistant *Burkholderia* sp. from heavy metal-contaminated paddy field soil and its potential in promoting plant growth and heavy metal accumulation in metal-polluted soil, *Chemosphere*, **72**, 157-164.
- Jing Y.X., Yan J.L., He H.D., Yang D.J., Xiao L., Zhong T., Yuan M., Cai X.D., Li S.B., (2014), Characterization of bacteria in the rhizosphere soils of *Polygonum pubescens* and their potential in promoting growth and Cd, Pb, Zn uptake by *Brassica napus*, *International Journal of Phytoremediation*, **16**, 321-333.
- Kamran M.A., Amna, Mufti R., Mubariz N., Syed J.H., Bano A., Javed M.T., Munis M.F., Tan Z., Chaudhary H.J., (2014), The potential of the flora from different regions of Pakistan in phytoremediation: a review, *Environmental Science and Pollution Research International*, **2**, 801-812.
- Kamran M.A., Syed J.H., Eqani S.A., Munis M.F., Chaudhary H.J., (2015), Effect of plant growth-promoting rhizobacteria inoculation on cadmium (Cd) uptake by *Eruca sativa*, *Environmental Science and Pollution Research International*, **22**, 9275-9283.
- Kamran M.A., Eqani S.A.M.A.S., Bibi S., Xu R.K., Amna, Monis M.F.H., Katsoyiannis A., Bokhari H., Chaudhary H.J., (2016), Bioaccumulation of nickel by *E. sativa* and role of plant growth promoting rhizobacteria (PGPRs) under nickel stress, *Ecotoxicology and Environmental Safety*, **126**, 256-263.
- Kamran M.A., Bibi S., Xu R.K., Hussain S., Mehmood K., Chaudhary H.J., (2017), Phyto-extraction of chromium

- and influence of plant growth promoting bacteria to enhance plant growth, *Journal of Geochemical Exploration*, **182**, 269-274.
- Karthik C., Oves M., Thangabalu R., Sharma R., Santhosh S.B., Arulselvia P.I., (2016), *Cellulosimicrobium funkei*-like enhances the growth of *Phaseolus vulgaris* by modulating oxidative damage under Chromium(VI) toxicity, *Journal of Advanced Research*, **7**, 839-850.
- Karthik C., Elangovan N., Kumar T.S., Govindharaju S., Barathi S., Oves M., Arulselvia P.I., (2017a), Characterization of multifarious plant growth promoting traits of rhizobacterial strain AR6 under Chromium (VI) stress, *Microbiological research*, **204**, 65-71.
- Karthik C., Oves M., Sathya K., Ramkumar V.S., Arulselvia P.I., (2017b), Isolation and characterization of multi-potential *Rhizobium* strain ND2 and its plant growth-promoting activities under Cr(VI) stress, *Archives of Agronomy and Soil Science*, **63**, 1058-1069.
- Khan M.S., Zaidi A., Wani P.A., Oves M., (2009), Role of plant growth promoting rhizobacteria in the remediation of metal contaminated soils, *Environmental Chemistry Letters*, **7**, 1-19.
- Lin Y.-F., Aarts M.G.M., (2012), The molecular mechanism of zinc and cadmium stress response in plants, *Celular and Molecular Life Sciences CMLS*, **69**, 3187-3206.
- Miransari M., (2011), Hyperaccumulators, arbuscular mycorrhizal fungi and stress of heavy metals, *Biotechnology Advances*, **29**, 645-653.
- Nagajyoti P.C., Lee K.D., Sreekanth T.V.M., (2010), Heavy metals, occurrence and toxicity for plants: a review, *Environmental Chemistry Letters*, **8**, 199-216.
- Oves M., Khan M.S., Qari H.A., (2017), *Ensifer adhaerens* for heavy metal bioaccumulation, biosorption, and phosphate solubilization under metal stress condition, *Journal of the Taiwan Institute of Chemical Engineers*, **80**, 540-552.
- Sessitsch A., Kuffner M., Kidd P., Vangronsveld J., Wenzel W.W., Fallmann K., Puschenreiter M., (2013), The role of plant-associated bacteria in the mobilization and phytoextraction of trace elements in contaminated soils, *Soil Biology and Biochemistry*, **60**, 182-194.
- Sharma S.S., Dietz K.-J., (2006), The significance of amino acids and amino acid-derived molecules in plant responses and adaptation to heavy metal stress, *Journal of Experimental Botany*, **57**, 711-726.
- Sun L.N., Zhang Y.F., He L.Y., Chen Z.J., Wang Q.Y., Qian M., Sheng X.F., (2010), Genetic diversity and characterization of heavy metal-resistant-endophytic bacteria from two copper-tolerant plant species on copper mine wasteland, *Bioresource Technology*, **101**, 501-509.
- Tiwari S., Singh S.N., Garg S.K., (2012), Stimulated phytoextraction of metals from fly ash by microbial interventions, *Environmental Technology*, **33**, 2405-2413.
- Ullah A., Heng S., Munis M.F.H., Fahad S., Yang X., (2015), Phytoremediation of heavy metals assisted by plant growth promoting (PGP) bacteria: A review, *Environmental and Experimental Botany*, **117**, 28-40.
- Wilkins D.A., (1978), The measurement of tolerance to edaphic factors by means of root growth, *New Phytologist*, **86**, 623-633.
- Zhang X., Li C., Nan Z., (2012), Effects of cadmium stress on seed germination and seedling growth of *Elymus dahuricus* infected with the *Neotyphodium* endophyte, *Science China Life Sciences*, **55**, 793-799.



“Gheorghe Asachi” Technical University of Iasi, Romania



EFFECTIVENESS FACTOR APPROACH FOR CHEMICAL ABSORPTION PROCESS

Maria Harja¹, Gabriela Ciobanu¹, Lăcrămioara Rusu^{2*}, Liliana Lazăr¹

¹“Gheorghe Asachi” Technical University of Iasi, Faculty of Chemical Engineering and Environmental Protection, 73 Prof. dr. doc. D. Mangeron Street, 700050 Iasi, Romania,

²“Vasile Alecsandri” University of Bacau, Faculty of Engineering, 157 Mărășești Blvd., 600115, Bacau, Romania

Abstract

Absorption of gases into liquids, with chemical reaction, is an important unit operation useful in many fields, especially synthesis of new products and waste gas treatment. Gas treatment means the separation of pollutants: acid gases, organic sulphur compounds, and other contaminants which may be found in gaseous streams. The absorption into liquid is a process almost exclusively used for removal of contaminants. The removal refers to retention of the majority of acid gases present in high concentration down to a level such as 0.1 % in the treated gas. The gas-liquid processes are carried out in a variety of equipment's including packed towers, bubbling absorbers, spray columns, falling film contactors etc. The absorber selection and design require models describing the interaction between mass transfer and chemical reaction. For design purposes, it may be used the concept of enhancement factor (E), related to the positive effect of the reaction rate on the physical mass transfer.

The aim of this paper is to develop a mathematical model that allows the analysis of gas-liquid processes in the intermediate reaction regime. The effectiveness factor approach for gas liquid reactions is developed in this paper by using the concept of fractional conversion in the liquid film (X_F), which precisely indicates the kinetic regime. This new approach for gas-liquid reactions is presented in the current study. When reaction rate does not improve the mass transfer (slow and very slow reaction) the effectiveness factor concept can be used to describe this interaction.

The elaborated mathematical model allows the determination of effectiveness factor values for practical intervals of Hatta (Ha) modulus and modified Sherwood (Sh) number. The development concept is similar with model used in the modelling of the heterogeneous catalytic reactions.

The proposed mathematical model has shown that in the intermediate regime (when $0.01 < X_F < 0.99$), the effectiveness factor approach is more convenient.

Key words: chemical absorption, effectiveness factor, gas-liquid processes, modelling

Received: May, 2017; *Revised final:* January, 2018; *Accepted:* March, 2018; *Published in final edited form:* April 2018

1. Introduction

Absorption of gaseous pollutants into liquid phase is widely used in environmental engineering for different contaminants removal (Biard and Couvert 2013; Roustan, 2003; Yildirim et al., 2012). Air pollution is a local, pan-European and hemispheric issue. Sources of air pollution can be natural, anthropogenic, or both. Emissions from industry,

transport activities, combustion system of diesel engine, wastewater treatment plants or from agriculture, are only a few examples of sources of anthropogenic pollution (Ge et al., 2016; Su et al., 2016; Wang et al., 2016). Nitrous oxide, methane and carbon dioxide (CO_2) exhibit greenhouse effect and, among these, CO_2 is considered the main greenhouse gas with negative impact over climate change (Bucur and Harja, 2012; Harja and Szep, 2013). CO_2 is

* Author to whom all correspondence should be addressed: e-mail: lacraistrati04@yahoo.com; Phone: +40744598363

typically used as a reference for global warming approaching (Jongartklang et al., 2016; Qin et al., 2016; Tan et al., 2012) and is believed to be responsible for about 64% of the greenhouse effect (Ramazani et al., 2016).

Gas treating is the term used to describe the separation of acid gases (CO_2 , H_2S , SO_2), organic volatile compounds (VOC), organic sulphur compounds and certain other gases (HCN, NH_3 , NO_x etc.) from gaseous wastes (Cai et al., 2017; Favier et al., 2016a, 2016b; Szep and Harja, 2007). There are four main categories of gas treating processes: absorption into a physical or chemical liquid agent; adsorption onto solids (zeolites, activated carbon); cryogenic separation; chemical conversion to other compounds. When the gas compound reacts with the liquid phase, the process is called chemical absorption. Chemical absorption is currently believed to be the most suitable method in the case of post-combustion power plants (Behr et al., 2011; Harja et al., 2008). On the other hand, chemical absorption process between gases and liquids are extensively applied in chemical engineering (Zhao et al., 2017). Significant chemical processes as: wet flue gas desulphurization, carbon capture by absorption, syngas purification, manufacturing of nitric or sulphuric acid, chlorination, hydrogenation, ammonization etc. involve an absorption process for manufacturing new products or for treating waste gases (Gaspar and Fosbøl, 2015; Qin et al., 2016; Yildirim et al., 2012).

This unit operation consists in pollutant transfer from the gas phase to a liquid phase; gas dissolution in liquid phase and chemical reaction at interface or in bulk liquid phase. The absorption into liquids is the process almost exclusively used for bulk removal of acid contaminants. Bulk removal refers to removal of the majority of acid gases present in high concentration down to a level such as 0.1 % in the treated gas.

There are different models that describe the absorption accompanied by chemical reaction process, which is based mainly on three theories: the two-films, the penetration and the surface renewal (Koronaki et al., 2015; Molga and Westerterp, 2013). The two films theory was developed by Whitman (1924), the equations being established by assuming a stagnant film of liquid and one of gas on each of the two sides of the interface area (Astarita, 1967; Morsi and Basha, 2015; Noeres et al., 2003). The resistance to mass transfer is concentrated in these films. Higbie (1935) proposed the penetration theory, where is considered that the gas-liquid interface is not stagnant but liquid packages remain at the interface for a period of time – named contact time, then migrate back into the solution. Higbie's model was modified by Danckwerts (1955) resulting in the surface renewal theory that assumes a contact time distribution of the liquid elements.

The chemical absorption processes are carried out in a variety of equipments ranging from a bubble absorber to a packed column, a spray tower, a Venturi scrubber, or a falling film contactor (Kening et al.,

2003; Petrescu and Harja, 2006). Chemical absorption processes are intensively used; however, the modelling is still approximate. Other accurate models are necessary in order to improve the absorber design, to upgrade the technical level and to perform a better economic optimization. A balance between modelling accuracy and computational requirements has to be found for simulations and applications of absorber (Gaspar and Fosbøl, 2015). Solving the numerical model is still computationally difficult.

The absorber selection and design require models characterizing the interaction between mass transfer and chemical reaction. Two approaches may be used to describe interaction between mass transfer and chemical reaction.

The first approach, expressing the effect of the reaction on improvement of the physical mass transfer led to the older concept of the enhancement factor (E) (Petrescu et al., 1998; Ramazani et al., 2016). The enhancement factor diminishes the complexity of a mass transfer model. The Hatta number is a parameter which compares reaction rate and diffusion rate in a liquid film. An increased Hatta number indicates a higher reaction rate compared to diffusion. In this context, Hatta number (Ha) and the instantaneous enhancement factor have been used in the modelling. Gaspar and Fosbøl presented a fast and simple enhancement factor model and revealed that the model overlaps the numerical solution of the film model (Gaspar and Fosbøl, 2015).

The second approach, expressing decrease of the reaction rate by the mass transfer resulted in the effectiveness factor concept, which is widely used in the modelling of the heterogeneous catalytic reactions. This is a relatively new approach for gas-liquid reactions.

The design of the absorber requires knowledge of the kinetic regime and the kinetic equation (Petrescu and Harja, 2006). The effectiveness factor approach for gas liquid reactions is developed in this paper by using the concept of fractional conversion in the liquid film (X_F), which precisely indicates the kinetic regime. The fractional conversion in the liquid film (X_F) is a function of the Ha number. Within this work, the values of the effectiveness factor for practical intervals of Ha modulus and modified Sherwood number are determined, using a derived mathematical model. For the regime of intermediate reaction rates the effectiveness factor approach is more convenient. It is further solved for practical intervals of Hatta modulus and modified Sherwood number.

2. Mathematical modelling

2.1. The enhancement factor

Let A be the component of the gas phase reacting with a non-volatile compound B in the liquid phase. The reaction that takes place is confined to the liquid phase are presented in Eq. (1):



Considering the Whitman model (Ivaniciuc, 1999; Noeres et al., 2003), the concentration profile in the liquid phase is presented in Fig. 1.

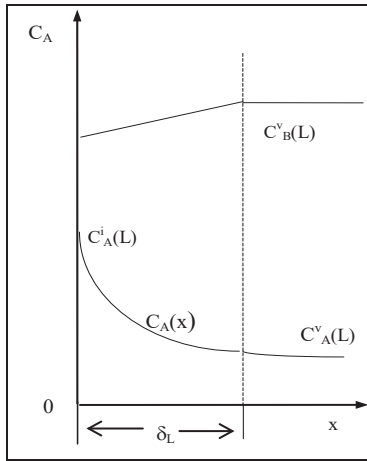


Fig. 1. Concentration profile in the liquid film

Since the two films theory involves a steady state, the mass balance of A in a slice of thickness dx and unit cross section in the liquid film may be written as Eq. (2):

$$D_A \frac{d^2 C_A}{dx^2} + k C_A^n C_B^m = 0 \quad (2)$$

For the component B the relation is similar (Eq. 3):

$$D_B \frac{d^2 C_B}{dx^2} + k C_A^n C_B^m = 0 \quad (3)$$

with the boundary conditions given by Eq. (4):

$$\begin{aligned} x=0; \quad C_A &= C_A^i \quad \frac{dC_B}{dx} = 0 \\ x=\delta_L; \quad C_A &= C_A^v; \quad C_B = C_B^v \end{aligned} \quad (4)$$

By integrating Eqs. (2-4), the concentration profiles of A and B in the liquid film are obtained. In general, Eqs. (2) and (3) cannot be integrated analytically, excepting the special cases of rate equations. For a pseudo-first-order reaction ($n = 1, m = 0$ or $C_B = \text{const.}$) the (Eq. 2) becomes Eq. (2'):

$$D_A \frac{d^2 C_A}{dx^2} + k_1 C_A = 0 \quad (2')$$

with the boundary conditions (Eq. 4'):

$$\begin{aligned} x=0; \quad C_A &= C_A^i \\ x=\delta_L; \quad C_A &= C_A^v \end{aligned} \quad (4')$$

At the interface ($x = 0$), Eq. (5) was obtained:

$$\left[\frac{dC_A(x)}{dx} \right]_{x=0} = \sqrt{\frac{k_1}{D_A}} \left[\frac{C_A^v - C_A^i \cosh(\delta_L \sqrt{\frac{k_1}{D_A}})}{\sinh\left(\delta_L \sqrt{\frac{k_1}{D_A}}\right)} \right] \quad (5)$$

The modulus $\delta_L \sqrt{\frac{k_1}{D_A}}$ is Hatta number (Ha):

$$\delta_L \sqrt{\frac{k_1}{D_A}} = \frac{D_A}{k_L^0} \sqrt{\frac{k_1}{D_A}} = \frac{\sqrt{k_1 D_A}}{k_L^0} = Ha \quad (6)$$

The flux of A transferred through the gas film boundary in the presence of the chemical reaction in the liquid phase is:

$$N'_A = D_A \left(\frac{dC_A(x)}{dx} \right)_{x=0} = k_L^0 \frac{H}{t} \frac{H}{\mathcal{H}o} \left(C_A^i - \frac{a}{c} \frac{C_A^v}{\mathcal{H}o} \right) \quad (7)$$

In the absence of the reaction, the mass flux physically transferred is given by Eq. (8):

$$N_A = k_L^0 (C_A^i - C_A^v) \quad (8)$$

The enhancement factor (E) may be defined as the ratio N'_A/N_A (Eq. 9):

$$E = \frac{N'_A}{N_A} = \frac{Ha}{\tanh(Ha)} \left(\frac{1 - \frac{\gamma}{\cosh(Ha)}}{1 - \gamma} \right) \quad (9)$$

$$\text{where: } \gamma = \frac{C_A^v}{C_A^i} \quad (10)$$

If $C_A^v \ll C_A^i$, $\gamma \rightarrow 0$ then (Eq. 9) becomes:

$$E = \frac{Ha}{\tanh(Ha)} \quad (11)$$

There is no agreement in the literature concerning the values of Ha at which the reaction is completed in the film ($Ha > 3.0$ or $Ha > 5.0$) or takes place mainly in the bulk liquid.

In order to determine these limits, one can define the fraction of A consumed in the liquid film (X_F) (Eq. 12):

$$X_F = \frac{(N'_A)_{x=0} - (N'_A)_{x=\delta_L}}{(N'_A)_{x=0}} = 1 - \frac{(N'_A)_{x=\delta_L}}{(N'_A)_{x=0}} \quad (12)$$

The mass flux of A which was not consumed in the film is Eq. (13):

$$(N'_A)_{x=\delta_L} = k_L^0 \frac{Ha}{\tanh Ha} \left(\frac{C_A^i}{\cosh Ha} - C_A^v \right) \quad (13)$$

Combining Eqs. (7), (12), and (13) leads to Eq. (14):

$$X_F = 1 - \frac{1 - \gamma \cosh Ha}{\cosh Ha - \gamma} \quad (14)$$

Eqs. (9) and (13) include the ratio γ which cannot be directly determined but correlated with

other readily measurable amounts. A material balance of A at the film - bulk boundary gives Eq. (15):

$$-S_v D_A \left(\frac{dC_A}{dx} \right)_{x=\delta_L} = (\varepsilon_L - S_v \delta_L) k_1 C_A^v \quad (15)$$

from which Eq.(16) is found by integration:

$$\gamma = \frac{1}{1 + Ha(\beta - 1) \tanh(Ha)} \quad (16)$$

where: $\beta = \frac{\varepsilon_L k_L^0}{S_v D_{A_1}} \quad (17)$

This β may be considered a modified Sherwood number. The system Eqs. (14-17) gives X_F as a function of Ha and β .

2.2. Effectiveness factor

The effectiveness factor or **liquid utilization factor** (η_L) may be defined as the ratio (Eq. 18):

$$\eta_L = \frac{(r_A)_{ef}}{(r_A)} \quad (18)$$

where the effective rate of gas-liquid reaction is (Eq. 19):

$$(r_A)_{ef} = -\frac{dn_A}{V d\tau} = S_v k_L^0 E (C_A^i - C_A^v) \quad (19)$$

and the reaction rate in the liquid phase is (Eq. 20):

$$(r_A) = -\frac{d_A n}{V \tau d} = \varepsilon_L k_1 C_A^i \quad (20)$$

By combining Eqs. (18- 20) results Eq. (21):

$$\eta_L = \frac{S_v k_L^0 E (1 - \gamma)}{\varepsilon_L k_1} \quad (21)$$

Since E and β are correlated by Eqs. (9) and (16) respectively, then Eq. (21) could be written as Eq. (22):

$$\eta_L = \frac{1}{Ha\beta} \left[\frac{\tanh Ha + Ha(\beta - 1)}{1 + Ha(\beta - 1)\tanh Ha} \right] \quad (22)$$

3. Results and discussion

3.1. Experimental and numerical validation of equations

Validation of Eqs. (15) and (22), must be based on experimental values of the kinetic parameters and transfer properties including: k_1 , k_L , ε_L , S_v . The determination of these coefficients by the chemical

method, using a model reaction as sulphite oxidation, has been presented in a previous paper (Ivaniciuc and Siminiceanu, 2000). For systems generally found in gas treatment technologies, their values are ranged within the following intervals (Ivaniciuc, 1999):

$$5 \times 10^{-5} < k_L < 5 \times 10^{-4}; \quad 10 < S_v < 10000$$

$$0.20 < \varepsilon_L < 0.99; \quad 10^{-9} < D_A < 5 \times 10^{-9}$$

From here one may assess the limits of the Hatta and modified Sherwood numbers:

$$1.0 < \beta < 10000.0$$

$$0.1 < Ha < 10.0$$

The practical values of β are frequently ranged between 10 and 5000, whereas those of Ha may exceed 10 and even 100 for very fast reactions.

By solving the Eqs. (14-17), in Mathcad 7, the values of X_F have been obtained. These values are of a great importance for the determining the kinetic regime of a given process and the rational design of the industrial gas-liquid contactor. According to the data presented in Fig. 2, three kinetic regimes can be distinguished, depending on the values of Ha and β :

- When $Ha < 0.3$, for practical values of β ($5 < \beta < 5000$), more than 99% of A is consumed in the bulk liquid ($X_F < 0.01$). This is the **slow reaction regime**. For this regime, from the Eq. (9) results:

$$Ha < 0.3 \quad \tanh Ha = Ha \quad E = 1.0 \quad (23)$$

A contactor with a large liquid holdup which, according to the Eq. (20), that accelerates the reaction, will be the best choice. This could be a bubble column or a stirred reactor.

Values of $1 - X_F = f(Ha, \beta)$ are presented in Fig. 2, considering: $Ha=0.1-10$, $\beta = 1.0-10,000$, $\varepsilon_L=0.2-0.99$, $D_A = (1-5) 10^{-9}$, $S_v = 10-1000$, $k_L^0 = (0.5-5) 10^{-4}$.

- When $Ha > 5.0$, the fractional conversion of A in the liquid film exceeds 99% for all values of β greater than 5.0. This is the **fast reaction regime**. From Eq. (11) results Eq. (24) (Hagiu and Ivaniciuc, 1997):

$$Ha > 5.0 \quad \tanh Ha = 1 \quad E = Ha \quad (24)$$

The rate of the gas-liquid reaction becomes Eq. (25):

$$N_A S_v = S_v \sqrt{k_1 D_A C_A^i} \quad [\text{kmol m}^{-3} \text{ s}^{-1}] \quad (25)$$

A contactor with as great as possible interfacial areas (S_v) will be the best choice. This could be a packed column, a plate column, a Venturi scrubber or a falling film contactor.

- When $0.3 < Ha < 5.0$ the values of X_F are ranged between 0.1 and 0.99 and depend on both Ha and β . This is the **intermediate reaction regime**, most frequently found in practice.

3.2. The effectiveness factor approach

For these intermediate reaction rates the use of the enhancement factor is not always in agreement with the standard approach of diffusional limitations in reactor design and may be somewhat confusing. Moreover, there are cases where there simply is no purely physical mass transfer process to refer to, as CO₂ absorption in aqueous alkali solutions.

The **effectiveness factor approach** is more convenient in these cases. For pseudo-first-order reactions this approach leads to a simple kinetic equation (Eq. 26):

$$(r_A)_{ef} = \eta_L \varepsilon_L k_1 C_A^i \tag{26}$$

The values of the effectiveness factor (η_L) resulted from Eq. (22) are presented in Fig. 3, for $\beta = 1 - 1000$ și $Ha = 0.3 - 10$.

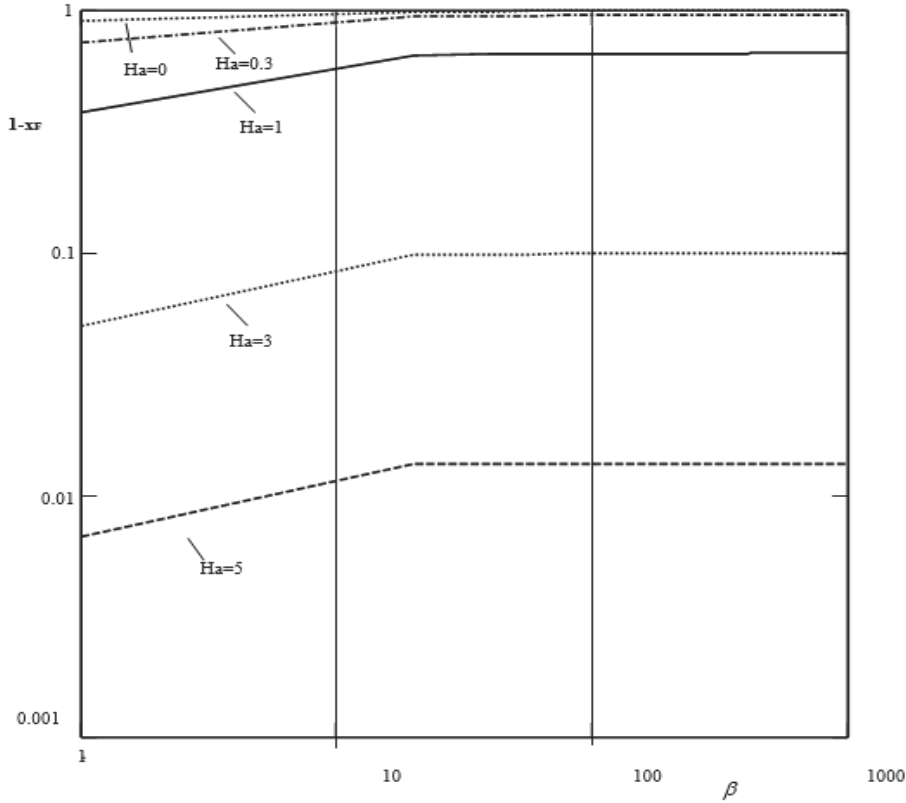


Fig. 2. Fraction of A consumed in the liquid film as a function of Ha and β

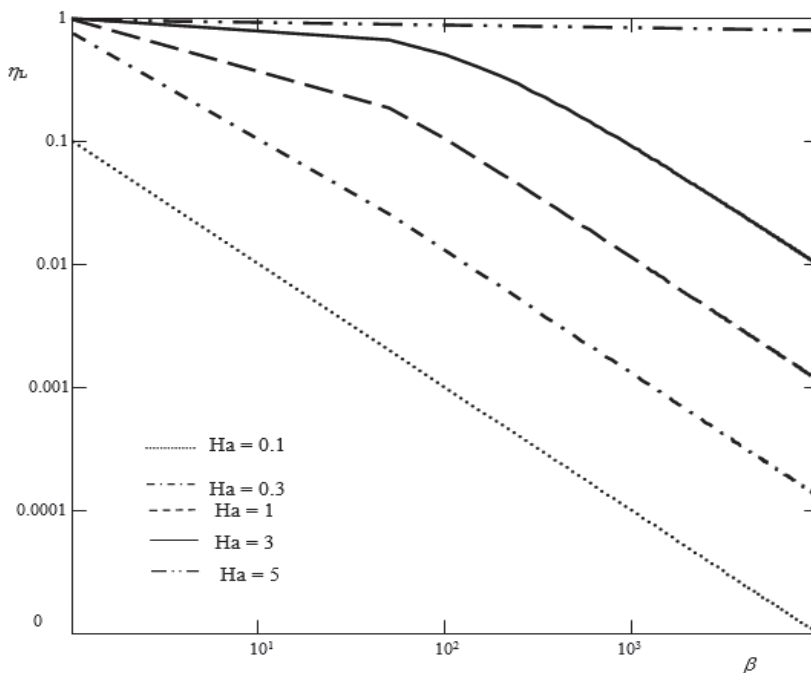


Fig. 3. Effectiveness factor for gas-liquid absorption with pseudo-first-order chemical reaction as a function of β and Ha

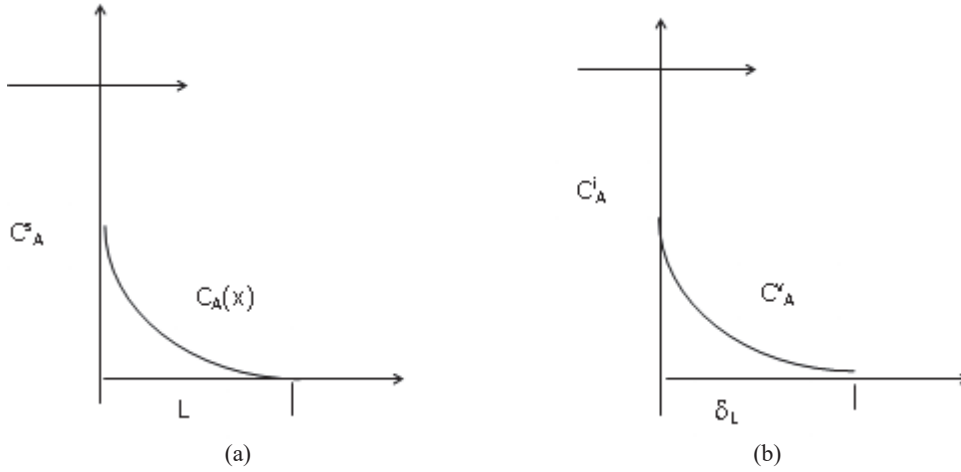


Fig. 4. Concentration profiles for the catalytic process (a) and the gas liquid absorption process (b)

3.3. Analogy between absorption and catalysis processes

In order to study the analogy between the Hatta and Thiele modulus, the model of a grain catalyst plate by length equal to L and the two films model for chemical absorption with film thickness equal to δ_L have been considered (Fig. 4). In the case of liquid-gas processes we have demonstrated that the liquid utilization factor can be calculated with the (Eq. 22), which for $\beta = 1$ has the form given by Eq. (27):

$$\eta_L = \frac{thHa}{Ha} \tag{27}$$

For catalytic processes, the mass balance of A in a catalyst plate by length equal to L may be written as:

$$D_{ef} \frac{d^2 C_A}{dx^2} + k_1 C_A = 0 \tag{28}$$

Thiele modulus has the form of Eq. (29):

$$\Phi = L \sqrt{\frac{k_1}{D_A}} \tag{29}$$

For catalytic process η_{cat} has the same form with liquid utilization factor for $\beta_{cat} = \beta = 1$ (Eq. 30):

Table 1. Absorption versus catalytic process

Catalytic	Absorption
$D_{ef} \frac{d^2 C_A}{dx^2} + k_1 C_A = 0$	$D_A \frac{d^2 C_A}{dx^2} + k_1 C_A = 0$
$\Phi = L \sqrt{\frac{k_1}{D_A}}$	$Ha = \delta_L \sqrt{\frac{k_1}{D_A}}$
$\beta_{cat} = \frac{\epsilon_p}{S_v L}$	$\beta = \frac{\epsilon_L k_L^0}{S_v D_{A_i}} = \frac{\epsilon_L}{S_v \delta_L}$
It can observe similarity: δ_L equivalent with L ϵ_L equivalent with ϵ_p	
$\eta_{cat} = \frac{th\Phi}{\Phi}$ for $\beta_{cat}=1$	$\eta_L = \frac{thHa}{Ha}$ for $\beta=1$

$$\eta_{cat} = \frac{th\Phi}{\Phi} \tag{30}$$

It must be demonstrated that $\beta_{cat} = 1$.

$$\beta_{cat} = \frac{\epsilon_p}{S_v L} \tag{31}$$

But:

$$\epsilon_p = \frac{\sum V_{S_i}}{V} = \frac{\sum S_i L}{V} = \frac{L \sum S_i}{V} = L S_v \tag{32}$$

By replacing in Eq. (31), it was obtained $\beta_{cat} = 1$, which demonstrates the perfect similarity.

Perfect similarity between models is presented in Table 1. From Table 1 it can be seen that even if there are major phenomenological differences between these processes, the mathematical model in simplified form is similar.

Analogy between models leads off a variety of perspectives. This conducted, in collaboration between different scientists, to provide a valuable source of intuitions which have led to a profounder theoretical understanding of processes. Analogy involves the comparison of two different domains:

catalysis and absorption. Indeed, the models can be expanding in unknown process.

4. Conclusions

Reactions between gases and liquids are extensively applied in gas purification and synthesis of new products. The rational design of the absorbers requires knowledge of the kinetic regime and the kinetic equation.

The classical mathematical model, based on Ha and the enhancement factor, E , can be used in the case of fast and very fast reactions. The kinetic regime can be determined by means of the fractional conversion in the liquid film (X_F) as a function of the Ha number.

For the intermediate reaction rates (when $0.01 < X_F < 0.99$), it is recommended to use the effectiveness factor approach. Based on the experimentally data, for various practical applications, the variation ranges of the effectiveness factor were calculated. The values of the effectiveness factor for practical intervals of Ha modulus and modified Sherwood number are determined, using a derived mathematical model.

The graphical representations presented in the paper allow the first approximation of a new process, the data read on the diagram can be used as a basis for modeling new reactors/absorbers.

This study demonstrated that two different processes can be study on the base of similar model and knowledge can be share between processes. Finally, these results provide additional valuable information about the possibility of using the effectiveness factor approach for the intermediate reaction regime, which can lead to viable application in environmental engineering for mathematical modelling and design of removal processes of the contaminants from gaseous streams.

Notation

A , component of the gas phase, dissolved in the liquid;
 B , component of the liquid phase reacting with A ;
 C_A , C_B , molar concentration of A , and B (mol L^{-1});
 C_A^i , C_A^b , concentration of A at the interface, and in the liquid bulk, respectively (mol L^{-1});
 D_A , D_B , molecular diffusivities of A and B in the liquid film ($\text{m}^2 \text{s}^{-1}$);
 E , enhancement factor;
 Ha , Hatta number;
 k_L , mass transfer coefficient of A from interface to liquid bulk (m s^{-1});
 k_t , rate coefficient for the pseudo-first-order reaction between A and B (s^{-1});
 n , m , reaction orders;
 n_A , moles number of component A ;
 N_A , molar rate of physical absorption per unit gas-liquid interface area ($\text{mol m}^{-2} \text{s}^{-1}$);
 N_A^c , molar rate of chemical absorption per unit gas-liquid interface area ($\text{mol m}^{-2} \text{s}^{-1}$);
 r_A , reaction rate of component A per unit of liquid volume ($\text{mol m}^{-3} \text{s}^{-1}$);
 $(r_A)_{ef}$, effective reaction rate ($\text{mol m}^{-3} \text{s}^{-1}$);
 S_v , gas-liquid interfacial area per unit of liquid volume ($\text{m}^2 \text{m}^{-3}$);
 V , volume of liquid phase (m^3);

X_F , fractional conversion of A in the liquid film;
 x , coordinate perpendicular to gas-liquid interface (m);
 β , modified Sherwood number for liquid film;
 γ , the ratio C_A^i/C_A^b ;
 δ_L , liquid film thickness for mass transfer (m);
 ε_L , liquid holdup;
 η_L , effectiveness factor/ liquid utilization factor;
 ν_B , stoichiometric coefficient of component B ;
 τ , time (s).

References

- Astarita G., (1967), *Mass Transfer with Chemical Reaction*, Elsevier, Amsterdam-London.
- Behr P., Maun A., Deutgen K., Tunnat A., Oeljeklaus G., Görner K., (2011), Kinetic study on promoted potassium carbonate solutions for CO₂ capture from flue gas, *Energy Procedia*, **4**, 85-92.
- Biard P.F., Couvert A., (2013), Overview of mass transfer enhancement factor determination for acidic and basic compounds absorption in water, *Chemical Engineering Journal*, **222**, 444-453.
- Bucur R., Harja M., (2012), Homogeneous areas delimitation by considering the energy demand for plants growing in covered spaces, *Environmental Engineering and Management Journal*, **11**, 253-257.
- Cai X., Zheng J.L., Wärnå J., Salmi T., Taouk B., Leveneu S., (2017), Influence of gas-liquid mass transfer on kinetic modeling: Carbonation of epoxidized vegetable oils, *Chemical Engineering Journal*, **313**, 1168-1183.
- Dankwerts P.V., (1955), Gas absorption accompanied by chemical reaction, *AIChE Journal*, **1**, 456-463.
- Favier L., Simion A.I., Matei E., Grigoras C.G., Kadmi Y., Bouzaza A., (2016a), Photocatalytic oxidation of a hazardous phenolic compound over TiO₂ in a batch system, *Environmental Engineering and Management Journal*, **15**, 1059-1067.
- Favier L., Harja M., Simion A.I., Kadmi Y., Pacala M.L., Rusu L., Bouzaza A., (2016b), Advanced oxidation process for the removal of chlorinated phenols in aqueous suspensions, *Journal of Environmental Protection and Ecology*, **17**, 1132-1141.
- Gaspar J., Fosbøl P.L., (2015), A general enhancement factor model for absorption and desorption systems: A CO₂ capture case-study, *Chemical Engineering Science*, **138**, 203-215.
- Ge Z., Wan H.F., Zhong J., Zhao C.Y., Wei Y.S., Zheng J.X., Wu Y.L., Han S.H., Zheng B.F., (2016), Emission of CH₄, N₂O and NH₃ from vegetable field fertilized with animal manure composts, *Environmental Engineering and Management Journal*, **15**, 2205-2213.
- Hagiu C., Ivaniciuc M., (1997), Determination of the enhancement factor for CO₂ absorption in activated potassium carbonate solution, *Revista de Chimie*, **10-11**, 856-862.
- Harja M., Szep Al., (2013), *Solid-Fluid Non-Catalytic Heterogeneous Processes*, Ecozone Publishing House, Iasi, Romania.
- Harja M., Rusu L., Barbuta M., (2008), The viscosity and density of the aqueous solutions used for the absorption accompanied by chemical reaction, *The Bulletin of the Polytechnic Institute of Iasi. Chemistry and Chemical Engineering Section*, **9**, 55-62.
- Higbie R., (1935), The rate of absorption of a pure gas into still liquid during short periods of exposure, *Transaction of the American Institute of Chemical Engineers*, **31**, 365-389.
- Ivaniciuc M., (1999), *Contributions to the modeling of gas-liquid absorption with chemical reaction*, PhD Thesis,

- “Gheorghe Asachi” Technical University of Iasi, Romania.
- Ivaniciuc M., Siminiceanu I., (2000), Modelling and simulation of the industrial reactor for carbon dioxide absorption into activated potassium carbonate aqueous solution, *Ovidius University Annals of Chemistry*, **XI**, 135-137.
- Jongartklang N., Chanchairoek S., Piumsomboon P., Chalermssinsuwan B., (2016), Correlations of kinetic parameters with various system operating conditions for CO₂ sorption using K₂CO₃/Al₂O₃ solid sorbent in a fixed/fluidized bed reactor, *Journal of Environmental Chemical Engineering*, **4**, 1938-1947.
- Kenig E.Y., Kucka L., Górak A., (2003), Rigorous modeling of reactive absorption processes, *Chemical Engineering Technology*, **26**, 631-646.
- Koronaki I.P., Prentza L., Papaefthimiou V., (2015), Modeling of CO₂ capture via chemical absorption processes: An extensive literature review, *Renewable and Sustainable Energy Reviews*, **50**, 547-566.
- Molga E.J., Westerterp K.R., (2013), *Principles of Chemical Reaction Engineering*, Ullmann's Encyclopedia of Industrial Chemistry, Wiley-VCH Verlag GmbH & Co. KGaA.
- Morsi B., Basha O., (2015), *Mass Transfer in Multiphase Systems*, In: *Mass Transfer - Advancement in Process Modelling*, Solecki M. (Ed.), Intec, Rijeka, Croatia, 189-217.
- Noeres C., Kenig E., Gorak A., (2003), Modelling of reactive separation processes: reactive absorption and reactive distillation, *Chemical Engineering and Processing: Process Intensification*, **42**, 157-178.
- Petrescu S., Mămăligă I., Ivaniciuc M., (1998), Enhancement factor of the mass transfer for chemical adsorption process, *Revista de Chimie*, **1**, 64-67.
- Petrescu S., Harja M., (2006), *Chemical Reactor for Heterogeneous Systems*, Venus Publishing House, Iasi, Romania.
- Qin J.Y., Xie J.L., Fu D., (2016), *Absorption Rate of CO₂ in DEA Promoted K₂CO₃ Solution at High Temperatures*, International Conference on Civil, Transportation and Environment, China, 1160-1164.
- Ramazani R., Mazinani S., Hafizi A., Jahanmiri A., Van der Bruggen B., Darvishmanesh S., (2016), Solubility and absorption rate enhancement of CO₂ in K₂CO₃, *Separation Science and Technology*, **51**, 327-338.
- Roustan M., (2003), *Gas-Liquid Transfer in the Treatment of Water and Gaseous Effluents*, Lavoisier, Paris.
- Su L., Li X., Gao H., Zhao L., Liu F., (2016), Emission characteristics of double swirl combustion system for a diesel engine, *Environmental Engineering and Management Journal*, **15**, 1611-1616.
- Szep Al., Harja M., (2007), Study of the absorption of sulfur dioxide in residual calcium carbonate slurries, *Revista de Chimie*, **10**, 870-874.
- Tan L.S., Shariff A.M., Lau K.K., Bustam M.A., (2012), Factors affecting CO₂ absorption efficiency in packed column: A review, *Journal of Industrial and Engineering Chemistry*, **18**, 1874-1883.
- Wang E., Xing L., Wu G., Guan Y., (2016), Nitrous oxide emission during nitrification of influents with different ammonium concentrations, *Environmental Engineering and Management Journal*, **15**, 19-25.
- Yildirim Ö., Kiss A. A., Hüser N., Leßmann K., Kenig E.Y., (2012), Reactive absorption in chemical process industry: A review on current activities, *Chemical Engineering Journal*, **213**, 371-391.
- Zhao W.L., Buffo A., Alopaeus V., Han B., Louhi-Kultanen M., (2017), Application of the compartmental model to the gas-liquid precipitation of CO₂-Ca(OH)₂ aqueous system in a stirred tank, *AIChE Journal*, **63**, 378-386.



“Gheorghe Asachi” Technical University of Iasi, Romania



MULTIPLE LINEAR REGRESSION (MLR) MODELS USED TO PREDICT THE THERMAL STABILITY OF SOME POLYIMIDES

Cătălin Lisa^{1*}, Corneliu Hamciuc², Elena Hamciuc², Gabriela Lisa¹

¹“Gheorghe Asachi” Technical University, Iasi, Faculty of Chemical Engineering and Environmental Protection “Cristofor Simionescu”, 73 Prof.dr.doc. Dimitrie Mangeron, 700050 Iasi, Romania

²“Petru Poni” Institute of Macromolecular Chemistry, Aleea Gr. Ghica Voda 41A, 700487 Iasi, Romania

Abstract

Two multiple linear regression (MLR) models were developed with the aim to estimate the decomposition temperature of a series of polyimides. Two parameters, T_{ni} and T_{ai} , corresponding to the temperature of 10 % weight loss of the sample, determined by dynamic thermogravimetric analysis under conditions of N_2 inert atmosphere and air, respectively, were used as a criterion for thermal stability. The obtained MLR models correlate thermostability with a series of characteristics of the studied polymers, such as Van der Waals volume, density, molecular weight, number of aromatic cycles, number of C=O bonds, number of CH_3 groups and the number of CF_3 groups. The results showed that the MLR models can be successfully used to predict the thermal stability of polyimides, the mean percentage errors being below 3%, regardless of the work environment.

Key words: MLR models, polyimides, prediction, thermal stability

Received: May, 2017; *Revised final:* February, 2018; *Accepted:* March, 2018; *Published in final edited form:* April 2018

1. Introduction

Polyimides are performance materials used in various fields, such as: microelectronics (Cha et al., 1996; Hokazono et al., 2014; Olariu et al., 2017; Park et al., 2012), aerospace (Yu et al., 2004), automotive industry (Yano et al., 1997), environmental protection (Bi et al., 2010; Li et al., 2004; Xiao et al., 2005), in obtaining biofuel (Ong et al., 2012), as well as in medicine, in the treatment of neurological disorders (Chen et al., 2009). Many of the practical applications of polyimides are a consequence of their special properties, namely: high thermal stability, good processability and mechanical properties, fire and wear resistance, high glass transition temperature, low dielectric constants and high chemical resistance. All these properties turn them into good insulators, widely used as dielectric layers manufacturing semiconductor chips and multichip packaging structures (Lisa et al.,

2009). However, there are certain limits that restrict their use in actual practice, encouraging further research in the field for the purpose of developing new materials as well as improving existing materials (Lisa et al., 2009). This study follows the same direction of research. As it has already been mentioned, one of the most important properties of polyimides is their high thermal stability. Certain types of polyimides are the only commercially available polymers that can withstand temperatures above 400°C (Lisa et al., 2009). In a previous study, with the help of various types of neural networks, Lisa et al. determined the relationship between structure and thermostability for a series of polyimides and demonstrated that neural networks offer the possibility to replace experiments with estimations (Lisa et al., 2009). An alternative to applying neural models is the statistical processing of experimental data using the multiple linear regression method (MLR).

*Author to whom all correspondence should be addressed: e-mail: clisa@ch.tuiasi.ro; Phone: +40232278683; Fax: +40232271311

The advantage of MLR models stands in their simplicity and ease with which they can be applied by other researchers as well in the possibility to estimate various properties (Lisa et al., 2015). Fayet et al. (Fayet et al., 2009; Fayet et al., 2010) used the quantitative structure-property relationship (QSPR) methodology to predict the thermal stability of a number of 22 nitroaromatic derivatives, while Lu et al., (2011) used it to study the thermal decomposition of 16 organic peroxides. Decomposition enthalpy, or T_{onset} temperature, experimentally determined by differential scanning calorimetry (DSC), were used as indicators of thermal stability for these compounds. The semi-empirical models containing equations with three or more parameters obtained by these authors offer a good correlation between the calculated values and those experimentally determined, correlation coefficients being above 0.9.

Pucci et al. (2016) used both neural and MLR models to predict the melting temperature (T_m) of the wild-type protein. The root-mean-square deviation between the values calculated using the models obtained and the experimental ones for ΔT_m is reduced from 4.2°C to 2.9°C when the authors eliminate 10% of the abnormal values. MRL models have been successfully used by researchers in the field of environmental protection, as well. Mokarram (2016) used such models for the prediction of groundwater quality, while Cemek et al. (2016) used them for the prediction of nutrient concentrations in runoff from feedlots to facilitate management practices.

Recently, He et al. (2018) compared the performance of two different models: MLR and support vector machine (SVM) designed to determine the self-accelerating decomposition temperature (SADT) for a series of organic peroxides. SADT is an important parameter for the description of the thermal hazard of organic peroxides in process industries. The average absolute error obtained with the MLR model is approximately 8.5°C, while with SVM it is 8.1°C.

In this paper, the experimental data referring to various polyimides were statistically processed using the *SigmaPlot 11.2* software. Multilinear regressions between the parameters that characterize thermostability (T_{ni} or T_{ai}) and molecular descriptors (Van der Waals volume, density, molecular weight, number of aromatic cycles, number of C=O bonds, number of CH₃ groups and the number of CF₃ groups) were obtained. The results were comparable with previous ones (Lisa et al., 2009) obtained by modelling with the help of neural networks. However, the advantage of the MLR models is the ease with which they can be applied by other researchers to predict the thermal stability of polyimides.

2. Data and methodology

2.1. Data

The used database contains information regarding the thermal stability of a number of 54 polyimides with a wide structural variety (Lisa et al.,

2009). Some of the analysed polyimide structures are selectively in Table 1.

2.2. Methodology

The *Multiple Linear Regression (MLR)* module of the *SigmaPlot 11.2* software allows to develop models of the following type: Property = f (characteristics). The models obtained have the following form: $Y = A_0 + A_1X_1 + A_2X_2 + \dots + A_nX_n$ where Y is the modelled property – *dependent variable*, X_i are characteristics of the systems – *independent variables* and A_i are coefficients of the models. Apart from the possibility to obtain MLR models, this software also allows to carry out a rigorous analysis of their performances.

With the help of the *Materials Studio 4.0 – Accelrys* software, various molecular descriptors were calculated and selected to study the relationship between structure and thermostability for polyimides. The Open Force Field (OFF) module was used to simulate properties. This uses a polymer consistent force field (PCFF) parameterized for a wide variety of organic compounds, for biopolymers and synthetic polymers. Moreover, the 15.5 Å cut-off parameter was used to estimate remote interactions. The load distribution, due to Coulomb-type interactions, was estimated using the Rappe-Goddard method. The molecular dynamics calculations (MD) were done at 298 K for every simulated structure, using the isothermal and isochoric ensemble (NVT) module. The simulation times used for MD-NVT were of 500 - 1000 ps, depending on the size of the investigated system (frequency of up to 2000 steps).

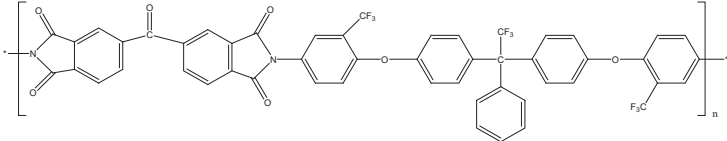
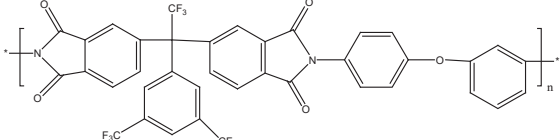
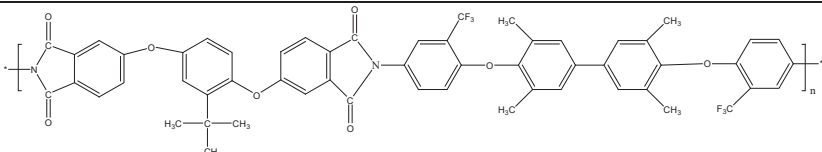
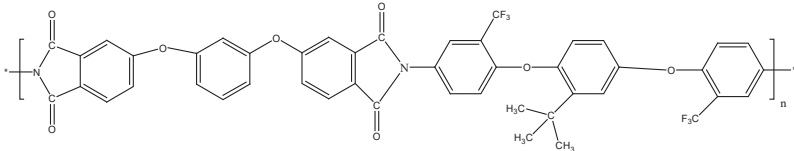
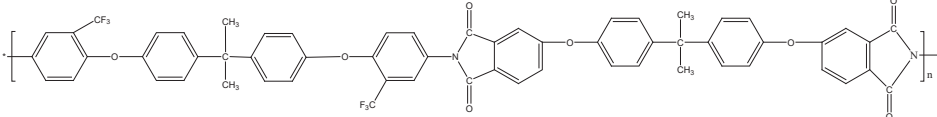
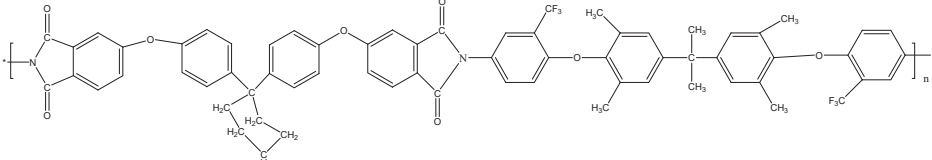
The following molecular descriptors obtained using the *Synthia* model of the *Materials Studio* software: Van der Waals volume - **V**, density - **D**, molecular weight - **M**, and a series of structural parameters, such as: number of aromatic cycles - **N_{ac}**, number of C=O bonds - **N_{C=O}**, number of CH₃ - **N_{CH3}** groups and the number of CF₃ - **N_{CF3}** groups, were selected as *independent variables* in the MLR models.

The temperatures at which 10% of the initial amount of the sample subjected to a thermal degradation process was lost under an inert atmosphere of N₂ (T_{ni}) and air (T_{ai}) were used as a criterion for thermal stability (*dependent variables*) by the built MLR models.

3. Results and discussion

With the help of the *Materials Studio* software, the optimized structures for the 54 analysed polyimides were obtained, and molecular descriptors were determined on this basis. Table 2 presents, for some of the studied polyimides, the optimized structures, the molecular descriptors selected as *independent variables* in MLR models, and the *dependent variables* quantifying thermal stability, respectively, the temperature at which, following degradation, 10% of the initial amount of the sample subjected to analysis under an inert atmosphere of N₂ (T_{ni}) and air (T_{ai}) is lost.

Table 1. The structure of polyimides whose thermal stability was modelled using the MLR module from the *SigmaPlot 11.2* software package

No.	Chemical structure of the analysed compounds
5.	
13.	
23.	
34.	
45.	
54.	

The values of the Van der Waals volume marked with **V** and those of the molecular weight marked with **M** were normalized. In Figs. 1 and 2, the experimental values for T_{ni} and T_{ai} , as well as the corresponding calculated values using the obtained MLR models are comparatively presented. The mathematical expressions for the MLR models have the form given by Eq. (1):

$$Y(T_{ni} \text{ or } T_{ai}) = A_0 + A_1X_1 + A_2X_2 + A_3X_3 + A_4X_4 + A_5X_5 + A_6X_6 + A_7X_7 \quad (1)$$

where X_1 is $V \times 10^{-3}$; X_2 is **D**; X_3 is $10^6/\mathbf{M}$; X_4 is **N_{ac}**; X_5 is **N_{C=O}**; X_6 is **N_{CH3}**, and X_7 is **N_{CF3}**.

Table 3 shows the values of the constants A_0, A_1, \dots, A_7 and the obtained mean values of the percentage estimation errors ($Ep\%$) (Eq. 2).

$$Ep\% = \left| \frac{(Y_{model} - Y_{experimental}) \cdot 100}{Y_{experimental}} \right| \quad (2)$$

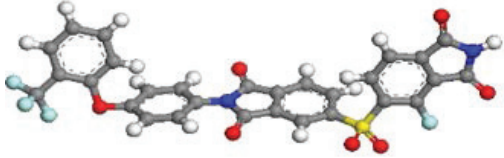
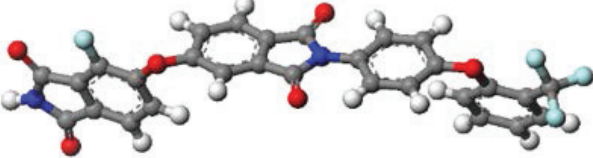
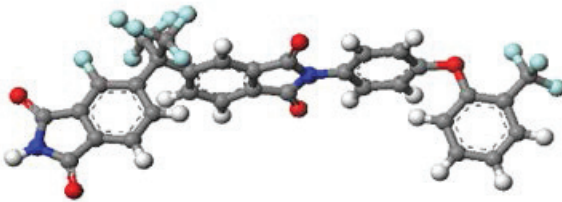
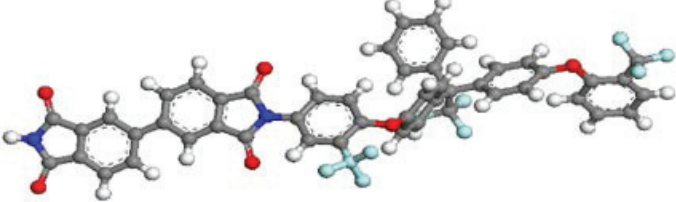
The mean percentage errors are comparable with those reported in a previous study (Lisa et al., 2009) having the same database, but using feed forward neural networks and modular neural networks. The advantage of the two MLR models

developed in this paper consists in the fact that they can be easily used by other researchers in order to estimate the decomposition temperature of a series of polyimides. It was calculated by means of Eq. (3), where n represents the number of experimental data for the two MLR models obtained and the average absolute error. In that way, for T_{ni} we obtained AAM = 12.2°C and for T_{ai} AAM = 10.8°C.

$$AAM = \frac{\sum_{i=1}^n |Y_{model} - Y_{experimental}|}{n} \quad (3)$$

The performances obtained in this work, respectively an average absolute error (AAM) of approximately 11.5°C, for the prediction of the initial decomposition temperature for a series of polyimides by applying MLR models, are comparable to those presented by other researchers in specialized literature. He et al. (2018) obtained, for a larger experimental database, an average absolute error of about 8.5°C for the prediction of the self-accelerating decomposition temperature (SADT) for a series of organic peroxides. They also achieved promising results with the support of a vector machine (SVM) model, i.e. an average absolute error of 8.1°C.

Table 2. Optimized structures of polyimides and values of the *dependent and independent variables* used to obtain the MLR models

Optimized structures	Dependent and independent variables from the MLR models built
	$V \times 10^{-3} = 0.2675$; $D = 1.57$; $10^6/M = 1.873$ $N_{ac} = 4$; $N_{C=O} = 4$; $N_{CH_3} = 0$; $N_{CF_3} = 1$ $T_{ni} = 515^\circ\text{C}$; $T_{ai} = 546^\circ\text{C}$
	$V \times 10^{-3} = 0.2513$; $D = 1.514$; $10^6/M = 2.6596$ $N_{ac} = 4$; $N_{C=O} = 4$; $N_{CH_3} = 0$; $N_{CF_3} = 1$ $T_{ni} = 591^\circ\text{C}$; $T_{ai} = 584^\circ\text{C}$
	$V \times 10^{-3} = 0.2964$; $D = 1.599$; $10^6/M = 1.3193$ $N_{ac} = 4$; $N_{C=O} = 4$; $N_{CH_3} = 0$; $N_{CF_3} = 3$ $T_{ni} = 555^\circ\text{C}$; $T_{ai} = 545^\circ\text{C}$
	$V \times 10^{-3} = 0.4274$; $D = 1.467$; $10^6/M = 5.882$ $N_{ac} = 7$; $N_{C=O} = 4$; $N_{CH_3} = 0$; $N_{CF_3} = 3$ $T_{ni} = 588^\circ\text{C}$; $T_{ai} = 568^\circ\text{C}$

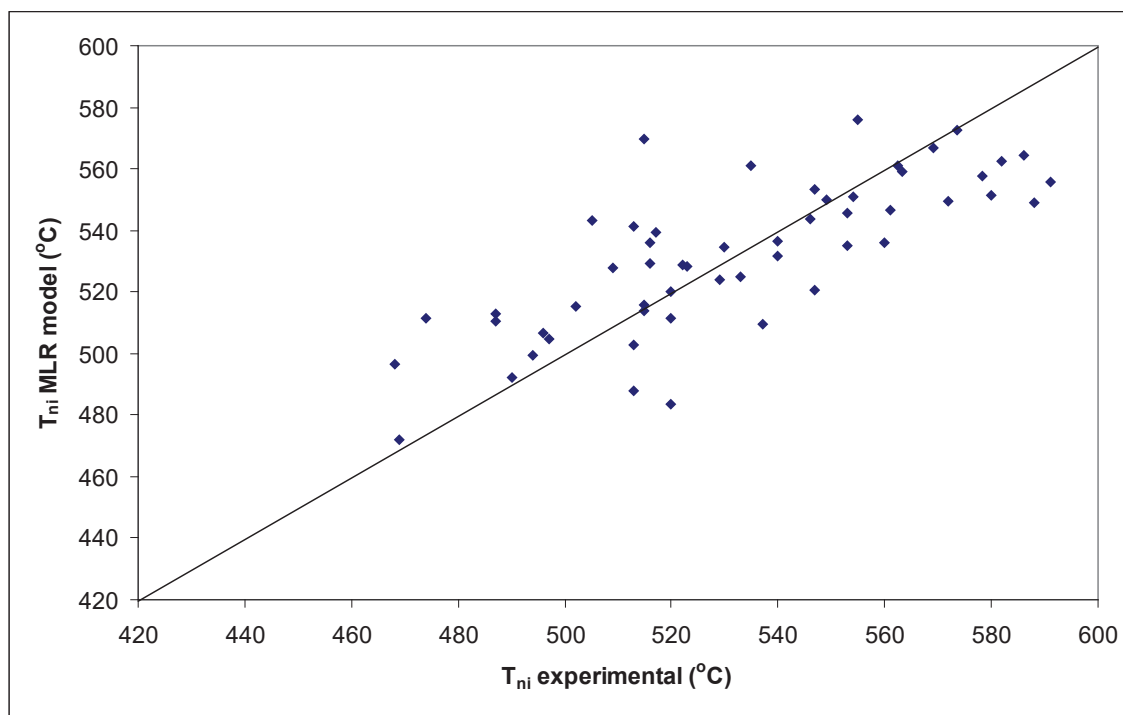


Fig. 1. Comparing the experimental values with those calculated using the MLR model for the temperature at which, following the degradation process, 10% of the initial amount of the sample subjected to analysis under an inert atmosphere of N_2 (T_{ni}) is lost

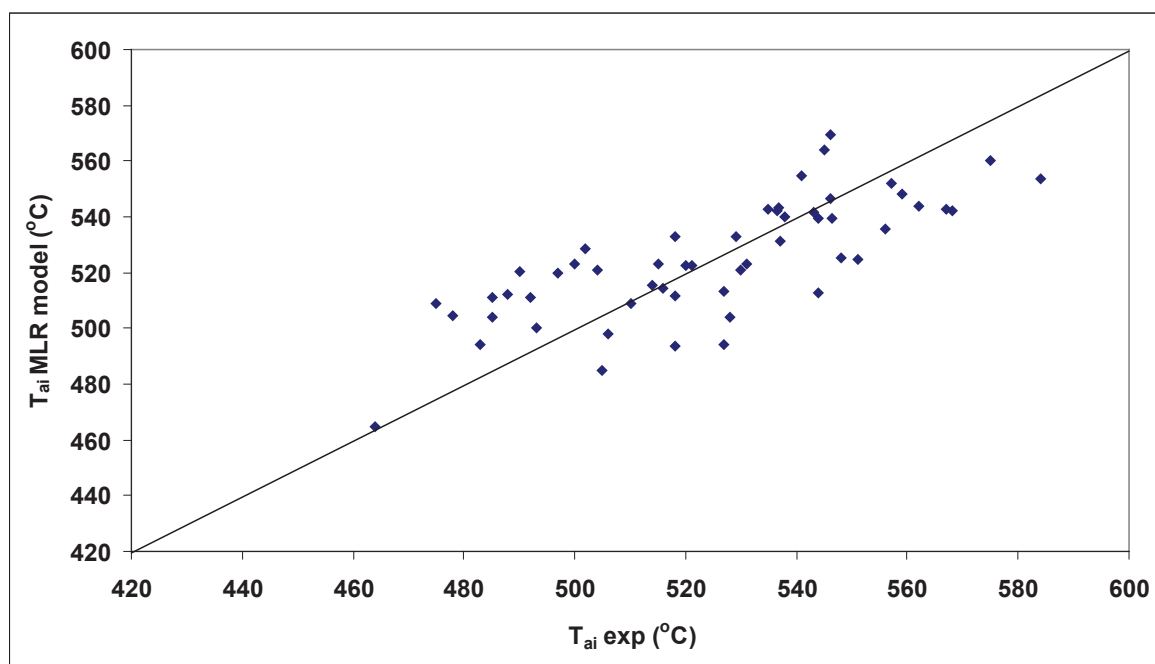


Fig. 2. Comparing the experimental values with those calculated using the MLR model for the temperature at which, following degradation, 10% of the initial amount of the sample subjected to analysis in air (T_{ai}) is lost

Table 3. Parameters of the obtained MLR models

Y	A_0	A_1	A_2	A_3	A_4	A_5	A_6	A_7	Ep (%) average
T_{ni}	212.318	30.674	199.519	-3.374	3.688	7.228	-5.709	-1.293	2.97
T_{ai}	151.559	90.556	239.338	-1.183	1.072	5.845	-4.151	-7.738	2.82

4. Conclusions

The research undertaken in this paper is in line with recent concerns to reduce the number of experimental tests by applying modern methods of modelling to correlate the relationship between structure and properties. Thus, two MLR models were developed to predict the thermal stability of polyimides.

The mean percentage errors estimating the temperature at which, following the degradation process, 10% of the initial amount of the sample subjected to thermogravimetric analysis is lost were below 3%, regardless of work environment.

The advantage of the two MLR models presented here consists in the fact that they can be easily used by other researchers in order to estimate the decomposition temperature of a series of polyimides.

References

- Bi H., Wang J., Chen S., Hu Z., Gao Z., Wang L., Okamoto K., (2010), Preparation and properties of cross-linked sulfonated poly(arylene ether sulfone)/sulfonated polyimide blend membranes for fuel cell application, *Journal of Membrane Science*, **350**, 109-116.
- Cemek B., Rahman S., Rahman A., (2013), Artificial neural network for predicting nutrients concentration in runoff

from beef cattle feedlot, *Environmental Engineering and Management Journal*, **12**, 2385-2396.

- Cha H.J., Hedrick J., DiPietro R.A., Blume T., Beyers R., Yoon D.Y., (1996), Structures and dielectric properties of thin polyimide films with nano-foam morphology, *Applied Physics Letters*, **68**, 1930-1932.
- Chen Y.-Z., Lai H.-S., Lin S.-H., Cho C.-W., Chao W.-H., Liao C.-H., Tsang S., Chen Y.-F., Lin S.-Y., (2009), Design and fabrication of a polyimide-based microelectrode array: Application in neural recording and repeatable electrolytic lesion in rat brain, *Journal of Neuroscience Methods*, **182**, 6-16.
- Fayet G., Rotureau P., Joubert L., Adamo C., (2009), On the prediction of thermal stability of nitroaromatic compounds using quantum chemical calculations, *Journal of Hazardous Materials*, **171**, 845-850.
- Fayet G., Rotureau P., Joubert L., Adamo C., (2010), QSPR modeling of thermal stability of nitroaromatic compounds: DFT vs. AM1 calculated descriptors, *Journal of Molecular Modeling*, **16**, 805-812.
- He P., Pan Y., Jiang J.-c., (2018), Prediction of the self-accelerating decomposition temperature of organic peroxides based on support vector machine, *Procedia Engineering*, **211**, 215-225.
- Hokazono M., Anno H., Toshima N., (2014), Thermoelectric properties and thermal stability of PEDOT: PSS films on a polyimide substrate and application in flexible energy conversion devices, *Journal of Electronic Materials*, **43**, 2196-2201.
- Li Y., Lu Q., Qian X., Zhu Z., Yin J., (2004), Preparation of surface bound silver nanoparticles on polyimide by surface modification method and its application on

- electroless metal deposition, *Applied Surface Science*, **233**, 299-306.
- Lisa C., Lisa G., Curteanu S., (2009), Neural networks used for the prediction of the structure-thermal stability relation, *Revue Roumaine de Chimie*, **54**, 1133-1142.
- Lisa C., Ungureanu M., Cosmațchi P.C., Bolat G., (2015), The density, the refractive index and the adjustment of the excess thermodynamic properties by means of the multiple linear regression method for the ternary system ethylbenzene-octane-propylbenzene, *Thermochimica Acta*, **617**, 76-82.
- Lu Y., Ng D., Mannan M.S., (2011), Prediction of the reactivity hazards for organic peroxides using QSPR approach, *Industrial & Engineering Chemistry Research*, **50**, 1515-1522.
- Mokarram M., (2016), Modeling of multiple regression and multiple linear regressions for prediction of groundwater quality (case study: north of Shiraz), *Modeling Earth Systems and Environment*, **2**, 1-7.
- Olariu M., Hamciuc C., Okrasa L., Hamciuc E., Dimitrov L., Kalvachev Y., (2017), Electrical properties of polyimide composite films containing TiO₂ nanotubes, *Polymer Composites*, **38**, 2584-2593.
- Ong Y.K., Wang H., Chung T.-S., (2012), A prospective study on the application of thermally rearranged acetate-containing polyimide membranes in dehydration of biofuels via pervaporation, *Chemical Engineering Science*, **79**, 41-53.
- Park J.-H., Cho J.-H., Kim S.-B., Kim W.-S., Lee S.-Y., Lee S.-Y., (2012), A novel ion-conductive protection skin based on polyimide gel polymer electrolyte: application to nanoscale coating layer of high voltage LiNi_{1/3}Co_{1/3}Mn_{1/3}O₂ cathode materials for lithium-ion batteries, *Journal of Materials Chemistry*, **22**, 12574-12581.
- Pucci F., Bourgeas R., Rooman M., (2016), Predicting protein thermal stability changes upon point mutations using statistical potentials: Introducing *HoTMuSiC*, *Scientific Reports*, **6**, 23257, 1-9, doi: 10.1038/srep23257.
- Xiao Y., Chung T.-S., Chng M.L., Tamai S., Yamaguchi A., (2005), Structure and properties relationships for aromatic polyimides and their derived carbon membranes: experimental and simulation approaches, *The Journal of Physical Chemistry B*, **109**, 18741-18748.
- Yano K., Usuki A., Okada A., (1997), Synthesis and properties of polyimide-clay hybrid films, *Journal of Polymer Science Part A: Polymer Chemistry*, **35**, 2289-2294.
- Yu Y.-H., Yeh J.-M., Liou S.-J., Chen C.-L., Liaw D.-J., Lu H.-Y., (2004), Preparation and properties of polyimide-clay nanocomposite materials for anticorrosion application, *Journal of Applied Polymer Science*, **92**, 3573-3582.



“Gheorghe Asachi” Technical University of Iasi, Romania



MASS TRANSFER IN SOLID-LIQUID EXTRACTION AT HIGH SOLUTE CONCENTRATIONS

Marcela Popa, Eugenia Teodora Iacob Tudose*, Ioan Mamaliga

“Gheorghe Asachi” Technical University of Iasi, Faculty of Chemical Engineering and Environmental Protection,
Chemical Engineering Department, 73 Prof. dr. docent Dimitrie Mangeron Street, 700050 Iasi, Romania

Abstract

The solid-liquid extraction process and some of its influencing factors such as solid-liquid ratio, temperature and salt initial amount have been investigated. Also, mathematical modeling for mass transfer coefficients calculation was applied.

An inert porous solid material (coal), impregnated with 10% and 20% mass NaCl or 15% and 30% mass CaCl₂, was used. The leaching was conducted in a fixed bed column, in laminar flow. The CaCl₂ impregnated samples were investigated in a column with a height/diameter ratio of 2.5, at 20°C, 30°C, and 40°C and the NaCl samples, in a 4.16 height/diameter ratio column, at 30°C, 40°C, 50°C, 60°C. In both cases, liquid flow rates of 3.8 L/h, 7 L/h, 10.6 L/h, 13.3 L/h were used.

An increase of the extraction degree with the washing liquid flow rate (up to 10.6 L/h) indicated that the solid-liquid ratio is a crucial factor. Temperature increase has a positive influence on the extraction degree.

At the beginning of the process, the salt quantity extracted from the high salt amount sample, using the lowest water flow rate has a similar value to the one extracted from the low salt amount sample, using the highest flow rate. At larger time values ($t > 500$ s), the extraction degree dependence on the liquid flow rate is similar for the high and low salt samples.

Based on the proposed mathematical model, mean time mass transfer coefficient values k_a were calculated and compared to the experimental obtained data.

Key words: diffusion, porous materials, kinetics, liquid- solid extraction, mass transfer coefficient

Received: May, 2017; *Revised final:* February, 2018; *Accepted:* March, 2018; *Published in final edited form:* April 2018

1. Introduction

Studies of a primary separation process of some components from a mixture in a solid matrix subjected to contact with a suitable liquid medium, have found applications in various processes such as metallurgical (Cojocaru et al., 2017; Kim et al., 2009; Nagaphani Kumar et al., 2010; Padilla et al., 2008; Predescu et al., 2017; Sokić et al., 2009; Xu et al., 2010), food, pharmaceutical and cosmetics industries (Bucić-Kojić et al., 2007; Chetan and Rastogi, 2013; Evon et al., 2009; Jerman et al., 2010; Librán et al., 2013; Loginova et al., 2011; Radojkovic et al., 2012; Simeonov and Koleva, 2012; Tzima et al., 2014;

Vázquez et al., 2012; Vítková et al., 2011; Wu et al., 2011), as well as environmental protection and biotechnology (Bucar et al., 2013; Costa et al., 2015; Galvín et al., 2012; Grathwohl and Susset, 2009; Sun et al., 2008; Wijngaard and Brunton, 2010; Wijngaard et al., 2012) or metal recovery (Kumar, 2014).

As a result of the diversity of the applicability areas, there are numerous studies focused on process kinetics, modeling and optimization, and also, on factors that influence the solid-liquid extraction (Bucić-Kojić et al., 2007; Chetan and Rastogi, 2013; Evon et al., 2009; Jerman et al., 2010; Librán et al., 2013; Loginova et al., 2011; Padilla et al., 2008; Radojkovic et al., 2012; Simeonov and Koleva, 2012;

* Author to whom all correspondence should be addressed: e-mail: etudose@ch.tuiasi.ro; Phone: +40 232278683; Fax: +40 232271311

Sokić et al., 2009; Wu et al., 2011). The solid-liquid extraction characterization is difficult due to the high number and type of influencing factors: the form of solid particles, the pore structure and size, the amount of substance to be extracted that varies from particle to particle, but also, during the process, the solid / liquid phase ratio, the type of liquid solvent used, the variation of its concentration, the temperature and the extraction method.

There are good extraction methods for the separation of compounds from ores, but not as effective for the extraction of plant or animal constituents.

In practical terms, there is a great interest in the extraction of higher quantities of the desired compound (solute) in the shortest time period and with reduced costs. Extraction speed is one of the criteria considered when an extraction method is applied (Bucić-Kojić et al., 2007; Radojkovic et al., 2012; Senol and Aydin, 2006). Its value is limited by the mass transfer at the small pores level. The intensity of mass transfer is determined on one hand, by the mass transfer coefficient, the mass transfer area which depends on the form of solid particles, the pore geometry and the contact method and, on the other hand, by a number of other operating factors.

Mathematical modeling allows optimization, simulation and evaluation of mass transfer coefficients and effective diffusion coefficients (Espinoza-Perez et al., 2007; Jokić et al., 2010; Larrard et al., 2010; Nayl et al., 2014; Padilla et al., 2008; Reinheimer et al., 2014; Senol and Aydin, 2006; Tiruta-Barna et al., 2006). Most mathematical models take into account the following stages of solid-liquid extraction process:

- Solvent transfer from the liquid bulk to the surface of the solid;

- Solvent penetration into the solid matrix;
- Liquid phase diffusion in the solid matrix over an increasing distance, depending on the particle shape and porous material structure;
- Solubilization of valuable component from the solid matrix;
- Solute diffusion from the solid phase (intraparticle diffusion);
- Migration of the solute from the liquid surface into the liquid bulk.

This work focuses on the experimental results obtained for the CaCl₂ and, respectively, NaCl extraction from a porous carbon matrix, using demineralized water as a solvent.

The research aim was to investigate some extraction influencing factors such as the rate and the extent of extraction, the temperature, the solid / liquid ratio and the initial amount of salt in the solid sample. A self designed set-up, with a fixed bed column, was used to obtain experimental data and use them to perform process optimization using mathematical modeling and calculate the mass transfer coefficients.

2. Material and methods

The solid-liquid extraction in a fixed bed was investigated using an experimental set-up, presented in Fig. 1, consisting of a thermoresistant glass column (1) with an inner diameter of 0.036 m and total height of 0.2 m. The column has a thermo-resistant glass mantle (1a) for the heating liquid (20-60°C). The fixed bed (1c), which contains the sample to be extracted, is made from active charcoal particles with $d = 3.0$ mm and $l = 3.5$ -4 mm. It is supported by a stainless steel sieve (1b), fixed at the bottom of the column.

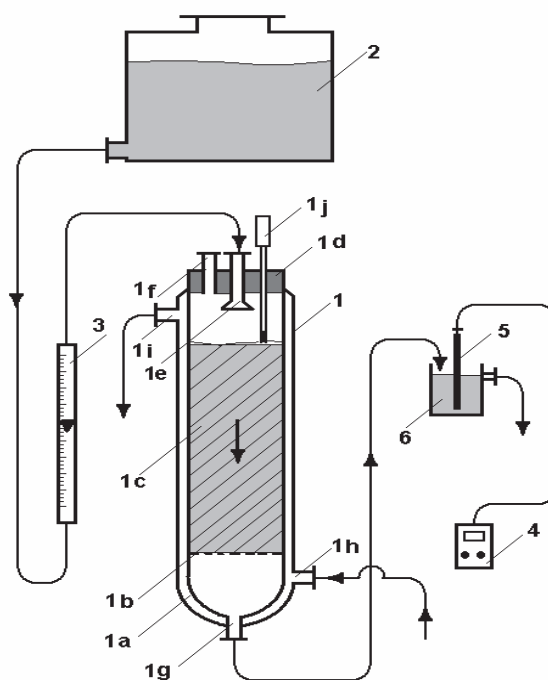


Fig. 1. Experimental set-up

The sample was washed with demineralized fresh water measured using a flowmeter (3). At the column input and output of the liquid phase, the temperatures were measured with digital thermometers with an accuracy of ± 0.1 degrees. At the top, the column is covered with a rubber stopper (1d), provided with three inlets for the solvent distribution (1e), a thermometer (1j) and a connection with the outside (1f). The liquid phase resulting from extraction is removed through the connection located at the bottom of the column (1g). Investigations were conducted at atmospheric pressure. Every 30 seconds, the conductivity of the solution obtained after the solvent passed the porous solid bed, was measured.

Extraction of the solid-liquid in a fixed bed was investigated on charcoal samples in the form of cylindrical granules, impregnated with a solution of CaCl_2 with two concentrations (15% and 30%) and a NaCl solution of 10% and respectively, 20% concentration, resulting in samples with different concentrations of salt (for NaCl : $C_1 = 0.08726$ g NaCl /g coal, $C_2 = 0.151203$ g NaCl /g coal; for CaCl_2 : $C_1 = 0.1334$ g CaCl_2 /g coal, $C_2 = 0.2884$ g CaCl_2 /g coal). The height of the active carbon fixed bed was 90 mm for the calcium chloride - impregnated coal and 150 mm for the sodium chloride - impregnated coal. For samples impregnated with CaCl_2 , three temperature values of 20°C, 30°C and respectively, 40°C were used, the flow of demineralized water was 3.8 L/h, 7 L/h, 10.6 L/h, 13.3 L/h, and the layer height/diameter ratio (H/D) was 2.5. For samples impregnated with NaCl , the investigation was done at 30°C, 40°C, 50°C, 60°C, with flow rates of 3.8 L/h, 7 L/h, 10.6 L/h, 13.3 L/h and the ratio H/D = 4.16.

Mathematical model

The degree of extraction i.e. the leaching degree, defined by the extracted quantity of calcium chloride (which has passed from the solid into the water), related to the calcium chloride mass which was initially in the extracted solid sample, is calculated with the Eq. (1):

$$\eta = \frac{M_v \rho}{m_s^0 x_A} \sum_i \bar{Y}_{Ai} \Delta t_i \quad (1)$$

$$\bar{Y}_{Ai} = \frac{c_{Ai}}{\rho_l - c_{Ai}}$$

where:

The extraction rate i.e. the leaching rate, defined as the calcium chloride mass extracted from the sampling bed unit per unit of time, is given by the Eq. (2):

$$v_e = \frac{M_v (c_{A_{t-I}} - c_{A_i})}{V_{ST}} \quad (2)$$

For the mathematical modeling, the following aspects were taken into consideration:

- the extracted salt diffusion takes place according to the second Fick's law (see Eq. 3),

$$N_A = k \cdot A (c_A^* - c_A) = k \cdot a \cdot V_{ST} (c_A^* - c_A) \quad (3)$$

where:

- mass transfer surface was written as a product between the specific area, a , and the solid bed volume, V_{ST} ;
- particles retain their shape and size;
- all particles have the same specific surface;
- the liquid flow is laminar;
- the transfer surface is perfectly wetted by the liquid;
- the salt concentration is the same at any point in the liquid phase.

The transferred flux can be expressed also as a minute solute concentration time variation over the bed volume, as in the Eq. (4):

$$\frac{V_{ST} dc_A}{dt} = N_A = kA(c_A^* - c_A) \quad (4)$$

Integrating the Eq. (4), between the limits $t = 0$; $c_A = c_{A0}$ and $t = t$; $c_A = c_A$,

$$\int_{c_{A0}}^{c_A} \frac{dc_A}{(c_A^* - c_A)} = k \frac{A}{V_{ST}} \int_0^t dt \quad (5)$$

The solid-liquid extraction mathematical model is attained (Eq. 6):

$$\ln(c_A^* - c_A) = -\frac{kA}{V_{ST}} t + \ln(c_A^* - c_{A0}) = -k \cdot a \cdot t + \ln(c_A^* - c_{A0}) \quad (6)$$

According to the Eq. (6), when a representation of $\ln(c_A - c_A^*)$ as a function of t was performed, the obtained slope, $tg\alpha$, is given by the Eq. (7),

$$tg\alpha = k \cdot a \quad (7)$$

and contains the mass transfer coefficient value, k , which can be expressed, based on the Eq. (6), using the Eq. (8):

$$k \cdot a = \frac{1}{t} \ln \frac{(c_A^* - c_{A0})}{(c_A^* - c_A)} \quad (8)$$

All variables are presented below:

- η - extraction degree (leaching degree), dimensionless;
- M_v - liquid flow rate (demineralized water) at the entrance in the sampling bed, m^3/s ;
- ρ - demineralized water density, kg/m^3 ;
- m_s^0 - solid mass of the sampling bed at the initial moment, kg ;
- x_A - salt mass fraction from the sampling bed at baseline;

\bar{Y}_{A_i} - salt concentration in the liquid phase at the exit from the bed (kg salt/kg water);
 Δt_i - the period between the two readings, s;
 $c_{A_{i-1}}, c_{A_i}$ - salt concentrations at the bed exit, kg/m³;
 V_{ST} - solid bed volume, m³;
 v_e - extraction rate (leaching rate), kg/m³s;
 ρ_l - density of the liquid phase out of the sampling bed, kg/m³;
 k - mass transfer coefficient, s⁻¹;
 A - mass transfer surface (external and internal of the porous solid particle), m²;
 a - specific surface of the porous solid particles, m²/m³;
 c_A - extracted salt concentration at equilibrium, kg/m³;
 c_{A_i} - extracted salt concentration at the moment i , kg/m³;
 c_{A_0} - extracted salt concentration at the initial moment, kg/m³;
 t - extraction time, s.

3. Results and discussion

3.1. Influence of water flow on extraction degree

The degree of extraction was calculated, using the Eq. (1) for concentration values c_i of the salt in the liquid phase, corresponding to the values of conductivity measured in the discharged liquid from the bottom of the column (1) after passing the sampling bed, using calibration graphs obtained at the experimental temperature.

The calculated extraction degree values, using the Eq. (1), were tabulated and graphically represented. From Figs. 2, 3 and 4 one can observe the

extraction degree increase at the same time with the washing liquid flow rate increase, but at values greater of 10.6 L/h, the liquid flow rate influence on the extracted salt quantity is decreasing, very small differences being recorded for $t > 700$ s at the CaCl₂ extraction, while for the NaCl extraction, the smallest differences are recorded for the first extraction stage ($t < 500$ s). The difference between the values obtained for the extraction degree at 30°C from the coal samples impregnated with 30% CaCl₂ solution is significantly higher compared to the difference between the values obtained for the extraction at 30°C from the coal samples impregnated with the solution of 15% CaCl₂ (Figs. 2 and 3). The extraction degree profile is different, depending on the initial amount of salt from the sample. This could be explained by the way the extraction mechanism is carried out.

In the first stage, at $t < 500$ s (for large flow rate values, even at small time values), the salt is washed from the particle exterior by molecular diffusion and convection, afterwards the salt diffusion begins from within the porous particles towards the outside, in the liquid mass. At this stage, the extraction process is determined by a number of factors such that: the solid-liquid contact manner, the process temperature (through its influence on the density and viscosity of the liquid phase), the liquid phase flow rate and the solid granules form.

For the samples with large initial salt concentration, in the time range of $t = 500 - 1600$ s, the extraction of the largest salt amount, mainly from the large pores, is taking place, after which (at a time longer than 1600 s) the salt extraction from medium and small pores takes place. The medium and small pores extraction is slow and is determined by the solid particles size, porosity and pore shape. For samples with low initial salt concentration, the extraction time for the salt from the large pores is longer.

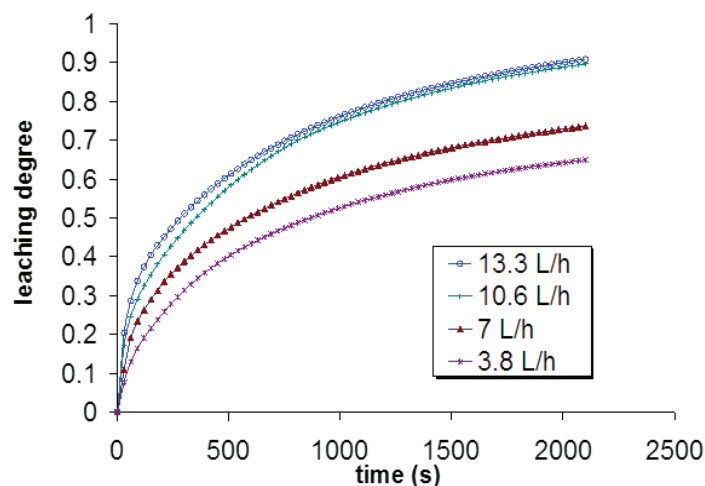


Fig. 2. Extraction degree at 30°C and different liquid flow rates, for the extraction from the samples with CaCl₂ C₂ concentration

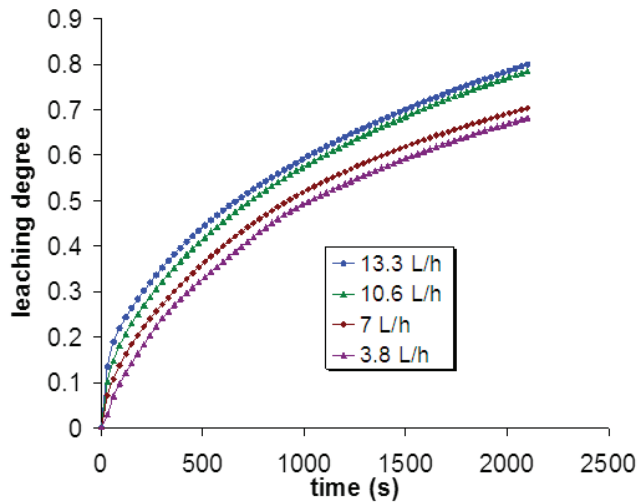


Fig. 3. The extraction degree at a temperature of 30°C and different liquid flow rates, for a CaCl_2 sample concentration

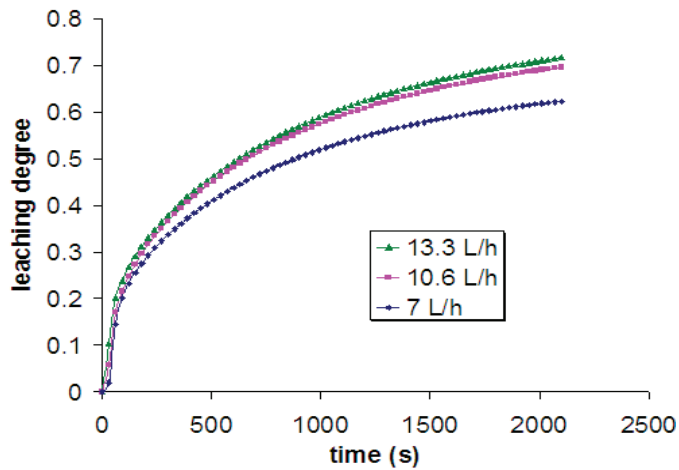


Fig. 4. Extraction degree at a temperature of 40°C and different liquid flow rates for NaCl C_2 sample concentration

The extraction process is completed within a time period slightly larger than 2100 s. The curves profile in Figs. 2, 3 and 4, indicate that the extraction time extent will be much higher for samples with lower initial salt amount. For the NaCl extraction, the extraction curves overlap for the 0-210 s time period which corresponds to the washing stage of porous granules exterior surface. For larger extraction periods, the profiles are similar to the previous ones.

3.2. Influence of temperature on extraction rate

On one hand, temperature increase has a positive influence on the extraction rate due to the washing liquid viscosity decrease, fact that causes an intensification of the particle external diffusion and, on the other hand, due to the increased diffusion coefficient in the solid pores, as one can observe in Fig. 5.

At the largest liquid flow rate (13.3 L/h) one can observe an increase in the extraction degree up to a temperature of 30°C, afterwards, a temperature increase up to 40°C determines a decrease of the

extraction degree (Figs. 6, 7). This could be due to the decreased solid – liquid contact time. A temperature increase causes a stronger diffusion, and, at the same time, a significant decrease in viscosity, which leads to a reduction of the liquid phase - solid granules contact time.

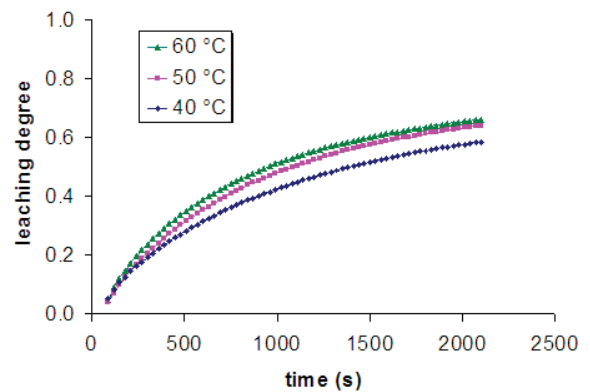


Fig. 5. Extraction degree at a liquid flow rate of 7 L/h and different temperatures for NaCl C_1 sample concentration

As a result of the contact time decrease, the extracted salt amount will be reduced despite the increased diffusion coefficient due to a higher temperature, which suggests that the contact time influence is more important than the one of the diffusion coefficient.

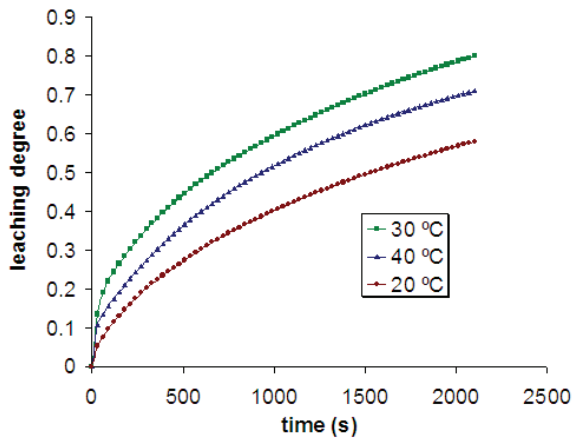


Fig. 6. Extraction degree at 13.3 L/h and three different temperatures, for CaCl_2 C₁ sample concentration

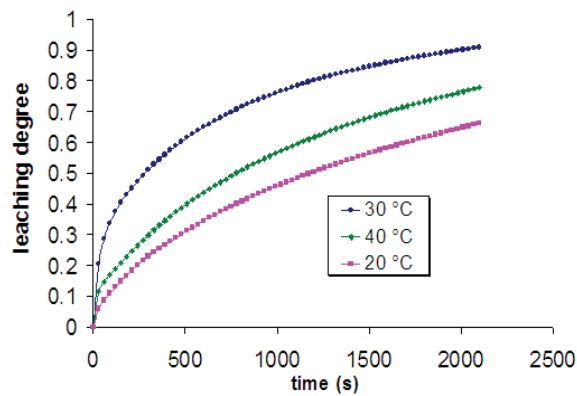


Fig. 7. Extraction degree at different temperatures and 13.3 L/h liquid flowrate, for CaCl_2 C₂ sample concentration

3.3. Influence of the salt amount on extraction degree

Fig. 8 summarizes the extraction degree for the minimum (3.8 L/h) and maximum (13.3 L/h) liquid extraction flow rates during the extraction from the samples containing different amounts of the initial salt.

In the first stage (at small time values) the amount of the extracted salt from the sample richer in salt using a water minimum flow rate is close to the one extracted from the sample with a lower salt amount using a maximum water flow rate. In the second stage (time greater than 500 s) the water flow rate influences the values of the extraction degree in a similar manner for the two samples. Also, the slope of the extraction degree variation with time is higher in samples with greater amount of salt (0.2884 g CaCl_2 /g coal), for the first extraction stage ($t < 500$ s) and decreases in the second stage when compared to the samples with smaller amount of salt (0.1334 g CaCl_2 /g carbon).

From Fig. 9, one can observe that an increase of the amount of NaCl by 1.73 times (for samples impregnated with 10% and 20% NaCl solution, respectively, a mass ratio of 0.08726 g NaCl/g coal and 0.151203 g NaCl/g coal, respectively, was determined) leads to an increase of the extracted salt by 1.3 times, under the same conditions of water flow rate, temperature and extraction time (from the maximum value of 0.4782 for the samples with small amount of NaCl to the maximum value of 0.6236 for higher NaCl concentration samples).

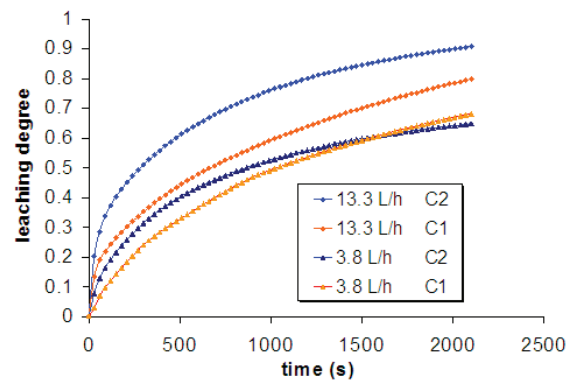


Fig. 8. The extraction degree at 30 °C, at 3.8 L/h and 13.3 L/h liquid flow rates, for CaCl_2 C₁ and C₂ sample concentrations

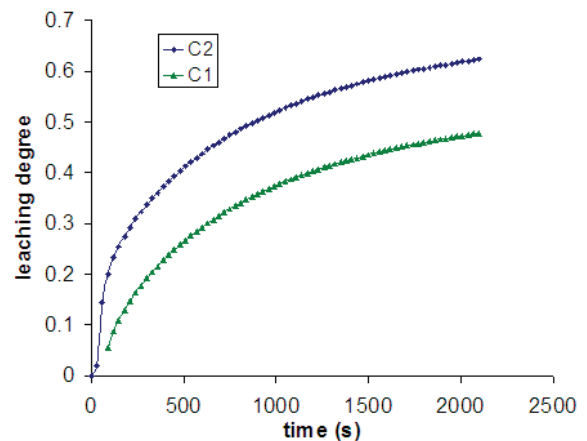


Fig. 9. The extraction degree, for a 7 L/h flow rate and 40 °C, for C₁ and C₂ NaCl sample concentrations

3.4. Influence of the fluid flow on extraction rate

Studying the variation of the extraction rate obtained when the equation (2) is applied to the experimentally determined values, one can observe that it reaches a maximum, at small values of the extraction time, typically within the first 250 s, as seen in Figs. 10, 11. The maximum values are influenced by the demineralized water flow rate used to wash the salt. The higher the flow rate, the greater the peak recorded for the extraction rate. The peak obtained at the beginning of the extraction is tall and narrow for large flow rates and decreases in height, becoming wider, as the flow rate decreases. At larger time values, the flow rate does not significantly influence the rate of extraction.

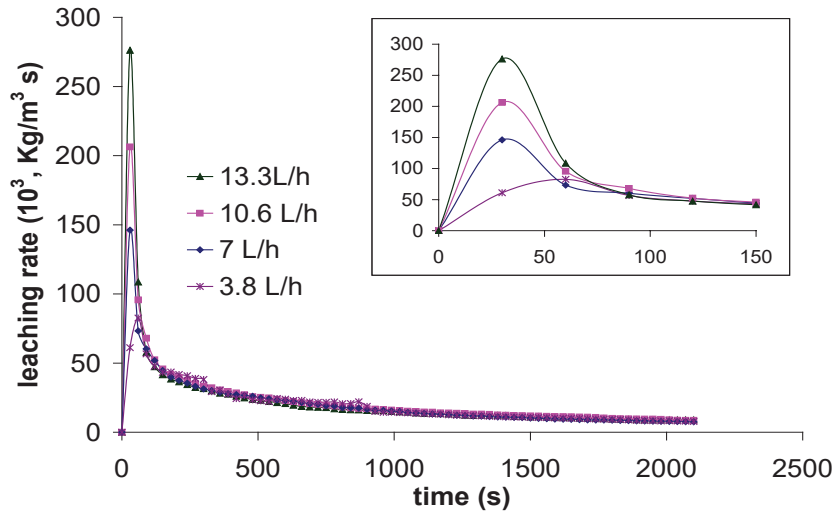


Fig. 10. Extraction rate at 30°C and different liquid flow rates for CaCl_2 C_1 sample concentration

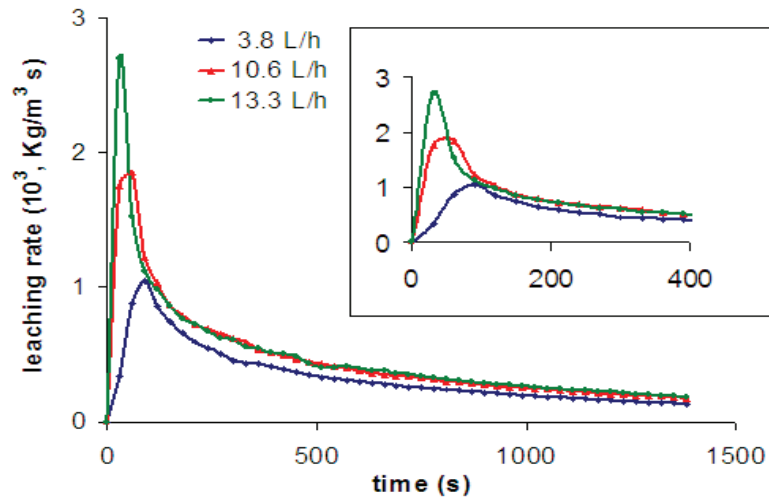


Fig. 11. Extraction rate at 40°C and different flow rates, for the NaCl C_1 sample concentration

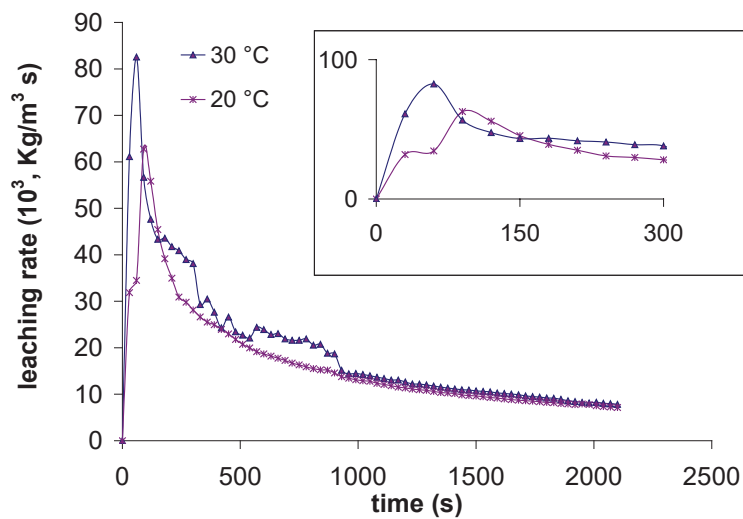


Fig. 12. Extraction rate at small liquid flow rates (3.8 L/h) and different temperatures, for the CaCl_2 C_1 concentration samples

Two stages of extraction can be distinguished:

1. In the first stage, corresponding to a range of 0-500s, the particle is washed on the outside and the process rate is determined by the washing demineralized water flow rate.
2. In the second stage, at times greater than 500 s, the diffusion inside the active carbon particle is decisive for the extraction, such that the liquid phase flow rate value influences to a lesser extent the extraction process rate.

3.5. Influence of temperature on extraction rate

The temperature increase has a double positive influence, on one hand on the liquid viscosity and on the other hand on the diffusion coefficient, both causing an intensification of the extraction process. Thus, the process takes place even at low liquid flow rates, as shown in Fig. 12. At a high flow rate, the extraction process rate is determined by the contact time between the solid - liquid phases, the obtained data rendered an optimum extraction temperature of 30°C, as indicated in Fig. 13.

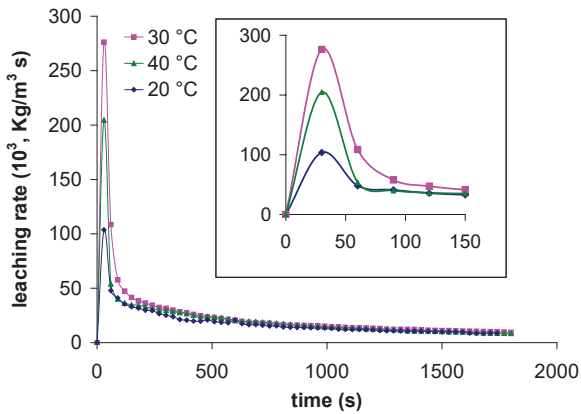


Fig. 13. The extraction rate at 13.3 L/h and different temperatures, for the C₁ CaCl₂ concentration samples

3.6. Variation of extraction rate with sample salt amount

Figs. 14 and 15 show the extraction rate variation with respect to the increase in the initial sample salt amount. For a NaCl sample increase by 1.73, the extraction rate at 40°C increases by 5.12 times, at a flow rate of 3.8 L/h and by 3.91 times, at a flow rate of 10.6 L/h, as shown in Fig. 14. A positive influence of the initial salt amount in the sample on the extraction rate is recorded at CaCl₂ extraction too. In Fig. 15, the CaCl₂ extraction rate, at 30°C, with a flow rate of 13.3 L/h demineralized water, is shown. For a sample salt amount increase by 2.16 times, an increase in the extraction rate by 4.1 times is recorded.

All of the above measurements were performed twice or, for some investigated parameters, even three times, the data reproducibility was very good, with a difference of maximum 1% between two runs of identical parameter values.

To our best knowledge, there is no literature study that investigates the NaCl or CaCl₂ leaching from impregnated coal, at large solute concentrations, thus, we could not render any comparison to other experimental data. However, leaching experiments, performed on other systems (Bouffard and Dixon, 2009; Srithammavut et al., 2011), and the obtained leaching degree/rate curves in time indicate similar behaviors to our study.

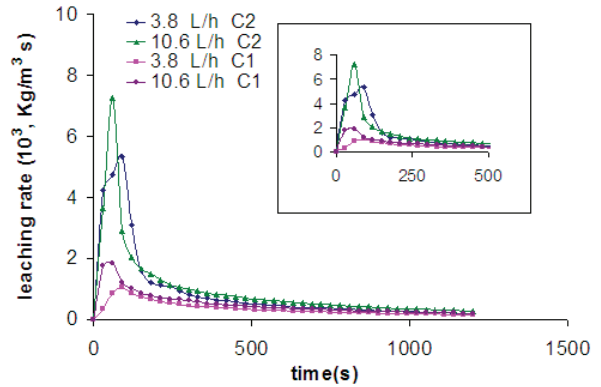


Fig. 14. The extraction rate at 40°C, for different NaCl concentration samples

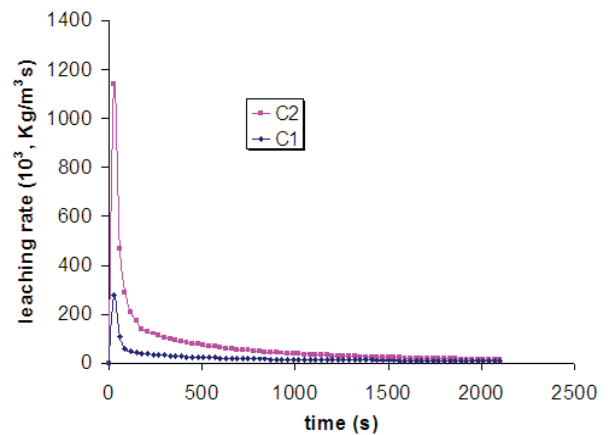


Fig. 15. The extraction rate, at a water flow rate of 13.3 L/h, at 30°C, at different CaCl₂ salt amounts of the samples

3.7. Extraction assessment based on mass transfer coefficient

The extraction process can be assessed by comparing the mass transfer coefficient values, namely the *k*·*a* products. It can be calculated using either the model applied to the current experimental data and proposed by the Eq. (6) or, directly, from the transferred salt flux from the solid particle to the liquid phase, according to the Eq. (9):

$$k \cdot a = \frac{\Delta m_{CaCl_2}}{\Delta t} \cdot \frac{1}{\Delta c_m} \tag{9}$$

where:

$$\Delta c_m = C_{sat} - \sum c_i \tag{10}$$

$$\Delta m_{CaCl_2} = M_v \Delta t \cdot \sum c_i - M_v \Delta t \cdot \sum c_{i-1} \quad (11)$$

3.7.1. Mass transfer coefficient for a $C_1=0.1334$ $CaCl_2$ sample concentration, at 30°C

If the mathematical model given by the Eq. (6) is applied and plotted graphically, for the concentration variation in the time interval of 500-2100 seconds, a straight line is obtained. The slopes of the regression lines, for different flow rates, yielded a quantitative assessment of the mass transfer coefficients, namely the $k \cdot a$. The $k \cdot a$ product can be also obtained as a ratio between the $CaCl_2$ extracted quantity in a short period of time (30 s) and the average variation of $CaCl_2$ quantity in the sample, at a certain temperature. These values are given in Table 1 and plotted in Fig. 17, for the time interval of 210-2100 seconds, at 30°C.

It was found that the $k \cdot a$ product values fall within $2.7 \cdot 10^{-4} - 7.7 \cdot 10^{-6} \text{ s}^{-1}$ range. The $k \cdot a$ value obtained according to the mathematical model (according to the Eq. 6) falls within this range. Note that this value is an average of the calculated $k \cdot a$ values for the time intervals of 30 s.

The $k \cdot a$ values obtained when the Eq. (9) is applied are higher at small flow rates, however they increase, at all three temperatures, according to the influence exerted by the convective diffusion and the liquid quantity that runs through the sample bed.

In the second stage of the process, the fluid flow does not influence any longer the solute diffusion and as a result, at the end of the interval, the $k \cdot a$ values are close, no matter the liquid flow rate. From Table 1, it is observed that the $k \cdot a$ values calculated based on the Eq. (6), at high flow rates, are very close to the lower limit of the range obtained base on the Eq. (9). This is due to the influence exerted by the internal diffusion on the solute extraction.

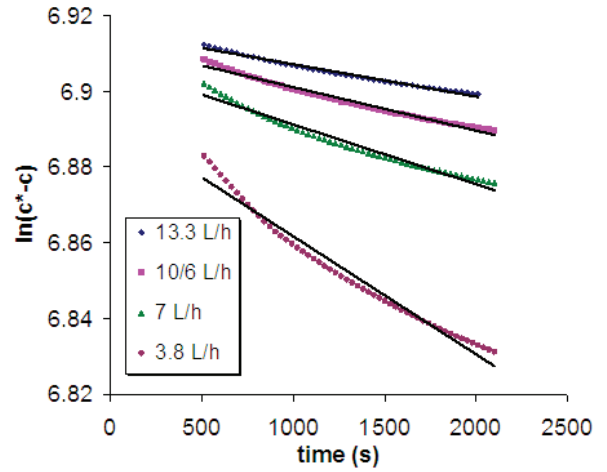


Fig. 16. Mass transfer coefficient at 30°C, small salt sample amount, different flow rates

Table 1. $k \cdot a$ product values for $CaCl_2$, calculated based on the experimental data

$T(^{\circ}C)$	M_v (L/h)	$k \cdot a$ (Eq. 6) (s^{-1})	Trendline equation (Eq. 6)	R^2	$k \cdot a$ (Eq. 9) (s^{-1})
30°C	3.8	$3.11 \cdot 10^{-5}$	$y = -3.11E-05x + 6.89$	0.987	$6.0 \cdot 10^{-5} - 8.4 \cdot 10^{-6}$
	7	$1.58 \cdot 10^{-5}$	$y = -1.58E-05x + 6.91$	0.984	$1.4 \cdot 10^{-4} - 7.7 \cdot 10^{-6}$
	10.6	$1.15 \cdot 10^{-5}$	$y = -1.15E-05x + 6.91$	0.975	$2.1 \cdot 10^{-4} - 8.9 \cdot 10^{-6}$
	13.3	$0.852 \cdot 10^{-5}$	$y = -8.52E-06x + 6.92$	0.975	$2.7 \cdot 10^{-4} - 9.0 \cdot 10^{-6}$
20 °C	3.8	$3.75 \cdot 10^{-5}$	$y = -3.75E-05x + 6.57$	0.984	$4.3 \cdot 10^{-5} - 1.1 \cdot 10^{-5}$
	13.3	$1.2 \cdot 10^{-5}$	$y = -1.20E-05x + 6.61$	0.966	$1.4 \cdot 10^{-4} - 1.1 \cdot 10^{-5}$
40 °C	7	$1.25 \cdot 10^{-5}$	$y = -1.25E-05x + 7.00$	0.985	$1.6 \cdot 10^{-4} - 6.2 \cdot 10^{-6}$
	13.3	$7.56 \cdot 10^{-6}$	$y = -7.56E-06x + 7.01$	0.975	$1.8 \cdot 10^{-4} - 6.5 \cdot 10^{-6}$

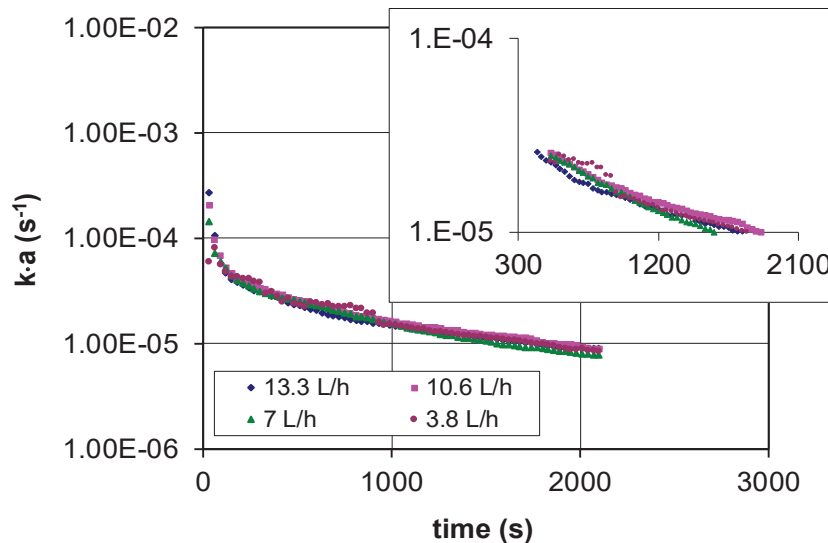


Fig. 17. Mass transfer coefficient $k \cdot a$ for $CaCl_2$ extraction, at 30°C, different liquid flow rates and small sample salt amount, $C_1=0.1334$

Table 2. *k*·*a* values for CaCl₂ calculated based on the experimental data

<i>T</i> (°C)	<i>M</i> , L/h	<i>k</i> · <i>a</i> (Eq. 6)(s ⁻¹)	Trendline equation(Eq. 6)	<i>R</i> ²	<i>k</i> · <i>a</i> (Eq. 9)(s ⁻¹)
20 °C	3.8	2·10 ⁻⁴	$y = -1.89E-04x + 6.14$	0.947	6.5 · 10 ⁻⁴ ÷ 3.0 · 10 ⁻⁵
	7	7.37·10 ⁻⁵	$y = -7.37E-05x + 6.39$	0.962	1.0 · 10 ⁻³ ÷ 3.0 · 10 ⁻⁵
	10.6	4.45·10 ⁻⁵	$y = -4.45E-05x + 6.50$	0.967	1.6 · 10 ⁻³ ÷ 2.8 · 10 ⁻⁵
	13.3	3.21·10 ⁻⁵	$y = -3.21E-05x + 6.53$	0.963	1.6 · 10 ⁻³ ÷ 2.4 · 10 ⁻⁵
30 °C	3.8	6.86·10 ⁻⁵	$y = -6.86E-05x + 6.78$	0.962	4.3 · 10 ⁻⁴ ÷ 1.5 · 10 ⁻⁵
	7	4.16·10 ⁻⁵	$y = -4.16E-05x + 6.83$	0.960	6.8 · 10 ⁻⁴ ÷ 1.7 · 10 ⁻⁵
	10.6	2.73·10 ⁻⁵	$y = -2.73E-05x + 6.85$	0.949	9.5 · 10 ⁻⁴ ÷ 1.5 · 10 ⁻⁵
	13.3	1.90·10 ⁻⁵	$y = -1.90E-05x + 6.86$	0.967	1.1 · 10 ⁻³ ÷ 1.6 · 10 ⁻⁵
40 °C	3.8	6.62·10 ⁻⁵	$y = -6.62E-05x + 6.88$	0.960	2.8 · 10 ⁻⁴ ÷ 1.6 · 10 ⁻⁵
	7	3.43·10 ⁻⁵	$y = -3.43E-05x + 6.93$	0.954	8.9 · 10 ⁻⁴ ÷ 1.3 · 10 ⁻⁵
	10.6	3.16·10 ⁻⁵	$y = -3.16E-05x + 6.87$	0.944	1.1 · 10 ⁻³ ÷ 1.7 · 10 ⁻⁵
	13.3	2.13·10 ⁻⁵	$y = -2.13E-05x + 6.97$	0.954	9.4 · 10 ⁻⁴ ÷ 1.6 · 10 ⁻⁵

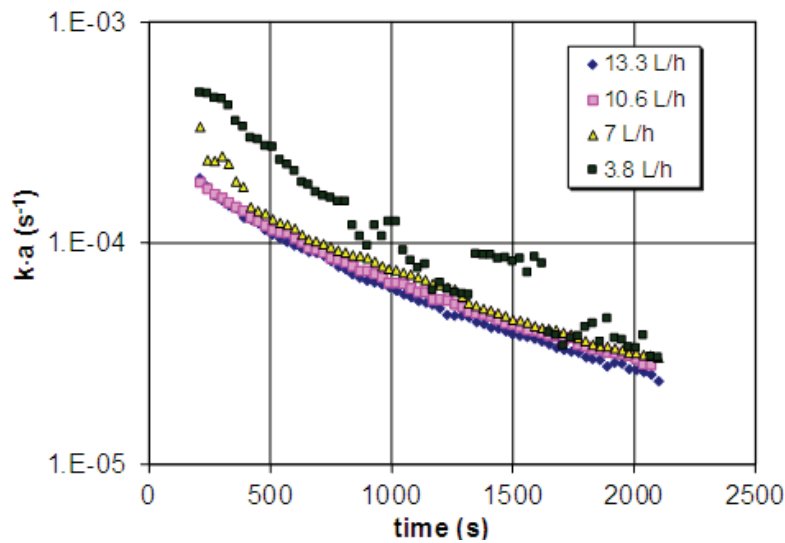


Fig. 18. *k*·*a* for CaCl₂ extraction, at 20°C, different liquid flow rates and large salt sample amount, C₂=0.2884

3.7.2. Mass transfer coefficient for a sample CaCl₂ concentration of C₂ =0.2884, at 20 °C

At 20°C and a CaCl₂ concentration of C₂ = 0.2884, at t>100 seconds, the mass transfer coefficient determined as the *k*·*a* product (Eq. 6), at different flow rates of 3.8 L/h, 7 L/h, 10.6 L/h, 13.3 L/h, takes values in the range of 2·10⁻⁴ - 7.37 · 10⁻⁵ s⁻¹. These values are consistent with those calculated for the *k*·*a* product using the Eq. (9), which gives values in the range of 1.6·10⁻³ - 3 · 10⁻⁵ (Fig. 18).

At the smallest flow rate (3.8 L/h), the *k*·*a* product has a much higher value than for the other three flow rates. At higher flow rates, the mass transfer coefficient values are quite close. For temperatures of 30°C and 40°C and t<1200 seconds, the *k*·*a* product values are dispersed. Looking at the data presented in Table 2, one can observe that the *k*·*a* values, obtained using the Eq. (9), are almost similar for the same temperature, with a maximum value at 20°C.

3.7.3. Mass transfer coefficient for different initial sample salt concentrations

According to the results in Fig. 8, (at point C, where an increase of the extraction rate due to an increase of the sample initial CaCl₂ amount was

presented), the values for the *k*·*a* product, shown in Fig. 19, indicate also an intensification in the mass transfer with an increase in the sample salt concentration.

The *k*·*a* product, at a liquid flow rate of 13.3 L/h and 30°C, increases by 7.46 times at t = 210 seconds and only by 1.69 times at t = 2100 s, the decrease being due to the increased internal diffusion contribution to the extraction process. An increase by 1.73 times of the sample NaCl amount leads to an increase by 1.5 - 1.7 times of the mass transfer coefficient, at the same values of the liquid flow rate, temperature and time.

3.7.4. Influence of temperature on mass transfer coefficient

At the same liquid flowrate, the *k*·*a* product increases with the temperature decrease. The increase is larger at higher extraction time periods, as presented in Fig. 21, which is due to the internal diffusion influence.

For NaCl samples, in the first stage (t < 500 s), a higher temperature causes a higher mass transfer coefficient, afterwards its values decrease, as seen in Fig. 22. The temperature influence is particularly clear at time values greater than 700 s.

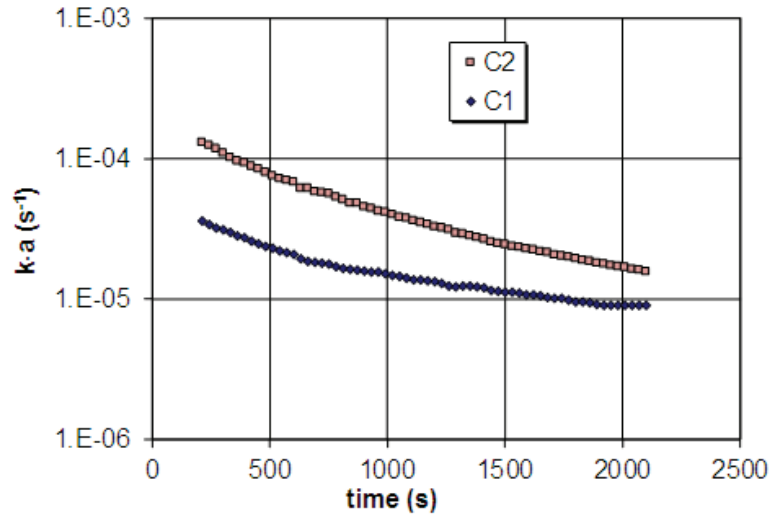


Fig. 19. Mass transfer coefficient, $k \cdot a$, for CaCl₂, at 30°C, 13.3 L/h liquid flow rate, different sample salt concentrations

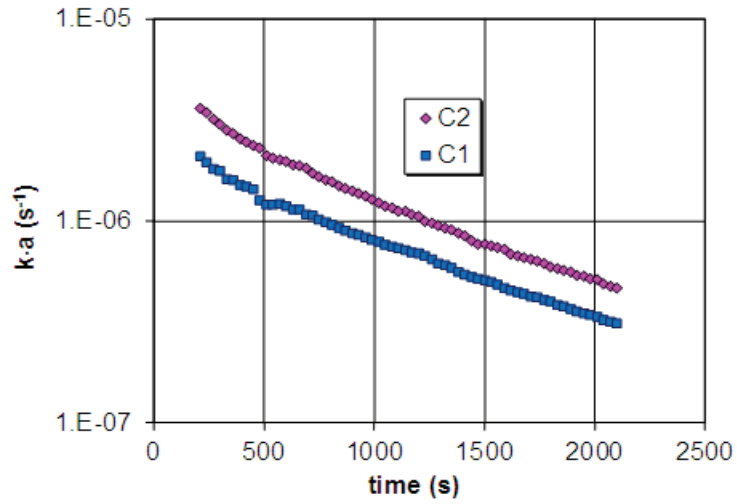


Fig. 20. Mass transfer coefficient, $k \cdot a$, for different sample NaCl concentrations, at 40°C, 13.3 L/h liquid flow rate

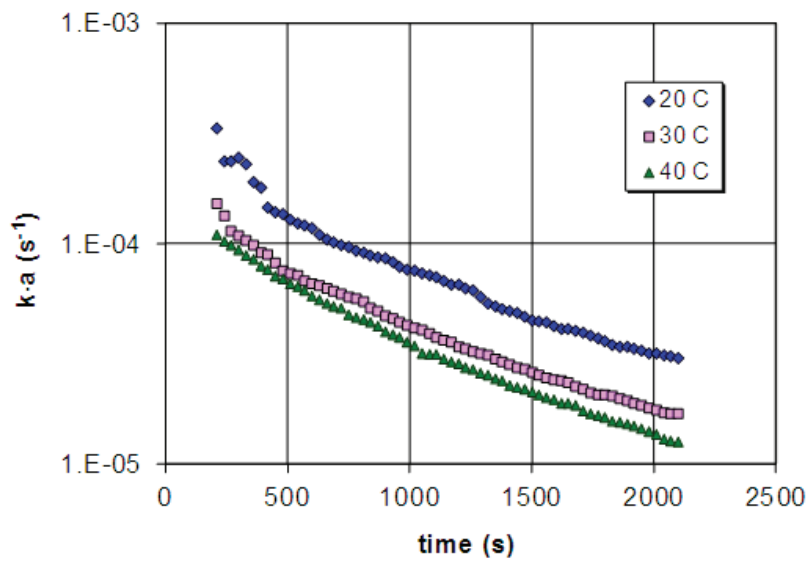


Fig. 21. Mass transfer coefficient, $k \cdot a$, for large CaCl₂ sample amount, at different temperatures, 7 L/h liquid flow rate

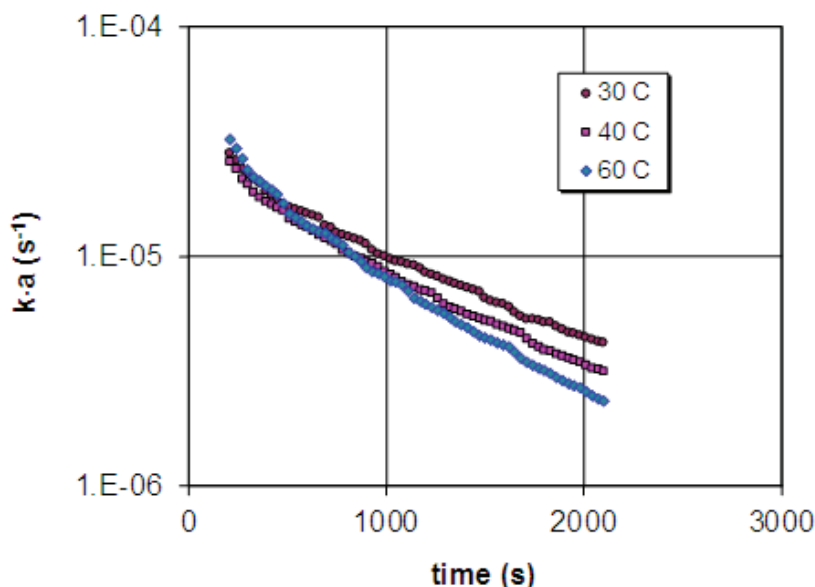


Fig. 22. Mass transfer coefficient, $k \cdot a$, for sample large NaCl amounts, at different temperatures, 7 L/h flow rate

4. Conclusions

The solid-liquid extraction is a complex process, influenced by many factors. Our studies have shown that the liquid flow rate, sample solute amount and temperature are the key factors which determine a particular solute to be obtained. An optimum temperature for the extraction process has been recorded, which could be determined by the decrease of the solid-liquid contact time, although a temperature increase intensifies the diffusion.

The mass transfer coefficient value is difficult to obtain because it is not easy to appreciate the liquid phase - solid granules contact surface. That is why this was estimated by the $k \cdot a$ product, obtained using a mathematical model. The $k \cdot a$ product has been calculated, on one hand, as the average value for the time interval when the extraction is determined by the internal diffusion. On the other hand, the same $k \cdot a$ product was calculated for small time intervals, these values being determined by the temperature and the sample initial salt amount.

The used flow rate value in the extraction has an insignificant influence, the process being determined by the internal diffusion.

References

- Bucar F., Wube A., Schmid M., (2013), Natural product isolation-how to get from biological material to pure compounds, *Natural Product Report*, **30**, 525-545.
- Bucić-Kojić A., Planinić M., Srećko T., Bilić M., Velić D., (2007), Study of solid-liquid extraction kinetics of total polyphenols from grape seeds, *Journal of Food Engineering*, **81**, 236-242.
- Bouffard S.C., Dixon D.G., (2009), Modeling the performance of pyritic biooxidation heaps under various design and operating conditions, *Hydrometallurgy*, **95**, 227-238.
- Chetan N., Rastogi N.K., (2013), Optimization of solid-liquid extraction of phytochemicals from *Garcinia indica* Choisy by response surface methodology, *Food Research International*, **50**, 550-556.
- Cojocaru P., Stătescu F., Biali G., (2017), Quantification of effects produced by the extraction of mineral aggregates towards water bodies, *Environmental Engineering and Management Journal*, **16**, 897-903.
- Costa A.I.G., Queiroz M.E., Neves A., de Sousa F.A., Zambolim L., (2015), Determination of pesticides in lettuce using solid-liquid extraction with low temperature partitioning, *Food Chemistry*, **181**, 64-71.
- Espinoza-Perez J.D., Vargas A., Robles-Olvera V.J., Rodriguez-Jimenes G.C., Garcia-Alvarado M.A., (2007), Mathematical modeling of caffeine kinetic during solid-liquid extraction of coffee beans, *Journal of Food Engineering*, **81**, 72-78.
- Evon P., Vandebossche V., Pontalier P.Y., Rigal L., (2009), Aqueous extraction of residual oil from sunflower press cake using a twin-screw extruder: Feasibility study, *Industrial Crops and Products*, **29**, 455-465.
- Galvín A.P., Ayuso J., Jiménez J.R., Agrela F., (2012), Comparison of batch leaching tests and influence of pH on the release of metals from construction and demolition wastes, *Waste Management*, **32**, 88-95.
- Grathwohl P., Susset B., (2009), Comparison of percolation to batch and sequential leaching tests, *Waste Management*, **29**, 2681-2688.
- Jerman T., Trebše P., Vodopivec M.B., (2010), Ultrasound-assisted solid liquid extraction (USLE) of olive fruit (*Olea europaea*) phenolic compounds, *Food Chemistry*, **123**, 175-182.
- Jokić S., Velić D., Bilić M., Bucić-Kojić A., Planinić M., Srećko T., (2010), Modeling of the process of solid-liquid extraction of total polyphenols from soybeans, *Czech Journal Food Science*, **28**, 206-212.
- Kim H.I., Park K.H., Mishra D., (2009), Influence of sulfuric acid baking on leaching of spent Ni-Mo/Al₂O₃ hydro-processing catalyst, *Hydrometallurgy*, **98**, 192-195.
- Kumar M., Lee J.C., Kim M.S., Jeong J., Yoo K., (2014), Leaching of metals from waste printed circuit boards

- (WPCBs) using sulfuric and nitric acids, *Environmental Engineering and Management Journal*, **13**, 2601-2607.
- Larrard T., Benboudjema F., Colliat J.B., Torrenti J.M., Deleruyelle F., (2010), Concrete calcium leaching at variable temperature, *Computational Materials Science*, **49**, 35-45.
- Librán C.M., Mayor L., Garcia-Castello E. M., Vidal-Brotos D., (2013), Polyphenol extraction from grape wastes: Solvent and pH effect, *Agricultural Sciences*, **4**, 56-62.
- Loginova K.V., Vorobiev E., Bals O., Lebovka N.I., (2011), Pilot study of countercurrent cold and mild heat extraction of sugar from sugar beets, assisted by pulsed electric fields, *Journal of Food Engineering*, **102**, 340-347.
- Nagaphani Kumar B., Radhika S., Reddy B.R., (2010), Solid-liquid extraction of heavy rare-earths from phosphoric acid solutions using Tulsion CH-96 and T-PAR resins, *Chemical Engineering Journal*, **160**, 138-144.
- Nayl A.A., Elkhatab R.A., Badawy S.M., El-Khateeb M., (2014), Acid leaching of mixed spent Li-ion batteries, *Arabian Journal of Chemistry*, **30**, 620-625.
- Padilla G.A., Cisternas L.A., Cueto J.Y., (2008), On the optimization of heap leaching, *Minerals Engineering*, **21**, 673-678.
- Predescu C., Vlad G., Matei E., Predescu A., Sohaciu M., Coman G., (2017), Methods for heavy metals (HM) extraction from sludge samples and their use for soil upgrading, *Environmental Engineering and Management Journal*, **16**, 2469-2474.
- Radojkovic M., Zekovic Z., Jokic S., Vidovic S., Lepojevic Z., Milosevic S., (2012), Optimization of solid-liquid extraction of antioxidants from black mulberry leaves by response surface methodology, *Food Technology & Biotechnology*, **50**, 167-176.
- Reinheimer M.A., Medina J.R., Scenna N.J., Mussati S.F., Freyre M., Pérez G.A., (2014), Mathematical modeling and simulation of soluble protein extraction during leaching process in surimi elaboration, *Journal of Food Engineering*, **120**, 167-174.
- Senol A., Aydin A., (2006), Solid-liquid extraction of caffeine from tea waste using battery type extractor: Process optimization, *Journal of Food Engineering*, **75**, 565-573.
- Simeonov E., Koleva V., (2012), Solid-liquid extraction of tannins from *Geranium Sanguineum L.* - Experimental kinetics and modeling, *Chemical Biochemistry Engineering Quarterly*, **26**, 249-255.
- Sokić M. D., Marković B., Živković D., (2009), Kinetics of chalcopyrite leaching by sodium nitrate in sulphuric acid, *Hydrometallurgy*, **95**, 273-279.
- Sun X., Peng B., Ji Y., Chen J., Li D., (2008), The solid-liquid extraction of yttrium from rare earths by solvent (ionic liquid) impregnated resin coupled with complexing method, *Separation and Purification Technology*, **63**, 61-68.
- Srithammavut W., Luukkanen S., Laari A., Kankaanpää T., Turunen I., (2011), Kinetic modelling of gold leaching and cyanide consumption in intensive cyanidation of refractory gold concentrate, *Journal of the University of Chemical Technology and Metallurgy*, **46**, 181-190.
- Tiruta-Barna L., Fantozzi-Merle C., de Brauer C., Barna R., (2006), Leaching behaviour of low level organic pollutants contained in cement-based materials, *Journal of Hazardous Materials B*, **138**, 331-342.
- Tzima K., Kallithraka S., Kotsieridis Y., Makris D. P., (2014), Kinetic modelling for flavanol extraction from red grape (*Vitis vinifera L.*) pomace using aqueous organic acid solutions, *International Food Research Journal*, **21**, 1919-1924.
- Vázquez G., Fernández-Agulló A., Gómez-Castro C., Freire M.S., Antorrena G., González-Álvarez J., (2012), Response surface optimization of antioxidants extraction from chestnut (*Castanea sativa*), *Industrial Crops and Products*, **35**, 126-134.
- Vítková M., Ettler V., Mihaljevic M., Sebek O., (2011), Effect of sample preparation on contaminant leaching from copper smelting slag, *Journal of Hazardous Materials*, **197**, 417-423.
- Wijngaard H.H., Ballay M., Brunton N., (2012), The optimisation of extraction of antioxidants from potato peel by pressurised liquids, *Food Chemistry*, **133**, 1123-1130.
- Wijngaard H.H., Brunton N., (2010), The optimisation of solid-liquid extraction of antioxidants from apple pomace by response surface methodology, *Journal of Food Engineering*, **96**, 134-140.
- Wu C.R., You-Cheng H., Jin-Cheng L., Li-Wei L., Yung-Ta L., Hui C., (2011), Triterpenoid contents and anti-inflammatory properties of the methanol extracts of *Ligustrum species* leaves, *Molecules*, **16**, 1-15.
- Xu H., Wei C., Li C., Fan G., Deng Z., Li M., Li X., (2010), Sulfuric acid leaching of zinc silicate ore under pressure, *Hydrometallurgy*, **105**, 186-190.



“Gheorghe Asachi” Technical University of Iasi, Romania



VALORIZATION OF MICROALGAL BIOMASS

Alexandra Cristina Blaga¹, Dan Cascaval^{1*}, Lenuta Kloetzer¹, Alexandra Tucaliuc¹,
Anca Irina Galaction²

¹“Gheorghe Asachi” Technical University of Iasi, Faculty of Chemical Engineering and Environmental Protection, Organic, Biochemical and Food Engineering Department, 73 Prof. Dr. Docent Dimitrie Mangeron Street, 700050 Iasi, Romania

²“Grigore T. Popa” University of Medicine and Pharmacy, Faculty of Medical Bioengineering, Biomedical Science Department, 9-13 M. Kogalniceanu Street, 700454 Iasi, Romania

Abstract

Microalgae can be considered as significant sources of sustainable and beneficial biocompounds such as carotenoids, lipids, proteins, polysaccharides, pigments, vitamins etc., with many uses in energy production (biofuels), pharmaceutical, cosmetic and food industries. This class of microorganisms are considered as sustainable feedstock due to some major advantages related to metabolism modulation, faster growth rate compared to plants, no use of terrestrial land. This review will present the most important bioactive compounds founded in microalgae, with high potential impact in industry and the technologies used for cultivation and downstream processes.

Key words: biomass, bioproducts, microalgae, valorisation

Received: May, 2017; *Revised final:* January, 2018; *Accepted:* March, 2018; *Published in final edited form:* April 2018

1. Introduction

Microalgae are a large and very diverse group of photosynthetic microorganisms, characterised by some features, that make them extremely interesting for food, cosmetic, pharmaceutical industries and agriculture, because they have high growth rates, do not require soil or fertilizer and pesticides, they can be grown all the year depending on the climate, have the ability to fix CO₂ with higher rate than the terrestrial plants, and are highly biodegradable (Jankowska et al., 2017; Luangpipat and Chisti, 2017).

Algae are an important resource for numerous natural products used in different industries (Table 1), some with exceptionally high market values: algal biomass of *Chlorella* and *Spirulina* costs about 40 to 50 US-\$/kg for human nutrition or 10 US-\$/kg, for animal feeding and aquaculture; the price of microalgal β-carotene is estimated at 300 to 3000 US-

\$/kg and astaxanthin about 2500 to 7000 US-\$/kg determined by the purity (Koller et al., 2014).

1.1. Growth systems

The chemical composition of algae is very different in its main components (proteins, carbohydrates and lipids), depending on the species (Table 2), availability of nutrients, and environmental factors.

The selection of an appropriate strain of microalgae, which can be used for food, feed, or biofuel production, must take into account several characteristics (Rajauria et al., 2015):

- can be cultivated constantly and continuously either in an open pond or a closed photobioreactor (PBR);
- produces high and constant quantities of desirable bioactive compounds;

*Author to whom all correspondence should be addressed: e-mail: dancasca@tuiasi.ro; Phone: +40 0232 278683/2260; Fax: +40 0232 271311

- survives and grows in spite of seasonal differences and daily climate changes;
- produces biomass at a large scale;
- provides high photosynthetic efficiency and energy conversion rate;
- generates minimal fouling from attachment to the sides or bottom of the production vessel;
- it can be easily harvested and submitted to different methods of extraction (soft or flexible cell walls).

Table 1. Bioactive compounds separated from microalgae (Priyadarshani and Rath, 2012; Raposo et al., 2013)

Product group	Application	Product	Algae
Pigments/ carotenoids	Cosmetics, Food industry, Pigmentation	β-carotene	<i>Dunaliella salina</i> , <i>Nannochloropsis gaditana</i>
		Astaxanthin, Lutein Canthaxanthin	<i>Haematococcus pluvialis</i> , <i>Chlorella vulgaris</i>
Polyunsaturated fatty acids	Food additives	Eicosapentaenoic acid, omega-3, docosahexaenoic acid	<i>Chlorella minutissima</i> , <i>Phaeodactylum tricornutum</i> , <i>Porphyridium cruentum</i>
		Arachidonic acid	<i>Parietochlorisincise</i> , <i>Porphyridium cruentum</i>
		Docosahexanoic acid	<i>Schizochytrium sp.</i>
		γ-Linoleic acid	<i>Arthrospira</i> , <i>Porphyridium</i>
Vitamins	Nutrition	Biotin	<i>Euglena gracilisa</i>
		Vitamin C	<i>Prototheca moriformis</i> , <i>Chlorella vulgaris</i>
		Vitamin B ₁₂	<i>Cylindrospermum sp.</i> , <i>Tolypothrix tenuis</i> , <i>Nostoc muscorum</i> , <i>Spirulina</i>
		Vitamin D ₂	<i>Chlorella sp.</i> , <i>Spirulina</i>
Sterols	Nutrition	Brassicasterol, stigmasterol	<i>I. galbana</i> , <i>Chaetoceros</i> , <i>Skeletonema</i> , <i>P. lutheri</i>
Polysaccharides	Pharmaceuticals	β-glucan, spirulan, homogalactan, (1,4)-D-glucan	<i>Chlorella vulgaris</i> , <i>Spirulina platensis</i> , <i>Gyrodinium impudicum</i> , <i>Porphyridium cruentum</i> , <i>Dunaliella tertiolecta</i>
Enzymes	Nutrition, Pharmaceuticals	Carbonic anhydrase	<i>I. galbana</i> , <i>Amphidinium carterae</i> , <i>Prorocentrum minimum</i>
		Superoxide dismutase (SOD)	<i>P. tricornutum</i> , <i>Porphyridium</i> , <i>Anabaena</i> , <i>Synechococcus</i>

Table 2. Microalgae composition (Priyadarshani et al., 2012; Rajauria et al., 2015)

Microalgae strain	Proteins, % d.w.	Carbohydrates, % d.w.	Lipids, % d.w.
High amounts of proteins			
<i>Synechococcus sp.</i>	73	15	11
<i>Arthrospira maxima</i>	61 – 71	13 – 14	6 – 7
<i>Spirulina platensis</i>	61 – 64	15 – 16	7 – 8
<i>Spirulina maxima</i>	60–71	13–16	6–7
<i>Aphanizomenon flos-aquae</i>	62	23	3
<i>Dunaliella salina</i>	57	32	6
<i>Scenedesmus obliquus</i>	50 – 56	10 – 17	12 – 14
<i>Chlamydomonas reinhardtii</i>	48	17	21
<i>Anabaena cylindrica</i>	43–56	25–30	4–7
<i>Botryococcus braunii</i>	40	2	33
<i>Chlorella pyrenoidosa</i>	57	26	2
<i>Chlorella vulgaris</i>	41–58	12–17	10–22
High amounts of carbohydrates			
<i>Spirogira sp.</i>	6 – 20	33 – 64	11 – 21
<i>Nostoc commune</i>	20.9	55.7	1.2
<i>Porphyridium cruentum</i>	28 – 39	40 – 57	9 – 14
<i>Scenedesmus dimorphus</i>	8 – 18	21 – 52	16 – 40
<i>Navicula sp.</i>	12.7	46.9	31.7
<i>Nitzschia sp.</i>	31.4	36.4	28.5
High amounts of lipids			
<i>Schizochytrium sp.</i>	13.2	19.4	50 – 77
<i>Nannochloropsis sp.</i>	18 – 46	3	31 – 68
<i>Botryococcus braunii</i>	5 – 45	15 – 20	35 – 75
<i>Neochloris oleoabundans</i>	26 – 42	4 – 39	35 – 54

The main nutritional factors that influence the microalgae growth are the C-source, the N-source, the minerals, trace-elements (iron, manganese, molybdenum, nickel) and vitamins, and the manipulation of these factors can increase biomass productivity. In many strains the nitrogen: phosphorus ratio plays a significant role in both biomass and hydrocarbon production, while the trace elements play critical roles in the metabolic pathways involving the utilization of light, nitrogen, phosphorus, and CO₂. Different nutrient concentration (e.g., nitrogen, phosphorus, sulphate, calcium), high salinity, high temperature, light intensity, and alternative sources of organic carbon can induce stress in microalgae cultivation that will increase the accumulation of some compounds but reducing the growth rate simultaneously.

For the production of the bioactive compounds it is important to consider not only microalgae cultivation but also the processes used for separation and purification, both being highly expensive and requiring intensive energy consumption. The microalgae's bioactive compound composition is

strongly influenced by species, location, growing conditions but also by the composition of the culture medium and the conditions used for growth (nutritional stress: reduction of nitrogen or phosphate content in the culture media, the presence of salts, strong light conditions) (Fig. 1) (Raposo et al., 2013; Silva Vaz et al., 2016).

Considering the cultivation systems (Fig. 2), microalgae can be grown in open ponds or open basins (Cheah et al., 2016) and closed photobioreactors with different configurations (Fig. 3), but also in hybrid systems (two types of reactors are used for two different growth stages) currently used in research (pilot and laboratory).

Algae culturing in one of these systems requires analysis of both configurations (Table 3) and selection of the most appropriate one in relation to their properties. Microalgae are able to grow and develop in very different conditions, but in order to obtain high productivity and the consistency of the structure and composition of the bioactive compounds, it is important to have a very good control of the process.

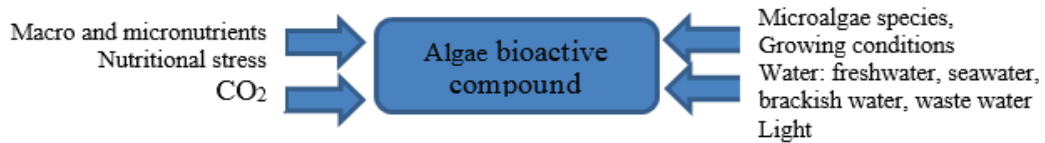


Fig. 1. Factors that influence microalgae growth and composition

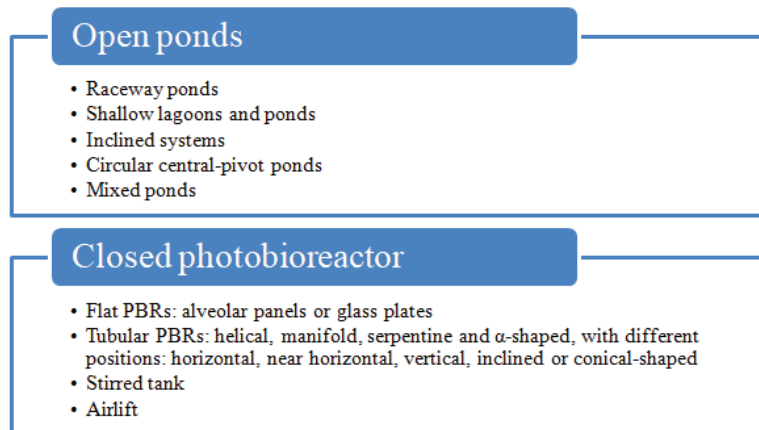


Fig. 2. Main systems for cultivation of microalgae

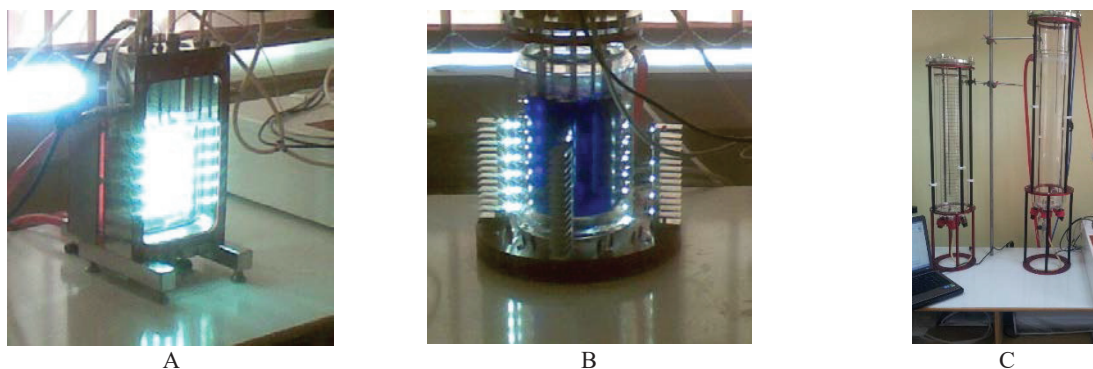


Fig. 3. Closed photobioreactors: A - Flat-vessel; B – Stirred tank; C – Airlift column

Table 3. Comparison between open ponds and closed photobioreactors (Blaga et al., 2016; Cascaval et al., 2007)

Open ponds		Closed photobioreactors (PBRs)	
Advantages	Disadvantages	Advantages	Disadvantages
- lower cost compared to PBRs; - easier to build and to operate than PBRs.	- low productivity; - high contamination risk; - low gas-liquid mass transfer rate; - huge water evaporation; - poor mixing, controllable light penetration; - require large area of land and high harvesting cost.	- low contamination risk; - control and enhancement of gas-liquid mass transfer rate; - reduction of water loss; - high biomass density - high volumetric and areal productivity; - low harvesting costs.	- low light penetration; - oxygen inhibition due to its accumulation in the tubes; - difficult to scale up; - sophisticated construction.

Table 4. Content of bioactive compounds in microalgae (Ahmed et al., 2014; Foo et al., 2017; Goiris et al., 2012; Koller et al., 2014; Kent et al., 2015; Maadane et al., 2015; Morais et al., 2015; Rodrigues et al., 2015; Sloth et al., 2006)

Bioactive compound	Concentration	Algae strain
C-phycoyanin	46.0 % w/w	<i>Spirulina fusiformis</i>
	15–28 mg/g d.w.	<i>Galdieria sulphuraria 074G</i>
Alkaloids	3.02 % w/w	<i>Spirulina platensis</i>
Terpenoids	0.14 % w/w	<i>Spirulina platensis</i>
Lutein	6.55 ± 0.92 mg/g	<i>Dunaliella salina</i>
	128.56 ± 0.5 µg/g d.w.	<i>Phormidium autumnale</i>
Zeaxanthin	11.27 ± 1.58 mg/g	<i>Dunaliella salina</i>
	88.46 µg/g	<i>Phormidium autumnale</i>
β-carotene	138.25 ± 10.03 mg/g	<i>Dunaliella salina</i>
	225.44 µg/g	<i>Phormidium autumnale</i>
Astaxanthin	6.4 ± 1.2 mg/g	<i>Nannochloopsis sp.</i>
Linoleic acid	8.43 ± 3.72 mg/g	<i>Dunaliella sp.</i>
Arachidonic acid	7.45 ± 1.79 mg/g	<i>Nannochloopsis sp.</i>
Eicosapentaenoic acid	36.76 ± 2.93 mg/g	<i>Nannochloopsis sp.</i>
Carotenoids	5.8 mg/g d.w.	<i>Tetraselmis sp.</i>
	1.1 mg/g d.w.	<i>Dunaliella tertiolecta</i>
	5.0 mg/g d.w.	<i>Isochrysis sp.</i>
	6.1 mg/g d.w.	<i>Phaeodactylum tricornutum</i>
Fucoxanthin	2.2 mg/g d.w.	<i>Nannochloopsis sp.</i>
	2.33 ± 0.44 mg/g d.w.	<i>Chaetoceros calcitrans</i>
	2.19 ± 0.02 mg/g d.w.	<i>Isochrysis galbana</i>
Poly(hydroxyalkanoates) (PHA)	1.18 ± 0.00 mg/g d.w.	<i>Odontellasinensis</i>
	77 % d.w.	<i>Aulosira fertilissima</i>
	55 % d.w.	<i>Synechococcus sp. MA19</i>

Recently, researchers worldwide have been investigating cultivation systems based on the use of wastewater, trying to achieve waste reduction and renewable energy production in one-step. Such studies used species like: *Chlorella* and *Scenedesmus*, for biofuel production (Cheah et al., 2016). Effective bioreactors design needs to be focused on minimizing energy consumption, increasing productivity, and reducing total cost of the production process (Manirafasha et al., 2016).

Over the last years, photobioreactor design has evolved especially for improved control and for long-term stability and reliability of operations. In order to choose the most appropriate bioreactor it is necessary to consider not only the yield, but also the increase in photosynthetic efficiency and enhancement of gas exchange rate, as well as the capital investment and operating costs, for a commercially feasible choice. Many challenges are still to be overcome in investigating models for radiative transfer mechanism, hydrodynamics, but also for photosynthetic and growth kinetics (Hallenbeck et al., 2016; Lamand Lee,

2012; Olivieri et al., 2014). Efficient large scale cultivation, but also appropriate techniques for harvesting and post-processing are necessary for providing a feasible commercial manufacture process.

2. Bioactive compounds

Microalgae are highly efficient photosynthetic species fast-growing, very rich in bioactive compounds (Table 4) that can be used in several applications related with health benefits.

The following microalgae: *Spirulina*, *Chlorella*, *Dunaliella*, *Nostoc*, *Botryococcus*, *Haematococcus* (Koller et al., 2014; Silva Vaz et al., 2016), are grown at commercially scale for food supplements.

2.1. Carotenoids

There is an increasing interest in finding natural, safe and powerful antioxidants in order to minimize oxidative damage to living cells and prevent

oxidative deterioration in commercialized products such as food, pharmaceuticals or cosmetics. The major carotenoids that were obtained and tested for human use are: β -carotene, astaxanthin, lutein, lycopene, fucoxanthin and canthaxanthin (Vigani et al., 2015).

Microalgae have a higher specific carotenoid content (compared to terrestrial plants). Species like: *Dunaliella salina*, *Haematococcus pluvialis*, *Porphyridium cruentum*, *Chlorella vulgaris*, *Chlorella zofingiensis* and *Chlorella pyrenoidosa* have been successfully used for the mass production of β -carotene, astaxanthin, canthaxanthin, lutein and other carotenoids (Gong and Bassi, 2016). Even if the use of microalgae as a source of carotenoids (given their antioxidant activity, nutritional value and as a food colorant) is justified by many advantages of this process: no requirement for storage or potential degradation of carotenoids in time, due to the possibility to grow algae during all year and the fact that synthetic carotenoids (cheaper) were incriminated for several undefined diseases: β -carotene and lung cancer (Goralczyk, 2009; Omenn, 1996), the cost of the process, mainly related to the harvesting and post-processing, is still very high (Foo et al., 2017). The diagram of the process is presented in Fig. 4.

Carotenoids can be divided into primary carotenoids (growth-coupled metabolites): lutein, β -

carotene (but under stress conditions act as secondary metabolite) and secondary carotenoids: astaxanthin. For the primary carotenoids a cultivation process in one step is recommended, due to the degradation of carotenoids under stress (lutein, for example), while for the secondary carotenoids, like astaxanthin or β -carotene, the recommended process implies two steps: in the first one the optimum conditions for growth and multiplication are provided, while the second step will be realised under extreme stress conditions (reduction of nitrogen, phosphate, or the presence of salts: sodium chloride or ferrous salts, strong light conditions).

The downstream part includes harvesting the cells by different physical and chemical methods (Fig. 4), with a cost contribution in the overall process of 20-30%. Flocculation has attracted much interest recently due to some major advantages: the ability to treat large scale suspensions with low cost and less energy consumption (Gong and Bassi, 2016). Cell disruption, due to the presence of a thick rigid cell wall, is often suggested as a necessary step to increase the carotenoids recovery yield by several times. Even if it introduces additional processing cost, the pre-treatment step is still viewed as mandatory. The methods used for this step could be of mechanical and non-mechanical type.

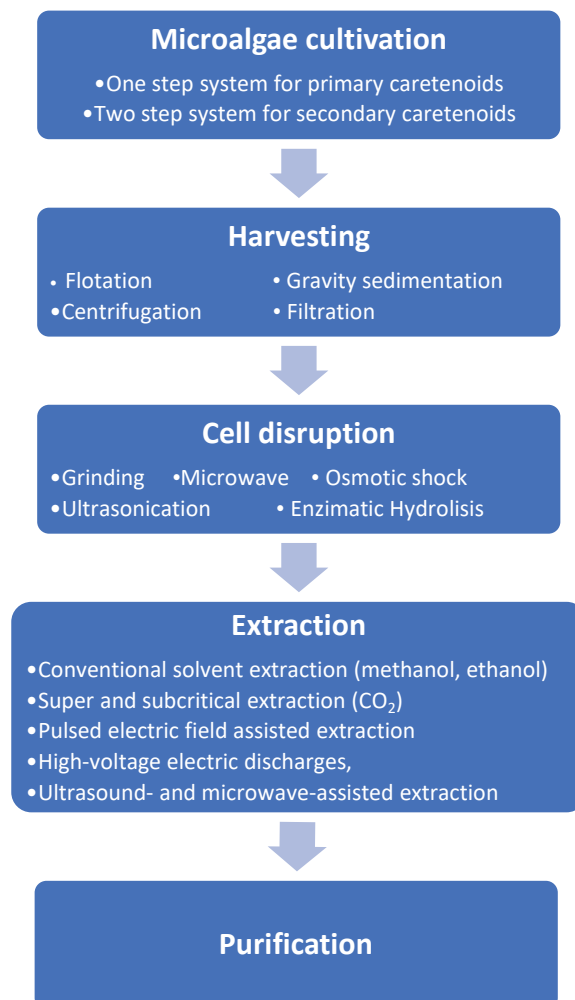


Fig. 4. Process diagram of carotenoids production

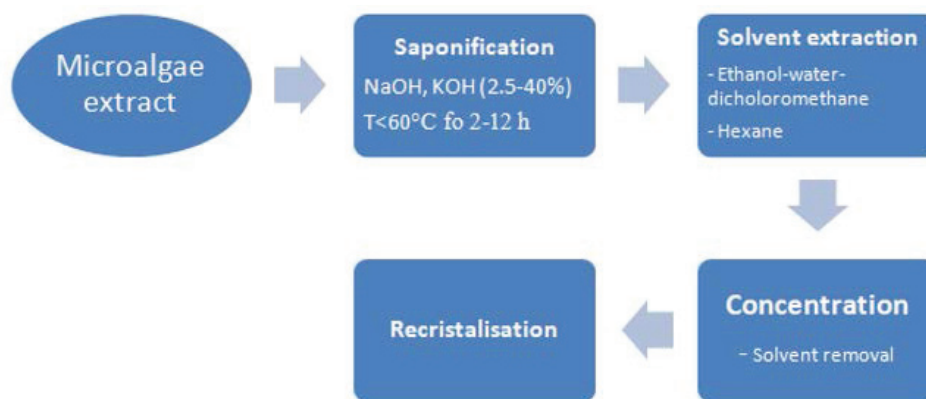


Fig. 5. Process diagram of carotenoids purification

Mechanical methods including high pressure homogenisers, grinding and bead milling are easy to scale up, but have high energy requirements (Taucher et al., 2016), while the non-mechanical one, like microwave, ultrasonication or enzymatic hydrolysis have great potential requiring less energy. However, the non-mechanical methods present some drawbacks: the first two needs a very efficient temperature control as the carotenoids start to degrade at 60°C and the last one is quite expensive due to enzyme price (Kim et al., 2015). Due to the lack of specificity of these cell disruption methods that causes the release of cell debris or other impurities, a pulsed electric fields (PEF) assisted extraction has been investigated for the extraction of nutritionally valuable compounds (total chlorophylls, carotenoids, proteins, phenolic compounds) from microalgae *Nannochloropsis sp.* using the binary mixture of organic solvents (dimethyl sulfoxide, DMSO and ethanol, EtOH) and water (Parniakov et al., 2015a). Pulsed electric fields (PEF) can increase the cell membrane permeability (electroporation), by high-intensity electric field pulses of short duration (microseconds to milliseconds) and can facilitate the purification steps, and also minimizing the energetic costs and losses due to the drying of the biomass (Barba et al., 2015; Parniakov et al., 2015b).

Carotenoids extraction can be achieved by conventional solvent extraction, but recently supercritical solvents (especially CO₂) are investigated, due to the possibility to conduct a process that avoids heat-degradation of active compounds, and offers higher selectivity, shorter extraction times and does not use toxic organic solvents (Millao and Uquiche, 2016a). Trying to overcome the limitations of batch operation related to high-pressure conditions, ways to increase the load of extraction equipment were investigated, namely: pelletization of the microalgae, method that also prevents filter clogging (Millao and Uquiche, 2016a).

Carotenoids purification process is based on a multi-step Willstatter method (Fig. 5), but recently other techniques were investigated: selective absorption, supercritical anti-solvent precipitation, expanded bed coupled column chromatography or reversed phase HPLC (Gong and Bassi, 2016).

Maadane et al. (2015) performed the extraction of bioactive compounds from nine marine microalgae: *Nannochloropsis gaditana*, *Dunaliella sp.*, *Dunaliella salina*, *Phaedactylum tricorutum*, *Isochrysis sp.*, *Navicula sp.*, *Chaetoceros sp.*, *Chlorella sp.* and *Tetraselmis sp.*, grown in sterile natural seawater using conventional solvent extraction with ethanol, water and a mixture of ethanol and water, for different polarities. The authors obtained higher antioxidant activities for the ethanolic extracts of all tested microalgae: *Dunaliella sp.* - 10.8 mg/g carotenoids and 14.5 mg/g phenolic content, *Tetraselmis sp.* - 4.6 mg/g carotenoids and 25.5 mg/g phenolic content and *Nannochloropsis gaditana* - 3.02 mg/g carotenoids and 32.0 mg/g phenolic content (Maadane et al., 2015).

Foo et al. (2017) have investigated the carotenoids extraction in several tropical microalgae species: *C. calcitrans*, *Isochrysis galbana*, *Saccharina japonica*, *Skeletonema costatum*, *Odontella sinensis*, *Phaeodactylum tricorutum* using methanol as a solvent. Methanol has the most suitable polarity in extracting antioxidants especially from brown microalgae (Foo et al., 2015). Thus, they obtained the highest amount of carotenoids (6.13 ± 0.25 mg/g d.w.) and fucoxanthin (5.13 ± 0.19 mg/g d.w.) in the extract from *C. calcitrans*, followed by 4.33 ± 0.04 mg/g d.w. carotenoids and 2.19 ± 0.02 mg/g d.w. fucoxanthin in *I. galbana*, and 2.66 ± 0.10 mg/g d.w. carotenoids for *O. sinensis*.

Millao and Uquiche (2016) studied the effects of temperature (36 – 64°C) and CO₂ density (914 – 956 kg/m³) on the content of carotenoids from *N. gaditana* with a moisture content of 30%. The performance of the process increased with CO₂ density and temperature, the highest values for antioxidant activities being obtained at 64°C and CO₂ density of 956 kg/m³ (Millao and Uquiche, 2016b).

Rodrigues et al. (2015) obtained twenty-four carotenoids, being the most important: all-trans- β -carotene (225.44 μ g/g), all-trans-lutein (117.56 μ g/g) and all-trans-zeaxanthin (88.46 μ g/g) from microalgae *Phormidium autumnale* grown in a bubble column photobioreactor, separated by centrifugation and using ethyl acetate and methanol as solvents for carotenoids extraction.

2.2. Phycobiliproteins - Phycocyanin

Phycocyanin is a photosynthetic blue pigment, water soluble, highly fluorescent and a major antioxidative protein from the phycobiliprotein family, composed of an α - and a β -subunit with 1 (α) and 2 (β) phycocyanobilin groups attached covalently. Commercially, phycocyanin is produced using the cyanobacterium *Spirulina platensis* (blue green algae with a long, thin, monocellular structure) and sunlight as energy source. Beside these microalgae, species of *Galdieria sulphuraria* (phycocyanin shows similar properties to cyanobacterial one and can be purified to the same standards), *Aphanizomenon flosaquae*, *Pyrophyridium sp.* (maximum concentration obtained was 10.2 % d.w. using a two variables experimental design: light and NaHCO_3 feeding and proving that irradiance is a determining factor in the high phycobiliprotein accumulation), *Synechocystis sp.* (a maximum yield of 12% d.w. was obtained in BG-11 medium at optimized conditions of pH 10 and 16 h light), *Phormidium ceylanicum* (purity 4.58 obtained by freezing and thawing method), *Limnothrix sp.*, *S. lividus*, *Nostoc sp.* (maximum yield 0.13 g/g d.w. was obtained for the following optimum conditions: initial pH 8, light intensity: $40 \mu\text{mol}/\text{m}^2 \text{ s}$, temperature 35°C , diurnal cycle of 16:8 h (light:dark regime), $75.48 \mu\text{M}$ Na_2CO_3 and 17.65 mM NaNO_3) and *Arthronema africanum* were also studied (Johnson et al., 2014; Manirafasha et al., 2016; Martínez et al., 2017; Nakagawa et al., 2016).

Phycocyanin properties proved important activities in medicine and pharmaceuticals: antioxidant, anti-inflammatory, anti-tumor, immunomodulating, atheroprotective, hepatoprotective, neuroprotective, antiviral and antifungal (Manirafasha et al., 2016). The cultivation of a microalgae strain that has the potential to offer high phycocyanin content requires choosing an appropriate system: open ponds or closed

photobioreactor (tubular and flat panel configuration seem to be more effective due to better biomass quality) (Carvalho et al., 2014), and heterotrophic, photoautotrophic and mixotrophic (facilitates faster growth with increased phycobiliproteins accumulation, but is not applicable to all microalgae) conditions. It is also important to control other parameters such as: medium composition (e.g. modified Zarrouks medium, artificial sea water, BG 11 medium, SOT medium), temperature, intensity and quality of light, pH, CO_2 availability, and residence time (Manirafasha et al., 2016). The production of phycocyanin requires two main consecutive steps (Fig. 6): upstream process including microalgae biomass production and phycobiliprotein accumulation and downstream processing including harvesting, separation and purification methods.

The upstream process implies the growth of cells in optimum conditions and the accumulation of high content of phycobiliprotein under stress determined by lower nitrate concentration or moderate light intensity (Rio-Chanona et al., 2015). After the biomass production a step of harvesting/dewatering is required, that can be realized by different methods chosen in relation with the microalgae properties, phycocyanin concentration but also taking into account the cost benefits and environmental impact (flocculation is preferred due to less energy demands and scale up possibility).

Phycocyanin can be separated from dry or wet microalgae, the last being economic (reduces the cost associated with drying) but also productive (dry biomass leads to 50 % lost in phycocyanin). After cell-disruption (the freezing and thawing method was considered a good option, robust, simple, fast and reproducible) phycocyanin is extracted using diluted sodium or potassium phosphate buffer (5 – 50 mM, pH 6.0 – 7.5), followed by precipitation by salting out with ammonium sulphate (Sørensen et al., 2013), and dialysis or gel filtration (for desalting).

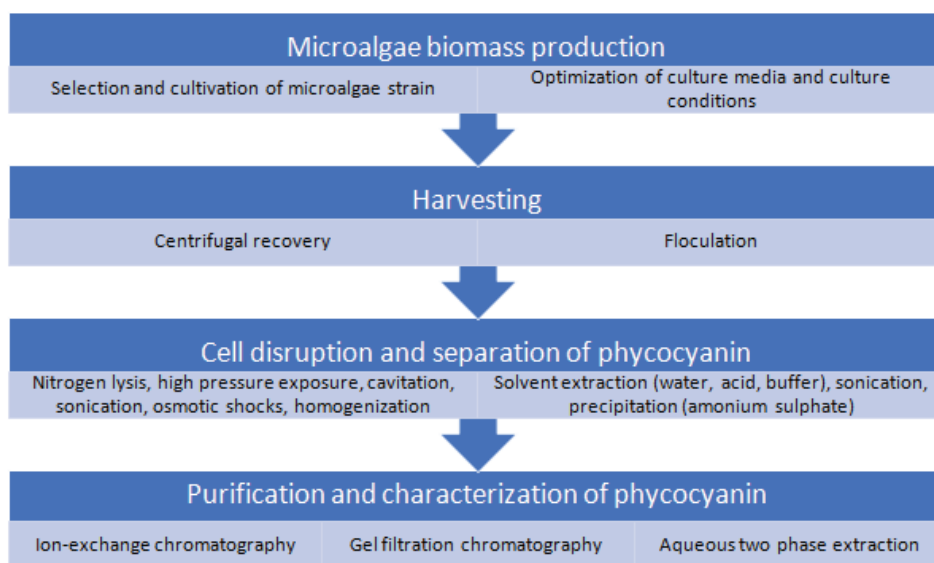


Fig. 6. Process diagram of phycocyanin production

The final step is purification by column chromatography (ion exchange chromatography using DEAE-cellulose DE-52 and hydroxyapatite) from desalted extract. Recently, other methods for separation have been investigated including ultrafiltration, aqueous two phase extraction, ultrasonication, homogenization and different types of chromatography (Chen et al., 2016; Manirafasha et al., 2016), the first offers the advantages of being applicable at large scale and it does not require preliminary stages (precipitation, centrifugation and dialysis).

Chen et al. (2016) used CO₂ feeding, instead of acid/alkaline titration, to control the pH of the culture (pH controlled at 9.5 for *Spirulina platensis* grown in a 1L flat photobioreactor), and a two-stage purification process: fractional precipitation (with (NH₄)₂SO₄ 40 %) combined with ion exchange chromatography and obtained a phycocyanin content and productivity enhanced to 16.8 % and 0.17 g/L/d, respectively.

Chaiklahan et al. (2011) investigated a membrane process using microfiltration and ultrafiltration for the purification of phycocyanin from *Spirulina sp.* cultured in Zarrouk's medium in 100 L open raceway ponds (culture depth of 15 cm, outdoor ambient temperatures, mixed with paddle wheels at 12 rpm). After extraction with phosphate buffer and centrifugation they obtained 82 % recovery, 6.17 mg/mL phycocyanin concentration, and 1.07 of the purity ratio. The authors observed a 5 % loss of phycocyanin in sun dried biomass compared to around 80 % loss in oven dried biomass.

Xie et al. (2015) analysed the influence of light intensity and initial biomass concentration on the cultivation of microalgal strain *Spirulina platensis* WH879 in a 1-L photobioreactor (15.5 cm height and 9.5 cm diameter) equipped with an external light source, operated at 28°C, pH 9.0, agitation rate of 400 rpm and 75 – 450 µmol/m²/s light intensity. The best results were obtained for 300 µmol/m²/s light intensity and an initial biomass concentration of 0.24 g/L in a fed-batch system: phycocyanin content - 16.1 %, and productivity - 94.8 mg/L/d.

Martinez et al. (2017) studied the application of pulsed electric fields on the extraction of phycocyanin into aqueous media from fresh biomass of *Arthrospira platensis* grown photoautotrophically in 2-L bubble column photobioreactor (8 cm diameter and 53 cm height), bubbled with air at 6 mL/s, working at 30°C, in light:dark cycles of 12:12 h with a light intensity of 15 mmol/m² s. The maximum amount of extracted phycocyanin (70 % of the total content with a purity of 0.46 ±0.019) was obtained for microalgae under most intensive treatment: 25 kV/cm, 150 µs at 40°C.

2.3. Polysaccharides

Microalgae polysaccharides are renewable materials, biodegradable and generally non-toxic. Due to their properties like water retention capacity, film-

forming ability, and rheology they are used as emulsifiers, stabilizers, plant bio-stimulants or thickening agents in a wide variety of industrial applications: food, cosmetics, agriculture, textiles, painting, paper, and pharmaceuticals. Polysaccharides isolated from *Chlorella sp.* have been shown to exhibit strong anti-inflammatory and immunomodulatory properties with important applications in medicine (Chakraborty et al., 2012; Elarroussi et al., 2016). Microalgae can produce two main types of exopolysaccharides: totally released into the environment (that offers an advantage in separation) and associated with the cell surface. The exopolysaccharides are predominantly heteropolysaccharides that include in their structure: sulphates, proteins, pyruvate, methylated sugars and uronic acids.

The main algae strains that can be used for the production of these complex and heterogeneous macromolecules are: *Chlorella vulgaris* – β-glucan, *Spirulina platensis* – spirulan, *Gyrodinium pudicum* – homogalactan, *Dunaliella tertiolecta* - (1,4)-D-glucan, but for the majority of microalgae the polysaccharides are divided in sulphated and extracellular. For the cell bound polysaccharides the main strains of microalgae producers are: *Cylindrotheca closterium*, *Navicula salinarum*, *Chlorella stigmatophora*, *Isochrysis sp.*, *Porphyridium sp.*, *Rhodella reticulata*, *Cochlodinium polykrikoides* (Raposo et al., 2015). For the extracellular polysaccharides, produced in a range from about 0.5 g/L up to 20 g/L, the following microalgae can be used: *Hasleaostrearia*, *Nitzschia closterium*, *Skeletonema costatum*, *Chaetoceros spp.*, *Amphora sp.*, *Dunaliella salina*, *Ankistrodesmus angustus*, *Botryococcus braunii*, *Nostoc sp.*, *Cosmarium sp. etc.* (Delattre et al., 2016).

The biological and pharmacological activities of polysaccharides depend strongly on types of glycosidic linkages and the contents and positions of the sulphate groups which depend on species, but also on growing conditions and extraction procedures (Qi and Kim, 2017). The process for obtaining algal polysaccharides without degradation implies microalgae cultivation, extraction and purification (Fig. 7).

Microalgae cultivation is extremely important for the production of polysaccharides, due to an extremely important effect of the environmental conditions on productivity. Nutrient limitation (nitrogen, sulphate, calcium or phosphorous starvation) is usually used to accumulate large amounts of exopolysaccharides, but this determine a negative effect on cell growth. Since for most exopolysaccharides, synthesis occurs along with growth phase (during all growth phases, or just exponential or stationary), research has focused on maximizing different conditions of the culture medium such as: irradiance, carbon dioxide supply, pH and temperature to increase productivity (Delattre et al., 2016).

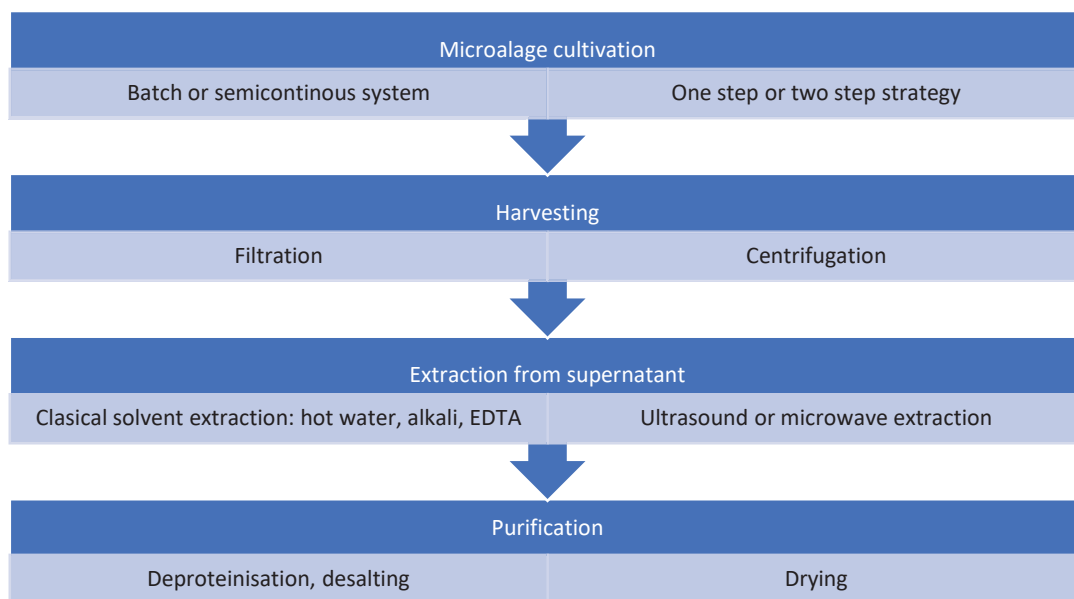


Fig. 7. Process diagram of polysaccharides production

The culture media optimized to increase the polysaccharides production that is usually used for microalgae growth are: BG11, Hemerick, F/2, Provasoli, ASW etc. (Gonzalez-Fernandez and Ballestros, 2013). The downstream part of the process implies the polysaccharides separation using centrifugation or microfiltration to remove microalgae (Li et al., 2011). The extraction of polysaccharides can be made using hot water or alkali solution (the conventional extraction method but with low extraction efficiency), or by microwave or ultrasonic assisted techniques (Patil et al., 2011; Yongjiang et al., 2009) with better performances, shorter time and increased selectively. Next, a precipitation step of the soluble fraction (supernatant or filtrate) using absolute alcohols (methanol, ethanol or isopropanol) at a temperature between -20°C and 20°C is required and followed by desalting by dialysis and membrane techniques.

Qi and Kim (2017) investigated polysaccharides extraction from green alga *Chlorella ellipsoidea*, grown on BG-11 medium at 25°C and $100\ \mu\text{E}/\text{m}^2\text{s}$ illumination with a light/dark cycle of 12:12 h, using hot water and fractionated with anion-exchange chromatography. They analyzed the molecular characteristics of exopolysaccharides that contained 68.1 – 89.7 % carbohydrate, 2.0 – 11.8 % protein, 1.9 – 6.1 % sulphate and 0.5 – 6.1 % uronic acid, with strong immunomodulatory activity.

Chakraborty et al. (2012) analyzed a unique two-step sequential hydrothermal liquefaction process for the simultaneous production of polysaccharides and bio-oil from green alga *Chlorella sorokiniana* (UTEX 1602) cultivated in a 5L fermenter. The polysaccharide rich extract (26 % polysaccharides) obtained by a subcritical water extraction at 160°C , was precipitated with ethanol thus proving that concomitant production of value co-products is feasible.

Balavigneswaran et al. (2013) optimized the polysaccharide extraction conditions from microalgae *Isocrysis galbana*, grown using Walne's medium enriched with vitamins: extraction time 3.6 h, temperature 67.02°C , and ratio between water and raw material 10 : 43.

2.4. Peptides

Microalgae biomass contains important quantities of proteins, and due to the fact, that is capable to synthesize all 20 essential amino acids it can become an unconventional source for human nutrition, but also for medicine due to their antihypertensive, antitumoral, antioxidative, and antimicrobial effect. Bioactive peptides (used as growth factors, hormones and immunomodulators) derived from microalgae proteins have natural bioactivities with beneficial health effects on hypertension and oxidative stress, besides the nutritional benefits. These peptides remain inactive until an enzymatic hydrolysis process followed by the isolation of peptides from the enzymatic extracts (process that provides higher yield and purity compared to the organic solvent extractions). The main microalgae strains that could be used for peptides extraction are: *Anabaena cylindrica*, *Aphanizomenonflos aquae*, *Arthrospira maxima*, *Chlorella ellipsoidea*, *Chlorella pyrenoidosa*, *Chlorella vulgaris*, *Dunaliella salina*, *Spirulina maxima*, *Spirulina platensis*, *Scenedesmus obliquus*, *Synechococcus sp*, *Navicula incerta* (Ejike et al., 2017). The schematic diagram for the recovery of peptides from marine algae is presented in Fig. 8.

The proteins and other components from the microalgae are released from the cells either by proteolytic enzymes (cellulase) or by sonication, the by-products (especially lipids) are removed by extraction and the proteins are converted to peptides

using proteolytic microorganisms or purified enzymes. Processing of the peptides is done by fractionation and purification techniques, particularly membrane ultrafiltration and chromatographic techniques using ion-exchange, affinity, and gel-permeation platforms, whose choice depends on the peptide structure, but also yield and feasibility for industrial scale-up (Samarakoon and Jeon, 2012).

An algal peptide: taurine (used in beverages, foods and nutritional supplements) with several functional and biological applications, has been separated from *Ulva pertusa* (Bellou et al., 2014).

Ko et al. (2012) investigated the peptic hydrolysis (using Protamex, Kojizyme, Neutrase, Flavourzyme, Alcalase, trypsin, α -chymotrypsin, pepsin and papain) of *Chlorella ellipsoidea* obtaining a pentapeptide (Leu-Asn-Gly-Asp-Val-Trp) with scavenging antioxidant activities in vitro, suggesting that *C. ellipsoidea* microalgae could become an attractive raw material for antihypertensive nutraceutical ingredients.

Kose and Oncel (2015) have analysed the effect of environmental conditions and nutritional mode on the biochemical composition of *Chlorella vulgaris* SAG 211-12 cells in photomixotrophic cultivation, using a continuous 2L stirred tank photobioreactor in the scope of protein synthesis used as supplemental nutrition for cystic fibrosis patients. The authors used a modified BG11 culture medium, different organic carbon sources: glucose, sucrose, fructose, glycerol and xylose, and organic nitrogen sources such as yeast extract, peptone and urea. The results showed that carbon sources did not have a significant effect on protein synthesis, unlike nitrogen source: urea inhibited cell growth and the yeast extract and peptone increased the quantity of protein accumulated in the microalgae. The enzymatic hydrolysis was realised with pancreatin (mixture of amylases, lipases and proteases) and hydrolysis yielded over 50 %.

Functional foods containing microalgae-derived peptides have the potential to ameliorate cardiovascular disease, but in order to be largely used more studies that could prove the beneficial health, are required and also the development of feasible technologies need to be addressed (Ejike et al., 2017).

2.5. Lipids

Microalgae are excellent sources of lipids (up to 50 – 75 % of dry matter), making them useful organisms as source of long chain fatty acids, (used for the treatment of various diseases, including thrombosis, arthritis, atherosclerosis, and a variety of cancers) or as feedstock for biodiesel production. Lipids, especially ω -3 and ω -6 fatty acids (long-chain ω -3 and ω -6 fatty acids, like arachidonic acid, docosahexaenoic acid, eicosapentaenoic acid, gamma-linolenic acid) that cannot be synthesized by humans, but necessarily especially for babies, are produced by: *Arthrospira platensis*, *Cryptocodinium cohnii*, *Chaetoceros constrictus*, *Gloeobacter violaceus*, *Isochrysis galbana*, *Odontella sp.*, *Oscillatoria agardhii*, *Tetraselmis viridis* and *Porphyridium cruentum* (Raposso et al., 2016).

Several microalgae species are able to accumulate appreciable (between 20 and 50 %) lipids quantities: *Porphyridium*, *Dunaliella*, *Isochrysis*, *Nannochloropsis*, *Tetraselmis*, *Phaeodactylum*, *Chlorella* and *Schizochytrium*. The schematic diagram for the recovery of lipids from marine algae is presented in Fig. 9.

The two main systems that can be used for microalgae growth are both applicable for lipids: for biodiesel production, the most appropriate would be open ponds, due to a low capital investment and operating cost of these systems, while for the production of polyunsaturated fatty acids closed photobioreactors are recommended (the higher cost can be covered by the high price of the products). As for the other presented compounds, the accumulation of lipids is increased under specific environmental stress conditions like nitrogen or phosphate limitation, high salinity, high temperature (Bellou et al., 2014; D'Alessandro and Filho, 2016). A number of processes can be applied for the harvest of biomass (depending on cell size and density, characteristics of the interest product), including those based on chemical, mechanical, physical, and biological methods, but for biodiesel production filtration, the combination of two processes seems to be preferred in order to reduce the cost of harvesting large quantities of algal biomass.

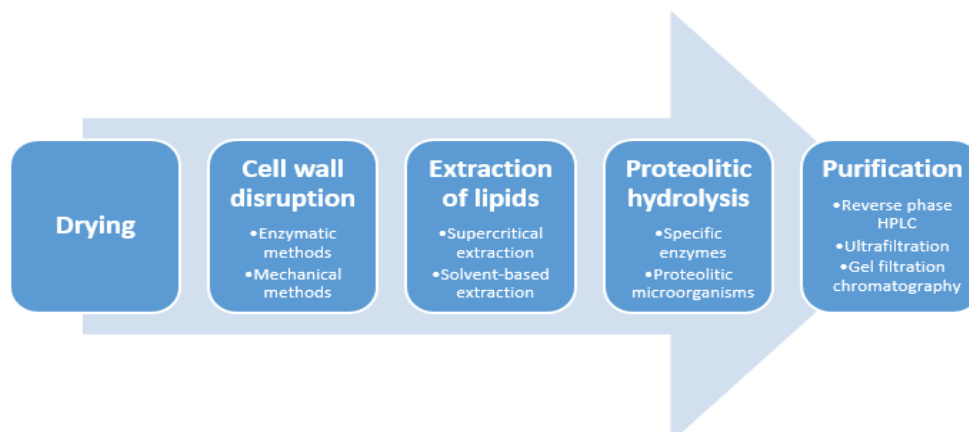


Fig. 8. Process diagram of bioactive peptides production

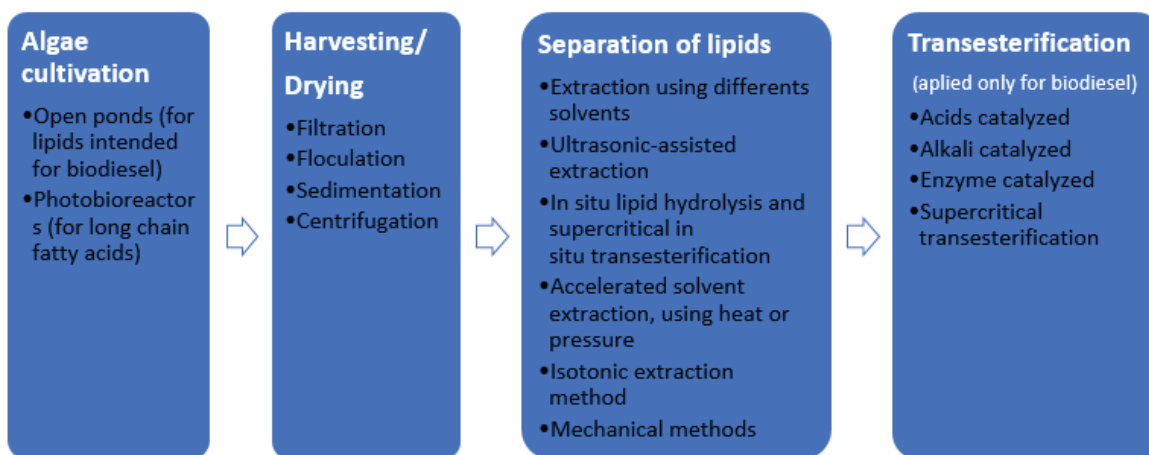


Fig. 9. Process diagram of polyunsaturated fatty acids and biodiesel production

For the extraction of lipids several techniques can be applied (some requires removing water from the biomass prior to lipid extraction for optimum results): organic solvents extraction with n-hexane, chloroform–methanol, methyl tert-butyl ether, 2-ethoxyethanol, electroporation, ultrasonic, and supercritical CO₂ methods (Kumar et al., 2015).

Biodiesel production from the lipids extracted is performed via a chemical conversion process known as transesterification, catalysed by acids, alkali or by enzymes. Recently an in-situ transesterification process with a strong catalyst dissolved in alcohol has been developed that does not require the lipids extraction from the biomass, but need to use dried microalgae (Du et al., 2016). Huang et al. (2016) investigated a thermochemical process including pyrolysis and hydrothermal liquefaction to transform all the organic components of wet microalgae rich in proteins: *Cyanobacteria sp.* and *Bacillariophyta sp.*, into oils with a yield of 21.1% d.w. and 18.2 respectively, at 325°C and 45 – 60 minutes. Moon et al. (2014) used a culture medium based on wastewater from a sugar factory (20 %) and hydrolysate of lipid extracted algal biomass (50 %) for the cultivation of *Ettlia sp.*, and obtained increased lipid productivity (from 5.8 to 95.5 mg/L/d). Du et al. (2017) analyzed the influence of freeze drying and cell breaking on lipids extraction efficiency from *Neochlorisoleo abundans*, proving that drying and cell breaking are not necessary for extraction with N-ethyl butylamine.

The biodiesel process can be more economical by combining lipid production with other applications: separation of carotenoids or polysaccharides, or an integration of wastewater as a medium for microalgal cultivation (Cheah et al., 2016). Millao and Uquiche (2016) studied lipids and carotenoids extraction from microalgae *Nannochloropsis gaditana* pelletized by supercritical CO₂, for the following conditions: 64°C and 956 kg/m³ CO₂ density, obtaining a maximum yield of 152.9 g/kg d.w. for lipids and 773.7 mg/kg d.w. for carotenoids.

Although microalgae biodiesel production presents many advantages and it is well studied, due to high cost (especially for dewatering the biomass

after harvest) there are no large scale algal biodiesel production facilities (Bellou et al., 2014). In order to reduce the cost for the process many efforts have been made for increasing by genetic mutations the lipids accumulation in the microalgae cell (more than 50 %), or to develop different separations methods: in situ lipid hydrolysis and supercritical in situ transesterification applied for wet microalgae (Levine et al., 2010;Valverde et al., 2016).

3. Conclusions

The technological importance of microalgae is clearly demonstrated by the multitude of high value compounds with wide applications in different areas: food additives, health food, cosmetic, pharmaceutical and medicine. The microalgal market is in continuous growth: *Chlorella* and *Spirulina sp.* were the main algae grown industrially for human use (as nutritional supplement), but now *Dunaliella salina* is used to obtain beta-caroten, (1 million \$/ton), or *Haematococcus pluvialis* for producing astaxanthin (10 millions \$/ton). Carotenoids are the most important molecules extracted from microalgae, and even if a high productivity can be achieved due to optimized growth conditions and very efficient photobioreactors, a great interest still remains on the downstream part of the process.

High expectations are associated with the microalgae biotechnological field, and for this a number of challenges will need to be solved in the near future: optimization both of the production step (using **genetic mutation** to increase the content in a specific compound, **solid understanding** of intracellular activities and **process design** for industrial scale that allows the use of all by-products for sustainable and economically feasible production) and the downstream processes with minimal energy consumption, for the development of efficient processes for expansion at commercially scale.

Acknowledgments

This research was supported by ENERED, POSCCE-A2-O2.2.1-2009-4, ID no. 911.

References

- Ahmed F., Fanning K., Netzel M., Turner W., Li Y., Schenk P.M., (2014), Profiling of carotenoids and antioxidant capacity of microalgae from subtropical coastal and brackish waters, *Food Chemistry*, **65**, 300-306.
- Balavigneswaran C.K., Kumar S.J.T., Packiaraj R.M., Veeraraj A., Prakash S., (2013), Anti-oxidant activity of polysaccharides extracted from *Isocrysis galbana* using RSM optimized conditions, *International Journal of Biological Macromolecules*, **60**, 100-108.
- Barba F.J., Grimi N., Vorobiev E., (2015), New approaches for the use of non-conventional cell disruption technologies to extract potential food additives and nutraceuticals from microalgae, *Food Engineering Reviews*, **7**, 45-62.
- Bellou S., Baeshen M.N., Elazzazy A.M., Aggeli D., Sayegh F., Aggelis G., (2014), Microalgal lipids biochemistry and biotechnological perspectives, *Biotechnology Advances*, **32**, 1476-1493.
- Blaga A.C., Kloetzer L., Tucaliuc A., Caşcaval D., Galaction A.I., (2016), Third generation biotechnol production, *The Bulletin of the Polytechnic Institute from Iaşi*, **62**, 39-62.
- Carvalho M.E.A., de Camargo e Castro P.R., Gallo L.A., de Castro Ferraz M.V., (2014), Seaweed extract provides development and production of wheat, *Dourados*, **7**, 166-170.
- Cascaval D., Galaction A.I., Blaga A.C., (2007), Photobioreactors, *Romanian Biotechnological Letters*, **12**, 3377-3388.
- Chaiklahan R., Chirasuwan N., Loha V., Tia S., Bunnag B., (2011), Separation and purification of phycocyanin from *Spirulina sp.* using a membrane process, *Bioresource Technology*, **102**, 7159-7164.
- Chakraborty M., Miao C., McDonald A., Chen S., (2012), Concomitant extraction of bio-oil and value added polysaccharides from *Chlorella sorokiniana* using a unique sequential hydrothermal extraction technology, *Fuel*, **95**, 63-70.
- Cheah W.Y., Ling T.C., Show P.L., Juan J.C., Chang J.S., Lee D.J., (2016), Cultivation in wastewaters for energy: A microalgae platform, *Applied Energy*, **179**, 609-625.
- Chen C.Y., Kao P.C., Tan C.H., Show P.L., Cheah W.Y., Lee W.L., Ling T.C., Chang J.S., (2016), Using an innovative pH-stat CO₂ feeding strategy to enhance cell growth and C-phycocyanin production from *Spirulina platensis*, *Biochemical Engineering Journal*, **112**, 78-85.
- D'Alessandro B.E., Filho N.R.A., (2016), Concepts and studies on lipid and pigments of microalgae: A review, *Renewable and Sustainable Energy Reviews*, **58**, 832-841.
- Delattre C., Pierre G., Laroche C., Michaud P., (2016), Production, extraction and characterization of microalgal and cyanobacterial exopolysaccharides, *Biotechnology Advances*, **34**, 1159-1179.
- Du Y., Schuur B., Kersten S.R.A., Brillman D.W.F., (2016), Microalgae wet extraction using N-ethyl butylamine for fatty acid production, *Green Energy & Environment*, **1**, 79-83.
- Ejike C.E.C.C., Collins S.A., Balasuriya N., Swanson A.K., Mason B., Udenigwe C.C., (2017), Prospects of microalgae proteins in producing peptide-based functional foods for promoting cardiovascular health, *Trends in Food Science & Technology*, **59**, 30-36.
- Elarroussi H., Elmernissi N., Benhima R., El Kadmiri I.M., Bendaou N., Smouni A., Wahby I., (2016), Microalgae polysaccharides a promising plant growth biostimulant, *Journal of Algal Biomass Utilization*, **7**, 55-63.
- Foo S.C., Yusoffa F.M., Ismail M., Basri M., Yau S.K., Khong N.M.H., Chan K.W., Ebrahimi M., (2017), Antioxidant capacities of fucoxanthin-producing algae as influenced by their carotenoid and phenolic contents, *Journal of Biotechnology*, **241**, 175-183.
- Goiris K., Muylaert K., Fraeye I., Foubert I., De Brabanter J., De Cooman L., (2012), Antioxidant potential of microalgae in relation to their phenolic and carotenoid content, *Journal of Applied Phycology*, **24**, 1477-1486.
- Gong M., Bassi A., (2016), Carotenoids from microalgae: A review of recent developments, *Biotechnology Advances*, **34**, 1396-1412.
- Gonzalez-Fernandez C., Ballesteros M., (2013), Microalgae autoflocculation: an alternative to high-energy consuming harvesting methods, *Journal of Applied Phycology*, **25**, 991-999.
- Goralczyk R., (2009), Beta-carotene and lung cancer in smokers: review of hypotheses and status of research, *Nutrition and Cancer*, **61**, 767-774.
- Hallenbeck P.C., Grogger M., Mraz M., Veverka D., (2016), Solar biofuels production with microalgae, *Applied Energy*, **179**, 136-145.
- Huang Y., Chen Y., Xie J., Liu H., Yin X., Wu C., (2016), Bio-oil production from hydrothermal liquefaction of high-protein high-ash microalgae including wild *Cyanobacteria sp.* and cultivated *Bacillariophyta sp.*, *Fuel*, **183**, 9-19.
- Omenn G., Goodman G., Thornquist M., Balmes J., Cullen M., Glass A., Keogh J., Meyskens F., Valanis B., Williams J., Barnhart S., Hammar S., (1996), Effects of a combination of Beta carotene and vitamin A on lung cancer and cardiovascular disease, *The New England Journal of Medicine*, **334**, 1150-1155.
- Jankowska E., Sahub A.K., Oleskowicz-Popiela P., (2017), Biogas from microalgae: Review on microalgae's cultivation, harvesting and pretreatment for anaerobic digestion, *Renewable and Sustainable Energy Reviews*, **75**, 692-709.
- Johnson E.M., Kumar K., Das D., (2014), Physicochemical parameters optimization, and purification of phycobiliproteins from the isolated *Nostoc sp.*, *Bioresource Technology*, **166**, 541-547.
- Kent M., Welladsen H.M., Mangott A., Li Y., (2015), Nutritional evaluation of australian microalgae as potential human health supplements, *PLoS ONE*, **10**, 1-14.
- Kim J.K., Mao Y., Kraemer G., Yarish C., (2015), Growth and pigment content of *Gracilariatikvahiae* McLachlan under fluorescent and LED lighting, *Aquaculture*, **436**, 52-57.
- Ko S.C., Kang N., Kim E.A., Kang M.C., Lee S.H., Kang S.M., Lee J.B., Jeon B.T., Kim S.K., Park S.J., Park P.J., Jung W.K., Kim D., Jeon Y.J., (2012), A novel angiotensin I-converting enzyme (ACE) inhibitory peptide from a marine *Chlorella ellipsoidea* and its antihypertensive effect in spontaneously hypertensive rats, *Process Biochemistry*, **47**, 2005-2011.
- Koller M., Muhr A., Braunegg G., (2014), Microalgae as versatile cellular factories for valued products, *Algal Research*, **6**, 52-63.
- Kose A., Oncel S.S., (2015), Properties of microalgal enzymatic protein hydrolysates: Biochemical composition, protein distribution and FTIR characteristics, *Biotechnology Reports*, **6**, 137-143.

- Kumar R.R., Rao P.H., Arumugam M., (2015), Lipid extraction methods from microalgae: a comprehensive review, *Frontiers in Energy Research*, **2**, 1-9.
- Lam M.K., Lee K.T., (2012), Microalgae biofuels: A critical review of issues, problems and the way forward, *Biotechnological Advances*, **30**, 673-90.
- Levine R.B., Pinnarat T., Savage P.E., (2010), Biodiesel production from wet algal biomass through in situ lipid hydrolysis and supercritical transesterification, *Energy Fuels*, **24**, 5235-5243.
- Li J., Zhu D, Niu J., Shen S., Wang G., (2011), An economic assessment of astaxanthin production by large scale cultivation of *Haematococcus pluvialis*, *Biotechnology Advances*, **29**, 568-574.
- Luangpipat T., Chisti Y., (2017), Biomass and oil production by *Chlorella vulgaris* and four other microalgae - Effects of salinity and other factors, *Journal of Biotechnology*, **257**, 47-57.
- Maadane A., Merghoub N., Ainane T., Arroussi H.E., Benhima R., Amzazib S., Bakrib Y., Wahbya I., (2015), Antioxidant activity of some Moroccan marine microalgae: Pufa profiles, carotenoids and phenolic content, *Journal of Biotechnology*, **215**, 13-19.
- Manirafasha E., Ndikubwimana T., Zeng X., Lua Y., Jing K., (2016), Phycobiliprotein: Potential microalgae derived pharmaceutical and biological reagent, *Biochemical Engineering Journal*, **109**, 282-296.
- Martínez J.M., Luengo E., Saldaña G., Álvarez I., Raso J., (2017), C-phycoyanin extraction assisted by pulsed electric field from *Arthrospira platensis*, *Food Research International*, **99**, 1042-1047.
- Millao S., Uquiche E., (2016a), Extraction of oil and carotenoids from pelletized microalgae using supercritical carbon dioxide, *Journal of Supercritical Fluids*, **116**, 223-231.
- Millao S., Uquiche E., (2016b), Antioxidant activity of supercritical extracts from *Nannochloropsis gaditana*: Correlation with its content of carotenoids and tocopherols, *Journal of Supercritical Fluids*, **111**, 143-150.
- Moon M., Kim C.W., Farooq W., Suh W.I., Shrivastav A., Park M.S., Mishra S.K., Yang J.W., (2014), Utilization of lipid extracted algal biomass and sugar factory wastewater for algal growth and lipid enhancement of *Ettlia sp.*, *Bioresource Technology*, **163**, 180-185.
- Morais M.G., Silva Vaz B., Morais E. G., Vieira Costa J.A., (2015), Biologically active metabolites synthesized by microalgae, *BioMed Research International*, **2015**, 1-15.
- Nakagawa K., Ritcharoen W., Sri-Uam P., Pavasant P., Adachi S., (2016), Antioxidant properties of convective-air-dried *Spirulina maxima*: Evaluation of phycocyanin retention by a simple mathematical model of air-drying, *Food and Bioprocess Technology*, **100**, 292-302.
- Olivieri G., Salatino P., Marzocchella A., (2014), Advances in photobioreactors for intensive microalgal production: configurations, operating strategies and applications, *Journal of Chemical Technology and Biotechnology*, **89**, 178-195.
- Parniakov O., Barba F.J., Grimi N., Marchal L., Jubeau S., Lebovka N., Vorobiev E., (2015a), Pulsed electric field assisted extraction of nutritionally valuable compounds from microalgae *Nannochloropsis* spp. using the binary mixture of organic solvents and water, *Innovative Food Science & Emerging Technologies*, **27**, 79-85.
- Parniakov O., Barba F.J., Grimi N., Marchal L., Jubeau S., Lebovka N., Vorobiev E., (2015b), Pulsed electric field and pH assisted selective extraction of intracellular components from microalgae *Nannochloropsis*, *Algal Research*, **8**, 128-134.
- Patil P.D., Gude V.G., Mannarswamy A., Cooke P., Munson-McGee S., Nirmalakhandan N., Lammers P., Deng S., (2011), Optimization of microwave-assisted transesterification of dry algal biomass using response surface methodology, *Bioresource Technology*, **102**, 1399-1405.
- Priyadarshani I., Rath B., (2012), Commercial and industrial applications of micro algae – A review, *Journal of Algal Biomass Utilisation*, **3**, 89-100.
- Qi J., Kim S.M., (2017), Characterization and immunomodulatory activities of polysaccharides extracted from green alga *Chlorella ellipsoidea*, *International Journal of Biological Macromolecules*, **95**, 106-114.
- Rajauria G., Cornish L., Ometto F., Msuya F.E., Villa R., (2015), *Identification and Selection of Algae for Food, Feed, and Fuel Applications*, In: *Seaweed Sustainability Food and Non-Food Applications*, Tiwari B.K., Troy D.J. (Eds.), Elsevier, 315-345.
- Raposo M.F.J., Bernardo de Morais A.M., Costa de Morais R.M.S., (2015), Marine polysaccharides from algae with potential biomedical applications, *Marine Drugs*, **13**, 2967-3028.
- Raposo M.F.J., Costa de Morais R.M.S., Bernardo de Morais A.M.M., (2013), Health applications of bioactive compounds from marine microalgae, *Life Sciences*, **93**, 479-486.
- Rio-Chanona E.A., Zhang D., Xie Y., Manirafasha E., Jing K., (2015), Dynamic simulation and optimization for *Arthrospira platensis* growth and 23 C-phycoyanin production, *Industrial Engineering Chemistry Research*, **54**, 10606-10614.
- Rodrigues D., Menezes C.R., Mercadante A.Z., Jacob-Lopes E., Zepka L.Q., (2015), Bioactive pigments from microalgae *Phormidium autumnale*, *Food Research International*, **77**, 273-279.
- Samarakoon K., Jeon Y.J., (2012), Bio-functionalities of proteins derived from marine algae - A review, *Food Research International*, **48**, 948-960.
- Silva Vaz B., Moreira J.B., Greque de Morais M., Costa J.A.V., (2016), Microalgae as a new source of bioactive compounds in food supplements, *Current Opinion in Food Science*, **7**, 73-77.
- Sloth J.K., Wiebe M.G., Eriksen N.T., (2006), Accumulation of phycocyanin in heterotrophic and mixotrophic cultures of the acidophilic red alga *Galdieria sulphuraria*, *Enzyme and Microbial Technology*, **38**, 168-175.
- Sørensen L., Hantke A., Eriksen N.T., (2013), Purification of the photosynthetic pigment C-phycoyanin from heterotrophic *Galdieria sulphuraria*, *Journal of the Science of Food and Agriculture*, **93**, 2933-2938.
- Taucher J., Baer S., Schwerna P., Hofmann D., Hümmer M., Buchholz R., Becker A., (2016), Cell disruption and pressurized liquid extraction of carotenoids from microalgae, *Journal of Thermodynamic Catalysis*, **7**, 1-7.
- Valverde F., Romero-Campero F.J., León R., Guerrero M.G., Serrano A., (2016), New challenges in microalgae biotechnology, *European Journal of Protistology*, **55**, 95-101.
- Vigani M., Parisia C., Rodriguez-Cerezo E., Barbosa M.J., Sijtsma L., Ploeg M., Enzing C., (2015), Food and feed products from microalgae: Market opportunities and challenges for the EU, *Trends in Food Science & Technology*, **42**, 81-92.

Xie Y., Jin Y., Zeng X., Chen J., Lu Y., Jing K., Fed-batch strategy for enhancing cell growth and C-phycoerythrin production of *Arthrospira (Spirulina) platensis* under phototrophic cultivation, *Bioresource Technology*, **180**, 281-287.

Yongjiang W., Zhong C., Jianwei M., Minger F., Xueqian W., (2009), Optimization of ultrasonic-assisted extraction process of *Poria cocos* polysaccharides by response surface methodology, *Carbohydrate Polymers*, **77**, 713-717.



“Gheorghe Asachi” Technical University of Iasi, Romania



STUDY OF DIFFERENT ENCAPSULATING AGENTS FOR THE MICROENCAPSULATION OF VITAMIN B12

Ioana C. Carlan, Berta N. Estevinho*, Fernando Rocha

LEPABE, Departamento de Engenharia Química, Faculdade de Engenharia da Universidade do Porto, Rua Dr. Roberto Frias,
4200-465 Porto, Portugal

Abstract

Recently, the studies about vitamin B12 increased due to the high number of people who can develop vitamin B12 deficiency, namely: vegetarians, pregnant women or with vitamin B12 malabsorption. One solution to correct the low nutritional intake of vitamin B12 can be using food supplements or pharmaceuticals, based on the vitamin B12 microencapsulation. In the present research, the vitamin B12 microencapsulation and the controlled release of fresh and 4 months' storage samples of vitamin B12 microcapsules were studied. The microcapsules were prepared using a spray-drying technique, and 7 biopolymers were used as encapsulating agents: arabic gum, sodium alginate, carrageenan, maltodextrin, modified starch, xanthan and pectin. The product yield of the spray-dryer ranged from 20 to 50%. The microparticles were also characterized in terms of size and morphology. The vitamin B12 release profiles from microcapsules were assessed by spectrophotometric analysis, at 361.4 nm, in deionized water at 22°C and simulated gastric fluid at 37°C. This study showed that the vitamin B12 microcapsules, with good stability properties, can be produced with several encapsulating agents and proved the possibility of releasing the vitamin in different periods of time.

Key words: A biopolymers, encapsulating agents, microencapsulation, spray drying, vitamin B12

Received: May, 2017; *Revised final:* February, 2018; *Accepted:* March, 2018; *Published in final edited form:* April 2018

1. Introduction

Vitamins delivery systems used for health maintenance improved significantly in the last decades, due to the new food diet varieties and the challenge of treating diseases in a fast and less painful way possible. Daily administration of vitamins is mandatory (Ball, 2006; Pressman and Buff, 1997) therefore it is a constant “battle” for the industry fields to produce new food and pharmaceutical products with vitamin content (Dordevic et al., 2014; Teleki et al., 2013). The main problem of these essential organic compounds is their stability, so a protective system to keep their properties active and to avoid any type of degradation is necessary (Teleki et al., 2012).

Microencapsulation is a method widely used for drug controlled delivery and is suitable also for vitamins, since it was tested with success for many

sensitive bioactives (Abbas et al., 2012; Carvalho et al., 2016; Dordevic et al., 2014; Estevinho et al., 2014a; Estevinho et al., 2016; Gonçalves et al., 2017; Rosiński et al., 2008; Teleki et al., 2013).

This research work chose vitamin B12 as a model core material to be tested by spray-drying technique with several encapsulating agents within the biopolymers class. Known also as cyanocobalamin, vitamin B12 is a water-soluble vitamin, stable in normal conditions if not exposed to direct light (Ball, 2006; Combs, 2008; Eitenmiller and Landen, 1999; Pressman and Buff, 1997).

In the case of balanced diet, which includes also products of animal origin, people are rarely found to suffer from vitamin B12 deficiency, since the human body can store more than the required amount. However, vegetarians and pregnant women or during lactation are predisposed to suffer from this type of

* Author to whom all correspondence should be addressed: e-mail: berta@fe.up.pt; Phone: +351225081678, Fax: +351225081449

deficiency. For them and those patients who suffer from vitamin B12 malabsorption, a way to correct the level of vitamin must be found (Combs, 2008; Herrmann and Geisel, 2002; Longmore et al., 2014; Okuda, 1999; Robert and Brown, 2003; Watanabe et al., 2013).

Spray-drying is known as the most used microencapsulation method for food industry applications. Stable powders can be obtained from a one-step process of atomization. Also because of the low cost, continuous work mode, easy handling of equipment, spray-drying process is preferred among other microencapsulation techniques (Abbas et al., 2012; Comunian and Favaro-Trindade, 2016; Desai and Park, 2005; Gharsallaoui et al., 2007; Oliveira et al., 2010; Teleki et al., 2013).

There is a big interest in changing the synthetic materials used for microencapsulation, so biopolymers will be a good alternative (Estevinho et al., 2012; Paiva et al., 2015). The option of using biopolymers, as encapsulating agents for the spray-drying process, can bring several advantages: bioavailability, biocompatibility, stability and no toxicity (Fathi et al., 2014; Freiberg and Zhu, 2004). For all these reasons, biopolymers can be considered suitable for the protection of vitamin B12, and further use of the microcapsules for applications of food and pharmaceutical industry, since the consumer is not exposed to any risks (Dordevic et al., 2014; Murugesan and Orsat, 2012).

The aim of this study was to investigate possible shell materials suitable for vitamin B12 oral delivery systems. These biopolymers materials are carbohydrates of different origin plants: arabic gum, maltodextrin and pectin; marine: sodium alginate and carrageenan; and also microbial origin: xanthan (Dordevic et al., 2014; Oliveira et al., 2010; Teleki et al., 2013). Microparticles were prepared by spray-drying method and then characterized regarding their size and surface aspect, using laser granulometry analysis and scanning electron microscopy (SEM). Finally, release profiles were evaluated by spectrophotometric analysis: tests were performed in deionized water at ambient room temperature (22°C) and in simulated gastric fluid (SGF) at the human body temperature (37°C).

The microencapsulation of vitamin B12 can be an option to integrate the vitamin in products that belong to the class of food supplements and pharmaceuticals, like: enriched food products, instant drinks, effervescent capsules, ready to eat cereal-bars, and multivitamin compressed caps.

2. Material and methods

2.1. Material

High purity and pharmaceutical grade reagents were selected for this work. Vitamin B12 was provided from Sigma-Aldrich, China (V2876, Lot # MKBQ9972V). Arabic gum from acacia tree was acquired from Fluka, Germany (30888, Lot

#BCBK8649V), pectin from apples was obtained from Sigma-Aldrich, Switzerland (101582340 76282, Lot #BCBN5335V) and modified starch from Alfa Aesar GmbH&Co KG, Germany (36673, Lot D04X013). From Sigma-Aldrich, USA were purchased: sodium alginate (1001503523 180947, Lot # MKBH8463V), maltodextrin (1001841656 419672, Lot # MKBN6629V), carrageenan (1001761179 C1013 - 1006, Lot # SLBH9868V) and xanthan gum from *Xanthomas campestris* (1001900732 G1253, Lot # MKBQ9467V).

For the formulation of the simulated gastric fluid, hydrochloric acid from Sigma-Aldrich (25,814-8) and sodium chloride from AppliChem Panreac ITW Companies (131659.1211, Lot 0000542745) were used.

2.2. Preparation of solutions

A different spray-drying feed solution was prepared for each one of the 7 encapsulating agents. Solutions with a content of 1% (w/V) encapsulating agent (placed under stirring for 2 hours at a speed of 1200 rpm), and solutions with 2% (w/V) of vitamin B12 (mixed in the shaker for 10 minutes) were prepared.

For the microencapsulation experiments, the encapsulating agent samples were mixed with vitamin B12 samples to obtain feed solutions for the spray-dryer. 100 mL of encapsulating agent solution were mixed with 10 mL of vitamin B12 solution. The stirring was made for 30 minutes at a speed of 500 rpm. Feed solutions without vitamin content were prepared for the analysis of empty microcapsules.

The formulation of simulated gastric fluid (SGF) followed the European Pharmacopeia 7.0 (2010). A stock solution of SGF (1 L - aqueous solution) was prepared with 2.0 g of sodium chloride and 7.0 mL of hydrochloric acid 37%. Additional pH corrections were done with a pH-meter until a final pH value of 1.2 was reached.

All solutions were prepared at room temperature with deionized water.

2.3. Spray-drying process

The microparticles (empty and with vitamin B12) were prepared by a spray-drying technique in a Mini Spray Dryer B-290 from BÜCHI (Flavil Switzerland) with a standard 0.5 mm nozzle. For the shell materials, the following 7 biopolymers were used: arabic gum, sodium alginate, carrageenan, maltodextrin, modified starch, xanthan and pectin.

Each solution was fed up under the following experimental conditions: solution and air flow rates - 4 mL/min (15%), 32 m³/h (80%), air pressure and inlet temperature - 6 bar and 120°C, respectively. The outlet temperature varied between 56 and 67°C, in the case of vitamin B12 microcapsules, and between 60 and 68°C, for the empty microcapsules. The same experimental conditions were applied for all the samples and were selected based on the literature and

some previous studies (Abbas et al., 2012; Casanova et al., 2016; Estevinho et al., 2013b; Estevinho et al., 2016).

The final products were stored and kept for further tests at 4°C, protected from light, to avoid degradation processes.

2.4. Microparticles characterization

The characterization of microparticles followed 2 types of analysis: surface morphology and particle size distribution. The surface morphology was examined by Scanning Electron Microscopy (SEM) and was performed with a Fei Quanta 400 FEG ESEM/EDAX Pegasus X4M equipment (Eindhoven, The Netherlands) at Centro de Materiais da Universidade do Porto (CEMUP). The powder samples (microparticles) were previously fixed on a brass stub using double-sided adhesive tape and then were made electrically conductive by coating, in vacuum, with a thin layer of gold in a Jeol JFC 100 equipment.

For the determination of particle size distribution, a Coulter-LS 230 Particle Size Analyzer (Miami, USA) was used. By laser granulometry, particles were characterized by number and volume average. For each sample an average of three 30 seconds runs was set. The procedure was made after each sample was ultrasound-irradiated, and ethanol was used as dispersant solution to avoid the microparticles aggregation.

2.5. Analytical method for controlled release profile studies

An analytical method was chosen to confirm, by spectrophotometry, the presence of vitamin B12, as an active core inside the microcapsules. The release tests were carried out in 2 types of dissolution mediums at different temperatures: deionised water at 22°C and SGF at 37°C. The evaluation of vitamin B12 was done by measuring the absorbance with a spectrophotometer from Sarspec SPEC RES+ UV/VIS (Portugal), equipped with an external device for heating and stirring of the analyzed solution. For

each test, readings were done in the UV domain at 361.4 nm wavelength and the data acquisition was set for continuous recording every 30 seconds in the case of the following encapsulating agents: arabic gum, sodium alginate, carrageenan, maltodextrin, xanthan and pectin, and every 5 seconds just for modified starch.

This method was first validated to prove the possibility of running the release studies. 13 standard solutions, in the range of 0.0025 g/L to 0.1000 g/L, were analyzed at room temperature. A linear calibration curve was obtained, with a good correlation coefficient $R^2 = 0.9918$. The limit of detection (LOD) was estimated to be 0.0563 µg/mL and the limit of quantification (LOQ) 0.1876 µg/mL.

For the release studies, 3 mg of microparticles were placed inside the cuvette filled with 3 ml of analyzing liquid. The quantity of vitamin B12 microcapsules was selected according to the methodology described in a previous work (Estevinho et al., 2016), being determined by mass balance of reagents used, assuming that during the spray-drying process the ratio of core material/encapsulating agent remained constant. Continuous stirring mode was set on for the cuvette and, depending on the type of analysis, temperature was adjusted (first round of experiments at 22°C, second one at 37°C). Tests were considered finished when all the vitamin content was released, corresponding to the stabilization in time of the value of absorbance. Samples were stored protected from light, in the fridge (4°C) for 4 months and then were tested as described in this section, to check the stability of the samples.

All release tests and the calibration solutions were performed in triplicate, showing coefficients of variation smaller than 10%.

3. Results and discussion

3.1. Product yield

The product yield (%) of the spray drying process was determined for each system studied and was expressed as a ratio of recovered powder reported to the introduced amount of raw materials (Fig. 1).

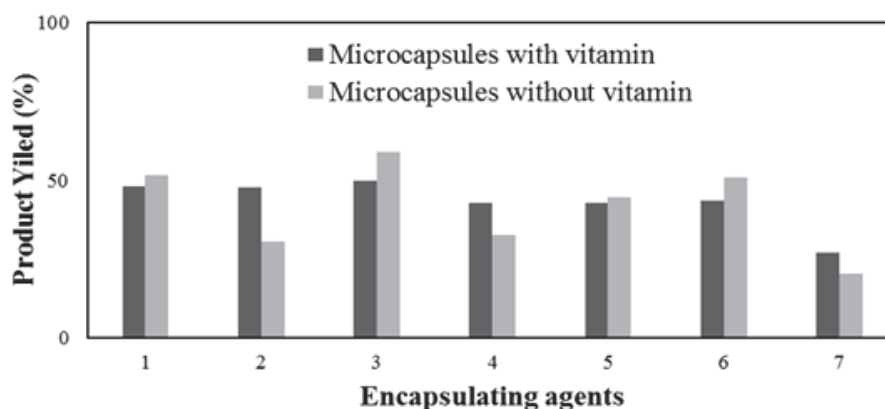


Fig. 1. Product yield for spray-drying process

(1 – arabic gum, 2 – carrageenan, 3 – maltodextrin, 4 – modified starch, 5 – pectin, 6 – sodium alginate, 7 – xanthan)

The results obtained for both types of microparticles are between 27 and 50% for vitamin B12 microparticles, and between 20 and 59 % for empty ones, as shown in Fig. 1. These values are acceptable compared with previous works: 41 – 56% for vitamins B12 and C (Estevinho et al., 2016), and 30 – 50% for food flavours (Estevinho et al., 2013a) and enzymes (Estevinho et al., 2014a; Estevinho et al., 2015). The only encapsulating agent having a low product yield is xanthan: 27% for microparticles with vitamin B12 and 20% for the empty ones.

3.2. Microparticles characterization in terms of size and morphology

All microparticles, with or without vitamin B12, were characterized regarding their surface morphology and their size. The specific morphology

for each biopolymer was observed in SEM images. In Fig. 2, microcapsules with spherical shape and smooth surface, corresponding to sodium alginate, carrageenan, maltodextrin and pectin, are presented. Microcapsules for the other 3 encapsulating agents, arabic gum, modified starch and also xanthan, presenting spherical shape with rough surface, can be observed in Fig. 3. The morphology found in the first group of microparticles was also obtained for vitamin B12 microparticles with modified chitosan and sodium alginate (Estevinho et al., 2016) and with poly (acrylic acid)-cysteine (Sarti et al., 2012).

On the other hand, similar morphology to the second group of encapsulating agents was obtained with chitosan capsules (Estevinho et al., 2016). Size characterization of microparticles performed by laser granulometry shows different sizes for microcapsules with and without vitamin B12 (Table 1).

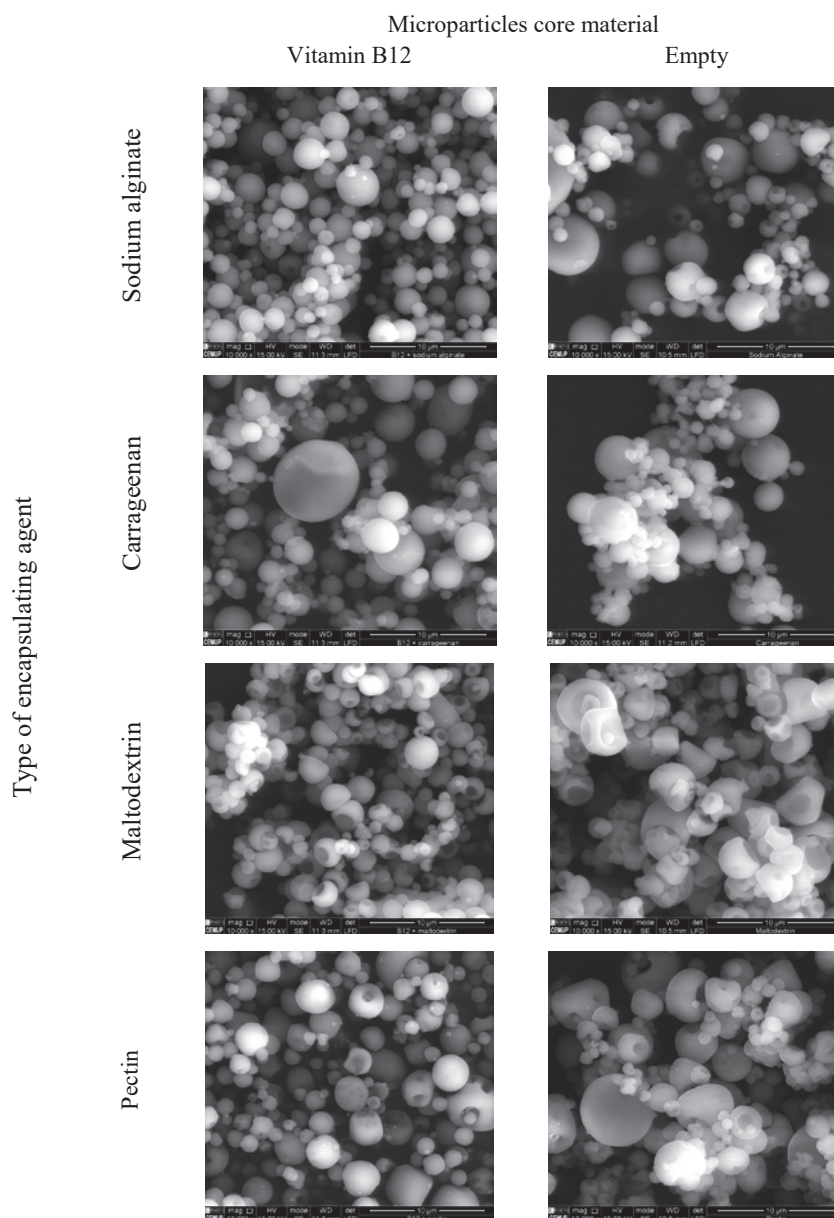


Fig. 2. SEM images of sodium alginate, carrageenan, maltodextrin and pectin microcapsules, with and without vitamin B12. Magnification = 10. 000 times, beam intensity (HV) 15.00 kV, distance between the sample and the lens (WD) around 10 mm

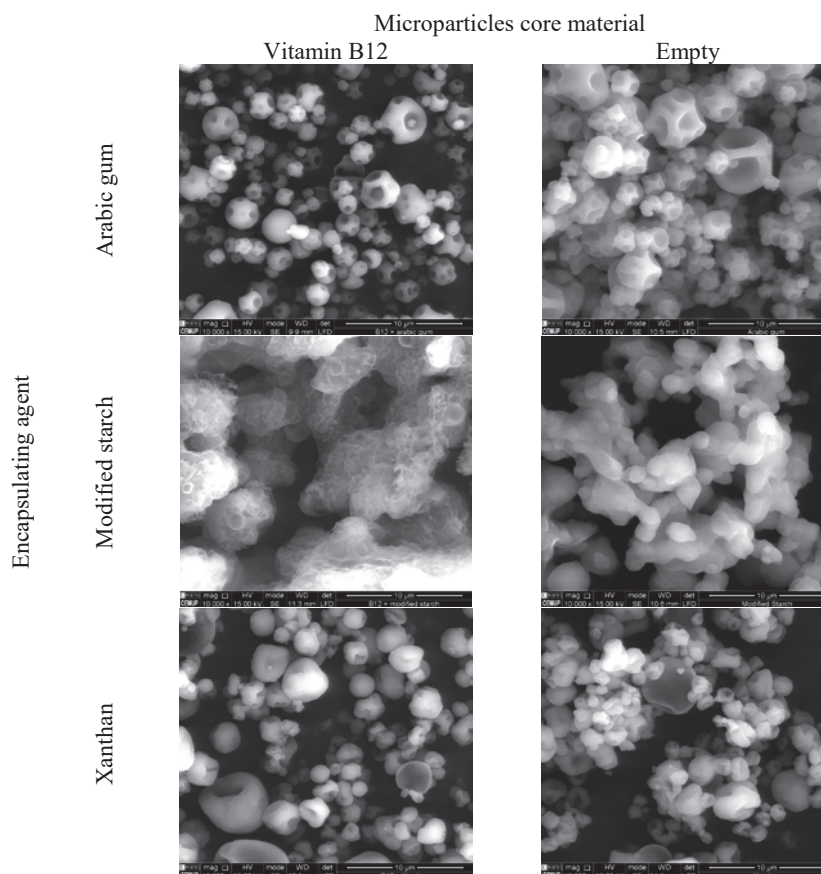


Fig. 3. SEM images of arabic gum, modified starch and xanthan microcapsules with and without vitamin B12. Magnification = 10. 000 times, beam intensity (HV) 15.00 kV, distance between the sample and the lens (WD) around 10 mm

Table 1. Particle mean size by laser granulometry considering volume and number distribution for microcapsules with vitamin B12 and for empty microcapsules

		<i>Differential volume distribution (µm)</i>		<i>Differential number distribution (µm)</i>	
		<i>Microparticle core material</i>			
		<i>Vitamin B12</i>	<i>Empty</i>	<i>Vitamin B12</i>	<i>Empty</i>
<i>Encapsulating agent</i>	Arabic gum	3.17	4.22	0.96	0.57
	Sodium alginate	3.35	10.18	0.93	0.60
	Maltodextrin	4.83	-	0.94	-
	Carrageenan	5.16	7.44	0.98	0.54
	Xanthan	6.58	7.56	0.93	0.72
	Pectin	6.67	4.66	0.99	1.77
	Modified starch	32.17	42.00	2.74	3.62

For microparticles with active core material the average diameter according to volume distribution increases from 3.17 up to 6.67 µm in this order: arabic gum, sodium alginate, maltodextrin, carrageenan, xanthan and pectin. As for the number distribution, the value of average diameter is maintained constant at approximately 1 µm, suggesting aggregation processes, fact highlighted also by the SEM images.

Empty microcapsules present mean sizes, for volume distribution, higher than the microcapsules with vitamin content. Regarding the number distribution of empty microcapsules, it can be observed that the behavior is the opposite; all the values are smaller than 1 µm excepting the sizes of pectin and modified starch capsules, 1.77 and 3.62, respectively. It was not possible to obtain the size distribution of the empty maltodextrin capsules.

Regarding modified starch microparticles, the sizes found are much higher than for the other encapsulating agents, even in the case of empty microcapsules. As shown in the Table 1, for vitamin B12 capsules the obtained values are 32.17 µm for volume distribution and 3.62 µm for number distribution. SEM images for this biopolymer, Fig. 3, show a significant particle aggregation.

3.3. Controlled release studies for fresh and 4 months samples

The controlled release profiles of vitamin B12 from biopolymers microcapsules were evaluated based on spectrophotometric measurements done at vitamin's specific wavelength: 361.4 nm. Release tests were performed using two different solvents:

deionized water at room temperature to simulate the main conditions at food industry, and SGF solution at 37°C to recreate human gastric conditions. Different release profiles behaviors were observed, demonstrating the effect of the type of microparticle, pH and temperature. The evaluation of the release of vitamin B12 was considered to be complete when the value of the absorbance remained stable.

Taking into account the different types of found morphologies, the release profiles are presented in two figures. In Fig. 4, one can observe the release profiles for the following encapsulating agents: sodium alginate, carrageenan, maltodextrin and pectin. In this figure, the profiles obtained in the two solvents, water and SGF, for fresh samples, are presented. In Fig. 5 the same is made for the other three encapsulating agents: arabic gum, modified starch and xanthan.

As can be observed in Figs. 4 and 5, microparticles tend to dissolve gradually, some of them slowly, some moderately or very fast. The microparticles of arabic gum, carrageenan, maltodextrin and modified starch present fast releases, very fast in the case of modified starch, and similar profiles. In all these cases, the release profiles in water and in SGF are almost equal and the release is completed in less of 5 min. The type of release is provoked by the type of encapsulating agent used, the sensibility of the biopolymer to the change of the pH, and the type of interactions between the encapsulating agent and vitamin that are established. In these specific cases the release profile had the same behaviour in water and in SGF for each encapsulating agent used. So, for these specific cases the type of solvent is irrelevant. Regarding sodium alginate microparticles the release is moderate, less than 15 min in both solvents, and one observes a different profile in the release in water, this release being also slower.

In the case of pectin microparticles, the release is completed in less than 70 min in water, faster in SGF, but the release profile is similar for the two solvents. Xanthan showed to be the most sensitive polymer to pH and temperature changes. The release is slower, and the effect of the solvent is pronounced: the release changes from 1 h in SCF to about 15 h in water, and the profile is different.

Comparing Figs. 4 and 5, with Figs. 2 and 3, it is not possible to relate the morphology with the release profile. The properties of encapsulating agents will reflect on the capacity of entrapping the core material protecting it and avoiding mass losses over time. The encapsulating agent will also, affect, the morphology and size of the particles.

Another information that can be obtained from the release profiles is the encapsulation efficiency that is the percentage of drug that is successfully entrapped into the particle. About the encapsulation efficiency there are different methods and strategies to determine it: in this case and considering the specifications of our experimental design, the encapsulation efficiency can

be calculated considering the release profiles, and corresponds to the amount of compound that is encapsulated in the time zero. For these experiments these values correspond to encapsulation ratios around 100% for the microparticles prepared with all the encapsulating agents, except for the case of the microparticles prepared with maltodextrin and modified starch and released in SGF, where this value is lower, around 60%.

Targeted delivery systems for bioactive compounds, like vitamin B12, can be a good solution for creating new food and pharmaceutical products. One of the big advantages of the microencapsulation is the protection. For example: a commercial instantaneous gelatin in powder can be fortified with vitamins; in this case a fast release is desired for the gelatin be homogeneous for the consumption. But during the time that it was in the package, stored, was protected from oxidation, light and interaction with other components. In other cases, as for example in pharmaceutical products, a slow release can be desired, in order to promote a more efficient absorption in the intestinal tract.

Therefore, it is important to choose effective wall materials capable to prevent or minimize the losses until they are utilized. This research work showed good results in what concerns the capsule stability for samples stored for 4 months. In Table 2, the mass loss of vitamin B12 is presented in percentage for each wall material. The stability of the microparticles over the time was evaluated with SGF. The losses of vitamin ranged from 6.2 to 22.4%, the smallest value corresponding to arabic gum and the highest to pectin.

4. Conclusions

The encapsulation of vitamin B12 was performed using 7 different biopolymers as encapsulating agents, using a spray-drying technique. The product yield for the spray-drying process is between 27 and 50% depending on the encapsulating agent.

Good microparticles were produced, with different morphologies and sizes. All particles show a spherical shape, the particle surface being smooth for sodium alginate, carrageenan, maltodextrin and pectin microparticles, and rough for the other 3 biopolymers, arabic gum, modified starch and xanthan. The average diameter of vitamin B12 microparticles according to volume distribution ranges from 3.17 to 6.67 μm .

Different release profiles were found, depending on the encapsulating agent and the release conditions, pH and temperature.

In terms of stability over time it can be concluded that the shelf life of microcapsules can be extended at least until 4 months. The encapsulating agents used show good protective effect. This study proved that vitamin B12 can be microencapsulated by spray-drying technique using several biopolymers as encapsulating agents.

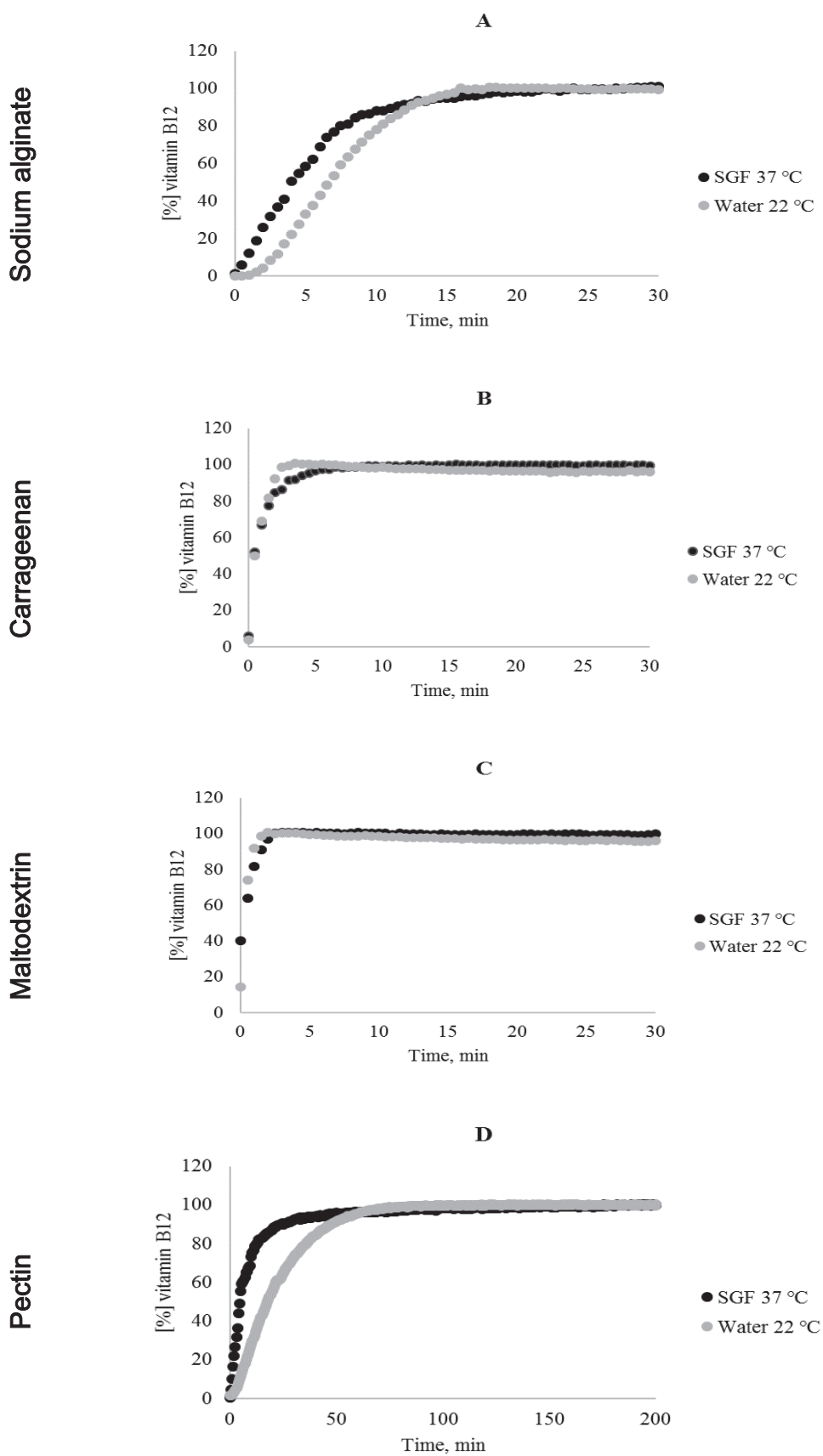


Fig. 4. Vitamin B12 release profile performed in: SGF at 37°C and deionized water at 22°C from microcapsules of (A) – sodium alginate, (B) – carrageenan, (C) – maltodextrin and (D) – pectin

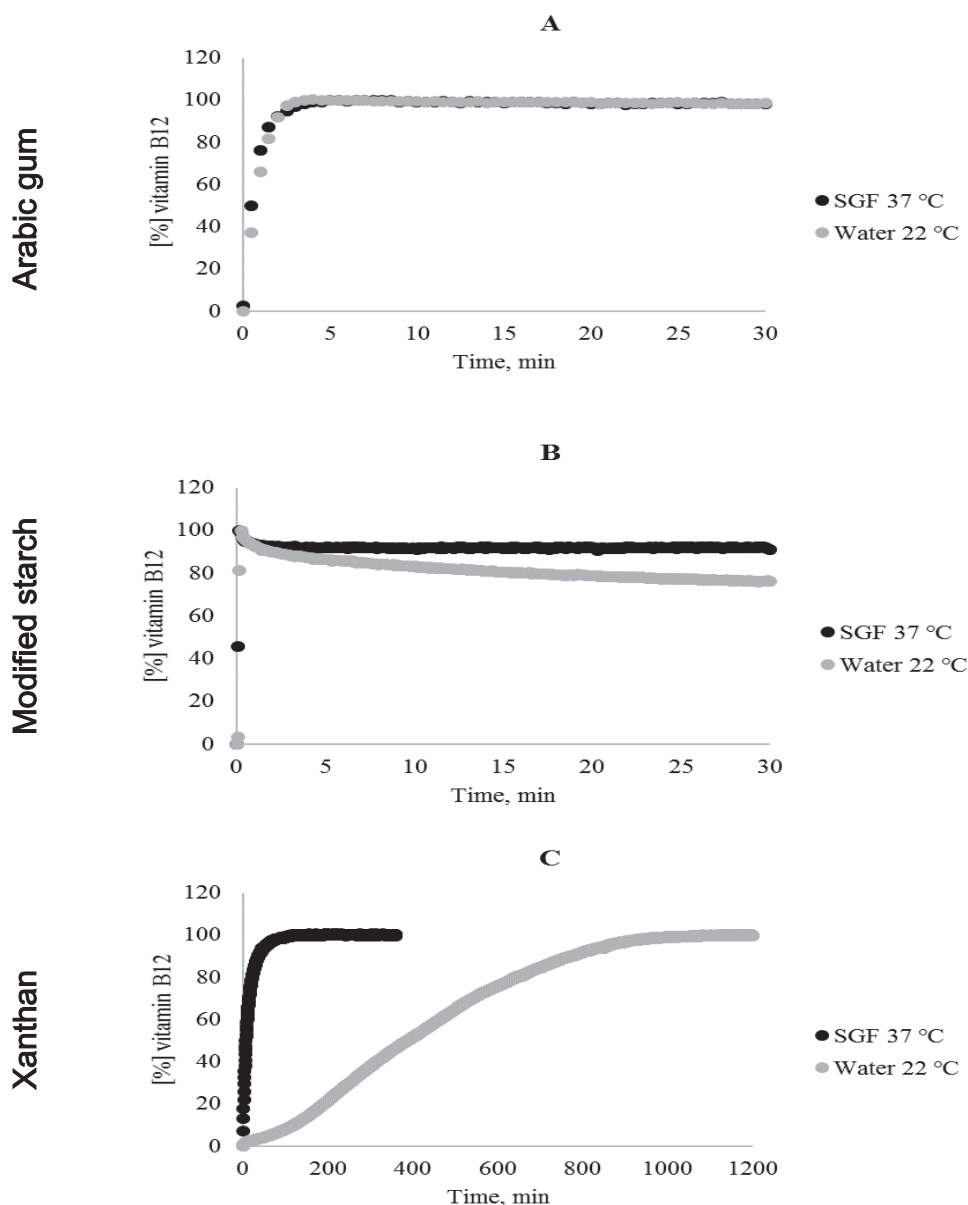


Fig. 5. Vitamin B12 release profile performed in: SGF at 37°C and deionized water at 22°C from microcapsules of (A) – arabic gum, (B) – modified starch and (C) – xanthan

Table 2. Mass loss of vitamin B12 after 4 months of storage in percentage for each type of biopolymers used as an encapsulating agent

Encapsulating agent	Mass loss of vitamin B12 (%) after 4 months of storage for samples released in SGF:
Arabic gum	6.2
Sodium alginate	7.7
Carrageenan	12.0
Maltodextrin	11.7
Modified starch	7.6
Pectin	22.4
Xanthan	12.7

The microparticles prepared with different encapsulating agents present different behaviours, and this fact can lead to different future applications, according to what it is expected from the final product (size and morphology of the microcapsules, needed

time for the complete release of vitamin from the protective layer, type of solvent used to evaluate the release). Further, it is shown that these products are a promising solution to be used for the formulation of oral delivery systems with good stability properties.

Acknowledgments

This work was the result of projects (i) POCI-01- 0145-FEDER- 006939 (Laboratory for Process Engineering, Environment, Biotechnology and Energy – UID/EQU/00511/2013) funded by the European Regional Development Fund (ERDF), through COMPETE2020 - Programa Operacional Competitividade e Internacionalização (POCI) and by national funds, through FCT - Fundação para a Ciência e a Tecnologia. and (ii) NORTE-01-0145-FEDER-000005 – LEPABE-2- ECO-INNOVATION, supported by North Portugal Regional Operational Programme (NORTE 2020), under the Portugal 2020 Partnership Agreement, through the European Regional Development Fund (ERDF). Berta Estevinho would also like to thank the Fundação para a Ciência e a Tecnologia (FCT) for the postdoctoral grant SFRH/BPD/73865/2010 and Ioana C. Carlan thanks for the doctoral grant PD/BD/105986/2014.

References

- Abbas S., Wei C.D., Hayat K., Xiaoming Z., (2012), Ascorbic acid: microencapsulation techniques and trends-A review, *Food Reviews International*, **28**, 343-374.
- Ball G.F.M., (2006), *Vitamin B12 (Cobalamins)*, In: *Vitamins in Foods. Analysis, Bioavailability and Stability (Food Science and Technology)*, CRC Press, Taylor & Francis, 339-368.
- Carvalho I.T., Estevinho B.N., Santos L., (2016), Application of microencapsulated essential oils in cosmetic and personal healthcare products – A review, *International Journal of Cosmetic Science*, **38**, 109-119.
- Casanova F., Estevinho B.N., Santos L., (2016), Preliminary studies of rosmarinic acid microencapsulation with chitosan and modified chitosan for topical delivery, *Powder Technology*, **297**, 44-49.
- Combs G.F., (2008), *Chapter 17 Vitamin B12*, In: *The Vitamins. Fundamental Aspects in Nutrition and Health*, Elsevier, Third Edition, Elsevier Academic Press, New York, 381-398.
- Comunian T.A., Favaro-Trindade C.S., (2016), Microencapsulation using biopolymers as an alternative to produce food enhanced with phytosterols and omega-3 fatty acids: A review, *Food Hydrocolloids*, **61**, 442-457.
- Desai K.G.H., Park H.J., (2005), Recent developments in microencapsulation of food ingredients, *Drying Technology: An International Journal*, **23**, 1361-1394.
- Dordevic V., Balanc B., Belscak-Cvitanovic A., Levic S., Trifkovic K., Kolusevic A., Kostic I., Komes D., Bugarski B., Nedovic V., (2014), Trends in encapsulation technologies for delivery of food bioactive compounds, *Food Engineering Reviews*, **7**, 452-490.
- Eitenmiller R.R., Landen W.O., (1999), *Chapter 12 Vitamin B12, Biotin and Pantothenic Acid*, In: *Vitamin Analysis for the Health and Food Science*, CRC Press LLC, 471-505.
- Estevinho B.N., Damas A.M., Martins P.M., Rocha F.A., (2012), Study of the inhibition effect in the microencapsulated enzyme β -Galactosidase, *Environmental Engineering and Management Journal*, **11**, 1923-1930.
- Estevinho B.N., Rocha F., Santos L., Alves A., (2013a), Using water-soluble chitosan for flavour microencapsulation in food industry, *Journal of Microencapsulation*, **30**, 571-579.
- Estevinho B.N., Rocha F., Santos L., Alves A., (2013b), Microencapsulation with chitosan by spray drying for industry applications - A review, *Trends in Food Science*, **31**, 138-155.
- Estevinho B.N., Damas A.M., Martins P., Rocha F., (2014a), Microencapsulation of β -galactosidase with different biopolymers by a spray-drying process, *Food Research International*, **64**, 134-140.
- Estevinho B.N., Damas A.M., Martins P., Rocha F., (2014), The influence of microencapsulation with a modified chitosan (water soluble) on β -galactosidase activity, *Drying Technology*, **32**, 1575-1586.
- Estevinho B.N., Ramos I., Rocha F., (2015), Effect of the pH in the formation of β -galactosidase microparticles produced by a spray-drying process., *International Journal of Biological Macromolecules*, **78**, 238-242.
- Estevinho B.N., Carlan I.C., Rocha F., (2016), Soluble vitamins (vitamin B12 and vitamin C) microencapsulated with different biopolymers by a spray drying process, *Powder Technology*, **289**, 71-78.
- Fathi M., Martín Á., McClements D.J., (2014), Nanoencapsulation of food ingredients using carbohydrate based delivery systems., *Trends in Food Science and Technology*, **39**, 18-39.
- Freiberg S., Zhu X.X., (2004), Polymer microspheres for controlled drug release., *International Journal of Pharmaceutics*, **282**, 1-18.
- Gharsallaoui A., Roudaut G., Chambin O., Vailley A., Remi S., (2007), Applications of spray-drying in microencapsulation of food ingredients: An overview, *Food Research International*, **40**, 1107-1121.
- Gonçalves A., Estevinho B.N., Rocha F., (2017), Design and characterization of controlled-release vitamin A microparticles prepared by a spray-drying process, *Powder Technology*, **305**, 411-417.
- Herrmann W., Geisel J., (2002), Vegetarian lifestyle and monitoring of vitamin B12 status, *Clinica Chimica Acta*, **326**, 47-59.
- Longmore M., Wikinson I., Baldwin A., Wallin E., (2014), *Chapter 8: Haematology*, In: *Oxford Handbook of Clinical Medicine*, Ninth Edition, Oxford University Press Inc., New York, 382-383.
- Oliveira W.P., Souza C.R.F., Kurozawa L.E., Park K.J., (2010), *Spray Drying of Food and Herbal Products*, In: *Spray Drying Technology*, Woo M.W., Mujumdar A.S., Daud W.R.W. (Eds.), 113-156.
- Murugesan R., Orsat V., (2012), Spray drying for the production of nutraceutical ingredients - A review, *Food and Bioprocess Technology*, **5**, 3-14.
- Okuda K., (1999), Discovery of vitamin B12 in the liver and its absorption factor in the stomach: A historical review, *Journal of Gastroenterology and Hepatology*, **4**, 301-308.
- Paiva M., Estevinho B.N., Rocha F., Nunes O.C., (2015), Development and validation of UV spectrophotometric method for determining the herbicide molinate with and without alginate microparticles, *Environmental Engineering and Management Journal*, **14**, 303-309.
- Pressman A.H., Buff S., (1997), *Cobalamin: The B for Healthy Blood*, In: *Vitamins and Minerals*, Alpha Books, New York, 107-115.

- Robert C., Brown D.L., (2003), Vitamin B12 deficiency, *American Family Physician*, **67**, 979-987.
- Rosiński S., Grigorescu G., Lewinska G., Ritzen L.G., Viernstein H., Teunou E., Poncelet D., Zhang Z., Fan X., Serp D., Morison I., Hunkeler D., (2008), Characterization of microcapsules: recommended methods based on round-robin testing, *Journal of Microencapsulation*, **19**, 641-659.
- Sarti F., Iqbal J., Muller C., Shahnaz G., Rahmat D., (2012), Poly(acrylic acid)-cysteine for oral vitamin B12 delivery, *Analytical Biochemistry*, **420**, 13-19.
- Teleki A., Hitzfeld A., Eggersdorfer M., (2013), 1000 years of vitamins: the science of formulation is the key to functionality, *Kona Powder and Particle Journal*, **30**, 144-163.
- Watanabe F., Yabuta Y., Tanioka Y., Bito T., (2013), Biologically active vitamin B12 compounds in foods for preventing deficiency among vegetarians and elderly subjects, *Journal of Agriculture and Food Chemistry*, **61**, 6769-6775.



“Gheorghe Asachi” Technical University of Iasi, Romania



PASSENGER CAR DEPENDENCY AND CONSEQUENT AIR POLLUTANTS EMISSIONS IN IASI METROPOLITAN AREA (ROMANIA)

Lucian Roșu¹, Marinela Istrate^{1,2}, Alexandru Bănică^{1,2*}

¹“Faculty of Geography and Geology, “Alexandru Ioan Cuza” University of Iasi, 11 Carol I Bvd., 700505 Iasi, Romania

²“Alexandru Ioan Cuza” University of Iasi, CERNESIM, 11 Carol I Bvd., 700506 Iasi, Romania

Abstract

Urban expansion, often seen as an indicator of economic growth and a possible response to housing crisis in big cities, is the main driver for carbon emissions in the metropolitan area due to higher values of household income, vehicle ownership and home size. The transport related pollution includes over 200 different compounds: besides CO₂ emissions, CO, NO_x, BTX and dust resulting from exhausting processes, from abrasive wear of brakes, tires and road surfaces. The expansion of the urban areas in Romania has faced similar patterns in all major cities in Eastern Europe. Traffic congestion and increasing pollution became common aspects of urban life, as most big cities were not prepared for this fast change in urban land use. The present paper proposes to highlight which communes from the Iasi metropolitan area contribute the most to air pollution due to car commuting. The results highlight the negative effects of urban sprawl upon air pollution and the challenges raised by residential mobility. The above-mentioned aspects were analyzed using surveys, statistical data, pollutants inventory and GIS related simulations for commuting in order to highlight patterns of peri-urban air pollution due to car commuting. The results suggest that the Iasi metropolitan area is confronted with an important sprawl which results in high values of different air pollutant emissions originating from extensive passenger car use in the peri-urban area.

Key words: commuting, Iasi pollutants emissions inventory, urban sprawl

Received: May, 2017; Revised final: February, 2018; Accepted: March, 2018; Published in final edited form: April 2018

1. Introduction

Urban sprawl is a multifaceted concept which has been intensely researched in the last decades mainly because of the issues associated with ecological stress in fast-changing patterns of land use due to the accelerated growth of liberal economies (Fina and Siedentop, 2008; Gonzalez, 2005; Muñiz and Galindo, 2005; Mironiuc and Huian, 2017). Analysing air pollution expressed by the expansion of the built-up area and car dependency has an increasing role as the effects of air pollution on public health are being observed worldwide. Road traffic emissions represent an increasingly major part of air pollutants

emissions in Romanian urban areas, a fact that is enhanced by peri-urbanisation/sprawl processes within the Metropolitan areas.

Besides fragmentation of natural landscape (Park et al., 2014), diminution of natural habitats (Alberti and Marzluff, 2004; Su et al., 2010) or biodiversity, other major problems are associated with this concept and are highly researched. Urban expansion has a direct negative impact on traffic congestion (Ciobanu and Benedek, 2015), high oil consumption (Aftabuzzaman and Mazloumi, 2011; Novelli et al., 2017), increased level of automobile travel (Petrescu et al., 2015) or car dependency (Newman and Kenworthy, 2011), air pollution

* Author to whom all correspondence should be addressed: e-mail: alexandrubanica@yahoo.com; Phone: +40 232 201 479

(Stankovic et al., 2015; Stefan et al., 2015) and related health problems (Frumkin, 2002), thus affecting the human condition.

Urban automobile transport has become the dominant source of air pollution in larger urban cities (Jensen, 1998; Takucev et al., 2014). Moreover, peri-urban areas are responsible for more than 50 % of all household emission (Jones and Kammen, 2014). Intense traffic air pollution is usually considered to result from high population density (Stankovic et al., 2015), which makes urban areas to gather the largest number of population subject to automobile pollution exposure (Banica et al., 2016). Meanwhile, it is often stated that compact urban areas address better environmental issues related to air emissions (Wang et al., 2016), while more dispersed development of cities is beneficial in terms of reducing the impact of localized pollution (De Ridder et al., 2008; Martins, 2012; Schindler et al., 2017; Schindler and Caruso, 2014). Nevertheless, both urban and peri-urban traffic (Kim, 2016) contribute to harmful effects on both human health and environment (WHO, 2016). One of the reasons of urban sprawl is represented by the choice of the population to leave the crowded urban centre in order to look for less polluted neighbourhoods (Lera-López et al., 2012). Meanwhile, this relocation is in itself creating additional pollution, by longer commuting trips to their workplaces and to service areas, which modifies the spatial patterns of urban pollution (Schindler et al., 2017). The fact is reflected by transport performance and accessibility which were debated by many studies focusing on the impact of mode choice on energy efficiency and atmospheric emissions. Some of these studies focus on the structure of vehicles (sizes and ages of engines) and travel behaviour, concluding that there is an obvious need to integrate urban development and transport systems in order to reduce pollution (Ambarwati et al., 2016; Chiou et al., 2009; Chiou and Chen, 2010). There is even a study that proposes numerical simulations of an urban model where residents are homogeneously harmed by the 'total pollution' generated by commuters (Verhoef and Nijkamp, 2004). Other different approaches assess the vehicular contribution to higher concentrations of nitrogen dioxide (NO₂) and suspended particles (PM₁₀) in traffic-related areas (Oprea et al., 2017; Vasilescu et al., 2017), especially referring to diesel vehicles in spite of the fact that more stringent emission standards had already been implemented (Borken-Kleefeld and Chen, 2015; Carslaw et al., 2011; Carslaw and Rhys-Tyler, 2013; Franco et al., 2014; Stefan et al., 2015; Zhang et al., 2016). Eastern Europe has been facing an important extension of functional urban areas in the last decade and is expected to go through the same pollution problems (Sailer-Fliege, 1999), as the highest values for air pollutants are recorded in the major cities across Eastern Europe (EEA, 2016; Manolache et al., 2017). The issue of sustainability of human-environment interaction represents a priority research topic, especially in the areas where urban expansion has

recorded important changes, as it is the case of the Iasi Metropolitan Area, in the North-Eastern Region of Romania.

The aim of the research is to investigate the relation between the urban sprawl, commuting and air pollution using a GIS integrative approach, based on network analysis, qualitative and quantitative surveys and official statistical data, in order to evaluate the impact of the urban expansion in the Metropolitan Area of Iasi on air pollution. Several objectives create the guidelines of the research in order to determine the degree of air pollution in the Metropolitan Area of Iasi Municipality. The first objective is to determine the extent of the urban sprawl based on accessibility measures, thus highlighting the existing pattern of the peri-urbanization process. The second objective aim is to determine the degree of car dependency using a survey applied for each settlement from the Metropolitan Area. The third objective targets to estimate the quantity of different pollutants generated by the daily use of personal cars on a detailed level, based on commuting data and the results of the survey.

2. Material and methods

2.1. Study area

Urban sprawl, a phenomenon with different levels of intensity and generated by different factors, has its beginnings during the post-Fordism period (Iatu and Eva, 2016). Romania (Grigorescu et al., 2012) and most of Eastern European (Brade et al., 2009) countries have experienced the process of urban expansion while changing the political and economic ideology from socialist to capitalist economies. The spatial frame of urban sprawl of the Iasi Municipality falls under these characteristics which are different from the western or American models and different from one city to another located in Eastern Europe.

The present research takes into consideration the Metropolitan Area of the Iasi Municipality, the first entity of this kind established in Romania in 2004 (Clipa, 2012). Located in the North-Eastern Romania, the study area comprises the Iasi Municipality (the second largest city in Romania) and 76 settlements grouped in 13 communes (Cimpianu and Corodescu, 2013) (Fig. 1). The entire area has a population of more than 400.000 inhabitants on a relatively small area (800 km²), forming one the densest, most active and complex functional urban area in Romania and on the Eastern border of the European Union. The positive effect of this urban agglomeration is represented by being considered the main economic engine of the entire North-East Development Region, clustering important IT&C services, high educational services, retail and industrial platforms.

The Iasi Municipality had a compact form until the late '90s. Even though the city faced a rapid urbanization, the extension was mainly vertical, densifying and creating compact districts, which are now seen as a sustainable urban form (Burton et al., 2013).

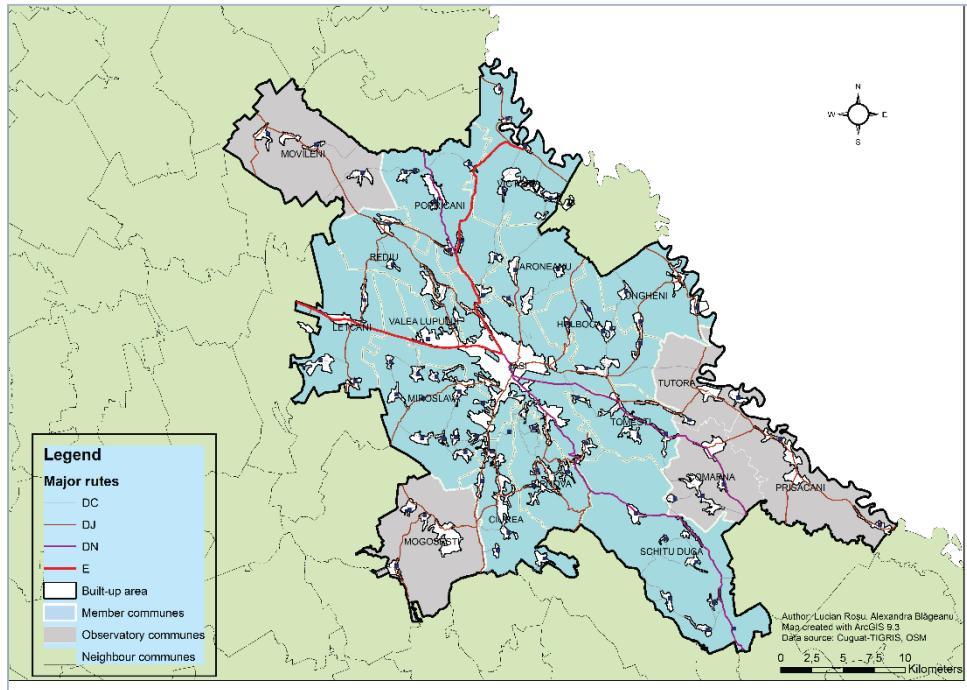


Fig. 1. Iasi Metropolitan Area

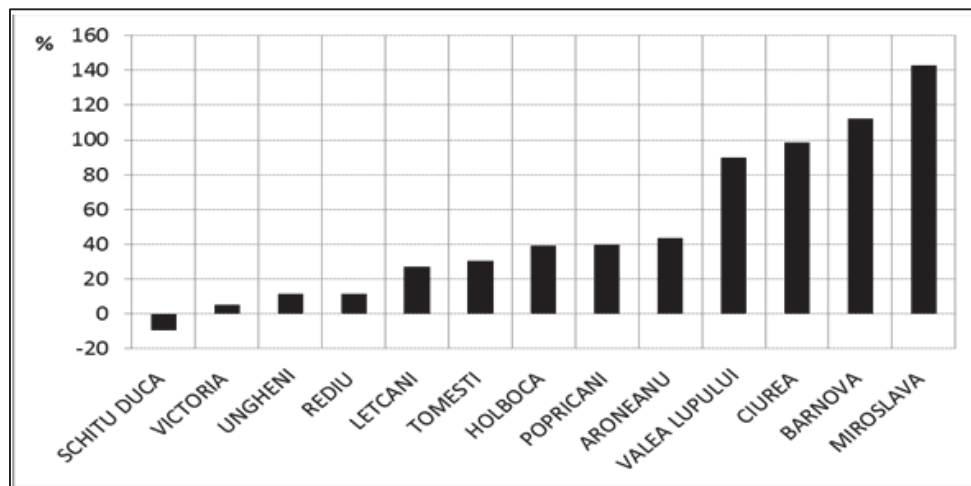


Fig. 1. Population growth rate (%) of the communes from Iasi Metropolitan Area (1992 – 2016)

The entire functional urban area faces a slow process of post-communist transition (Rosu and Blageanu, 2015). The actual form of the city and its surroundings has been influenced by rapid and visible changes in the last two decades, mainly due to the relocation of industry and housing in the peri-urban areas, where the new industry and retail economy are located.

During the last 25 years, the city has ceased growing (from a demographical perspective) even though its polarization force attracts more and more people from the surrounding areas (Blageanu et al., 2012). On the other hand, the fast growth of the peri-urban areas determined the local administration to create the Metropolitan Area of Iasi in order to fill the gap between the compact city and the undeveloped rural regions. As a consequence 12 of the 13

communes which are part of the Metropolitan Area experienced significant population growth, some of them doubling their population in the last 14 years, while the only commune showing a decrease (Schitu-Duca) is also the most remote from the city (Fig. 2 and Fig. 3). The constant movement towards the fringe of the city resulted in the occurrence of residential districts outside the city limits. On the other hand, most of the services are being clustered in the city centre, the economic integration leading to a dramatic increase in the geographic concentration of facilities via self-reinforcing agglomeration process (Forslid and Ottaviano, 2003).

Therefore a rather obvious monocentric development model can be observed (Mihai, 2015), resulting in planning problems such as a chaotic urban sprawl which generates, inter alia, massive traffic jams

(Ursu et al., 2016), especially at the main entrances towards the urban core, high values for air pollutants (Banica et al., 2017; Luca and Ioan, 2012), and other specific problems. These issues are also generated by the lack of an integrated metropolitan public transport and an obvious car-dependency model (Rosu and Blageanu, 2015).

2.2. Data and methods

In order to evaluate the interaction between car dependency, urban sprawl and air pollutants, a comprehensive methodology based on integrative approach was applied. There are three phases of the methodological path: evaluating urban sprawl by using GIS-based accessibility assessment, applying a survey in order to estimate car dependency and, finally, making an inventory of the main air pollutants that result from the use of cars for commuting.

2.2.1. Evaluating urban sprawl using GIS accessibility assessment

The concept of accessibility is used to determine different levels of peri-urban development (Frenkel and Ashkenazi, 2008). Accessibility represents the main outcome derived from the spatial analysis of a transport system. It creates the main location advantage of an area in relation to other areas it is linked to. Accessibility indicators point out the returns of an actor in his location from the use of the transport infrastructure relevant in its hinterland (Spiekermann and Neubauer, 2002). In order to establish the degree of urban sprawl a time-travel model based on network analyses has been performed using GIS specific methods.

The model takes into account the road network, classified by type, speed limits and length, built up areas of settlements inside the Metropolitan Area and the communes' administrative limits.

Using this method, each settlement from the Metropolitan Area obtained a value of duration-distance to the city centre, according to the road network type. The results were clustered into three categories of settlements, according to different levels of accessibility to the city centre (high, medium and low).

2.2.2. Using surveys for estimating car dependency

In order to evaluate different characteristics of travel pattern and car dependence during commuting, a qualitative approach was used by applying questionnaires. The use of questionnaires was a requisite for linking official statistics of commuters with car travel patterns and its characteristics. The items of the survey covered the dimensions of the researched field, according to the objective mentioned afore (Table 1). Most of the questions used were factual ones, adding filtered and identification questions. For establishing the questions, several items such as importance, responsiveness, clarity, comprehensiveness, validity and policy relevance were taken into account (Fowler Jr, 2014)

The information was collected using questionnaire-based surveys applied between August 2016 and October 2016 for approximately 30 settlements from all 13 communes which are part of the Iasi Metropolitan Area using a random sampling technique. Surveys were conducted both on weekdays and weekends and were worked out both directly and via online platforms. The sample size for data collecting was estimated using the methodology offered by National Statistical Services (NSS, 2017). With a confidence level of 95 %, population size of 17,000 commuters (according to official statistics) and a sample size of 255 surveys, the relative standard error is 6.23% which is considered admissible and stands at the bases of our further analysis.

2.2.3. Estimating air pollutants generated by car-commuting

For estimating the quantity of each pollutant, average European emission factors, stated in units of grams per vehicle-kilometre, were taken into account for each given vehicle technology. Five pollutants that are relevant for traffic related impact were chosen (CO, NMVOC, NO_x, N₂O and PM_{2.5}) and estimated using the estimations from Guidebook inventory of atmospheric air pollutants 2016 in g/km (EEA, 2016) These average emission factors were determined by European Environment Agency taking into account the typical values for ambient temperatures, driving speeds, rural-urban-expressway mode mix, trip length, etc.

Table 1. Questions used in the survey

<i>Subject of interest</i>	<i>Type of question</i>	<i>Ex. of answer</i>
Place of living	Identification Question	Valea Lupului
Work place	Identification Question	Iasi, City Centre
Commuting frequency	Factual Question	Daily
Distance (time and km) covered	Factual Question	50 km / 60 minutes
Means of transportation	Filtered question	Personal car
Number of passengers (by car)	Factual Question	Two passengers
Displacement for the car (cc)	Factual Question	1500-2000 cc
Fuel Type	Factual Question	Diesel
Pollution norm	Factual Question	Euro 4
Family income	Factual Question	4,000 RON
Age	Identification Question	45
Sex	Identification Question	M

The input data also included the estimated vehicle stock involved in commuting by vehicle type/technology (Non-EURO, EURO 1 to 6), fuel type (gasoline, diesel, LPG, hybrid) and vehicle size, broken down by cylinder capacity.

The results of the above mentioned applied questionnaires were used in order to obtain the profile of each commune from the Metropolitan Area not only in what concerns the mobility behaviour, but also the passenger cars fleet structure. The data obtained from questionnaires' were extrapolated to the total number of commuters. Finally joining the commuting profile data (frequency, distance, no. of passengers, displacement for the car) and the emission factors for each type of car there was identified a raw assessment of the annual quantities of the main air pollutants (CO, NMVOC, NO_x, N₂O, PM_{2.5}).

3. Results and discussions

3.1. GIS Assessment of Urban Sprawl in Iasi Metropolitan Area

The process of expanding the urban influence area, while concentrating the facilities inside the city centre, leads to a strong core-periphery model based on the assessment of accessibility that was calculated

for each settlement from the Metropolitan Area (Fig. 3) and then averaged at communes level (Table 2). Applying the GIS accessibility model taking into account the existing configuration and quality of road network resulted in the delineation of three rings of settlements. The first ring includes localities accessible in less than 15 minutes by car from the city centre: the suburban localities such as Valea Lupului, Miroslava, Barnova, Aroneanu, Letcani etc.). The second ring mainly encloses localities with medium accessibility within 15 - 25 minutes from the urban chore that are also emitters (and sometimes receivers) of commuters towards (and from) the city (secondary settlements from Popricani Aroneanu, Holboca, Miroslava communes). Finally, the third ring delineates localities with lower accessibility outside the 25 minutes isochrone (Schitu Duca, Ungheni, Victoria etc.).

The ease of accessing the city (and its facilities) is also correlated to the degree of development which explains the fact that several settlements bounded to the city (with a high degree of accessibility) have also a high degree of development. In the same time, localities positioned between main transportation axes have, generally, a lower degree of development caused by higher values of duration-distances.

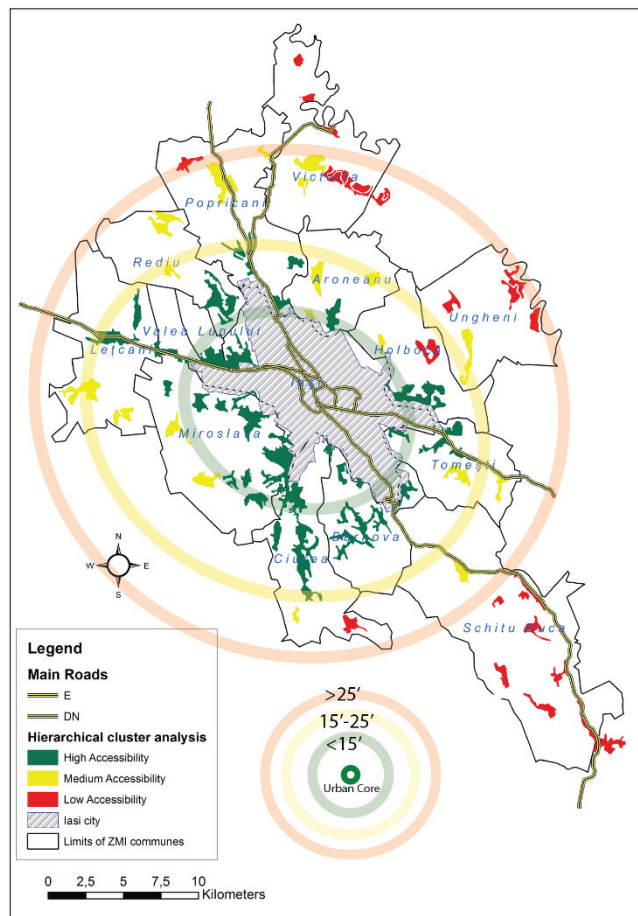


Fig. 3. Accessibility by duration-distance values in Iasi Metropolitan Area

Table 2. The relation between commuters and commuting distance to Iasi Municipality

Commune	No. of commuters	Commuters out of total employees (%)	Distance (km)	Time travel to city centre (min.)
Aroneanu	603	47.2	8	12
Barnova	1315	52.9	10	11
Ciurea	2256	49.3	13	10
Holboca	2962	58.2	11	12
Letcani	753	24.6	15	13
Miroslava	2117	51.7	5	10
Popricani	1089	39.2	19	14
Rediu	931	53.5	10	12
Schitu Duca	272	15.0	24	23
Tomesti	2674	52.6	11	12
Ungheni	453	24.9	21	20
Valea Lupului	1460	62.5	7	8
Victoria	190	12.0	25	22

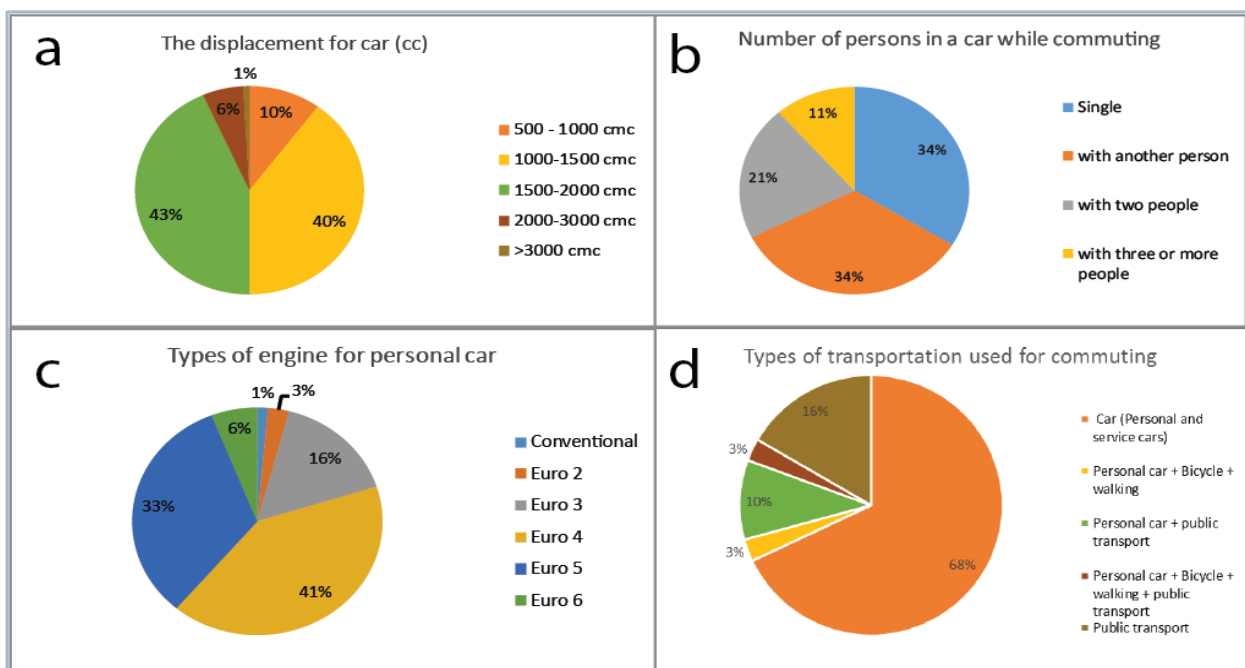


Fig. 2. Indicators of car dependency estimation using survey results

Therefore, these areas are considered peripheral and rural (even if they are 10 km away from the core), presenting typical characteristics and behaviours (lower frequency of commuting, less mobility, lower development). The accessibility model highlights a strong relation between the percentage of commuters working in Iasi and the time travel to city centre ($R^2 = 0.82$) (Table 2). It can be noticed that the longer the distance from the outskirts of the city, the lower the degree of mobility and usage of personal cars.

Nevertheless, there are cases of communes that are emitting fewer commuters even though they are relatively close to the city. For example in Letcani, local development absorbs a higher number of employees and the share of the commuters out of the total number of employees is at the same level with as the one in Ungheni, which is more than 21 km far from the city.

The negative effects are mainly caused by traffic agglomeration and longer trips which induce car dependency and generate increased air pollution. Therefore the relation discussed above, between the length of the trips and the number of commuters is highly important in order to understand and estimate car dependency in Iasi Metropolitan Area.

3.2. Estimating car dependency

Analysing the survey, the results highlighted that most commuters (68 %) are using their personal car, no matter their earnings, showing a car-dependency pattern which has its bases on the socialist regime, when having a car was considered a privilege (Fig. 4d). Most of the cars used by the commuters (83 %) have their displacement lower than 2,000 cc, emphasising a lower consumption of fuel (Fig. 4a). On the other hand, a reduced average income determines most of the commuters to buy used cars with a

moderate ecological footprint (Euro 5 – 33 % and Euro 4 – 41 %), resulting in negative effects upon traffic environment. Also, most of the respondents (34 %) are travelling alone or with another person (34%). The results of the survey demonstrate a high dependency on commuting by personal car. Most of the respondents possess a car (50 %) and 41 % possess two cars. Another reason for this dependency is related to a weak connectivity of the public transportation services to the suburbs (Rosu and Blageanu, 2015; Ursu et al., 2015) and within the Metropolitan Area.

The rapid growth of the income determines purchasing a car and locating in the peri-urban areas, thus establishing the car dependency no matter the time or distance. However, the accessibility model and the official statistics highlight a decrease in the number of commuters along with the increase in the distance to city centre.

To conclude, one can emphasise that the Metropolitan Area of Iasi city has known a strong increase in population, and, together with this, a high level of mobility by using their private cars. These behaviours are related to and have direct consequences on environmental pollution and the degradation or air quality.

3.3. Pollution resulted from using passenger cars for commuting

According to the previous assessment, a high number of commuters are located in the very proximity of the city (Valea Lupului, Miroslava, Ciurea), but fewer in the Northern and Eastern area. Nevertheless, the highest number of commuters are located in the Eastern part of the Metropolitan Area (Tomesti and Holboca) that are, in fact, neighbourhoods of Iasi city. The issue is reflected in the estimated annual emissions of exhausted gases from passenger cars, which are higher in the nearby communes also because of the high number of displacements per day except for the communes efficiently linked to the city by public transport and those with commuters owning new cars of high quality

technology (EURO 5 and 6- for example in Valea Lupului). The second ring of communes around Iasi has lower emissions, except for Schitu Duca (PM_{2.5}). There are differentiations that appear when it comes to communes where commuters usually use Diesel cars or cars with older and lower technology (Schitu Duca, Popricani, Holboca). For CO, the highest estimated emissions are originating from the peri-urban communes that are the closest to the city due to the high number of cars and daily trips: Ciurea (28.85 % of the total metropolitan rural areas), followed by Valea Lupului (18.08 %) and Tomesti (15.55 %). They are also the main emitters of NMVOC compounds (Table 3). If one refers to the main pollutant from transport activities – NO_x, the highest emitted quantities are caused by commuters from Tomesti (about 18 %), Ciurea and Valea Lupului (about 14 % each), followed by Barnova, Holboca and Popricani, which are farther from the city and, therefore, the travel distances are longer.

An important greenhouse gas, N₂O is emitted mainly by passenger cars from Ciurea (about 24 %) while other communes have a rather similar contribution of about 10% (Tomesti, Barnova, Valea Lupului, Holboca). In the case of fine particulate matter (PM_{2.5}), the higher values are from Ciurea and Holboca (about 33% from the total amount) because of high usage of diesel engines, followed by Barnova and Valea Lupului (large number of cars – different types). The lowest values for all analysed pollutants come from Aroneanu (smaller number of cars, predominantly with gasoline engines), Victoria and Ungheni (lower flows of commuters).

One can assess that the urban sprawl itself is mainly induced by the wealthiest people who can afford to commute by using their personal cars. They are, at the same time, the main contributors to the alteration of the air quality by using personal cars and having car-dependency behaviour. Meanwhile the results of our calculations indicate that even though the highest numbers of cars per family are in Valea Lupului and Barnova, there are also the newest types of cars that pollute less (Euro 5 and EURO 6).

Table 3. The estimated annual amount of pollutants by rural communes of Iasi Metropolitan Area

Commune	CO (kg/year)	NMVOC (kg/year)	NO _x (kg/year)	N ₂ O (kg/year)	PM _{2.5} (kg/year)
Aroneanu	356.49	27.19	456.78	3.24	1.71
Barnova	2766.49	237.19	1013.98	16.85	42.17
Ciurea	6671.86	610.45	1398.40	36.49	59.39
Holboca	147.61	22.46	930.56	16.04	50.38
Letcani	477.86	59.97	272.47	2.67	23.51
Miroslava	2076.13	160.45	299.70	8.05	4.42
Popricani	1142.23	62.99	922.51	12.90	32.73
Rediu	1503.14	127.68	712.68	10.60	32.21
Schitu Duca	65.78	12.36	491.70	6.18	25.62
Tomesti	3595.46	425.12	1718.58	19.45	12.32
Ungheni	31.96	3.78	77.30	0.54	5.92
Valea Lupului	4182.05	307.81	1363.49	16.28	38.01
Victoria	111.79	9.76	118.97	1.29	5.77

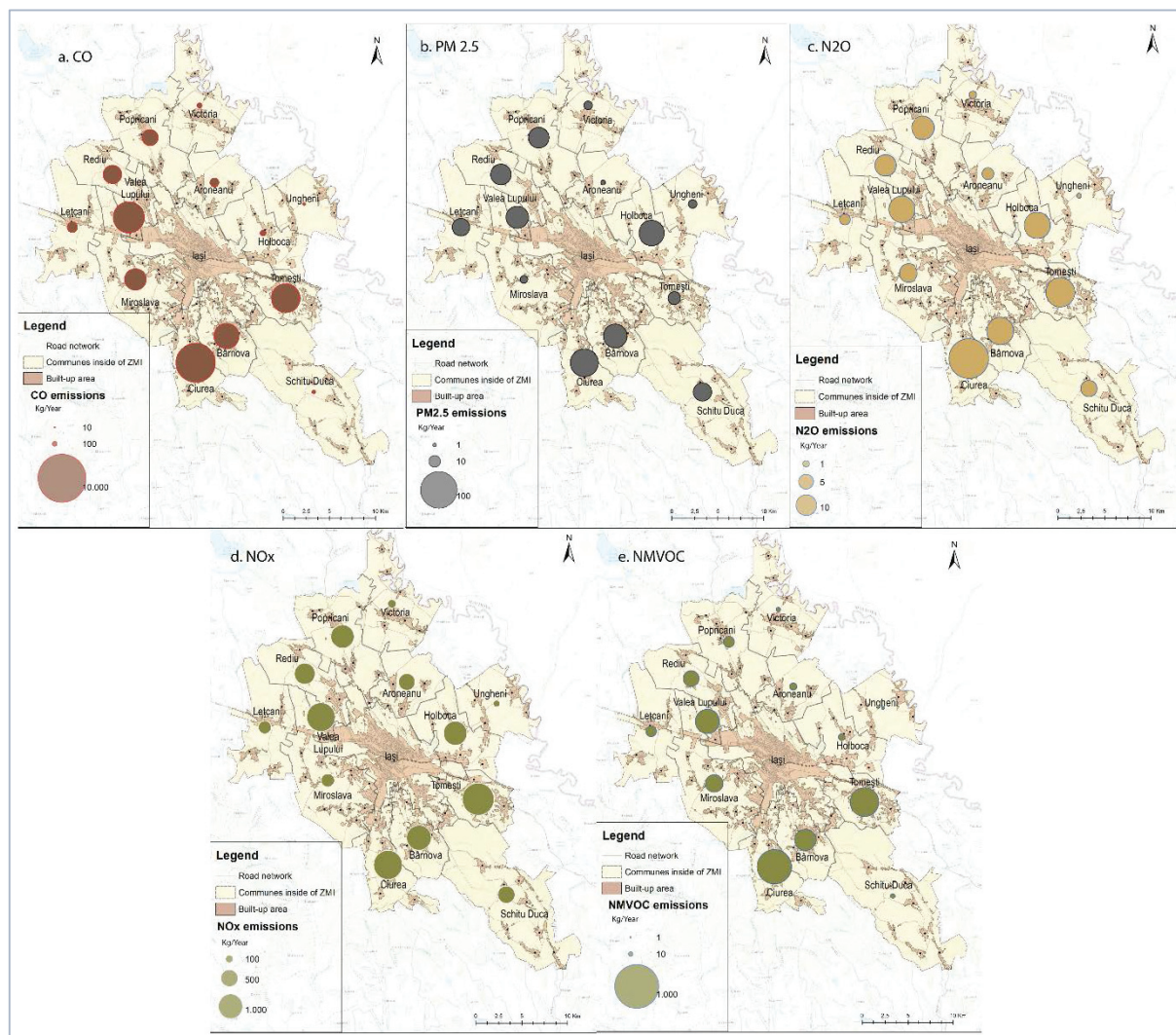


Fig. 3. The estimated annual emissions of CO(a), PM2.5(b), N₂O (c), NO_x (d), NMVOC (e) resulting from the use of personal car for commuting in Metropolitan Area of Iasi

On the other hand, there are rural areas with fewer commuters, but using older cars which pollute more (Ungheni, Victoria, Schitu Duca). Therefore, no direct correlation can be made between the number of cars and the relative atmospheric emissions.

The daily displacements of peri-urban population from Iasi Metropolitan area are an important cause of air pollution especially at peak hours, when it comes to more than 2,000 commuters (Holboca, Tomesti, Ciurea and Miroslava). The pollution is reduced if the commuters associate in using fewer cars for travelling to work, when the public transport has an acceptable quality and frequency or when commuters use new cars with environmentally friendly technology and fuel. The local policies are very important, stimulation of using public transport, smoothing the traffic flow or renewing the car fleet are to be considered by the local stakeholders in order to reduce the effects upon the quality of local environment.

Overall, without planning the areas of present urban sprawl, the Metropolitan Area of Iasi cannot face a farther extension of urban built area, the

explosion of commuting surpassing the real possibilities of the infrastructure and environment to bear the consequences.

The current assessment of spatial distribution of estimated air pollution in Iasi peri-urban metropolitan area does not comprise an actual modelling of pollution or an assessment of its actual impact, but the results do indicate the main directions (axis) that contribute to general pollution (Southern, Eastern and Western). The emissions inventory is a preliminary but useful tool in assessing car dependency environmental impact by increased air pollution. It is only a raw assessment that has to be integrated in larger studies. Unfortunately, the lack of monitoring stations in the peri-urban area – except for IS-5, Tomesti station - makes it impossible, at this phase, to perform the validation of data or finding a clear relation between air pollutant emissions and the corresponding air pollutants levels.

Nevertheless, it estimates the passenger cars used for commuting in each administrative unit and the annual amount of emissions that cumulate and contribute to background pollution in the metropolitan

area. It gives opportunity for further studies to evaluate the actual concentration of pollutants, the need for monitoring and implementing strategies for pollution abatement.

The resulting assessment should be completed by adding more precise and detailed long term data from traffic monitoring in the car-commuting areas. In practice, the decision-making process of obtaining these data is stopped by budget constraints (Vlachokostas et al., 2011).

4. Conclusions

The fast extension of the built-up area and uncontrolled peri-urbanization lead to specific issues of urban sprawl. The relation between this process, on the one hand, and car dependency and air pollution, on the other hand, was examined in the present study by using official statistical data and the results of our own survey for evaluating the commuter's flows and consequent atmospheric emissions.

It was observed that communes located in the proximity of urban core contribute the most to the air pollution caused by the usage of personal cars for commuting as their inhabitants have the highest number of cars per family, the highest number of daily trips to and from the city, therefore the highest car dependency. Meanwhile, the fact that they have newer cars reduces their overall contribution to general pollution. Contrary to this trend, the rural areas that are more remote from the city centre – more than 25 minutes car travel distance from the city – have a lower number of commuters, a higher use of public transport, while having fewer cars per family and a lower car dependency. However, their contribution to air pollution is increased by longer travel distances and the use of older and more polluting cars.

The results of this integrative approach estimate the quantities of air pollutants generated by the daily use of cars for commuting by each commune from Iasi Metropolitan Area, creating a spatial image of the air pollution footprint caused by car commuting.

The present study has several implications for policy analysis. It represents a starting point for further studies that could also imply measurements, dispersion modelling and public health assessments that could have in view the actual transformations in urban sprawl in order to ground coherent strategies for an effective air pollution abatement strategy in Iasi City, one of the most polluted urban areas in Romania.

Acknowledgments

This work was financially supported by the Department of Geography from the "Alexandru Ioan Cuza" University of Iasi, and the infrastructure was provided through the POSCCE-O 2.2.1, SMIS-CSNR 13984-901, No. 257/28.09.2010 Project, CERNESIM.

Author Contributions

All three authors equally contributed to the development of the framework and writing of the manuscript.

References

- Aftabuzzaman M., Mazloumi E., (2011), Achieving sustainable urban transport mobility in post peak oil era, *Transport Policy*, **18**, 695-702.
- Alberti M., Marzluff J.M., (2004), Ecological resilience in urban ecosystems: linking urban patterns to human and ecological functions, *Urban Ecosystems*, **7**, 241-265.
- Ambarwati L., Verhaeghe R., van Arem B., Pel A.J., (2016), The influence of integrated space-transport development strategies on air pollution in urban areas, *Transport Research Part D: Transport and Environment*, **44**, 134-146.
- Banica A., Bobric E., Breaban I.G., (2016), *Issues related to air quality monitoring in North-East region (Romania)*, SGEM 2016 Conference Proceedings, **2**, 451-458.
- Banica A., Bobric E.D., Cazacu M.M., Timofte A., Gurlui S., Breaban I.G., (2017) Integrated assesment of exposure to traffic-related air pollution in Iasi city, Romania, *Environmental Engineering and Management Journal*, **16**, 2147-2163.
- Blageanu A., Iacob I.C., Rosu L., (2012), Simulation of suburban development features based on scenarios in the Eastern side of Iasi city, *Geographia Napocensis*, **6**, 130-139.
- Borken-Kleefeld J., Chen Y., (2015), New emission deterioration rates for gasoline cars—Results from long-term measurements, *Atmospheric Environment*, **101**, 58-64.
- Brade I., Herfert G., Wiest K., (2009), Recent trends and future prospects of socio-spatial differentiation in urban regions of Central and Eastern Europe: A lull before the storm?, *Cities*, **26**, 233-244.
- Burton E., Jenks M., Williams K., (2013), *Achieving Sustainable Urban Form*, Routledge, New York.
- Carslaw D.C., Beevers S.D., Tate J.E., Westmoreland E.J., Williams M.L., (2011), Recent evidence concerning higher NOx emissions from passenger cars and light duty vehicles, *Atmospheric Environment*, **45**, 7053-7063.
- Carslaw D.C., Rhys-Tyler G., (2013), New insights from comprehensive on-road measurements of NOx, NO₂ and NH₃ from vehicle emission remote sensing in London, UK, *Atmospheric Environment*, **81**, 339-347.
- Chiou Y.-C., Chen T.-C., (2010), Direct and indirect factors affecting emissions of cars and motorcycles in Taiwan, *Transportmetrica*, **6**, 215-233.
- Chiou Y.-C., Wen C.-H., Tsai S.-H., Wang W.-Y., (2009), Integrated modeling of car/motorcycle ownership, type and usage for estimating energy consumption and emissions, *Transportation Research Part A: Policy and Practice*, **43**, 665-684.
- Cimpianu C., Corodescu E., (2013), Landscape dynamics analysis in Iasi Metropolitan Area (Romania) using remote sensing data, *Cinq Continents*, **3**, 18-32.
- Ciobanu S.M., Benedek J., (2015), Spatial characteristics and public health consequences of road traffic injuries in Romania, *Environmental Engineering and Management Journal*, **14**, 2689-2702.
- Clipa R.I., (2012), Attempts to estimate the sources of agglomeration economies in Iasi metropolitan area, *Anale. Seria Stiinte Economice.Timisoara*, **18**, 352-358.
- De Ridder K., Lefebre F., Adriaensen S., Arnold U., Beckroeghe W., Bronner C., Damsgaard O., Dostal I., Dufek J., Hirsch J., IntPanis L., Kotek Z., Ramadier T., Thierry A., Vermoote S., Wania A., Weber C., (2008),

- Simulating the impact of urban sprawl on air quality and population exposure in the German Ruhr area. Part I: Reproducing the base state, *Atmospheric Environment*, **42**, 7059-7069.
- EEA, (2016), EMEP/EEA air pollutant emission inventory guidebook - 2016 - European Environment Agency, Copenhagen, On line at: <http://www.eea.europa.eu/publications/emep-eea-guidebook-2016>.
- Fina S., Siedentop S., (2008), *Urban Sprawl in Europe—Identifying the Challenge*, REAL CORP 008 Proceedings/Tagungsband, Vienna, May 19-21 2008, On line at: http://realcorp.at/archive/CORP2008_34.pdf.
- Forslid R., Ottaviano G.I., (2003), An analytically solvable core-periphery model, *Journal of Economic Geography*, **3**, 229-240.
- Fowler, F. J., (2014), *Survey Research Methods*, Fifth Edition, Los Angeles, SAGE.
- Franco V., Sánchez, F.P., German, J., Mock, P., (2014), Real-world exhaust emissions from modern diesel cars, *Communications*, **49**, 1-53.
- Frenkel A., Ashkenazi M., (2008), Measuring urban sprawl: how can we deal with it?, *Environment and Planning B: Planning and Design*, **35**, 56-79.
- Frumkin H., (2002), Urban sprawl and public health, *Public Health Reports*, **117**, 201-2017.
- Gonzalez G.A., (2005), Urban sprawl, global warming and the limits of ecological modernisation. *Environmental Politics*, **14**, 344-362.
- Grigorescu I., Mitrica B., Kucsicsa G., Popovici E.-A., Dumitrascu M., Cuculici R., (2012), Post-communist land use changes related to urban sprawl in the Romanian Metropolitan Areas, *Human Geographies*, **6**, 35-46.
- Iatu C., Eva M., (2016), Spatial profile of the evolution of urban sprawl pressure on the surroundings of Romanian cities (2000-2013), *Carpathian Journal of Earth and Environmental Sciences*, **11**, 79-88.
- Jensen S.S., (1998), Mapping human exposure to traffic air pollution using GIS, *Journal of Hazardous Materials*, **61**, 385-392.
- Jones C., Kammen D.M., (2014), Spatial distribution of US household carbon footprints reveals suburbanization undermines greenhouse gas benefits of urban population density, *Environmental Science & Technology*, **48**, 895-902.
- Kim J., (2016), Vehicle fuel-efficiency choices, emission externalities, and urban sprawl, *Economics of Transportation*, **5**, 24-36.
- Lera-López F., Faulin J., Sánchez M., (2012), Determinants of the willingness-to-pay for reducing the environmental impacts of road transportation, *Transportation Research Part D: Transport and Environment*, **17**, 215-220.
- Luca F.A., Ioan C.A., (2012), Air quality management in Iasi city, *Environmental Engineering and Management Journal*, **11**, 377-383.
- Manolache G., Voinea S., Skliros D., Stefan S., (2017), Comparative study of urban and rural atmospheric aerosols in and near Bucharest, *Environmental Engineering and Management Journal*, **16**, 2381-2389.
- Martins H., (2012), Urban compaction or dispersion? An air quality modelling study, *Atmospheric Environment*, **54**, 60-72.
- Mihai C., (2015), *Morpho-functional dynamics of Iasi municipality after 1990 - process, structures and spatial challenges*, PhD Thesis (in Romanian), Alexandru Ioan Cuza University, Faculty of Geography and Geology, Iasi, Romania.
- Mironiuc M., Huian M.C., (2017), Empirical study on the interdependence between environmental wellbeing, financial development and economic growth, *Environmental Engineering and Management Journal*, **16**, 2625-2635.
- Muñiz L., Galindo A., (2005), Urban form and the ecological footprint of commuting. The case of Barcelona, *Ecological Economics*, **55**, 499-514.
- Newman P., Kenworthy J., (2011), Peak car use: Understanding the demise of automobile dependence, *World Transport Policy and Practice*, **17**, 31-42.
- Novelli V., Geatti P., Ceccon L., Toscani L., (2017), Low environmental impact of alternatively supplied cars. Results of an investigation carried out in the North-East of Italy.
- NSS, (2017), National Statistical Service-Sample Size Calculator, On line at: <http://www.nss.gov.au/nss/home.nsf/pages/Sample+size+calculator>.
- Oprea M., Dunea D., Liu H.-Y., (2017), Development of a knowledge based system for analyzing particulate matter air pollution effects on human health, *Environmental Engineering and Management Journal*, **16**, 669-676.
- Park S., Hepcan Ç.C., Hepcan S., Cook E.A., (2014), Influence of urban form on landscape pattern and connectivity in metropolitan regions: a comparative case study of Phoenix, AZ, USA, and Izmir, Turkey, *Environmental Monitoring and Assessment*, **186**, 6301-6318.
- Petrescu V., Ciudin R., Isarie C., Cioca L.I., Trif, B., Nederita, V., (2015), The impact of traffic related pollution on air quality in Sibiu region, *Environmental Engineering and Management Journal*, **14**, 2637-2642.
- Rosu L., Blageanu A., (2015), Evaluating issues and performance of a public transport network in a post-communist city using a quantitative spatial approach, *Urbani Izziv*, **26**, 103-116.
- Sailer-Fliege U., (1999), Characteristics of post-socialist urban transformation in East Central Europe, *GeoJournal*, **49**, 7-16.
- Schindler M., Caruso G., (2014), Urban compactness and the trade-off between air pollution emission and exposure: Lessons from a spatially explicit theoretical model, *Computers, Environment and Urban Systems*, **45**, 13-23.
- Schindler M., Caruso G., Picard P., (2017), Equilibrium and first-best city with endogenous exposure to local air pollution from traffic, *Regional Science and Urban Economics*, **62**, 12-23.
- Spiekermann K., Neubauer J., (2002). *European Accessibility and Peripherality: Concepts, Models and Indicators*, Working Paper 02-09, Nordregio, Stockholm.
- Stankovic S., Vaskovic V., Petrovic N., Radojicic Z., Ljubojevic M., (2015), Urban traffic air pollution: case study of Banja Luka, *Environmental Engineering and Management Journal*, **14**, 2783-2791.
- Stefan S., Barladeanu R., Andrei S., Zagar L., (2015), Study of air pollution in Bucharest, Romania during 2005-2007, *Environmental Engineering and Management Journal*, **14**, 809-818.
- Su W., Gu C., Yang G., Chen S., Zhen F., (2010), Measuring the impact of urban sprawl on natural landscape pattern of the Western Taihu Lake watershed, China, *Landscape and Urban Planning*, **95**, 61-67.

- Takuchev N., Vasileva I., Petrova S., (2014), Dispersion modelling of the air pollution, emitted by the traffic in the transport tunnel under the old town of Plovdiv, Bulgaria, *Ecologia Balkanica*, **6**, 73-86.
- Ursu A., Andrei M., Chelaru D.A., Ichim P., (2016), Built-up area change analysis in Iasi city using GIS, *Present Environment and Sustainable Development*, **10**, 201-216.
- Ursu A., Burtila R., Minea V., Marius A., Ichim P., (2015), *Urban Public Transportation System Changes, in Post-Communist Period in Iasi Municipality*, SGEM 2016 Conference Proceedings, **6**, 615-622.
- Vasilescu J., Marmureanu L., Nemuc A., Nicolae D., Talianu C., (2017), Seasonal variation of the aerosol chemical composition in a Romanian peri-urban area, *Environmental Engineering and Management Journal*, **16**, 2491-2496.
- Verhoef E.T., Nijkamp P., (2004), *Spatial Externalities and the Urban Economy*, In: *Urban Dynamics and Growth: Advances in Urban Economics*, Capello R., Nijkamp P. (Eds.), Elsevier, Amsterdam, 87-120.
- Vlachokostas C., Achillas C., Moussiopoulos N., Banias G., (2011), Multicriteria methodological approach to manage urban air pollution, *Atmospheric Environment*, **45**, 4160-4169.
- Wang X., Wang Y., Xu C., Chen L., Guo S., (2016), Convergence of human populations in China: impact on sustainable development, *Environmental Engineering and Management Journal*, **15**, 2375-2382.
- WHO, (2016), World Health Organization, Ambient (outdoor) air quality and health, On line at: <http://www.who.int/mediacentre/factsheets/fs313/en/>.
- Zhang S., Wu Y., Huang R., Wang J., Yan H., Zheng Y., Hao J., (2016), High-resolution simulation of link-level vehicle emissions and concentrations for air pollutants in a traffic-populated eastern Asian city, *Atmospheric Chemistry and Physics*, **16**, 9965-9981.



“Gheorghe Asachi” Technical University of Iasi, Romania



ANTIBACTERIAL ACTIVITIES OF BEECH BARK (*Fagus sylvatica* L.) POLYPHENOLIC EXTRACT

Corneliu Tănase^{1*}, Sanda Coșarcă¹, Felicia Toma¹, Anca Mare¹, Adrian Man¹,
Amalia Miklos², Silvia Imre¹, Irina Boz^{3,4}

¹University of Medicine and Pharmacy of Tirgu Mures, Gheorghe Marinescu, 38, 540139,
Tirgu Mures, Mures, Romania

²Center for Advanced Medical and Pharmaceutical Research (CCAMF), University of Medicine and Pharmacy of Tirgu Mures,
Gheorghe Marinescu, 38, 540139, Tirgu Mures, Mures, Romania

³Integrated Centre for Environmental Science Studies in the North-East Development Region – CERNESIM, Alexandru Ioan Cuza
University of Iasi, Bd. Carol I, 11, 700506, Iasi, Romania

⁴Institute of Biological Research, Lascar Catargi 47, 700107 Iasi, Romania

Abstract

The study provides information about separation and identification of natural bioactive compounds from beech (*Fagus sylvatica* L.) bark with potential therapeutic applications such as antibacterial activity against human pathogens. Beech is a common material used in the wood industry, but its bark is separated from the wood and is considered a by-product. In this study, natural compounds with biological activity were obtained from beech bark by hot water extraction. The high-performance liquid chromatography (HPLC) was used to analyze the phenolic compounds in the beech bark extracts. Spectrophotometric methods were employed for the determination of total phenolic content. Microdilution technique was used for testing the antimicrobial activity of the extract. The following strains were tested: *Staphylococcus aureus*, *Methicillin-resistant Staphylococcus aureus*, *Klebsiella pneumoniae*, *Escherichia coli* and *Pseudomonas aeruginosa*. The yield of extracted polyphenols was of 22.952 mg gallic acid/g dry bark. The compounds identified by HPLC were vanilic acid, catechin, taxifolin and syringin. The extracts were active against *Staphylococcus aureus* and *Methicillin-resistant Staphylococcus aureus*. The effect of polyphenolic extract on Gram-negative bacteria was absent at a concentration of 30 mg/mL beech bark extract. Altogether, the use of pure water for extraction of polyphenols from beech bark proved to be an effective eco-friendly method. This method sustains the concept of “green” chemistry by involving the use of renewable plant resources and also by using water as solvent.

Key words: antibacterial, beech bark, green biotechnology, biorefinery, polyphenols

Received: May, 2017; Revised final: February, 2018; Accepted: March, 2018; Published in final edited form: April 2018

1. Introduction

Today, with the evolution of technology triggering a great number of changes, humankind has adopted an attitude of returning to nature. The active principles of plants can represent a real alternative, with applications in different subject areas, tied to the specialty of the biologist (medicine, pharmacy, the food industry, cosmetics, and agriculture). Currently

great interest is given to the separation and characterization of the natural compounds. Also their application and introduction in different research fields is intended using the principles of green chemistry and biorefinery in the context of sustainable development (Barbosa-Pereira et al., 2014; Fierascu et al., 2017; Huang et al., 2010; Pereira et al., 2016; Shahina et al., 2006). Plants are an inexhaustible sources of bioactive compounds with antioxidant

* Author to whom all correspondence should be addressed: e-mail: corneliu.tanase@umftgm.ro; Phone: +40 265 215 551

properties. In the literature of specialty, there are several studies dealing with separation and augmentation of the polyphenolic compounds from waste resulting from different manufacturing processes (Balasundram et al., 2006; Ignat et al., 2013; Moure et al., 2001; Tanase et al., 2014). Studies have revealed the importance of waste from the timber industry. The rhytidome, the nodes of spruce (Ignat et al., 2013; Tanase et al., 2014) and the wood (red heart) of the common beech (*Fagus sylvatica* L.) contain important quantities of chlorogenic acid, catechin, quercetin, kaempferol (Hofmann et al., 2008; Hoppe et al., 2016; Omar et al., 2000; Vek et al., 2013a; 2013b).

The phenolic compounds present in plants have an important role in the protection against abiotic stress (UV rays) and biotic factors with negative influence (predators, pathogen attacks) (Ignat et al., 2013). The emergence of infectious diseases caused by drug resistant bacteria has become one of the most serious problems in medicine. Although the use of antibiotics has reduced the incidence of these diseases, nowadays, there are a number of bacterial strains resistant to antibiotics (Lazau et al., 2013).

Phenolic compounds (polyphenolic acids, tannins, flavonoids, anthocyanins), synthesized by plants as a response to microbial infections, have a high capacity for action against a wide range of microorganisms. Several studies have been reported about the use of polyphenolic plant extracts in medicine (Carraturo et al., 2014; Friedman et al., 2006; Hagi, 2008; Huang et al., 2010; Morteza-Semnani et al., 2011; Omar et al., 2000; Pereira et al., 2016; Szabo et al., 2010).

The majority of phenolic compounds are found in the leaf and stem of the plants. In stem, polyphenols are especially concentrated in the rhytidome. Thus, the extracts obtained from the rhytidome have a high antibacterial and antifungal activity (Omar et al., 2000). For example, it was found that the ethanolic extract obtained from the *Picea abies* L. rhytidome presents antibacterial activity against Gram-positive and Gram-negative bacteria (Ignat et al., 2013). The aqueous and alcoholic extract obtained from the bark of the common beech (*Fagus sylvatica* L.) were also biologically tested. It was found that these beech bark extracts present a high antioxidant activity (Hofmann et al., 2015b).

The aims of this study were: (1) to provide information on separation and identification of natural bioactive compounds with potential therapeutic applications from beech (*Fagus sylvatica* L.) bark, a renewable plant resources, using water as solvent; (2) to test the antibacterial activity of the beech bark extract on human pathogens like methicillin-sensitive *Staphylococcus aureus* (MSSA), methicillin-resistant *Staphylococcus aureus* (MRSA), *Klebsiella pneumoniae*, *Escherichia coli* and *Pseudomonas aeruginosa*.

2. Material and methods

2.1. Materials

Beech (*Fagus sylvatica* L.) bark was provided as waste by a wood processing company (Vatra Dornei, Romania). Prior to extraction, the beech bark was air-dried at room temperature (10.5 % humidity) and milled in a GRINDOMIX GM 2000 mill to a mean particle size diameter of 0.5 mm. The biomass was directly used without any pre-treatments.

To determine the antibacterial activity, the following bacterial strains were used: methicillin-sensitive *Staphylococcus aureus* (MSSA) ATCC 25923, methicillin-resistant *Staphylococcus aureus* (MRSA) ATCC 43300, *Escherichia coli* ATCC 25922, *Klebsiella pneumoniae* ATCC 13883, and *Pseudomonas aeruginosa* ATCC 27853. The bacterial strains were selected from the collection of Laboratory of Microbiology, Virology and Parasitology (Faculty of Medicine - University of Medicine and Pharmacy, Tîrgu Mureş).

2.2. Aqueous extraction

Extractions were performed using 20 g of ground and dried beech bark placed in an Erlenmeyer flask over which 125 mL distilled water was added. The mixture was introduced and kept for 45 min in a water bath at 85 – 90°C, shaking from time to time. Collected extract were filtered and the extracted material was subjected to a second extraction with fresh distilled water. This operation was repeated 2 or 3 times until full beech bark exhaustion (colorless extract). All extracts were cumulated in a 500 mL volumetric flask and marked up to volume with distilled water.

2.3. Characterization of the extract

The aqueous extract from beech bark (EAF) was characterized in terms of total dry matter and organic matter content, and total polyphenolic content using Folin Ciocalteu (FC) method. Dry matter content in the extract was determined by evaporation of 25 mL extract on water bath and drying at 105°C till constant mass, using a porcelain crucible. After that, the crucible was placed into a muffle furnace at 600°C for 6 hours to establish dry and organic matter content. Spectrophotometer readings at 420, 520, 620 nm, of the extract were cumulated to determine the color intensity. Folin Ciocalteu (FC) method was used to determine the total polyphenolic content (TPC). The principle of this colorimetrically method is based on the reducing properties of phenolic compounds in contact with FC reagent, which present a dark blue coloration with a maximum absorbance at 765 nm. About 1 mL of plant extract was mixed with 500 µL of the FC reagent, 2 mL of 10 % sodium carbonate and 5 mL of water.

The mixture was shaken thoroughly and was left to stand for 90 minutes. Then the absorbance at 765 nm was determined against a blank which contain all reagents without the samples or the gallic acid in the same conditions. The total phenolic content was expressed as the number of equivalents of gallic acid (GAE).

For qualitative analysis of beech bark extract by HPLC with multiple wavelength detection an UHPLC system, Flexar FX – 10 (Perkin Elmer) was used, consisting of binary pump, inline degaser, autosampler, column thermostat and PDA detector. All solvents were HPLC grade and the used reagents presented the highest available purity. The chromatographic conditions were: column - Luna C18 (Phenomenex), 150x4.6 mm, 3 µm; mobile phase A – formic acid 0.1 % V/V and B – acetonitrile; the elution gradient program: 0 – 0.1 min: 90 % A, 10 % B; 0.1 – 20.1 min: 90 % to 20 %A; 20.1 – 25.1 min: 20 %A; 25.1 – 26.1 min: 20 %A to 90 %A; 26.1 – 30.1 min: 90 %A. The mobile phase was delivered at a flow rate of 1 mL/min and the column was maintained at 35 °C. The monitoring wavelengths were 270 nm, 280 nm, 324 nm and 370 nm. A methanol-water mixture of Sigma Aldrich reference substances containing gallic acid monohydrate (GAL) (99%), eleutheroside B (ELE B) (98%), catechin (CAT) (99%), epicatechin (EPICAT) (90%), vanillic acid (VANIL) (97%), sinapic acid (SINAP) (99%), taxifolin (TAXI) (85%) and quercetin (QUER) (95%), with the concentration about 20 µg/mL for each substance, was analyzed after injecting a volume of 20 µL. Autosampler temperature was set at 20°C.

2.4. Microbiological activity

2.4.1. Minimum inhibitory concentration (MIC)

The microplate method was used to test the antimicrobial activity of the obtained extract, based on CLSI (2015). In order to establish the minimum inhibitory concentration (MIC) of the tested substance, 96 wells microplates were used. The bacterial inoculum was prepared by mixing 10 µL of bacterial suspension (0.5 McFarland) with 9990 µL of Muller-Hinton broth medium. In the first well of the microplate, 100 µL from the bacterial inoculum were mixed with 100 µL of the tested extract. From this well, binary dilutions were performed in Muller-Hinton broth medium. Control wells were also prepared: two for negative controls (culture medium and culture medium plus beech bark extract) and growth controls for each of the five bacteria (culture medium plus bacterial inoculum). The microplates were incubated at 37°C for 24 hours, in normal atmosphere. The minimum inhibitory concentration of the substance (MIC) was assessed in the first well (dilution), where no visible bacterial growth was detected by the unaided eye. For calculation of the MIC in mg of dry matter/mL, the concentration was adjusted mathematically by the dilution factor.

2.4.2. EAF growth rate effect

The growth rates were assessed for MSSA and MRSA by Spread Plate Procedure (Sanders, 2012). From fresh bacterial culture, a 0.5 McFarland suspension in sterile saline was prepared, and 10 µl of suspension was transferred into 9990 µL liquid culture medium (Muller Hinton broth). In Eppendorf tubes, 2 mL working solution of EAF was prepared, with a concentration corresponding to the well where the MIC was noted in the microplate assay. In the control solution the tested extract was substituted with sterile saline solution. From both control and sample, a series of dilutions in sterile saline were prepared.

From the dilution 1/100, 50 µL was seeded on Mueller Hinton agar plates (previously maintained at 37 °C). The seeded media were incubated at 37°C for 18 – 24 hours. This first phase was used to assess the total number of colony forming units/mL (CFU/mL) at time 0 (H0). The working solution and the control were incubated at 37°C for 3 hours and 6 hours, and in each of these time points, a new series of serial dilutions and seeding were performed. This allowed the assessment of CFU/mL after 3 hours and 6 hours of incubation (H1, H2). At the 3-hour time point, the 1/100 dilution was used for seeding, while at the 6-hour time point, the 1/100.000 dilution was used.

After 18 – 24 hours of incubation at 37°C, from the plates corresponding to each dilution and each time, the colonies were counted automatically using the "IUL Flash & Grow" colony counter. Mathematical adjustments were performed to compensate the dilution and the inoculation volume, using the formula:

$$\frac{CFU}{mL} = \text{number of colonies} \times \text{dilution factor} \times A \times B \quad (1)$$

A = dilution adjustment in the MH media = 100 at H0 and H1/10000 at H2;

B = volume of inoculation adjusting = 20 (mL).

Absolute growth curves were plotted using the CFU/mL numbers from each time point. The specific growth rates r for the tested sample and control were assessed using the CFU/mL values obtained after 6 hours of incubation, by the formula:

$$r = \frac{\ln(CFU/mL \text{ for } H2 - CFU/mL \text{ for } H0)}{\text{no.hours for } H2} \quad (2)$$

2.5. Statistical analysis

The statistical significance was assessed by GraphPad InStat 3 software, at a significance threshold value of $p < 0.05$.

3. Results and discussion

3.1. Extract characterization

The beech bark aqueous extract (EAF) was characterized in terms of dry matter and organic

matter, and total content of polyphenols. The results are summarized in Table 1. Beech bark extract contain considerable quantities of bioactive aromatic compounds. The total polyphenolic content for EAF was 0.918 mg GAE/mL.

3.2. Identification of phenolic compounds using HPLC

The chromatograms of a mixture of standards at different wavelengths are shown in Fig. 1. It can be observed that almost all components/peaks of interest are revealed at 270 nm and 280 nm, respectively. On the other hand, 324 nm seems to be the specific wavelength for SINAP and 370 nm for QUER. Based on the studies of Dübeler et al. (1997) and Hofmann (2015a) the major phenolic compounds from beech bark have been tentatively identified, including: (+)-catechin, (-)-epicatechin, quercetin-O-hexoside, taxifolin-O-hexosides, taxifolin-O-pentosides, B-type and C-type procyanidins, syringic acid and coumaric acid-di-O-glycosides, coniferyl alcohol and sinapyl

alcohol-glycosides, (+) and (-) glucodistylin (Dübeler et al., 1997; Hofmann et al., 2015a). Comparing to this results the compounds identified in our extract by HPLC were catechin, vanillic acid, taxifolin and eleutheroside B (syringin) in small amounts.

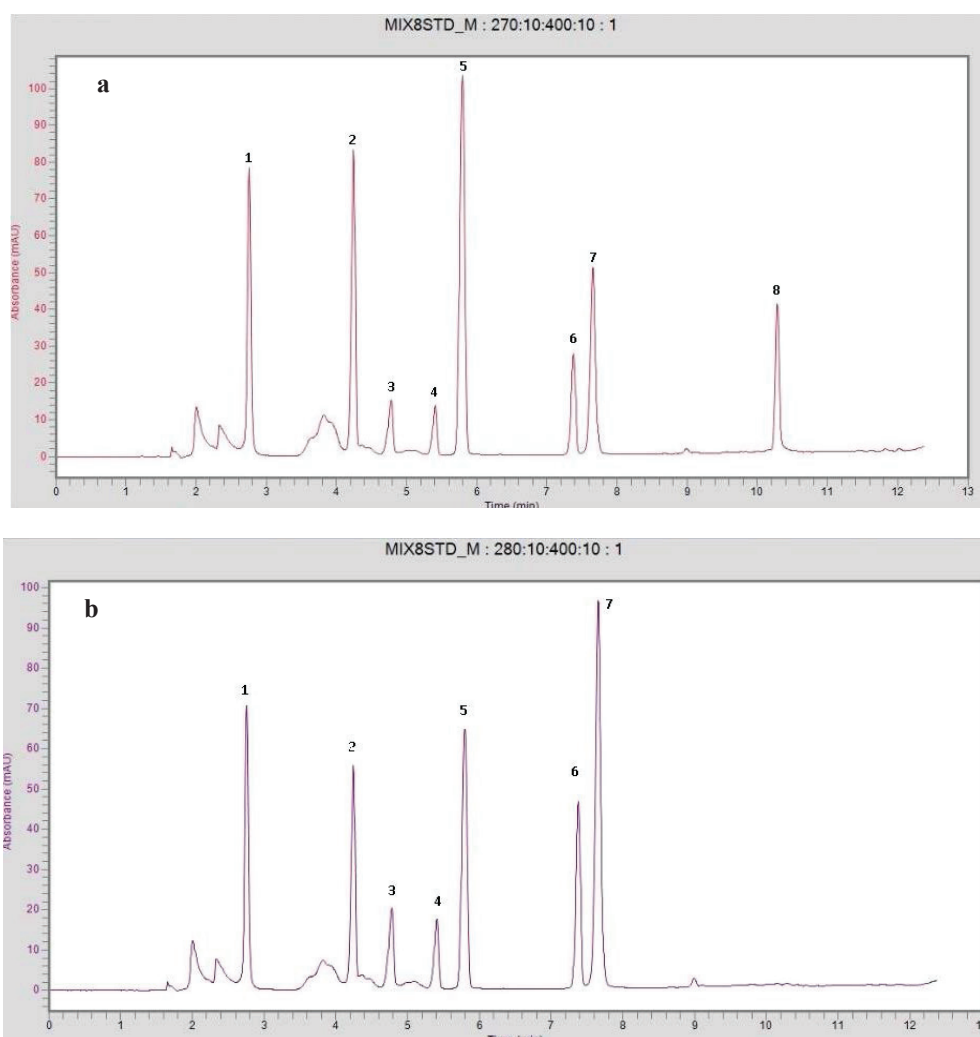
Vanillic acid being for the first time reported in the beech bark aqueous extract. The identification has been made by retention time's correspondence, multiwavelength analysis and addition standard method.

3.3. Microbiological activity

The minimum inhibitory concentrations (MICs) of polyphenolic extract required for growth inhibition of the Gram-negative and Gram-positive bacteria are presented in Table 2 and in a supportive image from Fig. 2. It was found, that EAF have antibacterial capacity against MSSA and MRSA. The effect of polyphenolic extract on Gram-negative bacteria was absent at a concentration of 30 mg/mL.

Table 1. Characteristics of beech bark aqueous polyphenolic extract

Dry matter content, g/L extract	Organic matter content, g/L extract	Color intensity	pH (at 25°C)	TPC, mg GAE/g dry bark
0.58 ± 0.09	0.41 ± 0.04	0.27 ± 0.03	4.5 ± 0.15	22.95 ± 0.07



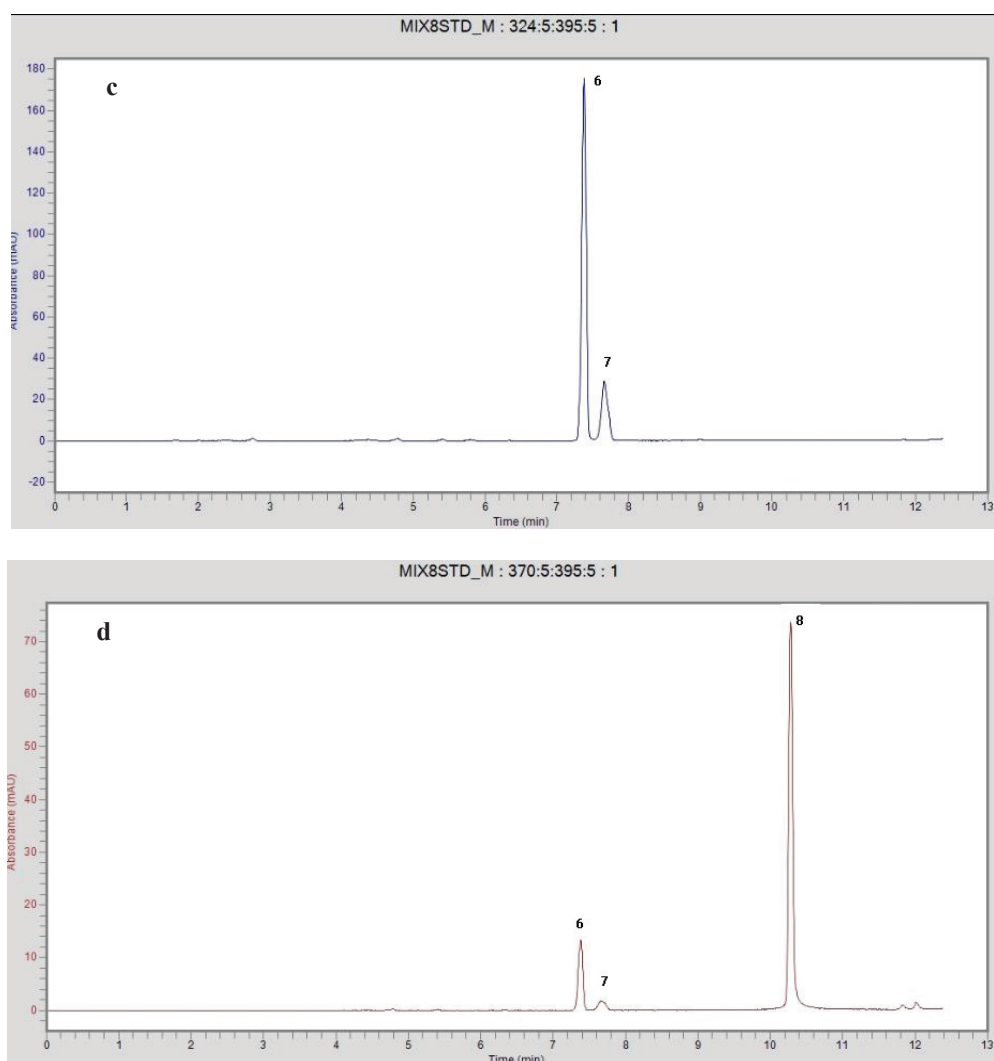


Fig. 1. Chromatograms of a mixture of eight standards, at different wavelengths: a) 270 nm; b) 280 nm; c) 324 nm; d) 370 nm. Order of elution: 1- gallic acid GAL, $t_R=2.76$ min; 2 – eleutheroside B ELE B, $t_R=4.24$ min; 3 – catechine CAT, $t_R=4.78$ min, 4 – epicatechine EPICAT $t_R=5.41$ min; 5 - vanillic acid VANIL, $t_R=5.79$ min, 6 - sinapic acid SINAP, $t_R=7.38$ min, 7 – taxifoline TAXI, $t_R=7.65$ min; 8 – quercetin QUER, $t_R=10.28$ min

Table 2. Minimum inhibitory concentrations (mg/mL) of EAF against the tested bacteria

<i>Bacteria</i>	<i>MICs – aqueous extract, mg/mL</i>
(A) <i>Staphylococcus aureus</i>	15
(B) <i>Methicillin-resistant Staphylococcus aureus</i> (MRSA)	30
(C) <i>Escherichia coli</i> ATCC 25922	-
(D) <i>Klebsiella pneumoniae</i> ATCC 13883	-
(E) <i>Pseudomonas aeruginosa</i> ATCC 27853	-

Thus, compared with MSSA and MRSA, which are gram-positive bacteria that only have the plasma membrane as their cell wall but do not have the bacterial outer membrane, it took longer for EAF compounds to penetrate into and interact with *E. coli*, *K. pneumoniae*, *P. aeruginosa*; thus, it may take a longer time for the gram-negative bacteria to be killed.

As shown in Fig. 3 and Table 3, when the growth medium was enriched with EAF, the bacterial growth was significantly inhibited within 6 hours compared to the control. After three hours of incubation (H1), EAF significantly inhibited the

bacterial growth for both MSSA and MRSA ($p < 0.0001$). After six hours of incubation (H2) EAF presented bactericidal effect on MRSA and further inhibited MSSA growth (Figs. 3 and 4). Beside the bactericidal effect, the growth rate r was also negatively affected by EAF. Fig. 5 presents a supportive image of the inoculated plates after 24 hours of incubation (MSSA and MRSA), corresponding to the tree time-points (initial time, 3 hours and 6 hours). In a study by Friedman et al. (2006) it was shown the antimicrobial activities of catechin from tea extract. Most phenolic compounds

presented a higher activity than antibiotics used in medicine, such as tetracycline or vancomycin, at comparable concentrations. The conclusion of this study was that the bactericidal activities of the teas are due to the presence of catechins. The antimicrobial activity of EAF consists in its phenolic nature. The antibacterial activity of any compound from EAF (CAT, VANIL, TAX or ELEB) against Gram-positive bacteria is partly due to their ability to reach the site of action. In bacteria, various enzymes, especially

components of energy-converting systems such as electron transport chains and ATPases, are embedded in the plasma membrane (Shahina et al., 2006). The extract of the beech bark have good efficacy of inhibiting bacterial growth and can be considered a potential pharmaceutical or food preservative.

Chemical constituents like catechin, vanillic acid, taxifolin, and syringin (found in EAF) have an antibacterial activity which leads to the increase of susceptibility of bacterial cells to these compounds.

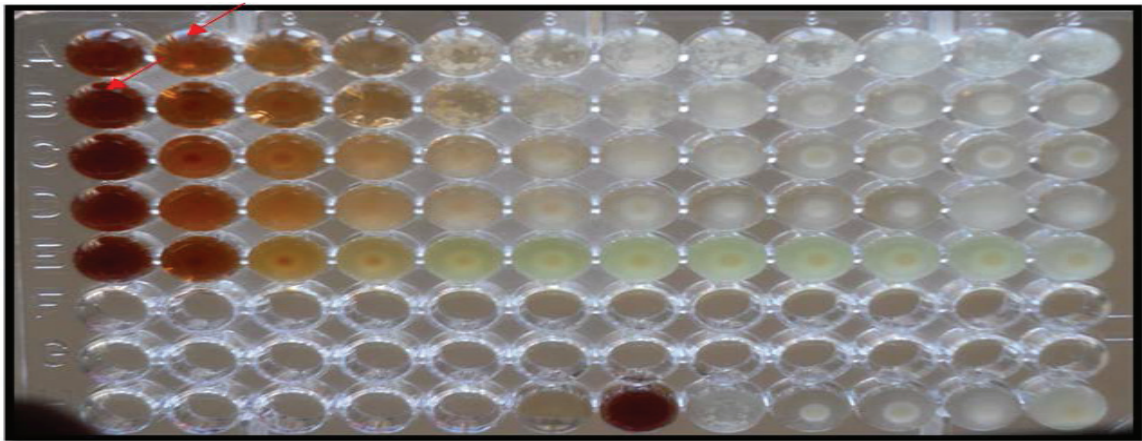


Fig. 2. Aspect of microplate for determined of MIC of beech bark polyphenolic extract obtained by hot water. Rows A-E: MSSA, MRSA, *E. coli*, *K. pneumoniae*, and *P. aeruginosa* respectively. Columns 1-12: Descending concentrations (binary dilutions) of beech bark extract, starting with 30 mg/mL (column 1) down to 0.015 mg/mL (column 12)

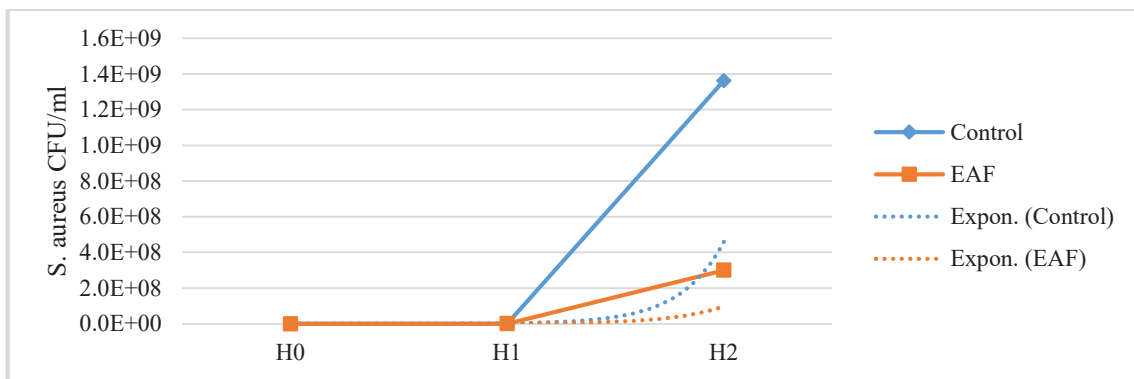


Fig. 3. The graphic representation of the growth rate for MSSA in the presence of EAF and Control (initial time – H0, 3 hours – H1 and 6 hours – H2)

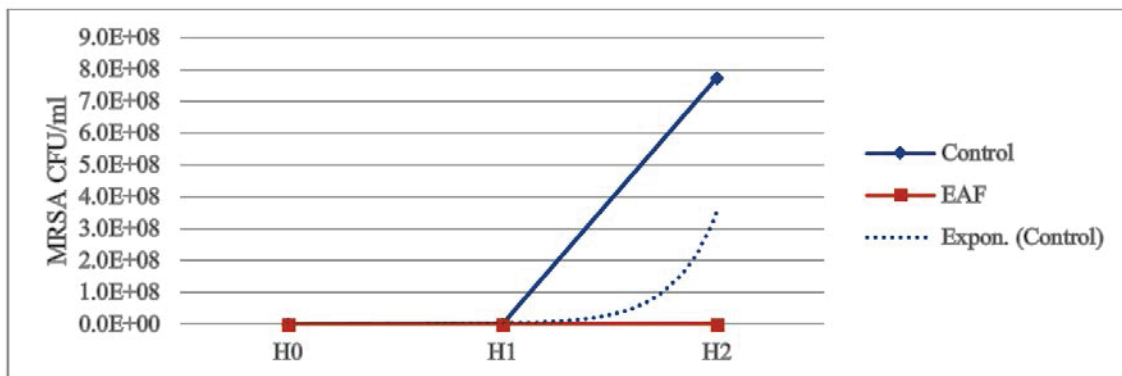


Fig. 4. The graphic representation of the growth rate for MRSA in the presence of EAF and Control (initial time – H0, 3 hours – H1 and 6 hours – H2)

Table 3. Data presenting the growth rate of *S. aureus* and MRSA in presence of EAF

		CFU/mL			Specific Growth rate, h ⁻¹	Generation time, min
		H0	H1	H2	r	g
MSSA	EAF	6.2 x 10 ⁴	1.5 x 10 ⁵	3 x 10 ⁸	1.41	29.40
	Control	7 x 10 ⁴	3.72 x 10 ⁵	1.36 x 10 ⁹	1.65	25.26
	p < 0.0001					
MRSA	EAF	3.8 x 10 ⁴	2.6 x 10 ⁴	0	N/A	N/A
	Control	4 x 10 ⁴	5.3 x 10 ⁵	7.74 x 10 ⁸	1.65	25.28
	p < 0.0001					

Taxifolin extracted from *Hypericum japonicum* Thunb., inhibits the growth of *S. aureus* (MRSA) by delaying the protein synthesis and adversely affecting the synthesis of enzymatic systems and nucleic acids (Grosso et al., 2007). These plant compounds also increase the membranes permeability to drugs, leading to a bacteriostatic effect. It was found that aromatic compounds have a good ability to link with bacteria cell walls and can exert bacteriostatic effect (Mahboubi and Haghi, 2008; Morteza-Semnani et al., 2011). Thus, plant extracts with high content of phenolic compounds (e.g. beech bark aqueous extract) can be efficient when used in complementary with commercial drugs due to their bactericidal effect.

It was found that recently work has been done on the antioxidant properties of hot water beech bark extracts (Hofmann et al., 2015b, 2017). According to Hofmann et al. (2017) the most efficient antioxidants in beech bark were found to be the (+) catechin, procyanidin B dimer 2, (-) epicatechin and coniferin isomer 2. The authors conclude that under high temperature pressurized environments water can be an extraction solvent as effective as solutions containing alcohols. The positive results related to antioxidant

activity could be closely connected to the antibacterial properties of the EAF on *S. aureus* including methicillin-resistant strains.

Our results have shown that EAF can be effective against both MRSA and MSSA due to high content of phenolic compounds, which can act synergistically with each other against those bacteria. Further research is needed to elucidate accurately their pathways and mechanisms of action against bacteria.

4. Conclusions

The results of this study reveal that the beech bark extract contains a considerable amount of phenolic compounds. Pure water can be an efficient solvent, supporting the concept of green extraction. The compounds identified by HPLC were vanilic acid, catechin, taxifolin and syringin. The antimicrobial tests demonstrated antimicrobial activity against *Staphylococcus aureus* including methicillin-resistant strains.

The results of this study have led to a new research direction orientated on reducing the pharmacological resistance of microorganisms to antibiotics, by using polyphenolic plant extracts.

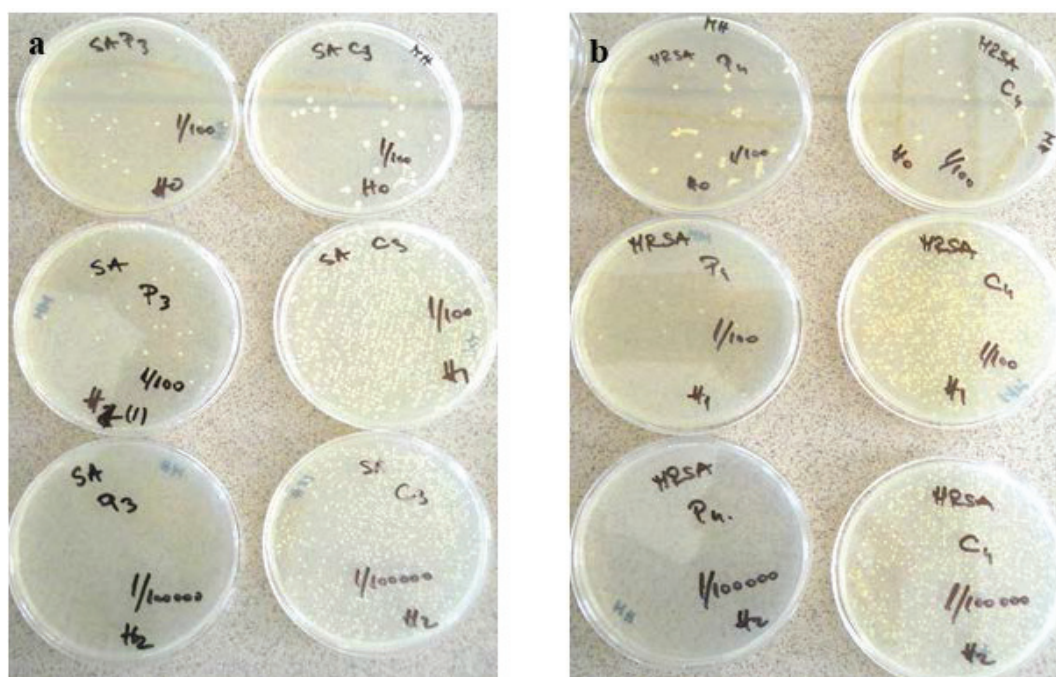


Fig. 5. Supportive image of the inoculated plates after 24 hours of incubation, corresponding to the tree time-points (initial time – H0, 3 hours – H1 and 6 hours – H2) for MSSA (a) MRSA (b) and Control

Acknowledgments

This work was supported by the University of Medicine and Pharmacy of Tîrgu Mureş Research Grant number 17800/3/22.12.2015. For this project, the infrastructure of Chromatography and mass spectrometry laboratory of the Center for Advanced Medical and Pharmaceutical Research (CCAMF), University of Medicine and Pharmacy of Tîrgu Mureş, was used.

References

- Balasundram N., Sundram K., Samman S., (2006), Phenolic compounds in plants and agri-industrial by-products: Antioxidant activity, occurrence, and potential uses, *Food Chemistry*, **99**, 191-203.
- Barbosa-Pereira L., Bilbao A., Vilches P., Inmaculada A., Jaime L.L., Perfecto P., Cruz J.M., (2014), Brewery waste as a potential source of phenolic compounds: Optimisation of the extraction process and evaluation of antioxidant and antimicrobial activities, *Food Chemistry*, **145**, 191-197.
- Carraturo A., Raieta K., Tedesco I., Kim J.R., Russo G.L., (2014), Antibacterial activity of phenolic compounds derived from *Ginkgo bilobasarcotestas* against food-borne pathogens, *British Microbiology Research Journal*, **4**, 18-27.
- CLSI, (2015), *Methods for Dilution Antimicrobial Susceptibility Tests for Bacteria that Grow Aerobically, 11th Edition*, CLSI Standard M07, Wayne, Pennsylvania, USA.
- Dübeler A., Voltmer G., Gora V., Lunderst J., Zeeck A., (1997), Phenols from *Fagus sylvatica* and their role in defence against *Cryptococcus fagisuga*, *Phytochemistry*, **45**, 51-57.
- Fierascu R.C., Ion R.M., Fierascu I., (2017), Antifungal effect of natural extracts on environmental biodeteriogens affecting the artifacts, *Environmental Engineering and Management Journal*, **16**, 2435-2442.
- Friedman M., Henika P.R., Levin C.E., Mandrell R.E., Kozukue N., (2006), Antimicrobial activities of tea catechins and theaflavins and tea extracts against *Bacillus cereus*, *Journal of Food Protection*, **69**, 354-361.
- Grosso A.C., Costa M.M., Ganc L., Pereira A.L., Teixeira G., Lavado J.M., Figueiredo C., Barroso J.G., Pedro L., (2007), Essential oil composition of *Pterospartum tridentatum* grown in Portugal, *Food Chemistry*, **102**, 1083-1088.
- Hofmann T., Tálos-Nebehaja E., Alberta L., Németh L., (2017), Antioxidant efficiency of beech (*Fagus sylvatica* L.) bark polyphenols assessed by chemometric methods, *Industrial Crops and Products*, **108**, 26-35.
- Hofmann T., Tálos-Nebehaja E., Albert L., (2015a), The high-performance liquid chromatography/multistage electrospray mass spectrometric investigation and extraction optimization of beech (*Fagus sylvatica* L.) bark polyphenols, *Journal of Chromatography A*, **1393**, 96-105.
- Hofmann T., Tálos-Nebehaja E., Stefanovits-Bányai É., Albert L., (2015b), Antioxidant capacity and total phenol content of beech (*Fagus sylvatica* L.) bark extracts, *Industrial Crops and Products*, **77**, 375-381.
- Hofmann T., Albert L., Retfalvi T., Visi-Rajczi E., Brolly G., (2008), TLC analysis of the in-vitro reaction of beech (*Fagus sylvatica* L.) wood enzyme extract with catechins, *Journal of Planar Chromatography*, **21**, 83-88.
- Hoppe B., Kahl T., Arnstadt T., Buscot F., Bauhus J., Wubet J., (2016), A pyrosequencing insight into sprawling bacterial diversity and community dynamics in decaying deadwood logs of *Fagus sylvatica* and *Picea abies*, *Scientific Reports*, **5**, 9456-9457.
- Huang W.Y., Cai Y.Z., Zhang Y., (2010), Natural phenolic compounds from medicinal herbs and dietary plants: potential use for cancer prevention, *Nutrition and Cancer*, **62**, 1-20.
- Ignat I., Radu D., Volf I., Pag I.A., Popa I.V., (2013), Antioxidant and antibacterial activities of some natural polyphenols, *Cellulose Chemistry and Technology*, **47**, 387-399.
- Lazau C., Misca C., Orha C., Bandas C., Olariu S., (2013), Synthesis of titanium dioxide with hydrothermal method and antibacterial activity against *E. coli*, *Environmental Engineering and Management Journal*, **12**, 234-242.
- Mahboubi M., Haghi G., (2008), Antimicrobial activity and chemical composition of *Mentha pulegium* L. essential oil, *Journal of Ethnopharmacology*, **119**, 325-327.
- Morteza-Semmani K., Saeedi M., Akbarzadeh M., (2011), Chemical composition and antimicrobial activity of the essential oil of *Mentha pulegium* L., *Journal of Essential Oil-Bearing Plants*, **14**, 208-213.
- Moure A., Cruz J.M., Franco D., Dominguez J.M., Dominguez H., Nunez M., Parajo C., (2001), Natural antioxidants from residual sources, *Food Chemistry*, **72**, 145-171.
- Omar S., Lemonnier B., Jones N., Ficker C., Smith M.L., Neema C., Towers G.H., Goel K., Arnason J.T., (2000), Antimicrobial activity of extracts of eastern North American hardwood trees and relation to traditional medicine, *Journal of Ethnopharmacology*, **73**, 161-170.
- Pereira C., Barros L., Ferreira I.C., (2016), Extraction, identification, fractionation and isolation of phenolic compounds in plants with hepatoprotective effects, *Journal of Science of Food and Agriculture*, **96**, 1068-1084.
- Sanders E.R., (2012), Aseptic laboratory techniques: plating methods, *Journal of Visualized Experiments*, **63**, e3064, doi: 10.3791/3064
- Shahina N., Samia A., Sheikh A.R., Syed A.S., Rahmanullah S., (2006), Antibacterial activity directed isolation of compounds from *Onosma hispidum*, *Microbiological Research*, **161**, 43-48.
- Szabo M.R., Radu D., Gavrilas S., Chambre D., (2010), Antioxidant and antimicrobial properties of selected spice extracts, *International Journal of Food Properties*, **13**, 535-545.
- Tanase C., Volf I., Popa V.I., (2014), Enhancing copper and lead bioaccumulation in rapeseed by adding hemp shives as soil natural amendments, *Journal of Environmental Engineering and Landscape Management*, **22**, 245-253.
- Vek V., Oven P., Poljanšek I., (2013a), Quantitative HPLC analysis of catechin in wound-associated wood and knots of beech, *Drvna industrija*, **64**, 231-238.
- Vek V., Oven P., Humar M., (2013b), Phenolic extractives of wound-associated wood of beech and their fungicidal effect, *International Biodeterioration & Biodegradation*, **77**, 91-97.



“Gheorghe Asachi” Technical University of Iasi, Romania



INFLUENCE OF HUSK ON GRAIN CONTAMINATION BY *Fusarium* spp. AND *Alternaria* spp. IN HULLED SPELT (*Triticum spelta* L.)

Karel Suchý¹, Petr Konvalina^{1*}, Ivana Capouchová², Dagmar Janovská³,
Leona Leišová-Svobodová³, Zdeněk Štěrba¹, Jan Moudrý jr.¹, Daniel Bucur⁴,
Jaroslav Bernas¹, Marek Kopecký¹, Dang Khoa Tran¹

¹“University of South Bohemia in Ceske Budejovice, Faculty of Agriculture, Studentska 1668,
370 05 Ceske Budejovice, Czech Republic

²Czech University of Life Sciences in Prague, Kamýcká 129, Prague, Czech Republic

³Crop Research Institute in Prague, Drnovska 507/73. 161 06 Praha 6 – Ruzyně, Czech Republic

⁴The University of Agricultural Sciences and Veterinary Medicine Iasi, Faculty of Agriculture,
Aleea Mihail Sadoveanu no.3, 700490Iasi, Romania

Abstract

Fusarium Head Blight is caused by several *Fusarium* species. Infections can result in mycotoxin contamination on cereals and associated foods. Harvested products are contaminated due to its secondary metabolites. The aim was to analyse the occurrence of spike *Fusarium* and *Alternaria* spp. in hulled *Triticum spelta* L. wheat species via polymerase chain reaction (PCR) method and the deoxynivalenol (DON) content analysis. Three varieties of spelt were used (Ceralio and Rubiota – winter and one spring form variety from genetics resources). Grains were sown in a randomized complete block design on organic certified experimental parcels during the years of 2011 and 2013. During the vegetation period plants were artificially inoculated with *Fusarium* spp. The occurrence of spike *Fusarium* and *Alternaria* spp. was assessed by the PCR method - DNA extracting and determination of *Fusarium* species and *Alternaria* spp. by the DNA markers and PCR method. DON content was analysed by ROSA®-DON Quantitative test. Strong infestation of grains with *Fusarium* spp. led to low contamination of grains with *Alternaria* spp. The technological operation of grain dehulling was performed and it was highly efficient there. The grain contamination by *Fusarium* spp. and *Alternaria* spp. decreased. Hulls protect grains to a certain point because of protection against *Fusarium* spp. and *Alternaria* spp. occurrence which produce harmful secondary metabolites. On the other hand the protection of grain by hulls only partly works. It is also important to pay attention to chemism of secondary metabolites in grain.

Key words: *Alternaria* spp., contamination, *Fusarium* spp., husk, wheat

Received: May, 2017; Revised final: February, 2018; Accepted: March, 2018; Published in final edited form: April 2018

1. Introduction

Microorganisms commonly found in grain include filamentous fungi, primarily those from the genera *Aspergillus*, *Fusarium* and *Penicillium* (Ostrowska-Kolodziejczak et al., 2016). They are responsible for the accumulation of mycotoxins in grain (Zain, 2011). Currently, over 31,000 known

metabolites produced by fungi occur in cereals. Some of these chemicals called mycotoxins are harmful to both humans and animals (AntiBase, 2005; Kuzdralinski et al., 2013). Mycotoxins produced by those pathogens lead to several health problems in humans and animals, and high mycotoxin concentrations in grain cause mycotoxicoses (Richard, 2007). Currently, there have been more than 400

* Author to whom all correspondence should be addressed: e-mail: konvalina@zf.jcu.cz; Phone: +420 387 772 547

known mycotoxins (Kuzdralinski et al., 2013). The most studied mycotoxins are aflatoxins, trichothecenes, zearalenone, and ochratoxins (Binder et al., 2007; Filtenborg et al., 2000). Biological and chemical properties of mycotoxins vary, as well as their toxicity (Salem and Ahmad, 2010). Many of these compounds have oestrogenic, teratogenic, mutagenic and carcinogenic effects (Binder et al., 2007; D'Mello et al., 1999; Prelusky et al., 1993). Mycotoxins can enter the human body in different ways, mainly through the consumption of contaminated food (Berthiller et al., 2005; Salem and Ahmad, 2010).

Due to the great economic significance of wheat, particular attention should be paid to its health management as well as to the threat posed by fungal pathogens, including species of the genus *Fusarium* causing *Fusarium* head blight (Ostrowska-Kołodziejczak et al., 2016). *Fusarium* head blight is one of the most severe diseases of small grain cereals. Four *Fusarium* species, *F. graminearum* Schwabe, *F. culmorum* (W.G. Smith) Sacc., *F. avenaceum* (Fr.) Sacc and *F. poae* (Peck) Wollenw. have been identified as important toxigenic pathogens that affect the heads of small grain cereals (Miedaner et al., 2008; Pasquali and Migheli, 2014).

Cereals produced in temperate zone climatic conditions can be frequently contaminated with mycotoxins (Zachariasova et al., 2014). Due to the fact that in the Central Europe climatic zone the most toxigenic fungi are *Fusarium culmorum* and *F. graminearum*, the presence of these fungi and also of chemotypes 3-acetyl-deoxynivalenol (3-AcDON) and 15-acetyl-deoxynivalenol (15-AcDON) in grain is increasingly often analysed (Ostrowska-Kołodziejczak et al., 2016). In particular *F. culmorum* has been a prevalent species in several countries in Europe and the species has been predominating especially in regions that have cooler climatic conditions while *F. graminearum* has been predominant in relatively warmer regions. However, generalisation about geographic region distribution of *Fusarium* spp. has been interrupted by several investigations in Europe (Yli-Mattila et al., 2013; Yörük et al., 2016). Formally in Central and Central-Eastern Europe, *Fusarium* head blight was caused primarily by *Fusarium culmorum* (W.G. Smith) Sacc. (Parry et al., 1995). Nowadays *Fusarium graminearum* predominates (Yli-Mattila et al., 2013) which attacks wheat spikes in the flowering stage. As a result, the grain may be shrivelled and discoloured, with a high toxin content, especially trichothecenes of group B (Chelkowski, 1989; Perkowski et al., 2002).

Organic farming is an alternative to the conventional cultivation system providing farm products of high quality, referred to as organic (Jelínková et al., 2016; Maeder et al., 2002). In organic farming, fungicides are not used as prevention against fungal diseases (Janovská et al., 2015). The FAO report (FAO, 2000) concerning the content of mycotoxins in agricultural crops showed no clear differences between organic and conventional farming

systems. It was stated however that in certain circumstances, such differences might occur. Most studies published after the FAO report (FAO, 2000) also failed to identify significant differences between organic and conventional cropping systems (Champeil et al., 2004; Cirillo et al., 2003; Jestoi et al., 2004). In some cases, the differences of mycotoxin levels between organic and conventional production systems, nevertheless, were reported (Knudsen et al., 1995; Kuzdralinski et al., 2013; Skaug, 1999; Woese et al., 1997).

The growing of resistant varieties is the best way to reduce *Fusarium* infection (Scholten et al., 2007). Bread wheat (*Triticum aestivum* L.) is the most frequent cereal species grown within the Czech organic farming system. Because in the Czech Republic are only available varieties bred in conventional breeding programmes, organic farmers use different species and crops (Konvalina et al., 2014). The information about the reaction of spikes of ancient wheat species to *Fusarium* spp. infection and toxin accumulation in grain is very important for growing systems limiting chemical plant protection. Hulled spelt wheat (*Triticum spelta* L.) is one from less bred among the *Triticeae* grown by farmers (Suchowilska et al., 2010). Information on the response of spelt cultivars to the infection by pathogens causing FHB is scant. Previous results (Wiwart et al., 2004) show that the response of this cereal to spike infection is slightly stronger than that of common wheat. Probably it is caused because of coverage of grain by hulls. Hulls can create more favourable conditions for *Fusarium* growth. But husks are removed from the grain before use and also an important part of contamination could be solved (Konvalina et al., 2011). There are many conflicting claims related to the role of husk as a protective factor against the secondary metabolites of *Fusarium* contamination. The example of *Alternaria* spp. contamination indicated significantly higher concentrations of Alternariatoxins in hulls than in dehulled kernels which implicate the possible protective effect of spelt wheat hulls (Vuckovic et al., 2013). Therefore, the contamination of the grain product, hulled wheat, by *Fusarium* and *Alternaria* toxins is an important question because of the safety of food and feed.

This study aimed to analyse the occurrence of *Fusarium* and *Alternaria* species in organic and conventionally produced hulled and dehulled grain of spelt wheat by DNA markers and PCR (polymerase chain reaction) method and deoxynivalenol (DON) content analysis by ROSA®-DON Quantitative test. The second aim was to analyse the role of the hull factor as potential protection against *Fusarium* spp. and *Alternaria* spp. contamination.

2. Material and methods

2.1. Plant material and field experiments

There were used two varieties of winter spelt (Rubiota and Ceralio) and one variety (spring form)

from the collection of genetic resources. The organic field trials were carried out from 2011 to 2013 as randomized complete block designs with three replications. The seeding rate was adjusted to a density of 350 germinating seeds per 1 m². Plot size was 12 m². Crop stands were treated in compliance with European Council regulations EC No. 834/2007 and EC No. 889/2008. The weather conditions of the years 2011 and 2012 were favourable for the *Fusarium* spp. development due to high temperatures and precipitation in comparison to the long term mean. The year 2013 was deficient in precipitation. All materials were harvested at maturation stage from small-scale field plots at the Experimental and Research Station of the Department of Crop Production, Czech University of Life Sciences, Prague and at the experimental areas of the University of South Bohemia in České Budějovice.

2.2. Artificial inoculation

The isolates of *F. culmorum* and *F. graminearum* used for the artificial inoculation were obtained from the mycological collection of the Crop Research Institute in Prague and cultivated on sterile wheat grains. More detailed information on isolates can be found in Leišová et al. (2006). The preparation of inoculums for the application: wheat grains with the cultures of *F. culmorum* and *F. graminearum* were put into a vessel with water and shaken for 15 minutes in a laboratory shaker to release the spores into the water. The obtained suspension was filtered through the gauze. Then artificial inoculation was done with the suspension of *F. culmorum* and *F. graminearum* spores in the ratio of 1:1, 10⁷ of spores/mL (Bürkerchamber was used for the verification of inoculum density), 2 litres of suspension per experimental plot (12 m²). The suspension was dosed according to the list of variants with a hand sprayer at the beginning and at the end of the wheat flowering.

During experiments we also inoculated spikes by inoculum contained *Alternaria* spp. The ability of *Alternaria* spp. isolates to produce mycotoxine was proved before. Inoculation was made during milky ripeness, but was not successful. There were no differences between inoculated plots and plots only after natural infection.

2.3. Processing of samples

For the dehulling of hulled grain, samples were used Wintersteiger LG 180 (Wintersteiger, Ried,

Austria) laboratory thresher. For the analysis were milled both – grain covered by hulls and dehulled (naked) grain. For the milling was used laboratory mill PSY MP 40 (holes in the sieve 0.8 mm).

2.4. Evaluation of spike *Fusarium* occurrence by the PCR method

DNA both from a mycelium of all tested fungi and from infected grain samples was extracted using DNeasy Plant Mini Kit (QIAGEN, Germany) according to the manufacturer instructions. The quality and the concentration of extracted DNA were verified electrophoretically in 0.8% agarose gel. DNA was visualized by ethidium-bromide and detected under a UV lamp. DNA extracted from infected seed samples was diluted to a concentration of 50 ng/μL using a GeneQuantPro spectrophotometer (Amersham, Cambridge, UK).

2.5. Species specific amplification

The markers specific to the species: *F. culmorum* (Fc), *F. graminearum* (Fg), *F. pseudograminearum* (Fpse), *F. poae* (Fp), *F. sporotrichioides* (Fsp), *F. equiseti* (Fe) and *F. avenaceum* (Fa) were borrowed from the literature (Aoki and O'Donnell, 1999; Demeke et al., 2005; Doohan et al., 1998; Leišová et al., 2006; Parry and Nicholson, 1996). Primers were designed based on the sequence of the ITS region of about 5 isolates of *Alternaria* spp. The sequence of primers is in Table 1.

PCR reactions were performed in a 15 μL reaction mixture (0.3 μM of each primer, 170 μM dNTP, 1x PCR buffer, 2 mM MgCl₂, 1U *Tth* DNA polymerase Biotools (DYNEX) and 50 ng of template DNA) in the cycler SensoQuest (Goettingen, Germany). The amplification products were separated in 1.6% agarose gel, stained with ethidium bromide and visualised under UV light. The size of the product was verified by comparing it with the size standard GeneRuler™ 100bp DNA Ladder (Thermo Fisher Scientific, USA).

Fusarium culmorum assay was used from a previous project (Leišová et al., 2006). *Fusarium graminearum* and *Alternaria* spp. specific primers for Real-time PCR were designed on the base of the sequences for elongation factor obtained from public databases using the Primer Express for Windows NT 1.5 software (Applied Biosystems, Foster City, CA, USA).

Table 1. The primer list

Name	Forward	Reverse
Fc92s1	TTCACTAGATCGTCCGGCAG	GAGCCCTCCAAGCGAGAAG
Fg	TTCCCTGGGCGCTCATC	GGCTTCCTATTGACAGGTGGTT
Fpse	CGGGGTAGTTTCACATTTCTY	GAGAATGTGATGAGGACAATA
Fp	CAAGCAAACAGGCTCTCACC	TGTTCCACCTCAGTGACAGGTT
Fsp	AAAAGCCCCAAATTGCTGATG	TGGCATGTTTATTGTACCT
Fe	CATACCTATACGTTGCCTCG	TTACCAGTAACGAGGTGTATG
Fa	CAAGCATTGTGCGCCACTCTC	GTTTGGCTTACCAGGACTG
Asp	TGGTGTGGGCGTCTTGTC	TAGGCCGGCTGCCAATTAC

In case of *F. graminearum* the assay contained also a MGB (minor groove binder) probe; in *Alternaria* spp. SYBR Green detection system was used because all *Alternaria* species should have been detected in one reaction without the necessity of species determination. The specificity of all primers and probes was verified in silico by blast analysis. After optimization, PCR reactions were carried out in a 25 μ L volume consisting of either 1x TaqMan Universal PCR Master Mix (Life Technologies, Foster City, CA, USA; in case MGB probe was used) or SYBR Green master mix (Life Technologies, Foster City, CA, USA; for *Alternaria* spp. detection), 0.3 μ M of each primer, 0.3 μ M Taq Man MGB probe and 250 ng of template DNA. Real-time quantitative PCR was performed using the cycler ABI PRISM 7900 (Life Technologies, Foster City, CA, USA) in MicroAmp optical 96-well plates. Reaction consisted of 2 min at 50°C, 10 min at 95°C and 40 cycles of 95°C for 15 s and 60°C for 1 min. followed only in SYBR Green detection system by dissociation stage (95°C for 15 s, 60°C for 15 s and then a slow increase to 95°C). The Sequence Detection Software (Life Technologies, Foster City, USA) collected data for the reported dye every 7 seconds from each well, generating a fluorescence profile for each amplification. The threshold cycle (Ct) was recorded for each dye as the cycle at which the fluorescent signal, associated with an exponential growth of PCR product, exceeded the background fluorescence. Dilution series of *F. culmorum*, *F. graminearum* and *A. alternata* isolates - DNA (from 0.1 pg to 100 ng) was included in triplicate as standard in every real-time PCR experiment. Standard curves for all assayed fungi were generated by plotting the known DNA amounts against the Ct values calculated by the SDS software. Unknown samples were quantified from measured Ct values by interpolation using the regression equation derived from standard curves. Final results of fungal content in samples were expressed in micrograms per 100 mg of groats.

2.6. Deoxynivalenol (DON) content

At first, toxin was extracted from the sample (deionized water was used as a solvent). 100 μ L of the extract was diluted in 1 mL of buffer. 300 μ L of the diluted extract was applied on the strip (ROSA®-DON Quantitative test). Incubation of the strip - 10 minutes at the temperature of 45°C (ROSA®-M Incubator). Assessment of the test – by ROSA®-M Reader (results in ppb).

2.7. Statistical analysis

In case of evaluation of the presence of DNA of pathogen – based on quantification of the intensity of the luminous band in relation to the marker for the statistical analysis, we used the following scale: 0 = no infection, 1 = weak infection, 2 = medium infection, 3 = strong infection.

The results were statistically evaluated by the Mann-Whitney Test (by variable organic system vs. conventional system, winter variety vs. spring variety, *Alternaria*+natural infection vs. *Fusarium* spp. inoculation, dehulled grain vs. hulled spikelets) and Kruskal-Wallis ANOVA evaluation of factor of variety. The selected factors are displayed in figures with the statistical significance expression on the level $p \leq 0.05$. The calculation was done by the software STATISTICA 12.0 CZ (StatSoft, Inc. USA).

3. Results and discussion

Degree of grain contamination (qualitative) with various *Fusarium* spp. (F.) and relationships between the contamination degree and other evaluated factors were evaluated at first (Tables 2 and 3). Farming system (organic or conventional one) is a statistically non-significant factor there. *Fusarium avenaceae*, *culmorum*, *equiseti* and *poae* infected the grains but they were statistically non-significant in our research. *Alternaria* spp. also infected the grains (Table 3) grown under both farming systems. The difference in DNA of *F. culmorum*, *F. graminearum* and *Alternaria* spp. was also statistically non-significant. Results of the Mann-Whitney test are shown in Table 4.

The difference in the degree of grain contamination with *Fusarium* spp. and *Alternaria* spp. toxins between the organic and conventional farming systems has already been noticed and discussed by many authors. Numerous surveys comparing mycotoxin content in organic and conventional production systems have already been conducted. The mycotoxin contamination of organic food products was reported to be either more or less equal to that of conventional systems (Magkos et al., 2006). Birzele et al. (2000) showed that contamination of conventional samples of winter wheat with DON and ochratoxin A (OTA) was comparable to that of the organic samples. In another study in Germany, comparable results for DON were obtained (Lücke et al., 2003). A study conducted in France revealed that organic cereals were contaminated with a higher level of mycotoxins but less frequently than cereals from conventional production (Malmauret et al., 2002). However, findings are not unequivocal in general. Works giving evidence of organic plants being as infected with *Fusarium* Head Blight as the conventional ones prevail.

The factor of variety has already been studied and evaluated with various methods. Table 6 (results of Kruskal-Wallis ANOVA) shows the factor of variety did not have any impact on the grain contamination with toxins in our research. Results were statistically non-significant. There was a minimum difference in the degree of grain contamination with toxins between winter and spring varieties (Tables 2 and 3). The same result was shown in the analysis of DON content in grain (Table 5).

Table 2. Grain contamination by different *Fusarium* species related to different factors

Factor		Fusarium			
		avenaceae	culmorum	equiseti	graminearum
System	Organic	1.9 ± 0.9	1.7 ± 1.0	0.7 ± 1.0	1.2 ± 1.2
	Conventional	2.4 ± 0.7	1.8 ± 1.0	0.8 ± 1.1	1.2 ± 1.2
Type of variety	Spring	1.5 ± 0.8	1.3 ± 1.1	0.3 ± 0.7	0.8 ± 0.9
	Winter	2.4 ± 0.7	2.0 ± 0.8	1.0 ± 1.1	1.4 ± 1.2
Year	2011	2.3 ± 0.5	1.8 ± 0.7	0.8 ± 1.0	1.3 ± 1.4
	2012	2.5 ± 0.8	1.9 ± 1.1	0.8 ± 1.1	1.5 ± 1.1
	2013	1.7 ± 1.0	1.7 ± 1.1	0.8 ± 1.1	0.9 ± 0.9
Processing	Dehulled	1.9 ± 0.8	1.7 ± 1.0	0.4 ± 0.8	1.1 ± 1.2
	Hulled	2.7 ± 0.6	2.0 ± 0.8	1.6 ± 1.1	1.4 ± 1.3
Inoculation	Natural	2.0 ± 0.9	1.2 ± 0.8	0.4 ± 0.8	0.5 ± 0.7
	<i>Fusarium</i> spp.	2.0 ± 0.8	2.5 ± 0.8	1.0 ± 1.2	2.1 ± 1.0
	<i>Alternaria</i> spp.	2.5 ± 0.7	1.5 ± 0.5	1.0 ± 1.1	0.9 ± 1.1

Note: 0 = no infection, 1 = weak infection, 2 = medium infection, 3 = strong infection

Table 3. Grain contamination by different *Fusarium* species and *Alternaria* spp. related to different factors

Factor		Fusarium			Alternaria spp.
		poae	pseudo-graminearum	sporotrichioides	
System	Organic	1.9±0.9	0.0±0.0	1.1±1.1	2.4±0.5
	Conventional	2.1±1.0	0.0±0.0	0.9±0.9	2.4±0.5
Type of variety	Spring	2.3±0.9	0.0±0.0	0.9±0.9	2.3±0.5
	Winter	1.9±0.9	0.0±0.0	1.0±1.1	2.4±0.5
Year	2011	2.3±0.6	0.0±0.0	1.4±1.0	2.0±0.2
	2012	2.0±1.2	0.0±0.0	0.5±0.8	2.0±0.0
	2013	1.7±1.0	0.0±0.0	0.8±1.0	3.0±0.0
Processing	Dehulled	1.8±1.0	0.0±0.0	0.6±0.8	2.3±0.5
	Hulled	2.5±0.7	0.0±0.0	1.8±1.0	2.5±0.6
Inoculation	Natural	1.9±1.0	0.0±0.0	0.6±0.8	2.3±0.5
	<i>Fusarium</i> spp.	2.1±0.9	0.0±0.0	1.2±1.1	2.4±0.5
	<i>Alternaria</i> spp.	2.0±1.0	0.0±0.0	1.1±1.1	2.4±0.5

Note: 0=no infection, 1=weak infection, 2 = medium infection, 3 = strong infection

Table 4. Mann-Whitney Test by variable Organic system vs. Conventional system of growing (concentration of DNA of pathogen in µg/100mg of grain)

Variable	Rank sum	Valid N	Rank sum	Valid N	U	Z	p-value	Z adjusted	2*1 sided exact p
	ORGANIC		CONVENTIONAL						
<i>F. culmorum</i>	919	30	911	30	446	0.052	0.959	0.052	0.959
<i>F. graminearum</i>	922	30	908	30	443	0.096	0.923	0.096	0.923
<i>Alternaria</i> spp.	906	30	924	30	441	-0.126	0.900	-0.126	0.900

Note: marked tests are significant at p<0.05; U = U value, Z = Z value

Table 5. Concentration of DNA of *F. culmorum*, *graminearum* and *Alternaria* spp. and DON content in grain

Factor		<i>Fusarium culmorum</i> (µg Fc DNA /100 mg of grain)	<i>Fusarium graminearum</i> (µg DNA Fg/100 mg of grain)	<i>Alternaria</i> spp. (µg DNA Asp/ 100 mg of grain)	DON (ppb)
System	Organic	5.39±16.68	0.54±1.61	0.04±0.05	2327±2774
	Conventional	3.69±8.66	0.72±2.21	0.04±0.05	2070±2606
Processing	Dehulled	2.07±4.85	0.29±0.87	0.02±0.02	2170±2780
	Hulled	10.72±22.72	1.47±3.23	0.09±0.06	2210±2660
Year	2011	6.72 ±12.09	0.73±1.67	0.06±0.04	2268±2459
	2012	2.05±2.60	0.31 ±0.52	0.01 ±0.01	2514±2924
	2013	3.92±17.59	0.73±2.62	0.03±0.06	1933±2788
Type of variety	Spring	1.47±2.39	0.05±0.09	0.02±0.02	2196±2614
	Winter	5.77±15.46	0.86±2.24	0.05±0.05	2199±2725
Inoculation	Natural	0.036±0.07	0.01±0.02	0.04 ±0.05	2660 ±358
	<i>Fusarium</i> spp.	11.801±19.53	1.63±2.87	0.03±0.05	5337±1613
	<i>Alternaria</i> spp.	0.136±0.23	0.02±0.03	0.05±0.06	2700 ±285

Note: Mean ± Standard deviation

There was practically the same mean but within the samples were differences (high standard deviation). *F. avenaceae*, *culmorum*, *equiseti* and *graminearum* infected more winter varieties (statistically non-significant occurrence). Winter wheat varieties were more infected by *Fusarium* spp. than spring wheat ones – it was registered by Etzeriod et al. (2016), for instance. Table 3 shows winter varieties were more seriously infected with *Fusarium culmorum* and *Fusarium graminearum* in our case (they contained more DNA of these two toxins). As there was a high variability between tested samples, it was a statistically non-significant result and finding (Mann-Whitney Test – Table 7).

All spikes were seriously infected with *Fusarium* Head Blight during every performed inoculation in our research. On the other hand, the tested inoculation with *Alternaria* spp. was not successful under field conditions. The inoculation with *Alternaria* spp. was also tested on the other crops (cumin or colza) (Khan et al., 2012; Özer and Bayraktar, 2015). It was tested on wheat with success – under laboratory conditions (Vergnes et al., 2006). Therefore, it was tested statistically with the natural infection together. All these results are shown in Table

8. A statistically significant difference between *F. culmorum* and *F. graminearum* DNA infestation rate was confirmed via Mann-Whitney test.

Testing and evaluation of the degree of grain contamination with pathogen produced the following results – a middle strong infestation with *F. graminearum* and a strong infestation with *F. culmorum* (Table 1). The artificial inoculation had a minimum impact on the degree of grain contamination with *Alternaria* spp. DNA. It caused neither higher contamination of grains with that pathogen (Table 3), nor a higher concentration of *Alternaria* spp. DNA in grains (Table 4). It brought about an inverse effect (Table 4). Compared to the natural conditions (0.039 µg DNA Asp/ 100mg of grain), the inoculation of grains with *Fusarium* spp. produced a slight decrease of *Alternaria* spp. DNA level in grains (0.033 µg DNA Asp/ 100 mg of grain). Such a decrease of the grain contamination with *Alternaria* spp. was provoked by a competitive interaction of *F. graminearum*. They occurred on wheat plants in the field, and therefore competed for the same resources. In the experiment done by Saß et al. (2007), *Alternaria alternata* was clearly suppressed when growing together with *F. graminearum*.

Table 6. Kruskal-Wallis ANOVA – evaluation of factor of variety of spelt (*Triticum spelta* L.)

<i>Fusarium culmorum</i> (µg DNA Fc/100mg of grain)			
Variety	N	Sum of scores	Mean score
Ceralio	18	633.0000	35.16667
Spring spelt	24	648.0000	27.00000
Rubiota	18	549.0000	30.50000
H (2, N = 60) = 2.249430 p = 0.3247			
<i>Fusarium graminearum</i> (µg DNA Fg/100mg of grain)			
Variety	N	Sum of scores	Mean score
Ceralio	18	661.0000	36.72222
Spring spelt	24	602.0000	25.08333
Rubiota	18	567.0000	31.50000
H (2, N = 60) = 4.652641 p = 0.0977			
<i>Alternaria</i> spp. (µg DNA Asp/ 100mg of grain)			
Variety	N	Sum of scores	Mean score
Ceralio	18	605.0000	33.61111
Spring spelt	24	614.0000	25.58333
Rubiota	18	611.0000	33.94444
H (2, N = 60) = 3.173588 p = 0.2046			

Table 7. Mann-Whitney Test by variable Winter variety vs. Spring variety (concentration of DNA of pathogen in µg/100mg of grain)

Variable	Rank sum	Valid N	Rank sum	Valid N	U	Z	p-value	Z adjusted	2*1 sided exact p
	WINTER		SPRING						
<i>F. culmorum</i>	1182	36	648	24	348	1.260	0.208	1.260	0.208
<i>F. graminearum</i>	1228	36	602	24	302	1.954	0.050	1.954	0.051
<i>Alternaria</i> spp.	1216	36	614	24	314	1.773	0.076	1.773	0.076

Note: marked tests are significant at $p < 0.050$; U = U value, Z = Z value

Table 8. Mann-Whitney Test by variable *Alternaria* natural infection vs. *Fusarium* spp. inoculation (concentration of DNA of pathogen in µg/100mg of grain)

Variable	Rank sum	Valid N	Rank sum	Valid N	U	Z	p-value	Z adjusted	2*1 sided exact p
	NATURAL		INOCULATION						
<i>F. culmorum</i>	792	36	1038	24	126	-4.610	0.001	-4.610	0.000
<i>F. graminearum</i>	864	36	966	24	198	-3.523	0.001	-3.523	0.001
<i>Alternaria</i> spp.	1192	36	638	24	338	1.411	0.158	1.411	0.159

Note: marked tests are significant at $p < 0.05000$; U = U value, Z = Z value

Table 9. Mann-Whitney Test by variable DEHULLED/HULLED (concentration of DNA of pathogen in µg/100mg of grain)

Variable	Rank sum	Valid N	Rank sum	Valid N	U	Z	p-value	Z adjusted	2*1 sided exact p
	DEHULLED		HULLED						
<i>F. culmorum</i>	565	24	611	24	265	-0.464	0.643	-0.464	0.646
<i>F. graminearum</i>	552	24	624	24	252	-0.732	0.464	-0.732	0.468
<i>Alternaria</i> spp.	423	24	753	24	123	-3.392	0.001	-3.391	0.001

Note: marked tests are significant at $p < 0.05000$; U = U value, Z = Z value

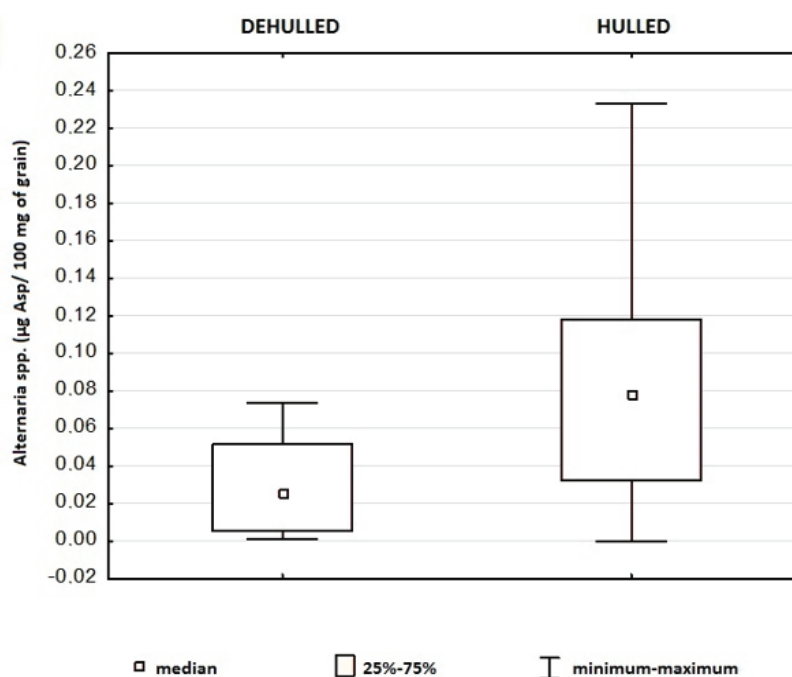


Fig. 1. Differences of grain contamination by the DNA of *Alternaria* spp. before and after dehulling (all the samples)

The factor of dehulling of the grain was studied and analysed in depth (when hulls were removed from spelt wheat spikes). It had the strongest and statistically significant effect (Mann-Whitney test – Table 9) and caused the contamination of grain with *Alternaria* spp. DNA to decrease (Table 4). Dehulled (peeled) grains were less contaminated with *Alternaria* spp. DNA (reduction from 0.09 µg DNA Asp/ 100mg of grain to 0.02 µg DNA Asp/ 100 mg of grain). Such a considerable reduction in the grain contamination with *Alternaria* spp. is shown in Fig. 1; the degree of contamination even decreased to zero in some tested samples. The dehulling of grain had a positive effect on individual years and inoculation options as well (Fig. 2). Released results of the research showed that hulls protected spelt kernels inside of *Alternaria* spp. from infection up to 50 %. The above-mentioned findings indicate that hulls

efficiently protect spelt kernels from *Alternaria* spp. infestation and their toxicological metabolites (Vuckovic et al., 2013).

The technological operation of grain dehulling had a strong impact on the degree of grain contamination with *Fusarium* spp. DNA; it was, nevertheless, non-significant (Table 9), as there was a wide range and high variability of tested samples (Table 4). There was an evident lower degree of grain contamination with *Fusarium avenaceae*, *equiseti* (Table 1), *poae*, and *sporotrichioides* (Table 3). The degree of grain contamination with *Fusarium culmorum* DNA decreased from 10.72 µg DNA Fc/100 mg of grain to 2.07 µg DNA Fc/100mg of grain (Table 4).

The reduction in contamination with *Fusarium culmorum* DNA is shown in Fig. 3. Our research produced similar results with *Fusarium graminearum*;

the degree of grain contamination with *Fusarium graminearum* decreased from 1.47 µg DNA Fg/100 mg of grain to 0.29 µg DNA Fg/100 mg of grain (Table 5). The degree of grain contamination with *Fusarium graminearum* DNA decreased dramatically in 2013 (Fig. 4). Previous research had indicated that hulls acted efficiently as barriers to *Fusarium* mycotoxins in hulled *Triticum* species (Castoria et al., 2005; Suchowilska et al., 2010; Wiwart

et al., 2004). Wiwart et al. (2011) compared *Fusarium* toxins in spelt and common wheat indicated that the concentrations of fungal metabolites were lower in spelt than in common wheat cultivars. There is a conclusion – dehulling can reduce contamination of fungi and toxins on spelt kernels. More surveys need to be conducted, considering the lack of knowledge on *Alternaria* toxins in food and feed in Europe and worldwide.

Wilks' lambda = 0.32268, F(6, 44) = 5.5764, p=0.00023

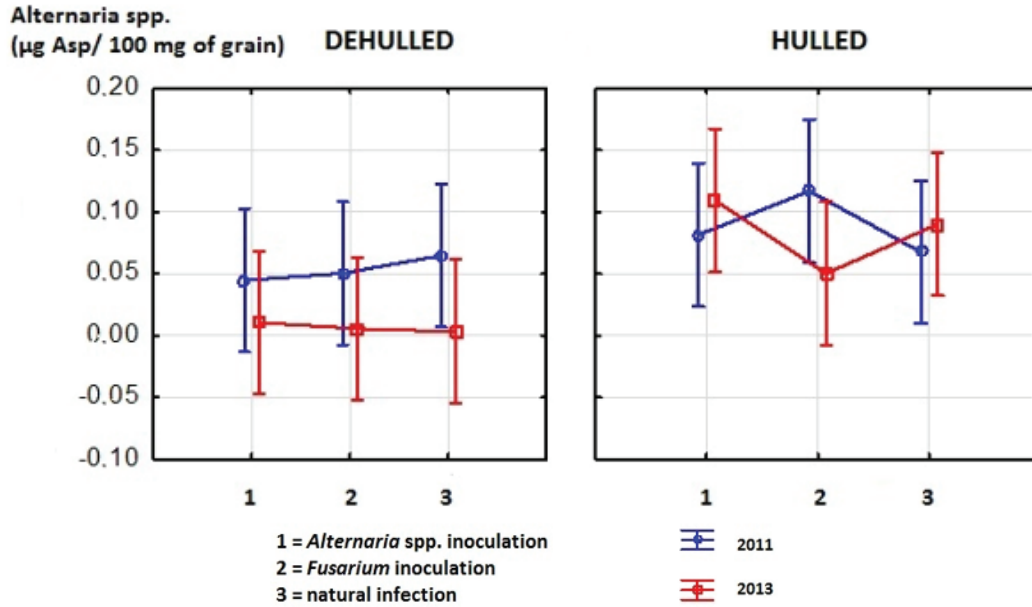


Fig. 2. Differences in grain contamination by DNA of *Alternaria* spp. in different years and grain treatment (results in 2011 were similar to 2012)

Wilks' lambda = 0.32268, F(6, 44) = 5.5764, p=0.00023

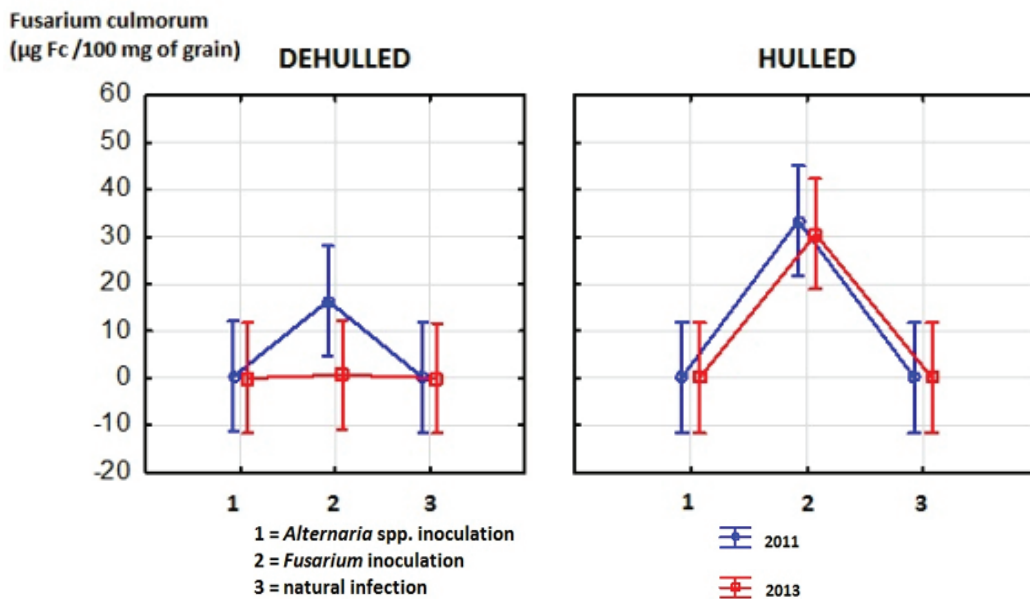


Fig. 3. Differences in grain contamination by DNA of *Fusarium culmorum* in different years and grain treatment

Wilks' lambda = 0.32268, F(6, 44) = 5.5764, p=0.00023

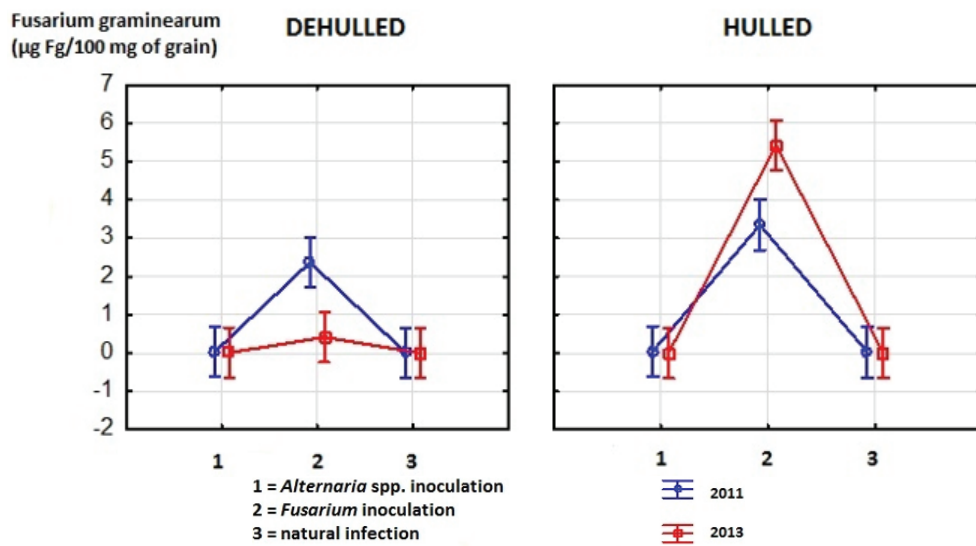


Fig. 4. Differences of grain contamination by DNA of *Fusarium graminearum* in different years and grain treatment

4. Conclusions

The degree of grain contamination with *Fusarium* spp. and *Alternaria* spp. was not influenced by the farming system. There were differences in the degree of grain contamination within individual years. Growing form (winter or spring) did not influence the degree of grain contamination either.

The artificial inoculation of grains with *Fusarium culmorum* and *graminearum* was successful. The natural infestation with *Alternaria* spp. was also studied and evaluated. The artificial inoculation with *Alternaria* spp. was not successful. Strong infestation of grains with *Fusarium* spp. led to low natural contamination of grains with *Alternaria* spp.

The technological operation of grain dehulling was performed and it was highly efficient there – the grain contamination with secondary metabolites and DNA of *Fusarium* spp. and DNA of *Alternaria* spp. decreased. The grain dehulling had a positive effect and reduced the degree of contamination of strongly infested varieties (that were infested artificially – by artificial inoculation). Therefore, it might be dangerous and risky to feed animals with whole spelt wheat spikes.

There are a lot of ambiguities about the biology of *Fusarium* spp. – how they develop in hulls and grains. Much more experiments with *Fusarium* spp. and *Alternaria* spp. involved have to be carried out in order to make the protecting role of hulls clear – if and how they protect spelt wheat and other hulled wheat species from *Fusarium* spp. and *Alternaria* spp. and possible contamination.

Acknowledgement

This work was supported by the research project No. NAZV QJ1310072 of the National Agency for Agricultural

Research of the Ministry of Agriculture of the Czech Republic and the University of South Bohemia in České Budějovice (project No. GAJU 094/2016/Z). I would like to thank Dr. Martin Šlachta for help with statistical data analysis.

References

- Aoki T., O'Donnell K., (1999), Morphological and molecular characterization of *Fusarium pseudograminearum* sp. nov., formerly recognized as the Group 1 population of *F. graminearum*, *Mycologia*, **91**, 597-609.
- Berthiller F., Dall'Asta C., Schumacher R., Lemmens M., Adam G., Krska R., (2005), Masked mycotoxins: determination of a deoxynivalenol glucoside in artificially and naturally contaminated wheat by liquid chromatography-tandem mass spectrometry, *Journal of Agricultural and Food Chemistry*, **53**, 3421-3425.
- Binder E.M., Tan L.M., Chin L., Handl J., Richard J., (2007), Worldwide occurrence of mycotoxins in commodities, feeds and feed ingredients, *Animal Feed Science and Technology*, **137**, 265-282.
- Birzele B., Prange A., Kramer J., (2000), Deoxynivalenol and ochratoxin A in German wheat and changes of level in relation to storage parameters, *Food Additives and Contaminants*, **17**, 1027-1035.
- Castoria X.X., Lima G., Ferracane R., Ritieni A., (2005), Occurrence of mycotoxin in farro samples from south Italy, *Journal of Food Protection*, **68**, 416-420.
- Champeil A., Fourbet J.F., Dore T., Rossignol L., (2004), Influence of cropping system on *Fusarium* head blight and mycotoxin levels in winter wheat, *Crop Protection*, **23**, 531-537.
- Chelkowski J., (1989), *Formation of Mycotoxins Produced by Fusarium in Heads of Wheat, Triticale and Rye*, In: *Fusarium - Mycotoxins, Taxonomy and Pathogenicity*, Chelkowski J. (Ed.), Elsevier, Amsterdam, 63-84.
- Cirillo T., Ritieni A., Visone M., Cocchieri R.A., (2003), Evaluation of conventional and organic Italian foodstuffs for deoxynivalenol and fumonisins B-1 and

- B-2, *Journal of Agricultural and Food Chemistry*, **51**, 8128-8131.
- Demeke T., Clear R.M., Patrick S.K., Gaba D., (2005), Species-specific PCR-based assays for the detection of *Fusarium* species and comparison with whole seed agar plate method and trichothecene analysis, *International Journal of Food Microbiology*, **103**, 271-284.
- D'Mello J.P.F., Placinta C.M., Macdonald A.M.C., (1999), *Fusarium* mycotoxins: a review of global implications for animal health, welfare and productivity, *Animal Feed Science and Technology*, **80**, 183-205.
- Doohan F.M., Parry D.W., Jenkinson P., Nicholson P., (1998), The use of species-specific PCR based assays to analyse *Fusarium* ear blight of wheat, *Journal of Plant Pathology*, **47**, 197-205.
- Janovská D., Leišová-Svobodová L., Capouchová I., Konvalina P., Káš M., (2015), Natural *Fusarium* occurrence qualitative evaluation on cereals under conventional and organic system in the Czech Republic, *Acta Fytotechnica et Zootechnica*, **18**, 19-21.
- Etzerodt T., Gislum R., Laursen B.B., Heinrichson K., Gregersen P.L., Jørgensen L.N., Fomsgaard I.S., (2016), Correlation of deoxynivalenol accumulation in *Fusarium* - infected winter and spring wheat cultivars with secondary metabolites at different growth stages, *Journal of Agricultural and Food Chemistry*, **64**, 4545-4555.
- FAO, (2000), Food safety and quality as affected by organic farming. FAO Regional Conference for Europe, Porto, On line at: <http://www.fao.org/docrep/meeting/X4983e.htm>.
- Filtenborg O., Frisvad J.C., Samson R.A., (2000), *Specific Associations of Fungi to Foods and Influence of Physical Environmental Factors*, In: *Introduction to Food and Airborne Fungi*, Samson R.A., Hoekstra E.S., Frisvad J.C., Filtenborg O. (Eds.), Centraal Bureau voor Schimmelcultures, Utrecht, 306-320.
- Jelínková Z., Moudrý J., Bernas J., Kopecký M., Moudrý J., Konvalina P., (2016), Environmental and economic aspects of *Triticum aestivum* L. and *Avena sativa* growing, *Open Life Sciences*, **11**, 533-541.
- Jestoi M., Somma M.C., Kouva M., Veijalainen P., Rizzo A., Ritieni, A., Peltonen K., (2004), Levels of mycotoxins and sample cytotoxicity of selected organic and conventional grain-based products purchased from Finnish and Italian markets, *Molecular Nutrition and Food Research*, **48**, 299-307.
- Knudsen I.M.B., Elmholt S., Hockenhull J., Jensen D.F., (1995), Distribution of saprophytic fungi antagonistic to *Fusarium culmorum* in two differently cultivated field soils, with special emphasis on the genus *Fusarium*, *Biological Agriculture and Horticulture*, **12**, 61-79.
- Konvalina P., Capouchová I., Stehno Z., Moudrý J. jr., Moudrý J., (2011), *Fusarium* identification by PCR and DON content in grain of ancient wheat, *Journal of Food, Agriculture and Environment*, **9**, 321-325.
- Konvalina P., Stehno Z., Capouchová I., Zechner E., Berger S., Grausgruber H., Janovská D., Moudrý J., (2014), Differences in grain/straw ratio, protein content and yield in landraces and modern varieties of different wheat species under organic farming, *Euphytica*, **199**, 31-40.
- Kuzdralinski A., Solarska E., Mazurkiewicz J., (2013), Mycotoxin content of organic and conventional oats from southeastern Poland, *Food Control*, **33**, 68-72.
- Leišová L., Kučera L., Chrpová J., Sýkorová S., Šíp V., Ovesná J., (2006), Quantification of *Fusarium culmorum* in wheat and barley tissues using real-time PCR in comparison with DON content, *Journal of Phytopathology*, **154**, 603-611.
- Lücke W., Steinbach P., Herten K., (2003), Phytosanitary observation in the organic farming of Mecklenburg-Vorpommern (in German), *Gesunde Pflanzen*, **55**, 117-120.
- Maeder P., Fliessbach A., Dubois D., Gunst L., Fried P., Niggli U., (2002), Soil fertility and biodiversity in organic farming, *Science*, **296**, 1694-1697.
- Magkos F., Arvantit F., Zampelas A., (2006), Organic food: buying more safety or just peace of mind? A critical review of the literature, *Critical Reviews in Food Science and Nutrition*, **46**, 23-56.
- Malmauret L., Parent-Massin D., Hardy J.L., Verger P., (2002), Contaminants in organic and conventional foodstuffs in France, *Food Additives and Contaminants*, **19**, 524-532.
- Miedaner T., Cumagun C.J.R., Chakraborty S., (2008), Population genetics of three important head blight pathogens *Fusarium graminearum*, *F. pseudograminearum* and *F. culmorum*, *Journal of Phytopathology*, **156**, 129-139.
- Khan M.M., Khan M.R., Mohiddin F.A., (2012), The relative performance of different inoculation methods with *Alternaria brassicae* and *A. brassicicola* on Indian Mustard, *Plant Pathology Journal*, **11**, 93-98.
- Ostrowska-Kołodziejczak A., Stuper Szablewska K., Kulik T., Buško M., Rissmann I., Wiwart M., Perkowski J., (2016), Concentration of fungal metabolites, phenolic acids and metals in mixtures of cereals grown in organic and conventional farms, *Journal of Animal and Feed Sciences*, **25**, 74-81.
- Özer G., Bayraktar H., (2015), Determination of fungal pathogens associated with *Cuminum cyminum* in Turkey, *Plant Protection Sciences*, **51**, 74-79.
- Parry D.W., Jenkinson P., McLeod L., (1995), *Fusarium* ear blight (scab) in small grain cereals - a review, *Plant Pathology*, **44**, 207-238.
- Pasanen A.L., Yli Pietilä K., Pasanen P., Kalliokoski P., Tarhanen J., (1999), Ergosterol content in various fungal species and biocontaminated building materials, *Applied Environmental Microbiology*, **65**, 138-142.
- Parry D.W., Nicholson P., (1996), Development of PCR assay to detect *Fusarium poae* in wheat, *Plant Pathology*, **45**, 872-883.
- Pasquali M., Migheli Q., (2014), Genetic approaches to chemotype determination in type B-trichothecene producing *Fusaria*, *International Journal of Food Microbiology*, **189**, 164-182.
- Perkowski J., Pavlova A., Šrobarova A., Stachowiak J., Golinski P., (2002), Group B trichothecenes biosynthesis in wheat cultivars after heads inoculation with *Fusarium culmorum* isolates, *Biologia*, **57**, 765-771.
- Prelusky D.B., Rotter B.A., Rotter R.G., (1993), *Toxicology of Mycotoxins*, In: *Mycotoxins in Grain: Compounds other than Aflatoxin*, Miller J.D., Trenholm H.L. (Eds.), Eagan Press, St. Paul, Minnesota, 359-404.
- Richard J.L., (2007), Some major mycotoxins and their mycotoxicoses: an overview, *International Journal of Food Microbiology*, **119**, 3-10.
- Salem N.M., Ahmad R., (2010), Mycotoxins in food from Jordan: preliminary survey, *Food Control*, **21**, 1099-1103.
- Scholten O.E., Steenhuis-Broers G., Timmermans B., Osman A., (2007), *Screening for Resistance to Fusarium Head Blight in Organic Wheat Production*, Proc. COST 860 SUSVAR workshop, Venence, vol. 1, 20-23.

- Skaug M.A., (1999), Analysis of Norwegian milk and infant formulas for ochratoxin A, *Food Additives and Contaminants*, **16**, 75-78.
- Suchowilska E., Kandler W., Sulyok M., Wiwart M., Krska R., (2010), Mycotoxin profiles in the grain of *Triticum monococcum*, *Triticum dicoccum* and *Triticum spelta* after head infection with *Fusarium culmorum*, *Journal of the Science of Food and Agriculture*, **90**, 556-565.
- Saß V., Milles J., Krämer J., Prange A., (2007), Competitive interactions of *Fusarium graminearum* and *Alternaria alternata* in vitro in relation to deoxynivalenol and zearalenone production, *Journal of Food, Agriculture & Environment*, **5**, 257-261.
- Vergnes D.M., Renard M.E., Duveiller E., Maraite H., (2006), Identification of *Alternaria* spp. on wheat by pathogenicity assays and sequencing, *Plant Pathology*, **55**, 485-493.
- Vuckovic J., Bodroza-Solarov M., Vujic D., Bocarov-Stancic A., Bagi F., (2013), The protective effect of hulls on the occurrence of *Alternaria* mycotoxins in spelt wheat, *Journal of the Science of Food and Agriculture*, **93**, 1996-2001.
- Wiwart M., Perkowski J., Budzynski W., Suchowilska E., Busko M., Matysiak A., (2011), Concentrations of ergosterol and trichothecenes in the grains of three *Triticum* species, *Czech Journal of Food Science*, **29**, 430-440.
- Wiwart M., Perkowski J., Jackowiak H., Packa D., Borusiewicz A., Buoeko M., (2004), Response of some cultivars of spring spelt (*Triticum spelta*) to *Fusarium culmorum* infection, *Die Bodenkultur*, **55**, 29-36.
- Woese K., Lange D., Boess C., Bogl K.W., (1997), A comparison of organically and conventionally grown foods-results of a review of the relevant literature, *Journal of the Science of Food and Agriculture*, **74**, 281-293.
- Yli-Mattila T., Rämö S., Hietaniemi V., Hussien T., Carlobos-Lopez A.L., Cumagun C.R.J., (2013), Molecular quantification and genetic diversity of toxigenic *Fusarium* species in northern Europe as compared to those in southern Europe, *Microorganisms*, **1**, 162-174.
- Yörük E., Tunali B., Kansu B., Ölmez F., Uz U., Zümrüt I.M., Sarıkaya A., Meyva G., (2016), Characterization of high-level deoxynivalenol producer *Fusarium graminearum* and *F. culmorum* isolates caused head blight and crown rot diseases in Turkey, *Journal of Plant Diseases and Protection*, **123**, 177-186.
- Zachariasova M., Dzuman Z., Veprikova Z., Hajkova K., Jiru M., Vaclavikova M., Zachariasova A., Pospichalova M., Florian M., Hajslova J., (2014), Occurrence of multiple mycotoxins in European feeding stuffs, assessment of dietary intake by farm animals, *Animal Feed Science and Technology*, **193**, 124-140.
- Zain E.M., (2011), Impact of mycotoxins on humans and animals, *Journal of Saudi Chemical Society*, **15**, 129-144.



“Gheorghe Asachi” Technical University of Iasi, Romania



CHEMICAL OXIDATION INTEGRATED INTO BIOLEACHING OF PYRITE AND CHALCOPYRITE USING IMMOBILIZED BIOMASS

Arevik Vardanyan*, Narine Vardanyan, Anna Khachatryan, Zaruhi Melkonyan

Laboratory of Geomicrobiology of SPC “Armbiotechnology” NAS of Armenia,
14 Gyurjyan Street, Yerevan, 0056, Armenia

Abstract

Chemical oxidation of pyrite and chalcopyrite by ferric sulfate ($\text{Fe}_2(\text{SO}_4)_3$) solution and biogenic ferric iron obtained by mixed culture of isolated thermotolerant *Acidithiobacillus* sp. 13Zn and *Leptospirillum ferriphilum* CC immobilized on natural carriers-zeolite and shungite was studied. Oxidation rate of sulfide minerals was estimated by the decrease of Fe^{3+} (oxidant) and increase of Fe^{2+} ions in the solution. It was revealed that chemical oxidation of chalcopyrite by biogenic ferric iron occurred 2-3 times more intensively than that by $\text{Fe}_2(\text{SO}_4)_3$ solution. Pyrite oxidation rate by biogenic ferric iron was twice higher than that by chemical ferric iron solution. It was shown that the treatment of pyrite and chalcopyrite by biogenic ferric iron allows to increase on average 1.5 - 2 times the bioleaching of iron from pyrite and iron and copper from chalcopyrite by the associations of iron and sulfur oxidizing bacteria.

Key words: *Acidithiobacillus* sp. 13Zn, biogenic ferric iron, chalcopyrite, chemical oxidation, immobilized biomass, pyrite

Received: May, 2017; *Revised final:* March, 2018; *Accepted:* March, 2018; *Published in final edited form:* April 2018

1. Introduction

Currently, it is accepted that there are two mechanisms for bioleaching of sulfide minerals: indirect “contact” and “non-contact” (Tributsch, 2001). According to indirect “contact” mechanism, the process of bioleaching occurs in the microenvironment - the reaction space between the surface of cell wall and mineral filled with extracellular polymeric substances (EPS) (Pace et al., 2005; Sand and Gehrke, 2006; Telegdi et al., 1998). Herneir et al. (2006) suppose that the complex of Fe (II) with glucuronic acid is unstable that allows Fe(II) ions to move freely within the EPS. Diffusing into the outer membrane of bacteria, Fe(II) can be oxidized by cell enzyme system and re-enter into the reduction-oxidation cycle (Herneir et al., 2006).

In case of “non-contact” mechanism, the mineral bioleaching is occurred in the liquid phase

through Fe (III) ions generated by bacteria. From this viewpoint the intensity of bioleaching is mainly determined by the regeneration of oxidizer – Fe (III) (Crundwell, 2003; Sand et al., 2001). Thus, the reduction of activity of leaching liquors or their bioregeneration is considered to be important for the development of efficient technology for the leaching of non-ferrous metals from minerals. At present, regeneration of ferric ion in operating leaching technologies realized by chemical methods, mainly by chlorine, ozone, hydrogen peroxide, makes the process more complicated and cost inefficient (http://www.khoamoitruonghue.edu.vn/courses/EnvTech/Fe_and_Mn_removal.pdf)

The use of chemolithotrophic microorganisms (CM) allows to simplify the process of regeneration of leaching solutions and significantly decrease its cost as microorganisms are considered to be unexhausted catalysts. On the other hand, to increase the intensity

* Author to whom all correspondence should be addressed: e-mail: avivardan@gmail.com; Phone: +374 94 900 931; Fax: +374 10 654 183

of bioregeneration of Fe(III), the method of immobilization of bacterial cells on porous solid carriers can be used. Immobilization of iron-oxidizing bacteria *At. ferrooxidans* and *L. ferrooxidans* on solid carriers allows to significantly increase the conversion rate of $\text{Fe}^{2+}/\text{Fe}^{3+}$ due to the concentration of bacterial cells (Armentia and Webb, 1992; Jaisankar and Modak, 2009; Nematy and Webb, 1996; Nikolov and Karamanev, 1992; Wood et al., 2001). Simultaneously, immobilization ensures long-term use of bacterial biomass (Gomez and Cantero, 1998; Ginsburg et al., 2009).

The process of immobilization of *At. ferrooxidans* is based on a number of factors, such as surface properties of adsorbent (Absolom et al., 1983), zeta potential (West et al., 1998), surface tension or moisture (Becker, 1998) and composition of nutrient media (An and Freidman, 1998; Li and Logan, 2004).

It has been revealed that the increase of temperature promotes the growth of free-living cells and oxidation of Fe (II) (Gomez and Cantero, 1998). However, unlike free-growing cells, the effect of the temperature on the immobilized cells of *At. ferrooxidans* is weaker (Nikolov and Karamanev, 1992). It is assumed that this is due to the physiological changes in the EPS of fixed cells, the nature and mechanism of which are not yet known (Gomez et al., 2000; Nikolov and Karamanev, 1992). Immobilization results in the increase of the oxidation rate of Fe (II) due to the enhancement of metabolic activity of *At. ferrooxidans* (Nemati and Webb, 1996, 1997; Wood et al., 2001; Zhong et al., 2004).

The immobilization mostly depends on the pH of the environment. The studies have shown that immobilization of *At. ferrooxidans* is 2 to 8 times more efficient at pH 2.0 as compared to pH 1.7 and 1.4, respectively (Gomez et al., 2000). It is assumed that under low pH conditions, the generation of jarosite is rapidly reduced. As the biofilm consists of the cells of *At. ferrooxidans* attached to the porous surface of jarosite, the biomass of immobilized cells on the carrier decreases at low pH ($\text{pH} < 2.0$). Thus, the temperature and pH may be used to control the processes of immobilization and biomass generation in the bioreactor (Nemati and Webb, 1997).

In this study for the first time natural inorganic carriers zeolite and shungite have been used for immobilization of the mixed culture of iron oxidizing bacteria *Acidithiobacillus* sp.13Zn and *L. ferriphilum*. Previously, the immobilization of *L. ferriphilum* CC was successfully implemented on the mentioned carriers (Vardanyan et al., 2013). It was shown that bacteria immobilized on zeolite and shungite might be prospective for regeneration of oxidant (Fe^{3+}) in bioleaching processes.

The objective of this paper is to study comparative activities of ferric sulfate ($\text{Fe}_2(\text{SO}_4)_3$) solution and biogenic ferric iron obtained by the isolated thermotolerant bacteria on chemical oxidation of pyrite and chalcopyrite. The studies will allow to reveal optimal conditions for the regeneration of leaching liquors. Based on the obtained results the

efficient integrated bioleaching technology for the extraction of non-ferrous and precious metals will be developed.

2. Material and methods

2.1. Microorganisms and media

In this study thermotolerant iron oxidizing CM *Acidithiobacillus* sp.13Zn (Stepanyan, 2016), *L. ferriphilum* CC (Vardanyan et al., 2013) and sulfur oxidizing bacteria *Acidithiobacillus albertensis* SO-2 (Vardanyan and Vardanyan, 2014) isolated in Armenia were used. For the growth of bacteria, Mackintosh medium (Mackintosh, 1978) with ferrous iron or sulfur as a source of energy was used.

2.2. Immobilization of microorganisms on natural carriers

For immobilization of iron oxidizing bacteria *Acidithiobacillus* sp.13Zn and *L. ferriphilum* CC natural inorganic carriers such as zeolite, shungite and activated carbon were tested. The mentioned carriers were provided by the Department of Mineralogy of Yerevan State University. The main features of the carriers are presented below.

Armenian natural zeolite (Clinoptilolite): chemical formula - $(\text{Na}, \text{K}, \text{Ca}) (\text{AlSi}_5\text{O}_{12}) \times 6\text{H}_2\text{O}$, bulk density-980 kg/m^3 , porosity - 60-63%, specific surface - $(50-65) \times 10^{-3} \text{ m}^2/\text{kg}$, Ion Exchange Capacity by Ca^{++} , K^+ , Na^+ mg eqv on 100g- 90-150.

Brilliant shungite (Karelsky Region, Russia): Carbon content 94 %, density 2.25 – 2.84 g/cm^3 , porosity 0.5 – 5 %.

Birch activated carbon BAU-A: Grains of black color, adsorption activity on iodine 60 %, total volume on water - no less than 1.6 cm^3/g , bulk density - no more than 240 g/dm^3 , mass fraction of ash - no more than 6.0 %, mass fraction of moisture - no more than 10 %.

Immobilization was performed according to the following procedure: 10g of each carrier was placed in 500 mL flask containing 200 mL Makintosh medium and 5 mL mixed culture of *Acidithiobacillus* sp.13Zn and *L. ferriphilum* CC in logarithmic phase of the growth. The flasks were shaken at 180 rpm on an orbital shaker at 35°C. In case of vessels stirring was performed through blowing. Ferrous iron oxidation by immobilized cells was monitoring by measuring its concentration. When ferrous iron was oxidized completely, the media were replaced with 200 mL fresh media. The procedure was continued several times until ferrous iron oxidation rate was stable.

The number of bacterial cells was determined using Thoma Chamber and the method of the most probable number (MPN). Obtained results were compared with standard McCrady's Table (Gerhardt et al., 1981). The number of adhered cells was determined as the difference between the number of inoculated cells and the cells remaining in the medium after immobilization.

2.3. Chemical and biogenic ferric iron (Fe^{3+}) solutions

As chemical ferric iron, $Fe_2(SO_4)_3$ salt solution was used. Biogenic ferric iron was obtained by the oxidation of ferrous iron ($Fe(II)$) by the biomass of newly isolated thermotolerant *Acidithiobacillus* sp. 13Zn and *L. ferriphilum* immobilized on zeolite and shungite.

2.4. Chemical oxidation of pyrite and chalcopyrite

Pyrite containing 43.8% Fe, 49% S and chalcopyrite containing 30.2% Cu, 29.7% Fe, 38% S from Shamlugh ore deposit (Armenia) were used. The minerals were ground to a size fraction of between 45-65 μm and sterilized at 112°C for 20 min.

Chemical oxidation of pyrite and chalcopyrite was carried out in 250 mL Erlenmeyer flasks containing 100 mL of Mackintosh medium, 5 and 10% of minerals and chemical and biogenic Fe^{3+} in concentration of 5 g/L. The experiments were performed under shaking conditions on rotary shaker (180 rpm) at 40°C. The rate of chemical oxidation was evaluated by either the increase of ferrous iron ($Fe(II)$) or decrease of ferric iron ($Fe(III)$) in the leaching solution. The amount of extracted iron from pyrite was calculated as the difference between total iron and added initial ferric iron concentrations (oxidant). Sampling was performed with an hour interval and ferric and ferrous ions were analyzed. The amount of copper and total iron in the leaching solution was determined by atomic absorption spectrometer AAS 1N (Carl Zeiss, Germany). Ferrous (Fe^{2+}) and ferric ions (Fe^{3+}) were determined complexometrically by titration with EDTA (Karavayko et al., 1989). The intensity of chemical oxidation was evaluated by the increase of $Fe(II)$ ions concentration in the leaching solution. The amount of extracted iron from pyrite was calculated as a difference between total iron and added initial ferric iron concentration.

2.5. Bioleaching of pyrite and chalcopyrite treated by ferric iron

For bioleaching of treated and untreated pyrite the association of iron oxidizing bacteria *Acidithiobacillus* sp. 13Zn and *L. ferriphilum* CC was used. Bioleaching of chalcopyrite was carried out by

the association of *Acidithiobacillus* sp. 13Zn, *L. ferriphilum* CC and sulfur oxidizing bacteria *At. albertensis* SO-2. The bioleaching experiments were carried out in 250 mL flasks in periodic mode of cultivation on a shaker (180 rpm) at 35°C.

The intensity of bioleaching of minerals was evaluated by the increase of copper and ferrous ions concentrations in the leaching solution. Sampling was performed with a 72 hour intervals and copper, total iron, ferric $Fe(III)$ and ferrous ($Fe(II)$) ions were analyzed. Ferric $Fe(III)$ and ferrous ($Fe(II)$) ions were determined complexometrically by EDTA. Total iron and copper were determined by atomic absorption spectrometer AAS 1N (Germany). The experiments were performed in triplicate. The data obtained were analyzed statistically by Excel.

3. Results and discussion

3.1. Immobilization of microorganisms

The studies have shown that the iron oxidation rate by the immobilized cells of *Acidithiobacillus* sp. 13Zn on zeolite, carbon and shungite in comparison with free-living cells increases about 2.3, 2 and 1.8 times, respectively. The most suitable carrier for *L. ferriphilum* CC is carbon followed by natural zeolite and shungite (Table 1).

Differences for carrier preference between *Acidithiobacillus* sp. 13Zn and *L. ferriphilum* can be explained by chemical composition of EPS produced by bacteria that mediate their adhesion on mineral and carrier surface (Harneit et al., 2006; Sand and Gehrke, 2006) as well as surface properties of carriers (Absolom et al., 1983).

To obtain biogenic ferric iron, the association of *Acidithiobacillus* sp.13Zn and *L. ferriphilum* CC immobilized on zeolite or shungite was used. Immobilization process was carried out at 37°C in a stirring mode for 10 - 15 days to achieve the maximum activity of iron oxidation (Fig. 1).

3.2. Chemical oxidation of pyrite and chalcopyrite

For chemical oxidation of pyrite, ferric sulfate ($(Fe_2(SO_4)_3 \times 9H_2O)$) salt solution and biogenic ferric iron obtained by mixed culture of *Acidithiobacillus* sp. 13Zn and *L. ferriphilum* immobilized on zeolite and shungite, were used. The initial concentration of ferric iron ($Fe(III)$) in both solutions was 5 g/L.

Table 1. Oxidation of ferrous iron by free-living and immobilized cells of *Acidithiobacillus* sp.13Zn and *L. ferriphilum* CC

Cells	<i>Acidithiobacillus</i> sp. 13Zn			<i>L. ferriphilum</i> CC		
	Oxidized Fe^{2+} , g/L in 48 h	Oxidation rate, g/L h	Adhered cell number, cells/mL	Oxidized Fe^{2+} , g/L in 48 h	Oxidation rate, g/L h	Adhered cell number, cells/mL
Free-living cells	1.8	0.038	-	0.62	0.013	
Cells Zeolite	4.5	0.09	6.2×10^7	1.34	0.028	1.2×10^6
Cells immobilized on shungite	3.4	0.07	5.26×10^7	0.86	0.018	2.6×10^6
Cells immobilized on activated carbon	3.6	0.075	5.8×10^6	2.42	0.05	5.0×10^6



Fig. 1. Immobilization of *Acidithiobacillus* sp. 13 Zn and *L. ferriphilum* CC on zeolite (37°C, stirring through blowing)

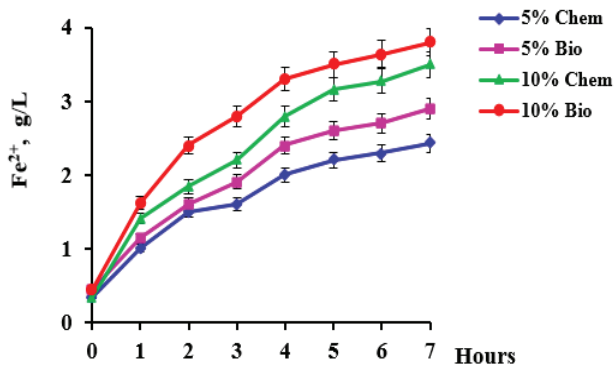


Fig. 2. Generation of Fe²⁺ during chemical oxidation of pyrite by solution of Fe₂(SO₄)₃ and biogenic ferric iron at 5 and 10% PD (initial concentration of Fe³⁺ - 5 g/L, pH 1.8, 40°C)

Chemical oxidation of pyrite was carried out under shaking conditions (180 rpm) at 5 and 10% pulp

density (PD) and 40°C. The intensity of chemical leaching was evaluated by the increase of Fe(II) ions concentration in the leaching solution (Fig. 2). As it can be seen from Fig. 3, the amount of iron leached from pyrite in the case of biogenic ferric iron is larger than in the case of Fe₂(SO₄)₃ solution (chemical solution). Besides, this regularity was observed at both 5 and 10% of the tested pulp densities (Figs. 3 a, b).

It should be noted that rapid extraction of iron was observed in the first 4 h, then the process was gradually slowed down. The maximum rate of iron extraction (2.4 - 2.5 g/L h) by chemical oxidation of pyrite was observed in the first hour and gradually declined to 0.2 - 0.3 g /L h for 6 hrs (Fig. 4). Direct dependence of iron extraction rate on the pulp density was also observed. Thus, the maximum rate of iron extraction at 10% pulp density was 2.52 g/L h and 1.6 times higher than that observed at 5% pulp density (1.4 g/L h) (Fig. 4).

The studies of several authors (Fomchenko and Biryukov, 2009; Muravev et al., 2009) have revealed that culture liquid containing ferric iron obtained by biooxidation of ferrous iron is a more active oxidizer for pyrite than the solution of Fe₂(SO₄)₃·9H₂O. It is also shown that preliminary chemical leaching of pyrite concentrates by culture liquid containing ferric iron compounds increases the rate and depth of the subsequent biooxidation of pyrite. The results of the chemical oxidation of chalcopyrite are presented in Fig. 5 and Table 2.

According to the data presented, similar to pyrite the leaching of chalcopyrite by Fe³⁺ of bacterial origin as compared to chemical solution of Fe³⁺ proceeds more effectively regardless of pulp density. Thus, during leaching of chalcopyrite with Fe³⁺ of bacterial origin 2-3 times more copper passes into the medium than in the case of chemical solution of Fe³⁺ at 5% pulp density. The amount of extracted iron during leaching of chalcopyrite by Fe³⁺ of bacterial origin was twice higher than in the case of chemical solution of Fe³⁺ (Table 2, Fig. 5a).

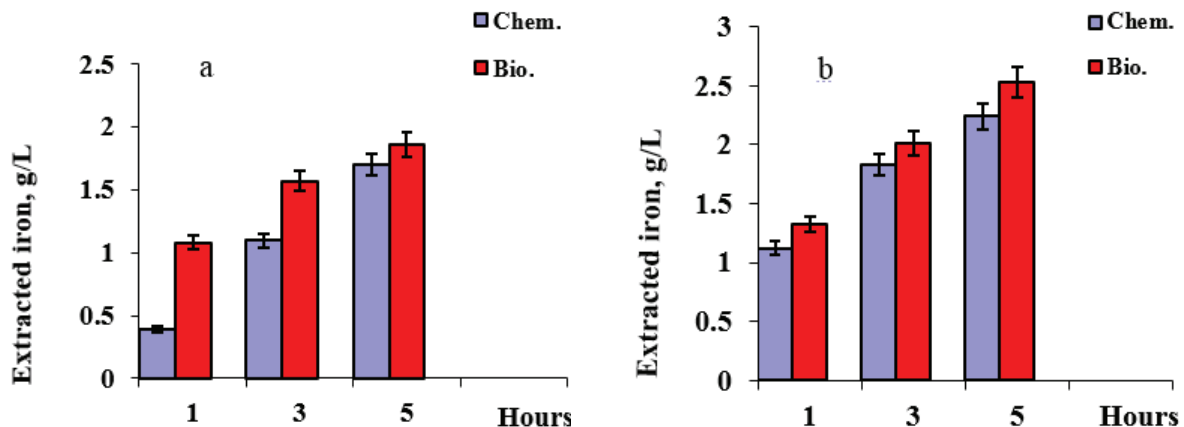


Fig. 3. Extraction of iron during chemical oxidation of pyrite at 5 % (a) and 10 % (b) pulp densities (PD) (initial concentration of Fe³⁺ - 5 g/L, pH 1.8, 40°C)

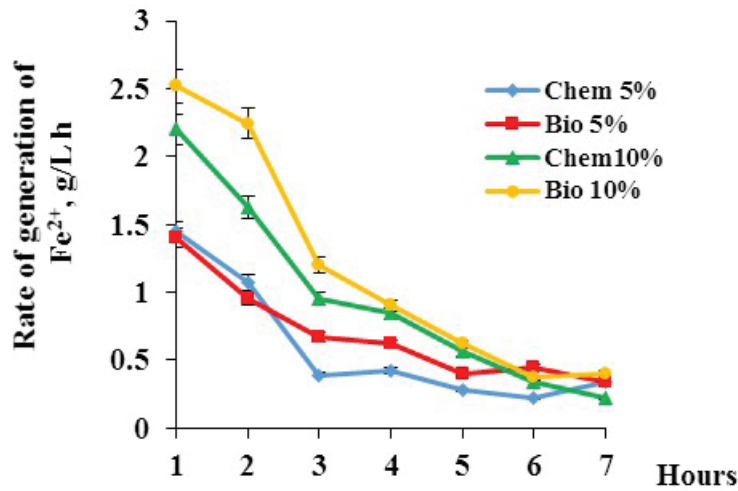


Fig. 4. Rate of generation of Fe²⁺ during chemical oxidation of pyrite at different pulp densities (initial concentration of Fe³⁺ - 5 g/L, pH 1.8, 40°C)

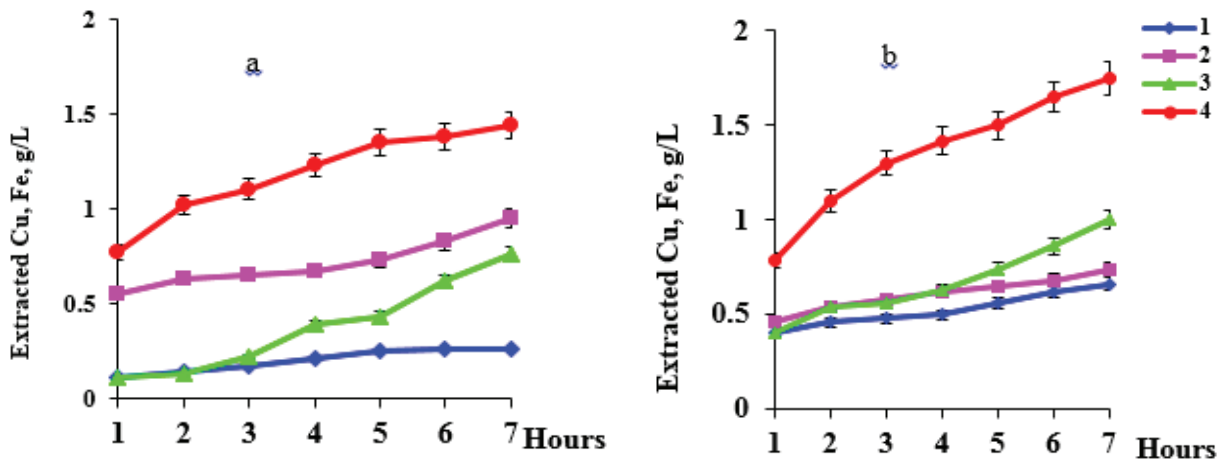


Fig. 5. Extraction of copper (1, 2) and iron (3, 4) during leaching of chalcopyrite by solution of Fe₂(SO₄)₃ (1, 3) and biogenic ferric iron (2, 4) at 5% (a) and 10% (b) PD (initial concentration of Fe³⁺ 5 g/L, pH 1.8, 40°C)

Table 2. Extraction of copper and iron during chemical oxidation of chalcopyrite

PD, %		Extraction of iron for 4h		Extraction of copper for 4h	
		g/L	%	g/L	%
5	Chem.	0.780	5.3	0.210	1.4
5	Bio.	1.232	8.3	0.650	4.3
10	Chem.	0.628	2.1	0.560	1.8
10	Bio.	1.434	4.8	0.670	2.0

The same pattern was observed at 10% pulp density, though the amount of leached copper was only 1.2 times higher. As a result, within 4 hours 4.3 and 2.0% of copper was leached from chalcopyrite when Fe³⁺ iron of bacterial origin was used and 1.4 and 1.8% in the case of chemical solution of Fe³⁺, respectively, at 5 and 10% pulp density (Fig. 5b, Table 2).

Oxidation of chalcopyrite by ferric iron can be presented by the following reaction:



Proceeding from this reaction some authors have concluded that “passivation” of chalcopyrite is

due to the formation of a layer of sulphur on the surface of mineral (Munoz, 1979). Another researchers have proposed that the passivating layer consists of jarosite that precipitate on the surface of the chalcopyrite particles thus preventing its further oxidation (Ahmadi et al., 2012; Cordoba, 2008; Yu et al., 2011). They have studied the effect of iron ions on the dissolution of chalcopyrite at low and high potential, and found that although Fe (III) ions are responsible for the oxidation of chalcopyrite, Fe (II) has an important role in controlling the formation and precipitation of the jarosite.

According to the another researchers’ data (Gusakov et al., 2011; Gusakov, 2012), the solutions of ferric sulfate (Fe₂(SO₄)₃) and biogenic ferric iron of

bacterial origin significantly differ by their ionic composition. It is revealed that unlike the chemical solution, in biogenic one ferric iron (Fe(III)) is connected with high-molecular organic compounds such as polysaccharides, able to form complexes with metal cations, including iron.

It is also shown that during the leaching of sulfide minerals by chemical solution ferric iron precipitates and iron concentration in leaching solution sharply reduces, which results in the decrease of its oxidation activity. In case of ferric iron of bacterial origin precipitation of Fe(III) does not occur, which results in the maintenance of oxidation activity at a high level.

3.3. Bioleaching of pyrite and chalcopyrite after treatment with biogenic ferric iron

A comparative study of microbiological leaching of untreated and treated with biogenic Fe³⁺ pyrite and chalcopyrite was carried out. For leaching of pyrite the mixed culture of *Acidithiobacillus* sp.13Zn with *L. ferriphilum* CC was used, for chalcopyrite – the mixed cultures of *Acidithiobacillus* sp.13Zn with *L. ferriphilum* CC and *At. albertensis* SO-2 were used. For bioleaching of pyrite the

association of iron oxidizing bacteria *Acidithiobacillus* sp. 13Zn and *L. ferriphilum* CC was used. Bioleaching of chalcopyrite was carried out by the association of *Acidithiobacillus* sp. 13Zn, *L. ferriphilum* CC and sulfur oxidizing bacteria *A. albertensis* SO-2 taking into consideration other author's research (Rawlings and Johnson, 2007; Watling et al., 2013; Zhou et al., 2009) as well as our previous research (Vardanyan et al., 2016). The results of bioleaching of pyrite are shown in Fig. 6.

As follows from the presented data, the amount of leached iron from pyrite treated with biogenic Fe³⁺ is about 1.3 times more than that of the untreated mineral. The extent of total iron extraction by the used mixed culture was 38.9% and 31.9% from both treated and untreated pyrite, respectively (Table 3). In general, after the chemical oxidation and subsequent bacterial leaching about 50% of iron from pyrite is extracted. The obtained results are in agreement with the research of other authors (Fomchenko and Biryukov, 2009). According to these studies, preliminary chemical leaching of pyrite concentrates by culture liquid, containing ferric iron compounds, increases the rate and depth of the subsequent biooxidation of sulfide mineral by moderate thermophilic bacteria.

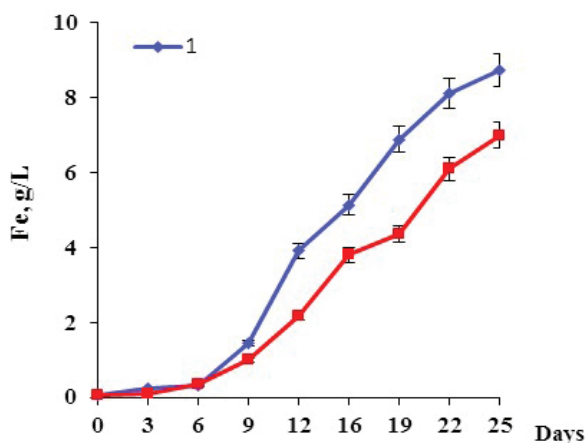


Fig. 6. Leaching of iron from treated (1) and untreated with biogenic Fe(III) (2) pyrite by the mixed culture of *Acidithiobacillus* sp.13Zn with *L. ferriphilum* CC (FeS₂ 5%, pH 1.8, 35°C)

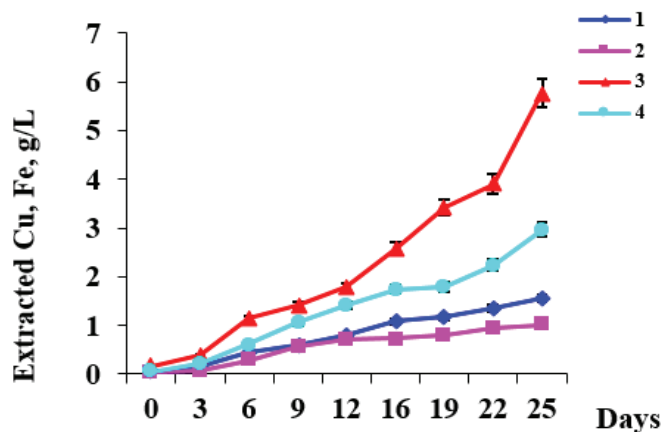


Fig 7. Leaching of copper (1, 2) and iron (3, 4) from treated (1, 3) and untreated with biogenic Fe(III) (2, 4) chalcopyrite by the mixed cultures of *Acidithiobacillus* sp.13Zn, *L. ferriphilum* CC and *At. albertensis* SO-2 (CuFeS₂ 5%, pH 1.8, 35°C)

Table 3. Extraction of copper and iron from untreated and treated pyrite and chalcopyrite by the mixed culture of *Acidithiobacillus* sp.13Zn, *L. ferriphilum* CC and *At. albertensis* SO-2 (for 25 days)

Mineral	Leached Cu, g/L	Extraction Cu, %	Leached Fe, g/L	Extraction Fe, %	Initial/final pH	Final ORP, mV
FeS ₂ , untreated	-	-	7.0	31.9	1.8 / 1.6	780
FeS ₂ , treated with Fe(III)	-	-	8.74	39.9	1.8 / 1.35	830
CuFeS ₂ , untreated	1.01	6.7	2.97	19.9	1.8 / 1.8	450
CuFeS ₂ , treated with Fe(III)	1.56	10.4	5.78	38.9	1.8 / 1.6	625

The results of bacterial leaching of chalcopyrite without pretreatment and after treatment with biogenic solution Fe(III) are shown in Fig. 7. As follows from the presented data, unlike untreated chalcopyrite, the treated one was leached more intensively. Thus, for 25 days of the experiment, from chalcopyrite treated with biogenic iron about 1.5 times more copper (1.56 g/L) was leached by the mixed cultures of *Acidithiobacillus* sp.13Zn with *L. ferriphilum* CC and *At. albertensis* SO-2 (Fig. 7) than that from the untreated mineral (1.01 g/L). In the same period the amount of leached iron was 5.8 g/L and 2.97 g/L from treated and untreated chalcopyrite, respectively (Fig. 7).

As a result, for 25 days of bioleaching from treated chalcopyrite 10.4% copper and 38.9% iron were leached (extracted) by the mixed culture of *Acidithiobacillus* sp. 13Zn with *L. ferriphilum* CC and *At. albertensis* SO-2, while from untreated mineral 6.3% and 31.9%, respectively (Table 3).

The intensity of chalcopyrite leaching also proved the changes in pH and ORP of the leaching medium. The more intensively the mineral is leached, the lower the final pH value and ORP of the leaching solution are (Table 3).

4. Conclusions

It can be concluded that mixed culture of *Acidithiobacillus* 13Zn and *L. ferrooxidans* CC immobilized on zeolite and shugite can be prospective for regeneration of oxidant (Fe³⁺) in the bioleaching processes. Results obtained show that during chemical leaching of pyrite and chalcopyrite by ferric iron Fe³⁺ of bacterial origin about twice more copper and iron pass into the medium than in case of chemical solution of Fe³⁺.

Treatment of pyrite and chalcopyrite with Fe(III) solution obtained by the immobilized mixed culture of *Acidithiobacillus* sp. 13Zn and *L. ferriphilum* allows to increase on average 1.5-2 times the extraction of iron and copper from chalcopyrite and iron from pyrite.

Thus, chemical oxidation of pyrite and chalcopyrite by biogenic ferric iron obtained by the immobilized biomass of CM integrated into biohydrometallurgical technology will allow to significantly increase the efficiency of subsequent bioleaching process and the extent of recovery of metals.

References

- Absolom D., Lamberti F., Policova Z., Zingg W., van Oss C.J., Neumann A., (1983), Surface thermodynamics of bacterial adhesion, *Applied and Environmental Microbiology*, **46**, 90-97.
- Ahmadi A., Schaffie M., Petersen J., Schippers A., Ranjbar M., (2011), Conventional and electrochemical bioleaching of chalcopyrite concentrates by moderately thermophilic bacteria at high pulp density, *Hydrometallurgy*, **106**, 84-92.
- An Y., Freidman R., (1998), Concise review of mechanisms of bacterial adhesion to biomaterial surfaces, *Journal of Biomedical Materials Research*, **43**, 338-348.
- Armentia H., Webb C., (1992), Ferrous sulfate oxidation using *T. ferrooxidans* cells immobilized in polyurethane foam support particles, *Applied Microbiology and Biotechnology*, **36**, 697-700.
- Becker K., (1998), Detachment studies on microfouling in natural biofilms on substrata with different surface tensions, *International Biodeterioration and Biodegradation*, **41**, 93-100.
- Cordoba E., (2008), Leaching of chalcopyrite with ferric ion. Part I: General aspects, *Hydrometallurgy*, **93**, 81-87.
- Crundwell F., (2003), How do bacteria interact with minerals?, *Hydrometallurgy*, **71**, 75-81.
- Fomchenko N., Biryukov V., (2009), Two-step technology of bacterial-chemical leaching of copper-zinc raw materials by Fe³⁺ ions with their subsequent regeneration by chemolithotrophic bacteria, *Applied Microbiology and Biotechnology*, **45**, 64-69.
- Gerhardt P., Murray R., Costilow R., Nester E., Wood W., Krieg N., Phillips G. (Eds.), (1981), *Manual of Methods for General Bacteriology*, American Society of Microbiology, Washington DC.
- Ginsburg M., Panev K., Karamanev D., (2009), Immobilization and ferrous ion bio-oxidation studies of a *Leptospirillum* sp. mixed-cell culture, *Minerals Engineering*, **22**, 140-148.
- Gomez J., Cantero D., (1998), Modelling of ferrous sulphate oxidation by *Thiobacillus ferrooxidans* in discontinuous culture: influence of temperature, pH and agitation rate, *Journal of Fermentation and Bioengineering*, **86**, 79-83.
- Gomez J., Canter D., Webb C., (2000), Immobilization of *T. ferrooxidans* cells on nickel alloy fibre for ferrous sulfate oxidation, *Applied Microbiology and Biotechnology*, **54**, 335-340.
- Gusakov M., Krylova L., Adamov E., (2011), The leaching of nickel from pyrrhotite concentrates by ferric iron obtained using immobilized biomass, *Non-Ferrous Metals*, **4**, 15-19.
- Gusakov M., (2012), *Development of the method of leaching of sulphide concentrates by ferric sulfate solution*

- obtained using immobilized biomass, PhD Thesis, National Research Technological University, MISA, Moscow, Russia.
- Harneit K., Goksel A., Kock D., Klock J., Gehrke T., Sand W., (2006), Adhesion to metal sulfide surfaces by cells of *Acidithiobacillus ferrooxidans*, *Acidithiobacillus thiooxidans* and *Leptospirillum ferrooxidans*, *Hydrometallurgy*, **83**, 245-254.
- Jaisankar S., Modak J., (2009), Ferrous iron oxidation by foam immobilized *Acidithiobacillus ferrooxidans*, *Experiments and modeling. Biocatalysts and Bioreactor Design*, **25**, 1328-1342.
- Karavayko G., Agate A., Grudev S., Avakyan Z. (Eds.), (1989), *Biogeotechnology of Metals*, Center of International Projects SCST, Moscow, Russia.
- Lancey E., Tuovinen O., (1984), Ferrous ion oxidation by *Thiobacillus ferrooxidans* immobilized in calcium alginate, *Applied Microbiology and Biotechnology*, **20**, 94-99.
- Li B., Logan B., (2004), Bacterial adhesion to glass and metal-oxide surfaces, *Colloids and Surfaces. B: Biointerfaces*, **36**, 81-90.
- Mackintosh M., (1978), Nitrogen fixation by *Thiobacillus ferrooxidans*, *Journal of General Microbiology*, **105**, 215-218.
- Nemati M., Webb C., (1996), Effect of ferrous iron concentration on the catalytic activity of immobilized cells of *Thiobacillus ferrooxidans*, *Applied Microbiology and Biotechnology*, **46**, 250-255.
- Nemati M., Webb C., (1997), Does immobilization of *Thiobacillus ferrooxidans* really decrease the effect of temperature on its activity, *Biotechnology Letters*, **19**, 39-43.
- Nikolov L., Karamanev D., (1992), Kinetics of the ferrous iron oxidation by resuspended cells of *Thiobacillus ferrooxidans*, *Biotechnology Progress*, **8**, 252-255.
- Pace D., Mielke R., Southam G., Porter T., (2005), Scanning force microscopy studies of the colonization and growth of *A. ferrooxidans* on the surface of pyrite minerals, *Scanning*, **27**, 136-140.
- Rawlings D., Johnson B., (2007), The microbiology of biomining: development and optimization of mineral-oxidizing microbial consortia, *Microbiology*, **153**, 315-324.
- Sand W., Gehrke T., Jozsa P., Schippers A., (2001), Biochemistry of bacterial leaching- direct vs. indirect bioleaching, *Hydrometallurgy*, **59**, 159-175.
- Sand W., Gehrke T., (2006), Extracellular polymeric substances mediate bioleaching/biocorrosion via interfacial processes involving iron (III) ions and acidophilic bacteria, *Research in Microbiology*, **157**, 49-56.
- Stepanyan S., (2016), Peculiarities of bioleaching of pyrite and chalcopyrite by new isolated *Acidithiobacillus* sp. strain 13Zn, *Biological Journal of Armenia*, **68**, 77-82.
- Telegdi J., Keresztes Z., Pálkás G., Kálmán E., Sand W., (1998), Microbially influenced corrosion visualized by atomic force microscopy, *Applied Physics*, **66**, 639-642.
- Tributsch H., (2001), Direct versus indirect bioleaching, *Hydrometallurgy*, **59**, 177-185.
- Yu R., Zhong D., Miao L., Wu F., Qiu G., Gu G., (2011), Relationship and effect of redox potential, jarosites and extracellular polymeric substances in bioleaching chalcopyrite by *Acidithiobacillus ferrooxidans*, *Transactions of Nonferrous Metals Society of China*, **21**, 1634-1640.
- Vardanyan A., Markosyan L., Vardanyan N., (2013), Immobilization of new isolated iron oxidizing bacteria on natural carriers, *Advanced Materials Research*, **825**, 388-391.
- Vardanyan N., Stepanyan S., Khachatryan A., Melqonyan Z., Vardanyan A., (2016), Biooxidation of chalcopyrite by iron and/or sulfur oxidizing bacteria isolated in Armenia, *Innovative Research in Science, Engineering and Technology*, **5**, 15901-15907.
- Vardanyan N., Vardanyan A., (2014), New sulphur oxidizing bacteria isolated from bioleaching pulp of zinc and copper concentrates, *Universal Journal of Microbiology Research*, **2**, 27-31.
- Watling H., (2006), The bioleaching of sulphide minerals with emphasis on copper sulphides – a review, *Hydrometallurgy*, **84**, 81-108.
- West R., Stephens G., Cilliers J., (1998), Zeta potential of silver absorbing *Thiobacillus ferrooxidans*, *Minerals Engineering*, **11**, 189-194.
- Wood T., Murray K., Burges J., (2001), Ferrous sulfate oxidation using *Thiobacillus ferrooxidans* cells immobilized on sand for purpose of treating acid mine drainage, *Applied Microbiology and Biotechnology*, **56**, 560-565.
- Zhong-Er L., Huang Y., Cai Z., Cong W., Ouyang F., (2004), Kinetics of continuous ferrous ion oxidation by *Acidithiobacillus ferrooxidans* immobilized in poly (vinyl alcohol) cryogel carriers, *Hydrometallurgy*, **74**, 181-187.
- Zhou H., Zeng W., Yang Z., Xie Y., Qiu G., (2009), Bioleaching of chalcopyrite concentrate by a moderately thermophilic culture in a stirred tank reactor, *Bioresource Technology*, **100**, 515-520.

Web sites:

http://www.khoamoitruonghue.edu.vn/courses/EnvTech/Fe_and_Mn_removal.pdf



“Gheorghe Asachi” Technical University of Iasi, Romania



INFLUENCE OF FARMING SYSTEM ON GREENHOUSE GAS EMISSIONS WITHIN CEREAL CULTIVATION

Jan Moudrý Jr.^{1*}, Jaroslav Bernas¹, Marek Kopecký¹, Petr Konvalina¹, Daniel Bucur²,
Jan Moudrý¹, Ladislav Kolář¹, Zdeněk Štěrbá¹, Zuzana Jelínková¹

¹University of South Bohemia in České Budějovice, Faculty of Agriculture, Studentská 1668, České Budějovice, CZ 37005, Czech Republic

²University of Agricultural Sciences and Veterinary Medicine Iasi, Faculty of Agriculture, Mihail Sadoveanu Alley 3, Iasi, 700490, Romania

Abstract

The emissions of greenhouse gases (GHG) from anthropogenic activities have still been a topical and much-discussed issue. In farming, room for reducing GHG emissions may also be available in crop farming. The measures aimed at the mitigation of GHG emissions may include a change in the farming system or partial switch to more extensive farming methods, including organic farming. The life cycle of oat, rye, wheat and spelt wheat cultivation in conventional and organic farming systems in the conditions of Central Europe was evaluated by LCA method, impact category: climate. The results clearly show that there are considerable differences between conventional and organic farming systems in individual subcategories of the farm phase of the production of cereals. The CO_{2e} emissions produced in the cultivation of the monitored cereals are lower in organic farming systems, both when converted to an area unit and when converted to a production unit.

Key words: cereals, emissions, greenhouse gases, LCA, organic farming

Received: May, 2017; *Revised final:* February, 2018; *Accepted:* March, 2018; *Published in final edited form:* April 2018

1. Introduction

In the course of the 20th century, the population grew from 1.6 to 6.1 billion (Lutz et al., 2013). This results in a steady rise in the consumption of natural sources and agricultural products (Foley et al., 2011). Since the population growth continues very rapidly, and the consumption of meat or other animal husbandry products as well as the consumption of energy in agriculture and food industry are on the increase, it cannot be expected that the trend of the growing environmental load would reverse spontaneously in the near future (Goodland, 1997; Schau and Fet, 2008). The global GHG emissions from agriculture amount to 5.1 – 6.1 billion tons of CO_2 equivalent (Niggli et al., 2011) [CO_{2e} in further

text]. Baumert et al. (2005) determine the shares of GHG (CO_2 , N_2O and CH_4) emissions produced in various branches of human activities. According to their findings agriculture accounted for a 13.5% share of the anthropogenic emissions in 2000. Friel et al. (2009) also claim that the share of agriculture in the global emissions is 10-12%, and an increase by half of those values can be expected to take place by 2030 (Smith et al., 2007).

According to IPCC report (IPCC, 2007) the share of agricultural production in the anthropogenic production of GHG emissions is 14%, and this share differs in various countries according to the intensity of the agricultural production. In general, carbon dioxide (CO_2) is the most important GHG generated as a result of human activity. It accounts for 82% of

* Author to whom all correspondence should be addressed: e-mail: jmoudry@zf.jcu.cz; Phone: +420723701768; Fax: +420387772456

all GHG emissions produced by the 27 EU member states, accounting for a 55% share in the total warming of all man-emitted gases (IPCC, 2014; Quashing, 2016). Agriculture is also a significant emission producer in the EU according to Brandt and Svendsen (2011). In the EU-27, the total share of GHG emissions from agriculture was 10.1% in 2011 (Pendolovska et al., 2013). Similar values can also be found in the UNFCCC report (2011), according to which this share amounted to 10.2% in 2009 in the EU-15. Therefore, ways to reduce greenhouse gas emissions are also searched for in agriculture.

In addition to animal husbandry, GHG emission savings may also be found in crop production, especially due to the large areal extent. Activities in the field of land use change, fertilizer use and production, fossil fuel burning and agricultural waste burning are the main sources of GHG emissions in the agricultural sector and they are presented as sources of CO_2 from agricultural production for example by (Nimkar et al., 2015). Another significant gas is N_2O , which is emitted in terms of production and utilization of nitrogen fertilizers and due to volatilization during various agricultural activities (Rees et al., 2013; Sutton et al., 2011). Last but not least, agricultural GHGs are associated with animal husbandry, especially beef cattle breeding and CH_4 production (Bellarby et al., 2013). The room for such measures is available in both non-food production, e.g. in the cultivation of energy crops (Bernas et al., 2016), and food production.

The most commonly grown groups of crops include cereals, which are very significant in terms of both the human nutrition and the size of the areas where they are grown (e.g. in the Czech Republic, the size of cereal fields constitutes more than half of the total arable land and, on a worldwide basis, wheat is one of the four crops that cover approximately 80% of the caloric consumption of mankind) (Šarapatka et al., 2008). This is also a reason why cereals constitute one of main groups in crop production, in respect of which it is possible to take mitigation measures. Cultivation of cereals in the conventional and organic farming system has its own specifics, which result in particular from a different approach to the protection and nutrition of plants in these systems of farming. Absence, or a very low rate of use of agrochemicals in organic farming often leads to an increase in the number of agrotechnical operations serving to protect plants; in terms of plant nutrition, in addition to the application of organic fertilizers, great emphasis is placed on proper selection of crops and securing of nitrogen from other sources (e.g. more frequent cultivation of leguminous plants).

The measures leading to a mitigation of GHG emissions may also include a change of the farming system or a partial switch to more extensive farming methods, including organic farming. Niggli et al. (2011) state that intensive crop production (often based on monocultures and high productivity) largely depends on external inputs, such as mineral fertilizers and chemical plant protection products. Sustainable

farming procedures, such as organic farming, greatly reduce such dependence on inputs. As presented by Lal (2004a), a system sustainability can be evaluated based on inputs and outputs and their conversion to CO_2e . The American research "Rodale Institute's Farming Systems Trial", which was focused on long-term comparison of the effects of organic and conventional farming, confirms that introduction of organic farming in the whole USA would reduce CO_2 emissions by as much as a fourth due to the increased carbon sequestration in soil (LaSalle and Hepperly, 2008). In order to be able to assess the efficiency of a change of the farming system, it is necessary to quantify the exact environmental load or rather the production of GHG in the given farming systems.

There are several suitable methods used for the assessment of environmental impacts of agricultural activities (Finnveden and Moberg, 2005), such as the Life Cycle Assessment (LCA), Ecological Footprint (EF) or Emergy Analysis (EA – analysis of direct and indirect energy flows) (Thomassen and De Boer, 2005; Van Der Werf and Petit, 2002). Cambria et al. (2016) or Ng et al. (2016) also present a suitable method for evaluating agricultural activities. Moreover, LCA, as one of the few tools, offers a comprehensive approach to the evaluation of environmental impacts at present (Kim and Dale, 2005; Nelson and Robertson, 2008; Requena et al., 2011; Wagner et al., 1998). LCA is also a very valuable tool due to its ability to include and compare various farming systems, their individual processes and products and most of their environmental impacts (Charles et al., 2006; Haas et al., 2000; Haas et al., 2001).

The aim of this paper is to quantify and assess the environmental aspects of growing of major cereal species in the conditions of the Czech Republic and Central Europe within the conventional and organic farming system, especially in terms of the impact of organic and conventional agriculture on greenhouse gas emissions.

2. Material and methods

The life cycle of growing oat, rye, wheat and spelt wheat in the conditions of Central Europe was modelled in the software SIMA Pro (method ReCiPe Midpoint (H) Europe) in accordance to the standards ČSN EN ISO 14040 (ISO, 2006a) and ČSN EN ISO 14044 (ISO, 2006b). As a functional unit, 1 kg of grain was used. The output was the yield per hectare, the inputs included technological operations, seed quantity, fertilizer quantity, and plant protection products. The LCA framework includes the farm phase (field emissions, seeds and seedlings, fertilizers, pesticides, and agrotechnical operations).

In addition to the emissions produced from the above stated inputs, there are also field emissions (N_2O emissions) released after the application of nitrogen fertilizers. They are quantified by the methods described in IPCC (*Intergovernmental Panel on Climate Change*) (De Klein et al., 2006).

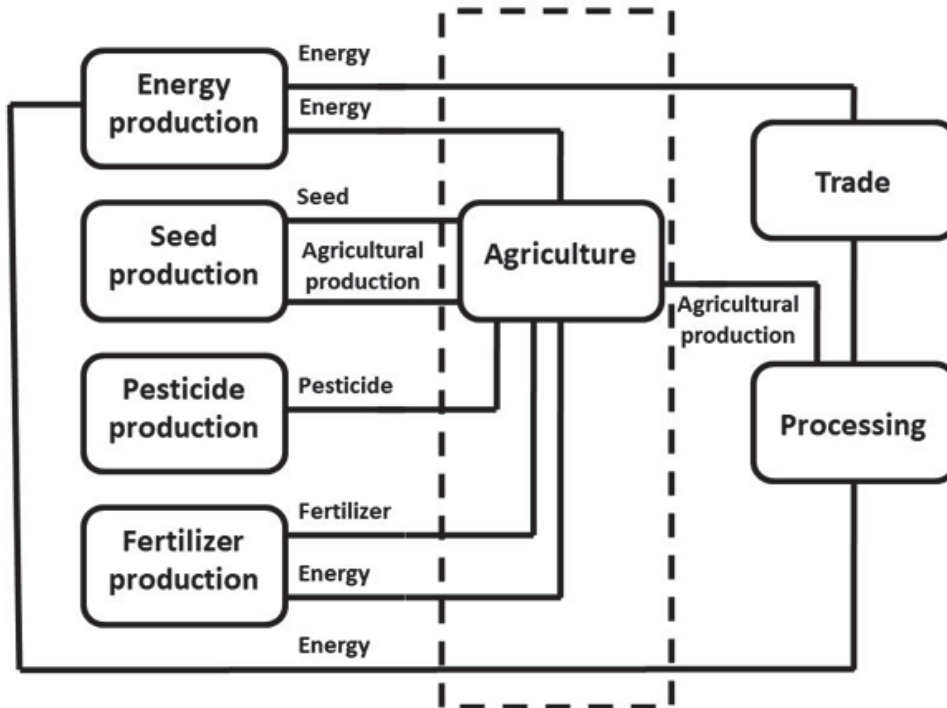


Fig. 1. Determination of the system boundaries – LCA framework

The greenhouse gases were converted to CO_{2e} based on the formula (Eq. 1):

$$CO_{2e} = 1 \times CO_2 = 23 \times CH_4 = 298 \times N_2O \quad (1)$$

The calculation of the emission load used the values obtained from the experimental cultivation of cereals in small experimental plots of the Faculty of Agriculture of the University of South Bohemia in České Budějovice (experiments were based both on an experimental plot certified in organic farming and on an experimental plot with conventional farming system) and referential operational and pilot stations, supplemented by the yield parameters from the selected set of 50 farms in the Czech Republic, the set comprising of 25 farms operating in organic farming and 25 farms operating in conventional farming system. The number of farms in the set was influenced by the total number of farms operating in organic farming system focusing on the cultivation of cereals and by the availability of the data from them. The basic data from the farms were supplemented from the Ecoinvent database (Ecoinvent, 2010).

The input data from the Ecoinvent database (2010) were adjusted to the farming conditions in the Czech Republic. The adjustments concerned mainly fuel consumption in individual agrotechnical operations. Based on the data from the selected set of farms, the most common agrotechnical procedures used in the cultivation of the monitored cereals in conventional and organic farming systems were identified. These procedures are a sequence of the most commonly used agrotechnical operations that are being carried out during cultivation, the most common

agrotechnical line being developed for each monitored cereal as well as farming system. Based on these operations, the technological chains of operations used for the calculation of greenhouse gas emissions were made up.

Wheat, rye and oat were evaluated in conventional and organic farming systems; in the Czech Republic, spelt wheat is grown almost solely in organic farming systems. The average yields in the evaluated selected set grown in a conventional farming system amounted to 5.6 t/ha for wheat, 3.7 t/ha for oat and 4.0 t/ha for rye, while the average yields of the crops grown in an organic farming system amounted to 3.5 t/ha for wheat, 2.6 t/ha for oat, 2.9 t/ha for rye and 3.3 t/ha for spelt wheat.

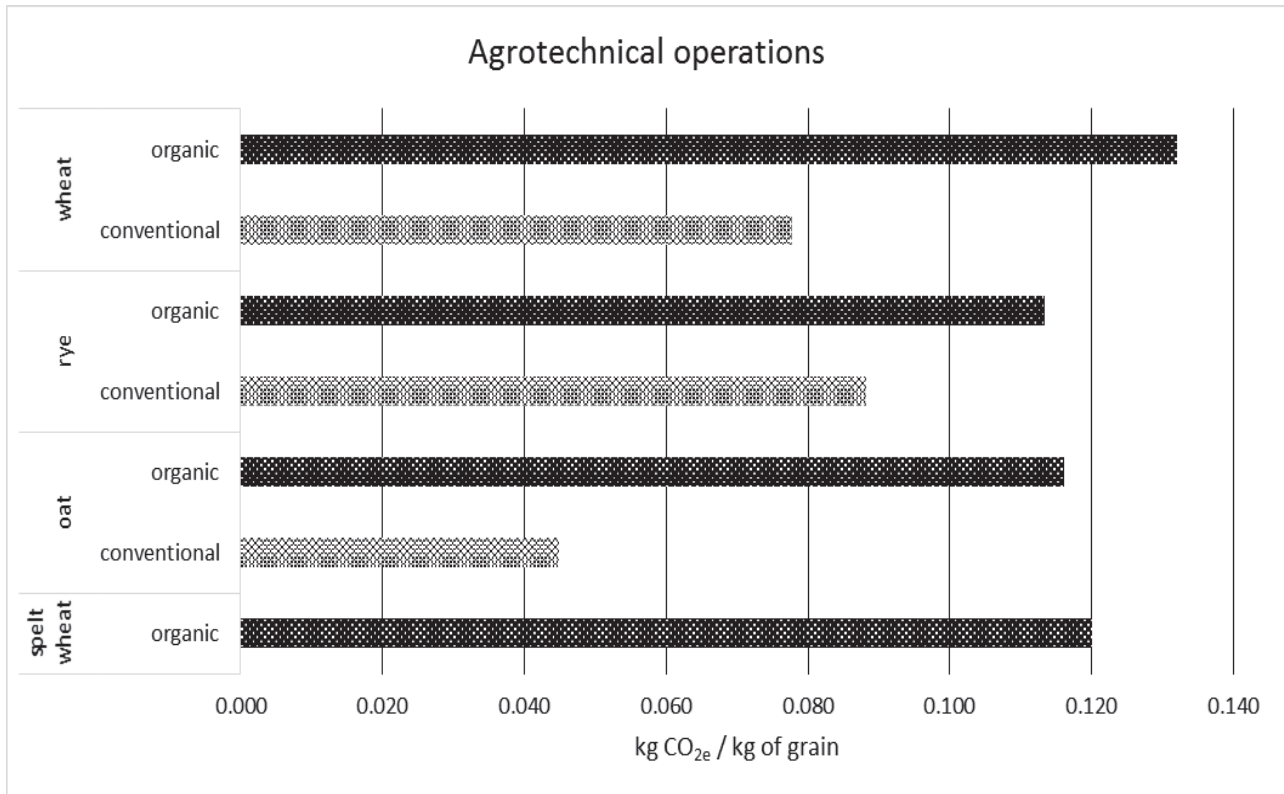
3. Results and discussion

In the Czech Republic, cereals are the most widely grown group of crops, and are grown on approximately 50 % of arable land (Capouchová et al., 2012; Konvalina et al., 2014; Moudrý and Konvalina, 2007; Stehno et al., 2010). Given the size of the area on which they are grown, they also rank among the crops significant in terms of a possible reduction of anthropogenic emissions of greenhouse gases.

In both organic and conventional farming systems, the growing of cereals have certain specifics leading to different environmental loads or rather different greenhouse gas emissions. The greenhouse gas emissions within the production of cereals vary in different regions due to differences in species, climatic conditions, soil conditions and production system (Barton et al., 2008).

Table 1. The yield parameters of the monitored cereals

Parameter	Unit	Wheat		Rye		Oat		Spelt wheat
		Conv.	Organic	Conv.	Organic	Conv.	Organic	Organic
average	t/ha	5.6	3.5	4.0	2.9	3.7	2.6	3.3
SD	t/ha	1.1	0.6	1.0	0.9	0.6	0.7	0.6
CV	%	19.9	18.6	24.6	32.3	17.0	27.1	17.0
Median	t/ha	5.8	3.5	4.1	2.7	3.7	2.6	3.4
Mode	t/ha	6.6	3.6	5.3	2.4	4.2	2.6	3.7

**Fig. 2.** GHG emissions from the basic category “agrotechnical operations”

The yield of individual crops is essential for the conversion of the emission load per unit of production. Table 1 summarizes the yield parameters of the monitored cereals in the conventional and organic farming system; the values were calculated from the yield data over the five-year period, and the average yield was used to calculate the emission load. Out of the 25 monitored conventional farms, 25 of them cultivated wheat, 19 rye, and 14 oat; out of 25 monitored organic farms, 25 of them cultivated wheat, 17 rye, 16 oat and 12 spelt wheat.

The results show that there are considerable differences between conventional and organic farming systems in individual subcategories of the farm phase of the cereals production. The production of emissions in a farming cycle is divided into the basic groups: agrotechnical operations, fertilizers, pesticides, seeds, and field emissions, and the load in those basic groups differs depending on the cultivated crop and the selected farming system.

In organic farming, a higher emission load is produced within the scope of agrotechnical operations,

which is due to a higher need of mechanical operations during vegetation and a lower production effectiveness, in particular. Within the framework of the group of agrotechnical operations, the evaluated operations included stubble plowing, plowing, application of synthetic fertilizers (several times during the agricultural cycle), application of farm fertilizers, preseed preparation and sowing, application of growth regulators, harrowing, treatment against weeds, diseases and pests, treatment against lodging, and harvesting. The conversion to the production unit, i.e. quantification of the emission load e.g. per kg of grain, in combination with the lower yields of organic farming cause that in this basic group the GHG emissions are lower for conventionally grown cereals than for those grown in organic farming systems (Fig. 2). Where the conversion involves GHG emissions produced per area unit (ha), the differences between the farming systems are considerably lower for individual cereals; as for rye, the load from the basic category “agrotechnical operations” is higher for a conventional farming system (Fig. 6).

In organic farming, the emission load from agrotechnical operations amounts to 0.132 kg CO_{2e} / kg of grain for wheat, 0.113 kg CO_{2e} / kg of grain for rye, 0.116 kg CO_{2e} / kg of grain for oat and 0.120 kg CO_{2e} / kg of grain for spelt wheat, while in conventional farming, the emission load amounts to 0.078 kg CO_{2e} / kg of grain for wheat, 0.088 kg CO_{2e} / kg of grain for rye and 0.045 kg CO_{2e} / kg of grain for oat.

A number of authors, such as Berner et al. (2008), Dorninger and Freyer (2008), Chen et al. (2013), Lal (2004b), and Teasdale et al. (2007), state changes of agrotechnical procedures as one of the ways how to reduce GHG emissions. The proposed measures are minimization, omission of plowing, limitation of the number of crossings by merging operations, but also deep application of fertilizers, incorporation of plant residues or changes in irrigation for some crops.

Another important basic group is field emissions. This fact is also confirmed by Mori et al. (2005), Tokuda and Hayatsu (2004) and Zou et al. (2005) who claim that a growing use of chemical fertilizers and manure is usually accompanied by a growing share of N_2O released from the soil. Determination of field emissions is difficult because field emissions are very varied, depending on a large number of variables, such as soil properties, climatic conditions, land management methods, etc. (Brentrup et al., 2000; Brentrup, 2003). Differences between individual farming systems are apparent even in this

group, and the differences after the conversion to a production unit are due to the different yields in individual farming systems as well as due to the different fertilization and subsequent soil processes. Fig. 3 clearly shows that in this basic group, GHG emissions are higher for wheat grown in an organic farming system (0.187 kg CO_{2e} / kg of grain) than for wheat grown in a conventional system (0.137 kg CO_{2e} / kg of grain). Contrarily, the field emissions from the growing of oat and rye in an organic farming system (0.123 kg CO_{2e} / kg of grain for oat, 0.116 kg CO_{2e} / kg of grain for rye) are lower than when grown in a conventional system (0.127 kg CO_{2e} / kg of grain for oat, 0.175 kg CO_{2e} / kg of grain for rye). As for spelt wheat grown in an organic farming system, this value amounts to 0.170 kg CO_{2e} /kg of grain.

Fertilization is regarded as the most significant basic group, which also accounts for the greatest difference in GHG emissions between conventional and organic farming systems, which is consistent also with the finding by Cambria et al. (2016). According to Fott et al. (2003), agricultural emissions are mostly released from the applied fertilizers and pesticides, which is also in line with the findings of Biswas et al. (2008). In organic farming, the main cause of the reduction of emissions in the basic group “fertilizers” is the elimination of synthetic fertilizers. The production and transport of such fertilizers consume a large amount of energy, thus creating a considerable environmental load (Cormack and Metcalfe, 2000; Williams et al., 2006).

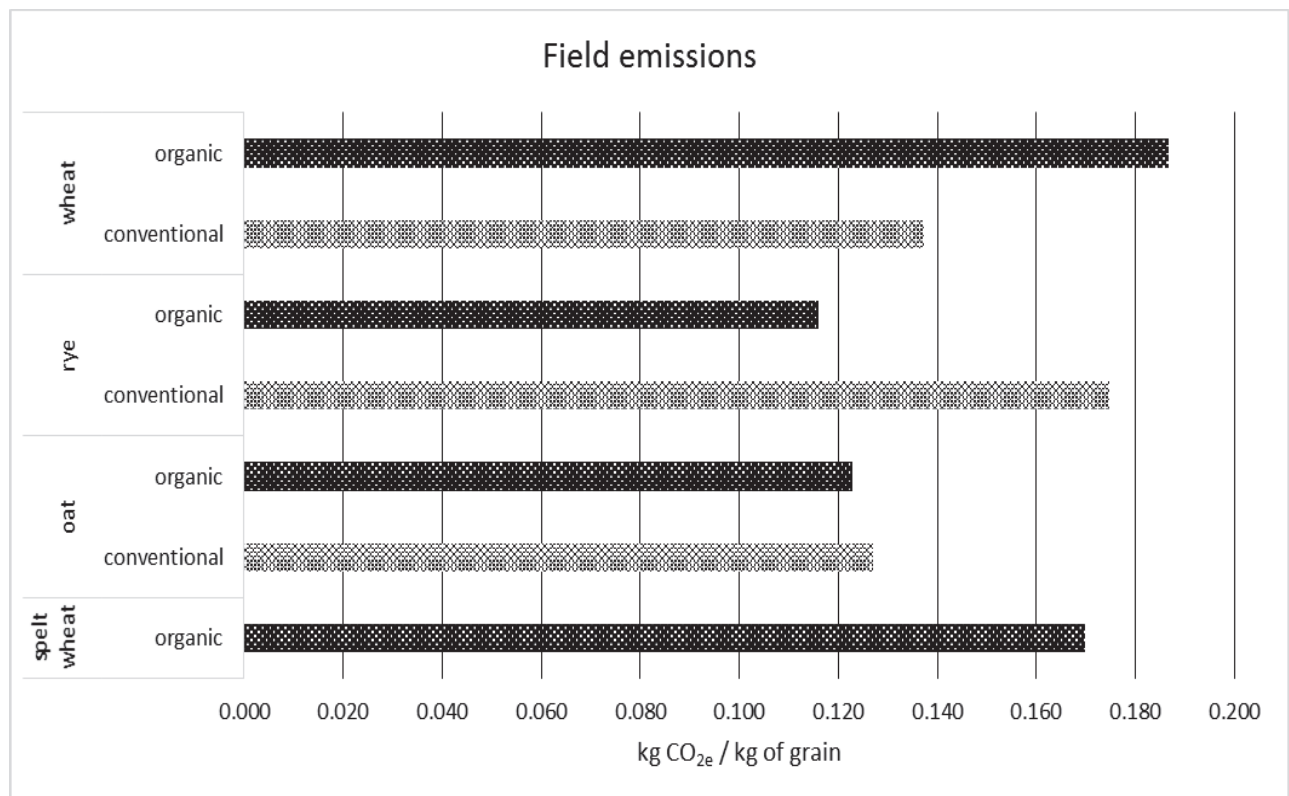


Fig. 3. GHG emissions from the basic category “field emissions”

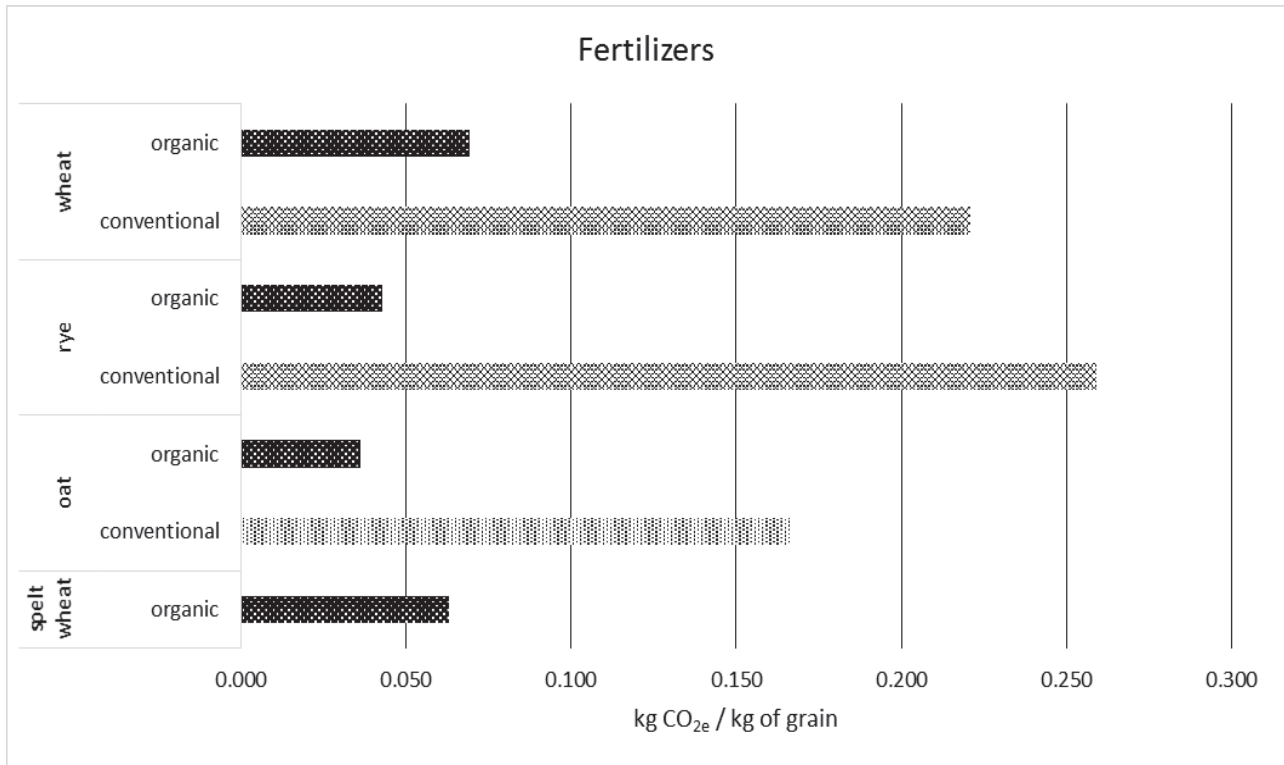


Fig. 4. GHG emissions in the basic category “fertilizers”

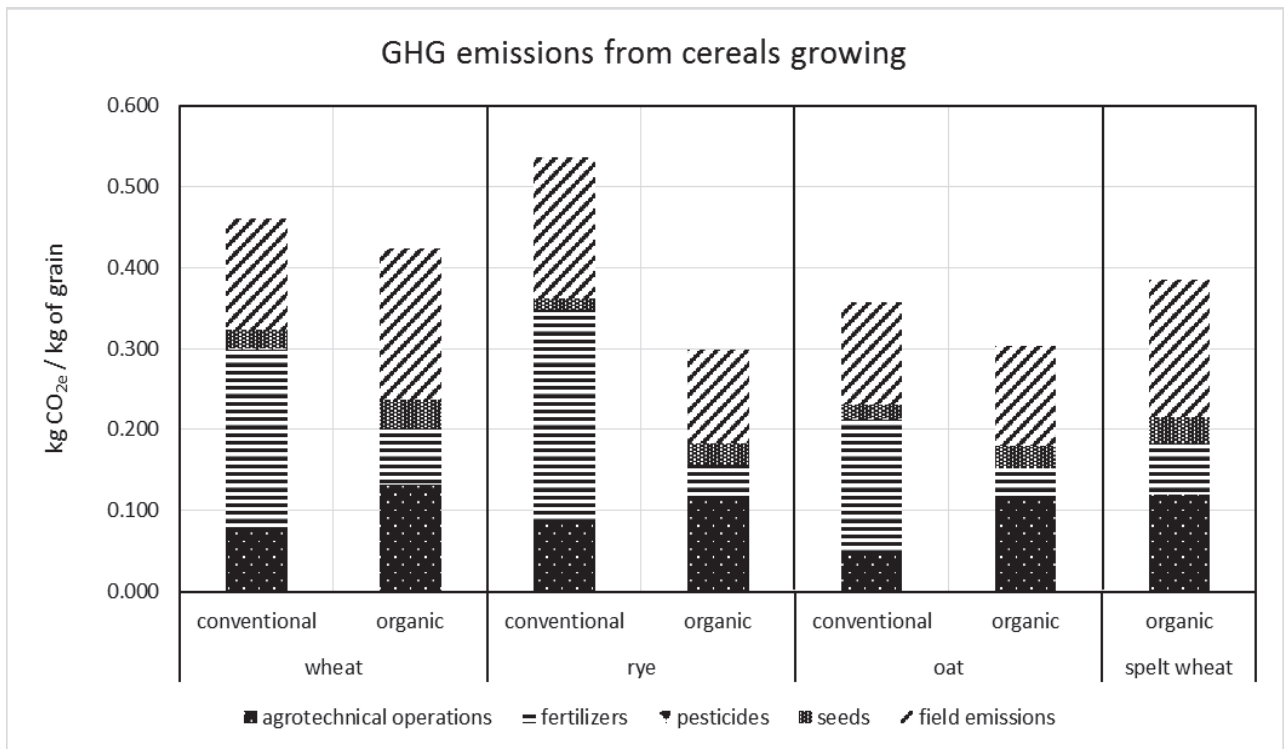


Fig. 5. GHG emissions from cereals growing – conversion to a production unit

Kindred et al. (2008) report that 11 kg CO_{2e} per kilogram of N are produced during the production, packing and transport of synthetic nitrogen fertilizers. In 2007, the total GHG emissions from the production and application of nitrogen fertilizers from fossil fuels amounted to 750-1080 million tons of CO₂ equivalent (1-2 % of the total global GHG emissions), while 47

years earlier, in 1960, it was less than 100 million tons of CO_{2e} (Niggli et al., 2011). Changes in fertilization, i.e. a certain degree of extensification and a correct use of organic fertilizers, may result in reduction of CO_{2e} emissions, which is in line with the statements of Johnson et al. (2007) and Smith et al. (2008). The need for more precise nitrogen management in organic

farming systems is also indicated by Kramer et al. (2006).

A considerably lower emission load generated by organic farming in the basic group “fertilizers” is evident for all the monitored cereals (Fig. 4). The highest load is produced in conventional farming as a result of application of synthetic nitrogen fertilizers. These values are 0.221 kg CO_{2e} / kg of grain for wheat, 0.259 kg CO_{2e} / kg of grain for rye, and 0.167 kg CO_{2e} / kg of grain for oat. In organic farming systems, these values are considerably lower – the emissions from fertilizers amount to 0.069 kg CO_{2e} / kg of grain for wheat, 0.043 kg CO_{2e} / kg for rye, 0.036 kg CO_{2e} / kg of grain for oat, and 0.063 kg CO_{2e} / kg of grain for spelt.

In terms of greenhouse gas emissions, the emissions from the basic group “seeds” appear to be less significant, and the emissions from the basic group “pesticides” seem to be almost negligible. As for seeds, the GHG emissions are always higher in organic farming systems due to lower yields (0.035 kg CO_{2e} / kg of grain for wheat, 0.026 kg CO_{2e} / kg of grain for rye, 0.027 kg CO_{2e} / kg of grain for oat, 0.032 kg CO_{2e} / kg of grain for spelt wheat) as compared to conventional farming systems (0.023 kg CO_{2e} / kg of grain for wheat, 0.014 kg CO_{2e} / kg of grain for rye, 0.018 kg CO_{2e} / kg of grain for oat), and the values are even considerably lower for pesticides. Pesticides are not applied in organic farming systems; in conventional systems, the emission load from pesticides is around 0.001 kg CO_{2e} / kg of grain for wheat and rye, and 0.002 kg CO_{2e} / kg of grain for oat.

The environmental impact of the use of pesticides consists especially in their toxicity (De Backer et al., 2009).

As evident from Fig. 5, there are also significant differences between individual cereal species; when comparing particular species in various farming systems, the total emission load is always higher in conventional farming, even when converted to a production unit. These values amount to 0.460 kg CO_{2e} / kg of grain for wheat, 0.537 kg CO_{2e} / kg of grain for rye and 0.358 kg CO_{2e} / kg of grain for oat. In organic farming, these values amount to 0.423 kg CO_{2e} / kg of grain for wheat, 0.298 kg CO_{2e} / kg of grain for rye, 0.303 kg CO_{2e} / kg of grain for oat and 0.385 kg CO_{2e} / kg of grain for spelt wheat.

A disadvantage of organic farming is a lower production per area unit, which increases the emission load per production unit. For example, in Europe, the average yields of wheat in organic farming amount to 80 % of the conventional production (Lackner, 2008). Differences in yields in conventional and organic farming are also expressed by Mondelaers et al. (2009) who state that the average yields of organic farms are 17 % lower than those of conventional farms. On the other hand, Pimentel et al. (2005) claim that organic farming systems may achieve yields comparable with those of conventional systems for some high-production plants, such as maize. Increasing the yields in organic farming while maintaining its environmental friendliness may further increase its efficiency as a tool for reducing greenhouse gas emissions in agriculture.

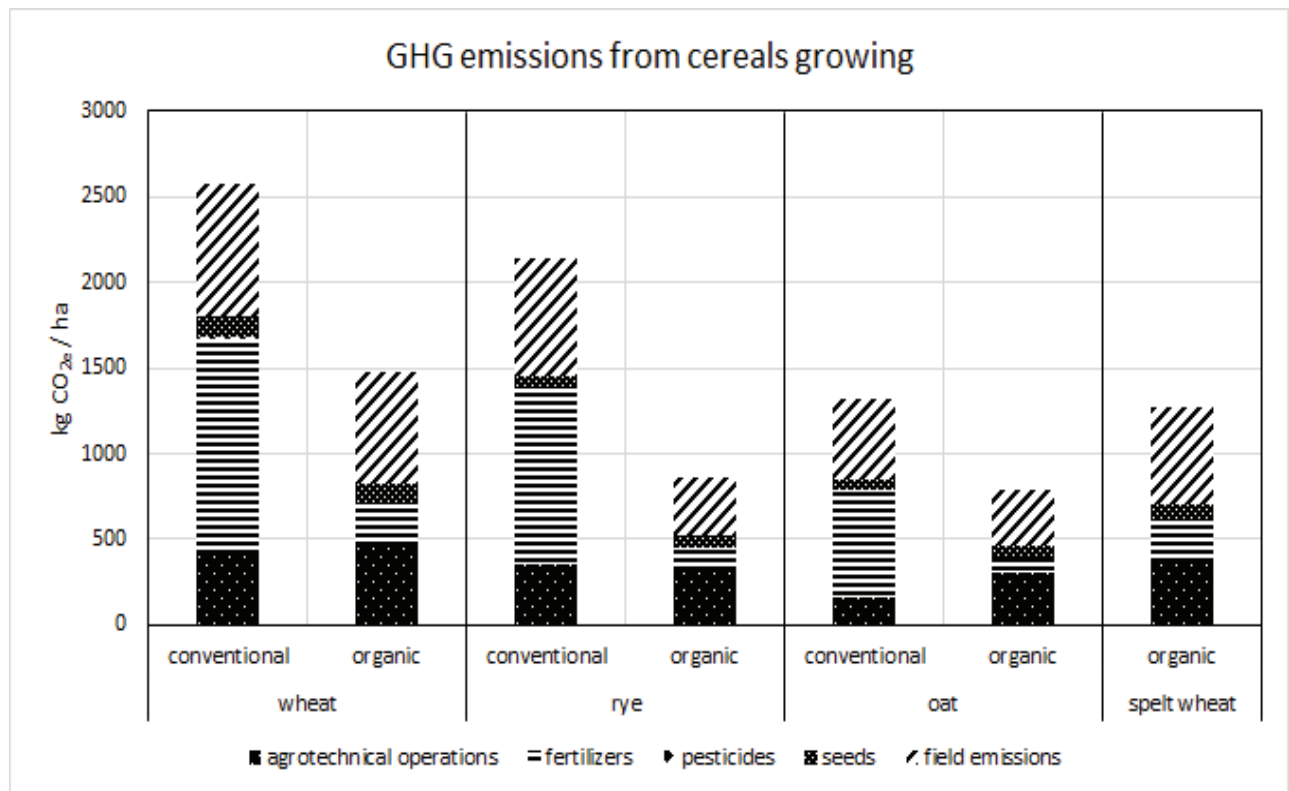


Fig. 6. GHG emissions from cereals growing – conversion to an area unit

Nemecek et al. (2005) argue that the environmental savings per area unit in organic farming are approximately double the savings calculated per production unit, which is due to the differences in yields. Knudsen (2010) also state that due to the lower yields in organic farming, the calculations of the production of greenhouse gas emissions per production unit show an increased environmental load in relation to conventional farming, so the resulting difference is lower than when converted to a unit of area.

This is in line with the findings of Mondelaers et al. (2009) who claim that due to the lower yields of organic farming, particularly in less developed countries, the environmental effect consisting in a reduction of greenhouse gas emissions is lower when converted to a production unit instead of an area unit, and in extreme cases it may even be negative. However, in both types of calculation the production of greenhouse gases remains lower in organic farming for many crops (Moudrý et al., 2013).

Considerable differences in GHG emissions after the conversion to an area unit are also well visible from Fig. 6. Given the average yields 5.6 t/ha for wheat, 3.7 t/ha for oat and 4.0 t/ha for rye, a conventional farming system produces 2577 kg CO_{2e} / ha for wheat, 2147 kg CO_{2e} / ha for rye and 1325 kg CO_{2e} / ha for oat. Similar figures (2330 kg CO_{2e} / ha for wheat, 2270 kg CO_{2e} / ha for rye and 1800 kg CO_{2e} / ha for oat) are also given by Rajaniemi et al. (2011). Given the average yields 3.5 t/ha for wheat, 2.6 t/ha for oat, 2.9 t/ha for rye and 3.3 t/ha for spelt wheat, an organic farming system produces 1482 kg CO_{2e} / ha for wheat, 865 kg CO_{2e} / ha for rye, 787 kg CO_{2e} / ha for oat and 1271 kg CO_{2e} / ha for spelt wheat.

So the evaluation of the emission load from the growing of cereals in conventional and organic farming systems in the conditions of Central Europe confirms the findings of Dorninger and Freyer (2008) who state that GHG emissions may be reduced by a correct choice of the farming system.

4. Conclusions

In crop production, a certain scope for reducing greenhouse gas emissions is also available in the growing of cereals, which are the most widely grown group of crops in many countries. The results show that the total emission load produced in organic farming systems is lower both when converted to an area unit and when converted to a production unit. Some savings may be achieved particularly by changes in the use of nitrogen fertilizers and partially by changes in agrotechnical measures.

In terms of agrotechnical operations, GHG emissions can be reduced in both conventional and organic farming, e.g. by omitting plowing and replacing it with shallow soil cultivation, another possibility is the use of tractors with lower performance and consumption, for example, during harrowing, or generally when working with lighter

tools. Savings can also be achieved by lowering the number of crossings by performance of multiple agrotechnical operations at the same time.

Yields are a key factor in organic farming. Their increase can be achieved by intensification of organic farming, with higher yields being supported, for example, by precise selection of varieties in view of their suitability for specific habitat conditions, nutrient requirements and resistance to weeds, diseases and pests, and also by observing suitable sowing dates, optimal sowing and plant placement or more precise plant nutrition.

In conventional farming, as a further measure, it is recommended to restrict plant production without any link to animal husbandry, to extend sowing practices, in particular by incorporating leguminous plants, including perennial plants (alfalfa, clover), or by cultivating varieties for better use of nutrients. Reducing the need for synthetic fertilizers, especially nitrogen fertilizers, leads to a significant reduction of the emission load. Based on the results, it can be stated that a change in the farming system may help reduce the emission load in agriculture.

Acknowledgements

This work was supported by the University of South Bohemia in České Budějovice research project GAJU 094/2016/Z.

References

- Barton L., Kiese R., Gatter D., Butterbach-Bahl K., Buck R., Hinz C., Murphy D., (2008), Nitrous oxide emissions from a cropped soil in a semi-arid climate, *Global Change Biology*, **14**, 177-192.
- Baumert K.A., Herzog T., Pershing J., (2005), *Navigating the Numbers Greenhouse Gas Data and International Climate Policy*, World Resources Institute, USA.
- Bellarby J., Tirado R., Leip A., Weiss F., Lesschen J.P., Smith P., (2013), Livestock greenhouse gas emissions and mitigation potential in Europe, *Global change biology*, **19**, 3-18.
- Bernas J., Moudrý jr. J., Jelínková Z., Kopecký M., Konvalina P., Moudrý J., (2016), Energy crops growing - impact on greenhouse gases emissions, *Journal of Environmental Protection and Ecology*, **17**, 950-960.
- Berner R.A., Hildermann I., Fließbach A., Pfiffner L., Niggli U., Mäder P., (2008), Crop yield and soil fertility response to reduced tillage under organic management, *Soil & Tillage Research*, **101**, 89-96.
- Biswas W.K., Barton L., Carter D., (2008), Global warming potential of wheat production in south western Australia: A life cycle assessment, *Water and Environment Journal*, **22**, 206-216.
- Brandt U.S., Svendsen G.T., (2011), A project-based system for including farmers in the EU ETS, *Journal of Environmental Management*, **92**, 1121-1127.
- Brentrup F., (2003), *Life cycle assessment to evaluate the environmental impact of arable crop production*, PhD Thesis, University of Hannover, Hannover, Germany.
- Brentrup F., Küsters J., Lammel J., Kuhlmann H., (2000), Methods to estimate on-field emissions from crop productions as an input to LCA studies in the agricultural sector, *International Journal of Life Cycle Assessment*, **5**, 349-357.

- Cambria D., Vázquez-Rowe I., González-García S., Moreira M.T., Feijoo G., Pierangeli D., (2016), Comparative life cycle assessment study of three winter wheat production systems in the European Union, *Environmental Engineering and Management Journal*, **15**, 1755-1766.
- Capouchová I., Konvalina P., Honsová H., Stehno Z., Chaloupský R., (2012), Influence of seed's biological traits of oat on next seed generation in organic farming, *Journal of Food, Agriculture & Environment*, **10**, 551-555.
- Charles R., Jolliet O., Gaillard G., Pellet D., (2006), Environmental analysis of intensity level in wheat crop production using life cycle assessment, *Agriculture, Ecosystems & Environment*, **113**, 216-225.
- Chen H., Zhu Q., Peng C., Wu N., Wang Y., Fang X., Jiang H., Xiang W., Chang J., Deng X., Yu G., (2013), Methane emissions from rice paddies natural wetlands, and lakes in China: Synthesis and new estimate, *Global Change Biology*, **19**, 19-32.
- Cormack W., Metcalfe P., (2000), *Energy Use in Organic Farming Systems*, Cranfield University, Cranfield, UK.
- De Backer E., Aertsens J., Vergucht S., Steurbaut W., (2009), Assessing the ecological soundness of organic and conventional agriculture by means of life cycle assessment (LCA): A case study of leek production, *British Food Journal*, **111**, 1028-1061.
- De Klein C., Novoa R.S.A., Ogle-Smith K.A., Rochette-Wirth T.C., McConkey B.G., Mosier A., Rypdal K., (2006), *N₂O Emissions from Managed Soils, and CO₂ Emissions Managed from Lime and Urea Applications*, In: *2006 IPCC Guidelines for National Greenhouse Gas Inventories: Volume 4 - Agriculture, Forestry and other Land Use*, Eggleston S., Buendia L., Miwa K., Ngara T., Tanabe K. (Eds.), IGES, Kanagawa, Japan, 11.1-11.54.
- Dorning M., Freyer B., (2008), *Current achievements and future potential of organic agriculture for climate protection in Austria* (in German), BOKU, IFOL, Wien, Austria.
- ECOINVENT, (2010), The Ecoinvent Database, Ecoinvent Centre, Zurich, Switzerland, Online at: www.ecoinvent.ch
- Finnveden G., Moberg Å., (2005), Environmental systems analysis tools: an overview, *Journal of Cleaner Production*, **13**, 1165-1173.
- Foley J.A., Ramankutty N., Brauman K.A., Cassidy E.S., Gerber J.S., Johnston M., Mueller N.D., O'Connell C., Ray D.K., West P.C., Balzer C., Bennett E.M., (2011), Solutions for a cultivated planet, *Nature*, **478**, 337-342.
- Fott P., Pretel J., Neuzil V., Blaha J., (2003), *National report of the Czech Republic on the inventory of greenhouse gases* (in Czech), ČHMÚ, Praha, Czech Republic.
- Goodland R., (1997), Environmental sustainability in agriculture: diet matters, *Ecological Economics*, **23**, 189-200.
- Haas G., Wetterich F., Geier U., (2000), Life cycle assessment framework in agriculture on the farm level, *International Journal of Life Cycle Assessment*, **5**, 345-348.
- Haas G., Wetterich F., Köpke U., (2001), Comparing intensive, extensified and organic grassland farming in southern Germany by process life cycle assessment, *Agriculture, Ecosystems & Environment*, **83**, 43-53.
- IPCC, (2014), *Climate Change 2014: Mitigation of Climate Change, Working Group III Contribution to the Fifth Assessment Report of the Intergovernmental Panel on Climate Change*, Edenhofer O., Pichs-Madruga R., Sokona Y., Farahani E., Kadner S., Seyboth K., Adler A., Baum I., Brunner S., Eickemeier P., Kriemann B., Savolainen J., Schlömer S., von Stechow C., Zwickel T., Minx J.C., (Eds.), Cambridge University Press, Cambridge, United Kingdom and New York, NY, USA., On line at: https://www.ipcc.ch/pdf/assessment-report/ar5/wg3/ipcc_wg3_ar5_frontmatter.pdf.
- IPCC, (2007), *Climate Change 2007: Synthesis Report. Contribution of Working Groups I, II and III to the Fourth Assessment Report of the Intergovernmental Panel on Climate Change*, Core Writing Team, Pachauri R.K., Reisinger A. (Eds.), Intergovernmental Panel on Climate Change, Geneva, Switzerland, On line at: https://www.ipcc.ch/pdf/assessment-report/ar4/syr/ar4_syr_full_report.pdf.
- ISO, (2006a), Environmental management – Life cycle assessment – Principles and framework, ISO 14040, International Organization for Standardization, Geneva, Switzerland.
- ISO, (2006b), Environmental management – Life cycle assessment – Requirements and guidelines, ISO 14044, International Organization for Standardization, Geneva, Switzerland.
- Johnson J., Franzluebbers A.J., Weyers S.L., Reicosky D.C., (2007), Agricultural opportunities to mitigate greenhouse gas emissions, *Environmental Pollution*, **150**, 107-124.
- Kim S., Dale B.E., (2005), Life cycle assessment of various cropping systems utilized for producing biofuels: bioethanol and biodiesel, *Biomass & Bioenergy*, **29**, 426-439.
- Kindred D., Berry P., Burch O., Sylvester-Bradley R., (2008), Effects of nitrogen fertiliser use on greenhouse gas emissions and land use change, *Aspects of Applied Biology*, **88**, 1-4.
- Knudsen M.T., (2010), *Environmental assessment of imported organic products - focusing on orange juice from Brazil and soyabeans from China*, PhD Thesis, Aarhus University, Aarhus, Denmark.
- Konvalina P., Stehno Z., Capouchová I., Zechner E., Berger S., Grausgruber H., Janovská D., Moudrý J., (2014), Differences in grain/straw ratio, protein content and yield in landraces and modern varieties of different wheat species under organic farming, *Euphytica*, **199**, 31-40.
- Kramer S.B., Reganold J.P., Glover J.D., Bohannon B.J.M., Mooney H.A., (2006), *Reduced Nitrate Leaching and Enhanced Denitrifier Activity and Efficiency in Organically Fertilized Soils*, Proc. of the National Academy of Sciences of the USA, **103**, 4522-4527.
- Lackner M., (2008), *Social-ecological dimensions of nutrition in Austria: A scenario analysis* (in German), Institute of Social Ecology, Klagenfurt University, Vienna, Austria.
- Lal R., (2004a), Carbon emission from farm operations, *Environment International*, **30**, 981-990.
- Lal R., (2004b), Soil carbon sequestration impacts on global climate change and food security, *Science*, **304**, 1623-1627.
- LaSalle T., Hepperly P., (2008), *Regenerative Organic Farming: A Solution to Global Warming*, Rodale Institute, Kutztown, Pennsylvania, USA.
- Lutz C., Sanderson W.C., Scherbov S., (2013), *The End of World Population Growth in 21st Century*, Routledge, New York, USA.
- Mori A., Hojito M., Kondo H., Matsunami H., Scholefield D., (2005), Effects of plant species on CH₄ and N₂O fluxes from a volcanic grassland soil in Nasu, Japan, *Soil Science & Plant Nutrition*, **51**, 19-27.

- Mondelaers K., Aertsens J., Van Huylenbroeck G., (2009), A meta-analysis of the differences in environmental impacts between organic and conventional farming, *British Food Journal*, **111**, 1098-1119.
- Moudrý jr. J., Jelinková Z., Jarešová M., Plch R., Moudrý J., Konvalina P., (2013), Assessing greenhouse gas emissions from potato production and processing in the Czech Republic, *Outlook on Agriculture*, **42**, 179-183.
- Moudrý jr. J., Konvalina P., (2007), *Systems of Farming and Rural Landscape in Czech Republic*, International Scientific Conference Research for Rural Development 2007, Jelgava, Latvia, 7-13.
- Nelson G.C., Robertson R.D., (2008), Green gold or green wash: environmental consequences of biofuels in the developing world, *Review of Agricultural Economics*, **30**, 517-529.
- Nemecek T., Huguenin-Elie O., Dubois D., Gaillard G., (2005), *Life cycle assessment of cultivation systems in Swiss arable and forage cultivation* (in German), Agroscope FAL Reckenholz, Zürich, Switzerland.
- Ng T., Ya Hong Dong S., Kumaraswamy M.M., (2016), Critical analysis of the life cycle impact assessment methods, *Environmental Engineering and Management Journal*, **15**, 879-890.
- Niggli U., Fliessbach A., Hepperly P., Scialabba N., (2011), *Low greenhouse gases emissions agriculture* (in Czech), Bioinstitut, Olomouc, Czech Republic.
- Nimkar I., Singh A., Unnikrishnan S., Naik N.S., (2015), Potential of GHG emission reduction from agriculture sector, *International Journal of Global Warming*, **8**, 31-45.
- Pendolovska V., Fernandez R., Mandl N., Gugele B., Ritter M., (2013), *Annual European Union Greenhouse Gas Inventory 1990-2011 and Inventory Report 2013*, European Environment Agency, Copenhagen, Denmark.
- Pimentel D., Hepperly P., Hanson J., Doubs D., Seidel R., (2005), Environmental, energetic, and economic comparisons of organic and conventional farming systems, *BioScience*, **55**, 573-582.
- Rajaniemi M., Mikkola H., Ahokas J., (2011): Greenhouse gas emissions from oats, barley, wheat and rye production, *Agronomy Research - Biosystem Engineering (Special Issue)*, **1**, 189-195.
- Quashing V., (2016), *Understanding Renewable Energy Systems*, Routledge, London, UK.
- Rees R.M., Agustín J., Alberti G., Ball B.C., Boeckx P., Cantarel A., Gordon H., (2013), Nitrous oxide emissions from European agriculture-an analysis of variability and drivers of emissions from field experiments, *Biogeosciences*, **10**, 2671-2682.
- Requena J.F.S., Guimaraes A.C., Alpera S.Q., Gangas E.R., Hernandez-Navarro S., Gracia L.M.N., Martin-Gil J., Guesta H.F., (2011), Life Cycle Assessment (LCA) of the biofuel production process from sunflower oil, rapeseed oil and soybean oil, *Fuel Processing Technology*, **92**, 190-199.
- Šarapatka B., Niggli U., Čížková S., Dyrtrtová K., Fišer B., Hluchý M., Just T., Kučera P., Kuras T., Lyth P., Potočiarová E., Salaš P., Salašová A., Chlatter Ch., Van Elsen T., Weibel F.P., Wilfling A., Wyss E., Zámečník V., (2008), *Agriculture and Landscape – pathways to mutual compliance* (in Czech), Univerzita Palackého v Olomouci, Olomouc, Czech Republic.
- Schau E.M., Fet A.M., (2008), LCA studies of food products as background for environmental product declarations - literature review, *International Journal of Life Cycle Assessment*, **13**, 255-264.
- Smith P., Martino D., Cai Z., Gwary D., Janzen H., Kumar P., (2008), Greenhouse gas mitigation in agriculture, *Biological Sciences*, **363**, 789-813.
- Smith P., Martino D., Cai Z., Gwary D., Janzen H., Kumar P., McCarl B., Ogle S., O'Mara F., Rice Ch., Scholes B., Sirotenko O., (2007), *Agriculture*, In: *Climate Change 2007: Mitigation, Contribution of Working Group III to the Fourth Assessment Report of the Intergovernmental Panel on Climate Change*, Metz B., Davidson O.R., Bosch P.R., Dave R., Meyer L.A. (Eds.), Cambridge University Press, Cambridge, UK, 497-540.
- Stehno Z., Bradová J., Dotlačil L., Konvalina P., (2010), Landraces and obsolete cultivars of minor wheat species in the Czech collection of wheat genetic resources, *Czech Journal of Genetics and Plant Breeding*, **46**, 100-105.
- Sutton M.A., Howard C.M., Erisman J.W., Billen G., Bleeker A., Grennfelt P., Grizzetti B., (Eds.), (2011), *The European Nitrogen Assessment: Sources, Effects and Policy Perspectives*, Cambridge University Press, 664.
- Teasdale J.R., Coffmann C.B., Magnum R.W., (2007), Potential long-term benefits of no-tillage and organic cropping systems for grain production and soil improvement, *Agronomy Journal*, **99**, 1297-1305.
- Thomassen M.A., De Boer I.J.M., (2005), Evaluation of indicators to assess the environmental impact of dairy production systems, *Agriculture, Ecosystems and Environment*, **111**, 185-199.
- Tokuda S., Hayatsu M., (2004), Nitrous oxide flux from a tea field amended with a large amount of nitrogen fertilizer and soil environmental factors controlling the flux, *Soil Science & Plant Nutrition*, **50**, 365-374.
- UNFCCC, (2011), National Inventory Submission 2011, United Nations Framework Convention on Climate Change, Bonn, Germany, On line at: http://unfccc.int/national_reports/annex_i_ghg_inventories/national_inventories_submissions/items/5888.ph
- Van der Werf H.M.G., Petit J., (2002), Evaluation of the environmental impact of agriculture at the farm level: A comparison and analysis of 12 indicator-based methods, *Agriculture Ecosystems & Environment*, **93**, 131-145.
- Wagner U., Geiger B., Dreier T., (1998), *Environmental Impacts and System Analysis of Biofuels*, International Conference Biomass for Energy and Industry, Würzburg, Germany, 544-548.
- Williams A.G., Audsley E., Sandars D.L., (2006), *Determining the Environmental Burdens and Resource Use in the Production of Agricultural and Horticultural Commodities*, Cranfield University, Cranfield, UK.
- Zou J., Huang Y., Lu Y., Zheng X., Wang Y., (2005), Direct emission factor for N₂O from rice-winter wheat rotation systems in Southeast China, *Atmospheric Environment*, **39**, 4755-4765.



“Gheorghe Asachi” Technical University of Iasi, Romania



APPLICATION OF *Sphagnum moss* PEAT IN ECOLOGICAL REMEDIATION OF OXYANIONS CONTAMINATED AQUEOUS SOLUTIONS

Gabriela Ungureanu¹, Catalin D. Balan², Irina Volf^{2*}

¹University of Porto, Faculty of Engineering, Laboratory of Separation and Reaction Engineering - Laboratory of Catalysis and Materials (LSRE-LCM), Department of Chemical Engineering, Rua Dr. Roberto Frias, 4200-465 Porto, Portugal

²“Gheorghe Asachi” Technical University of Iasi, Faculty of Chemical Engineering and Environmental Protection, Department of Environmental Engineering and Management, 73 Prof. Dr. docent Dimitrie Mangeron Street, 700050 Iasi, Romania

Abstract

The potential of *Sphagnum* moss peat to adsorb oxyanions (As(III), As(V), Sb(III), Sb(V) and Se(VI)) from aqueous solution was studied in batch mode. For arsenic (both species) and selenium, the results were negative: moss peat is not able to retain these oxyanion. For antimony, the hydroxyl and carboxyl groups from the *Sphagnum* moss peat surface seems to be responsible for Sb uptake. Kinetic studies were conducted for both Sb(III) and Sb(V) and a fast uptake process was observed, equilibrium being achieved in about 2 hours. Equilibrium studies reveals considerable adsorbed amounts of Sb(III) and Sb(V). The experimental sorption capacity resulted for Sb(III) was around 3 mg/g and nearly 3.3 mg/g for Sb(V), at pH 2 and 23 ± 1°C. The influence of pH (in the 2-8 range) is modest in case of Sb(III) and insignificant for Sb(V) sorption. Following the results, it is possible to conclude that *Sphagnum* moss peat could be used in ecological remediation of antimony contaminated aqueous solutions.

Key words: oxyanions, remediation, sorption, *Sphagnum* moss peat

Received: May, 2017; *Revised final:* February, 2018; *Accepted:* March, 2018; *Published in final edited form:* April 2018

1. Introduction

The toxic metals and metalloids, frequently found in wastewaters, represent an important class of environmental contaminants. Arsenic, antimony and selenium occur naturally, arsenic being the most abundant of them, but environmental contamination may occur also due to anthropogenic sources including coal combustion, mining, agriculture, industry (Ungureanu et al., 2015b). Arsenic and antimony have chemical and toxicological similarities, and they usually co-occur as pollutants (Fu et al., 2010). Toxicity of As(III) is referred to be nearly 70 times higher than organic forms of As and 10 times higher than As(V) (Ben Issa et al., 2011; Jain and Ali, 2000; Larios et al., 2012). Antimony trioxide

(Sb₂O₃) and antimony trisulfide (Sb₂S₃) are respectively assigned by IARC, as “possibly carcinogenic to humans” (group 2B), and “not classifiable as to its carcinogenicity to humans” (group 3). Selenium is quite different from arsenic and antimony; it is an essential micronutrient and a trace element with biological importance for humans and animals. A particularity of selenium is that the boundary between toxicity and deficiency is narrow (Thiry et al., 2012) and still not clarified. The toxicity of selenium is not only related to its chemical similarity to sulphur and to its ability to be substituted during the assembly of proteins, but also to the oxidative stress (Lavado et al., 2012).

In order to remove arsenic, antimony and selenium from contaminated waters, several methods

* Author to whom all correspondence should be addressed: e-mail: iwolf@tuiasi.ro

are available namely coagulation/flocculation, ion-exchange and adsorption, oxidation, electrochemical methods and membrane processes (Santos et al., 2015; Ungureanu et al., 2015b), but also phytoremediation or bioremediation. Adsorption has been noticed as a simple and relative low-cost process appropriate for removing low levels of contaminants. A good adsorbent must guarantee good removal efficiency with a low cost of use. The removal capacity of natural sorbents can be improved by surface modification treatments, but any intervention to alleviate this capacity involves an increase in costs. The use of pre-treatments is economically unadvisable in cases where the increase in process efficiency is not significant.

The sorption of various toxic metals, anions, but especially the cationic ones (Moța et al., 2017; Rashed et al., 2017), has been widely investigated using various adsorbents (Ahmed et al., 2017; Bulgariu et al., 2015; Carolin et al., 2017). Nonetheless, studies regarding the sorption of toxic metallic/metalloid oxyanions using natural sorbents are quite limited, especially using sorbents without any previous treatment (Tuzen and Sari, 2010; Ungureanu et al., 2015a). Ungureanu et al. (2015b) and Santos et al. (2015) published comprehensive reviews about adsorption capacity for arsenic, antimony and selenium, detailing the maximum adsorption capacities reported for different sorbents.

The high availability around the world makes the moss peat an interesting resource for adsorption studies. The removal of oxyanions on *Sphagnum* moss peat has never been tested and published until now. The aim of this study is to investigate the efficiency of Romanian moss peat in removal of oxyanions from polluted aqueous solutions in order to provide useful information about the mechanism of the process.

2. Material and methods

2.1. Chemicals and glassware preparation

The sorption process of arsenic was tested for the main oxidation states, As(III) and As(V); similarly, the two antimony predominant oxidation states Sb(III) and Sb(V) were studied. In case of selenium, only Se(VI) was tested because of its high solubility in aqueous solutions and also due to its low adsorption capacity that made this oxyanion more problematic to be removed. Adsorbate solution was prepared by diluting an appropriate volume of AAS commercial standards: As(III) from 1000 ± 1 mg As(III)/L in 2-5 % HCl (*ChemLab*), As(V) from As₂O₃ solution, 1001 ± 3 μg As(V)/L in HNO₃ 4 % (*SCP Science*), Sb(III) from K₂SbO₄·H₂O solution 1000 ± 2 mg Sb(III)/L, in 2-5 % HCl (*Carlo Erba*); Sb(V) from 1000 ± 2 mg Sb(V)/L, in 4 % HNO₃ (*Chem Lab*) and Se(VI) from 1000 ± 2 mg Se(VI)/L, in 2-5 % HNO₃ (*SCP Science*). The pH was adjusted to the required values using diluted solutions of NaOH and HCl or HNO₃ prepared from analytical grade chemicals: NaOH pellets (purity $\geq 99.0\%$, *Merck*), concentrated HNO₃ 65% analytical grade (*Sigma*

Aldrich) and concentrated HCl 37% p.a. (*Merck*). All solutions were prepared in distilled water. Glassware and plastic material were acid-washed (soaked for 24 hours in HNO₃ 20% solution) and rinsed with distilled water.

2.2. Sorbent preparation

The *Sphagnum* moss peat, collected from Poiana Stampei – Romania, was initially air-dried and ground (3-6 mm), using an electric grinder (*GM-100 Retsch Knife Mill Grindomix*). The moss peat was dried again, at 40 °C and stored in a desiccator until use.

2.3. Moss peat characterization

2.3.1. Humidity content

For the determination of physically bound water from moss peat and moisture content (MC) calculation the method described by Balan et al. (2012) was followed. Approximately 2 g of peat was weighed into a pre-weighed weighing bottle. The weighing bottle with the sample was maintained at 105°C in an oven for 4 hours, then cooled in a desiccator and weighed again. The moisture content of the analysed sample is calculated by:

$$MC \text{ (wt \%)} = \frac{A-B}{A} * 100 \quad (1)$$

where *A* is the mass of the moss peat sample before drying (g) and *B* represents the sample mass after drying at 105°C (g).

2.3.2. Ash content

The identification of mineral (inorganic) composition of moss peat was performed as previously (Balan et al., 2012) using an electric furnace *Nabertherm L3/11/B180*. In a porcelain crucible (previously calcined at 600°C and weighed) a sample of about 2 g of moss peat was weighed and firstly dried at 105°C and weighed again, then calcined in an electric furnace at 600°C for 2 hours. After calcination, the ash crucible was cooled in a desiccator and weighed. The ash content was calculated with the relation:

$$Ash, \% = \frac{B-C}{A} * 100 \quad (2)$$

where *A* is the mass of initial sample of moss peat (g), *B* represents the sample mass after drying at 105°C (g), and *C* is the sample mass after calcination at 600°C (g).

By the difference from 100%, the organic material content of the moss peat is calculated (Eq. 3):

$$Organic \text{ substances, \%} = 100 - moisture\% - ash\% \quad (3)$$

2.3.3. pH

The pH of the aqueous solution of moss peat was measured by immersing a sample of 1 g of moss peat in a beaker with 50 mL double distilled water.

After 24 hours with intermittent stirring, the pH of the suspension was measured with a pH meter equipped with a combined glass electrode.

2.3.4. Infrared spectroscopy

Fourier Transform Infrared Spectroscopy (FTIR) was used to identify the functional groups presented on the moss peat surface. Infrared spectra were obtained by a Shimadzu FTIR, model IR Affinity equipment, in triplicate readings, on a sample of moss peat ground to finer and homogeneous particles, in a wave number range from 400 to 4000 cm^{-1} , 50 scans, with a resolution of 8.0 cm^{-1} .

2.4. Adsorption studies

2.4.1. Analytical procedures

Adsorption tests were conducted using solutions with 2-50 mg/L contaminant concentration since these levels are typically found in wastewaters. Equilibrium and kinetic studies were performed in batch, testing the effect of pH and initial contaminant concentration. The concentration of arsenic, antimony and selenium in aqueous solution was measured by flame AAS (GBC 932 plus), deuterium background correction, in triplicate readings. As, Sb and Se were measured at wavelengths of 193.7 nm, 217.6 nm and 196.0 nm, respectively, with a lamp current of 5.0 mA and slit widths of 0.5 nm for arsenic, 0.2 nm for antimony and 1.0 nm for selenium. Acetylene and dinitrogen monoxide were used as combustible/oxidant gases for As and Se determinations, and acetylene/air for Sb analysis. Calibration curves were obtained and accepted for a determination coefficient $R^2 > 0.995$. All experiments were performed under orbital agitation at 120 rpm (orbital rotator GFL 3031), at constant temperature (23 ± 1 °C). Before AAS analysis, the samples were filtered using cellulose acetate membrane filters (45 μm porosity).

2.4.2. Screening tests

Preliminary assays were performed in order to test the sorption ability of moss peat for As(III), As(V), Sb(III), Sb(V) and Se(VI) removal. The experiments were conducted in duplicate, at constant pH 5.0 ± 0.5 . Contaminant solutions of 25 mg/L concentration were stirred with rigorously recorded moss peat mass of 10 g/L, in 100 mL capped Erlenmeyer flasks. After 6h-contact time, samples were filtered and final concentrations of the contaminant were analysed. The adsorbed amount per unit mass of adsorbent (q , mg/g) was calculated by mass balance (Eq. 4):

$$q = \frac{c_{in} - c_f}{m} * v \quad (4)$$

where C_{in} is the initial concentration (mg/L), C_f is the final concentration (mg/L), m is the mass of moss peat used (g) and v is the volume of solution (L).

2.4.3. Effect of pH

The pH conditions are known to have a significant influence in the adsorption process. In order to study the influence of this variable on the

sorption of Sb(III) and Sb(V) by moss peat, adsorption tests were conducted at different pH values. The experiments were carried out in duplicate, following the procedure described previously (section 2.4.2). The pH was adjusted in the initial solution, to values between 2 and 8, and was regularly controlled throughout the experiment, in order to be approx. constant (± 0.5).

2.4.4. Kinetic studies

The effect of contact time on the biosorption of Sb(III) and Sb(V) on moss peat was studied in batch mode, at pH 2 for both Sb(III) and Sb(V). The experimental conditions were 25 mg Sb(III) and Sb(V)/L, using 10 g/L moss peat dosage. Sb solution with the pH selected after preliminary tests (regularly controlled) and the sorbent were stirred for different pre-established contact times. Suspensions were filtered and antimony in the liquid phase analysed.

2.4.5. Equilibrium adsorption isotherm

Biosorption isotherms were performed for Sb(III) and Sb(V), at pH 2, adjusted regularly, in duplicate. Experimental data was obtained by stirring Erlenmeyer flasks containing Sb solutions, with different initial concentrations (2-50 mg/L), with 10 g/L of sorbent, for 6 hours (enough to reach the equilibrium state). The suspensions were filtered and Sb was analysed in the liquid phase. The amount of Sb(III) and Sb(V) adsorbed in equilibrium was calculated by (Eq. 4). In this case, q and C_f are the values observed at equilibrium (q_e and C_e , respectively).

2.4.6. Desorption studies

Experiments regarding the desorption of Sb(V) from loaded-moss peat were performed. Initially, simple tests were conducted using four different eluents (NaOH 0.1 mol/L, HCl 0.1 mol/L, NaCl 0.5 mol/L and Na_2HPO_4 0.5 mol/L) and a dosage of 10 g of loaded-peat per L of eluent, for 6 h-contact time. For further experiments, NaOH 0.1 mol/L was selected as eluent. Three adsorption/desorption cycles were then carried out. The contact time for each adsorption/desorption process was 4 hours. In the adsorption step, initial Sb(V) concentration and moss peat dosage were 25 mg/L and 10 g/L, respectively. For desorption assays, loaded-moss peat dosage was 15 g/L.

3. Results and discussion

3.1. Biomass characterization

3.1.1. Physical-Chemical analysis

The moss peat from Poiana Stampei is exploited since 1950. The peat deposits from Dorna watershed, falls into the category of oligotrophic peat deposits, characterized by the existence in the region of rich precipitations, cold climate, bulging appearance of peat lands and by characteristic vegetation which consists mainly of *Sphagnum* and

spruce. The main peat characteristics (Table 1) suggest a peat with a low degree of decomposition.

Table 1. Characteristics of *Sphagnum* moss peat

Properties	Value
Moisture content (wt %)	10.5
Ash content (wt %)	4.85
Organic matter (wt %)	84.65
pH (1:50, w:v deionized water)	4.00 ± 0.05

3.1.2. FTIR analysis

Fourier Transform Infrared Analysis (FTIR) (Fig. 1) permits the registration of infrared spectra for *Sphagnum* peat moss.

The main constituents of moss peat - cellulose, lignin, humic and fulvic acids - contain a large number of carbon, hydrogen, oxygen atoms bound together, and their valence and deformation vibrational movements are connected together in a complex way. As a result, the infrared spectrum has a very complex structure and is quite difficult to assign all the absorption bands to specific vibration from molecule or groups of atoms.

IR spectra of *Sphagnum* moss peat can be divided into several areas highlighting bands with different intensities of valence vibration and deformation of the groups OH, CH, CH₂, CO, COOH, etc. (Balaban et al., 1983; Romao et al., 2007).

Absorption band from 3410-3420 cm⁻¹ is assigned to the valence vibrations of hydroxyl groups involved in the inter- and intra-molecular hydrogen bonds. Valence vibrations of the CH₂ and CH groups determine the absorbance at 2920 cm⁻¹. The area between 2000 - 1500 cm⁻¹ is characterized by the valence vibrations of the double bonds C = O (carboxyl, aldehyde, ketone groups 1732 cm⁻¹) or aromatic structures (lignin or other compounds with low molecular weight, 1514 cm⁻¹).

The area between 1500 - 1200 cm⁻¹ includes absorption bands attributed to deformation vibrations of different atomic groups such as CH₂, CH, OH. The adsorption band of 1200-950 cm⁻¹ is characterized by a very broad absorption band assignable to the valence vibrations of the bonds C-O, C-C in the cyclic structure. Strong absorption in this spectral range is characteristic for all polysaccharides. Between 900-400 cm⁻¹, among a broad absorption, more peaks caused by vibrations of OH group are observed.

3.2. Adsorption studies

3.2.1. Screening Tests

Preliminary adsorption tests were carried out in order to compare the performance of *Sphagnum* moss peat as regards the adsorption of As, Sb and Se. Different species, with different charges and oxidation states, can be present in aqueous solution, depending on the pH and redox potential, which determines their chemistry to be complex. Fig. 2 presents a simplified diagram for As(III), As(V), Sb(III), Se(IV) and Se(VI) in water, as a function of pH (Filote et al., 2017); these diagrams can help to a better understanding of the results from these preliminary experiments.

Preliminary tests performed with *Sphagnum* moss peat and arsenic, antimony and selenium revealed that the moss peat is unable to remove both As(III) and As(V) and also Se(VI). According to the speciation diagram, at pH 5, As(III) mainly exists as a neutral compound (H₃AsO₃) and As(V) as an oxyanion (H₂AsO₄⁻). In case of antimony, the adsorption capacity of moss peat was 1.5 mg/g for Sb(III) and 2 mg/g for Sb(V). At pH 5, Sb(III) is present in aqueous solution as a neutral specie (Fig. 3) but, contrarily to As(III), it was removed considerably. Possibly, the electrostatic attraction is not the adsorption mechanism in this case, but most probably the complexation reactions between Sb(III) and carboxylic and hydroxyl groups is the explanation.

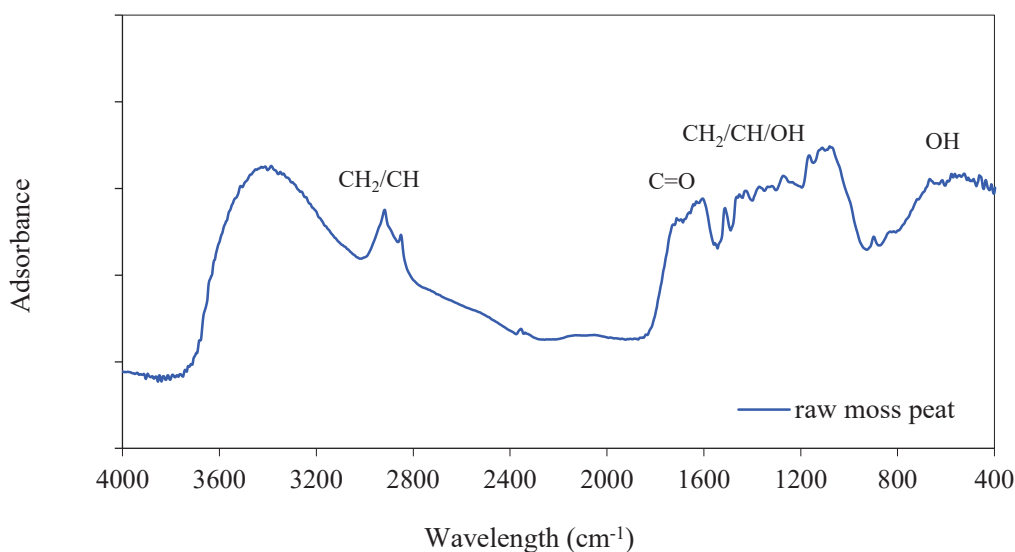


Fig. 1. FTIR spectra of raw peat moss

pH	2	7	9	11	13
As(III)	H_3AsO_3			$H_2AsO_3^-$	$HAsO_3^{2-}$
As(V)	H_3AsO_4	$H_2AsO_4^-$	$HAsO_4^{2-}$		AsO_4^{3-}
Sb(III)	$Sb(OH)_2^+$	H_3SbO_3 $Sb(OH)_3$		$H_2SbO_3^-$ $Sb(OH)_4^-$	
Sb(V)	$Sb(OH)_5$	$Sb(OH)_6^-$			
Se(IV)	H_2SeO_3	$HSeO_3^-$		SeO_3^{2-}	
Se(VI)	$HSeO_4^-$	SeO_4^{2-}			

Fig. 2. Schematic diagrams for speciation of As(III), As(V), Sb(III), Sb(V), Se(IV) and Se(VI) in aqueous solution (adapted upon Filote et al., 2017)

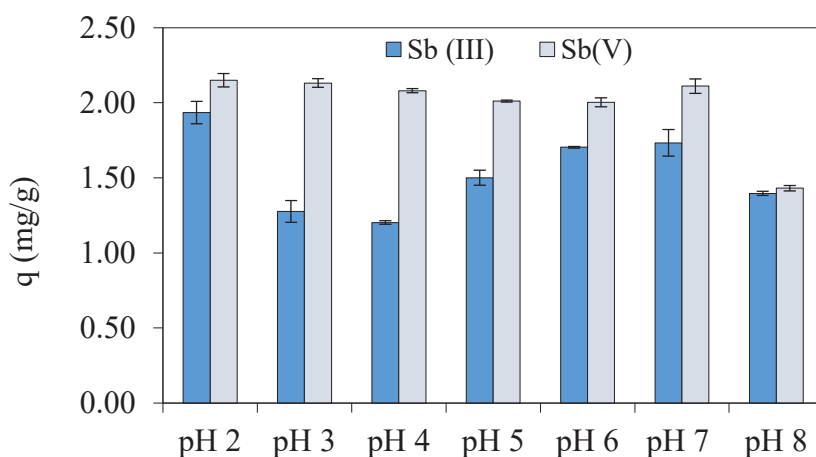


Fig. 3. Biosorption of Sb(III) and Sb(V) on *Sphagnum* moss peat as a function of pH (initial solution concentration 25 mg/L, moss peat dosage 10 g/L, 4 h contact time)

Tella and Pokrovski (2009) also observed the formation of complexes in solution, between antimonite and poly-functional carboxylic and hydroxy-carboxylic acids. Similarly, Wu et al. (2012) proposed for the adsorption of Sb(III) on *Microcystis* biomass the complexation reactions as the dominant mechanism, but additionally, considering that $Sb(OH)_3$ possesses three OH^- ligands, hydrogen bonding may also be involved in the adsorption process.

3.2.2. Effect of pH

The pH influences the chemical form of the adsorbate and the charge of the functional groups on the sorbent surface and for this reason it is an important parameter that usually affects the adsorption of metal ions in solution. The results found for sorption tests in different pH conditions are described in Fig. 3, as amount of antimony adsorbed, q (mg/g), calculated by mass balance equation (Eq. 3).

The error bars presented in Fig. 4 were calculated considering the maximum error in the measurements involved in the calculation of the adsorbed amount (i.e., error in volumes measurement, mass of moss peat and in the Sb concentration readings) and explains the global uncertainty of each result.

$$q = \frac{C_0 - C}{C_s} \quad (5)$$

In Eq. (5), C_0 and C are the initial and the final Sb concentrations (mg/L) in the liquid phase, respectively, and C_s the moss peat dosage (g/L). The sorption of antimonite by moss peat is modestly affected by pH (Fig. 3). The amounts of Sb(III) adsorbed ranged between 1.2 and 1.94 mg/g. Regarding Sb(V), the sorption was less influenced by pH, with sorbed amounts around 2 mg/g (from pH 2 to pH 7), but at pH 8, the amount of Sb(V) adsorbed reduced evidently. These results demonstrate that Sb(III) and especially Sb(V) uptake by moss peat is significant over the entire pH range studied (pH 2-8), which is an important advantage. Many sorbents require an optimum pH to achieve a maximum (or a considerable) uptake. In a practical situation, considering the huge volume of wastewater generated, it is impractical to alter the pH of solutions (Vijayaraghavan and Balasubramanian, 2015).

According to the speciation diagram from Fig. 2, neutral $Sb(OH)_3$ is the predominant form of antimonite in solutions in the whole pH range studied. Concerning antimonate, for pH 2-3 it is predominantly in neutral form ($Sb(OH)_5$), but for higher pH it acquires the form of the oxyanion $Sb(OH)_6^-$.

This confirms that electrostatic attraction is not involved in the uptake of Sb(III) or Sb(V), since there are not opposite charges (adsorbate/adsorbent) at any pH value. Previous works (Tella and Pokrovski, 2008; 2009; 2012) have provided an important support to the proposed adsorption mechanisms and to the results obtained in this study. The authors demonstrated the construction of stable complexes of Sb(III) and Sb(V) with poly-functional carboxylic, hydroxyl carboxylic acids and phenolic hydroxyl in aqueous solution. Considering the functional groups of the moss peat, the mechanism for sorption is probably the surface complexation, involving carboxylic and hydroxyl groups.

Other studies have reported comparable results concerning the pH effect on Sb(III) uptake. Iqbal et al. (2013) described a constant uptake by green bean husk between pH 3 and 10, and a diminution for pH below 3 or above 10. Wu et al. (2012) have also found an irrelevant dependence on the pH in the range from 2.0 to 7.0, but they obtained an optimum at pH 4. The studies regarding Sb(V) uptake by natural sorbents are very scarce, but Sun et al. (2014) reported a decrease of the sorption as pH increased in pH 3-10.

3.2.3. Kinetics studies

The kinetic study represents the first step in determining the inter-dependencies between equilibrium phenomenon and mass transfer, establishing a predictive model of the sorption behaviour.

Experimental results obtained in the kinetic study of Sb(III) and Sb(V) sorption by *Sphagnum* moss peat are presented in Fig. 4 as the amount of Sb adsorbed (q) as a function of contact time (t). The biosorption of antimony is a fast process (Fig. 4). The contact time required to reach equilibrium is about 120 min. In the first 30 min, the process is very quick; more than 60 % of the maximum adsorbed amount was already attained. The kinetic curves can be divided into two phases, a first phase very fast (0 – 30 minutes) when more than 60 % of the maximum adsorbed amount was already attained and a second slower phase (30 – 120 minutes).

The equilibrium time, for both systems is about 2-3 hours, since there were no further significant changes on the adsorbed amount of Sb. Various authors described fast kinetics for antimony removal, with contact times lower than few hours (Uluzlu et al., 2010; Ungureanu et al., 2015a; Ungureanu et al., 2016; Vijayaraghavan and Balasubramanian, 2011; Wu et al., 2012). Speedy sorption kinetics of metals/metalloids is very important in practical terms, allowing the use of smaller columns with continuous operation, in an efficient and economical way (Aksu, 2001). The most known models used to describe adsorption kinetics are the Lagergren's pseudo-first-order (Lagergren, 1898) and the pseudo-second order (Ho et al., 1996). Both models were fitted to the experimental data by non-linear regression using *CurveExpert* software (Ungureanu et al., 2016;

Ungureanu et al., 2017). Pseudo-2nd order showed much better results, higher correlation coefficients, lower standard error (SE) and a predicted value for the equilibrium adsorbed amount (q_e) closer to the experimental ones. Pseudo-2nd order model, expressed by (Eq. 5), was then selected to describe the experimental data for Sb(III) and Sb(V) biosorption.

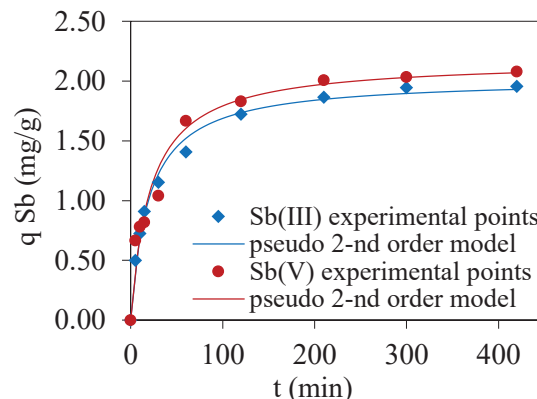


Fig. 4. Biosorption kinetics for Sb(III) and Sb(V) (pH 2) at 23 ± 1 °C and initial Sb concentrations of $C_{in}=25$ mg/L and $C_s=10$ g/L moss peat. Experimental data and pseudo-second-order model

This model assumes a homogeneous surface and metal binding to two active centres. In Eq. (6), q_e (mg g⁻¹) denotes the biosorbed amount in equilibrium and k_2 (g mg⁻¹ min⁻¹) the pseudo-second order kinetic constant. The initial rate of biosorption (r , mg g⁻¹ min⁻¹) was also calculated, using the parameters of pseudo-second order model (Eq. 7).

$$q = \frac{q_e^2 \cdot k_2 \cdot t}{1 + k_2 \cdot q_e \cdot t} \quad (6)$$

$$r = k_2 \cdot q_e^2 \quad (7)$$

The pseudo-2nd order model parameters were presented in Table 2.

3.2.4. Equilibrium studies

Isotherm provides information about the attraction of the adsorbent to the adsorbate and about the maximum sorption capacity, at a specified temperature. Equilibrium isotherms for Sb(III) and Sb(V) sorption on the moss peat were determined at constant pH 2 with synthetic antimony solutions, varying the initial concentration of antimony from 2 to 50 mg/L and using an adsorbent dosage of 10 g/L. The equilibrium results are described in Fig. 5, as Sb sorbed amount in equilibrium (q_e), calculated by (Eq. 3), where C was replaced by the equilibrium Sb concentration in the liquid phase (C_e).

Considerable adsorbed amounts were reached in the concentration range studied (Fig. 5). The experimental adsorbed amount obtained for Sb(III) was approx. 3 mg/g, whereas for Sb(V) nearly 3.3 mg/g was observed, at pH 2.

Table 2. Parameters for pseudo-second order kinetic model (value± 95 % confidence)

C_{in} (mg/L)	C_s (g/L)	k_2 (g mg ⁻¹ min ⁻¹)	q_e (mg/g)	r (mg g ⁻¹ min ⁻¹)	SE (mg/g)
Sb(III)					
25	10	0.025 ± 0.006	2.02 ± 0.09	0.102	0.06
Sb(V)					
25	10	0.02 ± 0.01	2.1 ± 0.2	0.1016	0.13

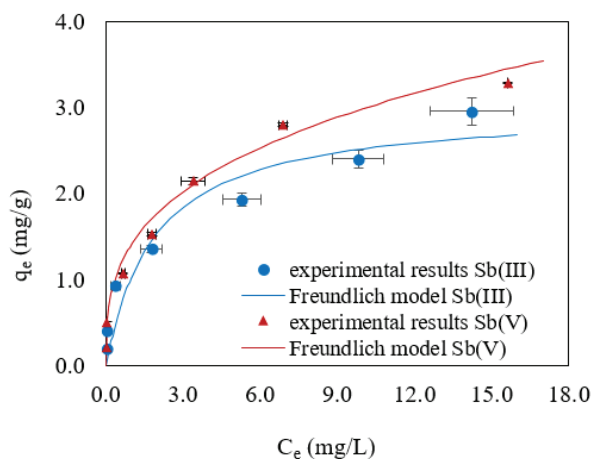


Fig. 5. Equilibrium isotherms for Sb(III) and Sb(V) biosorption on *Sphagnum* moss peat, experimental data and Freundlich model

For both Sb(III) and Sb(V), Langmuir and Freundlich models were adjusted to experimental data by non-linear fitting CurveExpert software and Freundlich model shows a better fitting. The Freundlich isotherm (1906) is an empirical expression (Eq. 8) that assumes a heterogeneous sorption surface with different energy active centres.

$$q_e = K_F C_e^{1/n_F} \quad (8)$$

where K_F ((mg g⁻¹)(L m⁻¹)^{1/n_F}) is a constant for the adsorbate-adsorbent system and n_F is a constant that indicates the intensity of adsorption ($n_F > 1$ favorable isotherm; $n_F \leq 1$ unfavorable isotherm). The values calculated are presented in Table 3.

The standard errors of the regressions have a reasonably low value, indicating a good agreement between observations and Freundlich predictions. The adsorbed amounts obtained in this study are comparable with adsorption capacities reported in literature. The maximum adsorption capacity of raw *Sargassum muticum* for Sb(III) (Ungureanu et al., 2015a) was 5.5 mg/g at pH 5, 2 g/L alga and initial concentration of 10 mg/L Sb(III) solution. Wu et al. (2012) testing the affinity of *Microcystis* biomass found a removal capacity of 4.88 mg/g for Sb(III), at pH 4. This value is slightly higher than the one reported in the present study, but it was achieved using much higher initial concentration in ranges 0 to 400 mg/L. *Cyanobacteria Synechocystis* sp. was tested by Mu (2011) and a maximum adsorption capacity of 4.68 mg/g was reported, using an initial Sb(III) concentration range from 5 to 100 mg/L. Other authors

presented higher adsorption capacities, such as 81.1 mg/g, for lichen, *Physcia Tribacia* (Uluozlu et al., 2010) and 14.9 mg/g (at pH 6) for the brown alga *Sargassum* sp. (Vijayaraghavan and Balasubramanian, 2011). Considerable higher adsorption capacities have been reported in case of binary metal oxides, for example 214 mg/g, at pH 3, for a Fe-Mn oxide (Xu et al., 2011); this category of material requires however, synthesis and consequently implies high costs of preparation.

Table 3. Parameters for Freundlich equilibrium model (values ± confidence intervals for 95 % confidence)

	n_F	$K_F = \text{mg g}^{-1} (\text{mg.L}^{-1})^{-1/n}$	SE (mg/g)
Sb(III)	2.9 ± 0.1	1.1 ± 0.5	0.23
Sb(V)	3.1 ± 0.4	1.4 ± 0.1	0.24

3.2.6. Desorption and reuse

Sphagnum moss peat is a material with several possible utilisations and for this reason the reuse potential of a loaded-*Sphagnum* moss peat might be an essential condition to evaluate the process design for a practical application. Considering that the *Sphagnum* moss peat is a natural and available adsorbent and its cost is low, the relevance of biomass regeneration might be questionable depending in the efficiency of the process. Preliminarily, desorption experiments were conducted with *Sphagnum* moss peat loaded with Sb(V) and different eluents. The results are revealed in Fig. 6. The eluents provided desorption levels ranging between 2 and 31 % for Sb(V) loaded in the moss peat and sodium hydroxide solution 0.1 M was the best desorbent.

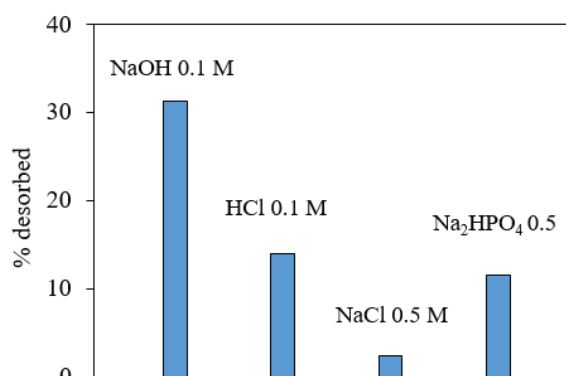


Fig. 6. Desorption percentages from Sb(V)-loaded *Sphagnum* moss peat (dosage 25 g/L), using different eluents

The process was repeated in three adsorption/desorption cycles and results are depicted

in Fig. 7. The adsorbed amount of Sb(V) was practically the same for the first two cycles but in the third cycle, the adsorption capacity of the moss peat decreased to 36 % of the initial capacity. The batch desorption studies also evaluate the strength of the interaction between Sb and moss peat. The amount of desorbed Sb, moderately increased from the first cycle to the second one, from 19 % to 34 %, respectively. In the third step, the desorption of loaded Sb(V) grew drastically, to 71 %.

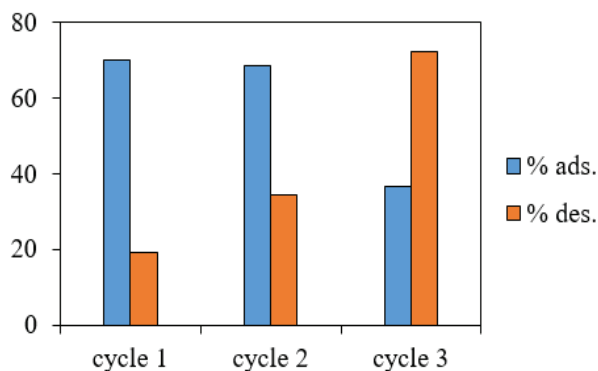


Fig. 7. Adsorbed and desorbed amounts, in repeated Sb(V) adsorption-desorption cycles, using *Sphagnum* moss peat

Iqbal et al. (2013) described a marginal reduction (less than 10 %) over seven repeated reuse cycles of the adsorption capacity of green bean husk, using HCl 0.1 M as eluent. Wu et al. (2012) used HCl 4.0 M as eluent and found a constant Sb(III) removal in the first four cycles on *Microcystis* biomass and reports approx. 20 % decrease only in the fifth cycle.

4. Conclusions

Sb(III) and Sb(V) biosorption from aqueous solutions was studied using *Sphagnum* moss peat. Infrared spectra showed the presence of carboxylic and hydroxyl groups, which were proposed to be involved in antimony uptake by surface complexation. Regarding the effect of pH, a moderate effect was visible for Sb(III) and no significant effect was recorded for Sb(V) biosorption.

Biosorption kinetics of both Sb(III) and Sb(V) were fast and well described by pseudo-second-order model. For both Sb(III) and Sb(V), Freundlich model shows a good fitting. The experimental adsorbed amount found for Sb(III) was around 3 mg/g and nearly 3.3 mg/g for Sb(V), at pH 2. Regeneration and reutilization of the moss peat with NaOH solution is possible, but limited to very few adsorption/desorption cycles, and is not encouraged.

Considering that the *Sphagnum* moss peat is a natural widespread material and requires a reduced number of operations for preparation, it can be considered a good sorbent; the good capture capacity revealed in this study and the weak influence of pH are positive arguments for a real utilisation of the *Sphagnum* moss peat for remediation of antimony-contaminated waters.

With consecutive regeneration, the sites on *Sphagnum* moss peat that become available to uptake Sb(V) will provide weaker interactions. It is probable that from cycle to cycle, the adsorption was established by weaker interactions and then the efficiency of desorption increased. The results of the desorption study are much more limited than others reported in literature.

References

- Aksu Z., (2001), Equilibrium and kinetic modelling of cadmium(II) biosorption by *C. vulgaris* in a batch system: effect of temperature, *Separation and Purification Technology*, **21**, 285-294.
- APHA, (1999), *Standard Methods for the Examination of Water and Wastewater*, 20th APHA/AWWA/WEF, American Public Health Association (APHA), Washington, DC.
- Balaban A.T., Banciu M., Pogany I., (1983), *Applications of Physical Methods in Organic Chemistry* (in Romanian), Scientific and Encyclopaedic Publishing House, Bucharest, Romania.
- Ben Issa N., Rajakovic-Ognjanovic V.N., Marinkovic A.D., Rajakovic L.V., (2011), Separation and determination of arsenic species in water by selective exchange and hybrid resins, *Analytica Chimica Acta*, **706**, 191-198.
- Ahmed M.B., Zhou L.J., Ngo H.H., Guo W., Thomaidis N.S., Xu J., (2017), Progress in the biological and chemical treatment technologies for emerging contaminant removal from wastewater: A critical review, *Journal of Hazardous Materials*, **323**, 274-298.
- Bulgariu L., Gavrilescu M., (2015), *Bioremediation of Heavy Metals by Microalgae*: In: *Handbook of Marine Microalgae. Biotechnology Advances*, Kim S.-K. (Ed.), Elsevier, 457-469.
- Carolin C.F., Kumar P.S., Saravanan A., Joshiba G.J., Naushad Mu., (2017), Efficient techniques for the removal of toxic heavy metals from aquatic environment: A review, *Journal of Environmental Chemical Engineering*, **5**, 2782-2799.
- Filote C., Ungureanu G., Boaventura R., Santos S., Volf I., Botelho C., (2017), Green macroalgae from the Romanian coast of Black Sea: Physico-chemical characterization and future perspectives on their use as metal anions biosorbents, *Process Safety and Environmental Protection*, **108**, 34-43.
- Fu Z.Y., Wu F.C., Amarasiriwardena D., Mo C.L., Liu B.J., Zhu J., Deng Q.J., Liao H.D., (2010), Antimony, arsenic and mercury in the aquatic environment and fish in a large antimony mining area in Hunan, China, *Science of the Total Environment*, **408**, 3403-3410.
- Ho Y.S., Wase D.A.J., Forster C.F., (1996), Kinetic studies of competitive heavy metal adsorption by *Sphagnum* moss peat, *Environmental Technology*, **17**, 71-77.
- Iqbal M., Saeed A., Edyvean R.G.J., (2013), Bioremoval of antimony(III) from contaminated water using several plant wastes: Optimization of batch and dynamic flow conditions for sorption by green bean husk (*Vigna radiata*), *Chemical Engineering Journal*, **225**, 192-201.
- Jain C.K., Ali I., (2000), Arsenic: occurrence, toxicity and speciation techniques, *Water Research*, **34**, 4304-4312.
- Lagergren S., (1898), About the theory of so-called adsorption of soluble substances, *Kungliga Svenska Vetenskapsakademiens Handlingar*, **24**, 1-39.
- Larios R., Fernandez-Martinez R., Lehecho I., Rucandio I., (2012), A methodological approach to evaluate arsenic speciation and bioaccumulation in different plant

- species from two highly polluted mining areas, *Science of the Total Environment*, **414**, 600-607.
- Lavado R., Shi D., Schlenk D., (2012), Effects of salinity on the toxicity and biotransformation of l-selenomethionine in Japanese medaka (*Oryzias latipes*) embryos: Mechanisms of oxidative stress, *Aquatic Toxicology*, **108**, 18-22.
- Moța A.S., Prodan M., Ghicioi E., Nălboc I., Moldovan C., (2017), Heavy metals removal from mining drainage acid water by use of natural zeolites, *Environmental Engineering and Management Journal*, **16**, 1383-1388.
- Rashed M.N., Soltan M., Ahmed M.M., Abdou A.N.E., (2017), Removal of heavy metals from wastewater by chemically activated sewage sludge, *Environmental Engineering and Management Journal*, **16**, 1531-1542.
- Romao L., Lead J.P., Rocha J.C., Oliveira L.C., Rosa A.H., Mendonca A.G.R., Ribeiro A.S., (2007), Structure and properties of Brazilian Peat: analysis by spectroscopy and microscopy, *Journal of the Brazilian Chemical Society*, **18**, 711-720.
- Santos S., Ungureanu G., Boaventura R., Botelho C., (2015), Selenium contaminated waters: an overview of analytical methods, treatment options and recent advances in sorption methods, *Science of the Total Environment*, **521-522**, 246-260.
- Sun H.J., Rathinasabapathi B., Wu B., Luo J., Pu L.P., Ma L.Q., (2014), Arsenic and selenium toxicity and their interactive effects in humans, *Environment International*, **69**, 148-158.
- Tella M., Pokrovski G.S., (2008), Antimony(V) complexing with O-bearing organic ligands in aqueous solution: an X-ray absorption fine structure spectroscopy and potentiometric study, *Mineralogical Magazine*, **72**, 205-209.
- Tella M., Pokrovski G.S., (2009), Antimony(III) complexing with O-bearing organic ligands in aqueous solution: An X-ray absorption fine structure spectroscopy and solubility study, *Geochimica Et Cosmochimica Acta*, **73**, 268-290.
- Tella M., Pokrovski G.S., (2012), Stability and structure of pentavalent antimony complexes with aqueous organic ligands, *Chemical Geology*, **292-293**, 57-68.
- Thiry C., Ruttens A., De Temmerman L., Schneider Y.J., Pussemier L., (2012), Current knowledge in species-related bioavailability of selenium in food, *Food Chemistry*, **130**, 767-784.
- Tuzen M., Sari A., (2010), Biosorption of selenium from aqueous solution by green algae (*Cladophora hutchinsiae*) biomass: equilibrium, thermodynamic and kinetic studies, *Chemical Engineering Journal*, **158**, 200-206.
- Uluozlu O.D., Sari A., Tuzen M., (2010), Biosorption of antimony from aqueous solution by lichen (*Physcia tribacia*) biomass, *Chemical Engineering Journal*, **163**, 382-388.
- Ungureanu G., Santos S.C.R., Volf I., Boaventura R.A.R., Botelho C.M.S., (2017), Biosorption of antimony oxyanions by brown seaweeds: Batch and column studies, *Journal of Environmental Chemical Engineering*, **5**, 3463-3471
- Ungureanu G., Filote C., Santos S.C.R., Boaventura R.A.R., Volf I., Botelho C.M.S., (2016), Antimony oxyanions uptake by green marine macroalgae, *Journal of Environmental Chemical Engineering*, **4**, 3441-3450.
- Ungureanu G., Santos S., Boaventura R., Botelho C., (2015a), Biosorption of antimony by brown algae *S. Muticum* and *A. Nodosum*, *Environmental Engineering and Management Journal*, **14**, 455-463.
- Ungureanu G., Santos S., Boaventura R., Botelho C., (2015b), Arsenic and antimony in water and wastewater: overview of removal techniques with special reference to latest advances in adsorption, *Journal of Environmental Management*, **151**, 326-342.
- Vijayaraghavan K., Balasubramanian R., (2011), Antimonite removal using marine algal species, *Industrial and Engineering Chemistry Research*, **50**, 9864-9869.
- Vijayaraghavan K., Balasubramanian R., (2015), Is biosorption suitable for decontamination of metal-bearing wastewaters? A critical review on the state-of-the-art of biosorption processes and future directions, *Journal of Environmental Management*, **160**, 283-296.
- Wu F.C., Sun F.H., Wu S., Yan Y.B., Xing B.S., (2012), Removal of antimony(III) from aqueous solution by freshwater cyanobacteria *Microcystis* biomass, *Chemical Engineering Journal*, **183**, 172-179.
- Xu W., Wang H.J., Liu R.P., Zhao X., Qu J.H., (2011), The mechanism of antimony(III) removal and its reactions on the surfaces of Fe-Mn Binary Oxide, *Journal of Colloid and Interface Science*, **363**, 320-326.



“Gheorghe Asachi” Technical University of Iasi, Romania



PREPARATION AND CHARACTERIZATION OF NANOCOMPOSITE MATERIAL BASED ON TiO₂-Ag FOR ENVIRONMENTAL APPLICATIONS

Catalina Nutescu Duduman¹, Jose Maria Gómez de Salazar y Caso de Los Cobos²,
Maria Harja^{1*}, Maria I. Barrena Pérez², Consuelo Gómez de Castro³, Doina Lutic⁴,
Olga Kotova⁵, Igor Cretescu^{6*}

¹“Gheorghe Asachi” Technical University of Iasi, Faculty of Chemical Engineering and Environmental Protection, Chemical Engineering Department, 73 Prof.dr.doc. Dimitrie Mangeron Street, 700050 Iasi, Romania

²Complutense University of Madrid, Faculty of Chemical, Department of Materials Science and Metallurgical Engineering Av. Séneca, 2, 28040 Madrid, Spain

³Complutense University of Madrid, Faculty of Chemical, Department of Materials and Chemical Engineering, Av. Séneca, 2, 28040 Madrid, Spain

⁴Alexandru Ioan Cuza University of Iasi, Bld. Carol I No 11, 700506 Iași, Romania

⁵Laboratory of Mineral Raw Materials Technology, Institute of Geology, Komi Science Center, Ural Branch of RAS, Syktyvkar, Komi Republic, Russia

⁶“Gheorghe Asachi” Technical University of Iasi, Faculty of Chemical Engineering and Environmental Protection, Department of Environmental Engineering and Management, 73 Prof.dr.doc. Dimitrie Mangeron Street, 700050 Iasi, Romania

Abstract

A simple and efficient method for preparing Ag-doped TiO₂ nanoparticles was successfully developed, by associating the sol-gel method and the impregnation-reduction. While titanium dioxide is one of the most used solids as photocatalyst, silver is particularly interesting for applications in biological and chemical detection and for its antibacterial properties. Moreover, in photocatalysis silver acts as an electron sink and donor in capturing the photogenerated electrons. The structural and morphological properties of the TiO₂-Ag samples were investigated by XRD, SEM, TEM, SAED and EDAX. The crystallinity degree increased by calcination at 650°C and the nature of the phases changed from anatase to a mixture of anatase, rutile and silver in metallic form and silver oxide. The photocatalytic properties of the synthesized product were evaluated in the UV-assisted photodegradation of Rhodamine 6G and Methyl Blue dyes. The photocatalytic performance in dyes decomposition of the doped samples was better than pure TiO₂.

Key words: nanocomposite, photocatalyst, silver, titanium dioxide

Received: May, 2017; *Revised final:* January, 2018; *Accepted:* March, 2018; *Published in final edited form:* April 2018

1. Introduction

Titanium dioxide (TiO₂) is widely used in environmental protection and energy applications (Nakata and Fujishima, 2012). Among the environmental protection applications, the air and

water purification systems, sterilization, manufacturing of self-cleaning surfaces, solar energy conversion, photo-electrochemical conversion can be mentioned (Liu and Bi, 2017; Wang et al., 2017). Another interesting and important application of titanium dioxide nanoparticles is its use in

*Author to whom all correspondence should be addressed: e-mail: mharja@tuiasi.ro; Phone: +40 747 909 645; Fax: +40 232 271 311; icre@tuiasi.ro; Phone: +40 741 914 342; Fax: +40 232 271 311

photocatalytic and photoelectrochemical applications, due to its convenient band gap value of 3.2 eV, non-toxic character, chemical and physical stability, high potential of capturing the solar energy and photocatalytic efficiency, low price etc. (Djoki et al., 2012; Ivanova et al., 2013; Kartal and Turhan, 2017; Liu et al., 2015). The semiconductive properties of TiO₂-based materials make them useful as sensitizers for redox processes activated by light, due to their electronic structure (Chen et al., 2010; Favier et al., 2016; Litic et al., 2017; Montazerzohori and Hoseinipour, 2017; Tobaldi et al., 2013).

Titanium dioxide exists in many polymorphs, but the most significant are anatase and rutile. These two polymorphs are semiconductors with rather large band gaps (3.23 and 3.02 eV respectively), therefore they can promote photocatalytic reactions in the presence of visible light (Tobaldi et al., 2013).

A convenient strategy to increase the visible light absorption is the incorporation of noble metals nanoparticles in titania (Cheriyian et al., 2017; Ivanova et al., 2013; Kochuveedu and Kim, 2012). Dopants such as Pt, Pd, Au, Ag improve the photocatalytic efficiency of TiO₂, by preventing the recombination of electron-hole pair (He et al., 2013; Sarina et al., 2013; Wei et al., 2013; Yin et al., 2014). Silver is suitable, nontoxic and much cheaper than the other mentioned noble metals, improving the TiO₂ bioactivity especially in water treatments, because of its intrinsic antibacterial activity against different microorganisms (Amin et al., 2009; Lee et al., 2005; Pham and Lee, 2004; Rupa et al., 2007; Liu et al., 2004). TiO₂-Ag and Ag nanoparticles can be relatively easily obtained by the sol-gel method (Behnajady et al., in press), a method widely employed in materials science. The formation of titanium oxide by the sol-gel method involves connecting Ti monomeric species by either oxo (Ti-O-Ti) or hydroxo (Ti-OH-Ti) bridges, generating polymers in solution. This technology allows obtaining a metal oxide matrix with the required characteristics and adding subsequently containing embedded nanoparticles (Galkina et al., 2011; Gomez de Salazar et al., 2016; Nutescu Duduman et al., 2016a, 2016b). Therefore, by the sol-gel method, TiO₂-Ag nanocomposites with easily controlled particle size can be obtained. The performance of TiO₂ in the photocatalytic processes is influenced by different factors: the nature of the phase, the crystallinity degree, the particles morphology and size, the active facet etc. (Hu et al., 2017; Niu et al., 2012; Vajda et al., 2016). Therefore, the preparation of anatase or rutile TiO₂ materials, with targeted properties is still a difficult task.

Organic dyes are widely used in textile industry, plastic, rubber, toys and many other industries. They have a major impact in the environment in generally, especially in wastewater (Ciobanu et al., 2013; Harja et al., 2011; Harja et al., 2016; Mahmoodi et al., 2017). The dyes originated from textile industry are a major source of water contamination, since, on one part, a lot of industries

use organic coloring agents resistant to the conventional treatments such as the common biologic conversion (Tian et al., 2014), and, on another part, because the amounts discharged are quite high (Ciobanu et al., 2014; Rusu et al., 2014).

Rhodamine 6 G (R6G) and Methyl Blue (MB) are usual and convenient model compounds for investigating the performance of semiconductive solids involved for their degradation by advanced methods as: chemical and electrochemical procedures, adsorption, ultrafiltration and photocatalytic degradation in the presence of UV or visible light (Bhakya et al., 2015; Litic and Cretescu, 2016; Litic et al., 2012), due to their high stability and coloring power even at concentrations of some ppm range.

In this paper we are describing the procedure for obtaining TiO₂-Ag nanocomposites by using an organic titanium salt as oxide precursor and hydrazine as reducing agent for Ag⁺ ions to metallic Ag. After the structural characterization, the solids were tested in the UV-assisted photocatalytic degradation of R6G and MB dyes from aqueous solutions simulating wastewaters.

2. Experimental

2.1. Samples preparation

Titanium tetra-isopropoxide (TIP-C₁₂H₂₈O₄Ti), Panreac was used as precursor for preparing the TiO₂-based materials. The other chemicals used in the preparation by sol-gel method: silver nitrate (AgNO₃), ethanol (C₂H₆O) 98%, and hydrazine (N₂H₄) 98%, all of analytical purity, were purchased from Pancreac. Nitric acid (HNO₃) 65% (w/w) was used as hydrolysis-condensation ratio controlling agent, ammonia solution (NH₄OH) 0.1 M as neutralization agent, and ethanol as solvent. Bidistilled water was used in all preparations employing aqueous media.

TIP was dissolved in ethanol under magnetic stirring, and then nitric acid was added drop wise until a pH value of 1.5 was reached, to induce the controlled hydrolysis of the titanium salt. After 30 minutes, the ammonia solution was added to neutralize the acid and settle the proper pH value (9-10) to initiate the polycondensation of Ti(OH)₄ and generate titania nanoparticles. After 2 h of stirring, the procedure of doping the particles with silver was started by adding AgNO₃ and ammonia solution, to bring the pH value to 10-11. After 1 h of stirring, the reducing agent was added and the stirring continued for another hour. The solid was recovered by filtration and dried in the oven at 110°C. A portion of this sample was calcined at 650°C. This calcination temperature was chosen in order to generate a convenient anatase/rutile ratio, since their mixture have, due to the easy different position and wideness of the band gap, the property to hinder the fast electron-hole recombination reaction (Atitar et al., 2015; He et al., 2014; Ibrahim et al., 2017).

Table 1. Synthesis conditions and samples labeling for the TiO₂-Ag nanocomposite

Samples	TiP, g	Ethanol, mL	HNO ₃ , mL	NH ₄ OH, mL	AgNO ₃ , g	Hydrazine, g	Calcined
TiO ₂	5.8	10	50	100	-	133	no
S1	5.8	10	50	100	0.418	133	no
S2	5.8	10	50	100	0.418	133	2h

In the meantime, the presence of some dopants induces the easier anatase-rutile transformation, while others inhibit it (Hanaor and Sorell, 2011). The detailed compositions of the synthesis mixtures and the samples labeling are summarized in Table 1.

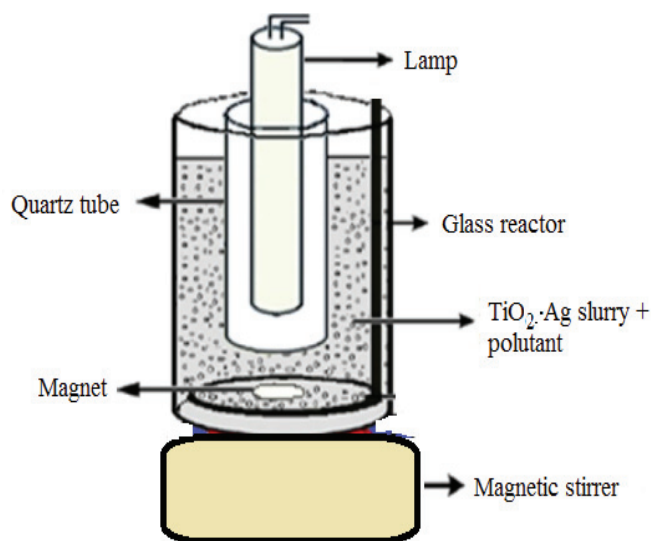
The samples morphology and chemical elementary composition were determined by Scanning Electron Microscopy (SEM) – Electron Dispersive Analysis by X-ray (EDAX) analysis, on a JEOL 6400 machine with an Oxford Link EDAX microanalyser and Pentafet light sensing with coupled EDSX-max (Oxford Instruments).

The chemical composition was obtained by performing minimum 5 determinations for each sample, in different points, and averaging the individual results, since EDAX analysis provides local concentrations. The transmission electron microscopy (TEM) and Selected Area Electron Diffraction (SAED) images were obtained on a JEOL JEM-2100 apparatus, working at accelerating voltage mode at 200 kV, obtaining a resolution of 0.14 x 0.25 nm. The X-ray diffraction (XRD) patterns were obtained on a Philips model X'Pert PDP3040 device with Cu K α 1 source ($\lambda = 1.5462 \text{ \AA}$), working at 40 kV and 40 mA, with curved single crystal monochromator of copper for eliminating the contributions of K α 2 radiation. The analysis of the diffraction patterns was realized with X'Pert High Score Plus PANalytical database software (version 2.0) (Nutescu Duduman et al., 2016).

2.2. Photocatalytic activity

The photocatalytic degradation was performed in a cylinder shape glass reactor (Fig. 1), equipped with a central quartz tube to host an Osram lamp of 9W and magnetic stirring. The pH value was measured by a Hanna HI 991003 pH-meter and set to the chosen value by adding nitric acid 0.1 M or sodium hydroxide 0.1 M. Prior to the photocatalytic run, the photocatalyst powder finely crushed in a mortar was dispersed in the dye solution, stirred for 30 minutes in dark at room temperature, to reach the adsorption/desorption equilibrium, then the UV lamp was turned on. The time zero concerning the behavior of the dye corresponds to the switch on of the lamp, therefore, the moment when the solid is contacted with the solution means – 30 minutes. Samples of approximately 5 mL mixture were withdrawn at defined time durations from the photo-reactor, filtered through 0.45 μm syringe filter to separate the solid and measured by spectrophotometry.

All experiments were run at ambient temperatures. Rhodamine 6G (R6G) and Methyl Blue (MB) were used as test dyes to evaluate the photocatalytic potential of the solids. The dye concentration were measured by UV-Vis spectroscopy on a Shimadzu UV-1700 spectrophotometer, on the basis of the main maxima of absorption in the visible region of the spectra, situated at 526.5 nm (R6G) and 568 nm (MB), respectively.

**Fig. 1.** Experimental setup for photocatalytic tests

The Lambert-Beer law is valid for R6G at concentrations below 12 ppm, therefore the dilution of the solutions of higher concentrations was made accordingly. The conversion degree of the dye was calculated as its decolorization yield, by measuring the concentrations values of the dye by spectrophotometry, using the (Eq. 1):

$$\text{Decolorization (\%)} = 100 (C_0 - C)/C_0, \% \quad (1)$$

where: C_0 is the initial concentration and C is the concentration at time t .

3. Results and discussion

3.1. Sample characterization

The nature of the phases and the crystallinity degree was analyzed by XRD, the patterns are shown in Fig. 2. The peak locations and relative intensities were fitted from the Joint Committee on Powder Diffraction Standards (JCPDS) database: TiO₂anatase (JCPDS 21-1272), TiO₂ rutile (JCPDS 21-1276), silver (JCPDS 04-0783) and silver oxide Ag₂O (JCPDS 00-076-139).

In all samples, the main peaks can be assigned to anatase by the following planes and corresponding 2θ angles: [101] (25.3°); [004] (38°); [200] (48°); [105] (54°); [204] (62.55°) and [116] (69°) (Sakurai and Mizusawa, 2010). The undoped TiO₂ is almost pure anatase, but the noisy pattern suggests the presence of significant amounts of amorphous phase. The larger width and the less sharpness of the peaks of sample S1 compared to S2 indicate that the first sample is less crystalline and has smaller particle size than the other. Also, S1 contains mostly anatase crystalline phase, while S2 is a mixture of anatase and rutile, as proved by the distinctive peaks at 27.5 and 36°, due to the rutile [110] and [101] planes. The lower position of the baseline for sample S2 indicates its higher crystallinity degree compared to S1. Silver was identified in S1 and S2, respectively, as metallic Ag by the peaks at 38.1° [111], 44.5° [200] and 64.4° [220] (Amin et al., 2009;

Brook et al., 2007), as AgO (32.8, 34, 38.2 and 40°) and as Ag₂O (38 and 44.5°) (Waterhouse et al., 2001). There are several overlapped peaks between silver and titania, therefore the individual contributions of the mentioned phases were labeled on Fig. 2. The unidentified peaks from S2 marked with asterisk (*) can be assigned to stable silver-organic combinations formed and stabilized during the thermal treatment (Gauri et al., 2016).

The SEM images and an exemplification of EDAX image for the as-synthesized and calcined samples are presented in Fig. 3. Sample S1 consists of compact agglomerations of small, irregularly shaped particles. The calcined sample S2 has a quite similar aspect, even more compact, with some small particles attached on the outer surface of the aggregates.

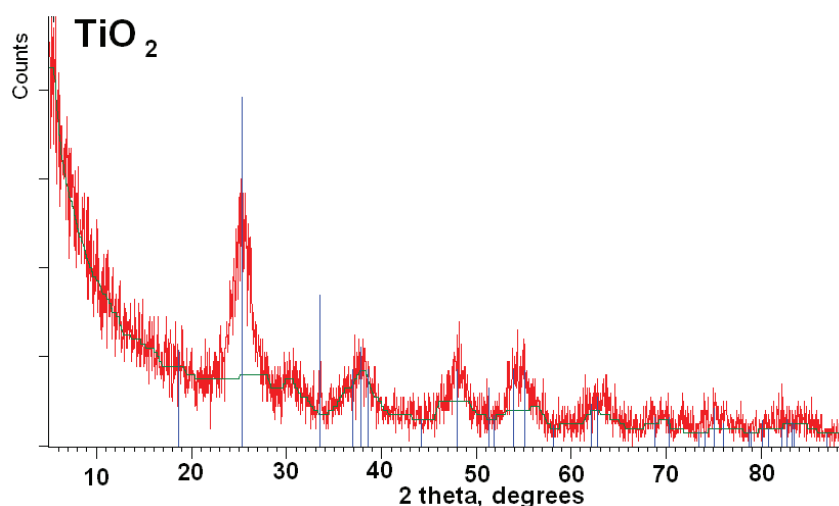
The EDAX analysis results (Table 2) show that upon calcination, the silver ratio at the surface decreases, indicating its migration inside the titania structure, as previously mentioned in literature (Amin et al., 2009; Hussain et al., 2016; Zhao and Chen, 2011).

Table 2. Elemental composition of samples S1 and S2

Element	Sample 1	Sample 2
O	51.78±1.2	51.53±1.45
Ti	41.29±0.5	44.29±0.9
Ag	6.94±0.85	4.17±0.4

The high resolution SEM images of samples S1 and S2 are presented in Fig. 4. The structure contains in both cases agglomerated nanoparticles, but their aspect changed significantly after the thermal exposure. In the case of as-synthesized sample, the surface is rather smooth, while during the calcination, the surface becomes rough and has the aspect of agglomerated small flakes.

The TEM and SAED images of samples S1 and S2 are shown in Fig. 5. The TEM images prove the uniform dispersion of the Ag nanoparticles, appearing as dark spots on the major TiO₂ phase. The crystallite size of TiO₂ increases after calcination.



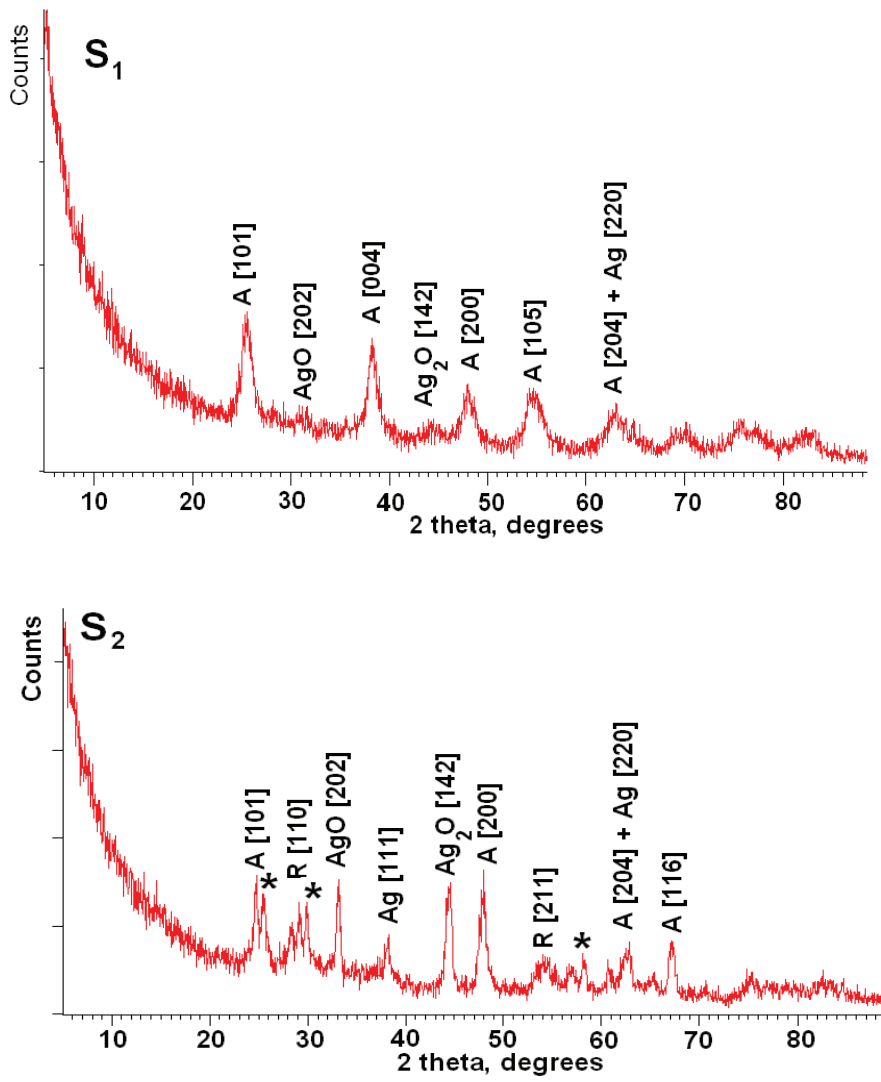
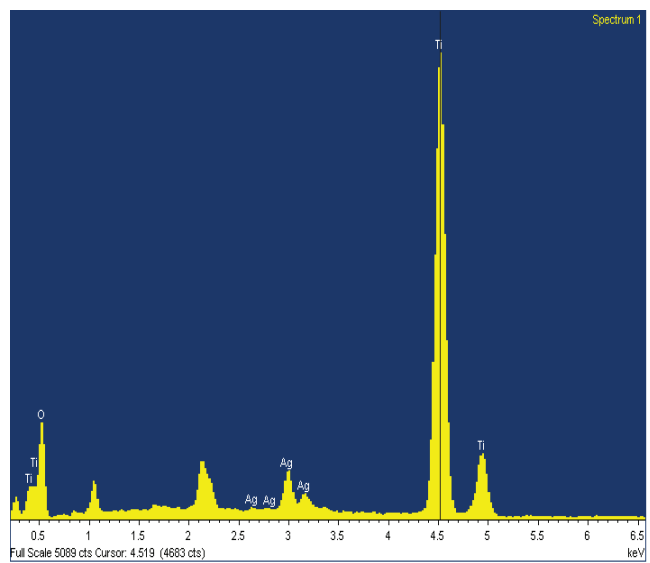
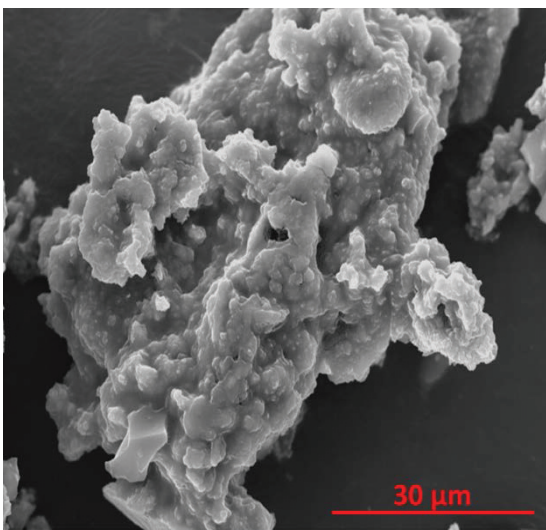
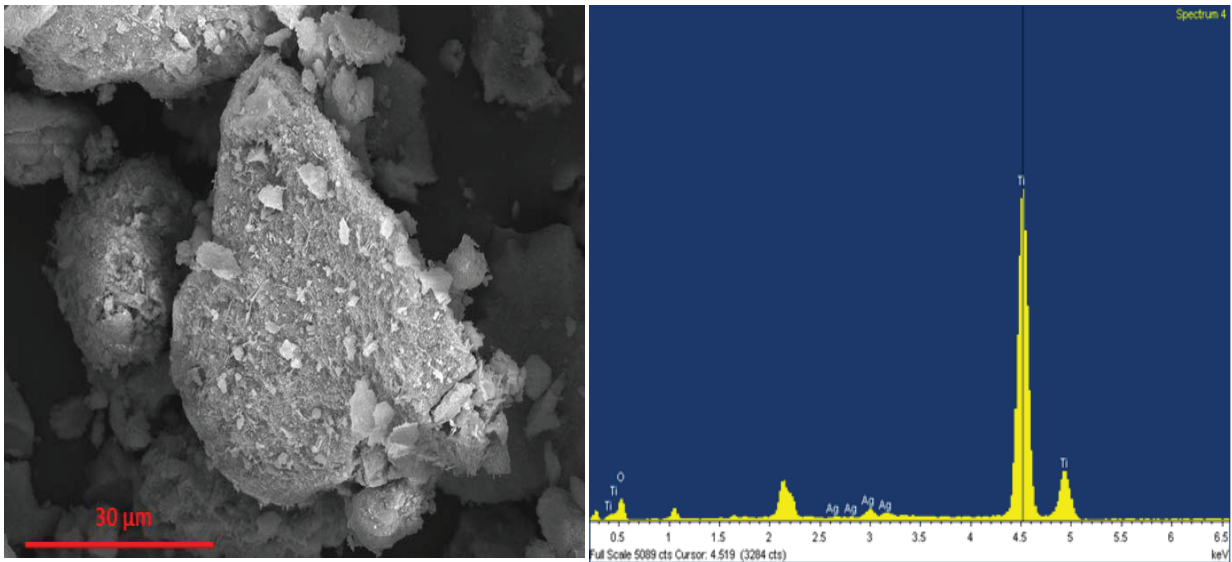


Fig. 2. Powder XRD patterns of synthesized samples: A – anatase, R – rutile



a - S1



b – S2

Fig. 3. SEM micrographs and EDAX snapshots of samples S1 and S2

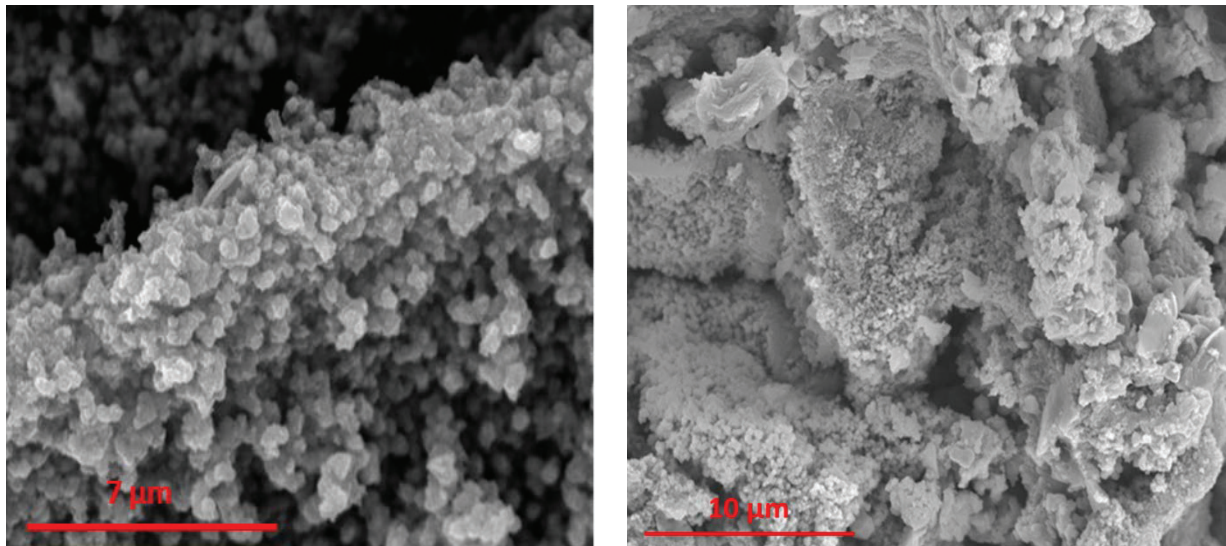
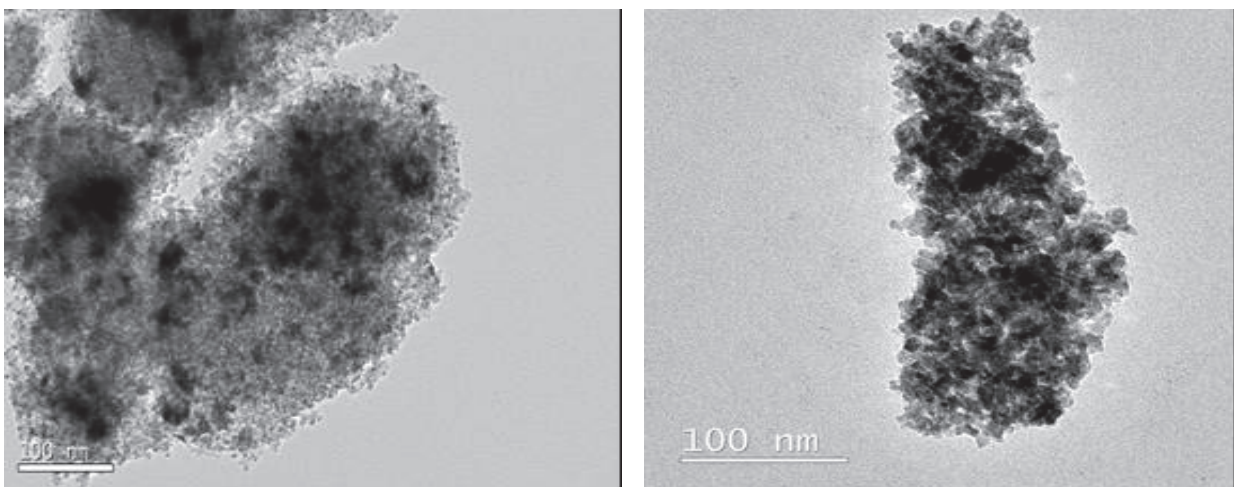


Fig. 4. Micrographs of samples S1 and S2 at high-resolution



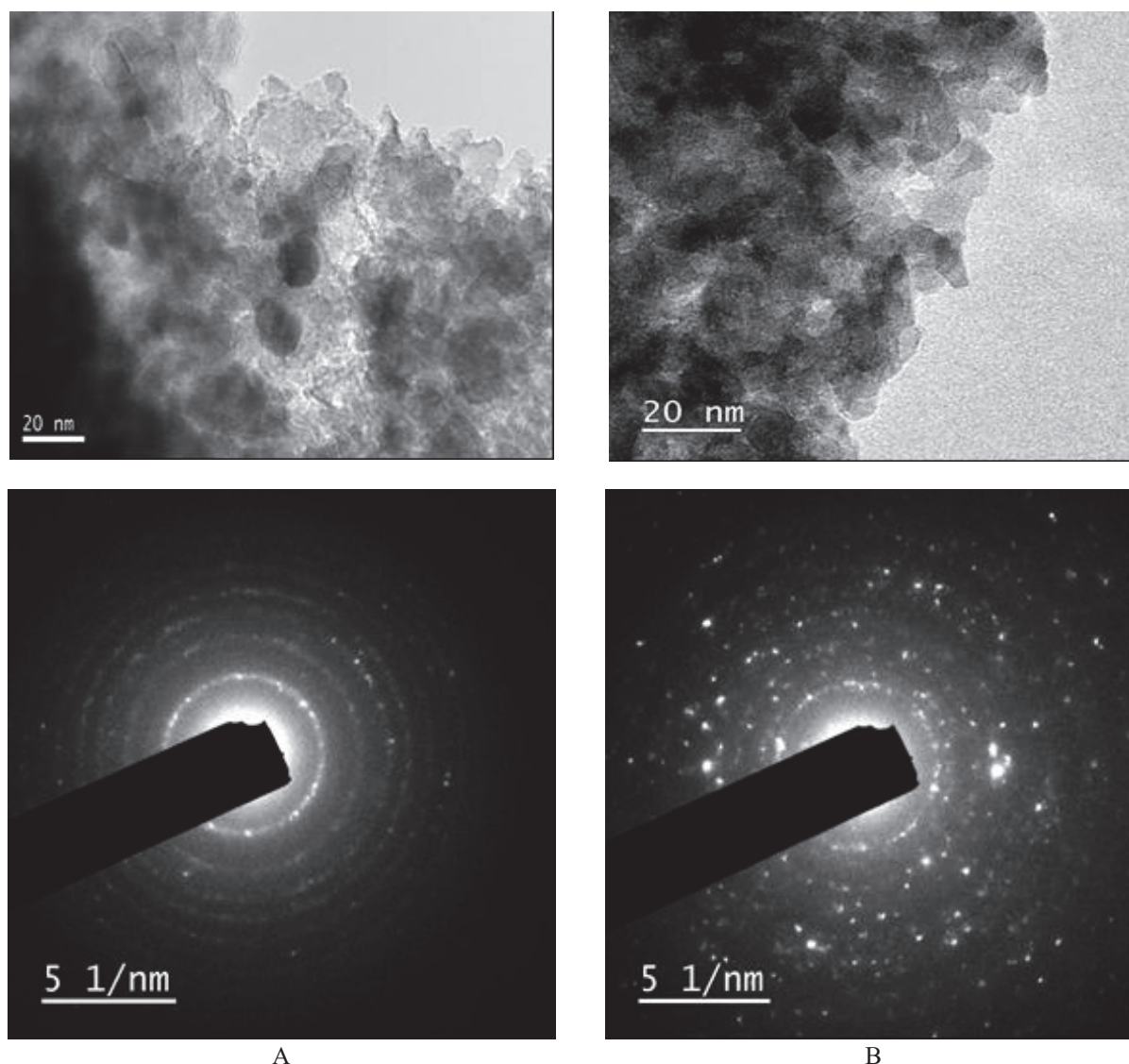


Fig. 5. TEM and SAED of samples S1 (A) and S2 (B)

Table 3. Interplanar distances (Å) for the nanoparticles of S1, deduced from SAED and XRD

<i>Distance from SAED</i>	3.525	2.363	1.90	1.66	1.458
<i>Distance from XRD</i>	3.517	2.366	1.893	1.696	1.483
<i>Interplanar distance from literature (Massard)</i>	3.51	2.33	1.89	1.66	-
<i>Miller indices</i>	[101]	[004]	[200]	[105]	[204]

The SAED pattern of S1 indicates that the crystallinity degree of the samples is not very high, since the rings are not continuous and bright, in line with the results from XRD. After the calcination, the sample becomes poly-nanocrystalline, as shown by the high number of light spots in Fig. 5B.

The SAED image of sample S1 was used to determine the values of the interplanar distances from the structure (Table 3). These values were compared with the theoretically calculated values available in literature (Massard et al., 2012) and the ones obtained from the XRD patterns using the relation of Bragg (Eq. 2):

$$\lambda = 2 D \sin \theta \quad (2)$$

where λ is the wavelength of X-Ray (1.5406 Å), D is the interplanar distance and θ the incidence angle.

The values from Table 3 correlate very well between the two analysis methods and are in agreement with literature data. The investigated area contained only TiO₂-anatase.

3.2. Environmental application

The heterogeneous photocatalytic degradation of organic dyes by TiO₂ and TiO₂-Ag nanocomposites was investigated in the photocatalytic degradation of Rhodamine 6 G (R6G) and Methyl Blue (MB) dyes.

The R6G concentrations were of 15 and 30 ppm, the photocatalyst dose of 1 g L⁻¹ and the pH was 4.2 (native value of the dye). In order to improve the

conductivity of the dye solution, a similar experiment was performed using sodium nitrate as an agent to introduce some extra ions in the reaction medium (Atitar et al., 2015).

A comparison between the two series of tests (15 and 30 ppm of dye), in terms of decolorization extent, performed on TiO₂, S1 and S2 of dye is displayed in Fig. 6. The results highlight the beneficial role of Ag doping of the TiO₂ sample. Both S1 and S2 samples have higher photocatalytic activities than the undoped sample, for both dye concentration values. The calcined form has a much better behavior, especially when the dye concentration is low, being able to decompose 85% of the dye in two hours of exposure to UV light from the 15 ppm solution and, respectively, 53% in the case of 30 ppm solution.

The higher activity of the doped titania samples compared with the pure TiO₂ can be explained by the contribution of the silver compounds (Jiang et al., 2015), which have a very low band gap (1.3 eV) and form boundaries by the aggregation of Ag₂O nanoparticles on the support, very efficient in escaping the photogenerated electrons and avoid the recombination electron-hole. On another part, the calcination generates a proper ratio between anatase and rutile (Dariani et al., 2016; Dorian et al., 2011; Ghazzal et al., 2012), which has an important role in the optimization of the electron-hole pair formation and avoiding the recombination process. The position of the energy levels of the valence band and conduction bands of the two phases favors the migration of the promoted electron from the anatase conduction band to the conduction band of rutile, instead allowing the recombination (Scanlon et al., 2013).

An example of the spectra evolution in time (Fig. 7) shows that the decrease of the main peak of R6G from 526.5 nm is strong, as well as that of the peak at 248 nm. Another peak increases progressively around 220 nm, due probably to nitrate ions issued during the degradation of the dye.

The photocatalytic reactions are usually strongly influenced by the pH value and by the conductivity of the solution. A test was made at 30 ppm of R6G at pH of 8 (Lutic and Cretescu, 2016). Some studies (Atitar et al., 2015) indicate that the increase the conductivity of the dye solution is beneficial on the organic compounds removal from solutions. In order to check this fact in our case, a similar experiment was performed using sodium nitrate (0.1 M) as an ions provider in the reaction medium. The decolorization of the dye in time is displayed in Fig. 8.

The results are highly similar in both cases, either using or not the sodium nitrate. The value of the initial solution conductivity did not influence the dye degradation efficiency. The decolorizing degree is of only 34% after 120 minutes and 41% after 180 minutes. So, in our case, the increase of conductivity did not bring any special progress of the decomposition reaction.

The MB dye was also tested as standard compound in the photodegradation. In this case, the initial value of the dye concentration was of 100 ppm and the photocatalyst dose of 0.2 g L⁻¹. The lower solid dose and higher dye concentration chosen are due to the very high efficiency of the photocatalyst in the decolorization. In Fig. 9 is displayed the evolution in time of the MB spectra and in the inset, the evolution in time of the dye concentration.

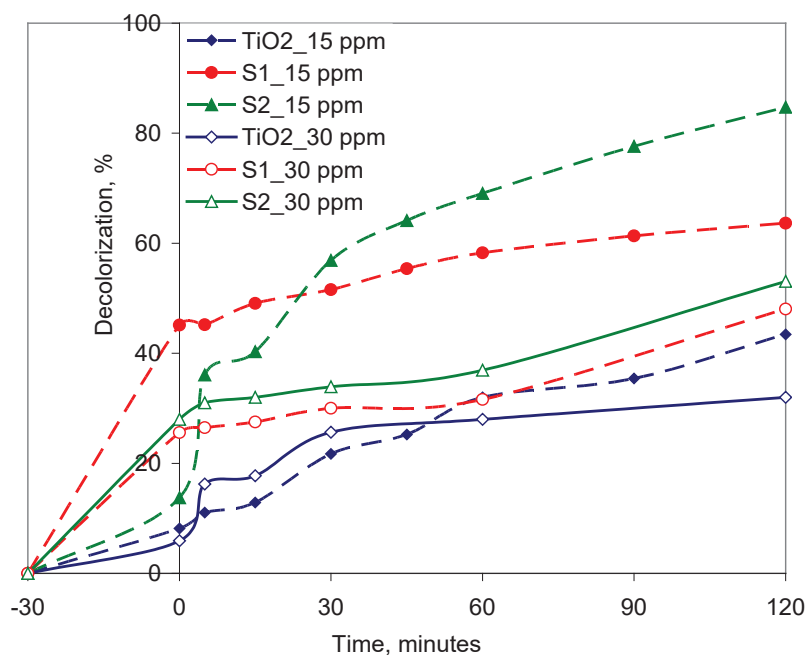


Fig. 6. Conversion versus time of the R6G by photocatalytic degradation on TiO₂-based samples (native dye pH, 1 g L⁻¹ photocatalyst dose)

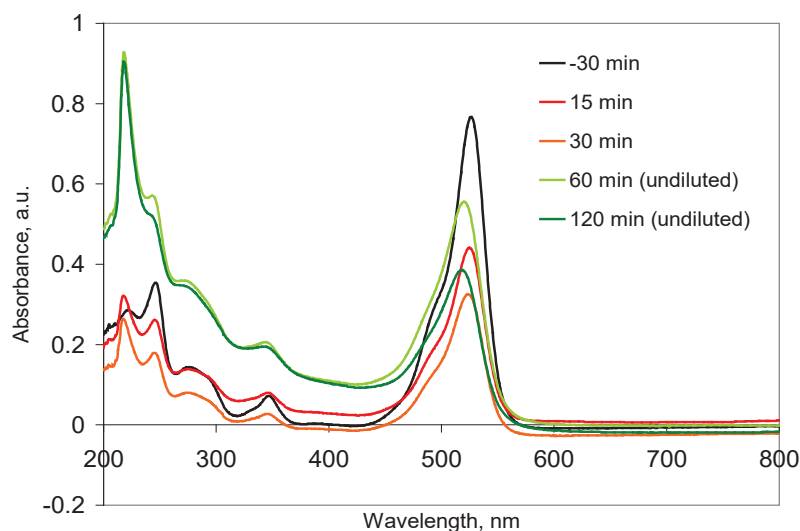


Fig. 7. Spectra evolution in time for 15 ppm of R6G decomposition on S2 (up to 60 min of photocatalysis the dye solution was diluted prior to measuring)

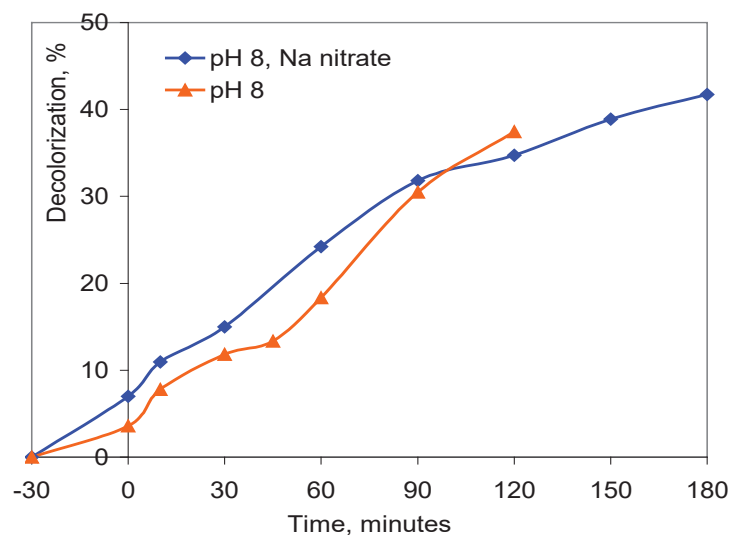


Fig. 8. Influence of sodium nitrate in the reaction medium at pH 8 (1 g L⁻¹ photocatalyst dose, 30 ppm R6G initial concentration; 0.1 mol L⁻¹ NaNO₃)

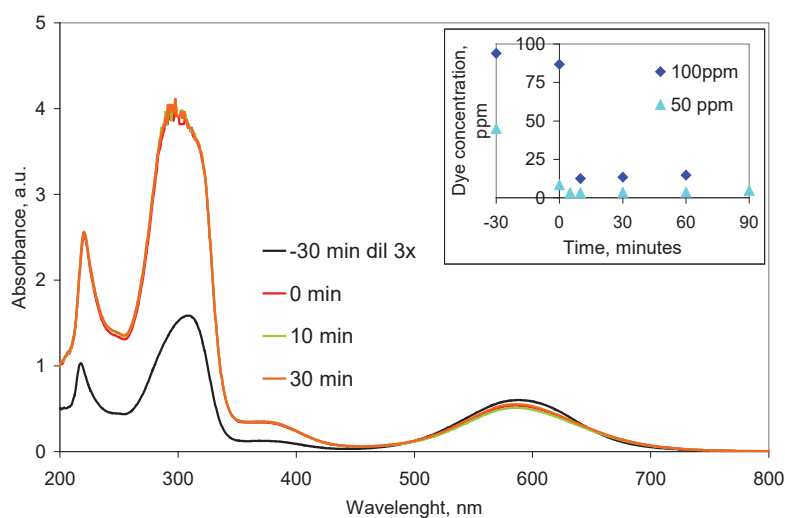


Fig. 9. Spectra in time during the photocatalytic conversion of MB dye (100 ppm MB, 0.2 g L⁻¹ solid) and dye concentrations during 120 min of reaction at 100 and 50 ppm of dye

The decomposition of MB is rapid after switching on the UV light. The decolorization is very fast, but only chromophore group is clearly affected in the process. The spectra provide the production of very large and intense peaks in the UV region of the spectrum, indicating that the initial molecule is only splitted in several fragments, not mineralized, as most photocatalytic reactions aim as the target in the environmental applications.

From these two examples, we can conclude that the structure of the dye is of prime importance in evaluating the behavior of the TiO₂-Ag nanocomposites. Despite the activity in the decomposition of R6G is remarkably high only at low dye concentrations, we should be aware of the antiseptic-disinfection potential of silver in real wastewaters treatment and consider this type of solids as interesting to investigate further.

4. Conclusions

The synthesis of a new photocatalyst with disinfection potential, based on Ag-doped TiO₂ nanoparticles was described. The sol-gel method was combined with impregnation-reduction, in order to obtain a good dispersion of the dopant as small nanoparticles on the surface of the majority phase.

Titanium tetra-isopropoxide was used as a TiO₂ precursor in the synthesis: hydrolyzed in nitric acid solution and precipitated by ammonia solution. The obtained solid was then doped with silver nitrate and the ions reduced to silver with hydrazine. The comparison in terms of structural investigation and photocatalytic testing was made between the as-synthesized product and the one obtained by calcination at 650°C.

The characterization of the prepared samples (simple or calcined) was performed by XRD, SEM, TEM and EDAX. The anatase phase was the main component of the as-synthesized product, while a mixture anatase-rutile was detected in the calcined phase. Silver is well dispersed as nanoparticles in the as-synthesized product, while a mixture of Ag, AgO and Ag₂O exists in the calcined product. Also, a migration of Ag inside the structure during the calcination was highlighted by EDAX.

The photocatalytic activity in the decolorizing of R6G dye indicates the beneficial roles of silver as a dopant and of the calcination process. The conversion degree of R6G (15 ppm aqueous solution) on undoped TiO₂ was only 42%, and reached 48% on the as-synthesized sample and respectively 84% on the calcined one. The attempt to enhance the reaction yield by changing the pH value and the conductivity of the reaction medium did not bring any further success.

The MB was decolorized almost totally in 10 minutes, at higher initial concentrations dye values (100 ppm) and lower photocatalyst dose (0.2 g L⁻¹). However, high amounts of organic intermediates absorbing in the UV region of the spectra were

produced in the solution, making unattractive an eventual application.

The high decomposition yield of organic dyes and the well-known disinfection potential of Ag-containing solids recommend them for testing in wastewaters needing complex treatments.

Acknowledgements

The authors are grateful for the partial support of this work by the Ministry of Economy and Competitiveness from Spain, Reference: MAT2013-46755-R, and grant POSDRU/159/1.5/S/133652.

References

- Amin A.S., Pazouki M., Hosseinnia A., (2009), Synthesis of TiO₂-Ag nanocomposite with sol-gel method and investigation of its antibacterial activity against *E. coli*, *Powder Technology*, **196**, 241-245.
- Atitar M.F., Ismail A.A., Al-Sayari S.A., Bahnemann D., Afanasev D., Emeline A.V., (2015), Mesoporous TiO₂nanocrystals as efficient photocatalysts: Impact of calcination temperature and phase transformation on photocatalytic performance, *Chemical Engineering Journal*, **264**, 417-424.
- Behnajady M., Bimeghdar S., Eskandarloo H., Photocatalytic activity of Ag/TiO₂-P25-modified cement: optimization using Taguchi approach (2018), *Environmental Engineering and Management Journal*, in press.
- Bhakya S., Muthukrishnan S., Sukumaran M., Muthukumar M., Senthil Kumar T., Rao M.V., (2015), Catalytic degradation of organic dyes using synthesized silver nanoparticles: a green approach, *Journal of Bioremediation & Biodegradation*, **6**, 1-9.
- Brook L.A., Evans P., Foster H.A., Pemble M.E., Steele A., Sheel D.W., Yates H.M., (2007), Highly bioactive silver and silver/titania composite films grown by chemical vapour deposition, *Journal of Photochemistry and Photobiology A: Chemistry*, **187**, 53-63.
- Chen C., Ma W., Zhao J., (2010), Semiconductor-mediated photodegradation of pollutants under visible-light irradiation, *Chemical Society Reviews*, **39**, 4206-4219.
- Cheriyian A.J., Shaik F., Baawain A., Said M., Sarkar J.P., (2017), A study on the removal of contaminants from secondary treated municipal wastewater by solar photocatalysis, *Environmental Engineering and Management Journal*, **16**, 1451-1456.
- Ciobanu G., Harja M., Rusu L., Mocanu A.M., Luca C., (2014), Acid Black 172 dye adsorption from aqueous solution by hydroxyapatite as low-cost adsorbent, *Korean Journal of Chemical Engineering*, **31**, 1021-1027.
- Ciobanu G., Ilisei S., Harja M., Luca C., (2013), Removal of Reactive Blue 204 dye from aqueous solutions by adsorption onto nanohydroxyapatite, *Science of Advanced Materials*, **5**, 1090-1096.
- Darriani R.S., Esmacili A., Mortezaali A., Dehghanpour S., (2016), Photocatalytic reaction and degradation of methylene blue on TiO₂nano-sized particles, *Optik - International Journal for Light and Electron Optics*, **127**, 7143-7154.
- Djoki V.R., Marinkovic A.D., Mitric M., Uskokovic P.S., Petrovic R.D., Radmilovic V.R., Janackovic D.T., (2012), Preparation of TiO₂/carbon nanotubes photocatalysts: the influence of the method of oxidation

- of the carbon nanotubes on the photocatalytic activity of the nanocomposites, *Ceramics International*, **38**, 6123-6129.
- Dorian A.H., Hanaor D.A.H., Sorrell C.C., (2011), Review of the anatase to rutile phase transformation, *Journal of Materials Science*, **46**, 855-874.
- Favier L., Harja M., Simion A.I., Rusu L., Kadmi Y., Pacala M.L., Bouzaza A., (2016), Advanced oxidation process for the removal of chlorinated phenols in aqueous suspensions, *Journal of Environmental Protection and Ecology*, **17**, 1132-1141.
- Galkina O.L., Vinogradov V.V., Agafonov A.V., Vinogradov A.V., (2011), Surfactant-assisted sol-gel synthesis of TiO₂ with uniform particle size distribution, *International Journal of Inorganic Chemistry*, **2011**, 1-8, Article ID 108087.
- Gauri B., Vidya K., Dagade S.P., Shobha W., (2016), Synthesis and characterization of Ag/AgO nanoparticles as alcohol sensor, *Research Journal of Chemistry and Environment*, **20**, 1-5.
- Ghazzal M.N., Kebaili H., Joseph M., Debecker D.P., Eloy P., De Coninck J., Gaigneaux E.M., (2012), Photocatalytic degradation of Rhodamine 6G on mesoporous titania films: Combined effect of texture and dye aggregation forms, *Applied Catalysis B: Environmental*, **115-116**, 276-284.
- Gómez de Salazar J.M., Nutescu Duduman C., Juárez Gonzalez M., Palamarciuc I., Barrena Pérez M. I., Carcea I., (2016), Research of obtaining TiO₂ by sol-gel method using titanium isopropoxide TIP and tetra-n-butyl orthotitanate TNB, *IOP Conference Series: Materials Science and Engineering*, **145**, Micro and Nano Technologies, 1-6.
- Hanaor A.H., Sorrell C.C., (2011), Review of the anatase to rutile phase transformation, *Journal of Materials Science*, **46**, 855-874.
- Harja M., Barbuta M., Rusu L., Munteanu C., Buema G., Doniga E., (2011), Simultaneous removal of Astrazone blue and lead onto low cost adsorbents based on power plant ash, *Environmental Engineering and Management Journal*, **10**, 341-347.
- Harja M., Ciobanu G., Favier L., Bulgariu L., Rusu L., (2016), Adsorption of crystal violet dye onto modified ash, *The Bulletin of the Polytechnic Institute from Iași. Chemistry and Chemical Engineering Section*, **62**, 27-37.
- He F., Fang Ma, Li J., Li T., Li G., (2014), Effect of calcination temperature on the structural properties and photocatalytic activities of solvothermal synthesized TiO₂ hollow nanoparticles, *Ceramics International*, **40**, 6441-6446.
- He Y., Basnet P., Murph S.E.H., Zhao Y., (2013), Ag nanoparticle embedded TiO₂ composite nanorod arrays fabricated by oblique angle deposition: toward plasmonic photocatalysis, *ACS Applied Materials & Interfaces*, **5**, 11818-11827.
- Hu J., Cao Y., Wang K., Jia D., (2017), Green solid-state synthesis and photocatalytic hydrogen production activity of anatase TiO₂ nanoplates with super heat-stability, *RSC Advances*, **7**, 11827-11833.
- Hussain M., Tariq S., Ahmad M., Sun H., Maaz K., Ali G., Zahid Hussain S., Iqbal M., Karim S., Nisar A., (2016), Ag-TiO₂ nanocomposite for environmental and sensing applications, *Materials Chemistry and Physics*, **181**, 194-203.
- Ibrahim A., Mekprasart W., Pecharapa W., (2017), Anatase/Rutile TiO₂ composite prepared via sonochemical process and their photocatalytic activity, *Materials Today: Proceedings*, **4**, 6159-6165.
- Ivanova T., Harizanova A., Koutzarova T., Vertruyen B., (2013), Optical and structural characterization of TiO₂ films doped with silver nanoparticles obtained by sol-gel method, *Optical Materials*, **36**, 207-213.
- Jiang W., Wang X., Wu Z., Yue X., Yuan S., Lu H., Liang B., (2015), Silver oxide as superb and stable photocatalyst under visible and near-infrared light irradiation and its photocatalytic mechanism, *Industrial and Engineering Chemistry Research*, **54**, 832-841.
- Kartal O.E., Turhan G.D., (2017), Determination of electrical energy cost of decolorization of C.I. Acid Orange 7 via TiO₂-assisted photocatalysis under UV illumination in the presence of H₂O₂, *Environmental Engineering and Management Journal*, **16**, 2045-2052.
- Kochuveedu S.T., Kim D.P., (2012), Surface-plasmon-induced visible light photocatalytic activity of TiO₂ nanospheres decorated by Au nanoparticles with controlled configuration, *The Journal of Physical Chemistry C*, **116**, 2500-2506.
- Lee M.S., Hong S.S., Mohseni M., (2005), Synthesis of photocatalytic nanosized TiO₂-Ag particles with sol-gel method using reduction agent, *Journal of Molecular Catalysis A: Chemical*, **242**, 135-140.
- Liu S.X., Qu Z.P., Han X.W., Sun C.L., (2004), A mechanism for enhanced photocatalytic activity of silver-loaded titanium dioxide, *Catalysis Today*, **93**, 877-884.
- Liu X., Bi Y., (2017), In situ preparation of oxygen-deficient TiO₂ microspheres with modified {001} facets for enhanced photocatalytic activity, *RSC Advances*, **7**, 9902-9907.
- Liu R., Ren F., Su W., He P., Shen C., Zhang L., Wang C., (2015), Synthesis of TiO₂ hollow spheres with tunable pore structure and enhanced photocatalytic activity, *Ceramics International*, **41**, 14615-14620.
- Lutic D., Cretescu I., (2016), Optimization study of Rhodamine 6G removal from aqueous solutions by photocatalytic oxidation, *Revista de Chimie (Bucharest)*, **67**, 134-138.
- Lutic D., Coromelci-Pastravanu C., Cretescu I., Poullos I., Stan C.D., (2012), Photocatalytic treatment of Rhodamine 6G in wastewater using photoactive ZnO, *International Journal of Photoenergy*, **2012**, 1-8.
- Lutic D., Coromelci C.G., Juzsakova T., Cretescu I., (2017), New mesoporous titanium oxide-based photoactive materials for the removal of dyes from wastewaters, *Environmental Engineering and Management Journal*, **6**, 801-807.
- Mahmoodi N.M., Khari F.A., Khatibzadeh M., Gharanjig K., (2017), Synthesis of alginate amide composite using microwave and its dye removal ability, *Environmental Engineering and Management Journal*, **16**, 1859-1866.
- Massard C., Bourdeaux D., Raspal V., Feschet-Chassot E., Sibaud Y., Caudron E., Devers T., Awitor K.O., (2012), One-pot synthesis of TiO₂ nanoparticles in suspensions for quantification of titanium debris release in biological liquids, *Advances in Nanoparticles*, **1**, 86-94.
- Montazerzohori M., Hoseinipour S.A., (2017), Decolorization of p-dimethylaminobenzal-rhodanine under photocatalytic process by use of titanium dioxide nanoparticles at various buffer pHs, *Environmental Engineering and Management Journal*, **16**, 1853-1858.
- Nakata K., Fujishima A., (2012), TiO₂ photocatalysis design and applications, *Journal of Photochemistry and Photobiology C: Photochemistry Reviews*, **13**, 169-189.
- Niu Y., Xing M., Tian B., Zhang J., (2012), Improving the visible light photocatalytic activity of nano-sized titanium dioxide via the synergistic effects between

- sulfur doping and sulfation, *Applied Catalysis B: Environmental*, **115-116**, 253-260.
- Nutescu Duduman C., Gómez De Salazar J.M., Barrena Pérez M.I., Harja M., Palamarciuc I., Gómez De Castro C., (2016a), Obtained of nanocomposites: Cu, CuO and Cu(OH)₂ - CNF by sol-gel method, *International Journal of Modern Manufacturing Technologies*, **VIII**, 13-18.
- Nutescu Duduman C., Gómez De Salazar J.M., Barrena Pérez M.I., Carcea I., Palamarciuc I., (2016b), Research on obtaining TiO₂-CNF nanocomposites, *International Journal of Modern Manufacturing Technologies*, **VIII**, 30-34.
- Pham T.D., Lee B.K., (2004), Effects of Ag doping on the photocatalytic disinfection of *E. coli* in bioaerosol by Ag-TiO₂/GF under visible light, *Journal of Colloid and Interface Science*, **428**, 24-31.
- Rupa V., Manikandan D., Divakar D., Sivakumar T., (2007), Effect of deposition of Ag on TiO₂ nanoparticles on the photodegradation of reactive yellow-17, *Journal of Hazardous Materials*, **147**, 906-913.
- Rusu L., Harja M., Simion A.I., Suteu D., Ciobanu G., Favier L., (2014), Removal of astrazone blue from aqueous solutions onto brown peat. Equilibrium and kinetics studies, *Korean Journal of Chemical Engineering*, **31**, 1008-1015.
- Sakurai K., Mizusawa M., (2010), X-ray diffraction imaging of anatase and rutile, *Analytical Chemistry*, **82**, 3519-3522.
- Sarina S., Waclawik E.R., Zhu H., (2013), Photocatalysis on supported gold and silver nanoparticles under ultraviolet and visible light irradiation, *Green Chemistry*, **15**, 1814-1833.
- Scanlon D.O., Dunnill C.W., Buckeridge J., Shevlin S.A., Logsdail A.J., Woodley S.M., Catlow C.R.A., Powell M.J., Palgrave R.G., Parkin I.P., Watson G.W., Keal T.K., Sherwood P., Walsh A., Sokol A.A., (2013), Band alignment of rutile and anatase TiO₂, *Nature Materials*, **12**, 798-801.
- Tian B., Dong R., Zhang J., Bao S., Yang F., Zhang J., (2014), Sandwich-structured AgCl@Ag@TiO with excellent visible-light photocatalytic activity for organic pollutant degradation and *E. coli* K12 inactivation, *Applied Catalysis B: Environmental*, **158-159**, 76-84.
- Tobaldi D.M., Pullar R.C., Gualtieri A.F., Seabra M.P., Labrincha J.A., (2013), Sol-gel synthesis, characterisation and photocatalytic activity of pure, W, Ag and W/Ag co-doped TiO₂ nanopowders, *Chemical Engineering Journal*, **214**, 364-375.
- Vajda K., Saszet K., Kedves E.Z., Kása Z., Danciu V., Baia L., Magyari K., Hernádi K, Kovács G., Pap Z., (2016), Shape-controlled agglomeration of TiO₂ nanoparticles, New insights on polycrystallinity vs. single crystals in photocatalysis, *Ceramics International*, **42**, 3077-3087.
- Wang M., Zhang W., Zheng X., Zhu P., (2017), Antibacterial and catalytic activities of biosynthesized silver nanoparticles prepared by using an aqueous extract of green coffee bean as a reducing agent, *RSC Advances*, **7**, 12144-12149.
- Waterhouse G.I.N., Bowmaker G.A., Metson J.B., (2001), The thermal decomposition of silver (I, III) oxide: A combined XRD, FT-IR and Raman spectroscopic study, *Physical Chemistry Chemical Physics*, **3**, 3838-3845
- Wei P., Liu J., Li Z., (2013), Effect of Pt loading and calcination temperature on the photocatalytic hydrogen production activity of TiO₂ microspheres, *Ceramics International*, **39**, 5387-5391.
- Yin H., Yu K., Song C., Huang R., Zhu Z., (2014), Synthesis of Au-Decorated V₂O₅@ZnO heteronanostructures and enhanced plasmonic photocatalytic activity, *ACS Applied Materials & Interfaces*, **6**, 14851-14860.
- Zhao B., Chen Y.W., (2011), Ag/TiO₂ sol prepared by a sol-gel method and its photocatalytic activity, *Journal of Physics and Chemistry of Solids*, **72**, 1312-1318.



“Gheorghe Asachi” Technical University of Iasi, Romania



INDICATORS SYSTEM FOR ASSESSING THE ORGANIZATIONAL KNOWLEDGE ACQUISITION PROCESS

Daniela Geanina Luca Cososchi, Alina Luca, Luminița Mihaela Lupu*,
Ionuț Viorel Herghiligiu

“Gheorghe Asachi” Technical University of Iași, Department of Engineering and Management,
29 Prof. Dr. Docent Dimitrie Mangeron Street, 700050 Iași, Romania

Abstract

In recent years the organizations' has gone from resource-based economy to a knowledge based economy. Likewise the organizations' success in this turbulent environment depends on its sustainable orientation which implies integration of various management practices. Such a management practices considered to be a driving force to sustainable development are environmental management system (EMS) and knowledge acquisition. In this context, it's required to measure the organizational knowledge management performance and to identify viable knowledge acquisition metrics.

This paper aim to develop a managerial instrument in order to measure each steps of knowledge acquisition process. Therefore the main objective is to elaborate an indicators system with the purpose to assess the environmental knowledge acquisition process. The main results of this approach are: (1) development of a methodology in order to elaborate an indicators system associated to knowledge acquisition process; (2) development of an indicators system in order to assess the steps which characterizes the environmental knowledge acquisition process. The results are based on a research that addresses knowledge acquisition process within organization from NE area of Romania; the research sample was 182 respondents. This research approach is innovative and original because in the literature are not being identified indicators which organizational assess each of the environmental knowledge acquisition stages.

Key words: environmental knowledge acquisition process, indicators system/ metrics, knowledge management

Received: May, 2017; *Revised final:* March, 2018; *Accepted:* March, 2018; *Published in final edited form:* April 2018

1. Introduction

The report “Climate change, impacts and vulnerability in Europe 2016 (<http://www.eea.europa.eu/ro/highlights/schimbarile-climatic-reprezinta-un-factor>), made public in January 2017, underlines the important impact which climatic changes have on ecosystems, economy and people's health. Likewise worldwide there exist an increasing concern regarding the companies' impact on the environment (Farneti and Guthrie, 2009; Comăniță et al., 2015; Dominguez et al., 2016; Ghinea et al., 2016; Istrate et al., 2017). Basically, this means that at each organization level the environmental

policies should become a daily activity vector, while the environmental management system (EMS) should become an important part of the general management system. Also, the environmental performance should be as close as possible to the imposed targets.

Likewise it should be mention that the success of any organization in this turbulent environment depends on its sustainable orientation which implies integration of various management practices. Such management practices considered to be a driving force to sustainable development and knowledge acquisition (Herghiligiu, 2017) is EMS - design according with ISO 14001 (Sebhatu and Enquist, 2007) or with EMAS (Wijesooriya et al., 2011). In this context, the

* Author to whom all correspondence should be addressed: e-mail: luminitalupu2011@gmail.com

ISO 14001 EMS implementation constitutes a desirable outcome that every organization has to reach. This organizational practice it's integrated in the context in which the society has evolved from the resource based economy to knowledge based economy; organizations leaders (i) have to deal every day with large amounts of information, (ii) have to select and manage it in order to identify and assimilate fast the necessary knowledge, and (iii) to adopt suitable decisions in order to achieve organizations' objectives.

Thus, in knowledge based economy paradigm, knowledge management is the organization performance core; also equally in environment management the correct interpretation and measurement regarding the knowledge acquisition process, it's a necessity.

In the literature we did not find representative researches regarding organizational knowledge acquisition assessment (associated to knowledge management field), and much less in the field of environment management. Therefore the aim of this paper is to present an evaluation indicators system for each of the stages associated to environmental knowledge acquisition that is considered to be a primordial process in the environmental knowledge management. Likewise it's should be mention the fact that a real organizational EMS integration it's based on an efficient and effective environmental knowledge management process that has as its core the knowledge acquisition. Also a real integration of such an environmental practice (EMS) bring multiple benefits such: market share, employees motivation, customer loyalty and trust, cost reductions, operation and process efficiency, business reputation, profitability, and so on (Halis and Halis, 2016; Herghiligiu, 2013; Tari et al., 2012; Vaute-Samanni and Grevêche, 2015).

Therefore, a clear and efficient evaluation indicators system associated to environmental knowledge acquisitions process can be considered a very useful managerial instrument, with direct correlation on environmental decision making processes.

The paper is structured in 3 sections, as follows: section 1 – Material and methods, which include (i) the literature review regarding the importance and necessity associated to the environmental knowledge acquisition process assessment, and (ii) the research methodology; section 2 – Results and discussions; and section 3 – Conclusions.

2. Material and methods

2.1. Importance and necessity of environmental knowledge acquisition process assessment

Environmental knowledge can be addressed in simple terms as “... *what people know about the environment, key relationships leading to environmental aspects or impacts, an appreciation of*

“whole systems”, and collective responsibilities necessary for sustainable development” (Fryxell and Lo, 2003). Taking into account the fact that managers can influence directly the organizational environmental orientation, the environmental knowledge acquisition and the organizational ability to assess such information “would appear to be inherently desirable” (Fryxell and Lo, 2003; Kaplan, 2000). Literature presents an increasing role of knowledge management in “key areas of environmental management” (Boiral, 2002). Roome and Wijen (2006) argue that a “superior environmental performance” requires capabilities “to process new information ... and to adapt the organization to contexts”. Organizational integration of different knowledge management instruments associated to environmental issues becomes an essential process for SMEs (Roy and Thérin, 2008). Even if the literature on environmental management and SMEs is growing (Hitchens et al., 2003; McKeiver and Gadenne, 2005; Rothenberg and Becker, 2004), few studies have focused on the knowledge acquisition process (Roy and Thérin, 2008). For elaborating this paper we started with a more extensive previous researches (Luca, 2016; Luca et al., 2016a, 2016b, 2016c) that addresses (investigation, analysis and improvement) knowledge acquisition process within organization from NE area of Romania; the research sample was 182 respondents. This research involves elaboration of quantitative and qualitative working instruments, methodologies and methods (Fig. 1). The research aimed a qualitative and quantitative analysis regarding the relation between various organizational components (intellectual capital) and the stages of the organizational knowledge acquisition process.

The statistical study established the influences between the variables that describe these connections, leading to various solutions with the main purpose to improve the organizational knowledge acquisition process. Following this extensive analysis the necessity of elaborating an evaluation indicators system for the organizational knowledge acquisition process became obvious.

In this context, the main objective of the paper consists in elaborating an evaluation indicators system for the process of organizational environmental knowledge acquisition.

Economic realities place organizations in the situation in which they have to face a very large amount of information, and the competitive advantage nowadays is given by the originality of the way in which they use this information. Segarra-Cipres et al. (2014) notices the fact that the competitive advantage of an organization is directly linked to the capacity of identifying valuable external knowledge and integrated it in its own innovation process. Ulrey (2015) states the fact that the recent rebirth of the field of environmental knowledge acquisition is no coincidence, but rather the results of an explosion of the social medial and of the pressure placed on organizations by the economic crisis.

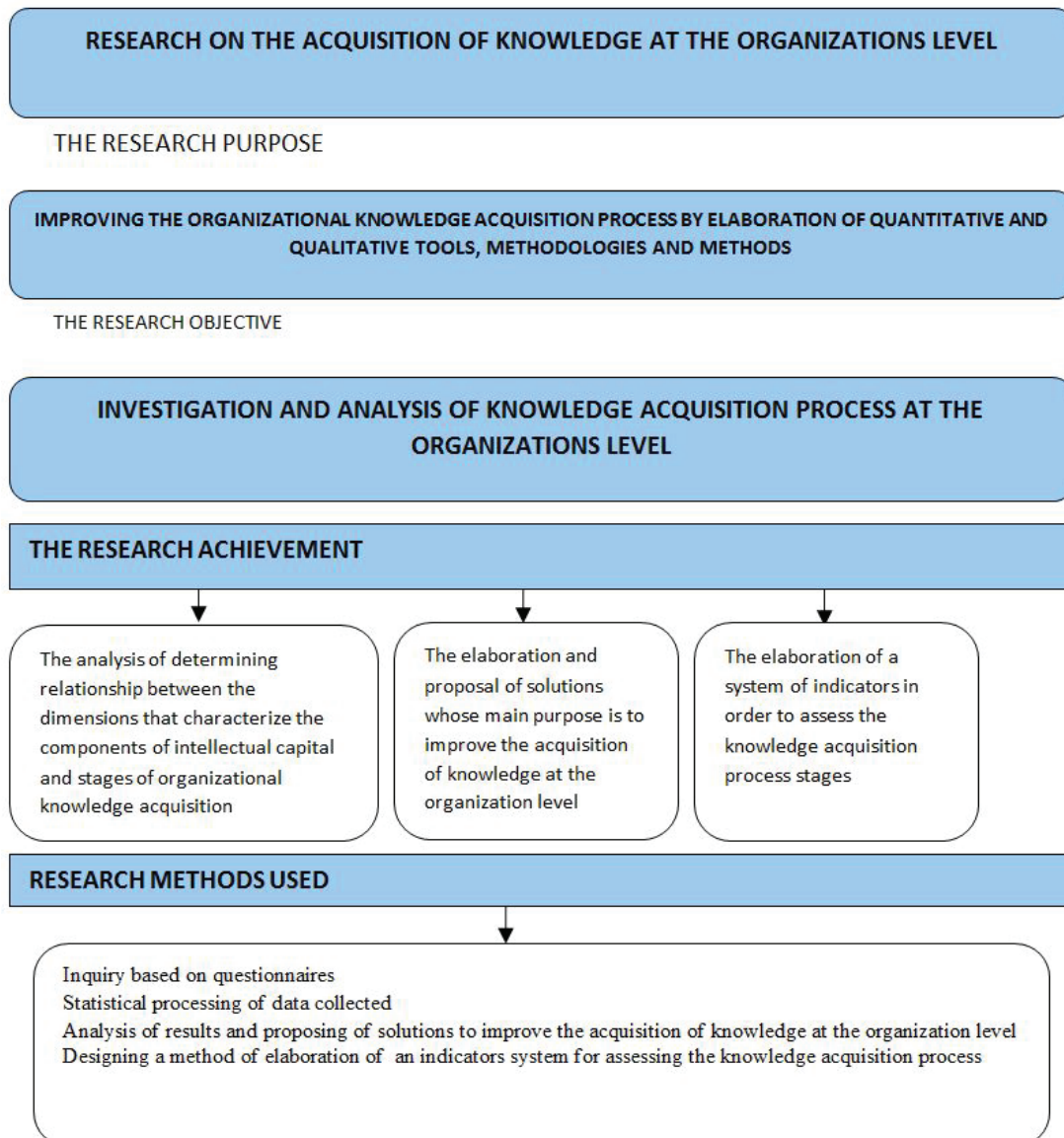


Fig. 1. General scheme regarding the research on organizational knowledge acquisition process

The literature provides numerous attempts to measure knowledge management, most of the times this being reflected by the number of innovations (Arvanitis et al., 2015; Segarra-Cipres et al., 2014; Silva et al., 2013 etc.), investments in research and development, number of researchers, number of patents, the existence of partnerships with research institutes and universities (Silva et al., 2013), the speed, frequency and magnitude of innovation, continuous or periodical expertise reports, technical reports, presentations, documents, task books, studies (Hawkins et al., 2014), business performance (financial performance), productivity, price, product mix, value created for clients, growth in core competences and promoting responsibility. A study conducted and published in 2014 by Andrea Hurtado-Ayala and Carlos Hernan Gonzalez-Campo (González-Campo and Ayala, 2014) notices that knowledge management was measured over time in the specialty literature through the research-development activity (the intensity of the research-

development process, investments in research-development, technological information, personnel and departments/ activities involved in research-development, investments in infrastructure), individual characteristics (technical and professional personnel and personnel training), scientific production (number of scientific publications and number of patents/ registers and trademarks), networks (number of partners/ affiliations, alliances with research institutes, use of scientific journals) and organizational structure (use of manuals / policies, human resources practices, organizational forms, bonus systems) (Luca, 2016).

The paper focuses on representative aspects related to knowledge acquisition process and associated to environment management practices. Taking into account the fact that EMS integration requires a substantial knowledge input, both to managers as well as non-management personnel, we considered absolutely relevant the evaluation associated to the environmental knowledge

acquisition process; thus providing a specific methodology to this evaluation, as a measuring instrument for the efficiency of the environmental knowledge acquisition process. Therefore the paper bring a methodological contribution to knowledge management and environment management fields; and propose a new metrics approach to knowledge – environmental issue “entities” (“organizational management entities” that have a direct influences in environmental decision making process).

Based on extensive researches (Luca, 2016; Luca et al., 2016a, 2016b, 2016c; Lupu et al., 2006) and the previous brief literature review, it is evident the fact that few studies have focused on the knowledge acquisition process, and relevant metrics associated to organizational environmental knowledge acquisition stages, have not been developed/presented. For this reason, this paper presents/proposes a developed indicators system for measuring the process of environmental knowledge acquisition/stages of knowledge acquisition.

2.2. Research methodology

By designing this indicators system we intended the evaluation of each stage associated to the environmental knowledge acquisition process, as well as the possibility of weighing the importance of each of these indicators, according to the specificity and characteristics of each organization. This initiative is taken due to the fact that environmental knowledge acquisition process can be considered an essential stage in the environmental knowledge management,

with an extremely important impact over the environmental performance.

The elaboration of this indicators system started with evaluating the performance of each stage in the environmental knowledge acquisition process, viewed through the defining elements – the knowledge acquisition stage; the hierarchy of the indicators was established according to general criteria, as well as to specific criteria’s associated to organizations. Tracking the organizations general objectives, we could customize knowledge acquisitions, for linking it to organizational environment protections issues.

Therefore, the study aims to design an indicators system for evaluating the stages of the environmental knowledge acquisition process. When developing the methodology for designing **the indicators system for evaluating each stage of the of environmental knowledge acquisition process** we took into consideration the results of previous research (mentioned before) on knowledge acquisition. The methodology presents a phased approach according to figure below (Fig. 2).

3. Results and discussion

3.1. Indicators for evaluation of environmental knowledge acquisition process

The evaluation indicators of the environmental knowledge acquisition process are established according to the organizations’ environment policy, commitment, objectives and targets.

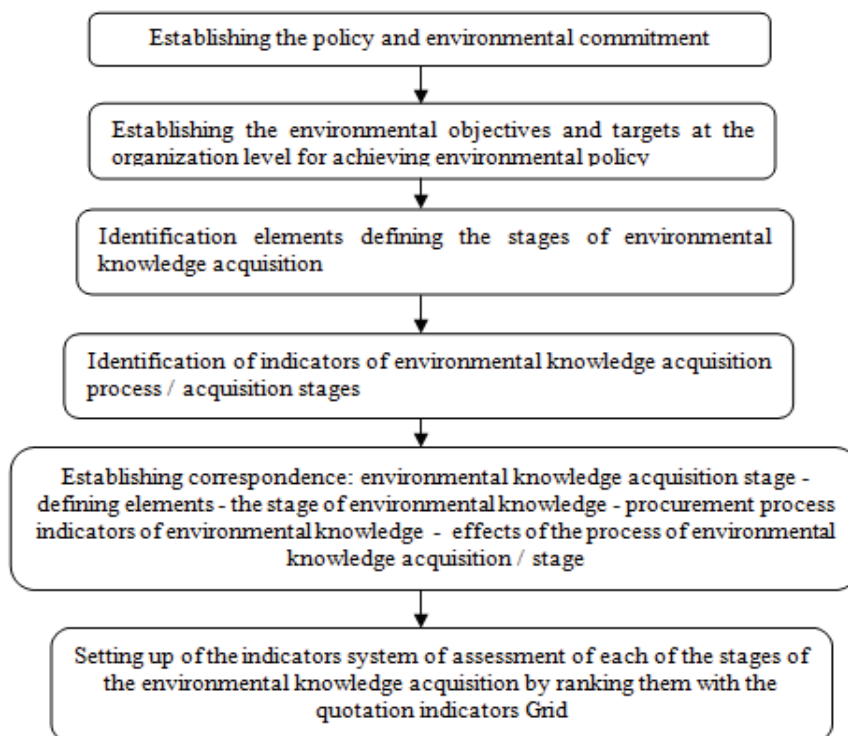


Fig. 2. The methodology for establishing the system of assessment indicators regarding each stages associated to organizational environmental knowledge acquisition

The stages are:

- *Establishing the organizations' environment policy, commitment, objectives and targets*

The purpose of these stages is to identify the necessary environment knowledge that should be acquired at the level of each organisation. The dimension and content of this was the object of previous research (Luca, 2016). Placing these stages within the methodology of designing the indicators system is necessary to underline the specific features of environmental knowledge which influence the accomplishment of the stages in the knowledge acquisition process.

- *Identifying defining elements of the environmental knowledge acquisition stages*

In accomplishing this stage, managers have to take into consideration a series of established general organizational objectives, such as reducing the costs involved in the phase of strategic search for knowledge at organisation level, reducing the time allotted to the phase of decoding/ recoding the acquired knowledge, increasing the revenues generated by the acquired environmental knowledge or reducing the costs generated by the environmental knowledge acquired and not yet capitalised. In general terms, this identification was performed according to (Table 1).

- *Identifying indicators for the environmental knowledge acquisition process/ acquisition stages*

The approach of this stage was based on an analysis of the requirements expressed by the respondents who participated in the survey that the methodology was built on (Luca, 2016). When analysing the answers we noticed a lack of correlation between the stages of the knowledge acquisition process found in literature and the practical process performed in organisations. Following the findings are based on a qualitative analysis of these expressed opinions, we proposed the indicators for the environmental knowledge acquisition process, structured on acquisition stages. The current paper constitutes a presentation of these indicators, the calculus, relationship and measurement unit.

- *Establishing the correspondence: environmental knowledge acquisition stages – defining elements – the acquiring environmental knowledge stage – indicators for the environmental knowledge acquisition process – effects of the environmental knowledge acquisition process/ stage – will take into consideration aspects connected to the relevance of the results returned by the respective indicators and to the resources implied by this correspondence.*

Within this approach we understood the necessity of quantifying through evaluation the knowledge acquisition process, and environmental knowledge implicitly. As a consequence, the design of indicators was performed for each stage in the knowledge acquisition process. The evaluation of the stages associated to the environmental knowledge management process follow the structure presented in (Fig. 3).

- *Constituting the indicators system for the evaluation of each stage in the environmental knowledge acquisition process, by hierarchizing those with the help of the indicators ranking grid.*

In order to facilitate the evaluation process of each of the stages associated to the knowledge management process, we propose a methodology of ranking the indicators according to their individual importance. The necessity of this stage resulted from the analyses undertook which led to the conclusion that not all evaluation indicators are relevant and necessary in relation (i) to the organisation particularity, (ii) to the environment issue development, (iii) to the degree of the knowledge acquisition process development.

The methodology for hierarchizing evaluation indicators for each of the stages associated to the knowledge acquisition process involved the identification of hierarchizing criteria's - the evaluation of each criteria of the indicators importance its' on 1 to 5 scale [1 meaning that the criteria have a very little importance for organisation, and 5 meaning that the criteria is very important; followed by the sum of scores]. The least important criteria will have the lowest score and the most important will have the highest score.

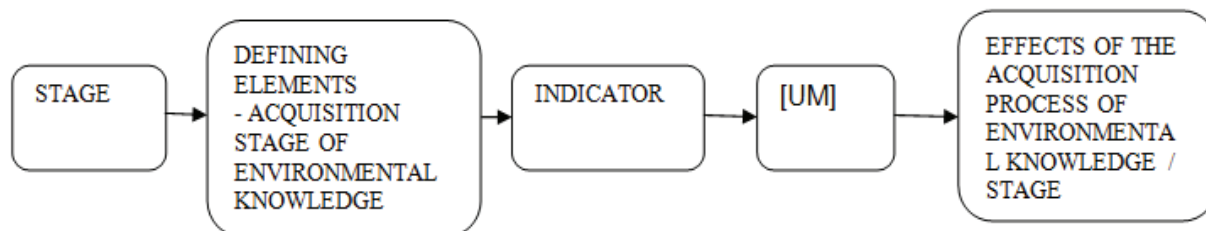


Fig. 3. Establishing correspondence: environmental knowledge acquisition stage - defining elements - the environmental knowledge stage - environmental knowledge indicators - effects of the environmental knowledge acquisition process/ stage (Table 1)

Table 1. Correspondence: environmental knowledge acquisition stage - defining elements - the environmental knowledge stage - environmental knowledge indicators - effects of the environmental knowledge acquisition process / stage

Stage	Defining elements - acquisition stage of environmental knowledge	Indicator	[UM]	Effects of the acquisition process of environmental knowledge / stage
Strategic stage for the environmental knowledges search needed to the organization	Share of time in which are identified the environmental knowledge necessary to the organization T_M	$T_M = T_{cMv} / T_{cMs} * 100$ (%) T_{cMv} – the time required to identify environmental knowledge which were valued (hours) T_{cMs} – time spent for the strategic search (hours) Ideal: $T_{cMv} = T_{cMs}$	[% hours] [% hours spent for identifying the environmental knowledge valued]	-reducing the time with identify the environmental knowledge acquired and unused - incorrect evaluation of the potential of some environmental knowledge with effects in losing sight of possibilities to organization development - loss of interest of employees on continuous learning
	Share costs with the environmental knowledge needed to identify the organization related to the cost with obtaining environmental knowledge valued C_M	$CM = CcMv / CcMs * 100$ (%) $CcMv$ – costs with identification of the environmental knowledge capitalized (lei) CcS – the costs of the strategic search stage of the environmental knowledge necessary to organization (lei) Ideal: $CcMv = CcMs$	[%Monetary units] [% expenditures achieved with identifying of environmental knowledge valued in the total amount of the expenditure achieved in obtaining environmental knowledge]	- identifying of the rhythm breaks for identification of the environmental knowledge needed by the organization
	Share costs with the infrastructure necessary to identify the environmental knowledge needed to organization I_{cMs}	$I_{cMs} = (I_{cMs_{n+1}} - I_{cMs_n}) / I_T * 100$ (%) I_{cMs} – value of infrastructure needed to identify the necessary environmental knowledge (lei) $I_{cMs_{n+1}}$ - value of existing infrastructure in the organization at the end of the identification phase of environmental knowledge (lei) I_{cS_n} – value of existing infrastructure organization at the beginning of the strategic search stage of environmental knowledge (lei) I_T – the total value of existing infrastructure within the organization (lei)	[%Monetary units] [% value of infrastructure used in the strategic search phase of environmental knowledge regarding with the total amount of organization infrastructure]	
Stage for the environmental knowledge acquisition through the purchase of environmental know-how	Share value of the environmental knowledge acquired through the acquisition of know-how and valued in relation to the total amounts budgeted for the environmental knowledge acquisition stage through acquisition of know-how V_{kMakh}	$V_{kMakh} = V_{khMv} / V_{khMb} * 100$ (%) V_{kMakh} – environmental knowledge acquisition value share through the acquisition of know-how (lei) V_{khMv} – the amounts resulting from valuing acquired of environmental know-how (lei) V_{khMb} – the amounts budgeted for the acquisition of environmental knowledge by acquiring know-how (lei)	[%Monetary units] [%amounts resulting of valuing knowledge acquired through the acquisition of know-how in relation to the amounts budgeted for acquisition of know-how]	- potential possibilities of organization development using the know-how acquired - the potential of know-how that the organization has
	The expected period of exploitation of the know-how in relation to the acquired of environmental know-how T_{expkhM}	$T_{expkhM} = T_{expkhMsf} - T_{expkhMif}$ T_{expkhM} - the exploitation period of the environmental know-how acquired (operating hours) $T_{expkhMsf}$ – the removal time from exploiting of the acquired environmental know-how $T_{expkhMif}$ - time of placing into exploiting of the acquired environmental know-how	[operating hours]	
	Identification number of activities that should be proceeding at the	$N_{pn} = N_{TaM} - N_{ap}$ N_{pn} – the number of procedures necessary due to the	[number of activities that require the	

	organization level due to acquisition of environmental knowledge through the acquisition of know-how Npn	knowledge acquisition by acquiring environmental know-how (number of activities that require the development of operational procedures) N _{TaM} – total environmental activity within the organization (number of activities) N _{ap} – number of procedural activities across the organization (number of operating procedures)	development of operational procedures]	
	The time preparation till entry into operation environmental know-how acquired TexplkhM	TexplkhM= TiexplkhM – TakhM TexplkhM – the time to set into operation of the acquired environmental know-how (hours) Tiexplkh – the time to set into operation of the acquired environmental know-how Takh – time of purchase of environmental know-how	[hours]	
	Share procedures that were changed along with the acquisition of environmental knowledge through the acquisition of environmental know-how in relation to the total number of activities across the organization Npkh	Npkh= Npn/ N _{Ta} *100 (%) Npkh - Share procedures that were changed along with the acquisition of knowledge by acquiring environmental know-how Npn – the number of procedures required due to knowledge acquisition through the purchase of environmental know-how (number of procedures) N _{Ta} – total number of procedural activities within the organization (number of procedures)	[%procedures] [%modified procedures in the total of procedures]	
	Number of workers who do not have coverage with loads within the organization along with the purchase of environmental know-how N _{LkhM}	N _{LkhM} = N _{Ln} -N _{Ln+1} N _{Lkh} - Number of workers who do not have coverage with loads within the organization along with the purchase of environmental know-how (no. workers) N _{Ln} – the number of workers in the organization before the acquisition of environmental know-how (no. workers) N _{Ln+1} - the number of workers in the organization after implementing of the existing environmental know-how acquired	[number of workers]	
	The environmental knowledge acquisition stage by hiring experts	Share of proceeds from valorisation acquired environmental knowledge by hiring experts in relation to the total budgeted amount of the environmental knowledge acquisition stage by hiring experts V _{kaMex}	V _{kaMex} =V _{Mexv} /V _{Mexb} *100 (%) V _{kaMex} – share acquisition of environmental knowledge by hiring experts V _{Mexv} – the amounts resulting from valorisation of environmental knowledge acquired through hiring experts (lei) V _{Mexb} – the budgeted amounts value for the acquisition of environmental knowledge by hiring experts (lei)	[%Monetary units] [%lei income generated by the acquisition of environmental knowledge by hiring experts compared with the amounts allocated to the acquisition of environmental knowledge by hiring experts]
The share of new /amended procedures at the		P _{pex} = N _{pMex} / N _{Ta} *100 (%) P _{pex} - Share procedures that were changed along with the	[%procedures] [% modified procedures across	

	experts proposal of total procedures P_{pex}	acquisition of environmental knowledge by hiring experts N_{pMex} – the number of new /modified procedures due to the acquisition of environmental knowledge by hiring experts, on their proposal (no. procedures) N_{Ta} – total number of procedural activities within the organization (no. procedures)	the organization due to environmental knowledge acquisition through employment of experts]	
The assimilation stage through the decoding / recoding of the acquired environmental knowledge	The share of employees who need training due to the acquisition of environmental knowledge in relation to the total number of employees within the organization A_{LsdrM}	$A_{LsdrM} = N_{Lsdr} / N_{Lo} * 100$ (%) A_{LsdrM} – the share of employees who need further clarifications following the acquisition of environmental knowledge N_{Lsdr} – the number of workers that require further clarification in the decoding / re-encoding stage (number of employees) N_{Lo} – number of employees within the organization (number of employees)	[% employees] [% employees who need training due to the acquisition of environmental knowledge in relation to the total number of employees within the organization]	- availability of language used in the stage decoding / encoding for other members of the organization - losing sight of the potential of some of the acquired environmental knowledge due to stage decoding / recoding - decoding / recoding erroneous of the environmental knowledge acquired - the time to required recoding / encoding when the operation is performed solitary
	The allotted time to the decoding / recoding operations of environmental knowledge in total acquisition time T_{drM}	$T_{drM} = (T_{imp} - T_{ach}) / T_{oka}$ T_{drM} - The allotted time to the decoding / recoding operations of environmental knowledge in total acquisition T_{imp} – time of implementation into procedures of the acquired knowledge T_{ach} – time of purchase T_{oka} – time spent on the acquisition of environmental knowledge within the organization	[hours]	
The assimilation stage through the implementation into procedures of acquired environmental knowledge	Share of time for implementing the environmental knowledge acquired in total time spent on the process of knowledge acquisition $T_{kasimpM}$	$T_{kasimpM} = (T_{ivM} - T_{fdrM}) / T_{oka} * 100$ (%) $T_{kasimpM}$ – Share of time for implementing the environmental knowledge acquired in total time spent on the process of knowledge acquisition T_{ivM} – the stage of the time of initiation of valuing the acquired environmental knowledge T_{fdrM} – the moment of the final stage of decoding / recoding of environmental knowledge T_{oka} – time spent on the acquisition of environmental knowledge within the organization	[% hours] [% hours needed to implement acquired environmental knowledge in relation to the total time allocated to acquisition of knowledge within the organization]	- the potential of the use of acquired environmental knowledge - freedom given to professionals in identifying of new ways of interpretation and use of the working procedures of the organization - the personality stamp of each worker in the knowledge domain
	Implementation degree in the work procedures of the organization of the acquired environmental knowledge GiM	$GiM = N_{pm} / N_{ap} * 100$ (%) GiM - Implementation degree in the work procedures of the organization of the acquired environmental knowledge N_{pm} – the number of modified procedures (number of procedures) N_{ap} – number of procedural activities within the organization (number of procedures) $N_{pm} = N_{pexM} + N_{pkhM}$ N_{pexM} – the number of new / modified procedures due to the acquisition of environmental knowledge by hiring experts on their proposal (no. procedures)	[%] [% share of modified procedures due to the acquisition of environmental knowledge in relation to all existing procedures within the organization]	

		NpkhM – the number of new / modified procedures due to the acquisition of environmental knowledge through the acquisition of know-how (no. procedures)		
The stage of valuing the acquired environmental knowledge	The time where the environmental knowledge are valued TvalM	TvalM= (TvM-Tcs)/Toka TvM – the time of valuing of acquisition environmental knowledge (the moment when the acquired environmental knowledge bring financial revenue to the organization) TcsM- the time when it was initiated the strategic environmental knowledge search	[hours]	- losing sight of new opportunities to value the acquired environmental knowledge - loss of market segments or even entire markets
	Share of revenues by valorisation environmental knowledge acquired in relation to the overall revenues of the organization VvM	VvM= (VvM _{n+1} -Vv _n)/V _T *100 (%) VvM - Share of revenues by valorisation environmental knowledge acquired VvM _{n+1} – company recorded income immediately after valuing of acquisition of environmental knowledge (lei) VvM _n - previously recorded income by the company before of valuing of acquisition environmental knowledge (lei) V _T – total revenues recorded in the organization (lei)	[%Monetary units] [% lei incomes obtained by valorisation the environmental knowledge acquired in relation to the total revenues generated by the organization]	

Table 2. Grid listing indicators

Process stage of environmental knowledge acquisition	Defining elements - acquisition stages of environmental knowledge	Indicator	Criteria of correspondence/ selection								Total score/ Indicator TI	Total score/stage TE	Share indicators in the system indicators
			Score										
			A	B	C	D	E	F	G	H			
Strategic stage for the environmental knowledges search needed to the organization	Share of time in which are identified the environmental knowledge necessary to the organization T _M	$T = T_{cM} / T_{cMs} * 100 (\%)$											
	Share costs with the environmental knowledge needed to identify the organization related to the cost with obtaining environmental knowledge valued C _M	$C_M = C_{cM} / C_{cMs} * 100 (\%)$											
	Share costs with the infrastructure necessary to identify the environmental knowledge needed to organization Ic _M s	$IcMs = (IcMs_{n+1} - IcMs_n) / I_T * 100 (\%)$											
Stage for the environmental knowledge acquisition through the purchase of environmental know-how	Share value of the environmental knowledge acquired through the acquisition of know-how and valued in relation to the total amounts budgeted for the environmental knowledge acquisition stage through acquisition of know-how V _{kMakh}	$V_{kMakh} = V_{khM} / V_{khMb} * 100 (\%)$											

	The expected period of exploitation of the know-how in relation to the acquired of environmental know-how TexpkhM	$TexpkhM = TexpkhMsf - TexpkhMif$													
	Identification number of activities that should be proceeding at the organization level due to acquisition of environmental knowledge through the acquisition of know-how Npn	$Npn = N_{TaM} - Nap$													
	The time preparation till entry into operation environmental know-how acquired TexplkhM	$TexplkhM = TiexplkhM - TakhM$													
	Share procedures that were changed along with the acquisition of environmental knowledge through the acquisition of environmental know-how in relation to the total number of activities across the organization Npkh	$Npkh = Npn / N_{Ta} * 100 (\%)$													
	Number of workers who do not have coverage with loads within the organization along with the purchase of environmental know-how N_{LkhM}	$N_{LkhM} = N_{Ln} - N_{Ln+1}$													
The environmental knowledge acquisition stage by hiring experts	Share of proceeds from valorisation acquired environmental knowledge by hiring experts in relation to the total budgeted amount of the environmental knowledge acquisition stage by hiring experts V_{kaMex}	$V_{kaMex} = V_{Mexv} / V_{Mexb} * 100 (\%)$													
	The share of new /amended procedures at the experts proposal of total procedures Ppex	$Ppex = NpMex / N_{Ta} * 100 (\%)$													
The assimilation stage through the decoding / recoding of the acquired environmental knowledge	The share of employees who need training due to the acquisition of environmental knowledge in relation to the total number of employees within the organization A_{LsdrM}	$A_{LsdrM} = N_{Lsdr} / N_{Lo} * 100 (\%)$													
	The allotted time to the decoding / recoding operations of environmental knowledge in total acquisition time T_{drM}	$T_{drM} = (T_{imp} - T_{ach}) / T_{oka}$													
The assimilation stage through the implementation into procedures of acquired environmental knowledge	Share of time for implementing the environmental knowledge acquired in total time spent on the process of knowledge acquisition $T_{kasimpM}$	$T_{kasimpM} = (T_{ivM} - T_{fdrM}) / T_{oka} * 100 (\%)$													

	Implementation degree in the work procedures of the organization of the acquired environmental knowledge GiM	$GiM = Npm / Nap * 100 (\%)$ $Npm = NpexM + NpkhM$																		
The stage of valuing the acquired environmental knowledge	The time where the environmental knowledge are valued TvalM	$TvalM = (TvM - Tcs) / Toka$																		
	Share of revenues by valorisation environmental knowledge acquired in relation to the overall revenues of the organization VvM	$VvM = (VvM_{n+1} - VvM_n) / V_T * 100 (\%)$																		
Total score																				
	<p>Notations:</p> <p>A - correct assessment of the degree of achievement of each of the stages of acquisition of environmental knowledge within the organization</p> <p>B - direct appreciation the degree of realization of each of the stages of acquisition of environmental knowledge within the organization</p> <p>C - easy appreciation the degree of achievement of each of the stages of environmental knowledge acquisition</p> <p>D - relevance in assessing the degree of achievement of each of the stages of environmental knowledge acquisition</p> <p>E - the indicator relevance for activity of the company</p> <p>F - availability of existing resources within the organization to allow monitoring the indicator</p> <p>G - availability of managers in assessing the impact of the indicator on the company activity</p> <p>H - possibilities for rapid assessment of evolution of the indicator</p> <p>Total indicator TI - is obtained by summing the scores given per element</p> <p>Total stage TE - is obtained by summing the scores given to each item, per stage</p> <p>Total Share of indicators in the total process – TI/ETE/100 (%)</p>																			

The criteria's proposed for this hierarchy should take into consideration general appreciation criteria (the returned results correctness, use and interpretation, and so on), and organisation specific criteria (relevance to the organisation activity, monitoring availability, managers' interest in evaluating the performances of each stage in the environmental knowledge acquisition process, possibilities for a rapid evolution of current situation and anticipation of the indicator evolution and so on).

In Table 2 we presented a ranking grid model with a view to select the indicators needed to evaluate in each stage in the environmental knowledge acquisition process, in accordance to/ and satisfying best the organisation needs.

All these methodologies are intended to be instruments which can facilitate the evaluation of each stage associated to the environmental knowledge acquisition process, and allow managers to adopt the best decisions in allotting time, financial and human resources for achieving the organisation environmental objectives.

3.2. Synthetic presentation of the evaluation indicators system for each stage associated to the environmental knowledge acquisition process

The framework from Fig. 4 and Fig. 5 presents a synthetic approach of the indicators for each stage. The indicators hierarchy is done according to their share, their importance and the detailed components of the environmental knowledge acquisition process.

This evaluation system of each stage in the process of environmental knowledge acquisition stage at organisation level allows managers to quantify and

establish with precision the important indicators in their own organisation and to act accordingly on them. Moreover, we elaborated a methodology for selecting the indicators used in the evaluation of each stage in the process of environmental knowledge management and a ranking grid for hierarchizing those indicators and their importance.

4. Conclusions

Knowledge management is a part of integrated management and environmental knowledge management and occupies an important place within the managerial strategy of each organisation. Measuring the organizational process of knowledge acquisition sits at the core of predicting its performance, and measuring each stage in the process of knowledge acquisition allows the identification of some instruments for the evaluation of each indicator in relation to organisation objectives.

EMS ISO 14001 implementation is worldwide important and environmental knowledge management it's relevant for any organisation. In this context, the organizational management staffs have to take into consideration the elaboration and use of an indicators system for evaluating the environmental knowledge acquisition process. Likewise such a managerial instrument could be used to anticipate the future evolution of this process, and basically for achieving the organisation objectives, with minimum time and financial resources. Thus, organizational managers (i) have the possibility to have an indicators system, according to their own necessities, and (ii) have the possibility to evaluate the importance of each indicator in relation to organisation objectives.

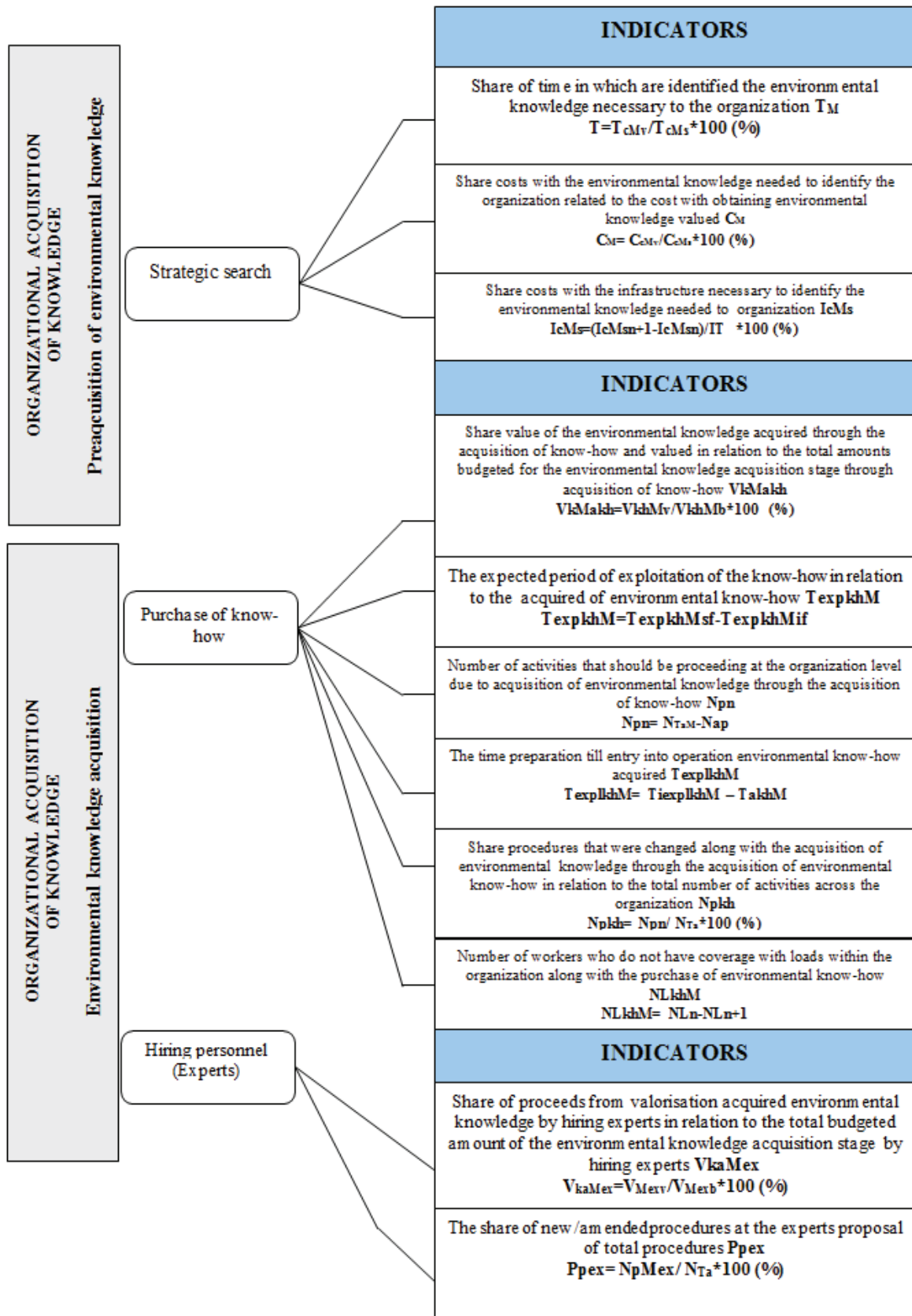


Fig. 4. Indicators proposed to evaluate each of the stages of knowledge acquisition process (pre acquisition stage and procurement stage)

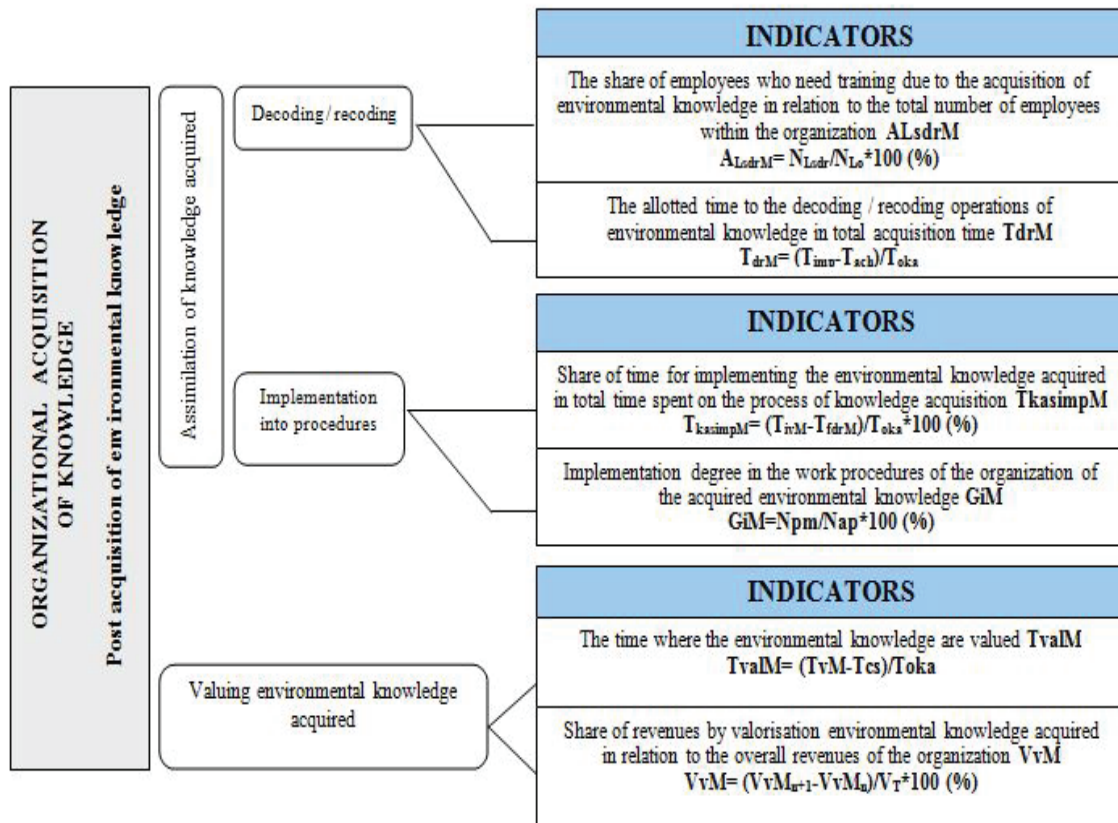


Fig. 5. Indicators proposed for the evaluation of the post-acquisition stage in the process of environmental acquisition stage

Following this indicator selection, organizations can weigh and identify those relevant to their objectives, within the environmental knowledge acquisition process. In this paper framework we approached aspects related to environmental knowledge acquisition, the stages of this process, the necessity of environmental knowledge acquisition, as well as the evaluation of each stage in the organizational knowledge acquisition process, based on the indicators necessary to this evaluation (1). This study was based on previous extensive research regarding organizational knowledge acquisition (2). The methodology for indicators hierarchy wishes to be a managerial instrument used by managers in order to identify correctly the most important indicators for each stage in the environmental knowledge acquisition process, according to the particularities and the needs of each organization (3).

The novelty of this approach resides from the fact that such aspects have not constituted the object of previous research. In addition, it equips managers with a methodology for designing an indicators system for the evaluation of each stage in the environmental knowledge acquisition process and for hierarchizing them according to their organizational needs.

Taking into account that reducing the environmental negative impact generates high costs and also must be one major objective of all organisations, the EMS ISO 14001 implementation represents a very important strategic objective. Consequently, environmental knowledge acquisition

must be an activity for which any organisation should allocate resources (4).

Concluding it could be said that “designing a system to connect data, analysis, and people presents an unprecedented opportunity to formalize ... in a business setting” the environmental issue (Wernick, 2002).

References

- Arvanitis S., Lokshin B., Mohnen P., Woerter M., (2015), Impact of external knowledge acquisition strategies on innovation: A comparative study based on Dutch and Swiss Panel Data, *Review of Industrial Organization*, **46**, 359-382.
- Boiral O., (2002), Tacit knowledge and environmental management, *Long Range Planning*, **35**, 291-317.
- Comăniță E.D., Ghinea C., Hlihor R.M., Simion I.M., Smaranda C., Favier L., Gavrilesco M., (2015), Challenges and opportunities in green plastics: an assessment using the ELECTRE decision-aid method, *Environmental Engineering and Management Journal*, **14**, 689-702.
- Dominguez C., Felgueiras J., Varajao J., (2016), Environmental management systems certification: insights from Portuguese construction companies, *Environmental Engineering and Management Journal*, **15**, 2383-2394.
- Farneti F., Guthrie J., (2009), Sustainability reporting by Australian public sector organizations: why they report, *Accounting Forum*, **33**, 89-98.
- Fryxell G.E., Lo C.W.H., (2003), The influence of environmental knowledge and values on managerial

- behaviours on behalf of the environment: An empirical examination of managers in China, *Journal of Business Ethics*, **46**, 45-69.
- Ghinea C., Dragoi E.N., Comanita E.D., Gavrilesco M., Campean T., Curteanu S., Gavrilesco M., (2016), Forecasting municipal solid waste generation using prognostic tools and regression analysis, *Journal of Environmental Management*, **182**, 80-93.
- González-Campo C.H., Ayala A.H., (2014), Influence of absorption capacity on innovation: An empirical analysis in Colombian SMES, *Estudios Gerenciales*, **30**, 277-286.
- Halis M., Halis M., (2016), Relationship between EMS implementation and environmental performance: Findings from Turkish EMS certificated businesses, *International Journal of Organizational Leadership*, **5**, 137-150.
- Hawkins T.G., Nissen M.E., Rendon R.G., (2014), Leveraging strategic sourcing and knowledge management to improve the acquisition of knowledge based services, *Journal of Public Procurement*, **14**, 215-253.
- Herghiligiu I.V., (2013), *Researches regarding environmental management system as a complex process at the organizational level*, PhD thesis, University of Angers, France and "Gheorghe Asachi" Technical University of Iasi, Romania.
- Herghiligiu I.V., (2017), Fractal design: a new path to improve EMS organizational integration assessment process, "Mircea cel Batran" Naval Academy Scientific Bulletin, **21**, 25-30.
- Hitchens D., Clausen J., Trainor M., Keil M., Thankappan S., (2003), Competitiveness, environmental performance and management of SMEs, *Greener Management International*, **4**, 45-57.
- Istrate C., Robu I.B., Păvăloaia L., Herghiligiu I.V., (2017), Companies sustainability analysis under the influence of environmental information disclosure, *Environmental Engineering and Management Journal*, **16**, 957-967.
- Kaplan S., (2000), Human nature and environmentally responsible behavior, *Journal of Social Issues*, **56**, 491-508.
- Luca A., Lupu M.L., Herghiligiu I.V., (2016a), *Theoretical Framework Regarding Organizational Knowledge Acquisition Evaluation Process*, 17th European Conference on Knowledge Management, 1- 2 September 2016.
- Luca A., Lupu M.L., Herghiligiu I.V., (2016b), *Organizational Knowledge Acquisition - Strategic Objective of Organization*, International Conference Innovations in Science and Education, March 23-25, 2016, Prague, Czech Republic.
- Luca A., Lupu M.L., Herghiligiu I.V., (2016c), *Knowledge Acquisition Process Metrics*, The 20th International Salon of Research, Innovation and Technological Transfer "Inventica 2016", 29 June-1 July 2016, Iasi, Romania.
- Luca A.P., (2016), *Researches on knowledge acquisition at organizations level*, PhD Thesis, "Gheorghe Asachi" Technical University of Iasi, Romania.
- Lupu M.L., Oniciuc N., Rusu B., Rusu C., (2006), *The System of Environmental Performance Indicators*, Performantica Publishing House, Iasi, Romania.
- McKeiver C., Gadenne D., (2005), Environmental management systems in small and medium business, *International Small Business Journal*, **23**, 513-536.
- Roome N., Wijen F., (2006), Stakeholder power and organizational learning in corporate environmental management, *Organization Studies*, **27**, 235-263.
- Rothenberg S, Becker M., (2004), Technical assistance programs and the diffusion of environmental technologies in the printing industry: the case of SMEs, *Business and Society*, **43**, 366-397.
- Roy M.J., Thérin F., (2008), Knowledge acquisition and environmental commitment in SMEs, *Corporate Social Responsibility and Environmental Management*, **15**, 249-259.
- Sebhatu S.P., Enquist B., (2007), ISO 14001 as a driving force for sustainable development and value creation, *The TQM Magazine*, **19**, 468-482.
- Segarra-Cipres M., Roca-Puig V., Bou-Llugar J.C., (2014), External knowledge acquisition and innovation output: an analysis of the moderating effect of internal knowledge transfer, *Knowledge Management Research & Practice*, **12**, 203-214.
- Silva D., Romero F., Vieira F., (2013), *Effects of Technological Innovation on Knowledge Acquisition Inside the Organization: A Case Study*, Proc. of The 8th European Conference on Entrepreneurship and Innovation (ECIE 2013), 791-796.
- Tari J.J., Molina-Azorin J.F., Heras I., (2012), Benefits of the ISO 9001 and ISO 14001 standards: A literature review, *Journal of Industrial Engineering and Management*, **5**, 297-322.
- Ulrey R.J., (2015), *Knowledge Acquisition Processes: Understanding the Communication Event*, Wayne State University Dissertations.
- Vaute-Samanni L., Grevèche M.P., (2015), *Au cœur de l'ISO 14001:2015: Le système de management environnemental au centre de la stratégie*, AFNOR 2015, France.
- Wernick I., (2002), Environmental knowledge management, *Journal of Industrial Ecology*, **6**, 7-9.
- Wijesooriya C., Xu D., Green P., (2011), *The Role of EMS in Environmental and Organizational Performance*, National EMS Conference, Geelong, Vic., Australia, 1-5.

Web sites:

<http://www.eea.europa.eu/ro/highlights/schimbarile-climatice-reprezinta-un-factor>



“Gheorghe Asachi” Technical University of Iasi, Romania



DIELECTRIC PROPERTIES OF SOME BENT CORE LIQUID CRYSTALS

Irina Carlescu^{1*}, Aurel Simion¹, Adrian Bele², Petru Marian Carlescu³,
Cristina Maria Herghiligiu¹, Dan Scutaru¹

¹“Gheorghe Asachi” Technical University of Iasi, “Cristofor Simionescu” Faculty of Chemical Engineering and Environmental Protection, 73 Prof. dr.docent Dimitrie Mangeron Street, 700050 Iasi, Romania

²Institute of Macromolecular Chemistry “Petru Poni” Iasi, Grigore Ghica Vodă Street, 41A, 700487 Iasi, Romania

³“Ion Ionescu de la Brad” University of Agricultural Sciences and Veterinary Medicine of Iasi, Faculty of Agriculture, 3 Mihail Sadoveanu Alley, 700490 Iasi, Romania

Abstract

Dielectric measurements were carried out on a series of bent-core liquid crystals based on resorcinol and 2, 7-dihydroxynaphthalene cores and presenting B mesophase in between 30-160°C. The dielectric constants in the liquid crystalline phase were measured as a function of frequency and temperature. The dielectric relaxation of bent-core compounds has been analyzed by dielectric constants/frequency curves. The variation of the dielectric strength with temperature has been determined as well. The frequency dependence of dielectric loss has also been analyzed by means of frequency exponent.

Key words: bent-core liquid crystals, dielectric spectroscopy, molecular reorientation

Received: May, 2017; *Revised final:* January, 2018; *Accepted:* March, 2018; *Published in final edited form:* April 2018

1. Introduction

The liquid crystalline phase is a thermodynamic stable state of matter that exhibits the anisotropic properties of crystals, due to the orientational ordering and flow properties of liquids, derived from the mobility of the molecules. The ordered structures of anisotropic molecules cause as well anisotropy in their physical properties, as the dielectric constant and optical birefringence. As a result, in the presence of an electric field, the anisotropy of the dielectric permittivity leads to the reorientation of liquid crystal molecules. In liquid crystals with positive dielectric anisotropy, the director reorients parallel to an applied electric field, while for negative dielectric anisotropy, the director is perpendicular to the electric field. Generally, liquid crystals which denote positive dielectric anisotropy at low frequencies are used for the most active matrix

displays for image quality of LCDs (Kelly and O’Neil, 2000).

The response of a liquid crystalline material is in concordance to the magnitude of the dielectric permittivity, which in turn depends on the temperature and the frequency of the applied field in the mesophase (Kundu et al., 2007; Marik et al., 2015; Sreenilayam et al., 2015; Yildiz et al., 2016a, 2016b; Yilmaz Canli et al., 2015). The relationship between dielectric constant and molecular properties of liquid crystals provides useful information in determining the electro-optical response of devices based on liquid crystals, which should combine birefringence, high dielectric anisotropy and low viscosity (Reddy and Tschierske, 2006; Takezoe and Takanishi, 2006; Tschierske, 2013). In this regard, dielectric spectroscopy is used to obtain reliable information towards the molecular structure, dynamics of polar structures, phase transitions and switching speed performances of liquid crystals. Parameters which

* Author to whom all correspondence should be addressed: e-mail: icarlescu@ch.tuiasi.ro

decide whether a material is suitable for technological applications are the real (ϵ') and imaginary (ϵ'') part of dielectric function, dielectric loss ($\tan\delta$) and conductivity (σ). For instance, relatively higher dielectric constants are used in microelectronics devices such as memory devices (Kelly and O'Neil, 2000).

After the discovery of electro-optical switching in the mesophases of bent core achiral molecules as a result of spontaneous chirality (Niori et al., 1996), numerous studies have been focused on designing of banana type molecules (Link et al., 1997; Sadashiva, 2014; Weissflog et al., 2001; Weissflog et al., 2006).

There are some factors that influence the mesomorphic properties and therefore the dielectric properties of liquid crystalline materials, as the geometry of molecules and the nature of rigid core, lateral polar substituents or terminal flexible chains (Demus, 1998). Although the structure-property correlations are well established for calamitic liquid crystals, for bent core liquid crystals steric effects exercise a significant influence on some of the physical properties such as viscosity. Consequently, factors as the size of the molecules, the position and the magnitude of the angle of bent central unit (135 to 140°) should be taken into account (Pelzl et al., 1999). However, because the mesophases formed by bent core molecules often occurs above 150°C , it is difficult to determine their physical properties. Among mesophases showed by banana-shaped molecules, the B2 phase has been associated with specific dielectric properties (Krishna Prasad et al., 2003; Pelzl et al., 1999). In the present study, the electric fields that induced effects on mesophases properties of some bent core liquid crystals based on resorcinol (DCB) and 2,7-dihydroxynaphthalene (RAC and CAN) (Fig. 1) were studied. In this regard, the relaxation behavior of static parameters as permittivity (ϵ) and dielectric loss tangent ($\tan \delta$) were measured as a function of frequency and temperatures into mesophase.

2. Material and methods

Synthesis and liquid crystalline properties of compounds DCB, RAC and CAN were previously reported (Simion et al., 2015, 2016). The dielectric measurements were conducted on a Novocontrol Alpha-A Frequency Analyzer, connected to planar cell filled with liquid crystalline material that was heat from 30°C to isotropization temperatures.

The experimental data were registered only on first heating in the frequency range 1 Hz and 10^6 Hz. The samples were grounded using an agate mortar and pressed between two electrodes using a 15T manual hydraulic press. The thickness was determined using a micrometer screw (Mitutoyo Absolute, model ID-C112X, $12.7 - 0.001$ mm range).

3. Results and discussion

3.1. The liquid crystalline properties of the investigated bent core compounds

The dielectric behavior of the compounds has been studied over a range of frequency and temperature mesophases. All the investigated bent-core compounds presented a good thermal stability and a convenient temperature range of liquid crystalline phase. According to DSC analysis correlated with POM textures, compound CAN exhibited the widest mesophase range (about 30°C) towards RAC and DCB, proving that the presence of disubstituted 2,7-naphthalene central unit better stabilizes mesophases than disubstituted 1,3-benzene core.

However, the presence of disubstituted 1,3-benzene core in compound DCB lowers the temperature when liquid crystalline phase appears on heating, with a temperature difference of about 40°C , if compared with the others two compounds (Fig. 2).

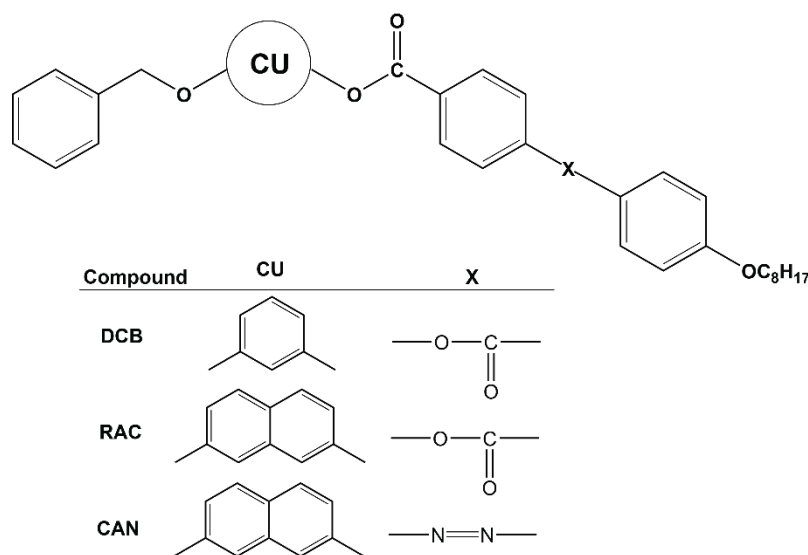


Fig. 1. General structure of studied bent core liquid crystals (CU: central unit)

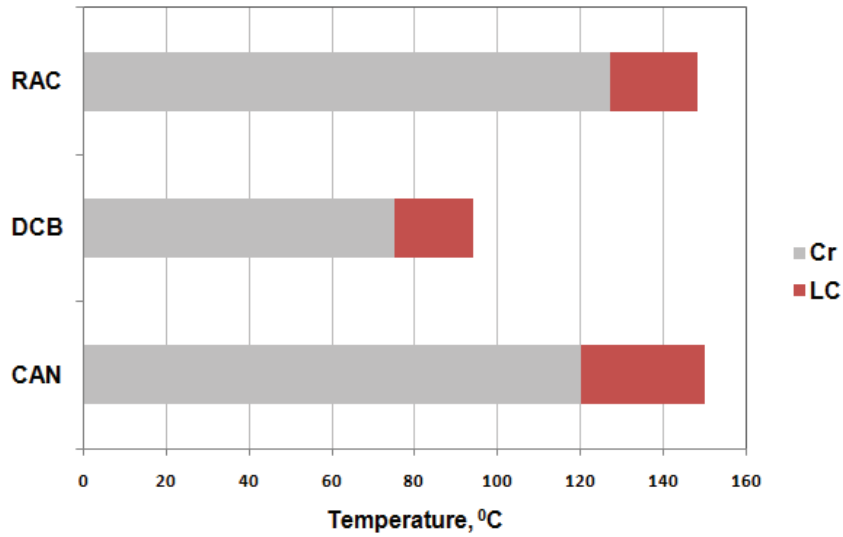


Fig. 2. The liquid crystalline domains of bent core compounds obtained by differential scanning calorimetry (10°C/min) on heating Cr = crystal, LC = liquid crystal

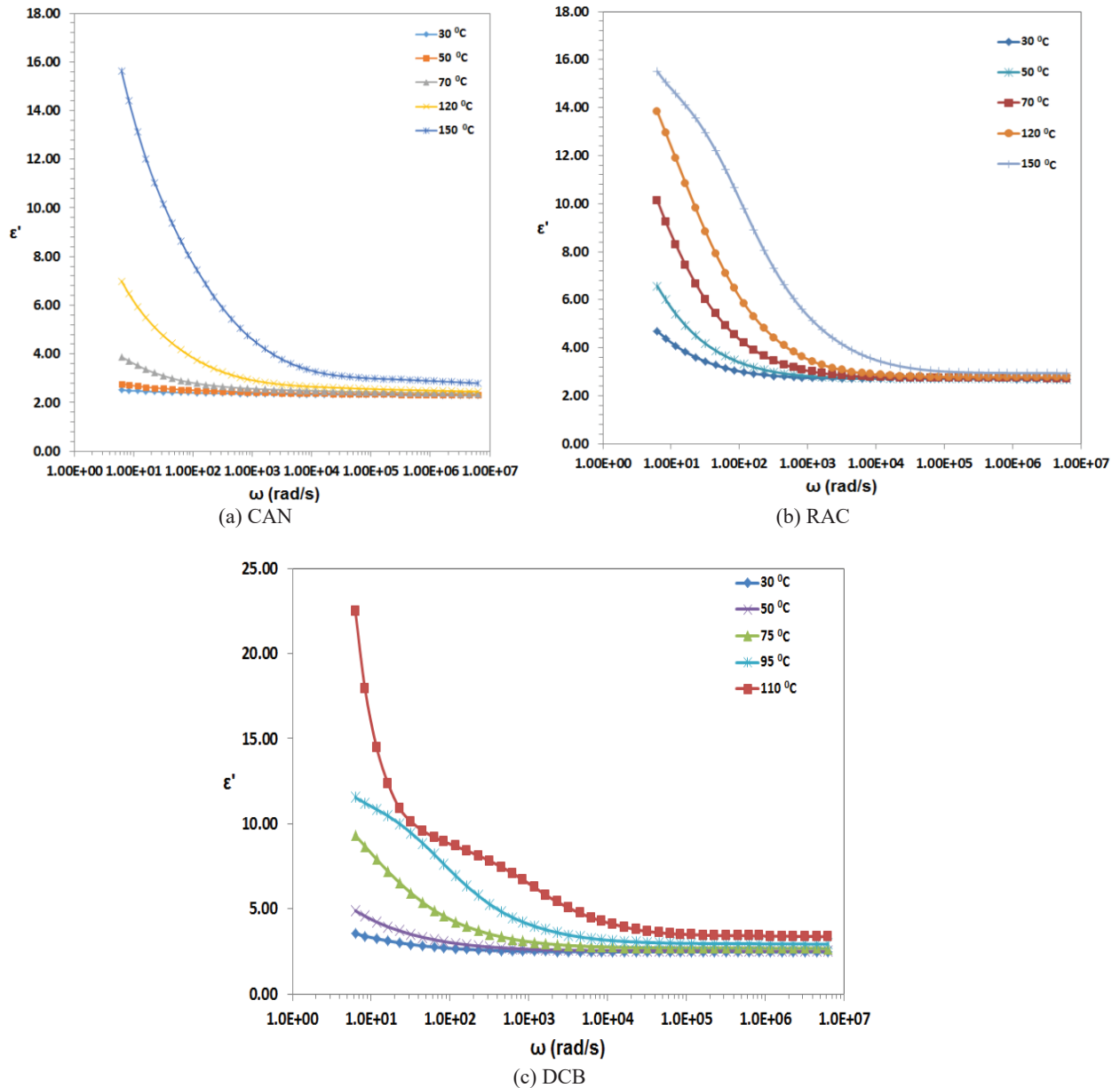


Fig. 3. The angular frequency dependence of the real parts of the dielectric constant of the investigated bent-core liquid crystals as a function of temperature

3.2. Analysis of temperature effect on dielectric parameters of the investigated bent-core liquid crystals

The dielectric parameters of the investigated bent-core liquid crystals have been measured within the frequency interval of 1 - 10⁶ Hz at various temperatures varying from 30°C to 160°C. In this respect, dielectric parameters of CAN have been compared with DCB and RAC. The frequency dependences of the real part of dielectric constant (ϵ') are presented in Fig. 3 (where $\omega=2\pi f$ and f is the linear frequency). The obtained data suggest that ϵ' shows dispersive behavior and decreases gradually with the increases of frequency and then attains to close values at high frequencies, a characteristic behavior of dielectric materials (Sinha et al., 2001). On the other hand, the real part of dielectric constant has its maximum value at low frequencies. The explanation is that at high frequencies (i.e. > 10⁴), the molecular agitation is high so there is no dipolar polarization. As a result, noticeable loss of stored energy appears; hence the ϵ' approaches the same low values. However, at low frequencies, the existence of a net molecular polarization leads to increases of the real parts of the dielectric constant that increases with temperatures, due to the molecular reorientation.

The variation of the real parts of the dielectric constant of the investigated bent-core compounds with temperature in different frequency regions (1 kHz, 5 kHz, 10 kHz, 100 kHz) is presented in Fig. 4, in the whole investigated temperature range in the heating process. The temperature dependence of dielectric permittivity shows potentially phase transitions.

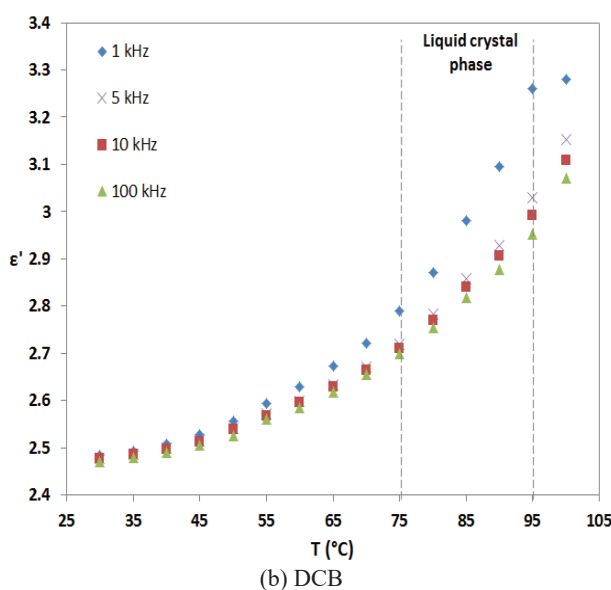
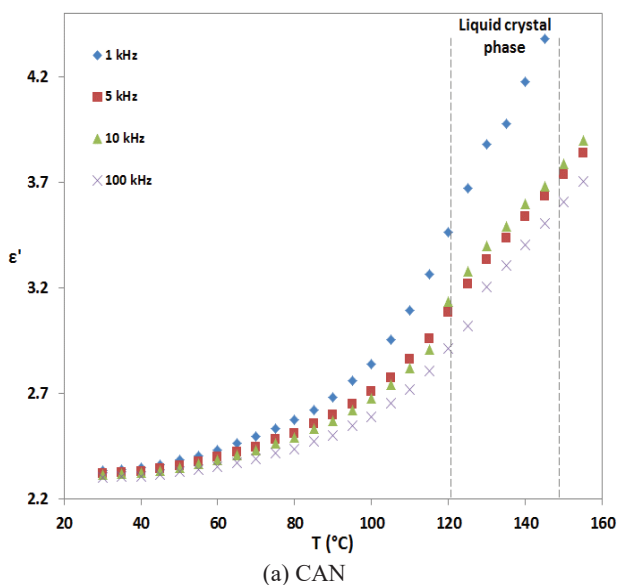
Although the three compounds have different liquid crystalline phase temperature domains, the dielectric constants deviate from the linear shape and start increasing gradually with temperature after 55°C, suggesting some similar phase transition of crystal-crystal type for all bent-core compounds, more

pronounced for RAC. In liquid crystalline phases, the dielectric constants reach the maximum values at 1 kHz, when the polarization is probably high as well.

The angular frequency dependence of the imaginary component of the dielectric constant (dielectric loss) has been given as well (Fig. 5). As shown, the magnitude of the imaginary parts of dielectric constant in the low frequency region is higher than that of high frequency region. In the high frequency regions, the imaginary components of dielectric constant have small hollows (more pronounced for RAC and DCB), between 10⁴ and 10⁶ Hz, corresponding to dielectric relaxations. Since the magnitude of ϵ'' is proportional to energy dissipation, it was assumed that bent-core liquid crystals are more stable in the high frequency region.

Moreover, the dissipation energy has been analyzed in the conduction process. The electrical conductivity σ is known to be related to dielectric loss ϵ'' , depending on frequency and temperature as well. As shown in Fig. 6, conductivity (σ) has a tendency of increase both with temperature and frequency. This phenomenon can be useful in liquid crystal device applications. In addition to this, as the frequency increases, the conductivity increases about linearly to 10⁵ Hz, when the growth deviates appreciably and attains to similar value.

It is noticeable that conductivity curves show similar behavior for RAC and DCB while the deviations for CAN are less evidenced. The highest conductivity values of corresponding mesophases, at the frequency of 10⁵ Hz have similar order sizes as follow: $\sigma_{RAC}= 2.39 \times 10^{-9}$ S/cm, $\sigma_{DCB}= 2.12 \times 10^{-9}$ S/cm and $\sigma_{CAN}= 1.108 \times 10^{-9}$ S/cm. One should point out that conductivities in crystalline phases (at 30 °C) are by two orders of magnitude smaller than that ones from mesophases: $\sigma_{RAC}= 8.95 \times 10^{-11}$ S/cm, $\sigma_{DCB}= 8.02 \times 10^{-11}$ S/cm and $\sigma_{CAN}= 7.08 \times 10^{-11}$ S/cm. These data are important for applications.



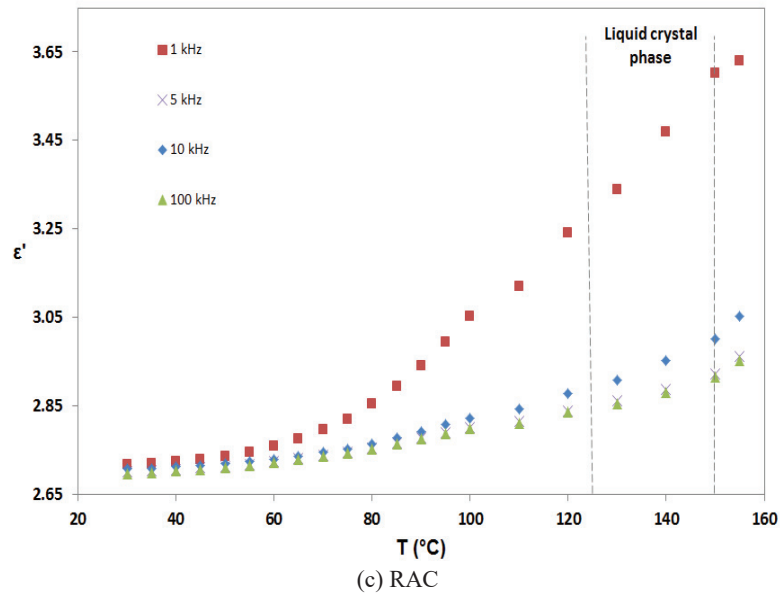


Fig. 4. Temperature dependence of the real parts of the dielectric constant of the investigated bent-core liquid crystals at different frequencies

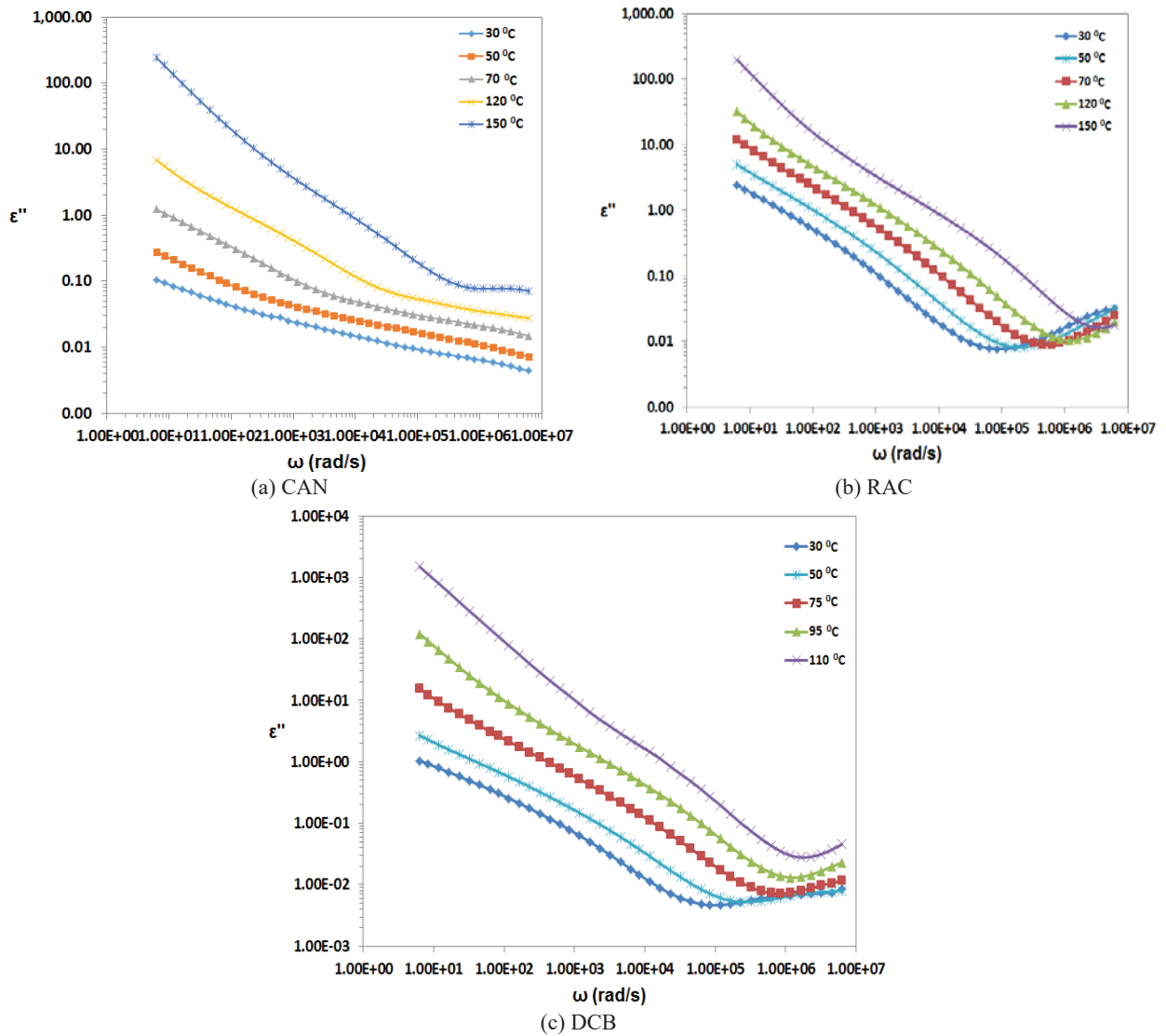


Fig. 5. The angular frequency dependence of the imaginary parts of the dielectric constant of the investigated bent-core liquid crystals at different temperatures

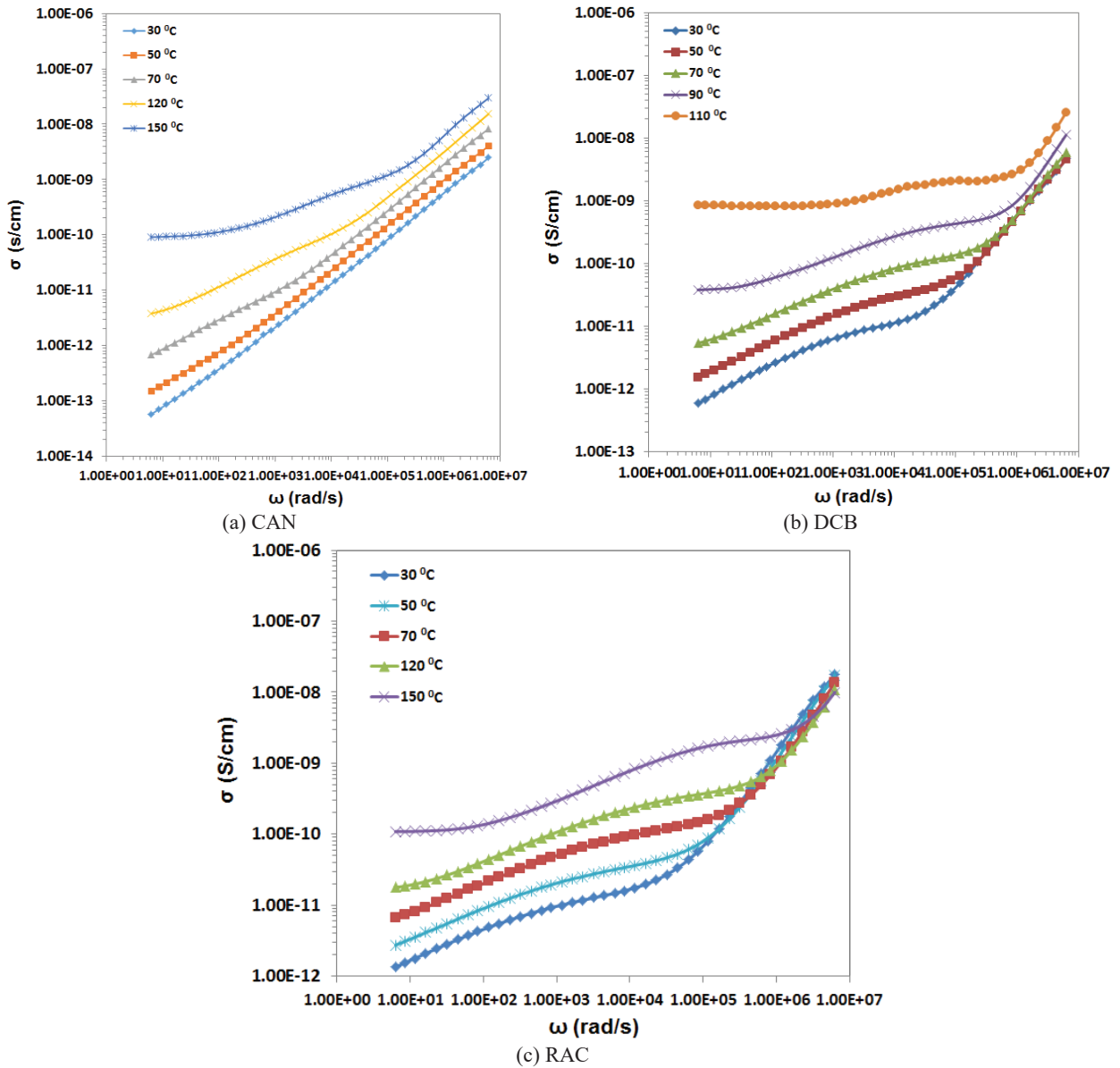
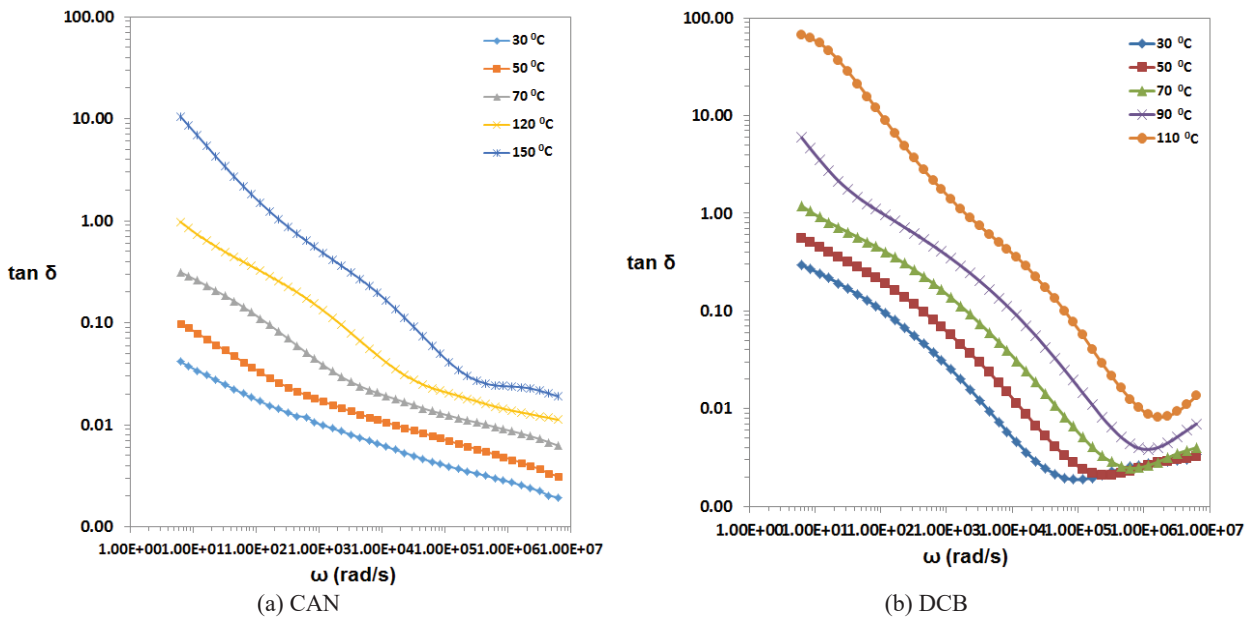


Fig. 6. Angular frequency dependence of the real part of conductivity for bent-core liquid crystals at different temperatures



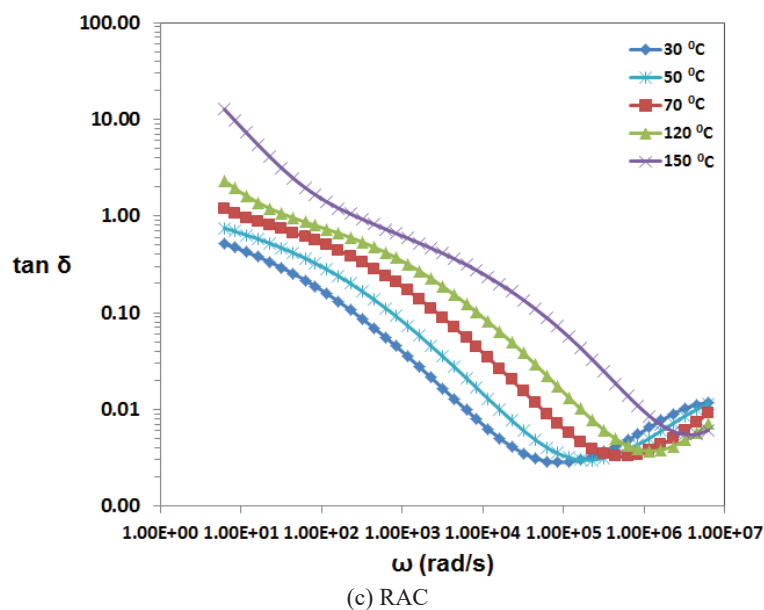


Fig. 7. The angular frequency dependence of the dissipation factor at different temperatures

3.3. Analysis of frequency effect on dissipation factor

The frequency and temperature dependence of dissipation factor (dielectric loss tangent) was also analyzed (Fig. 7). For all the compounds, the relaxation processes are found between 10^4 and 10^6 Hz. As shown in Fig. 7, the dissipation factors vary in about a similar way with the imaginary components of dielectric constant, but the loss peaks corresponding to dielectric relaxations are more pronounced. Thus, CAN show some poor relaxation peaks between 120°C and 150°C , the mesophase domain, where also has the highest values of $\tan \delta$. In contrast to CAN, the relaxation processes corresponding to DCB and RAC are more emphasized, and what is obvious, not only on mesophase domains. This different behavior between the compounds reflects the various physical interactions which take place, more intensive in DCB and RAC. It can be assumed that the presence of an esteric linkage between the two aromatic rings enhances the delocalization of the electronic cloud with the increase of the molecular dipole moment. As result, these molecules can be easily reoriented.

4. Conclusions

In the present study, the dielectric properties of some bent-core liquid crystals were studied as a function of temperature and frequency. The angular frequency dependence of the real and imaginary components of dielectric constant and the dielectric strength has been analyzed for the low and high frequency regions.

The investigated bent-core compounds are easier reoriented in the high frequency domain, where are more stable. The conductivity in mesophases is much higher than in crystalline state, proving the potential uses of bent-core liquid crystals in applications. Compounds with esteric linkage between

aromatic rings display more emphasized relaxation processes, for the whole temperature domains, probably due to electronic delocalization.

References

- Demus D., (1998), *Chemical Structure and Mesogenic Properties*, In: *Handbook of Liquid Crystals*, Demus D., Goodby J.W., Gray G.W., Spiess H.W., Vill V. (Eds.), Wiley-VCH, Weinheim, Germany, 133-188.
- Kelly S.M., O'Neil M., (2000), *Liquid Crystals for Electro-Optic Applications*, In: *Liquid Crystals, Display and Laser Materials, Handbook of Advanced Electronic and Photonic Materials and Devices*, Nalwa H.S. (Eds.), Academic Press, 2-61.
- Krishna Prasad S., Maeda Y.Y., Shankar Rao D.S., Anitha Nagamani S., Hiremath U.S., Yelamaggad C.V., (2003), Phase behavior of thermotropic banana-shaped compounds under pressure, *Liquid Crystals*, **30**, 1277-1283.
- Kundu S.K., Yagihara S., Yoshizawa A., (2007), Dielectric spectroscopy of a smectic liquid crystal, *Liquid Crystals*, **34**, 981-986.
- Link D.R., Natale G., Shao R., MacLennan J.E., Korblova E., Clark N.A., Walba D.M., (1997), Spontaneous formation of macroscopic chiral domains in a fluid smectic phase of achiral molecules, *Science*, **278**, 1924-1927.
- Marik M., Jana D., Majumder K.C., Chaudhuri B.K., (2015), Dielectric behavior in B1 and B2 phases composed of unsymmetrical bent shaped liquid crystal molecules, *Molecular Crystals and Liquid Crystals*, **606**, 111-125.
- Niori T., Sekine T., Watanabe J., Furukawa T., Takezoe H., (1996), Distinct ferroelectric smectic liquid crystals consisting of banana shaped achiral molecules, *Journal of Materials Chemistry*, **6**, 1231-1233.
- Pelzl G., Diele S., Weissflog W., (1999), Banana-shaped compounds - A new field of liquid crystals, *Advanced Materials*, **11**, 9, 707-724.
- Reddy R.A., Tschierske C., (2006), Bent-core liquid crystals: polar order, superstructural chirality and spontaneous desymmetrisation in soft matter systems, *Journal of Materials Chemistry*, **16**, 907-961.

- Sadashiva B.K., (2014), *Non-conventional Liquid-Crystalline materials. Biaxial Nematic Liquid Crystals*, In: *Handbook of Liquid Crystals*, Demus D., Goodby J., Gray G.W., Spiess H.W., Vill V. (Eds.), Wiley-VCH, Weinheim, Germany, 933-944.
- Simion A., Carlescu I., Lisa G., Scutaru D., (2016), Unsymmetrical bent-core liquid crystals based on resorcinol core, *Revista de Chimie*, **67**, 446-450.
- Simion A., Huzum C.C., Carlescu I., Lisa G., Balan M., Scutaru D., (2015), Unsymmetrical banana-shaped liquid crystalline compounds derived from 2, 7-dihydroxynaphthalene, *Journal of the Serbian Chemical Society*, **80**, 673-683.
- Sinha S.K., Choudhary S.N., Choudhary R.N.P., (2001), Structural and dielectric behavior of $Pb(Mn_{1/4}Zn_{1/4}W_{1/2})O_3$ ceramics, *Materials Chemistry and Physics*, **70**, 296-299.
- Sreenilayam S., Panarin Yu., Vij J.K., (2015), Dielectric study of nematic LC built with bent-core molecules, *Molecular Crystals and Liquid Crystals*, **610**, 63-67.
- Takezoe H., Takanishi Y., (2006), Bent-core liquid crystals: their mysterious and attractive world, *Japanese Journal of Applied Physics*, **45**, 597-625.
- Tschierske C., (2013), Development of structural complexity by liquid-crystal self-assembly, *Angewandte Chemistry International Edition*, **52**, 8828-8878.
- Weissflog W., Murthy S., Diele H.N.S., Pelzl G., (2006), Relationships between molecular structure and physical properties in bent-core mesogens, *Philosophical Transactions of the Royal Society A*, **364**, 2657-2679.
- Weissflog W., Nadasi H., Dunemann U., Pelzl G., Diele S., Eremin A., Kresse H., (2001), Influence of lateral substituents on the mesophase behavior of banana shaped mesogens, *Journal of Materials Chemistry*, **11**, 2748-2758.
- Yildiz A., Yilmaz Canli N., Karanlik G., Ocak H., Okutan M., Bilgin Eran B., (2016a), The determination of the phase transition temperatures of a semifluorinated liquid crystalline biphenyl ester by impedance spectroscopy as an alternative method, *Physica B*, **503**, 152-156.
- Yildiz A., Yilmaz Canli N., Guven Ozdemir Z., Ocak H., Bilgin Eran B., Okutan M., (2016b), The role of temperature on dielectric relaxation and conductivity mechanism of dark conglomerate liquid crystal phase, *Physica B*, **485**, 21-28.
- Yilmaz Canli N., Guven Ozdemir Z., Okutan M., Guzeller D., Ocak H., Bilgin Eran B., (2015), Dielectric Properties of 4-Cyano-4'-pentylbiphenyl (5CB): 4-[4-(S)-2-Methylbutoxybenzoyloxy]benzoic Acid (BAC) Composite, *Molecular Crystals and Liquid Crystals*, **623**, 17-30.



“Gheorghe Asachi” Technical University of Iasi, Romania



SOIL SEED BANK AND ITS RELATIONSHIP TO THE ABOVE-GROUND VEGETATION IN GRAZED AND UNGRAZED OXBOW WETLANDS OF THE YANGTZE RIVER, CHINA

Dong Yang¹, Wenzhi Liu¹, Hui Liu^{2,3}, Wei Li^{1,4*}

¹Key Laboratory of Aquatic Botany and Watershed Ecology, Wuhan Botanical Garden, Chinese Academy of Sciences, Wuhan 430074, P.R. China

²Institute of Hydroecology, Ministry of Water Resources and Chinese Academy of Sciences, Wuhan 430074, P.R. China

³Key Laboratory of Ecological Impacts of Hydraulic-projects and Restoration of Aquatic Ecosystem, Ministry of Water Resources, Wuhan 430074, P.R. China

⁴Hubei Key Laboratory of Wetland Evolution & Ecological Restoration, Wuhan Botanical Garden, Chinese Academy of Sciences, Wuhan, 430074, P.R. China

Abstract

Livestock grazing may have a great effect on both standing vegetation and soil seed bank. The present study investigated the characteristics of the soil seed bank and determined its relationship to the above-ground vegetation in grazed and ungrazed sites in the Hei-wa-wu oxbow wetland of the Yangtze River, China. A total of 3700 seedlings across 59 species germinated from the soil seed bank. Annuals and terrestrial species dominated the soil seed banks of both grazed and ungrazed sites. Grazing had no significant effect on the seed density and species richness, but altered the species composition of soil seed bank. Grazing tended to increase the floristic similarity between the soil seed bank and the above-ground vegetation. DCA ordination produced a clear separation of the soil seed bank and above-ground vegetation. Our results suggest that soil seed bank and its relation to standing vegetation in the Hei-wa-wu oxbow wetland are strongly influenced by livestock grazing.

Key words: flooding, human disturbance, vegetation, Yangtze River

Received: October, 2012; *Revised final:* February, 2014; *Accepted:* February, 2014; *Published in final edited form:* April 2018

1. Introduction

In temporary wetlands, plant species must have life cycle stages that ensure survival between the alternate wet and dry phases (Brock, 2011; MacGillivray and Grime, 1995; Van Der Valk, 2005). Seed banks are part of the life cycle (Harper, 1977) and provide a mechanism for regeneration of plant communities after natural or human disturbance, such as seasonal flooding, drought, prolonged inundation or grazing (Brock et al., 1994). Survival as vegetative propagules during prolonged disturbance is not feasible for the majority of wetland species. Therefore the soil seed bank may play a vital role in vegetation

establishment after disturbance (Liu et al., 2009; Nicol et al., 2007; Thompson, 2000).

The tendency of domestic livestock to congregate around water has meant that wetlands and riparian zones are often more heavily affected by grazing than adjacent terrestrial systems (Jansen and Robertson, 2001; Nicol et al., 2007). Domestic livestock such as cattle, sheep, goats, and horses are found to change the floristic composition of above-ground vegetation in freshwater and riparian systems by selective grazing and trampling (Jansen and Robertson, 2001). Grazing has been shown to affect plant community structure (Blanch and Brock, 1994), survival of species (Mulder and Ruess, 1998), plant

* Author to whom all correspondence should be addressed: e-mail: liwei@wbgcas.cn; Phone: +086 2787510140; Fax: +086 2787510298

growth rates (Moon et al., 2013; Zimmerman et al., 1996), resource allocation (Ehrlén, 1995), and the species composition of soil seed banks (Crossle and Brock, 2002; Osem et al., 2006; Tessema et al., 2012).

Grazing by domestic livestock may have various effects on the density and composition of soil seed banks in riparian or freshwater systems. For instance, studies have shown that seed density was reduced (Barnewitz et al., 2012; Erkkilä, 1998; Granström, 1988; McDonald et al., 1996; Vlad and Toma, 2017), hardly affected (Loydi et al., 2012; Ortega et al., 1997) or even increased (Levine et al., 2012; Russi et al., 1992) by grazing. Variation in patterns of seed bank response to grazing can be attributed to differences among the studied ecosystems in environmental conditions, grazing regimes and type of herbivore, as well as in vegetation composition and species traits (Osem et al., 2006). The interaction of grazing and water regime on soil seed bank has not been widely studied especially in riparian or freshwater systems (Crossle and Brock, 2002; Erkkilä, 1998; Nicol et al., 2007). Understanding the effects of grazing on the soil seed bank is of critical importance for conservation and grazing management.

The middle to lower reaches of the Yangtze River is the largest floodplain in China (Li et al., 2002). Many wetlands are distributed across this vast area, and almost all are directly or indirectly connected to the river (Li et al., 2008). The pattern of drawdown and flooding in these wetlands is predictable, due to seasonal rainfall (Liu et al., 2006a). The wetlands are often grazed by cattle or sheep during drawdown, as they are close to residential areas. Our previous studies have shown this area to have a large and persistent seed bank (Liu et al., 2005). However, the effect of grazing by domestic livestock on the soil seed bank and its relation to the above-ground vegetation has not been studied. Water level fluctuations and grazing on the wetlands offer an opportunity to study the effect of disturbances on soil seed banks.

This study investigated the soil seed bank and its relation to the above-ground vegetation of grazed and ungrazed oxbow wetlands of the Yangtze River, China. Our aims were to test the following hypotheses: (1) grazing by domestic livestock during dry phases will reduce seed density, species richness and change the floristic composition of the seed bank; (2) grazing will decrease the similarity between the soil seed bank and above-ground vegetation.

2. Material and methods

2.1. Study sites

This study was carried out in Hei-wa-wu oxbow wetland (29°45'–29°48' N, 112°41'–112°46' E) Shishou, China (Fig. 1), the most well-preserved floodplain wetland in the middle Yangtze River (Hao et al., 2004). The oxbow was cut off from the main course of the Yangtze River by purely man-made factors in 1968. It is connected to the Yangtze River during flooding (May to September) and remains

intact as a riparian wetland in the dry season. The length of Hei-wa-wu oxbow is about 30 km. The climate in this region is subtropical monsoon with a mean air temperature of 3.4°C in January and 28.5°C in July. Mean annual precipitation is approximately 1153 mm, and 80% of the total rainfall concentrates in the rainy season from May to October (Wu et al., 2006). The soil is a sandy clay loam with organic matter content of 1.75% and pH of 7.3. Clonal perennials (e.g., *Carex cinerascens*, *Hemarthria altissima*, and *Cynodon dactylon*) dominate the vast area and seed germination is mainly restricted by flooding.

The grazed and ungrazed sites were along the oxbow (Fig. 1) and their geomorphology, elevation (32–34 m above sea level), distance from the water (10–30 m) and slope (less than 5%) were similar. The grazed sites lie near populated areas and have been continuously grazed by domestic livestock such as cattle, sheep and horses since the 1970s. Grazing intensity during the time of the study (April 2009) was approximately 16–45 livestock per ha. Ungrazed sites were those where livestock grazing was typically excluded all year.

2.2. Seed bank sampling and germination

Soil seed banks were sampled at the beginning of April 2009, before the spring germination season in the field. Two grazed and ungrazed transects parallel to the flow direction were established along the Hei-wa-wu oxbow wetland, respectively (Fig. 1). Five 1×1 m plots were systematically placed along each transect. Each plot was generally separated by a minimum distance of 300 m from neighbouring plot (Fig. 1). After thoroughly removing the plant material from the soil surface, five soil cores of 10 cm depth were taken with an iron cylinder (diameter 8 cm) in each plot. The cores of each plot were then combined (TerHeerd et al., 1996). A total of 100 soil cores were sampled. The total surface area represented by the soil cores was 0.503 m² (0.025 m² per plot).

Methods for seedling emergence followed van der Valk and Davis (1978). Visible tubers, turions, roots, rhizomes and litter were removed carefully after washing the sediment. Each sample was wet-sieved (0.2 mm) and the retained material was spread in a layer (<1 cm deep) over 10 cm of sand in plastic trays (diameter 30 cm). The sand had previously been dried for 24 h at 75°C to kill any weed propagules. All trays were randomly arranged in an unheated greenhouse at the Wuhan Botanical Garden (30°32'82" N, 114°25'18" E) and were watered twice a week with tap water (Reiné et al., 2004). The climate in Wuhan is similar to that in Hei-wa-wu oxbow wetland. Seedlings were counted weekly and were removed as soon as they could be identified.

Seedlings that could not be identified were transplanted to empty trays and allowed to grow until they could be identified. Seedling emergence started in early May, reached a peak in mid-June, and ended in early September of 2009.

Germination was recorded until there had been no further germination for more than 1 month. Non-germinated seeds were considered to be dead or non-viable. Nomenclature followed the Flora of China (Wu and Peter, 2013).

2.3. Vegetation survey

In April 2009, 10 quadrats (50 cm × 50 cm) were established in the grazed and ungrazed sites, respectively. Within each quadrat, density and coverage of each species were recorded. Plant density was measured by directly counting the number of stems at a height of about 20 cm for ungrazed sites and 10 cm for grazed sites (Guan et al., 2013). Vegetation cover was visually determined in each quadrat by a 50 cm × 50 cm frame that was divided into 100 cells (5 cm × 5 cm).

2.4. Data analysis

Seed density was calculated as the density of seedlings per m² of a sample. Species were classified into different functional groups according to their life form and longevity (Liu et al. 2009). The percentage of annual and perennial species in each habitat (grazed and ungrazed) was determined. Prior to statistical analyses, data were transformed (log(x + 1)) to improve the normality of the distribution. The differences in seed density and species richness between grazed and ungrazed samples in seed bank were compared by the t-test using SPSS 19.0 (IBM Corporation, Armonk, New York). To compare the

species composition between the seed bank and the above-ground vegetation, Sørensen similarity index (S) was used on the total number of species present in the vegetation and seed bank of grazed and ungrazed sites (Eq. 1):

$$S = 2c/(a + b) \quad (1)$$

where: *a*= number of species in seed bank, *b*= number of species in vegetation and *c*= number of species common in both seed bank and vegetation.

We used permutation-based multivariate analysis of variance (PERMANOVA) to assess the effect of grazing on floristic composition of the seed bank using Bray–Curtis dissimilarities (McCune and Grace, 2002). The statistical significance of F values was tested with a randomization procedure with 4,999 runs. We further used indicator species analysis (ISA) to identify species that consistently differed in their seed density between grazed and ungrazed samples (Dufrene and Legendre, 1997). To compare the species composition in the above-ground vegetation and soil seed bank samples (grazed and ungrazed quadrats), a Detrended Correspondence Analysis (DCA) was conducted using species importance values (Hill and Gauch, 1980). Importance values of each species in the seed bank were calculated by averaging relative density and relative frequency, while importance values of above-ground vegetation were calculated by averaging relative density, relative coverage and relative frequency. PERMANOVA, ISA and DCA were performed using PC-ORD 5.0 (McCune and Mefford, 1999).

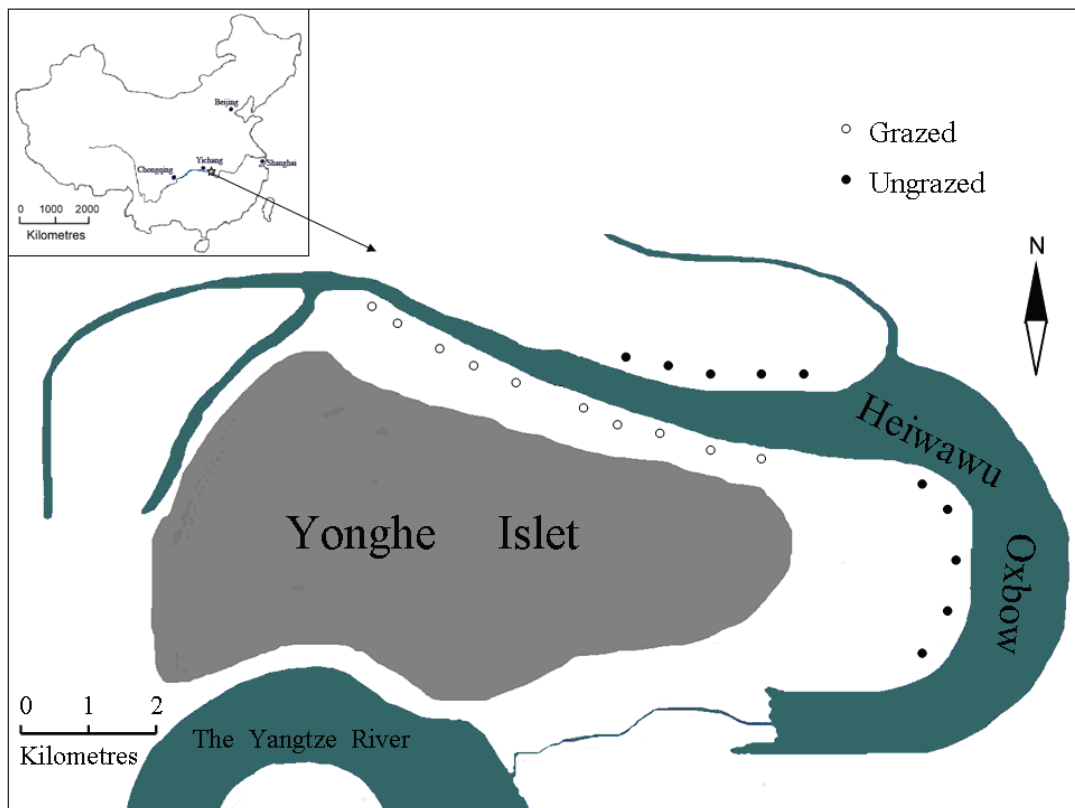


Fig. 1. Map of Hei-wa-wu oxbow wetland showing the grazed and ungrazed plots

3. Results and discussion

3.1. Soil seed bank size and composition

A total of 59 plant species, belonging to 19 families, were recorded in the soil seed bank from grazed and ungrazed plots (Table 1). The observed seed densities in this study (7361 ± 2170 seedlings/m²) were in the range of those observed in temporary wetlands from the middle to lower reaches of the Yangtze River. For example, 1227–10115 seedlings/m² from the lakeshore of Honghu, Longgan and Liangzi Lake have been reported (Li et al., 2008; Liu et al., 2006a; Yuan et al., 2007). However, the species richness found in this study was higher than that found in similar studies in the Yangtze River Basin. For example, 34, 22, and 31 species were recorded in the seed banks of Honghu, Longgan and Liangzi Lakes, respectively (Li et al., 2008; Liu et al., 2006a; Yuan et al., 2007).

The large number of species may be explained by the open nature of the oxbow into which seeds may disperse via wind, water and animals. The oxbow acts as a sink for seeds transported from the upstream of the river during flooding periods. Many wetland plants produce large numbers of seeds, which never have a chance to germinate due to water level fluctuation. The presence of a large and species-rich soil seed bank in the wetland will buffer vegetation change in the short term, although not in the long term (Hulme, 1996).

Annual species accounted for 66% (39 species) of species recorded in the seed banks (Table 1). The most abundant annual species was *Mazus japonicus* which accounted for 22% of total seed density in grazed sites. Consistent with previous studies (Liu et al., 2009; Yuan et al., 2007), annuals dominated the seed banks even though the predominant aboveground plant cover is characterized by perennial species in the oxbow wetland.

The low frequency of seeds of the dominant perennials indicates that many perennials commonly found in the oxbow wetland do not produce a persistent seed bank (Hartman, 1988; Hutchings and Russell, 1989). This was also found in the studies of Ungar and Woodell (1996) in coastal salt wetlands. Research has shown that plant communities are structured predominantly by water regimes and are generally dominated by flood-tolerant species and annuals that can complete their life cycles between the alternate wet and dry phases (Liu et al., 2006b). Annuals show adaptive responses to the seasonal flooding by producing dormant seeds that persist during periods of drought or long-term flooding (Parlak et al., 2011).

Moreover, the Hei-wa-wu oxbow wetland is frequently inundated by floods during spring and summer. Previous work indicated that annuals increased the number of flowers and biomass allocated to seed reproduction with increased duration of inundation (Mony et al., 2010).

3.2. Effect of grazing on size and composition of the seed bank

Although more than double the size, the soil seed bank density of the ungrazed plots (10309 ± 13273 seedlings/m²) was not significantly greater ($P = 0.196$) than grazed plots (4413 ± 1829 seedlings/m²; Table 1). This result may be due to the huge variability in seed bank size among plots. At the local scale, soil seed density can be influenced by many factors, including plant community types and soil physical properties (Csontos, 2007). Similarly, there were not significant differences ($P = 0.389$) in mean species richness of ungrazed (13.2 ± 6.6) versus grazed (15.4 ± 4.3) plots. The percentages of annuals in the grazed and ungrazed samples were 67% and 60%, respectively. Moreover, over 95% of the species recorded in the grazed samples were terrestrial species, compared with 84% in the ungrazed samples.

The size of the seed bank of several species, e.g. *Carex cinerascens*, *Cyperus michelianus*, *Ranunculus sceleratus* and *Veronica anagallis-aquatica*, was significantly reduced by grazing. These species accounted for 60% of total seed density in the ungrazed samples but only accounted for 9% of total seed density in the grazed samples. The reason for the larger soil seed bank in the ungrazed sites is that livestock intake and trampling may have reduced seed production of this species in grazed sites. Furthermore, taller vegetation collects more sediment and litter including seeds compared to the shorter vegetation in the grazed sites (Erkkila, 1998). In our study, water- and wind-dispersed seeds dominated the seed bank. These seeds can accumulate in local depressions, on the edge of tussocks etc. (Jerling, 1983). Osem et al. (2006) showed that grazing by domestic livestock may have various effects on the density and composition of seed banks. Variation in patterns of seed bank response to grazing can be attributed to differences among the studied ecosystems in environmental conditions, grazing regimes and type of domestic livestock, as well as in vegetation composition and species traits (Osem et al., 2006). Our results suggest that continuous grazing has a moderate effect on soil seed bank density of riverine wetlands.

The 28 species common to the grazed and ungrazed samples (Table 1) accounted for 96 % of total seed density in both grazed and ungrazed plots. However, PERMANOVA indicated that there was a significant difference in seed bank composition between the grazed and ungrazed plots ($F = 3.13587$; $P = 0.0004$). Indicator species analysis further indicated that this difference driven by five species (Table 2). Grazing by domestic livestock changed the species composition of the seed banks in the oxbow wetland. Most of the aquatic plants, e.g. *Hydrilla verticillata*, *Myriophyllum verticillatum*, *Nymphoides peltatum*, *Scirpus triquetrum* and *Typha orientalis*, were eliminated from the grazed samples, probably because livestock grazing limited the recruitment of seeds into the soil seed bank.

Table 1. Life form, longevity, absolute seed density (mean± SD), relative seed density (%), and species richness in the seed bank of grazed and ungrazed sites

Species	Life form	Longevity	Grazed		Ungrazed	
			Absolute density (n/m ²)	Relative density (%)	Absolute density (n/m ²)	Relative density (%)
<i>Alopecurus aequalis</i>	Ter	A	115 ± 58	2.6	36 ± 19	1.3
<i>Artemisia annua</i>	Ter	A			36 ± 36	0.6
<i>Artemisia selengensis</i>	Ter	P	4 ± 4	0.4		
<i>Arthraxon hispidus</i>	Ter	A			12 ± 8	0.8
<i>Astragalus sinicus</i>	Ter	A			4 ± 4	0.4
<i>Beckmannia syzigachne</i>	Ter	A			36 ± 28	0.9
<i>Bothriospermum tenellum</i>	Ter	A	44 ± 33	1.1		
<i>Capsella bursa-pastoris</i>	Ter	A			72 ± 72	0.7
<i>Cardamine hirsute</i>	Ter	A	44 ± 27	1.8	52 ± 47	1.0
<i>Cardamine lyrata</i>	Ter	A			115 ± 67	1.7
<i>Carex argyi</i>	Ter	P	12 ± 8	0.8	12 ± 8	0.8
<i>Carex dimorpholepis</i>	Ter	P	4 ± 4	0.4	48 ± 48	0.6
<i>Carex unisexualis</i>	Ter	P	247 ± 76	5.7	123 ± 83	2.1
<i>Carex cinerascens</i>	Ter	P	12 ± 8	0.8	1977 ± 1041	11.5
<i>Centella asiatica</i>	Ter	A	4 ± 4	0.4		
<i>Chenopodium album</i>	Ter	A	4 ± 4	0.4		
<i>Cnidium monnieri</i>	Ter	A	48 ± 19	2.5	203 ± 172	3.6
<i>Coryza canadensis</i>	Ter	A	8 ± 5	0.7	4 ± 4	0.4
<i>Cynodon dactylon</i>	Ter	P	143 ± 86	3.2	28 ± 28	0.5
<i>Cyperus michelianus</i>	Ter	A	16 ± 16	0.5	2427 ± 2423	12.5
<i>Digitaria ciliaris</i>	Ter	A			32 ± 32	0.5
<i>Echinochloa crusgali var. mitis</i>	Ter	A	8 ± 8	0.4	4 ± 4	0.4
<i>Eleusine indica</i>	Ter	A			12 ± 12	0.4
<i>Fimbristylis dichotoma</i>	Ter	A	8 ± 8	0.4		
<i>Gnaphalium affine</i>	Ter	A	159 ± 55	4.1	48 ± 40	1.0
<i>Heleocharis valleculosa f. setosa</i>	Ter	P	215 ± 116	5.4	207 ± 107	3.3
<i>Hemarthria altissima</i>	Ter	P	4 ± 4	0.4		
<i>Hemistepia lyrata</i>	Ter	A	8 ± 5	0.7		
<i>Hydrilla verticillata</i>	S	P			32 ± 32	0.5
<i>Lindernia antipoda</i>	Ter	A			36 ± 22	1.3
<i>Lindernia crustacea</i>	Ter	A	8 ± 8	0.4		
<i>Mazus japonicus</i>	Ter	A	975 ± 298	14.3	1631 ± 1255	10.9
<i>Medicago sativa</i>	Ter	P	48 ± 20	2.2	16 ± 9	1.2
<i>Myriophyllum verticillatum</i>	S	P			4 ± 4	0.4
<i>Nymphoides peltatum</i>	R	P			12 ± 12	0.4
<i>Oenanthe javanica</i>	Ter	P	8 ± 5	0.7		
<i>Paspalum thunbergii</i>	Ter	P			12 ± 12	0.4
<i>Poa annua</i>	Ter	A	318 ± 254	4.6	64 ± 51	1.4
<i>Polygonum hydropiper</i>	T	A	40 ± 21	1.7	12 ± 8	0.8
<i>Polygonum plebeium</i>	Ter	A	99 ± 32	3.1	92 ± 58	2.3
<i>Polypogon fugax</i>	Ter	A	517 ± 110	8.8	330 ± 189	3.9
<i>Potamogeton malaianus</i>	S	P	40 ± 40	0.8	44 ± 44	0.6
<i>Potentilla supine</i>	Ter	A	155 ± 49	4.4	322 ± 296	3.1
<i>Ranunculus chinensis</i>	Ter	A			4 ± 4	0.4
<i>Ranunculus sceleratus</i>	Ter	A	107 ± 46	3.5	943 ± 459	6.8
<i>Rorippa cantoniensis</i>	Ter	A	390 ± 209	6.4	203 ± 59	4.0
<i>Rorippa globosa</i>	Ter	A	24 ± 14	1.2		
<i>Rumex dentatus</i>	Ter	A	8 ± 8	0.4	72 ± 30	3.4
<i>Salvia plebeian</i>	Ter	A	16 ± 9	1.2	4 ± 4	0.4
<i>Scirpus triqueter</i>	T	P			8 ± 8	0.4
<i>Scirpus wallichii</i>	Ter	P	8 ± 8	0.4	16 ± 16	0.5
<i>Stellaria media</i>	Ter	A	4 ± 4	0.4		
<i>Torilis scabra</i>	Ter	A	4 ± 4	0.4		
<i>Triarrhena lutarioriparia</i>	Ter	P			12 ± 8	0.8
<i>Typha orientalis</i>	T	P			20 ± 9	1.6
<i>Veronica anagallis-aquatica</i>	Ter	P	259 ± 194	4.9	796 ± 593	6.5
<i>Veronica peregrina</i>	Ter	A	235 ± 94	5.6	139 ± 53	2.6
<i>Youngia heterophylla</i>	Ter	A	4 ± 4	0.4		
<i>Youngia japonica</i>	Ter	A	40 ± 19	1.7		
Total density			4413 ± 1829	100	10309 ± 13273	100
Species richness			42		45	

A = annual; P = perennial; R = amphibious-responders; S = submerged species; T = amphibious-tolerators; Ter = terrestrial species.

Table 2. Significant indicator species for the grazed and ungrazed soil seed bank community. To be significant, species had to have an indicator value of ≥ 25 and a P value ≤ 0.05

Plant species	Treatment	Indicator value	P value
<i>Carex unisexualis</i>	Grazed	69.0	0.0066
<i>Gnaphalium affine</i>	Grazed	61.9	0.0082
<i>Polypogon fugax</i>	Grazed	61.4	0.0406
<i>Rumex dentatus</i>	Ungrazed	73.1	0.0016
<i>Carex cinerascens</i>	Ungrazed	48.4	0.0444

C. cinerascens, *R. sceleratus* and *V. anagallisaquatica* were reduced by grazing both in the seed bank and in the vegetation. Selective grazing and trampling in freshwater and riparian systems gives less palatable species a competitive advantage (Lodge, 1991; Nicol et al., 2007). Grazing is known to increase the number of gaps in the vegetation and may be responsible for an increase in the cover of annuals (Ungar and Woodell, 1996). *Polypogon fugax*, *Rorippa cantoniensis*, and *Poa annua* benefited from grazing (Table 1). These species were dominant in grazed samples (28%) but rare in the ungrazed samples (6%). Grazing increases the number of ruderal species, such as these (Jutilla, 2003). Through selective grazing, livestock can reduce or eliminate the palatable species from the seed bank but increase the seed density of the unpalatable species in a managed ephemeral wetland (Nicol et al., 2007).

3.3. Effect of grazing on the similarity between the soil seed bank and above-ground vegetation

A total of 44 species were recorded in the above-ground vegetation (Table 3). Sørensen's coefficient of similarity between soil seed bank and above-ground vegetation showed that the grazed samples had a higher similarity value (0.62) than the ungrazed samples (0.47). Many terrestrial annuals in the seed bank of ungrazed samples, such as *Polypogon fugax*, *Rorippa cantoniensis*, *Cnidium monnieri*, and *Cyperus michelianus* were not found in above-ground vegetation. Different responses of species to grazing have been found previously depending on environmental conditions and whether the vegetation is dominated by annual or perennial communities (Bakker and Vries, 1992; Chaideftou et al., 2009; Erkkila, 1998; Peco et al., 1998; Ungar and Woodell, 1996).

In general, there are high similarities in annual-dominated vegetation, but low similarities in most perennial-dominated communities (Osem et al., 2006). In the oxbow wetland, grazing can increase the number of gaps in the vegetation and promote germination of species that are inhibited by dense sediment or plant cover (Peco et al., 1998; Ungar and Woodell, 1996).

The first two DCA axes accounted for 28% of the total variance in species composition among soil seed bank and above-ground vegetation. The distribution of above-ground vegetation samples was more dispersed than that of the seed bank samples (Fig. 2). This indicates greater heterogeneity in species

composition in the above-ground vegetation than in the seed bank. The first axis of the DCA separated grazed vegetation samples from ungrazed vegetation samples, while the second axis showed a clear separation of the seed bank and above-ground vegetation (Fig. 2). These results reflect the minor contribution of the dominant species to the seed bank (Chang et al., 2001; Xiao et al., 2010). *Phalaris arundinacea*, which was characteristic of the oxbow wetland vegetation, was not found in the seed bank.

Table 3. List of species found in the above-ground vegetation of grazed and ungrazed sites

Species	Grazed sites	Ungrazed sites
<i>Alopecurus aequalis</i>	√	√
<i>Alopecurus japonicus</i>	√	√
<i>Artemisia annua</i>		√
<i>Artemisia selengensis</i>	√	
<i>Astragalus sinicus</i>	√	
<i>Beckmannia syzigachne</i>		√
<i>Cardamine hirsuta</i>		√
<i>Cardamine lyrata</i>		√
<i>Carex argyi</i>	√	
<i>Carex unisexualis</i>	√	
<i>Carex cinerascens</i>	√	√
<i>Centella asiatica</i>	√	
<i>Centipeda minima</i>		√
<i>Cnidium monnieri</i>	√	
<i>Cynodon dactylon</i>	√	
<i>Cyperus rotundus</i>	√	
<i>Echinochloa crusgali var. mitis</i>	√	
<i>Euphorbia helioscopia</i>	√	
<i>Geranium wilfordii</i>	√	
<i>Gnaphalium affine</i>	√	
<i>Heleocharis valleculosa f. setosa</i>	√	√
<i>Hemarthria altissima</i>	√	
<i>Hemistepta lyrata</i>		√
<i>Kalimeris indica</i>	√	
<i>Lindernia antipoda</i>	√	
<i>Mazus japonicus</i>	√	√
<i>Medicago lupulina</i>	√	
<i>Medicago sativa</i>	√	
<i>Myriophyllum verticillatum</i>		√
<i>Phalaris arundinacea</i>	√	√
<i>Poa annua</i>	√	
<i>Polygonum hydropiper</i>	√	√
<i>Polygonum plebeium</i>	√	
<i>Polypogon fugax</i>	√	
<i>Potentilla supina</i>		√
<i>Ranunculus chinensis</i>	√	
<i>Ranunculus sceleratus</i>	√	√
<i>Rumex dentatus</i>		√
<i>Salvia plebeia</i>	√	
<i>Scirpus wallichii</i>	√	
<i>Trigonotis peduncularis</i>	√	
<i>Veronica anagallisaquatica</i>	√	√
<i>Veronica peregrina</i>	√	√
<i>Youngia heterophylla</i>	√	

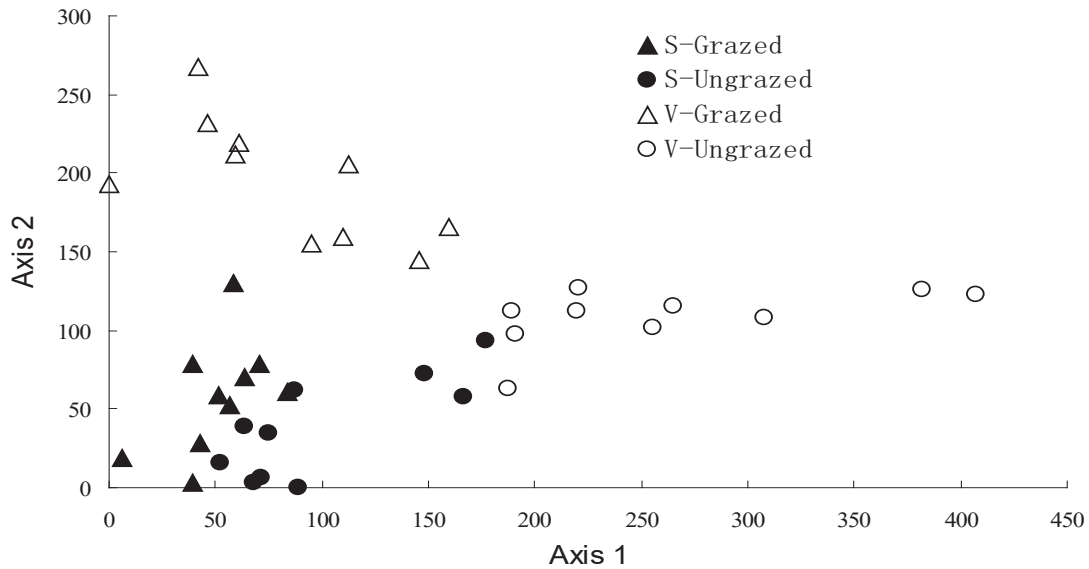


Fig. 2. Detrended Correspondence Analysis (DCA) ordination of seed bank and above-ground vegetation samples (S= seed bank; V= above-ground vegetation)

Carex cinerascens, *Carex argyi*, and *Heleocharis valliculosa* were frequently found in the above-ground vegetation, but they only accounted for 16 % of the total seed density.

The reason may be that these species have a limited seed production because they alternate between sexual reproduction and vegetative forms and their seeds persist in the soil for short periods of time (Boedeltje et al., 2003; Thompson, 2000; Touzard et al., 2002). In contrast, *M. japonicus*, *P. fugax*, and *C. michelianus* accounted for 40% of the total seed density, possibly due to a production of large numbers of small seeds. It is commonly believed that small-seeded species usually form more abundant seed banks than large-seeded species (Honda, 2008; Thompson et al., 2001).

4. Conclusions

In the Hei-wa-wu oxbow wetland of the Yangtze River, grazing by domestic livestock during dry phases does not significantly impact the seed density and species richness of the soil seed bank. However, grazing changes the species composition of both soil seed bank and standing vegetation. Moreover, the similarity between the soil seed bank and the above-ground vegetation in grazed samples was higher than that in ungrazed samples. We suggest that current grazing practices in the Hei-wa-wu oxbow wetland have moderate effects on the soil seed bank. Reduced grazing intensity or rotational grazing can increase the seed density of several annual species (e.g., *Cyperus michelianus* and *Ranunculus sceleratus*) in soils and may thus promote the development of above-ground vegetation in the Hei-wa-wu oxbow wetland.

Acknowledgments

We would like to thank Yu Cheng, Youping Liu, and Guang Deng for their help with field samplings. We also thank Prof. Stephen Maberly, Dr. Chris Hakkenberg and three anonymous reviewers who gave helpful comments on the manuscript. This research was supported by the National Key Technology R&D Program (2012BAC06B04), the Project of NSF-Hubei (2012FFA139), the Innovation Key project of CAS (KSCX2-YW-Z-1023-5), National Natural Science Foundation of China (51379133) and Young Talent Program of NSF-Hubei (2007ABB041).

References

- Bakker J., Vries Y., (1992), Germination and early establishment of lower salt-marsh species in grazed and mown salt marsh, *Journal of Vegetation Science*, **3**, 247-252.
- Barnewitz E., Klinkenberg A., Scheibel J., (2012), Effects of goat grazing and mowing on seed density and seed mass of *Lespedeza cuneata*, *Tillers*, **6**, 21-25.
- Blanch S.J., Brock M.A., (1994), Effects of grazing and depth on two wetland plant species, *Marine and Freshwater Research*, **45**, 1387-1394.
- Boedeltje G., Bakker J.P., ter Heerdt G.N.J., (2003), Potential role of propagule banks in the development of aquatic vegetation in backwaters along navigation canals, *Aquatic Botany*, **77**, 53-69.
- Brock M.A., (2011), Persistence of seed banks in Australian temporary wetlands, *Freshwater Biology*, **56**, 1312-1327.
- Brock M.A., Theodore K., O'Donnell L., (1994), Seed-bank methods for Australian wetlands, *Marine and Freshwater Research*, **45**, 483-493.
- Chaideftou E., Thanos C.A., Bergmeier E., Kallimanis A., Dimopoulos P., (2009), Seed bank composition and above-ground vegetation in response to grazing in sub-Mediterranean oak forests (NW Greece), *Plant Ecology*, **201**, 255-265.

- Chang E., Jefferies R., Carleton T., (2001), Relationship between vegetation and soil seed banks in an arctic coastal marsh, *Journal of Ecology*, **89**, 367-384.
- Crossle K., Brock M.A., (2002), How do water regime and clipping influence wetland plant establishment from seed banks and subsequent reproduction?, *Aquatic Botany*, **74**, 43-56.
- Csontos P., (2007), Seed banks: ecological definitions and sampling considerations, *Community Ecology*, **8**, 75-85.
- Dufrene M., Legendre P., (1997), Species assemblages and indicator species: the need for a flexible asymmetrical approach, *Ecological Monographs*, **67**, 345-366.
- Ehrlén J., (1995), Demography of the perennial herb *Lathyrus vernus*. II. Herbivory and population dynamics, *Journal of Ecology*, 297-308.
- Erkkilä H.M.J.B., (1998), Seed banks of grazed and ungrazed Baltic seashore meadows, *Journal of Vegetation Science*, **9**, 395-408.
- Granstrom A., (1988), Seed banks at six open and afforested heathland sites in southern Sweden, *Journal of Applied Ecology*, **25**, 297-306.
- Guan B., Yu J.B., Cao D., Li Y.Z., Han G.X., Mao P.L., (2013), The ecological restoration of heavily degraded saline wetland in the Yellow River delta, *CLEAN – Soil, Air, Water*, **41**, 690-696.
- Hao Y.J., Wang D., Wei Z., Zhu J., Wang L. M., Zhang X. Q., (2004), Problems and Countermeasures in Conservation of Tianezhou Oxbow Wetland of the Yangtze River, *Advances in Biodiversity Conservation and Research in China*, 319-328.
- Harper J.L., (1977), *Population Biology of Plants*, Academic Press, London.
- Hartman J.M., (1988), Recolonization of small disturbance patches in a New England salt marsh, *American Journal of Botany*, **75**, 1625-1631.
- Hill M.O., Gauch H., (1980), Detrended correspondence analysis: an improved ordination technique, *Plant Ecology*, **42**, 47-58.
- Honda Y., (2008), Ecological correlations between the persistence of the soil seed bank and several plant traits, including seed dormancy, *Plant Ecology*, **196**, 301-309.
- Hulme P.E., (1996), Herbivory, plant regeneration, and species coexistence, *Journal of Ecology*, **84**, 609-615.
- Hutchings M., Russell P., (1989), The seed regeneration dynamics of an emergent salt marsh, *The Journal of Ecology*, **77**, 615-637.
- Jansen A., Robertson A.I., (2001), Relationships between livestock management and the ecological condition of riparian habitats along an Australian floodplain river, *Journal of Applied Ecology*, **38**, 63-75.
- Jerling L., (1983), Composition and viability of the seed bank along a successional gradient on a Baltic sea shore meadow, *Ecography*, **6**, 150-156.
- Jutila H.M., (2003), Germination in Baltic coastal wetland meadows: similarities and differences between vegetation and seed bank, *Plant Ecology*, **166**, 275-293.
- Levine C.R., Winchcombe R.J., Canham C.D., Christenson L.M., Ronsheim M.L., (2012), Deer Impacts on Seed Banks and Saplings in Eastern New York, *Northeastern Naturalist*, **19**, 49-66.
- Li W., Huang B., Li R.R., (2002), Assessing the effect of fisheries development on aquatic vegetation using GIS, *Aquatic Botany*, **73**, 187-199.
- Li E.H., Liu G.H., Li W., Yuan L.Y., Li S.C., (2008), The seed-bank of a lakeshore wetland in Lake Honghu: implications for restoration, *Plant Ecology*, **195**, 69-76.
- Liu G. H., Zhou J., Li W., Cheng Y., (2005), The seed bank in a subtropical freshwater marsh: implications for wetland restoration, *Aquatic Botany*, **81**, 1-11.
- Liu G.H., Li W., Li E.H., Yuan L.Y., Davy A.J., (2006a), Landscape-scale variation in the seed banks of floodplain wetlands with contrasting hydrology in China, *Freshwater Biology*, **51**, 1862-1878.
- Liu G.H., Li W., Zhou J., Liu W.Z., Yang D., Davy A.J., (2006b), How does the propagule bank contribute to cyclic vegetation change in a lakeshore marsh with seasonal drawdown?, *Aquatic Botany*, **84**, 137-143.
- Liu W.Z., Zhang Q.F., Liu G.H., (2009), Seed banks of a river-reservoir wetland system and their implications for vegetation development, *Aquatic Botany*, **90**, 7-12.
- Lodge D.M., (1991), Herbivory on freshwater macrophytes, *Aquatic Botany*, **41**, 195-224.
- Loydi A., Zalba S.M., Distel R.A., (2012), Viable seed banks under grazing and enclosure conditions in montane mesic grasslands of Argentina, *Acta Oecologica*, **43**, 8-15.
- MacGillivray C., Grime J., (1995), Testing predictions of the resistance and resilience of vegetation subjected to extreme events, *Functional Ecology*, **9**, 640-649.
- McCune B., Mefford M.J., (1999), PC-ORD: Multivariate Analysis of Ecological Data. Version 4 for Windows; [user'S Guide], MjM Software Design.
- McCune B., Grace J.B., (2002), Analysis of ecological communities. Gleneden Beach, OR: MjM Software Design.
- McDonald A., Bakker J., Vegelin K., (1996), Seed bank classification and its importance for the restoration of species-rich flood-meadows, *Journal of Vegetation Science*, **7**, 157-164.
- Mony C., Mercier E., Bonis A., Bouzillé J.B., (2010), Reproductive strategies may explain plant tolerance to inundation: A mesocosm experiment using six marsh species, *Aquatic Botany*, **92**, 99-104.
- Moon J., Jung Y., Lee T., Kim T.C., Rho P., Shin Y.C., Ryu J., Lim K.J., (2013), Determining the effective width of riparian buffers in Korean watersheds using the swat model, *Environmental Engineering and Management Journal*, **12**, 2249-2260.
- Mulder C.P.H., Ruess R., (1998), Relationships between size, biomass allocation, reproduction, and survival in *Triglochin palustris*: implications for the effects of goose herbivory, *Canadian Journal of Botany*, **76**, 2164-2176.
- Nicol J., Muston S., D'Santos P., McCarthy B., Zukowski S., (2007), Impact of sheep grazing on the soil seed bank of a managed ephemeral wetland: implications for management, *Australian Journal of Botany*, **55**, 103-109.
- Ortega M., Levassor C., Peco B., (1997), Seasonal dynamics of Mediterranean pasture seed banks along environmental gradients, *Journal of Biogeography*, **24**, 177-195.
- Osem Y., Perevolotsky A., Kigel J., (2006), Size traits and site conditions determine changes in seed bank structure caused by grazing exclusion in semiarid annual plant communities, *Ecography*, **29**, 11-20.
- Parlak A.O., Gokkus A., Demiray H.C., (2011), Soil seed bank and aboveground vegetation in Grazing Lands of Southern Marmara, Turkey, *Notulae Botanicae Horti Agrobotanici Cluj-Napoca*, **39**, 96-106.
- Peco B., Ortega M., Levassor C., (1998), Similarity between seed bank and vegetation in Mediterranean grassland: a predictive model, *Journal of Vegetation Science*, **9**, 815-828.

- Reiné R., Chocarro C., Fillat F., (2004), Soil seed bank and management regimes of semi-natural mountain meadow communities. *Agriculture, Ecosystems & Environment*, **104**, 567-575.
- Russi L., Cocks P., Roberts E., (1992), Seed bank dynamics in a Mediterranean grassland, *Journal of Applied Ecology*, **29**, 763-771.
- TerHeerdt G.N.J., Verweij G. L., Bekker R. M., Bakker J. P., (1996), An improved method for seed-bank analysis: Seedling emergence after removing the soil by sieving, *Functional Ecology*, **10**, 144-151.
- Tessema Z.K., de Boer W.F., Baars R.M.T., Prins H.H. T., (2012), Influence of grazing on soil seed banks determines the restoration potential of aboveground vegetation in a semi-arid Savanna of Ethiopia, *Biotropica*, **44**, 211-219.
- Thompson K., (2000), *The Functional Ecology of Soil Seed Banks*, In: *Seeds: the Ecology of Regeneration in Plant Communities*, Fenner M., CAB International, Wallingford, UK, 215-235.
- Thompson K., Jalili A., Hodgson J.G., Hamzeh ee B., Asri Y., Shaw S., Shirvany A., Yazdani S., Khoshnevis M. and Zarrinkamar F., (2001), Seed size, shape and persistence in the soil in an Iranian flora, *Seed Science Research*, **11**, 345-356.
- Touzard B., Amiaud B., Langlois E., Lemauviel S., Clement B., (2002), The relationships between soil seed bank, aboveground vegetation and disturbances in an eutrophic alluvial wetland of Western France, *Flora*, **197**, 175-185.
- Ungar I.A., Woodell S.R.J., (1996), Similarity of seed banks to aboveground vegetation in grazed and ungrazed salt marsh communities on the Gower Peninsula, South Wales, *International Journal of Plant Sciences*, **157**, 746-749.
- van der Valk A.G., Davis C., (1978), The role of seed banks in the vegetation dynamics of prairie glacial marshes, *Ecology*, **59**, 322-335.
- van der Valk A.G., (2005), Water-level fluctuations in North American prairie wetlands, *Hydrobiologia*, **539**, 171-188.
- Vlad L., Toma D., (2017), Restoring wetlands and natural floodplain along the lower Baseu River in Romania, *Environmental Engineering and Management Journal*, **16**, 2337-2346.
- Wu M.W., Chen L., Yan L., Deng X.L., He X.H., (2006), Analysis of effect of a doption of fries by filling with river flows on water quality and sediment of Tianezhou wetland, *Engineering Journal of Wuhan University*, **39**, 36-40.
- Wu Z., Peter H.R., (2013), Flora of China, On line at: <http://foc.eflora.cn/>.
- Xiao C., Dou W.F., Liu G.H., (2010), Variation in vegetation and seed banks of freshwater lakes with contrasting intensity of aquaculture along the Yangtze River, China, *Aquatic Botany*, **92**, 195-199.
- Yuan L.Y., Liu G.H., Li W., Li E.H., (2007), Seed bank variation along a water depth gradient in a subtropical lakeshore marsh, Longgan Lake, China, *Plant Ecology*, **189**, 127-137.
- Zimmerman R.C., Kohrs D.G., Alberte R.S., (1996), Top-down impact through a bottom-up mechanism: the effect of limpet grazing on growth, productivity and carbon allocation of *Zostera marina* L. (eelgrass), *Oecologia*, **107**, 560-567.



“Gheorghe Asachi” Technical University of Iasi, Romania



ANALYSIS OF THE MATERIAL COMPOSITION OF MIXED MUNICIPAL SOLID WASTE IN THE KOŠICE REGION OF THE SLOVAK REPUBLIC

Takáčová Zita^{1*}, Vindt Tomáš¹, Havlík Tomáš¹, Kvokačka Jozef²

¹Technical University of Kosice, Faculty of Metallurgy, Department of Non-ferrous Metals and Waste Treatment,
Letna 9, 042 00 Kosice, Slovakia

²Cityhall of Košice, Department of Environment and Special Construction Authority, Tr. SNP 48 / A, 04011 Košice, Slovakia

Abstract

This work focuses on the analysis of material composition of mixed municipal solid waste (MSW) in the city of Košice, the second largest city in Slovakia, and in the village of Poproč, which is representative of the region. The paper describes the characteristics of the monitored localities, the methodology and the original evaluation procedure. The analysis of the mixed MSW composition in Poproč was performed in 2009-2010, and in Košice in 2011. In both cases, the analysis was carried out in each season in four campaigns according to a regular interval of waste collection. 36 samples were analyzed in Košice with an average weight of 236.1 kg, and 4 samples were analyzed in Poproč with an average weight of 208.2 kg. The mixed MSW was sorted into categories and subcategories. The biodegradable waste had the highest content at both sites. The content of the biodegradable MSW in Poproč was about 25% lower than in Košice because of the built-up area type. The content of packaging was 24% in Košice and 29% in Poproč.

Key words: analysis, material composition, mixed municipal solid waste (mixed MSW), sieving, sorting

Received: March, 2013; *Revised final:* June, 2014; *Accepted:* July, 2014; *Published in final edited form:* April 2018

1. Introduction

In Slovakia, about 1.2 million tons of mixed MSW are produced per year, which represents approximately 67% of the total amount of MSW (Fig. 1) (Klinda et al., 2010).

According to the Decree of the Ministry of Environment of the Slovak Republic No. 284/2001 Coll. which defines the Waste catalogue the mixed MSW belongs to a Group 20 - municipal wastes with the catalog number 20 03 01. MSW is defined as waste collected by a municipality. It refers to waste generated in households, small business, office buildings and institutions such as schools, hospitals, government buildings, waste from parks and street

cleaning. Mixed MSW is a part of municipal waste which consists of non-separated solid waste from households and waste with similar characteristics and composition.

In Slovakia, the mixed MSW disposal is carried out mainly in two ways: landfilling (86%) and incineration with or without energy recovery (Ministry of Environment of Slovak Republic, 2010). Slovakia has only two incineration plants (in Bratislava and Košice) for incineration of mixed MSW. The fees for landfilling are currently growing up. A fee for landfilling mixed municipal waste is in range of 5-10 euros per ton, depending on waste composition. On the other hand, one tone of mixed MSW has a caloric value of 8-12 MJ/kg (IEA, 2003),

* Author to whom all correspondence should be addressed: e-mail: zita.takacova@tuke.sk; Phone: +421556022427; Fax: +421556022428

which is comparable to a caloric value of brown coal. From that reason, mixed MSW can be considered as a secondary raw material for energy recovery.

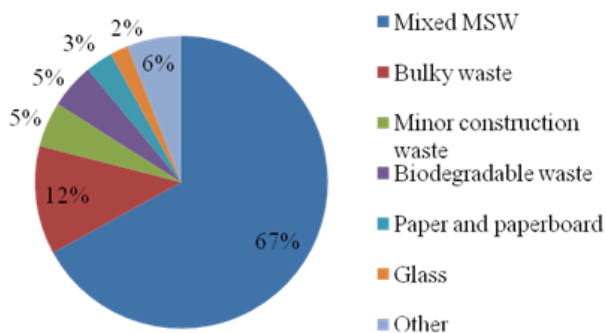


Fig. 1. The composition of MSW in Slovakia (Klinda et al., 2010)

The main component of mixed MSW is biodegradable waste. According to the EU, biodegradable MSW going to landfills must be reduced to 75% of the total amount (by weight) of biodegradable MSW produced in 1995 by the year 2006, to 50% by 2009 and to 35% by 2016 (EC Directive, 1999).

Slovakia is one of the EU Member States, which can take advantage of a four-year delay, considering the heavy reliance on landfilling. This means that the target years are 2010, 2013 and 2020. To meet the EU goals, Slovakia takes steps to reduce the amount of landfilled biodegradable MSW mainly through recycling, composting, biogas production or the use of waste as a source of secondary raw materials and energy. Since January 1st 2010, a separate collection of four components of MSW - paper, plastics, glass and metals is required for all municipalities in Slovakia. Directive 2008/98/EC of the European Parliament and of the Council of 19 November 2008 sets recycling goals for MSW disposal for the Member States, namely 50% for paper, metals, plastic and glass from households by 2020 (EC Directive, 2008). Simultaneously, it is necessary to meet the goals for the reduction of landfilled biodegradable MSW, as mentioned above. In this regard, the identification of the mixed MSW composition is the key factor from which all necessary steps and measures for the achievement of the defined goals are derived.

Mixed MSW is highly heterogeneous in terms of qualitative and quantitative material composition. Its amount and composition depend on the population size and demographic characteristic, and simultaneously on the market development and the community consumption. According to the mixed MSW composition it is possible to assume the yield of separated collection as well as to define the insufficiencies in this field.

There are many similar studies that have been carried out in different countries (Banar and Ozkan, 2008; Burnley et al., 2007; Riber et al., 2009), with either the original methodology, or the methodology

transposed from other sources. However, the local conditions must be taken into account.

The mixed MSW composition is influenced by several factors which must be considered in the planning, sampling and analysis process (ASTM D5231 – 92, 2008; Gidakaros et al., 2006; SAEFL, 2004). These are mainly: the seasons, the age structure of population, built-up area types and methods of heating, collection intervals and separate collection parameters (number and location of containers for separated waste, separately collected commodities) and so on. The analysis of the mixed MSW composition in Košice and Poproč was carried out for the following reasons:

- The long-term absence of relevant objective data about the mixed MSW composition in the region.
- The variability of the material composition and amount of mixed MSW produced under the influence of economic and social situation.
- New possibilities for mixed MSW disposal resulting from the European and Slovak standards.

In the years 2009 – 2011, the analysis of the mixed MSW composition was performed independently in the regional city of Košice in Eastern Slovakia and in Poproč village that is 37 km far from Košice. Poproč is a member of Regional Associations of Municipalities *Rudohorie* which includes 16 municipalities. This Association chose the village of Poproč as a representative of this region due to the number of inhabitants, their age structure and an established waste management system.

The main goal of the analysis was to define the material composition of the mixed MSW as well as the amount of packaging. In Poproč, other MSW streams were monitored too, such as bulky waste, separately collected fractions, etc. While the analysis in Košice was based on the SWA-Tool methodology recommendations (European Commission, 2004a, b), in Poproč the mixed MSW composition was analyzed according to the Kotoulová methodology (Kotoulová, 2001). The results could be compared, because the methodologies in the comparing parameters were not significantly different.

1.1. Characteristics of the studied region

Slovakia, a member of the European Union, is a landlocked country in Central Europe with the area of 49 035 km². About 5.4 million inhabitants live in Slovakia. Slovakia borders with the Czech Republic, Austria, Hungary, Ukraine and Poland. The capital city is Bratislava. The population density is approximately 110.8 inhabitants/km²; there are 2891 independent municipalities, including 138 towns (2010). Bratislava and Košice are the largest cities in population. More than 57% of population lives in cities. Slovakia is divided into 8 regions, and the Košice region is one of the regions with the largest population (Statistical Office of the Slovakia, 2012).

The Slovak Republic is a parliamentary democracy and the official language is Slovak. Since May 2004 it has been a member state of the European

Union, and since December 2007 it has been a member of the Schengen area. Since January 2009 it has been a member of the European Monetary Union with the official Euro currency (European Union, 2013). Slovakia is in the North Temperate Zone. Its geographical position is in the middle of Europe. The city of Košice, the second largest city in Slovakia, is located in the eastern part of Slovakia. The population of Košice is about 240000 (Statistical Office of the Slovakia, 2012). Of the total number of inhabitants, 15.4% is in the pre-productive age (persons aged 0-18 years), 62.8% in the productive age and 21.8% in the post-productive age.

The MSW disposal in Košice is carried out by Kosit, Inc. Company, whose amount of the MSW disposal was about 49000 t in 2011 (Kopernický, 2011). Separate collection of paper, plastic, glass and metal has been introduced there. In summer 2011, multilayer composite materials started to be separated as well (for example Tetra Pak packaging materials). In 2011, the total amount of separately collected MSW in Košice was nearly 5000 tons of paper and paperboard, 2500 t of glass, 1800 t of metals and 700 t of plastic (Kopernický, 2011). The mixed MSW is recovered/disposed in the MSW incinerator of Kosit, Inc. Company. Produced heat is used for purposes of an incineration plant and for heating one of the district of Košice. Currently, the Kosit, Inc. Company is starting a production of electricity from the mixed MSW. The mixed MSW collection and transport interval is 2-3 times a week depending on the district. For analysis of the mixed MSW composition, it was necessary to divide Košice area into three sections according to the building types and used waste containers:

- The section of multi-storey buildings – 4 districts mostly with 1100 l waste containers,
- The rural section – 11 districts mostly with 110 and 120 l litter bins,
- The mixed section – 4 districts with both built-up area types and both container types (waste containers and litter bins).

Poproč is in the Košice region, in the Košice-okolie district. Poproč has 2736 inhabitants (by December 31st 2009). Of the total number of inhabitants, 16.8% is in the pre-productive age, 62.9 % in the productive age and 20.3% in the post-productive age. Separate collection of paper, plastic, glass, multilayer composite materials and metal containers has been launched. The amount of the MSW disposal in 2009 was about 630 t, from which 85 t (13.5 %) was collected separately. Specifically, it was 19.5 t of paper and paperboard, 47.2 t of glass, 9.5t of plastic and 4.5 t of WEEE. At present, all generated mixed MSW is landfilled (Kvokačka, 2011). The rural buildings are very typical for Poproč. Therefore, there was no need to divide this area according to the built-up type. The mixed MSW is collected in 110 l litter bins at two-week intervals.

The map of Slovakia showing the studied localities is shown in Fig. 2.

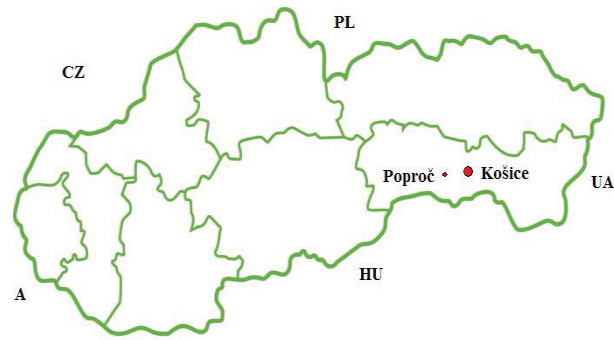


Fig. 2. The Slovakia map showing the studied locations

2. Experiments

2.1. Methodology for sampling and analysis

In both localities, the analysis of the mixed MSW composition was carried out during one year in each season. The cycle of sample collection was the same in each season, which followed a regular mixed MSW collection interval, thus representative sampling was ensured. In Košice, one part of the district from residential, rural and mixed section was selected based on the average age structure and number of inhabitants for sampling and analysis because of the impossibility to analyze all generated mixed MSW. In Poproč, all generated mixed MSW was analyzed for a specified time period.

One collecting vehicle was considered a general sampling unit, from which 200 kg samples were taken. The vehicle was emptied in an open area and the waste was homogenized. The samples with the total volume of about 1 m³ and a weight of 200 kg were taken from a pile of dumped waste by a hydraulic rotary loader from 5 different places. These samples were manually sorted into defined categories and subcategories. As a guide for separation of the finest fraction the screens were used. The finest fraction was a separate category.

In both localities, a similar approach for sampling was used, consisting of the following main steps:

1. Analyzed waste (one collecting vehicle) from the selected part/district of the city of Košice in each section was collected and transported to a designated location. The days of collection and analysis were the same as the days of the regular collection interval. In case of Poproč, the mixed MSW was collected from the whole village.

2. All the waste was weighed and the data were recorded in the form (date, district, weight of all waste, etc.).

3. The mixed MSW from the vehicle was dumped and homogenized and a sample with a total volume of about 1 m³ and weight of about 200 kg was taken by the hydraulic rotary loader.

4. Each sample was sorted separately. The sorting procedure was following (Fig. 3).

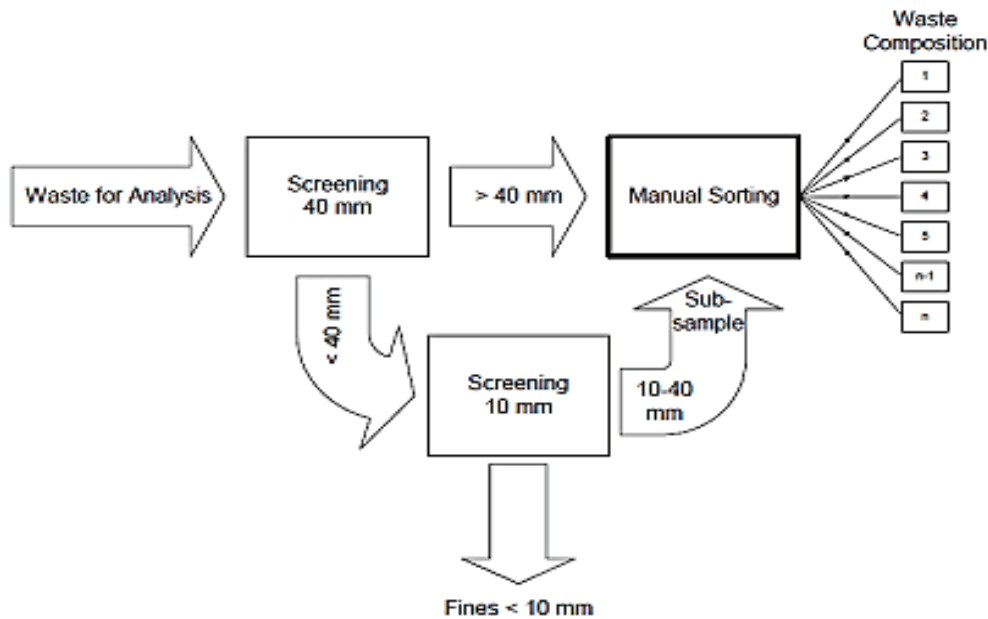


Fig. 3. The sorting procedure (Brasov Waste Analysis Final Report, 2004)

- Separation of the waste into the fractions + 4 cm and +1 - 4 cm by screening with 4 cm mesh screen-table.
- Sorting of the + 4 cm fraction into the waste categories mentioned above.
- Dividing of the +1 - 4 cm fraction into the fraction - 1 cm and fraction +1 - 4 cm by screening with 1 cm mesh screen-table.
- The - 1 cm fraction was reported as the category: fine fraction < 1 cm.

5. The obtained categories and subcategories were weighted; the data were recorded and statistically evaluated.

The following main sorting categories were adopted:

- Košice – 12 main categories: paper, glass, plastic, metals, biodegradable waste, multilayer composite materials, wood, textile and shoes, WEEE, inert waste, hazardous waste, and fine fraction < 1 cm.
- Poproč – 10 main categories: paper, glass, plastic, metals, biodegradable waste, textile, inert waste, hazardous waste, fine fraction, and combustible waste.

2.2. Sampling and analysis

The mixed MSW sampling and subsequent analysis was performed in each season in both localities using the same method. The data of each component weight were recorded in the protocol, they were evaluated separately for each section and season and subsequently the total results were calculated. Nine samples were analyzed in the Košice analysis in each season; it means 36 samples with the average weight of 236.2 kg altogether. Four samples (one for each season) with the average weight of 208.2 kg were analyzed in Poproč.

2.3. Analysis evaluation

2.3.1. Košice

The evaluation of the analysis of the mixed MSW material composition according to the sections, seasons and total was performed. The multi-storey building section results and rural section results in each season were obtained by a simple arithmetic average of the partial results. Another situation occurred in the case of the mixed section.

There the samples from the multi-storey building type (from 1100 l containers) and also from the rural building type (from 110 l litter bins) were taken and they were evaluated separately. For this reason it was impossible to carry out a simple arithmetic average for the mixed section. In order to gain the total results of the mixed section, it was necessary to consider the amount of the mixed MSW from one week from both types of containers, so that the results represented the real situation using the following formula (Eq. 1):

$$m1w1 + m2w2 = m3w3 \quad (1)$$

Therefore (Eq. 2):

$$w3 = (m1w1 + m2w2) / m3 \quad (2)$$

where:

$w1, w2, w3$ – wt. % of the waste category,

$m1$ – an average weight of the mixed MSW generated per one week (collected interval) in the mixed section from 110 l litter bins,

$m2$ – an average weight of the mixed MSW generated per one week (collected interval) in the mixed section from 1100 l containers,

$m3$ – an average weight of the mixed MSW generated per one week (collected interval) in the mixed section together.

A calculation of the average weight of the mixed MSW collected per one week was carried out by following (Eq. 3):

$$m_{1,2,3} = c_i * n_c * m \tag{3}$$

where: c_i – collection interval, n_c – a number of containers/bins, m – an average weight of one filled container/bin

Data was provided by Kosit, Inc. Company. In the analysis evaluation for one season from all sections together, the amount of generated mixed MSW in each section was calculated similarly as Eq. (1) (Eq. 4):

$$m_1w_1 + m_2w_2 + m_3w_3 = m_4w_4 \tag{4}$$

Therefore (Eq. 5):

$$w_4 = (m_1w_1 + m_2w_2 + m_3w_3) / m_4 \tag{5}$$

where: w_1, w_2, w_3, w_4 – wt. % of the waste category, m_1, m_2, m_3 – an average weight of the mixed MSW generated per one week in each section, m_4 – a total amount of the mixed MSW generated per one week together. The total year results were calculated by the arithmetic average of the particular season results.

2.3.2. Poproč

Due to the fact that in Poproč only one sample was analyzed each season, the evaluation of the analysis data was carried out by a simple arithmetic average of the partial results.

3. Results and discussion

3.1. Material composition of mixed MSW

The total results of the mixed MSW material composition analysis according to the seasons and the summary in Košice and Poproč are shown in Fig. 4 and Fig. 5. For the comparison of results, the

combustible waste from the Poproč analysis was divided into the categories of biodegradable waste and wood. Multilayer composite materials were removed from the paper category and evaluated as a separate category. The comparison between the composition of the mixed MSW from each section in Košice and in Poproč is shown in Fig. 6.

3.2. Representation of packaging

Packaging of various material composition comprised 29% of the total amount of the mixed MSW. In Košice, it was almost 24%. The comparison of packaging material representation from the both sites is shown in Fig. 7. The presented study aimed at the comparison of the mixed MSW material composition results of analysis, which was carried out in the city of Košice and the village of Poproč in the Slovak Republic. In terms of the generation and composition, the age structure is an important factor. From this perspective it is possible to say that the localities are very similar. At both localities approximately 17% of the population is in the pre-productive, 63% in the productive and 20% in the post-productive age.

Both analyses were carried out in each season. In the case of Košice, it was shown that the seasons had a minimal impact on the content of components in mixed MSW. As for Poproč, the situation was different. The biodegradable waste content was higher in autumn than in other seasons, and this fact can be related to the end of the gardening season and preparation of gardens for winter. The biodegradable waste had the highest content in both localities in each season, nearly 50% in Košice and about 25% in Poproč.

The reason for the high content of biodegradable waste is the absence of its separate collection and well-functioning separate collection of other commodities. On the other hand, 25 % difference between the content of biodegradable waste in Košice and Poproč is caused by the building type.

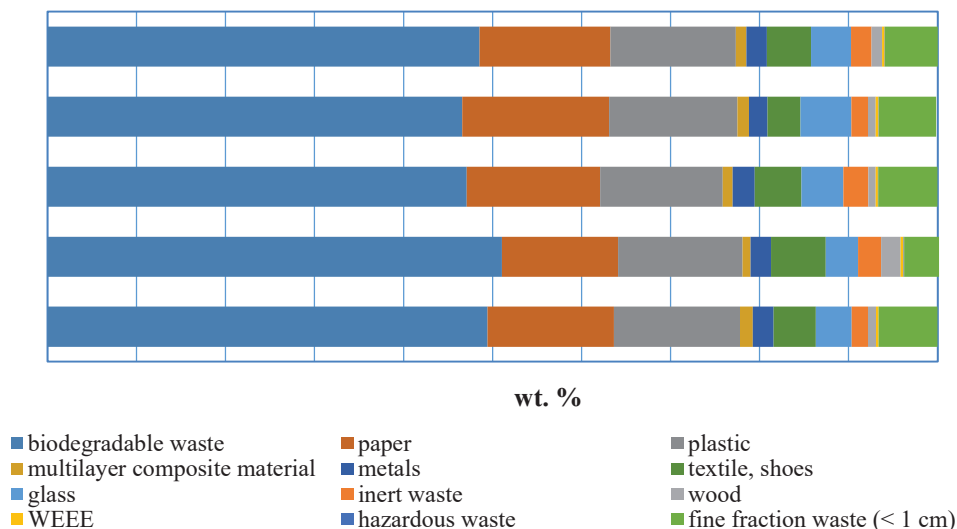


Fig. 4. The mixed MSW composition in each season and total - Košice

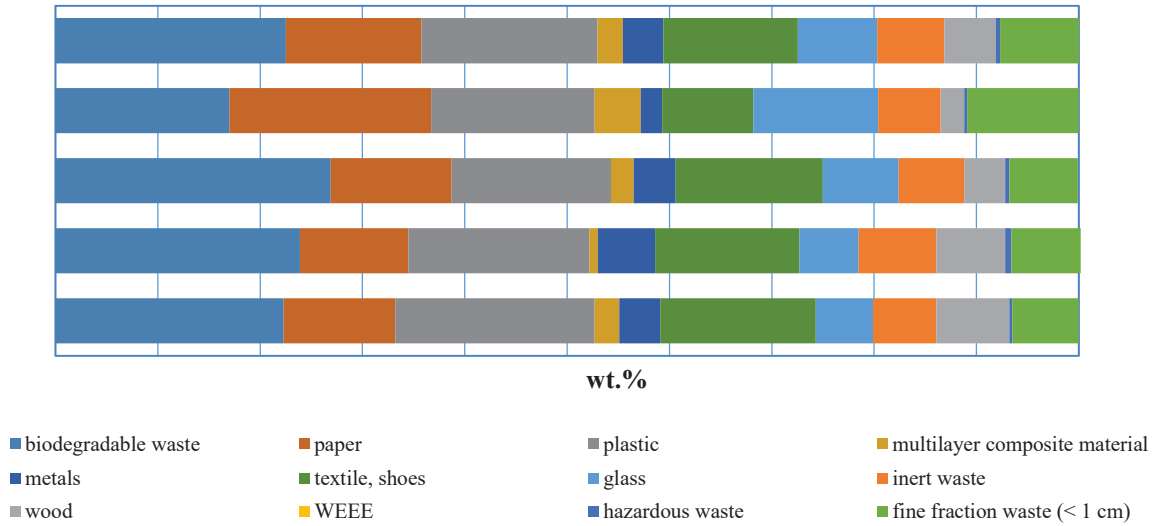


Fig. 5. The mixed MSW composition in each season and total – Poproč

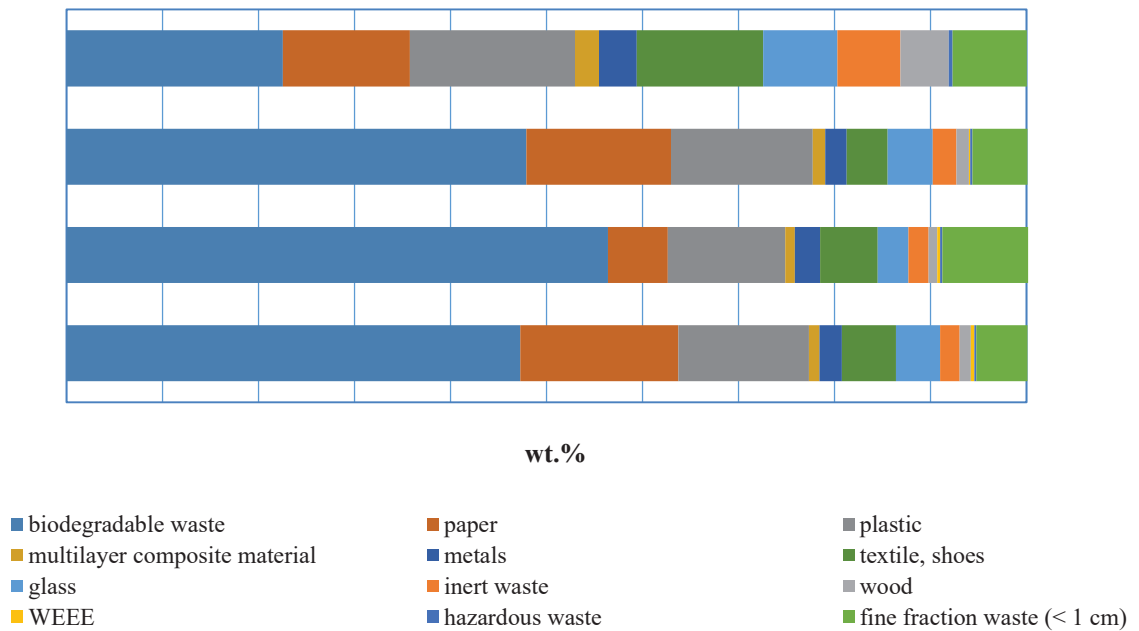


Fig. 6. The mixed MSW composition in each section in Košice and Poproč

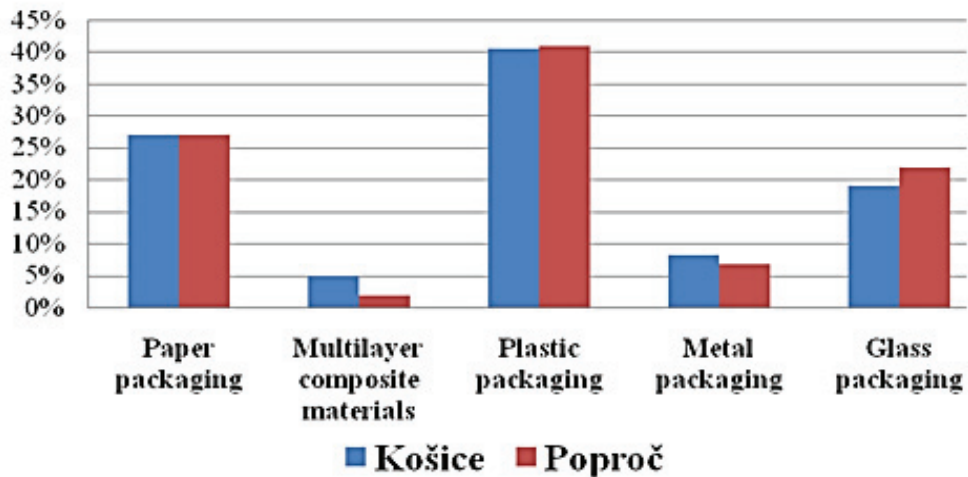


Fig. 7. Material composition of packaging in Košice and Poproč

In the rural section of the village Poproč probably more of this kind of waste is generated, but its lower content in the mixed MSW is caused by individual composting or feeding. The content of paper and plastic at both sites is comparable, as well as the amount of other minor commodities, with the exception of textiles, wood and inert waste. The above-mentioned commodities have a slightly higher content in the village of Poproč which is related to the low content of biodegradable waste. The relatively high content of textiles in both sites points to the absence of a possible introduction of separate collection of this commodity.

The comparison of the mixed MSW composition in various sections revealed that the built-up area type has a relatively high impact on the mixed MSW composition in Košice, in particular the content of biodegradable waste. In the multi-storey building section biodegradable waste was 47%, as for the rural section, it was 57%. This difference may be caused by the increased generation of biodegradable waste as a result of the private garden ownership. It is also obvious from the comparison of the biodegradable waste content between the rural sections of Košice and Poproč. In Poproč, where the rural section is predominant too, the content of biodegradable waste is less than 25% and in the same building type in Košice it is 57%. This fact points to the absolutely unsatisfactory situation in the area of separate collection of biodegradable waste and the absence of home composting by the population of Košice living in private houses.

In the future, this situation must be solved. A large part of such waste can be used for energy recovery. In Kosit, Inc. Company, a project for electricity production from the mixed MSW is currently being carried out. On the other side, the city of Košice has built a composting facility for composting of biodegradable waste from various sources. The analysis of the mixed MSW composition both in Košice and Poproč focuses on the packaging as well. The packaging content in Košice was 24% and in Poproč 29%. By comparing the material composition it was found out that in both cases plastic packaging had the highest content (40%). In Košice, a higher content of multilayer composite material was found than in Poproč. The reason was the later introduction of separate collection of this commodity in Košice. Paper packaging reached the second highest content (27%), followed by glass (19-22%) and metals (7-8%).

4. Conclusion

The results of the analysis of mixed MSW material composition in both localities showed high content of biodegradable waste and insufficiencies in separate collection. Effective separate collection can lead to the reduction of landfilled waste to a minimum, as it is required by the EU. However, the Košice city does not have an intention to separate the

biodegradable waste from the mixed MSW in the future. Anyway, Slovakia tries hard to comply with the EU waste requirements. The implementation of the results published in this paper could contribute to this effort.

Acknowledgements

This work was supported by Ministry of Education of Slovak Republic under Grant VEGA MS SR 1/0293/14. Article is the result of the Project implementation: **University Science Park TECHNICOM for Innovation Applications Supported by Knowledge Technology**, ITMS: **26220220182**, supported by the Research & Development Operational Programme funded by the ERDF."

References

- ASTM D5231 – 92, (2008), Standard test method for determination of the composition of unprocessed municipal solid waste, On line at: <http://www.astm.org/Standards/D5231.htm>.
- Banar M., Ozkan A., (2008), Characterization of the municipal solid waste in Eskisehir City, Turkey, *Environmental Engineering Science*, **25**, 1213-1219.
- Burnley S.J., Eliss J.C., Flowerdew R., Poll A.J., Prosser H., (2007), Assessing the composition of municipal solid waste in Wales, *Resources, Conservation and Recycling*, **49**, 264-283.
- EC Directive, (1999), Council Directive 1999/31/EC of 26 April 1999 on the landfill of waste, *Official Journal of European Communities*, L182/1, 16.07/1999.
- EC Directive, (2008), Directive 2008/98/EC of the European Parliament and of the Council of 19 November 2008 on waste and repealing certain Directives, *Official Journal of the European Union*, L 312/3, 22.11.2008, Brussels.
- European Commission, (2004), Methodology for the Analysis of Solid Waste (SWA-Tool). User Version, 5th Framework Program, EU, Project coordinator-iC consulenten ZT GmbH, Austria, On line at: <https://www.wien.gv.at/meu/fdb/pdf/swa-tool-759-ma48.pdf>.
- European Commission, (2004), Brasov Waste Analysis Final Report, On line at: http://www.wastesolutions.org/fileadmin/userupload/wastesolutions/BrasovFinal_Waste_Analysis_Report_March_2004.pdf.
- European Union, (2013), The euro, On line at: http://europa.eu/about-eu/basic-information/money/euro/index_en.htm.
- Gidakaros E., Havas G., Ntzamilis P., (2006), Municipal solid waste composition determination supporting the integrated solid waste management system in the island of Crete, *Waste Management*, **26**, 668-679.
- IEA, (2003), Municipal solid waste and its role in sustainability: A position paper, *Bioenergy*, On line at: www.ieabioenergy.com/media/40_IEAPositionPaperMSW.pdf.
- Klinda J., Lieskovská Z., (2010), *State of the Environment Report of the Slovak Republic 2010*, (in Slovak), Ministry of Environment of Slovak Republic, 192, ISBN 978-80-89503-19-3.
- Kopernický J., (2011), Internal report - Kosit Company, Košice, Slovakia.
- Kotoulová Z., (2001), Recommended methodology: Quantities and composition of municipal waste, (in Slovak), *Odpadové Fórum*, **10**, 10-13.

- Kvokačka J., (2011), *Methodology of Analysis of the Composition of Municipal Waste with Emphasis on the Presence of Packaging* (in Slovak), The 5th Annual Conference „Enviro-management 2011“, Štrbské Pleso, Slovakia, Environmental policy and Municipal Waste Management in Europe, 2011 XVII - 1/8.
- Ministry of Environment of Slovak Republic, (2010), Strategy for reduction of biodegradable MSW going to landfill, (in Slovak), Bratislava.
- Riber Ch., Petersen C., Christensen T.H., (2009), Chemical composition of material fractions in Danish household waste, *Waste Management*, **29**, 1251-1257.
- Statistical Office of the Slovakia, (2012), On line at: <http://portal.statistics.sk/showdoc.do?docid=10>.
- Slovak Hydrometeorological Institute, Climatic conditions of Slovak Republic, (2012), On line at: <http://www.shmu.sk/sk/?page=1064>.
- SAEFL, (2004), A survey of the composition of household waste 2001/02. Environmental Series no. 356. Swiss Agency for the Environment, Forests and Landscape, Bern, On line at: <https://www.bafu.admin.ch/bafu/en/home/topics/waste/publications-studies/publications/composition-household-waste-2001-02.html>.



“Gheorghe Asachi” Technical University of Iasi, Romania



FATE AND BIODEGRADATION OF ESTROGENS IN THE ENVIRONMENT AND ENGINEERING SYSTEMS – A REVIEW

Hai-Liang Song^{1,2*}, Shi-Bei Huang², Xiao-Li Yang³

¹School of Environment, Nanjing Normal University, Nanjing 210023, China

²School of Energy and Environment, Southeast University, Nanjing 210096, China

³School of Civil Engineering, Southeast University, Nanjing 210096, China

Abstract

Estrogens excreted by humans and animals are groups of endocrine disruptors, which degrade rapidly in soil and water as reported. This review focuses on biodegradation of estrone (E1), 17 β -estradiol (E2) and 17 α -ethynylestradiol (EE2) in surface water, STPs (sewage treatment plants), manure, soil and sediments, and illustrates possible pathways and mechanisms. In general, half-lives of EE2 are much longer than E1 and E2, because an ethinyl group at one hydroxyl group containing C-atom makes the cleavage of this ring rather difficult. Thus, EE2 has great estrogenic potential although the secreted amount is much smaller than that of E2 or E1. Various kinds of bacteria and fungus, *Cornybacterium* spp., *Nitrosomonas europaea* etc., are reported to be capable of degrading estrogens. Moreover, reports indicate that temperature, pH values etc. exert impacts on degradation to different extents. The biodegradation in the sludge phase was assumed by researchers to follow a pseudo-first-order reaction, and the sequence of K -values is $E2 > E1 \gg EE2$ for the same sludge. As for the pathways, it was found that E2 is oxidized to E1 by the first step. The half-life of this step is about 4 to 12 hours in aerobic water and soil. However, this step cannot remarkably reduce the estrogenic potential. Further degradation of E1 needs the cleavage of one ring. Therefore, half-lives and concentrations of E1 are much longer and higher than those of E2. As a matter of fact, pathways of EE2 are still controversial, as several incompatible theories have been proposed.

Key words: biodegradation, co-metabolism, endocrine disruption, estrogen

Received: July, 2013; *Revised final:* July, 2014; *Accepted:* July, 2014; *Published in final edited form:* April 2018

1. Introduction

Research about the occurrence and fate of estrogenic compounds in wastewater emerged in the mid-1990s (Anderson et al., 2003; Kumar et al., 2016; Matsui et al., 2000; Ternes et al., 1999a). In general, there are two kinds of estrogenic compounds, endogenous estrogens and xenoestrogens respectively. Human and animal waste-borne steroidal hormones, also called natural steroidal estrogens, belong to the group of endogenous steroidal Endocrine-Disrupting Compounds (EDCs), which have high estrogenic potency. These steroids have been detected in the effluent of sewage treatment

plants (STPs) and surface water (Desbrow et al., 1998; Kuch and Ballschmiter, 2001; Preda et al., 2011; Ternes et al., 1999a). Among the steroids, three sterols, the natural hormones 17 β -estradiol (E2), estrone (E1) and the synthetic hormone 17 α -ethynylestradiol (EE2), were isolated from the effluents of domestic STPs and identified as a dominating contributor to its estrogenic character (Chen et al., 2016; Desbrow et al., 1998; Körner et al., 2001; Onda et al., 2003; Routledge et al., 1998). Research has been conducted to quantify human-excreted estrogens in raw sewage and in treated effluent. It is found that natural estrogen hormones excreted by humans, e.g. 17 α -estradiol, have levels as

* Author to whom all correspondence should be addressed: e-mail: hlsong@njnu.edu.cn; Phone:+86 2585891849; Fax:+86 25 85891455

high as 5 mg/day for pregnant women. The estrogen (particularly 17 α -estradiol, estrone, and estriol) concentrations in the effluent of a conventional sewage treatment plant (STP) range from a few nanograms per liter (ng/L) to several μ g/L.

These micropollutants, which are at relatively low levels compared with other pollutants, have properties of EDCs which may modify diverse physiological functions, e.g. reproduction and development in different species including fish and humans (Nakamura et al., 2014; Sumpter et al., 1998; Zuo et al., 2013). Recent studies point out that estrogens affect the gene expression in fish (Joseph et al., 2014) and increase breast cancer risk in both exposed mothers and their daughters if they are exposed to synthetic estrogens during pregnancy (Hilakivi et al., 2013).

With the measurements by the MELN cell line in vitro test, the relative estrogenic activity for different EDCs, with the E2 estrogenicity arbitrarily fixed at 100, display values of 246 for EE2, 17.6 for estriol (E3), 2.5 for E1 (Balaguer et al., 1999; Pillon et al., 2005; Sarah and Guillermina, 2010). Such great estrogenic activity found in hormones underlines their possible negative impact on the natural environment.

Biodegradation has been reported the major removal mechanism that affects the fate and transfer of estrogenic compounds in the environment and engineering systems (Johnson and Sumpter, 2001; Writer et al., 2011). This article is mainly aimed to review the recent findings with respect to biodegradation pathways and mechanisms of estrogens, e.g., E1, E2, E3, EE2, in different phases and systems. Relevant background information, such as structure, physicochemical properties, sources, occurrences, and analytical techniques, is also briefly discussed.

2. Synthesis, structure and properties of estrogens

The principal estrogens of environmental concern are naturally occurring estrogens: estrone (E1), estradiol (E2), and estriol (E3) (Sarah and Guillermina, 2010), as well as a synthetic estrogen ethinylestradiol (EE2), which is used in the formulation of the contraceptive pill.

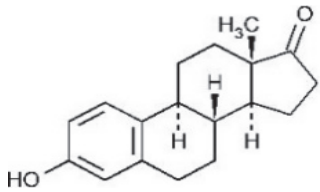
In general, estrogens dissolve poorly in water, as evidenced by Lai et al. (2000), with solubility of about 13 mg/L for the natural compounds, while EE2 display solubility of 4.8 mg/L, which is even lower. The octanol - water partition (K_{ow}) of the estrogens is between 2.8 and 4.2 (Lai et al., 2000). Both the vapor pressure and the volatility of these estrogens are relatively low. The relative estrogenic activity of E2 is around 100, while that of EE2 is as high as 246.

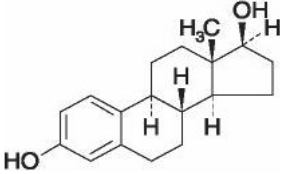
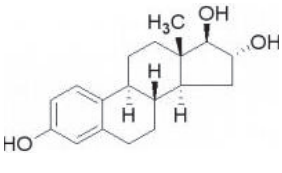
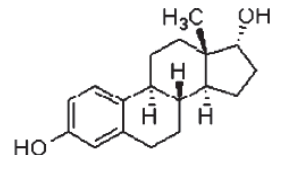
3. Estrogen sources and levels in the environment

Estrogens produced by human glands are excreted within urine and faeces. The synthetic EE2 is used in oral contraceptives world-wide (Williams and Stancel, 1996). Liver of humans and animals is the place where estrogens are enzymatically mediated and conjugated with either sulphate or glucuronide esters to the hydroxyl groups in the C3- and C7-position of the basic steroid structure (Williams and Stancel, 1996). Conjugation boosts the water solubility, which makes estrogens more mobile in the environment than free hormones. Natural hormones excreted in faeces, which occupies a very small proportion of effluent hormones, are mainly in an unconjugated form. The reason for the estrogens being unconjugated in faeces is the capability of bacteria, e.g. *E. coli*, to produce the enzyme β -glucuronidase, which can hydrolyse glucuronide conjugates back to their original form (Legler 2001; Ternes et al., 1999a).

To our knowledge, high performance liquid chromatography (HPLC) and gas chromatography-mass spectrometer (GC-MS) are appropriate for the determination of estrogens. Various preconcentration methods have been established, as well as other detection methods Zou et al. (2013) reported hollow-fiber-supported liquid-phase microextraction using an ionic liquid as the extractant for the preconcentration of estrogens from water samples with HPLC detection. Li et al. (2013a) optimized the solid-phase extraction for determining estrone in sewage. In addition, Owen and Keevil (2013) describe a sensitive and rapid Liquid Chromatography-Mass Spectrometry (LC-MS/MS) assay for the simultaneous measurement of serum estradiol and estrone, which is similar to the methods established by Szarka et al. (2013).

Table 1. Structure and properties of natural and synthetic steroidal estrogen hormones

Compound	Chemical structure	Molecular weight (g/mol)	Water solubility ^a (mg/L)	Log K_{ow} ^b	Vapor pressure (mmHg) ^c	Relative estrogenic activity ^d
Estrone(E1)		270.4	13	3.43	2.3×10^{-10}	2.54

17 β -estradiol(E2)		272.4	13	3.94	2.3×10 ⁻¹⁰	100
Estriol(E3)		288.4	13	2.81	6.7×10 ⁻¹⁵	17.6
17 α -Ethinylestradiol(EE2)		296.4	4.8	4.15	4.5×10 ⁻¹¹	246

a - solubility in water at 20°C (Lai et al., 2000); *b* - octanol-water partition coefficient (Lai et al., 2000); *c*(Lai et al., 2000); *d* (Pillon et al., 2005); MELN *in vitro* test

Table 2. Daily values of E1, E2 and E3 in urine and faeces excreted by women

Form	Carriers	E1(μ g)	E2(μ g)	E3(μ g)	References
unconjugated	urine	8.00	3.00	4.80	Fotsis et al., 1980
	urine	7.00	2.40	4.60	Adlercreutz et al., 1986
	faeces	0.50	0.40	1.25	Adlercreutz et al., 1994

According to Williams and Stancel (1996), the total daily excretion of natural estrogens ranges from 10 to 100 μ g for women, 5 to 10 μ g for women after the menopause and 2 to 25 μ g for men. Average excretion values of unconjugated natural estrogens and the synthetic EE2 were tested, as shown in Table 2. From Adlercreutz et al. (1986), women can excrete 7 μ g of E1, 2.4 μ g of E2, and 4.6 μ g of E3 of unconjugated forms daily via urine. Approximately 0.4 μ g E2, 1.25 μ g of E3 and 0.5 μ g E1 was excreted in faeces per day (Adlercreutz et al., 1994). Fotsis et al. (1980) reported a daily excretion in urine of unconjugated forms as 3.0 μ g of E2, 8.0 μ g of E1 and 4.8 μ g of E3. In addition, Johnson et al. (2000) reported that male excreted 1.6 μ g/day of E2, 3.9 μ g/day of E1 and 1.5 μ g/day of E3 in their urine. With that, the amount of E2 is relatively lower than E1 and E3. Additionally, the daily intake of EE2 ranges about 20-60 μ g for contraception while approximately 10 μ g to control menopausal disorders. This means that almost 30-90 percent of EE2 is excreted in urine and faeces (Johnson and Williams 2004; Sarah and Guillermina, 2010; Webb et al., 2003).

As for animals, E1, E2, and E3 are the main parts of natural estrogens excretion (Sarmah et al., 2006). The daily excretion of estrogens changes with animal species, sex, circadian rhythm, and reproductive state (Lange et al., 2001). The wide differences between species were evidenced by radiotracer studies, which showed that cattle excreted estrogens mostly in faeces (58%), whereas swine and poultry excreted estrogens mostly in urine (96% and

69%, respectively) (Ainsworth et al., 1962; Ivie et al., 1986; Palme et al., 1996). However, the ratio fluctuates during pregnancy (Hoffmann et al., 1997). Since urine and feces are not usually disposed separately in commercial animal production systems, the route of excretion would not appear to be an important environmental concern (Knight et al., 1980).

Estrogenic steroids have been measured in both STPs and surface water. In effluents of British STPs, the concentration of E1 and E2 ranged from 1 ng/L to almost 50-80 ng/L. The concentration of EE2 was generally below the limit of detection but was positively identified in three of the effluent samples at concentrations ranging from 0.2 to 7.0 ng/L (Desbrow et al., 1998). The concentrations reached 70 ng/L for E1, 64 ng/L for E2, 18 ng/L for E3 and 42 ng/L for EE2 in the effluents of sewage treatment plants (STPs) in different countries (Ying et al., 2002). In German river water, the concentrations reached 4.1 ng/L for E1, 3.6 ng/L for E2, and 5.1 ng/L for EE2 (Kuch and Ballschmiter, 2001). E2 reaches 27 ng/L in river waters from Japan, Italy, Germany and the Netherlands (Ying et al., 2002). Besides, E2 concentration measured in mantled karst aquifers in northwest Arkansas ranged from 6 to 66 ng/L (Peterson et al., 2000). In Lake Quinsigamond (Massachusetts, USA), EE2 was detected at a concentration up to 11.1 ng/L (Zuo et al., 2013). In wastewater from five sewage treatment plants (STPs) in Guangdong Province, China, E1 and E2 were detected in all influent samples at concentrations of

69.3–280 ng/L and 1.3–30 ng/L, respectively (Xu et al., 2014).

4. Degradation efficiency in the environment and in the engineered system

The biodegradation of unconjugated estrogens has been studied in soil, water, and manure for several years. It is obvious that biodegradation is not only an important process to remove estrogens in raw sewages of STPs, but also an enhancement to eliminate estrogens in the environment, thus reducing their risk via surface runoff and/or leaching. One key factor for hydrocarbon degradation in polluted habitats is the presence of an adequate electron acceptor (Berthel-Corti and Nachtkamp, 2010).

However, natural environments such as wet soils, swamps, fresh water, marine sediments and aquifers, are places where oxygen is often limited.

4.1. Degradation in surface water

Lai et al. (2002) reported that common freshwater algae (*Chlorella vulgaris*) were capable of oxidizing 17 β -estradiol to estrone. Jürgens et al. (2002) observed similar degradation rates for E2 in river water for a spiking concentration range of 20, 50 and 100 ng/L.

They suggested that even when insufficient E2 was present to stimulate the multiplication of bacteria, E2 were still transformed. Degradation studies carried out in waters from five English rivers indicate that E2 has a half-life of 3–27 days. E1 is the first degradation product of E2 but no investigations of the subsequent by-products has been conducted. The poorest degradation rate was observed in the estuary river water samples, where the high salt content might inhibit microbial degradation. Jürgens et al. (2002) reported that the half-lives of estradiol and estrone at 20°C ranged from 0.2 to 9 d and from 0.1 to 11 d, respectively. Temperature may have a significant impact on degradation efficiency. Shortest half-lives from 4 to 5 hours were found for the degradation of E2 in summer at 20°C (cf. longest half-lives around 40 hours), while half-lives in winter and spring were 2.5 to 8.5 times higher than in summer (also tested at 20°C). Kuster et al. (2004) pointed out that EE2 (half-life, 46 days) is more reluctant than E2 (half-life 4 days, e.g., in the River Thames). These half-life values have possible reasons corresponding to ideal summer temperatures. However, under winter conditions, these compounds could be twice as persistent. Explanation is that higher prior temperatures in summer or higher nutrient concentrations due to less dilution in summer, which means that microorganisms exposed to the test system have higher initial activity.

EE2 was studied with a long half-life up to 17 days, which was much longer than E2. (Jürgens et al., 2002). In other words, EE2 was more recalcitrant in the water. According to de Mes et al. (2005), the structure of EE2 is the critical factor of such characteristic, as EE2 has an ethinyl group at position

17 which hinders the oxidation at this C-atom. Hence, EE2 exerts significant impact on the environment due to its stability in spite of its low concentration. Another way how EE2 can be degraded is by photolysis. The half-life was estimated by Jürgens et al. (2002) as 124 h for E2 and 126 h EE2, respectively (at 12 hours sunshine per day). The photolysis is slower than biodegradation, although EE2 removal through photolysis may be more significant at places where the sun is often shining. Contrary to this notion, a case study conducted by Zuo et al. (2013) showed that the photodegradation of EE2 was faster than biodegradation in the lake surface water under sunlight, with a half-life of less than 2 days in summer sunny days, which means photodegradation may represent a dominant removal mechanism for EE2 in natural surface waters. In that study, under aerobic conditions, a half-life of 108 days was estimated. Under anaerobic conditions, microbial degradation in the lake water was even slower. However, photolysis of estrone generates estrogenic photoproducts with higher activity than the parent compound (Souissi et al., 2014).

4.2. Degradation in soils and sediments

Compared to the biodegradation by sewage microbes, which is fast and complete, biodegradation by soil microbes is rather slow and incomplete. Sediments may serve as both a sink and a source of more estrogenic compounds, as reported by Mashtare et al. (2013).

Das et al. (2004) examined the sorption and degradation of E2 during transport by column studies, packed with surface soil, freshwater sediment and two sands, utilizing model evaluation. Degradation-rate coefficient (k) is in the range 0.0003–0.075/h for E2 and the rate for the only metabolite found (E1) was 1–2 orders of magnitude larger.

Colucci et al. (2001a) studied the mineralization of ¹⁴C-E2 in loam, sandy loam, and silt loam soils from Canada. Only 11.5–17.1% of 1 mg/kg ¹⁴C-E2 was evolved as ¹⁴CO₂ after 3 months of incubation at 30°C. Similarly, the mineralization efficiency of ¹⁴C-E2 measured in terms of carbon dioxide released did not exceed 10% in both loam and silt soils with an initial concentration of 81.7 μ g/kg after 96 h of incubation (Jacobsen et al., 2005). Stumpe and Marschner (2007) reported that the mineralization of 1 mg/kg ¹⁴C-E2 in four agricultural topsoils with different soil properties and different site histories like wastewater irrigation and sewage sludge application reached 5.1–7.4% during incubations at 20°C over three weeks. Apart from mineralization to ¹⁴CO₂, most of the applied estrogens were incorporated into “bound” (i.e. non-extractable) residues. It has been suggested that the non-extractable residues were relatively nonbioavailable (Colucci et al., 2001b), but characterization of the unknown products is necessary. As expected, EE2 was found more persistent than E2 in aerobic experiments with river sediments (Jürgens et al., 2002). To the best of our knowledge, no data are available for the

mineralization of EE2 in soil though it is suggested that the dissipation of EE2 in soil was in part microbially mediated (Colucci and Topp, 2001).

Several factors may affect biodegradation of steroid hormones in environment including temperature, redox conditions, organic matter content and soil moisture.

4.2.1. Temperature

In the loamy soils studied by Colucci et al. (2001a) soil temperature was found to influence the total mineralization of E2. Mineralization (61 days) decreased with decreasing temperature, with measured values being 14.7%, 14.1%, 10.9%, 6.0%, and 3.6% at 37, 30, 19, 10, and 4°C, respectively. Not surprisingly, the rates of degradation were slower at reduced temperatures, presumably due to reduced microbial activity.

4.2.2. Redox conditions

The former research suggests that redox conditions (aerobic, anoxic, or anaerobic) are critical factors for degradation of estrogens, as evidenced by batch experiments in agricultural top soil (Fan et al., 2007; Ying and Kaakana, 2005), river bed material (Jürgens et al., 2002), marine sediment (Ying and Kaakana, 2003) and aquifer material (Ying et al., 2003). The total mineralization of estrogens is generally higher under aerobic conditions than under anoxic/anaerobic conditions. Half-lives for the natural estrogens in aerobic sediment have been reported as <1 day but can be longer in anaerobic sediments with reports of up to 14 days for E1 (Jürgens et al., 2002). In transport studies with repacked soil columns (Das et al., 2004) and aerobic batch experiments with agricultural topsoils (Ying and Kaakana, 2005), both E2 and E1 dissipated in a similar manner. Mineralization of E1 in particular was reported to be highly affected by redox conditions (Fan et al., 2007; Ying and Kaakana, 2005). Under aerobic conditions E2 (applied as 2.5 mg/kg soil) was rapidly biotransformed into E1 with a DT₅₀ (i.e., time to dissipate 50% of the initial concentration) of 3 days, and the generated E1 dissipated to an undetectable level of 0.1 mg/kg within 3 days. Under anaerobic conditions, however, E2 was transformed much more slowly (DT₅₀ 20 days) and the generated E1 persisted in the soil without further dissipation throughout the 70-day experiment (Ying and Kaakana, 2005).

Similar results are obtained by Czajka and Londry (2006), whose tests were conducted under strict anaerobic conditions including sulphate, nitrate and iron reducing, and methanogenic conditions with limited degradation of E2. The authors found even slower degradation of E2 under nitrate reducing conditions, while anaerobic degradation of EE2 was not observed over a 3 year time period (Czajka and Londry, 2006). Similar results indicated that approximately 50% of E2 was degraded after 70 d anaerobic incubation, while little or no degradation of EE2 was observed under anaerobic conditions (Ying and Kookana, 2003). Mashtare et al. (2013) reported

that under nitrate- and sulfate-reducing conditions, degradation followed similar trends in half-lives, E2 < EE2 < E1, with degradation much slower under sulfate-reducing conditions. Fan et al. (2007) reported that after 132 h of incubation, 6% of 375 µg/kg ¹⁴C-E2 could be mineralized to ¹⁴CO₂ in native soils under aerobic conditions while there were no ¹⁴CH₄ or other ¹⁴C-labeled volatile organic compounds detected under anaerobic conditions. The growth of microbes might be limited due to the lower level of electron acceptor under anaerobic conditions thus reducing the metabolism of these hormones. Considering that wet soils, swamps, fresh water or marine sediments and aquifers are frequently oxygen limited, sub-surface soil environments where anaerobic conditions often occur can be a potential source for steroid hormones.

4.2.3. Organic matter content

It is worth noting that neither low organic content nor high organic content is favorable to the degradation of estrogens. For instance, the half-lives of E2 in a loam soil with 3.2% organic matter and a silt loam soil with 2.9% organic matter were 61 and 72 h at room temperature (Jacobsen et al., 2005). According to Herman and Mills (2003), addition of 1 mg/L dissolved organic carbon increased the biotransformation of E2. The observed increase of degradation could be attributed to an enhanced microbial growth in the soils caused by the rise of organic matter concentrations, since the estrogens themselves as sole source of carbon and energy seem too low in concentration to support extensive microbial growth. In the case of carbon-deficient soils, therefore, small quantity of additional organic matter may enhance biodegradation of trace organic contaminants.

Unfortunately, the simultaneous monitor of the characteristics of microbial communities was often ignored in such studies. On the other hand, Herman and Mills (2003) also discovered that high concentrations of readily available carbon sources inhibited E2 degradation. This suggests that the availability of higher concentration of readily biodegradable organic carbon in water, as well as in soil or sediment may negatively affect the degradation of E2. This could be explained by that elevated levels of organic content decreased the extractability and bioavailability of estrogens, which have certainly a tendency to partition into organic matter due to their moderate lipophilicity. Nonetheless, this explanation comes to existence based on the assumption of degradation only proceeding in the liquid phase. In fact, Das et al. (2004) did indicate that strong sorption of E2 did not hinder degradation and they hypothesized that E2 either can be degraded while sorbed or rapidly desorbed from the solid phase and then degraded in the liquid phase. Systematic research addressing the impact of organic matter on biodegradation of estrogens is highly recommended. More importantly, it is necessary to distinguish the difference between the effect of dissolved and particulate organic matter.

4.2.4. Soil moisture

With regard to soil moisture, its effect on estrogen degradation parallels the effect of organic matter content. That is, neither very low nor very high soil moisture is beneficial to estrogen degradation. Colucci et al. (2001a) indicated that the mineralization of E2 increased from <1% to 20% after 73 d of incubation when the moisture content of the sandy loam soil was increased from air-dry to 15%. However, when moisture content of the same soil was increased to field capacity (24%), the amount of E2 mineralized decreased sharply to 8%. Note that soil moistened to field capacity limits oxygen supply to aerobic biodegradation. This suggests that the persistence of steroid hormones is more likely in dried sandy soil, moistened soil at field capacity or saturated soils, which is mainly due to the fact that appropriate moisture is indispensable to normal physiological functioning of living microorganisms while water-saturated condition limits oxygen supply to aerobic biodegradation.

In addition, natural and synthetic steroids are generally dispersed into the soil environment within a complex matrix of solid and soluble organic compounds due to the agricultural use of municipal sewage sludge (biosolids) and animal manures as fertilizer. These organic matrices, rich in nutrients, organic matter, and microorganisms, will profoundly change soil conditions following application, and therefore could influence the degradation of estrogens. A few studies have therefore been addressed about the impacts of these matrices on the behavior of the steroids in soils. Jacobsen et al. (2005) conducted various laboratory studies to investigate the influence of various organic matrices (e.g., swine manure slurry and municipal biosolids) on the aerobic degradation of E2 in three agricultural soils the same as that used formerly by Colucci et al. (2001a). Their results indicate that the municipal biosolids, and to a lesser degree manure slurry accelerated the mineralization of [¹⁴C]-E2 detected after 96 h of incubation. These results also indicate that microorganisms carried in manure can convert E2 to E1, and that mineralization of E2 requires a viable soil microbial population. Lucas and Jones (2006) similarly reported that the mineralization of E2 and E1 in the sheep manure amended soils was generally higher than in the non-amended soils. Additionally, in comparison to urine amended soil, the rate of estrogens mineralization is higher in cattle and sheep manure, which is also significantly affected by the age of the manures. It is well known that sorption of organic compounds increases with the organic contents of the soil.

The addition of manure or biosolids may, therefore, enhance the sorption of estrogens due to the combination of elevated levels of organic carbon content and higher adsorption surface area in soil. However, strong sorption of parent compound and transformation products was shown not to hinder degradation, as the high rate of degradation could only be reached if compounds were either degraded while sorbed or rapidly desorbed from the solid phase and

then degraded in the aqueous phase (Das et al., 2004). Two possible hypotheses explain the elevated degradation: Firstly, the introduction of the microorganisms inherent to organic matrices that are both adapted to the chemical conditions and possess the intrinsic capability for estrogen degradation; also, the microbial activity in the soil is stimulated due to the nutrient addition introduced by application of organic matrices.

The former presumption seems to be more rational (Das et al., 2004; Lucas and Jones, 2006). In the case of agricultural sites with different long-term treatment histories with wastewater and sewage sludge, however, Stumpe and Marschner (2007) reported that the long-term sewage sludge application had no effect on E2 mineralization whereas long-term wastewater irrigation significantly decreased E2 mineralization rate in soils compared to the corresponding soil with freshwater irrigation. Further work is needed to elucidate the discrepancy between the long-term and short-term effect of organic matrices application on the degradation of estrogens in soils. As a whole, given the complex nature of real-world situations where soil pH, redox conditions, temperature, prevailing soil water conditions, wetting and drying cycles, as well as the fact that the size and type of bacterial populations can vary, biodegradability of estrogens may likely to be different in the field than what has been observed under controlled conditions in the laboratory.

The degradation pathway, conversion of E2 to E1, and subsequent formation of non-extractable residues was observed consistent with three kinds of soils under all incubation conditions (Colucci et al., 2001a). A miscible-displacement column experiment indicated that E2 entered the soil column underwent rapid transformation to form at least three metabolites, E1, sporadic E3 and an unidentified high-polarity compound (Casey et al., 2003). Results from batch incubation experiment also indicated that E2 could be transformed to an unidentified polar compound through abiotic chemical processes in agriculture soil (Fan et al., 2007). Unfortunately, all of these studies failed to identify the unknown intermediate degradation products.

The authors concluded that estrogens are biodegradable in soils by ubiquitous microorganisms that require no prior adaptation (Colucci et al., 2001b). Stumpe and Marschner (2007) also indicated that two-week pre-incubation of the soils with 0.1 mg/kg unlabeled hormones or application of the hormones within a wastewater matrix had only minor effects on their mineralization.

While estrogens were studied to be biodegraded in soil, little was known about the soil microorganisms responsible for estrogen degradation. The first attempts to identify the microorganisms involved in estrogens biotic transformation, over 60 years ago, were based on culture-dependent techniques (Turffitt et al., 1947).

In this study, the biodegradation of E1 was examined using 355 different cultures of bacteria

isolated from five disparate soil types. No culturable bacteria were found in loam, marl, or alkaline peat soils that could metabolize E2. However, one *Proactinomyces spp.* was isolated from an acid sand, and two strains were found in arable soil that could use E2 as a carbon source. E1 was degradable by one species of *Proactinomyces spp.* in the arable soil, but no degradation was observed with organisms from the other four soils.

4.3. Comparison of degradation rates in the natural system

Half-lives of each estrogens in different natural systems vary. Research conducted by Moschet (2009) and Xuan et al. (2008) suggested that half-lives of E1 and E2 in aerobic water are pretty close, while degradation rate of E2 is significantly higher than that of E1 in aerobic soil and sediment. Generally, EE2 is harder to be degraded as compared to E2 and E1, as the ethinyl group makes it more recalcitrant (Colucci and Topp, 2001; Colucci et al., 2001b; Jürgens et al., 2002; Ying and Kookana, 2003).

On the other hand, degradation rate under anaerobic conditions is much lower than under aerobic conditions or sometimes degradation cannot even proceed, as evidenced by Ying and Kookana (2003) and Czajka and Londry (2006). Degradation of E2 in the anaerobic river sediment is much faster than that in the lake sediment and anaerobic marine, may due to that there was still a tiny amount of oxygen in the anaerobic river sediment because it is difficult to create a real anaerobic environment (Moschet, 2009).

4.4. Degradation in manure

Large estrogen loads associated with animal feeding operations (AFOs) arise not only from steroidal treatments given to livestock to enhance growth and fecundity, but also from the current trend towards concentrating animals into small geographic areas, magnifying waste related issues. Manure disposal presents a potential source for surface and groundwater contamination, consequently threatening human health and imperiling wildlife communities.

Bacteria in animal manure are capable of degrading estrogens. Soils amended with swine manure facilitate the biodegradation of estrogens, mainly due to the presence of fecal bacteria. Raman et al. (2001, 2004) tested estrogen degradation in cattle and swine manures. The authors found that the E2 concentration dropped sharply during the first 24 h of incubation under aerobic conditions; while E1 was accumulated and reached a peak concentration in 48 h. The total estrogenic activity measured by yeast screen decayed following first order kinetics, and the rate constants increased with temperature from 0.03 day⁻¹ at 3°C to 0.12 day⁻¹ at 5°C. The manure microorganism *Cornybacterium spp.* was believed to be responsible for the biodegradation of both E1 and E2. The complete biodegradation of estrogen compounds is largely dependent on the destruction of

the phenolic ring. The fungus group *Paecilomyces lilacinus* was found to be capable of cleaving the phenolic ring of biphenyl into five di- and trihydroxylated metabolites and thus was believed to have the capacity to degrade estrogen compounds as well (Gesell et al., 2001). *Fusarium proliferatum* isolated from a manure sample, could degrade EE2 with an initial concentration of 25 mg l⁻¹ (Shi et al., 2002).

The impacts of pH values, temperature, the presence of antibiotics, and incubation time on degradation efficiency of estrogens in manure have been observed in many studies. Shore et al. (1993) incubated broiler litter for 1 week at different pH values, with and without the addition of antibiotics (penicillin/streptomycin), and found significant reductions in estrogen concentrations at pH 5 and 7 but no change at pH 1 or 12.

When antibiotics were added to the litter, estrogens persisted. Similar results indicated that estrogens may have slower dissipation rates in soil particularly when manure is applied at high rates or not mechanically mixed in the surface horizon (Rose and Farenhorst, 2014). Tetracycline in manure induced a lag phase of 40 to 50 days, and tetracycline at 200 mg kg⁻¹ remarkably decreased maximum mineralization of E1 and E2 in manure. Schlenker et al. (1998) studied the degradation of estrogens in cattle feces by incubating manure samples for 12 weeks at 20-23°C. The median concentrations of total estrogens extracted from the manure were unchanged for 9 weeks but were reduced by 80% after 12 weeks. Schlenker et al. (1999b) tested *E. coli* and *Clostridium perfringens* for their ability to degrade fecal estrone in cattle manure. The *E. coli* had no effect on estrone concentrations, but the *C. perfringens* reduced the average concentration of estrone from ~16 µg L⁻¹ to ~11 µg L⁻¹ during the 48 h incubation. Schlenker et al. (1999a) evaluated the influence of temperature on the stability of estrogens in the feces of cattle. At 5°C, the median concentrations of total estrogens extracted from the manure fell below initial concentrations after 12 weeks of incubation. At 30 °C, however, estrogen was almost completely eliminated from the samples within 3 weeks. Similar studies of estrogen degradation in dairy cattle manure were done by Raman et al. (2001). Press cake samples were spiked with 17β-estradiol and incubated at temperatures ranging from 5 to 50°C. The effects of acidification on estrogen transformation and degradation during sample storage were also evaluated. At all temperatures, estradiol concentrations rapidly declined during the first 24 h of incubation, and estrone accumulated. Total estrogen removal rates followed the pattern of estrone degradation, and these data were fitted to a first-order decay model. Rate constants increased from ~0.03 d⁻¹ at 5°C to ~0.12 d⁻¹ at 50°C. Acidification to pH 2 reduced rates of estrogen transformations at both 5 °C and 30°C, but a 15% and 31% loss, respectively, of total estrogen was still observed when samples were stored for 7 days. The authors speculated that *Cornybacterium spp.* were

partially responsible for the estrogen transformations in their study (2001). Hakk et al. (2005) performed incubation experiments under aerobic conditions to assess the water extractability of E2 in chicken manure compost with 60% moisture. They concluded that the extractability of E2 decreased with time, and the first-order degradation rate constant for E2 was 0.010 d^{-1} , and the first-order degradation rate constant for E2 was 0.010 d^{-1} . Chun et al. (2005) suggested that the presence of antibiotics significantly decreased transformation of E2 to E1 upon recommendation that any study evaluating the fate and transport of estrogenic hormones in soil should include the effect of agricultural antibiotics because antibiotics and estrogenic hormones were commonly excreted together in environmental samples.

4.5. Degradation in biological wastewater treatment systems

4.5.1. Field monitor data

Different studies around the world agree on the aerobic degradation of estrogens underwent during aerobic biological treatment units in municipal STPs. Municipal STP is an important facility which markedly reduces the concentrations of estrogens, although its principal purposes are the removal of organic substances even nitrogen and phosphorus from wastewater, as well as the disinfection of the treated wastewater. There is abundant documentation about the overall removal efficiencies of estrogens, as determined from influent and effluent concentrations in actual STPs situated in Europe, North America, Australia and Japan. It was proved to be efficient in removing E2 and E3, but less effective in removing E1 and EE2 (Baronti et al., 2000), similar to the findings by Shi et al. (2004a). Moreover, this conclusion was confirmed by the experiment using two pilot-scale STPs free from the problems such as fluctuations in influent concentrations, cleavage of conjugated hormones, rainfall events, which were inevitably encountered when dealing with full-scale plants (Esperanza et al., 2004). In anaerobic condition, estrogens removals were in the range of 76-92% for E1, 58-90% for E2, 43-63% for E3, and 62-88% for EE2. In aerobic phase, removal of estrogens were ranging from 79-96% for E1, 76-96% for E2, 36-64% for E3, and 57-96% of EE2 (Ruchiraset and Chinwetkitvanich, 2014). To our best knowledge, among all of the published field monitor data all over the world, the Wiesbaden STP, a common municipal STP in German, with an activated sludge system for nitrification and denitrification including sludge recirculation, operated with a sludge retention time (SRT) of 11-13 d, had the best removal rate not only for E1 and E2, but also for EE2, which was more than 99%, 98% and 93% respectively (Andersen et al., 2003).

With the attempt to evaluate the importance of sorption and biodegradation, which are widely viewed as two principal mechanisms for estrogen removal by biological treatment, more detailed studies also have

been conducted on the fate of estrogens in each treatment step of specific STPs. A complete mass balance of Wiesbaden STP based on concentration profiles in both water and sludge showed that biodegradation was the main pathway for estrogens removal, which was responsible for above 80% removal for both natural and synthetic estrogens, whereas only approximately 5% of the estrogens entered the plant were removed with excess sludge (Andersen et al., 2003). Another study case of Danish Lundtofte STP suggested that removal of estrogens with excess sludge was less than 2% of the total amounts of estrogens that entered the STP (Andersen et al., 2005). However, in a sewage treatment plant in Centre Eastern Tunisia using simple activated sludge process, sorption onto sludge played a predominant role in the removal of estrogens in warm season, especially for E1 and E2 (69.5 and 66.3%, respectively) (Belhaj et al., 2013). This conclusion was evidenced by Xu et al. (2014), Zhang et al. (2014), Zeng et al. (2013) and Ruchiraset and Chinwetkitvanich (2014). So it is noteworthy that sorption may affect the fate of estrogens in STPs because estrogens are easily sorbed onto activated sludge (Zeng et al., 2013).

4.5.2. Lab-scale batch tests of sludge culture Aerobic degradation

To observe the biodegradation of estrogens under different conditions, extensive research has been performed with real activated sludge from various STPs. The efficiency of a STP to degrade estrogens is influenced by numerous parameters including microbial activity, sludge retention time (SRT) (Maeng et al., 2013), hydraulic retention time (HRT), temperature, and rainfall, all of which vary seasonally (Ternes, 1998). For example, SRT was proved to be a suitable operational parameter to remove estrogens in activated sludge system. Zeng et al. (2013) investigated the effect of SRT on the removal and fate of E2 and EE2 in an anaerobic-anoxic-oxic activated (A²/O) sludge system by lab-scale experiments. Optimal SRT was 20 days for E2, EE2 and nutrient removal. Mass balance calculation suggested that 99% of influent E2 was degraded by the activated sludge process, and 1% remained in excess sludge; of influent EE2, 62.0%-80.1% was biodegraded; 18.9%-34.7% was released in effluent; and 0.88%-3.31% remained in excess sludge. Different treatment systems may also affect microbial activity and therefore, estrogenic composition of STP effluents (Rodgers-Gray et al., 2000). The conventional activated sludge (CAS) process has been reported to have higher estrogen removal efficiency than trickling filter (Chimchirian et al., 2007). Furthermore, it appears that oxidation ditch (OD) process is better than CAS process, while the biological nitrogen removal process with high SRT removes natural estrogens as effectively as the OD plants (Hashimoto et al., 2007).

In batch experiments, Ternes et al. (1999b) investigated the basic aerobic microbial reactions of

estrogens in activated sludge taken from the old Wiesbaden plant with only BOD removal. Experiments were performed at 20°C with two starting concentrations of 1 µg/L and 1 mg/L for E2. At both spiking levels, E2 was almost quantitatively oxidized to E1. It was also found that the removal of E2, as well as the formation and elimination of E1 was accelerated at the lower spiking level, under which condition neither E2 nor E1 was to be found above the detection limits after 5h. Layton et al. (2000) conducted a similar study with estrogens using activated sludge from four municipal STPs in Tennessee U.S.A. The sludge from all of the municipal plants mineralized 70-80% of radio labelled ¹⁴C-E2 to ¹⁴C-CO₂ within 24 h. A recombinant yeast estrogen assay (YES assay) also confirmed that biological estrogenic activity was removed from the biosolid samples to below the detection limit (1.56 nM) indicating no accumulation of E1. In this study, ¹⁴C EE2 was found to mineralize much more slowly, even though 40% was mineralized in 24 h. The degradation activity of E1 and E2 is seen to be higher in the sludge from membrane bioreactor (MBR) plant than that from conventional activity sludge (CAS) plant by a factor of 2-3, which was attributable to either higher age of the sludge (30 d vs 11 d) resulting higher accumulation of specialist-degrading estrogens, or smaller sludge flocs size (80 vs 400 µm) with thinner boundary layer favoring the passive-diffusion mass transfer (Joss et al., 2004).

Essandoh et al. (2012) studied the removal of three potent EDCs including estrone (E1), 17β-estradiol (E2), and 17α-ethinylestradiol (EE2) in a wastewater using soil columns. E2 was the most easily removed estrogen, while EE2 was the least removed. Besides, novel bioreactors are efficient in removal of estrogens, such as membrane distillation bioreactor (MDBR) which can be operated at thermophilic conditions to facilitate the integration of biological treatment with membrane distillation (Wijekoon et al., 2014). In order to know the more exact behavior of estrogens in actual sewage when in contact with activated sludge, Suzuki and Maruyama (2006) conducted an experiment using filtered sewage and activated sludge that were both collected from STPs in Japan. E2 and E1 simultaneously decreased immediately after the beginning of the batch mixing. E2 rapidly decomposed completely within 4-6h, while E1 concentration remained constant at 2-5 ng/L following the incipient rapid descent during a period of 24h. The biodegradation in the sludge phase was assumed by many researchers following a pseudo-first-order reaction as given below (Eq. 1):

$$dC/dt = K \cdot TSS \cdot C \quad (1)$$

where K is the first-order biological degradation rate constant, in L/(g of TSS·d); TSS is the mixed liquor suspended solids, in g/L; and t is the time of degradation in sludge, in day.

The integration of Eq. (1) will result in:

$$C_t = C_0 \cdot \exp(-K \cdot TSS \cdot t) \quad (2)$$

where C_0 is the initial concentration and C_t is the concentration at time t (days), in ng/L.

All the K -values obtained directly or standardized from literature are summarized in Table 3. Despite that the K -values are markedly different, some conclusions can be generalized as following. Firstly, the sequence of K -values is E2>E1>>EE2 for the same sludge. Secondly, much lower were the initial estrogens concentrations; much higher K -values would be obtained, which indicate the sludge activity could be inhibited by high concentrations estrogens. Fortunately, the estrogens concentrations of actual sewage never exceed 200 ng/L according to all of the published monitor data up to the present. It is expected that estrogens could be biotransformed at relatively high rates. However, these previous batch tests tended to overestimate the true degradation rates, which could be attributed to two reasons. On the one hand, the experiments were carried out with the estrogens solution lacking organic substrates that could competitively inhibit the degradation of estrogens (Joss et al., 2004). On the other hand, these aeration experiments were likely to be consistently high in a shaking flask, which may not always be the case within an activated sludge aeration tank.

Moreover, the occurrence of nitrification in an activated sludge system seems to have a positive effect on the removal of hormones. For nitrification a longer SRT is required because the autotrophic bacteria involved grow very slow (de Mes et al., 2005).

It is noteworthy that heterotrophic populations, which are likely to affect estrogen degradation, can be influenced by the type of growth substrate. Ziels et al. (2014) reported that kinetic rate coefficient (k_b) values for EE2 biodegradation ranged from 5.0 to 18.9 L/g VSS/d at temperatures of 18°C to 24°C. EE2 k_b values for aerobic biomass growth at low initial food to mass ratio feeding conditions (F/M_f) were 1.4 to 2.2 times greater than that from growth at high initial F/M_f , which indicated that employing MBR processes (no gravitational settling) with low- F/M_f growth conditions facilitated EE2 biodegradation. Similarly, oxidation ditch (OD) processes, which can provide low- F/M_f substrate removal conditions, might promote higher EE2 biodegradation kinetics, while keeping acceptable sludge settling characteristics.

Tan et al. (2013) pointed out that further enrichment under starvation conditions may enhance E1 degradation capability via the growth and/or stimulation of multiple substrate utilizers rather than heterotrophs which are characterized by an r-strategist growth regime, although initial growth of biomass depends on the presence of sufficient organic carbon. More research is needed to determine whether and how estrogen degradation is affected by F/M_f conditions.

Anoxic and anaerobic degradation

Anoxic is most commonly defined as the absence of oxygen, while *anaerobic* indicates the absence of a common electron acceptor such as nitrate, sulfate or oxygen.

Table 3. K-values obtained directly or standardized from literature

Initial concentration	E2	E1	EE2	References
100 ng/L			8	Joss et al., 2004
500 ng/L	350	162		Joss et al., 2004
1µg/L	150	20	0	Ternes et al., 1999a
50µg/L			0.6	Vader et al., 2000
58µg/L	2.79			Layton et al., 2000
72µg/L			0.13	Layton et al., 2000
200µg/L	11.66	1.2	1.34	Shi et al., 2004a
1.0 mg/L	8.36	0.42	0.2	Shi et al., 2004a
20-25mg/L	0.22	0.16	0	Shi et al., 2004b

Matsui et al. (2000) is probably the first to suggest that estrogen activity was mainly reduced during the denitrification treatment step which was also the first step of the activated sludge treatment by performing a detailed profile of estrogen removal in a Japanese STP using an immunoassay for E2 in combination with the yeast estrogen screening (YES) assay for measuring estrogen activity. Then Andersen et al. (2003) further demonstrated that estrogens were mainly degraded during denitrification based on analysis of steroid estrogens in both water and sludge in a south German STP by GC-MS-MS. Afterwards, Joss et al. (2004) systematically investigated the degradation of estrogens under different redox conditions in batch experiments performed with same activated sludge originating from either CAS or MBR. The degradation rate of E1 and EE2 depended strongly on redox conditions, while E2 exhibited high rates anyway. For example, the K -value ($L \cdot gSS^{-1} \cdot d^{-1}$) of E1 degraded by CAS sludge was 10 under anaerobic conditions, 30 under anoxic and 162 under aerobic conditions (Joss et al., 2004). With regard to E2, the K -value was 350 and 460 with CAS sludge under aerobic and anoxic conditions respectively, while was 950 and 500 with MBR sludge under aerobic and anaerobic conditions respectively. In contrast, Dytczak et al. (2008) indicated that the conversion from E2 to E1 was faster under aerobic than anoxic conditions and removal of E1 was not observed over the 3-7 hour incubation times. The influence of oxidation-reduction conditions on E2 degradation currently remains ambiguous. The exiting data implied that EE2 was degraded under neither anoxic nor anaerobic conditions (Czajka and Londry, 2006; Dytczak et al., 2008; Joss et al., 2004).

A denitrifying bacterium was lately isolated from activated sludge of a municipal wastewater treatment plant using E2 as sole source of carbon and energy (Fahrbach et al., 2006).

Estrone was converted to 17 α -estradiol under either nitrate-reducing condition (Dytczak et al., 2008) or anaerobic condition (Czajka and Londry, 2006). In some respects this could be considered as a deactivation step, in that 17 α -estradiol is less biologically active than E2 (Hutchins et al., 2007). However, it is not known to what extent 17 α -estradiol remains stable in anaerobic/anoxic conditions, and the

potential therefore exists for reverse transformation back to E1 and ultimately back to E2.

However, little research has been conducted on the microbial degradation of estrogens under anaerobic conditions. Overall anaerobic conditions resulted in much slower conversion rates compared to the same experiments under aerobic conditions. For example, a half-life of 2.5 min for E1 under aerobic conditions, was 1.66 h under anaerobic conditions. No degradation of the three estrogens was found by Pakert et al. (2003) in batch experiments using sludge from anaerobic digester. Zhang et al. (2013) reported that the degradation rate constant of estrogens decreased with the original estrogen concentrations while increased with the sludge concentrations. Additionally, E1 was accumulated in the process of E2 degradation. The degradation rate of E1 decreased by a factor of between 3 and 5 in the transition from aerobic (O_2 available in solution) to anoxic (nitrate available but no molecular oxygen) as well as from anoxic to anaerobic (Joss et al., 2004).

Bed sediment was used to examine the potential for E2 to be degraded anaerobically at 20°C; and was fairly rapidly converted to E1, almost completely after an incubation of 2-days (Jürgens et al., 2002). In batch experiments with activated sludge supernatant under anaerobic conditions (purged with nitrogen gas), after 7 days, 50% of the spiked amount of E2 was converted into E1 and resulting in accumulation of E1 due to no further degradation (Lee and Liu, 2002).

EE2 tested under anaerobic conditions in river water samples showed no degradation over 46 days (Jürgens et al., 1999). Under strict anaerobic conditions, E1 is expected to convert into E2, rather than E2 is converted to E1 (Joss et al., 2004). So somehow under anaerobic conditions there are still electron acceptors available, like Fe^{3+} and various organic oxidative compounds, responsible for the conversion. Joss et al. (2004) also found the conversion of EE2 in MBR sludge under anaerobic conditions was nearly the same as that in the blank experiment where no sludge was present.

On the whole, the microbial conversion rates of estrogens under various oxidation-reduction conditions appeared to follow the order: aerobic > anoxic > anaerobic.

5. Metabolic pathways

5.1. Isolated organisms and enzymes involved in estrogens degradation

Several reports dealing with isolating and identifying microorganisms are involved in estrogens degradation. For instance, Yu et al. (2005) indicated that a frequent occurrence of *E.coli*, *Pseudomonas fluorescens* (gram negative), and *Bacillus thuringiensis* (gram positive) strains were probably responsible for the estrogen-degrading capacity in activated sludge by using the method of terminal restriction fragment length polymorphism (T-RFLP) assay. The bacterial strains that are capable of degrading estrogens are briefly summarized below in Table 4. A strain of the gram-negative, oval-shaped

aerobic bacterium genus *Novosphingobium tardaugens* sp. nov. isolated from activated sludge decomposes E1, E2, E3, except for EE2. In addition, this bacterium seemed to assimilate E2 as a preferred carbon source and the degradation activity was not accelerated by yeast extract or glucose (Fujii et al., 2002; Fujii et al., 2003), which was similar to what was observed in *Rhodococcus zopfii* (Yoshimoto et al., 2004).

Although bioreactors at a wastewater treatment plant were operated under eutrophic conditions, it was suggested that these bacterial strains possibly degrade estrogens selectively in such environment. Similarly, two another gram-negative bacillus, *Achromobacter xylooxidans* and *Ralstonia pickettii*, isolated from membrane bioreactor (MBR), were able only to degrade E1, E2, E3, but not EE2 (Weber et al., 2005).

Table 4. Microorganisms capable of biodegrading or metabolizing natural and synthetic estrogens

Resources	Strains	Generas	Gram Stain	E1	E2	E3	EE2	References
Sewage treatment plants	<i>Novosphingobium tardaugens</i> sp. nov.	<i>Novosphingobium</i>	negative	○ ^a	○	○	× ^b	Fujii et al., 2002, 2003
	<i>Rhodococcus zopfii</i>	<i>Rhodococcus</i>	- ^c	○	○	○	○	Yoshimoto et al., 2004
	<i>Rhodococcus equi</i>	<i>Rhodococcus</i>	-	○	○	○	○	Yoshimoto et al., 2004
	EMS-1	<i>Rhodococcus</i>	-	○	○	○	-	Villemur et al., 2013
	JEM-1	<i>Novosphingobium</i>	negative	○	○	○	○	Hashimoto et al., 2009
	<i>Achromobacter xylooxidans</i>	<i>Achromobacter</i>	negative	○	○	○	×	Weber et al., 2005
	<i>Ralstonia pickettii</i>	<i>Ralstonia</i>	negative	○	○	○	×	Weber et al., 2005
	E2Y1	<i>Bacillus</i>	-	○	○	- ^d	-	Jiang et al., 2010
	E2Y2	<i>Bacillus</i>	-	×	○	-	-	Jiang et al., 2010
	E2Y3	<i>Bacillus</i>	-	×	○	-	-	Jiang et al., 2010
	E2Y4	<i>Bacillus</i>	-	○	○	-	-	Jiang et al., 2010
	E2Y5	<i>Bacillus</i>	-	×	○	-	-	Jiang et al., 2010
	KC6	<i>Aminobacter</i>	negative	○	○	-	-	Yu et al., 2007
	KC7	<i>Aminobacter</i>	negative	○	○	-	-	Yu et al., 2007
	KC12	<i>Brevundimonas</i>	negative	×	○	-	-	Yu et al., 2007
	KC13	<i>Escherichia</i>	negative	×	○	-	-	Yu et al., 2007
	KC1	<i>Flavobacterium</i>	negative	×	○	-	-	Yu et al., 2007
	KC2	<i>Flavobacterium</i>	negative	×	○	-	-	Yu et al., 2007
	KC5	<i>Microbacterium</i>	positive	×	○	-	-	Yu et al., 2007
	KC3	<i>Nocardioides</i>	positive	×	○	-	-	Yu et al., 2007
	KC4	<i>Rhodococcus</i>	positive	×	○	-	-	Yu et al., 2007
	KC8	<i>Sphingomonas</i>	negative	○	○	-	-	Roh and Chu, 2010; Yu et al., 2007
	KC9-11	<i>Sphingomonas</i>	negative	×	○	-	-	Yu et al., 2007
KC14	<i>Sphingomonas</i>	negative	×	○	-	-	Yu et al., 2007	
<i>Nitrosomonas europaea</i>	<i>Nitrosomonas</i>	negative	○	○	○	○	Shi et al., 2004 Yi et al., 2007	
Soil samples from agricultural fields	ED8	<i>Sphingomonas</i>	negative	○	○	-	-	Kurusu et al., 2010
	ED9	<i>Sphingomonas</i>	negative	○	○	-	-	Kurusu et al., 2010
	ED7	<i>Rhodococcus</i>	positive	○	○	-	-	Kurusu et al., 2010
	ED10	<i>Rhodococcus</i>	positive	○	○	-	-	Kurusu et al., 2010
Marine sand and seawater	CYH	<i>Sphingomonas</i>	negative	○	○	×	×	Ke et al., 2007
	LHJ1	<i>Acinetobacter</i>	negative	×	○	×	×	Ke et al., 2007
	LHJ3	<i>Agromyces</i>	positive	×	○	○	×	Ke et al., 2007
	S19-1	<i>Buttiauxella</i>	negative	-	○	-	-	Zhang et al., 2011
	H5	<i>Vibrio</i>	negative	-	○	-	-	Sang et al., 2012

Wastewater treatment facility of contraceptive factory	<i>Sphingobacterium</i> sp. JCR5	<i>Sphingobacterium</i>	negative	○	○	○	○	Haiyan et al., 2007
Manure of cowshed compost	<i>Fusarium proliferatum</i> strain HNS-1	<i>Fusarium</i>	-	-	-	-	○	Shi et al., 2002
	<i>Phyllobacterium myrsinacearum</i> (BP1)	α-Proteobacteria	negative	○	○	○	○	Pauwels et al., 2008
	<i>Ralstonia pickettii</i> (BP2)	β-Proteobacteria	negative	○	○	○	○	Pauwels et al., 2008
	<i>Pseudomonas aeruginosa</i> (BP3)	γ-Proteobacteria	negative	○	○	○	○	Pauwels et al., 2008
	<i>Pseudomonas</i> sp. (BP7)	γ-Proteobacteria	negative	○	○	○	○	Pauwels et al., 2008
	<i>Acinetobacter</i> sp. (BP8)	γ-Proteobacteria	negative	○	○	○	○	Pauwels et al., 2008
	<i>Acinetobacter</i> sp. (BP10)	γ-Proteobacteria	negative	○	○	○	○	Pauwels et al., 2008

a: able to degrade the corresponding pollutant; b: disable to degrade the corresponding pollutant; c: unsuitable for Gram stain method or undetected; d: undetected

More recently, fourteen phylogenetically diverse E2-degrading bacteria, which widely distributed among eight different genera *Aminobacter*, *Brevundimonas*, *Escherichia*, *Flavobacterium*, *Microbacterium*, *Nocardioidea*, *Rhodococcus*, and *Sphingomonas* of three Phyla: Proteobacteria, Actinobacteria, and Bacteroidetes, were successfully isolated from activated sludge of a wastewater treatment plant (Yu et al., 2007).

So far, only a few strains, like *Rhodococcus zopfii* and *Rhodococcus equi*, isolated from activated sludge were found to degrade not only natural estrogens but also the synthetic estrogen EE2 (Yoshimoto et al., 2004). The rare presence of EE2-degrader in activated sludge can be applied to account in part for the frequent observation of inefficient removal in real-scale wastewater treatment plants and slow mineralization in batch experiments upon EE2. Larcher and Yargeau (2013) found that *R. rhodochrous* was able to degrade EE2 with no detectable EE2 after 48h, and that no additive or synergistic effects were observed due to the combination of the bacterial cultures with maximum EE2 removals of 43% after 300h. The two *Rhodococcus* strains degraded E2 and E1 by 99% or more, as well as degraded E3 and EE2 by 80% or more in 24h with an initial concentration of 100 mgL⁻¹ (Yoshimoto et al., 2004). In addition, *Rhodococcus zopfii*, one of the two *Rhodococcus* strains, showed particularly strong degrading activities, which degraded E2 (100 mg/L, 10 ml) by 81% in 2 h, E1 at the same concentration by 91% in 3 h, E3 by 96% in 4h, and EE2 by 70% in 6 h (Yoshimoto et al., 2004). *Rhodococcus* sp. strains have been reported to degrade cholesterol that possesses a steroidal skeleton and to degrade aromatic compounds such as 2,4-dinitrophenol, polychlorinated biphenyl (Maeda et al., 1995; Yazdi et al., 2001; Yoon et al., 2000). *Achromobacter* sp. and *Ralstonia* sp. are known to be able to degrade some pollutants, especially phenolic compounds (Bhushan et al., 2000; Shin et al., 2003). *Novosphingobium*, which is one of the recently proposed genera which were previously included in the genus *Sphingomonas* (Takeuchi et al., 2001), is also well known for including many species that can

assimilate biodegradation-resistant compounds such as chlorophenol (Nohynek et al., 1996), fluorene, biphenyl, dibenzothiophene (Frederickson et al., 1995), benzoate, cresol, naphthalene and xylene (Balkwill et al., 1997). Thus, it might be inferred that the known strains being able to degrade compound carrying phenolic group also could assimilate estrogens. It has been proved by Haiyan et al. (2007) that *Sphingobacterium* sp. JCR5 which grew on EE2 as sole source of carbon and energy could also degrade E1 and E2.

Besides activated sludge, some estrogen-degrading bacteria were also successfully isolated from soil, manure and compost. The first attempts to identify the microorganisms involved in estrogens biotic transformation in soil, over 60 years ago, were based on culture-dependent techniques (Turffitt et al., 1947). In this study, the biodegradation of E1 was examined using 355 different cultures of bacteria isolated from five disparate soil types. No culturable bacteria were found in loam, marl, or alkaline peat soils that could metabolize E2. However, one *Proactinomyces* spp. was isolated from an acid sand, and two strains were found in arable soil that could use E2 as a carbon source. E1 was degradable by one species of *Proactinomyces* spp. in the arable soil, but no degradation was observed with organisms from the other four soils. Three estrogen-degrading bacteria, LHJ1, LHJ3, and CYH, were isolated from microcosms constructed with marine sand and ultrafiltered (UF) secondary effluent (Ke et al., 2007). All three isolates were not capable of degrading EE2. Under aerobic condition, all three isolates oxidize E2 to E1, while only one of them, CYH, degraded E1, and only LHJ3 degraded E3. Furthermore, under aerobic condition, CYH was able to degrade E1 while LHJ3 was able to degrade E2.

Five species, i.e. *Phyllobacterium myrsinacearum*, *Ralstonia pickettii*, *Pseudomonas aeruginosa*, *Pseudomonas* sp. and *Acinetobacter* sp. isolated from compost were able to degrade E1, E2 and E3, while were not able to degrade EE2 except in the presence of E2 (Pauwels et al., 2008).

Moreover, fungi were found to be able to degrade estrogens as well. For example, an EE2-

degrading fungus (*Fusarium proliferatum*) was isolated from cowshed samples (Shi et al., 2002). Ligninolytic fungi (LF) or their enzymes can be actively used for decontamination because of their ability to either polymerize the target pollutants or to substantially decompose the original structure using ligninolytic enzymes and cytochrome P-450 (Cajthaml, 2015). Likewise, white-rot fungi (WRF) and their lignin modifying enzymes (LME) can degrade various kinds of trace organic contaminants (TrOC). Depending on the initial concentration of TrOC, WRF species and associated LME, addition of redox mediators can facilitate the removal of those compounds (Yang et al., 2013). *T. versicolor* was also able to degrade EE2 (Castellana and Loffredo, 2014). Many studies were also performed in order to determine the feasibility of applying fungal treatments to the biodegradation of estrogens, as shown in Table 5. In light of the recent success in the isolation of estrogen-degrading cultures from activated sludge and different environmental compartments, natural estrogen-degrading cultures are widespread in environment and engineered systems. Natural estrogens of human and animal origin are being delivered into the environment over thousands of years, especially due to growing population and more intensive farming.

It is therefore not surprising that a large number of bacteria have acquired pathways to make use of these compounds as growth substrates. Certain bacteria are able to grow on steroid hormones as the sole source of carbon and energy by the expression of a set of steroid-catabolizing enzymes. By contrast, so far only a small number of EE2 degrading microbes have been isolated. However, it remains uncertain whether the different degradation abilities of estrogen-degrading cultures toward estrogens contribute to the wide range of estrogen removal observed by many field studies.

Another important issue is to know whether these isolated strains are still active in the case estrogens at the environmentally relevant concentration, due to the fact that estrogens were generally found in natural environments in nanograms-per-liter concentrations.

5.2. Degradation pathways of E1 and E2

Although bacteria are generally capable of growing on either natural or synthetic estrogens as sole source of carbon and energy, only a few metabolic pathways have been proposed. Bolton et al. (1998) suggested a metabolic pathway where E2 is oxidized to E1 and then further oxidized to a more polar semiquinone or quinone. Only a small fraction of E3 is found in effluent probably due to the three hydroxyl groups in its structure, which makes it more susceptible of surface reactions.

E1 might be one of the common key intermediates involved in the degradation of E2, which was confirmed by both laboratory studies performed with either activated sludge or soil (Colucci et al., 2001a; Jacobsen et al., 2005; Johnson et al., 2001; Lee et al., 2002; Shi et al., 2013; Ternes et al., 1999a; Weber et al., 2005; Yu et al., 2007) and field monitor data (Baronti et al., 2000). In a pilot-scale step-feed anoxic/oxic (A/O) wastewater treatment system established by Shi et al. (2013), a linear relationship between the concentrations of E1 and E2 in the water phase indicated the transformation between E1 and E2. The equilibrium constant (K) for the transformation between E1 and E2 was remarkably higher in the anoxic zones (0.38–0.81) than in the aerobic zones (0.08–0.24). The frequently observed conversion of E2 to E1 is probably due to microbial enzymatic activity of an NADH-dependent hydroxysteroid dehydrogenase (Czajka and Londry, 2006). A miscible-displacement column experiment indicated that E2 entered the soil column underwent rapid transformation to form at least three metabolites, E1, sporadic E3 and an unidentified high-polarity compound (Casey et al., 2003). It is worth noting that, E2 also can be biotransformed in some other pathways not via E1. For instance, Degradation of E2 by neither *Rhodococcus zopfii* (Yoshimoto et al., 2004) nor commercial pure culture *Nitrosomonas europaea* (Shi et al., 2004) occurred with increasing of E1 concentration. In another study, a new metabolite, a steroid-D-ring lactone, was detected during the very early stages of E2 degradation by sewage bacteria (Lee and Liu, 2002).

Table 5. Fungal enzymes capable of biodegrading or metabolizing estrogens

Treatment	Fungal enzymes	Initial concentration	E1 removal rates	E2 removal rates	E3 removal rates	EE2 removal rates	References
Flask scale	VP from <i>B. adusta</i>	2.5 mg/L	100% after 15 min	100% after 15 min	-	100% after 15 min	Eibes et al., 2011
	LAC from <i>M. thermophila</i>	5 mg/L	100% after 24 h with mediators	100% after 3 h without mediators	-	100% after 5 h without mediators	Lloret et al., 2010
Stirred batch reactor with the compound spiked in wastewater	LAC from <i>Trametes sp.</i>	100 ng/L	100% after 1 h	100% after 1 h	100% after 1 h	100% after 1 h	Auriol et al., 2007
	LAC from <i>T. versicolor</i>	100 ng/L	100% after 1 h	100% after 1 h	100% after 1 h	100% after 1 h	Auriol et al., 2008

Furthermore, the scenario regarding the conversion of E2 to E1 in soil remains both controversial and elusive. Taking into consideration the less effective removal of E1 in STPs (Johnson and Sumpter, 2001) and batch experiments (Suzuki and Maruyama, 2006) in comparison to E2, we can postulate that the bacteria capable of transforming E2 directly to non-estrogenic compounds not via E1 either are not so prevailing in activated sludge as the bacteria that are able to transform E2 to E1 but are not able to further oxidize E1, or are inhibited by other unknown factors in the mixed culture.

Neither autoclaving (Colucci et al., 2001) nor oven-drying at 85°C for 24h (Casey et al., 2003) was able to prevent the oxidation of E2 to E1 in soil. These results suggest that either the enzyme responsible for E2 transformation in soils is able to survive from autoclaving and oven-drying process, or oxidation of E2 to E1 can proceed abiotically. But they were contradictory to a recent finding of Mashtare et al. (2013), who reported that transformation of amended hormones in autoclaved sediments was markedly slower than in nonautoclaved sediments. This result was consistent with a previous study which showed that E2 was only oxidized to E1 via biological processes (Fan et al., 2007).

The discrepancy could be attributed to the difference of adopted experimental strategy. In contrast to the research of Fan et al. (2007), where 500 mg HgCl₂ per kg soil was added to the autoclaved soil, no inhibitor was used in the research of Colucci et al. (2001a) and Casey et al. (2003), where the inadvertent introduction of airborne microorganisms could not be ruled out when periodically sampling. Although it is not understood how the relative rates of biotic and abiotic degradation rates influence the transform of E2 to E1, E1 was shown to degrade primarily through microbial processes under aerobic conditions (Colucci et al., 2001a). More studies further confirmed that microbial processes play a key role in E2 mineralization under aerobic conditions supported by the fact that no mineralization of E2 was observed in sterile soils (Fan et al., 2007; Jacobsen et al., 2005).

With regard to E1 mineralization, two different pathways have been thus far proposed. In the mineralization study using ¹⁴C-E2, which was labeled on the C-4 carbon, Layton et al. (2000) demonstrated that the conversion of E1 proceeded by a cleavage of the A-ring based on the release of ¹⁴C-CO₂. The possible metabolite resulted from A-ring cleavage was

suggested by an earlier study (Coombe et al., 1966) as showed in Fig. 1. Alternatively, Lee and Liu (2002) indicated that E2 was oxidized from the cyclopentane ring D at C17 into E1 during enzymatic degradation and then further degraded into metabolite X1 and finally to carbon dioxide through a tricarboxylic acid (TCA) cycle due to the detection of lactone as an intermediate. The pathway is given as Fig. 2. Additionally, dehydration was firstly reported as a mechanism of microbial estrogen degradation when Nakai et al. (2011) studied the degradation pathways of 17β-estradiol by *Nitrosomonas europaea* and determined whether the degradation products of 17β-estradiol had estrogenic activity. 1,3,5(10),16-Estratetraen-3-ol (estratetraenol) was newly recognized as a degradation intermediate produced by dehydration of 17β-estradiol. Its degradation rate was faster than that of 17β-estradiol. The yeast two-hybrid assay proved that estratetraenol acted as a ligand for the estrogen receptor; estratetraenol thus has potential estrogenic activity.

5.3. Degradation pathways of EE2

Degradation pathways of the natural estrogens as well as of EE2 are still controversial. In batch experiments with nitrifying activated sludge, Vader et al. (2000) found that EE2 was degraded completely within 6 days and an unidentified hydrophilic metabolite was produced and postulated that nitrifying bacteria were responsible for the steroid transformation by co-metabolism. Layton et al. (2000) indicated that the cleavage of the A-ring was involved in the mineralization of EE2 by conducting an experiment with ¹⁴C-EE2 labeled on the C-4 carbon. Recently, three catabolic intermediates, including E1, resulted from EE2 degradation, were identified during a study carried out with *Sphingobacterium* sp. JCR5 isolated from activated sludge obtained from a wastewater treatment plant of an oral contraceptives producing factory. According to Haiyan et al. (2007), in the first step EE2 is oxygenized to three main catabolic intermediates, namely, E1, 2-hydroxy-2,4-dienevaleric acid and 2-hydroxy-2,4-diene-1,6-dioic acid. The second compound shares the analogous route with a previously reported testosterone-degrading bacterium and the latter is a metabolite with a different cleavage position from the former. It is conceivable that the degradation pathways vary from microbe to microbe.

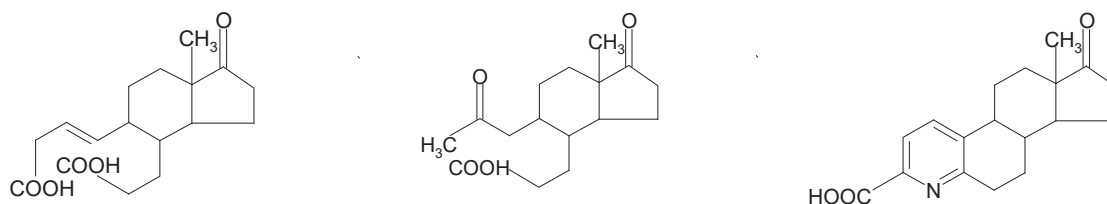


Fig. 1. Suggested intermediates as a result of ring cleavage of estrone (E1)

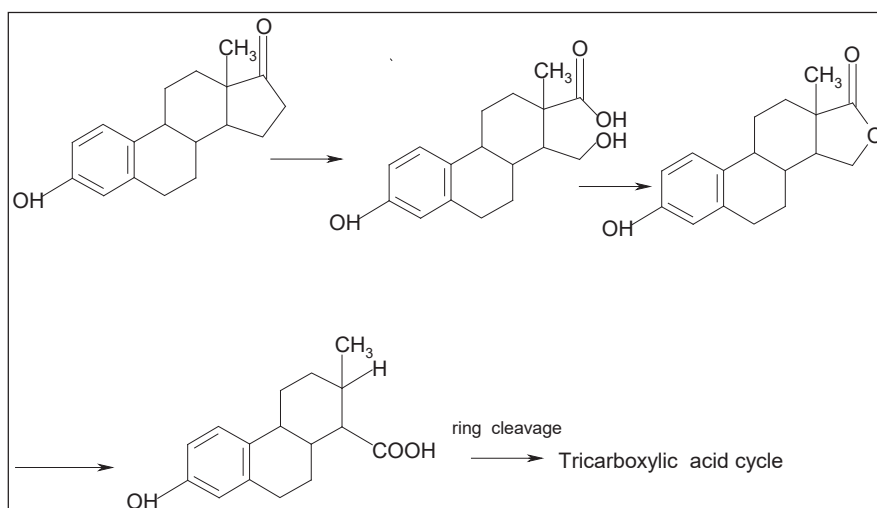


Fig. 2. A proposed route of ring cleavage of estrone (E1)

However, that the degradation of EE2 is firstly oxidized to E1 by the splitting of the ethynyl group suggested by Haiyan et al. (2007) is not in agreement with the study where two differently radiolabeled EE2 was applied continuously to a bench-scale membrane bioreactor with adapted industrial activated sludge (Cirja et al., 2007). A unique degradation product was identically detected in two experiments performed with the two differently radiolabeled EE2 labeled on the C-4 and C-20 carbon, respectively.

The authors consequently believed that the ethynyl group was not substituted due to no detection of ^{14}C -labelled ethynyl. Nevertheless, in terms of the downstream part of the whole degradation pathway, the oxidation of ethynyl group could not be ruled out due to that $^{14}\text{CO}_2$ was produced in both experiments using the different ^{14}C -EE2, though the percents of mineralization were both less than 1% (Cirja et al., 2007). Yi et al. (2007) suggested that ring A (aromatic ring) of EE2 was the site of electrophilic initiating reactions, including conjugation, hydroxylation and cleavage; due to electron density associated with ring A was significantly higher than that in other rings of EE2, which could be useful for further efforts to elucidate biodegradation pathway of EE2. In contrast, Haiyan et al. (2007) proposed that EE2 was initially oxidized to E1, and that the pathway continued with ring opening oxidation reactions on ring B, leaving ring A initially intact based on the detected daughter products in an isolation culture experiment. It can be seen that the degradation pathway by co-metabolism is different with that by isolated bacterium being able to utilize EE2 as growth substrate. Future work must identify daughter products to investigate the metabolic details.

6. Cometabolic steroid degradation especially by nitrifying microorganisms

Cometabolic transformations are reactions that are catalyzed by existing microbial enzymes and that yield no carbon or energy benefits to the transforming cells. Therefore, a growth substrate must be available

at least periodically to grow new cells, provide an energy source, and induce production of the cometabolic enzymes. Cometabolism- in which an organic compound is modified but not utilised for growth - is another important biodegradation process (Alexander, 1994), especially for micropollutants including estrogens present in significantly low concentration.

It is well documented that biodegradation of estrogens is clearly stimulated in the presence of nitrifying bacteria. Moreover, the enhancement was most probably due to co-metabolic effects. Several bacterial strains that produce monooxygenase enzymes are known to aerobically cometabolise organic compounds. *Nitrosomonas europaea* is a ubiquitous monooxygenase-producing bacterium catalyzing the oxidation of ammonium in soils, natural waters and nitrifying activated sludge (Shi et al., 2004b). It has often been demonstrated that ammonium monooxygenase (AMO) in the cells of *Nitrosomonas europaea* is capable of co-oxidising many organic compounds. Vader et al. (2000) used activated sludge in a laboratory reactor with ammonium and hydrazine as the energy sources and found approximately 28h half-life of EE2 by sludges that nitrified. The sludges that failed to nitrify significantly also failed to degrade EE2.

This result was afterwards supported by Shi et al. (2004a), who found that using allylthiourea (ATU), a chemical that inhibits the nitrification by blocking the ammonium monooxygenase (AMO), resulted in a decline of degradation rate for EE2 by about 80%, while that for E1 and E2 remained the same. Compared to the completely blocked in a culture of pure-strain *Nitrosomonas europaea* inhibited by ATU, the degradation of EE2 only slowed down in a mixed culture of nitrifiers and heterotrophs inhibited by ATU, which suggested that there were also other bacteria being able to convert EE2 in activated sludge (Shi et al., 2004a). It was demonstrated that the cometabolic degradation of E1, E2 and EE2 was the primary approach of their removal in nitrifying activated sludge and the activity of ammonia-

oxidizing bacteria dominating their degradation (Ren, et al., 2007). Although AMO may be inhibited by acetylene (Bollmann and Conrad, 1997; Teissier and Torre, 2002), the ethynyl group contained in EE2 did not appear to inhibit AMO activity (Yi et al., 2007). This conclusion was afterwards supported by Khunjar et al. (2011), who evaluated the biological fate of EE2 with flow through reactors containing an ammonia oxidizing bacterial (AOB) culture, two enriched heterotrophic cultures lack of nitrifier activity, and nitrifying activated sludge (NAS) cultures. It was found that EE2 removal slowed remarkably after AOBs were inhibited. It was worth noting that AOBs biotransformed EE2 five times faster than heterotrophs. Moreover, The cometabolic activity of AMO responsible for EE2 degradation is linearly correlated with ammonia oxidizing rate that usually regulated by initial ammonia concentration, temperature (Vader et al., 2000; Yi et al., 2006; Yi et al., 2007). Interestingly, Forrez et al. (2009) found that the elimination of EE2 was not affected by the absence of ammonium in the feed, suggesting that ammonia oxidizing bacteria (AOB) were able to maintain their population density and their activity, even after several months of starvation. Not only was AMO, but also other nonspecific monooxygenase enzymes were probably contributing to the degradation of estrogens. For instance, although the all 14 strains isolated by Yu et al. (2007) were capable of converting E2 to E1, only three of them (two strains of *Aminobacter* and one strain of *Sphingomonas*, all three strains belong to *Alphaproteobacteria*) showed the ability to degrade E1, which unexceptionally exhibited nonspecific monooxygenase activity rather than nonspecific dioxygenase activity.

Nonspecific monooxygenases are known to be responsible for metabolic and/or cometabolic reactions of a wide range of organics (Leahy et al., 2003; McCarty, 1997), including EE2 (Shi et al., 2004a). It is likely that nonspecific monooxygenase enzymes were responsible for estrogen degradation. It should be noted that the one strain of *Sphingomonas* mentioned above is unique with the ability to utilize E2 as a sole carbon source for growth. In other words, only one consortium of the fourteen isolates degraded E2 by growth linked metabolic reaction, while the other 13 isolates might via co-metabolic reaction. Afterwards, Roh (2009) found that *Sphingomonas* strain KC8 exhibited nonspecific monooxygenase activity but not dioxygenase activity via the results of enzymatic characterization. Nonspecific monooxygenase enzymes may be responsible for estrogen degradation by strain KC8, which supports the conclusion before.

Tran et al. (2013) suggested that cometabolism of EOCs (emerging trace organic contaminants), which includes estrogens, is widely noted in autotrophic microbes, such as autotrophic ammonia oxidizers via the non-specific enzymes, e.g. AMO. It is due to the fact that the autotrophic oxidizers utilize inorganic carbon and ammonia as the sole carbon and energy sources for their growth and induce AMO and

cofactors as well. However, heterotrophic microbes can get involved in both cometabolism and/or metabolism depending on both the concentration of EOCs in the environment and their toxicity to the microbes.

Interestingly, a particular co-metabolic transformation process was recently reported occurring between natural and synthetic estrogens (Pauwels et al., 2008). With the intention of isolating EE2-degrading microorganisms from compost, Pauwels and co-workers (Pauwels et al., 2008) not only successfully isolated six strains, but also discovered that all six isolates were only able to co-metabolize EE2 in the presence of E2 or E1, possibly even E3, while fail to metabolize EE2 as the sole carbon sources. In the co-metabolism experiment using E2 and EE2 as coexistent substrate, It was observed that EE2 remained constant until the depletion of E2, and was subsequently degraded as soon as the E1 began to decrease, which early accumulated as a temporary intermediate. The authors speculated that certain enzyme, produced by the isolate, involved in degradation of E1 was perhaps responsible for the degradation of EE2 simultaneously. Apparently, more focused research is highly desired, due to the ubiquitous coexistence of E2, E1 and EE2 in urine, activated sludge, soil and compost, etc.

7. Conclusion and outlook

Generally, the sequence of degradation efficiency is $E2 > E1 >> EE2$. Although E2 is fast degraded to E1, this does not reduce the estrogenic potential remarkably. E1 is quite persistent in the environment, while EE2 is even more recalcitrant because it contains an ethynyl group at the same C-atom. According to research by far, most important degradation process is the degradation by microorganisms. *Cornybacterium* spp., *Nitrosomonas europaea* etc. are proved to be able to degrade estrogens. Moreover, the degradation rates can be influenced by temperature, pH values, redox conditions, etc. In general, better results can be gained at relatively higher temperatures. Bacteria that can degrade steroid hormones metabolically under denitrifying conditions could be isolated. It is however not certain if these bacteria have a big influence in removing estrogens, or if other bacteria in the denitrifying tank is in favor of the degradation.

Although research has been done to determine removal rates of estrogens, their degradation pathways are still dubious. The oxidation from E2 to E1, also called the first step, is widely accepted. Nevertheless, it is still unclear at which ring the cleavage initially occurs and which enzymes are involved in the estrogens degradation pathway. Further studies are required to determine this pathway. Moreover, pathways of EE2 are still controversial, as several incompatible theories have been proposed.

Lastly, before being put into practical application, the ability of the organisms to degrade estrogens needs to be enhanced. As the ambient

concentrations of estrogens in wastewater are much lower than the concentrations used in published studies, further studies are needed to address the prevalence of the isolates in biological treatment processes as well as to determine the significance of the isolates in estrogen removal. Quite a few aspects, including the ability to utilize other available organics and other estrogenic compounds in wastewater, the pathways, enzymes, and kinetics of estrogen degradation, have to be investigated in order to fully capitalize the degradation ability of these strains for potentiating estrogen degradation.

Acknowledgements

The present work was supported by the National Science Foundation of China (Grant No. 41571476 and No. 51109038), the Qing Lan Project of Jiangsu Province, and Startup Fund for Talented Scholars of Nanjing Normal University.

References

- Adlercreutz H., Fotsis T., Bannwart C., Hamalainen E., Bloigu S., Ollus A., (1986), Urinary estrogen profile determination in young finnish vegetarian and omnivorous women, *Journal of Steroid Biochemistry*, **24**, 289-296.
- Adlercreutz H., Gorbach S.L., Goldin B.R., Woods M.N., Dwyer J.T., Hamalainen E., (1994), Estrogen metabolism and excretion in Oriental and Caucasian women, *Journal of the National Cancer Institute*, **86**, 1076-1082.
- Ainsworth L., Common R.H., Carter A.L., (1962), A chromatographic study of some conversion products of estrone-16-C-14 in the urine and feces of the laying hen, *Canadian Journal of Biochemistry and Physiology*, **40**, 123-135.
- Andersen H., Siegrist H., Halling-Sørensen B., Ternes T.A., (2003), Fate of estrogens in a municipal sewage treatment plant, *Environmental Science & Technology*, **37**, 4021-4026.
- Andersen H.R., Hansen M., Kjølholt J., Stuer-Lauridsen F., Ternes T., Halling-Sørensen B., (2005), Assessment of the importance of sorption for steroid estrogens removal during activated sludge treatment, *Chemosphere*, **61**, 139-146.
- Alexander M., (1994), *Biodegradation and Bioremediation*, Academic Press, San Diego, USA.
- Auriol M., Filali-Meknassi Y., Tyagi R.D., Adams C.D., (2007), Laccase-catalyzed conversion of natural and synthetic hormones from a municipal wastewater, *Water research*, **41**, 3281-3288.
- Auriol M., Filali-Meknassi Y., Adams C.D., Tyagi R.D., Noguero T.N., Piña B., (2008), Removal of estrogenic activity of natural and synthetic hormones from a municipal wastewater: Efficiency of horseradish peroxidase and laccase from *Trametes versicolor*, *Chemosphere*, **70**, 445-452.
- Balaguer P., Francois F., Comunale F., Fenet H., Boussioux A.M., Pons M., Nicolas J.C., Casellas C., (1999), Reporter cell lines to study the estrogenic effects of xenoestrogens, *Science of the Total Environment*, **233**, 47-56.
- Balkwill D.L., Drake G.R., Reeves R.H., Fredrickson J.K., White D.C., Ringelberg D.B., Chandler D.P., Romine M.F., Kennedy D.W., Spadoni C.M., (1997), Taxonomic study of aromatic-degrading bacteria from deep-terrestrial-subsurface sediments and description of *Sphingomonas aromaticivorans* sp. nov., *Sphingomonas subterranea* sp. nov., and *Sphingomonas stygia* sp. nov. *International Journal of Systematic and Evolutionary Microbiology*, **47**, 191-201.
- Baronti C., Curini R., D'Ascenzo G., Di Corcia A., Gentili A., Samperi R., (2000), Monitoring natural and synthetic estrogens at activated sludge sewage treatment plants and in a receiving river water, *Environmental Science & Technology*, **34**, 5059-5066.
- Belhaj D., Jaabiri I., Ayadi H., Kallel M., Zhou J.L., (2013), Occurrence and removal of steroidal estrogens in Centre Eastern Tunisia municipal sewage treatment plant, *Desalination and Water Treatment*, **14**, 2330-2339.
- Berthe-Corti L., Nachtkamp M., (2010), *54 Bacterial Communities in Hydrocarbon-Contaminated Marine Coastal Environments*, In: *Handbook of Hydrocarbon and Lipid Microbiology*, Kenneth N., Timmis (Eds.), Springer, Berlin Heidelberg New York, 2349-2359.
- Bhushan B., Samanta S.K., Chauhan A., Chakraborti A.K., Jain R.K., (2000), Chemotaxis and biodegradation of 3-methyl-4-nitrophenol by *Ralstonia* sp. SJ98, *Biochemical and Biophysical Research Communications*, **275**, 129-133.
- Bollmann A., Conrad R., (1997), Recovery of nitrification and production of NO and N₂O after exposure of soil to acetylene, *Biology and Fertility of Soils*, **25**, 41-46.
- Bolton J.L., Pisha E., Zhang F., Qiu S., (1998), Role of quinoids in estrogen carcinogenesis, *Chemical Research in Toxicology*, **11**, 1113-1127.
- Cajthaml T., (2015), Biodegradation of endocrine-disrupting compounds by ligninolytic fungi: mechanisms involved in the degradation, *Environmental Microbiology*, **17**, 4822-4834.
- Casey F.X.M., Larsen G.L., Hakk H., Simunek J., (2003), Fate and transport of 17 β -estradiol in soil-water system, *Environmental Science & Technology*, **37**, 2400-2409.
- Castellana G., Loffredo E., (2014), Simultaneous removal of endocrine disruptors from a wastewater using white rot fungi and various adsorbents, *Water, Air & Soil Pollution*, **225**, 1-13.
- Chen M.X., Fang H., Qi R., He S.X., Wei Y.S., (2016), 17 β -estradiol degrading bacteria in sequencing batch reactors for swine wastewater treatment, *Environmental Engineering and Management Journal*, **15**, 2273-2278.
- Chimchirian R.F., Suri R.P.S., Fu H.X., (2007), Free synthetic and natural estrogen hormones in influent and effluent of three municipal wastewater treatment plants, *Water Environment Research*, **79**, 969-974.
- Chun S., Lee J., Geyer R., White D.C., Raj Raman D., (2005), Effect of agricultural antibiotics on the persistence and transformation of 17 β -Estradiol in a sequatchie loam, *Journal of Environmental Science and Health, Part B: Pesticides, Food Contaminants, and Agricultural Wastes*, **40**, 741-751.
- Cirja M., Zuehlke S., Ivashechkin P., Hollender J., Schaffer A., Corvini P.F.X., (2007), Behavior of two differently radiolabelled 17 α -Ethinylestradiol continuously applied to a laboratory-scale membrane bioreactor with adapted industrial activated sludge, *Water Research*, **41**, 4403-4412.
- Colucci M.S., Bork H., Topp E., (2001a), Persistence of estrogenic hormones in agricultural soils: I. 17 β -estradiol and estrone, *Journal of Environmental Quality*, **30**, 2070-2076.

- Colucci M.S., Topp E., (2001b), Persistence of estrogenic hormones in agricultural soils: II 17 α -Ethinylestradiol, *Journal of Environmental Quality*, **30**, 2077-2080.
- Coombe R.G., Tsong Y.Y., Hamilton P. B., Sih C.J., (1966), Mechanisms of steroid oxidation by microorganisms. X. Oxidative cleavage of estrone, *Journal of Biological Chemistry*, **241**, 1587-1595.
- Czajka C.P., Londry K.L., (2006), Anaerobic biotransformation of estrogens, *Science of the Total Environment*, **367**, 932-941.
- Das B.S., Lee L.S., Rao P.S.C., Hultgren R.P., (2004), Sorption and degradation of steroid hormones in soils during transport: Column studies and model evaluation, *Environmental Science & Technology*, **38**, 1460-1470.
- de Mes, T., Zeeman G., Lettinga G., (2005), Occurrence and fate of estrone, 17 β -estradiol and 17 α -ethinylestradiol in STPs for domestic wastewater, *Reviews in Environmental Science and Bio/Technology*, **4**, 275-311.
- Desbrow C., Routledge E.J., Brighty G.C., Sumpter J.P., Waldock M., (1998), Identification of estrogenic chemicals in STW effluent. I. Chemical fractionation and *in vitro* biological screening, *Environmental Science & Technology*, **32**, 1549-1558.
- Dytczak M.A., Londry K. L., Oleszkiewicz J.A., (2008), Biotransformation of estrogens in nitrifying activated sludge under aerobic and alternating anoxic/aerobic conditions, *Water Environment Research*, **80**, 47-52.
- Eibes G., Debernardi G., Feijoo G., Moreira M. T., Lema J.M., (2011), Oxidation of pharmaceutically active compounds by a ligninolytic fungal peroxidase, *Biodegradation*, **22**, 539-550.
- Esperanza M., Suidan M.T., Nishimura F., Wang Z.M., Sorial G.A., (2004), Determination of sex hormones and nonylphenol ethoxylates in the aqueous matrixes of two pilot-scale municipal wastewater treatment plants, *Environmental Science & Technology*, **38**, 3028-3035.
- Essandoh H.M.K., Tizaoui C., Mohamed M.H.A., (2012), Removal of estrone (E1), 17 β -estradiol (E2) and 17 α -ethinylestradiol (EE2) during soil aquifer treatment of a model wastewater, *Separation Science and Technology*, **47**, 777-787.
- Fahrbach M., Kuever J., Meinke R., Kämpfer P., Hollender J., (2006), *Denitratisoma oestradiolicum* gen. nov., sp. nov., a 17 β -oestradiol-degrading, denitrifying betaproteobacterium, *International Journal of Systematic and Evolutionary Microbiology*, **56**, 1547-1552.
- Fan Z., Casey F.X.M., Hakk H., Larsen G.L., (2007), Persistence and fate of 17 β -estradiol and testosterone in agricultural soils, *Chemosphere*, **67**, 886-895.
- Fotsis T., Järvenpää P., Adlecreutz H., (1980), Purification of urine for quantification of the complete estrogen profile, *Journal of Steroid Biochemistry*, **12**, 503-508.
- Frederickson J.K., Balkwill D.L., Drake G.R., Romine M.F., Ringelberg D.B., White D.C., (1995), Aromatic-degrading *Sphingomonas* isolates from the deep substrate, *Applied and Environmental Microbiology*, **61**, 1917-1922.
- Fujii K., Kikuchi S., Satomi M., Ushio-Sata N., Morita N., (2002), Degradation of 17 β -estradiol by a gram-negative bacterium isolated from activated sludge in a sewage treatment plant in Tokyo, Japan, *Applied and Environmental Microbiology*, **68**, 2057-2060.
- Fujii K., Satomi M., Morita N., Motomura T., Tanaka T., Kikuchi S., (2003), *Novosphingobium tardegens* sp. nov., an oestradiol-degrading bacterium isolated from activated sludge of a sewage treatment plant in Tokyo, *International Journal of Systematic and Evolutionary Microbiology*, **53**, 47-52.
- Forrez I., Carballa M., Boon N., Verstraete W., (2009), Biological removal of 17 α -ethinylestradiol (EE2) in an aerated nitrifying fixed bed reactor during ammonium starvation, *Journal of Chemical Technology and Biotechnology*, **84**, 119-125.
- Gesell M., Hammer E., Specht M., Francke W., Schauer F., (2001), Biotransformation of biphenyl by *Paecilomyces lilacinus* and characterization of ring cleavage products, *Applied and Environmental Microbiology*, **67**, 1551-1557.
- Hakk H., Millner P., Larsen G., (2005), Decrease in water-soluble 17 β -estradiol and testosterone in composted poultry manure with time, *Journal of Environmental Quality*, **34**, 943-950.
- Haiyan R., Shulan J., ud din Ahmad N., (2007), Degradation characteristics and metabolic pathway of 17 α -ethinylestradiol by *Sphingobacterium* sp. JCR5, *Chemosphere*, **66**, 340-346.
- Hashimoto T., Onda K., Nakamura Y., Tada K., Miya A., Murakami T., (2007), Comparison of natural estrogen removal efficiency in the conventional activated sludge process and the oxidation ditch process, *Water Research*, **41**, 2117-2126.
- Hashimoto T., Onda K., Morita T., Luxmy B.S., Tada K., Miya A., Murakami T., (2009), Contribution of the estrogen-degrading bacterium *Novosphingobium* sp. strain JEM-1 to estrogen removal in wastewater treatment, *Journal of Environmental Engineering*, **136**, 890-896.
- Herman J.S., Mills A.L., (2003), Biological and hydrological interactions affect the persistence of 17 β -estradiol in an agricultural watershed, *Geobiology*, **1**, 141-151.
- Hilakivi-Clarke L., de Assis S., Warri A., (2013), Exposures to synthetic estrogens at different times during the life, and their effect on breast cancer risk, *Journal of Mammary Gland Biology and Neoplasia*, **18**, 25-42.
- Hoffmann B., Depinho T.G., Schuler G., (1997), Determination of free and conjugated oestrogens in peripheral blood plasma, feces and urine of cattle throughout pregnancy, *Experimental and Clinical Endocrinology Diabetes*, **105**, 296-303.
- Hutchins S.R., White M.V., Hudson F.M., Fine D.D., (2007), Analysis of lagoon samples from different concentrated animal feeding operations for estrogens and estrogen conjugates, *Environmental Science & Technology*, **41**, 738-744.
- Ivie G.W., Christopher R.J., Munger C.E., Coppock C.E., (1986), Fate and residues of [4-¹⁴C] estradiol-17 beta after intramuscular injection into Holstein steer calves, *Journal of Animal Science*, **62**, 681-690.
- Jacobsen A., Lorenzen A., Chapman R., Topp E., (2005), Persistence of testosterone and 17 β -estradiol in soils receiving swine manure or municipal biosolids, *Journal of Environmental Quality*, **34**, 861-871.
- Jiang L., Yang J., Chen J., (2010), Isolation and characteristics of 17 β -estradiol-degrading *Bacillus* spp. strains from activated sludge, *Biodegradation*, **21**, 729-736.
- Johnson A.C., Belfroid A., Di Corcia A., (2000), Estimating steroid oestrogen inputs into activated sludge treatment works and observations on their removal from the effluent, *Science of the Total Environment*, **256**, 163-173.
- Johnson A.C., Sumpter J.P., (2001), Removal of endocrine-disrupting chemicals in activated sludge treatment

- works, *Environmental Science & Technology*, **35**, 4697-4703.
- Joss A., Andersen H., Ternes T., Richle P.R., Siegrist H., (2004), Removal of estrogens in municipal wastewater treatment under aerobic and anaerobic conditions: consequences for plant optimization, *Environmental Science & Technology*, **38**, 3047-3055.
- Jürgens M.D., Holthaus K.I.E., Johnson A.C., Smith J.J.L., Hetheridge M., Williams R.J., (2002), The potential for estradiol and ethinylestradiol degradation in English rivers, *Environmental Toxicology and Chemistry*, **21**, 480-488.
- Ke J., Zhuang W., Gin K.Y., Reinhard M., Hoon L.T., Tay J.H., (2007), Characterization of estrogen-degrading bacteria isolated from an artificial sandy aquifer with ultrafiltered secondary effluent as the medium, *Applied Microbiology and Biotechnology*, **75**, 1163-1171.
- Khunjar W.O., Mackintosh S.A., Skotnicka-Pitak J., Baik S., Aga D.S., Love N.G., (2011), Elucidating the relative roles of ammonia oxidizing and heterotrophic bacteria during the biotransformation of 17 α -ethinylestradiol and trimethoprim, *Environmental Science & Technology*, **45**, 3605-3612.
- Knight W.M., (1980), Estrogens administered to food producing animals: environmental considerations, *Estrogens in the Environment*, Elsevier/North-Holland, New York, 391-402.
- Körner W., Spengler P., Bolz U., Schuller W., Hanf V., Metzger J.W., (2001), Substances with estrogenic activity in effluents of sewage treatment plants in southwestern Germany. 2. Biological analysis, *Environmental Toxicology and Chemistry*, **20**, 2142-2151.
- Kuch H.M., Ballschmitter K., (2001), Determination of endocrine-disrupting phenolic compounds and estrogens in surface and drinking water by HRGC-(NCl)-MS in the picogram per liter range, *Environmental Science & Technology*, **35**, 3201-3206.
- Kumar A.K., Sarma P.N., Venkata Mohan S.R., (2016), Incidence of selected endocrine disrupting estrogens in water bodies of Hyderabad and its relation to water quality parameters, *Environmental Engineering and Management Journal*, **15**, 315-325.
- Kurisu F., Ogura M., Saitoh S., Yamazoe A., Yagi O., (2010), Degradation of natural estrogen and identification of the metabolites produced by soil isolates of *Rhodococcus* sp. and *Sphingomonas* sp., *Journal of Bioscience and Bioengineering*, **109**, 576-582.
- Kuster M., López de Alda M.J., Barceló D., (2004), Analysis and distribution of estrogens and progestogens in sewage sludge, soils and sediments, *Trends in Analytical Chemistry*, **23**, 790-798.
- Lai K.M., Johnson K.L., Scrimshaw M.D., Lester J.N., (2000), Binding of waterborne steroid estrogens to solid phases in river and estuarine systems, *Environmental Science & Technology*, **34**, 3890-3894.
- Lange R., Hutchinson T.H., Croudace C.P., Siegmund F., Schweinfurth H., Hampe P., Panter G.H., Sumpter J.P., (2001), Effects of the synthetic estrogen 17 α -ethinylestradiol on the life-cycle of the fathead minnow (*Pimephales promelas*), *Environmental Toxicology and Chemistry*, **20**, 1216-1227.
- Larcher S., Yargeau V., (2013), Biodegradation of 17 α -ethinylestradiol by heterotrophic bacteria, *Environmental Pollution*, **173**, 17-22.
- Layton A.C., Gregory B.W., Seward J.R., Schultz T.W., Sayler G.S., (2000), Mineralization of steroidal hormones by biosolids in wastewater treatment systems in Tennessee U.S.A, *Environmental Science & Technology*, **34**, 3925-3931.
- Leahy J.G., Batchelor P.J., Morcomb S.M., (2003), Evolution of the soluble diiron monooxygenases, *FEMS Microbiology Reviews*, **27**, 449-479.
- Lee H.B., Liu D., (2002), Degradation of 17 β -estradiol and its metabolites by sewage bacteria, *Water Air and Soil Pollution*, **134**, 353-368.
- Legler J., (2001), *Development and application of in vitro and in vivo reporter gene assays for the assessment of (xeno-) estrogenic compounds in the aquatic environment*, PhD Thesis, Wageningen Universiteit, On line at: <https://edepot.wur.nl/199007>.
- Li G.P., Yang Z.Y., He Z., Chen M., Yang X.L., (2013a), Optimization of solid-phase extraction for determining estrone in sewage by response surface methodology, *Environmental Science & Technology*, **3**, 026.
- Lloret L., Eibes G., Lú-Chau T.A., Moreira M.T., Feijoo G., Lema J.M., (2010), Laccase-catalyzed degradation of anti-inflammatories and estrogens, *Biochemical Engineering Journal*, **51**, 124-131.
- Lucas S.D., Jones D.L., (2006), Biodegradation of estrone and 17 β -estradiol in grassland soils amended with animal wastes, *Soil Biology and Biochemistry*, **38**, 2803-2815.
- Maeda M., Chung S.Y., Song E., Kudo T., (1995), Multiple genes encoding 2,3-dihydroxybiphenyl 1,2-dioxygenase in the gram-positive polychlorinated biphenyl-degrading bacterium *Rhodococcus erythropolis* TA421, isolated from a termite ecosystem, *Applied and Environmental Microbiology*, **61**, 549-555.
- Maeng S.K., Choi B.G., Lee K.T., Song K.G., (2013), Influences of solid retention time, nitrification and microbial activity on the attenuation of pharmaceuticals and estrogens in membrane bioreactors, *Water research*, **47**, 3151-3162.
- Mashtare M.L., Lee L.S., Nies L.F., Turco R.F., (2013), Transformation of 17 α -Estradiol, 17 β -Estradiol, and estrone in sediments under nitrate-and sulfate-reducing conditions, *Environmental Science & Technology*, **47**, 7178-7185.
- Matsui S., Takigami H., Matsuda T., Taniguchi N., Adachi J., Kawami H., Shimizu Y., (2000), Estrogen and estrogen mimics contamination in water and the role of sewage treatment, *Water Science & Technology*, **42**, 173-179.
- McCarty P.L., (1997), Breathing with chlorinated solvents, *Science*, **276**, 1521-1522.
- Moschet C., (2009), *Microbial degradation of steroid hormones in the environment and technical systems*, PhD Thesis, Institute of Technology, Institute of Biogeochemistry and Pollutant Dynamics (IBP-ETH), Swiss.
- Nakai S., Yamamura A., Tanaka S., Shi J., Nishikawa M., Nakashimada Y., Hosomi M., (2011), Pathway of 17 β -estradiol degradation by *Nitrosomonas europaea* and reduction in 17 β -estradiol-derived estrogenic activity, *Environmental Chemistry Letters*, **9**, 1-6.
- Nakamura A., Tamura I., Takanobu H., Yamamuro M., Iguchi T., Tatarazako N., (2014), Fish multigeneration test with preliminary short-term reproduction assay for estrone using Japanese medaka (*Oryzias latipes*), *Journal of Applied Toxicology*, **35**, 11-30.
- Nohynek L.J., Nurmiaho-Lassila E.L., Suhonen E.L., Busse H.J., Mohammadi M., Hantula J., Rainey F., Salkinoja-Salonen M.S., (1996), Description of chlorophenol-degrading *Pseudomonas* sp. strains KF1T, KF3, and NK1F1 as a new species of the genus *Sphingomonas*,

- Sphingomonassubarctica* sp. nov, *International Journal of Systematic Bacteriology*, **46**, 1042-1055.
- Onda K., Nakamura Y., Takatoh C., Miya A., Katsu Y., (2003), The behavior of estrogenic substances in the biological treatment process of sewage, *Water Science & Technology*, **47**, 109-116.
- Owen L., Keevil B., (2013), A rapid and sensitive LC-MS/MS assay for the routine analysis of estradiol and estrone, *Endocrine Abstracts*, **31**, P35, DOI: 10.1530/endoabs.31.P35.
- Pakert M., Filipov E., Kunst S., (2003), Discharge of estrogens from sewage treatment plants II: Behavior during the digestion process, estimation of estrogen exposure (in German); poster 7, POSEIDON Symposium, On line at: http://www.bafg.de/portale/poseidon/Abstract_Book_Braunschweig_final.pdf.
- Palme R., Fischer P., Schildorfer H., Ismail M.N., (1996), Excretion of infused ¹⁴C-steroid hormones via faeces and urine in domestic livestock, *Animal Reproduction Science*, **43**, 43-63.
- Pauwels B., Wille K., Noppe H., De Brabander H., Van de Wiele T., Verstraete W., Boon N., (2008), 17 α -ethinylestradiol cometabolism by bacteria degrading estrone, 17 β -estradiol and estriol, *Biodegradation*, **19**, 683-693.
- Peterson E.W., Davis R.K., Orndorff H.A., (2000), 17 β -estradiol as an indicator of animal waste contamination in Mantled Karst Aquifers, *Journal of Environmental Quality*, **29**, 826-834.
- Pillon A., Servant N., Vignon F., Balaguer P., Nicolas J.C., (2005), *In vivo* bioluminescence imaging to evaluate estrogenic activities of endocrine disrupters, *Analytical Biochemistry*, **340**, 295-302.
- Preda C., Ungureanu M.C., Vulpoi C., (2012), Endocrine disruptors in the environment and their impact on human health, *Environmental Engineering and Management Journal*, **11**, 1697-1706.
- Raman D.R., Layton A.C., Moody L.B., Easter J.P., Sayler G.S., Burns R.T., Mullen M.D., (2001), Degradation of estrogens in dairy waste solids: effect of acidification and temperature, *Transactions of the ASAE*, **44**, 1881-1888.
- Raman D.R., Williams E.L., Layton A.C., Burns R.T., Easter J.P., Daugherty A.S., Mullen M.D., Sayler G.S., (2004), Estrogen content of dairy and swine wastes, *Environmental Science & Technology*, **38**, 3567-3573.
- Rodgers-Gray T.P., Jobling S., Morris S., Kelly C., Kirby S., Janbakhsh A., Harries J.E., Waldock M.J., Sumpter J.P., Tyler C.R., (2000), Long-term temporal changes in the estrogenic composition of treated sewage effluent and its biological effects on fish, *Environmental Science & Technology*, **34**, 1521-1528.
- Roh H.K., (2009), *Deciphering active estrogen-degrading microorganisms in bioreactors*, PhD Thesis, Texas A&M University, Texas, USA.
- Roh H., Chu K.H., (2010), A 17 β -estradiol-utilizing bacterium, *Sphingomonas* strain KC8: Part I-Characterization and abundance in wastewater treatment plants, *Environmental Science & Technology*, **44**, 4943-4950.
- Rose K.P., Farenhorst A., (2014), Estrone and 17 β -estradiol mineralization in liquid swine manure and soil in the presence and absence of penicillin or tetracycline, *Journal of Environmental Science and Health, Part B*, **49**, 331-337.
- Routledge E.J., Sheahan D., Desbrow C., Brighty G.C., Waldock M., Sumpter J.P., (1998), Identification of estrogenic chemicals in STW effluent: 2. *In vivo* responses in trout and roach, *Environmental Science & Technology*, **32**, 1559-1565.
- Ruchiraset A., Chinwetkitvanich S., (2014), Estrogens removal by sludge from enhance biological phosphorus removal system, *Advanced Materials Research*, **931**, 246-250.
- Sang Y., Xiong G., Maser E., (2012), Identification of a new steroid degrading bacterial strain H5 from the Baltic Sea and isolation of two estradiol inducible genes, *The Journal of Steroid Biochemistry and Molecular Biology*, **129**, 22-30.
- Sarmah A.K., Northcott G.L., Leusch F.D.L., Tremblay L.A., (2006), A survey of endocrine disrupting chemicals (EDCs) in municipal sewage and animal waste effluents in the Waikato region of New Zealand, *Science of the Total Environment*, **355**, 135-144.
- Sarah C., Guillermina H.R., (2010), Occurrence, fate, and biodegradation of estrogens in sewage and manure, *Applied Microbiology and Biotechnology*, **86**, 1671-1692.
- Schlenker G., Birkelbach C., Glatzel P.S., (1999a), Analysis of the influence of temperature on the stability of sex steroids in cow feces, *Berliner und Muenchener Tieraerztliche Wochenschrift*, **112**, 459-464.
- Schlenker G., Muller W., Birkelbach C., Glatzel P.S., (1999b), Experimental investigations into influence of *Escherichia coli* and *Clostridium perfringens* on the steroid estrone, *Berliner und Muenchener Tieraerztliche Wochenschrift*, **112**, 14-17.
- Schlenker G., Muller W., Glatzel P., (1998), Analysis for the stability of sexual steroids in feces of cows over 12 weeks, *Berliner und Muenchener Tieraerztliche Wochenschrift*, **111**, 248-252.
- Shi J., Chen Q., Liu X., Zhan X., Li J., Li Z., (2013), Sludge/water partition and biochemical transformation of estrone and 17 β -estradiol in a pilot-scale step-feed anoxic/oxic wastewater treatment system, *Biochemical Engineering Journal*, **74**, 107-114.
- Shi J., Fujisawa S., Nakai S., Hosomi M., (2004a), Biodegradation of natural and synthetic estrogens by nitrifying activated sludge and ammonia-oxidizing bacterium *Nitrosomonas europaea*, *Water Research*, **38**, 2323-2330.
- Shi J.H., Suzuki Y., Nakai S., Hosomi M., (2004b), Microbial degradation of estrogens using activated sludge and night soil-compositing microorganisms, *Water Science & Technology*, **50**, 153-159.
- Shi J.H., Suzuki Y., Lee B.D., Nakai S., Hosomi M., (2002), Isolation and characterization of the ethynylestradiol-biodegrading microorganism, *Fusarium proliferatum* strain HNS-1, *Water Science & Technology*, **45**, 175-179.
- Shin S.K., Kim J.E., Kwon G.S., Kwon J.W., Oh E.T., So J.S., Koh S.C., (2003), Isolation and identification of a pentachloronitrobenzene(PCNB) degrading bacterium *Alcaligenes xylosoxidans* PCNB-2 from agricultural soil, *Journal of Microbiology*, **41**, 165-168.
- Shore L.S., Harel-Markowitz E., Gurevich M., Shemesh M., (1993), Factors affecting the concentration of testosterone in poultry litter, *Journal of Environmental Science and Health A*, **28**, 1737-1749.
- Souissi Y., Kinani S., Bouchonnet S., Bourcier S., Malosse C., Sablier M., Ait-Aïssa S., (2014), Photolysis of estrone generates estrogenic photoproducts with higher activity than the parent compound, *Environmental Science and Pollution Research*, **21**, 7818-7827.
- Stumpe B., Marschner B., (2007), Long-term sewage sludge application and wastewater irrigation on the mineralization and sorption of 17 β -estradiol and

- testosterone in soils, *Science of the Total Environment*, **374**, 282-291.
- Sumpter J.P., (1998), Reproductive effects from oestrogen activity in polluted water, *Archives of Toxicology*, **20**, 143-150.
- Suzuki Y., Maruyama T., (2006), Fate of natural estrogens in batch mixing experiments using municipal sewage and activated sludge, *Water Research*, **40**, 1061-1069.
- Szarka S., Nguyen V., Prokai L., Prokai-Tatrai K., (2013), Separation of dansylated 17 β -estradiol, 17 α -estradiol, and estrone on a single HPLC column for simultaneous quantitation by LC-MS/MS, *Analytical and Bioanalytical Chemistry*, **405**, 3399-3406.
- Takeuchi M., Hamana K., Hiraishi A., (2001), Proposal of the genus *Sphingomonas* sensu stricto and three new genera, *Sphingobium*, *Novosphingobium*, and *Sphingopyxis*, on the basis of phylogenetic and chemotaxonomic analyses, *International Journal of Systematic and Evolutionary Microbiology*, **51**, 1405-1417.
- Tan D.T., Arnold W.A., Novak P.J., (2013), Impact of organic carbon on the biodegradation of estrone in mixed culture systems, *Environmental Science & Technology*, **47**, 12359-12365.
- Teissier S., Torre M., (2002), Simultaneous assessment of nitrification and denitrification on freshwater epilithic biofilms by acetylene block method, *Water Research*, **36**, 3803-3811.
- Ternes T.A., (1998), Occurrence of drugs in German sewage treatment plants and rivers, *Water Research*, **32**, 3245-3260.
- Ternes T.A., Kreckel P., Mueller J., (1999a), Behaviour and occurrence of estrogens in municipal sewage treatment plants. II. Aerobic batch experiments with activated sludge, *Science of the Total Environment*, **225**, 91-99.
- Ternes T.A., Stumpf M., Mueller J., Haberer K., Wilken R.D., Servos M., (1999b), Behavior and occurrence of estrogens in municipal sewage treatment plants. I. Investigations in Germany, Canada and Brazil, *Science of the Total Environment*, **225**, 81-90.
- Tran N.H., Urase T., Ngo H.H., Hu J., Ong S.L., (2013), Insight into metabolic and cometabolic activities of autotrophic and heterotrophic microorganisms in the biodegradation of emerging trace organic contaminants, *Bioresource Technology*, **146**, 721-731.
- Turfitt G.E., (1947), Microbiological agencies in the degradation of steroids II. Steroid utilization by the microflora of soils, *Journal of Bacteriology*, **54**, 557-562.
- Vader J.S., van Ginkel C.G., Sperling F.M.G.M., de Jong J., de Boer W., de Graaf J.S., van der Most M., Stokman P.G.W., (2000), Degradation of ethinyl estradiol by nitrifying activated sludge, *Chemosphere*, **41**, 1239-1243.
- Villemur R., dos Santos S.C.C., Ouellette J., Juteau P., Lépine F., Déziel E., (2013), Biodegradation of endocrine disruptors in solid-liquid two-phase Partitioning Systems By Enrichment Cultures, *Applied and Environmental Microbiology*, **79**, 4701-4711.
- Weber S., Leuschner P., Kämpfer P., Dott W., Hollender J., (2005), Degradation of estradiol and ethinyl estradiol by activated sludge and by a defined mixed culture, *Applied Microbiology and Biotechnology*, **67**, 106-112.
- Wijekoon K.C., Hai F.I., Kang J., Price W.E., Guo W., Ngo H.H., Nghiem L.D., (2014), A novel membrane distillation-thermophilic bioreactor system: Biological stability and trace organic compound removal, *Bioresource Technology*, **159**, 334-341.
- Williams C.L., Stancel G.M., (1996), *Estrogens and Progestins*, In: *The Pharmacological Basis of Therapeutics*, Hardman J.G., Limbird L.E., Molinoff P.B., Ruddon R.W., Goodman-Gilman A. (Eds), The McGraw-Hill Companies, USA, 1411-1440.
- Writer J.H., Ryan J.N., Keefe S.H., Barber L.B., (2011), Fate of 4-nonylphenol and 17 β -estradiol in the Redwood River of Minnesota, *Environmental Science & Technology*, **46**, 860-868.
- Xu Y., Xu N., Llewellyn N. R., Tao H., (2014), Occurrence and removal of free and conjugated estrogens in wastewater and sludge in five sewage treatment plants, *Environmental Science: Processes & Impacts*, **16**, 262-270.
- Xuan R.C., Blassengale A.A., Wang Q.Q., (2008), Degradation of estrogenic hormones in a silt loam soil, *Journal of Agricultural and Food Chemistry*, **56**, 9152-9158.
- Yang S., Hai F.I., Nghiem L.D., Price W.E., Roddick F., Moreira M.T., Magram S.F., (2013), Understanding the factors controlling the removal of trace organic contaminants by white-rot fungi and their lignin modifying enzymes: a critical review, *Bioresource Technology*, **141**, 97-108.
- Yazdi M.T., Malekzadeh F., Zarrini G., Faramarzi M.A., Kamranpour N., Khaleghparast S., (2001), Production of cholesterol oxidase by a newly isolated *Rhodococcus* sp., *World Journal of Microbiology and Biotechnology*, **17**, 731-737.
- Yi T., Harper W.F., Holbrook R.D., Love N.G., (2006), Role of particle size and ammonium oxidation in removal of 17 α -ethinyl estradiol in bioreactors, *Journal of Environmental Engineering*, **132**, 1527-1529.
- Yi T., Harper W.F., (2007), The link between nitrification and biotransformation of 17 α -ethinyl lestradiol, *Environmental Science & Technology*, **41**, 4311-4316.
- Ying G.G., Kookana R.S., (2003), Degradation of five selected endocrine-disrupting chemicals in seawater and marine sediment, *Environmental Science & Technology*, **37**, 1256-1260.
- Ying G.G., Kookana R.S., (2005), Sorption and degradation of estrogen-like-endocrine disrupting chemicals in soil, *Environmental Toxicology and Chemistry*, **24**, 2640-2645.
- Ying G.G., Kookana R.S., Ru Y.J., (2002), Occurrence and fate of hormone steroids in the environment, *Environment International*, **28**, 545-551.
- Ying G.G., Kookana R.S., Dillon P., (2003), Sorption and degradation of selected five endocrine disrupting chemicals in aquifer material, *Water Research*, **37**, 3785-3791.
- Yoon J.H., Cho Y.G., Kang S.S., Kim S.B., Lee S.T., Park Y.H., (2000), *Rhodococcus koreensis* sp. nov., a 2,4-dinitrophenol-degrading bacterium, *International Journal of Systematic and Evolutionary Microbiology*, **50**, 1193-1201.
- Yoshimoto T., Nagai F., Fujimoto J., Watanabe K., Mizukoshi H., Makino T., Kimura K., Saino H., Sawada H., Omura H., (2004), Degradation of estrogens by *Rhodococcus zopfii* and *Rhodococcus equi* isolates from activated sludge in wastewater treatment plants, *Applied and Environmental Microbiology*, **70**, 5283-5289.
- Yu C.P., Roh H., Chu K.H., (2007), 17 β -estradiol-degrading bacteria isolated from activated sludge, *Environmental Science & Technology*, **41**, 486-492.
- Yu Z., Huang W., (2005), Competitive sorption between 17 α -ethinylestradiol and naphthalene/phenanthrene by

- sediments, *Environmental Science & Technology*, **39**, 4878-4885.
- Zeng Q., Li Y., Yang S., (2013), Sludge retention time as a suitable operational parameter to remove both estrogen and nutrients in an anaerobic–anoxic–aerobic activated sludge system, *Environmental Engineering Science*, **30**, 161-169.
- Zhang T., Xiong G., Maser E., (2011), Characterization of the steroid degrading bacterium S19-1 from the Baltic Sea at Kiel, Germany, *Chemico-Biological Interactions*, **191**, 83-88.
- Zhang X., Li X., Zhang Q., Peng Q., Zhang W., Gao F., (2014), New insight into the biological treatment by activated sludge: The role of adsorption process, *Bioresource Technology*, **153**, 160-164.
- Zhang Z., Gao P., Su H., Zhan P., Ren N., Feng Y., (2013), Anaerobic biodegradation characteristics of estrone, estradiol, and 17 α -ethinylestradiol in activated sludge batch tests, *Desalination and Water Treatment*, **53**, 985-993.
- Ziels R.M., Lust M.J., Gough H.L., Strand S.E., Stensel H.D., (2014), Influence of bioselector processes on 17 α -ethinylestradiol biodegradation in activated sludge wastewater treatment systems, *Environmental Science & Technology*, **48**, 6160-6167.
- Zou Y., Zhang Z., Shao X., Chen Y., Wu X., Yang L., Zhang D., (2013), Hollow-fiber-supported liquid-phase microextraction using an ionic liquid as the extractant for the preconcentration of bisphenol A, 17- β -estradiol, estrone and diethylstilbestrol from water samples with HPLC detection, *Water Science & Technology*, **69**, 1028-1035.
- Zuo Y., Zhang K., Zhou S., (2013), Determination of estrogenic steroids and microbial and photochemical degradation of 17 α -ethinylestradiol (EE2) in lake surface water, a case study, *Environmental Science: Processes & Impacts*, **15**, 1529-1535.



“Gheorghe Asachi” Technical University of Iasi, Romania



COST-EFFECTIVENESS OF OPTIMIZING CONCENTRATED FEED BLENDS TO DECREASE GREENHOUSE GAS EMISSIONS

Ricardo F.M. Teixeira^{1,2*}

¹University of Antwerp, Department of Biology, Research Group of Plant and Vegetation Ecology; Campus Drie Eiken, Universiteitsplein 1, B-2610 Wilrijk, Belgium

²MARETEC – Marine, Environment and Technology Centre, Instituto Superior Técnico, Universidade de Lisboa; Av. Rovisco Pais 1, 1049-001 Lisboa, Portugal

Abstract

Livestock production is under growing public and scientific scrutiny for its greenhouse gas (GHG) emissions. This article contains a preliminary assessment of the inclusion of upstream life-cycle GHG emissions in concentrated feeds design, using the most common nonlinear programming optimization algorithms to determine feed composition. First, GHG emissions are included as costs in a single criteria optimization problem. The unit price of GHG emissions was obtained using a genetic algorithm. Second, GHG emissions are included as a target function to minimize in a multi criteria optimization problem using goal attainment programming. Results obtained after both optimization methods were applied to two case studies, namely fattening pigs and rabbit feeds. Changing ingredients in concentrated feed blends has a marginal effect on GHG emissions due to mandatory nutritional constraints. If the optimization is unconstrained, the maximum possible decrease in GHG emissions is 27.5% for the pigs feed, accompanied by increasing costs and a decrease in feed nutritional quality. To maintain nutritional integrity, the maximum possible reduction in GHG emissions is 7.5%. Considering cost as an optimization variable in the problem, the maximum decreases are even lower. It is possible to decrease emissions by 71% for the rabbits feed, but the cost of the reduction is higher than the opportunity cost for farmers to reduce GHG emissions using other strategies. These results are qualitatively robust but critically depend on feed ingredients GHG emissions and cost data.

Key words: genetic algorithm, goal programming, greenhouse gases, linear optimization, livestock feed

Received: May, 2013; *Revised final:* July, 2014; *Accepted:* July, 2014; *Published in final edited form:* April 2018

1. Introduction

Life Cycle Assessment (LCA) studies show that food and beverages are one of the three types of products with the largest environmental impacts in the European Union (Tukker et al., 2006). Meat production is particularly relevant for this score (Weidema et al., 2008). The contribution of the livestock sector to worldwide greenhouse gas (GHG) emissions is estimated in the range of 18% (Steinfeld et al., 2006) to 50% (Goodland and Anhang, 2010), although the upper estimate has been disputed (Herrero et al., 2011). Concentrated feed production (including sourcing of ingredients) and transportation

are often the hotspots in meat production (Cederberg and Mattsson, 2000; Lewandowski et al., 1999; van der Werf et al., 2005). This means feeds formulations are the first place to look for optimization options.

Livestock feed formulation is usually treated as a programming optimization problem. One of the most widely used approaches is the least-cost feed formulation method using the simplex method to derive solutions of a linear programming model (Peng and Li, 2011). The model combines ingredients to obtain the optimum composition, which minimizes costs, subject to nutritional and ingredient availability constraints (Saxena et al., 2016). Several initiatives related to environmental product labeling are

* Author to whom all correspondence should be addressed: e-mail: ricardo.teixeira@tecnico.ulisboa.pt; Phone: +351 218419438

underway and will likely steer the market towards more environmentally-friendly meat products. In the future, producers may have to minimize environmental impacts as well as costs. The recent literature has thus been flourishing with authors trying to expand the typical feed optimization algorithms by including environmental criteria. Oishi et al. (2011) used the least-cost feed formulation method applied to the Japanese beef fattening system. They considered nitrogen (N) and phosphorus (P) as additional costs and introduced them in the least-cost objective function. Dubeau et al. (2011) approached the same problem in France and Québec by adding N and P as part of a multi-objective minimization problem (Žgajnar and Kavčič, 2009). The authors minimized N and P as objectives (objective functions) to quantify the trade-off between excretions and costs, providing a tool for decision-makers. They did not point out one specific optimum feed formula. If the objective is to find optima considering more than one function to minimize (or maximize: e.g. nutritional quality), problems regarding simultaneous attainment arise (Peric and Babic, 2009). If functions are minimized in parallel (equal weights for all objectives), the final result may be neither optimum for any of them separately nor Pareto efficient. In optimizations that are not Pareto-efficient any improvement according to one criterion comes at the cost of another criterion.

To overcome this problem, Castrodeza et al. (2005) use a fractional model together with an Interactive Multiple Goal Programming (IMGP) decision method. With IMGP, each objective is optimized individually, and then the decision-maker, faced with the results, makes successive choices on which criteria to improve first, thus generating a second feasible solution space, and repeating the procedure until one solution remains. This method does not require the decision maker to know beforehand which goal is preferred, but it is not systematic and does not necessarily provide efficient results.

As an alternative, goal programming introduces preferences in problem formulations (Caballero et al., 2009). Farmers may have specific preferences that bias results towards their end. For example, Babic and Peric (2011) provide explicit goals for total feed cost, nutritional quality (share of nutrients) and water content, as well as several scenarios of farmer preference between criteria. Instead of relying on decision-maker *ad hoc* decisions, results can reflect the best feed formulation that respects optimization criteria in sequential order.

Using this framework, this article proposes methods to test the cost-effectiveness of decreasing upstream GHG emissions (i.e. considering life-cycle emissions for each feed ingredient) by replacing ingredients in feed blends. So far, the introduction of environmental variables in feed formulation problems has been restricted to N and P emissions or excretions (Finneran et al., 2010; Pomar et al., 2007) and methane (CH₄) emissions from enteric fermentation and manure management (Moraes et al., 2012). Moraes et

al. (2012) tested the influence of a GHG tax in direct CH₄ emissions management, but the research question here is different: can life-cycle GHG emissions from feeds be reduced by changing feed ingredients while maintaining the same nutritional restrictions, and if so at what cost? By analyzing both emissions reduction and cost simultaneously, the feed cost increase per unit of GHG emissions reduction can be compared with international carbon market prices, thus determining the cost-effectiveness of the approach. The following section proposes two alternative methods to address this question, while the results section deals with the application of the methods to specific datasets.

2. Material and methods

2.1. Nonlinear programming method

The most generic formulation for the feed optimization problem is to minimize an objective function F (Eq. 1):

$$\min_x F(X) \quad (1)$$

where F is a function of vector $X = (x_1, x_2, \dots, x_n)$ where x_j , $j = 1, \dots, n$ denotes the proportion of ingredient j in the diet and n is the total number of ingredients available (Castrodeza et al., 2005). F is a vector of the t target functions to minimize or maximize (Eq. 2):

$$F(X) = (f_1(X), f_2(X), \dots, f_t(X))^T \quad (2)$$

Note that if there is only one criteria to optimize (e.g., cost), $F = f_1$. Essential nutritional requirements of animals (protein, energy, calcium, etc.) are not objective functions, but rather interval constraints on the minimum and maximum values x can take (Eq. 3):

$$\underline{b}_i \leq \sum_{j=1}^n a_{i,j} x_j \leq \overline{b}_i \quad (3)$$

where $i = 1, \dots, k$. k is the number of nutrients (or constraints) considered, $a_{i,j}$ the amount of nutrient i in ingredient j , minimum and maximum b_i are the lower and upper bounds, respectively, of nutrient i in the diet. There may also be lower or upper thresholds for the amount of some ingredients in the feed. Considering s_j is the maximum proportion of ingredient j in the diet, the case where there is a maximum amount is translated by Eq. (4):

$$x_j \leq s_j \quad (4)$$

Two methodological possibilities were tested to introduce GHG emissions as an optimization parameter: (a) following Oishi et al. (2011), consider GHG as an additional cost in a single criterion optimization problem, as described in section 2.2

below; (b) following Babic and Peric (2011), consider GHG an additional target function, and apply goal attainment programming, as explained in section 2.3.

2.2. GHG emissions as part of least-cost optimization

In the least-cost optimization, Eq. (2) becomes (Castrodeza et al., 2005) (Eq. 5):

$$F(X) = f_1(X) = \sum_{j=1}^n c_j x_j \quad (5)$$

where c_j is the unit cost of ingredient j . Considering GHG emissions as an additional cost (Oishi et al., 2011), Eq. (5) becomes (Eq. 6):

$$F(X) = \sum_{j=1}^n (p_j + \beta \cdot GHG_j) x_j \quad (6)$$

where p_j is the unit price (i.e. per unit of mass) of ingredient j , GHG_j is the unit CO₂e emissions of ingredient j , and β is the cost of each unit of CO₂e emitted. β is calculated as the increase in feed cost needed for a given decrease in total emissions.

Eq. (6) can only be minimized as a single criteria optimization problem if β is known. There are two possible ways to estimate β . First, it could be introduced as an exogenous variable, in which case it would be the average cost of GHG emissions obtained from some external source. This is the approach followed by Oishi et al. (2011). The social cost of carbon and the international carbon market price are examples of external sources that could potentially be used. Alternative, it is possible to find β using the same datasets that are also employed in the optimization step. Since the meaning of β is narrower as it applies only to the price of carbon emitter due to feed blends ingredients, in this work the second strategy was chosen, using a genetic algorithm (GA). GA finds a Pareto-efficient solution space (Sahman et al., 2009) where both variables - cost and GHG emissions - are minimized simultaneously (Eq. 7):

$$\begin{cases} f_1(X) = \sum_{j=1}^n p_j x_j \\ f_2(X) = \sum_{j=1}^n GHG_j x_j \end{cases} \quad (7)$$

Both equations are optimized considering nutritional constraints. The result of the GA application is not one optimum feed mix that minimizes both simultaneously, but rather an “efficiency frontier” depicted by a curve whose points are all Pareto-efficient combinations. Eq. (7) is thus not an optimization problem since it does not yield a unique solution. Its objective is only to find β and use the parameter in Eq. (6).

2.3. Multi criteria optimization with goal attainments

Alternatively to the process described in section 2.2, where a single target function is

optimized, multi criteria optimization can also be performed using multiple target functions as depicted by Eq. (2). Multiple goal attainment requires *a priori* ranking between objectives. The objective is to minimize the deviations from the target function’s goals. Former objective functions are thus modified and become additional restrictions in the problem (Babic and Peric, 2011) (Eq. 8):

$$f_t(X) - w_t \gamma_t = G_t \quad (8)$$

and each function t is evaluated with vector solution X , minus the deviation γ weighed with the decision makers’ preference parameter w has to be equal to the goal G . Note that γ can be positive or negative (a negative deviation is an overshoot).

2.4. Data for case study comparisons

The methods in sections 2.2 and 2.3 were primarily applied to a case study feed for fattening pigs, as described by Babic and Peric (2011). Originally three criteria were optimized – water content, nutritional quality and cost of each ingredient in a pig growth feed, including nutritional and ingredient availability restrictions. The entire dataset can be found in the original paper. Babic and Peric (2011) assign dual role to nutritional requirements: they are constraints as well as an optimization goal. First, minimum or maximum nutritional restrictions are included for raw protein, pulp, calcium, phosphorus, ash, methionine, lysine, tryptophan, threonine, isoleucine, histidine, valine, leucine, arginine and phenylalanine. These restrictions ensure that the necessary dose of each ingredient is included in every feed. The amount of each nutrient in the feed is included as a fraction of the total amount needed to ensure maximum growth. Additionally, the sum of all nutrient fractions is itself a maximization goal to ensure weight gain. This means that feeds that contain high digestibility ingredients are favored. The present article also assumes this dual role of nutrition for the multi criteria optimization problem. For least-cost optimization, nutrition is only included as a constraint. Also similarly to Babic and Peric (2011), in this article ingredients add up to 97% of the mass of the feed. The additional 3% mass respects to minor ingredients and additives that must be part of the feed and cannot be optimized.

Data on GHG emissions of the ingredients was obtained as an average of all records of a similar type in the Carbonostics (www.carbonostics.com) proprietary database, adapted from results presented in Teixeira (2014). Carbonostics is an LCA tool specialized on the agri-food sector. Note that GHG emissions are the only LCA environmental indicator used due to data availability and also to maintain a minimum possible level of complexity (less parameters to optimize). Plus, this dataset considers the emissions up until the end of production of the ingredients of the feed. Emissions from the digestion of the feed and manure are not included (Table 1).

Table 1. Data on life cycle GHG emissions from the ingredients considered

Ingredient	GHG ^a Emissions (kg CO ₂ e/kg)
Barley	0.54
Maize	0.27
Lucerne	0.24
Powdered milk	9.11
Fish meal	1.60
Soya	0.68
Soya hulls	0.52
Dried whey	0.08
Rapepellets	0.30
Wheat	0.47
Rye	0.42
Millet	0.47
Sunflower pellets	0.13

^aGHG – Greenhouse gases. Source: adapted from the database used in Teixeira (2014)

For goal attainment, Babic and Peric (2011) indicate as goals for cost 1.85 monetary units (MU), for the share of nutrients 77%, and for the share of water 8.3%. This paper introduces a further objective for GHG emissions of 0 kg CO₂e. While zero emissions are an impossible target, it is the simplest number that guarantees the maximum priority for the goal of emissions reduction. Any number minor or equal than the minimum feasible solution for emissions provides the same result. Also, Babic and Peric (2011) test four scenarios (A-D), to which three more (E-G) are added, according to Table 2. To have a higher priority means to have the highest weight (w_i in Eq. (8)).

The GA, linear optimization and goal attainment methods were applied using the software

MATLAB 7, using the functions “gamultiobj”, “fmincom” and “fgoalattain”, respectively.

After examining data from Babic and Peric (2011), the same method was applied to datasets from two other research articles. The first one, Castrodeza et al. (2005), also targets growing pigs, but has a wider range of ingredients and different nutritional constraints since one of the goals of the work is to limit nitrogen pollution as ensured by a balanced pig diet. In this case the nutritional criteria are crude fiber, methionine plus cysteine, tryptophan, threonine, calcium, total phosphorus, available phosphorus, dry matter, crude protein, lysine, and digestible energy. The second dataset, Altun and Sahman (2013), focused on feeds for rabbits. The nutritional criteria are similar to Castrodeza et al. (2005). Furthermore, while Babic and Petric (2011) use unknown monetary units, Castrodeza et al. (2005) use Euros and Altun and Sahman (2013) use Turkish Liras.

3. Results and discussion

3.1. Application of the genetic algorithm

Application of the GA provided the Pareto frontier defined by the solutions depicted in Fig 1. The frontier can be depicted, in the simplest case, by a linear relation ($R^2=86.9\%$). A better fit is obtained when the curve is depicted as a second-order polynomial ($R^2=94.2\%$). In either case, the figure shows that increasing costs from 2.34 to 2.36 MU results in a significant decrease of GHG emissions (0.55 to 0.49 kg CO₂e). To further decrease emissions results in heavily increasing costs. Parameter β , the marginal cost of abating GHG emissions in feeds, is calculated the two possible fits in Fig. 1.

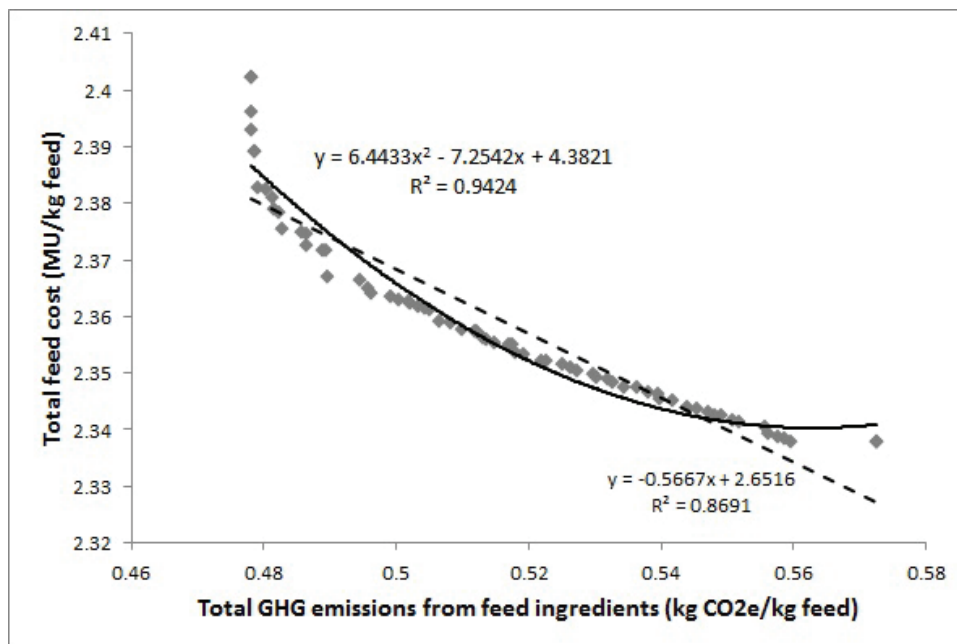


Fig. 1. Pareto frontier for the multi-objective optimization problem of minimizing feed cost and GHG emissions, using a genetic algorithm (MU – Monetary units)

Table 2. Objectives for the goal attainment problem

Scenario		A	B	C	D	E	F	G
Priority is to minimize:	1 st	Exceeding costs	Nutrient shortfall	Water excess	Exceeding costs & Exceeding raw protein	GHG emissions	GHG emissions	GHG emissions & Nutrient shortfall
	2 nd	Nutrient shortfall	Exceeding costs	Exceeding costs	Nutrient shortfall	Exceeding costs	-	-
	3 rd	Water excess	Water excess	Nutrient shortfall	Water excess	Nutrient shortfall	-	-
	4 th	-	-	-	-	Water excess	-	-

Using the linear expression (Eq. 9):

$$\beta_{linear} = -\frac{dC}{dCO_2e} = 0.5667 \quad (9)$$

The consequence of the linear factor is that the contribution of GHG emissions cost to the minimization function is always negative, i.e., to decrease emissions farmers must increase costs. Using the quadratic expression (Eq. 10):

$$\beta_{quad} = -\frac{dC}{dCO_2e} = -12.8866 \cdot CO_2e + 7.2542 \quad (10)$$

This approach makes the marginal effect dependent on the level of GHG emissions. It interprets the curve as making trade-offs otherwise hard to capture for very low or very high CO₂e emissions, which is where the curve in Fig. 1 is not linear. In Eq. (10), the role of GHG emissions in the minimization function is positive or negative depending on the ingredient. Ingredients with low cost and emissions have a positive contribution, i.e., increasing their share in the feed is a double positive contribution to cost minimization. This quadratic β estimation is thus qualitatively preferable to the linear approach, but quantitative differences in final results only arise when there is a large share of fringe (in terms of emissions) ingredients. The next section shows that this is never the case in the datasets used in this work.

3.2. GHG emissions as part of least-cost optimization

There are two options for replacing β in the Eq. (6) target function (Eqs. 11-12):

$$\min_x (p_i + 0.5667 \cdot CO_2e) x_i \quad (11)$$

$$\min_x (p_i + 12.8866 \cdot CO_2e^2 - 7.2542 \cdot CO_2e) x_i \quad (12)$$

Eqs. (11) and (12) are dimensionally correct optimization problems. There is no trade-off between cost and GHG emissions because the solution of the optimization problem is already the most efficient (the one that minimizes cost and GHG emissions), by definition of β . The application of the LP algorithm yields results shown in Table 3, which shows that the feed obtained for cost minimization without including GHG emissions in the objective function has the highest GHG and lowest cost. Results vary depending

on whether GHG costs change linearly or quadratically with ingredient cost. In the first case, the cost of reducing each kg CO₂e is 0.407 MU; the maximum reduction in GHG emissions that satisfies nutritional constraints is 3.1%. In the second case, the cost is 2.713 MU/kgCO₂e, and the maximum reduction in GHG emissions is 7.5%.

The high cost has to do with the strict restriction that all trade-offs during the application of the GA must be Pareto-optimal. The main differences in feed formulation is a shift towards the replacement of barley with soya hulls and rye, which are more efficient in terms of the balance nutrition/CO₂e emissions but also more expensive.

Table 3. Results of inserting GHG emission costs in the objective cost function to minimize

Ingredient/ Indicator	Only feed costs	Linear GHG, Eq. (11)	Quadratic GHG, Eq. (12)
Barley (%) ^a	0.15	0.06	0.09
Maize (%)	0.15	0.15	0.15
Lucerne (%)	0.03	0.04	0.03
Powdered milk (%)	0	0	0
Fish meal (%)	0	0	0
Soya (%)	0.12	0.12	0
Soya hulls (%)	0	0	0.11
Dried whey (%)	0	0	0
Rapepellets (%)	0.15	0.15	0.15
Wheat (%)	0.15	0.15	0.15
Rye (%)	0.07	0.15	0.15
Millet (%)	0	0	0
Sunflower pellets (%)	0.15	0.15	0.15
GHG^b emissions (kg CO₂e/kg feed)	0.377	0.365	0.349
Cost (MU/kg feed^c)	1.836	1.841	1.913
Nutrients (per kg feed)	71.898	71.983	70.562
Water (per kg feed)	9.721	9.713	9.871

^a The sum of all percentages is 97% because the additional 3% are minor ingredients and additives set aside from the optimization;

^b GHG – Greenhouse gases; ^c MU – Monetary Units

3.3. Multi criteria optimization with goal attainments

Results are shown in Table 4. Scenario A, which is a cost-first optimization, is comparable to the previous cost minimization approach. Results from Scenario A are similar to those in Table 3, indicating some mutual reinforcement of the two approaches.

The cost of reducing each unit of CO₂e in other scenarios is higher than in Scenario A: 7.7 MU for Scenario E, 10.9 MU for Scenario F and 47.5 MU for Scenario G. The relative decreases in GHG emissions are 19.1%, 27.5% and 7.5%, respectively. Feed quality always drops when GHG emissions decrease, and water consumption also seems to decrease with GHG emissions. Regarding feed formulations, in this case barley, powdered milk and fish meal are removed from the feed, and in Scenario F wheat is also reduced to a third. In Scenario G, in which GHG emissions reduction and maintaining feed quality are equally important, the decrease in GHG emissions is much lower than in Scenario F, but total nutrition is similar to Scenario B. This means that it is possible to reduce GHG emissions while maintaining quality standards, but at the expense of a 73.4% increase in costs. Results are shown in Table 4.

3.4. Application to other data sets and animal types

Data from Castrodeza et al. (2005) was analyzed using multi-objective goal attainment using two possible objectives: cost minimization and GHG emissions minimization. While weights may vary, there are only two feasible solutions, which correspond to cost-first and GHG reduction-first. It is possible to reduce GHG emissions by 18.5%, with a cost of 12.87 €/t feed. This means that the reduction of each ton of CO₂e costs 135.34 €.

Evaluating data from Altun and Sahman (2013) under multi-objective goal attainment also provides two feasible solutions only (cost-first and GHG reduction-first). This is when the highest improvement potential surfaces. Switching from Scenario A to B would decrease emissions by 73%, while increasing costs by 4.73 Krs/kg feed. This means that, under this method, the cost of reducing emissions is 5.09 Krs/kg

CO₂e, or, at the conversion rate of 1 Krs = 0.44 cents of €, 22.38 €/ t CO₂e.

3.5. Economic efficiency of replacing feed ingredients

Cost minimization results, in the case when GHG emissions are introduced as extra costs, produced a strict constraint on feed blend that required solutions to be Pareto-efficient. As a consequence, smaller reductions in GHG emissions are obtainable. A higher potential for decrease was obtained only when using multi objective optimization. Since this procedure does not discard Pareto-dominated solutions, it is possible to decrease GHG emissions more than with the GA cost minimization method, but also at much higher costs. The two methods are indeed convergent in comparable situations, i.e. when costs are the main variable to minimize. Multiple goal attainment should be used preferably when there is flexibility for more drastic (but ultimately constrained) changes in production. Results cast doubt over the cost-efficiency of switching ingredients in a feed to decrease its life-cycle emissions. Let us consider that the maximum opportunity cost for farmers is the reference cost for GHG emissions in the international carbon market (20 €/t CO₂e). It is possible that some farmers find even lower costs with other GHG minimization strategies (carbon sequestration in soils, change of tillage method etc.). For the rabbits feed, the result is similar to the reference cost (22.38 €/ t CO₂e), but for pigs feed it is much higher (135.34 €). Considering that the cost found for rabbits feed corresponds to a decrease in 71% in emissions, which is the maximum possible reduction considering the constraints, it is highly doubtful that a blend that uses different ingredients can be even more efficient, and thus more cost-effective in reducing emissions.

Table 4. Results of the application of the goal attainment algorithm to data from Babic and Petric (2011)

<i>Ingredient/Indicator</i>	<i>Scenario</i>						
	<i>A</i>	<i>B</i>	<i>C</i>	<i>D</i>	<i>E</i>	<i>F</i>	<i>G</i>
Barley (%) ^a	0.13	0.04	0.07	0.15	0	0	0
Maize (%)	0.15	0.15	0	0.15	0.15	0.15	0.15
Lucerne (%)	0	0	0.64	0	0	0.06	0
Powdered milk (%)	0	0.07	0.08	0.10	0	0	0
Fish meal (%)	0	0	0	0.02	0	0	0
Soya (%)	0.13	0.15	0.15	0	0.10	0	0.15
Soya hulls (%)	0	0.15	0	0.02	0.02	0.11	0.15
Dried whey (%)	0	0	0.15	0	0.15	0.15	0.15
Rapepellets (%)	0.15	0	0.15	0	0.15	0.15	0
Wheat (%)	0.15	0.15	0	0.15	0.15	0.05	0.15
Rye (%)	0.11	0.15	0.15	0.08	0.10	0.15	0.07
Millet (%)	0	0	0	0.15	0	0	0
Sunflower pellets (%)	0.15	0.11	0.15	0.15	0.15	0.15	0.15
GHG^b emissions (kg CO₂e/kg feed)	0.381	1.004	1.194	1.261	0.308	0.276	0.353
Cost (MU/kg feed^c)	1.850	2.409	3.299	2.580	2.410	2.996	3.208
Nutrients (per kg feed)	73.291	77.000	71.151	71.849	73.916	69.808	76.647
Water (per kg feed)	9.834	10.255	8.300	9.955	9.111	8.906	9.498

^a The sum of all percentages is 97% because the additional 3% are minor ingredients and additives set aside from the optimization; ^b GHG – Greenhouse gases; ^c MU – Monetary Units

Changes in pigs and rabbits feed blends can be considered a mildly cost-effective policy because it stands mid-range in estimates of cost-effectiveness of policies for GHG emissions mitigation. For example, in France for the year 2030, the cost-effectiveness of measures in the agricultural sector for GHG mitigation ranges from approximately negative 440€ to positive 460€ for each ton of CO₂e averted (the negative estimate meaning a cost and the positive revenue) (Pellerin et al., 2013). In the UK, there are measures for GHG mitigation that cost as much as 1750 British pounds per ton of CO₂e, and others that have a positive result of 300 pounds (Moran et al., 2011). In Ireland, the range is between minus 600 and 300€/ t CO₂e (Schulte et al., 2012). One of the measures indicated for France whose cost is similar to those obtained above for the optimization of these particular feed blends is to reduce the amount of protein in the diet of livestock to limit the quantity of nitrogen excreted in manure and the associated N₂O emissions (Pellerin et al., 2013). The similarity of the cost-effectiveness of the measure and the calculations in this work is an important source of validation for these results. Measures that are based on efficiency improvements, such as feed blend optimization, are typically more expensive than others based on land use change and technological innovation (Schulte et al., 2012).

In the future, the inclusion of GHG emissions can be tested in other feed optimization algorithms, like for example different variants of the Particle Swarm Optimization (PSO) method. Altun and Sahman (2013) applied PSO to cost minimization of rabbit feeds, and found that PSO is more efficient at computing stable optimum values than GA. However, the present article found remarkably similar results for rabbit feeds using multi-objective goal optimization: 25.34 Krs/kg feed for cost minimization and 30.08 krs/kg for GHG emissions minimization (against 26.73 and 30.17 Krs/kg feed for ingredients that minimize cost and ingredients that do not, obtained using PSO in the original Altun and Sahman (2013) article).

Introducing other objective functions (such as GHG emissions) to minimize in PSO requires multi-objective PSO (MOPSO) (Coello et al., 2004). MOPSO has been applied for the first time in fish feed design by Zhang and Wang (2010). The authors identify advantages in this method but ran into practical problems regarding convergence of solutions if running time is longer or if cost and nutritional goals are in conflict, despite having disregarded complex nutrient interactions. The optimum formulas found with MOPSO rely heavily on by-products, which have low GHG emissions if impacts are allocated economically, but also include fish meal which has high emissions (Zhang and Wang, 2010). The inclusion of a GHG reduction goal would thus provide more conflicting results, at least until preferences are included in the MOPSO objective functions (Mostaghim, 2010). All in all, MOPSO is more robust than GA but the results can be very similar, since both

consider only Pareto efficient solutions. This means that MOPSO models will likely not find other optimum solutions that minimize GHG emissions beyond the limits found in this work.

3.6. Limitations and future work

The present work is limited in scope to the analysis of directly replacing feedstocks in particular concentrated feed blends. The next step is to compare the potential for GHG reductions by replacing part of the feed with grazing. Another option is to test more ingredients and blends, since other ingredients may produce more drastic results. In fact, some minor ingredients (but nutritionally crucial) were ignored due to their residual contribution to the overall weight of the feed (and thus also to its life-cycle emissions). It is also relevant in the future to connect this work and the work by Moraes et al. (2012), because changing feed formulations also has an impact in its digestion by animals and ensuing enteric emissions and emissions from manure. Ideally, direct and life cycle emissions should be considered simultaneously. Digestion of feeds was not included in this analysis, only life-cycle emissions from feed ingredient production.

To minimize uncertainty from using secondary GHG emissions databases, it is preferable to perform a full LCA of the feed ingredients rather than rely on average GHG emissions as those presented in Table 1 when these methods are applied to optimize actual feeds. Despite the methodological consistency and relatively low uncertainty of these averages (Teixeira, 2014), there are different methodological choices that could provide different results (e.g. using consequential rather than attributional LCA). Despite the fact that this article does not include a quantitative analysis of uncertainty it is clear that results are crucially dependent on GHG emissions data, as well as the highly volatile feed ingredients prices.

Also regarding uncertainty, the convergence shown in the previous section between results obtained using both approaches in this article and other studies provides some degree of confidence in the robustness of the conclusions. For example, the GA used in the least-cost approach could have been replaced by other estimates for the price of carbon. This methodological choice is a source of uncertainty. Multi criteria optimization, however, does not require an explicit cost of GHG emissions in monetary units and still arrives at similar results in equivalent scenarios. In conclusion, it is plausible to assume high quantitative uncertainty in the results presented here and in similar studies but qualitatively the conclusions are robust.

Further datasets should also be explored. In this work pigs and rabbits feeds displayed different potential GHG emissions reduction estimates; this does not, however, translate into a general higher GHG reduction potential in rabbit production rather than pig. Results presented here are explained simply

by differences in ingredients used in these particular datasets. Since some ingredients with high or low GHG emissions are more common in feeds for rabbits or pigs, it may be the case that the potential for amelioration does depend on animal type – but this conclusion can only be drawn after more comprehensive datasets are explored.

Finally, since being able to pinpoint where in the life cycle of the production of the feed is more efficient to reduce emissions is of the utmost importance, the cost-effectiveness of improving feedstock production should be determined and compared with the results of this work. If it proves to be less costly to improve each crop's production than to change feed formulations, then that should be the target of farmers efforts.

4. Conclusions

Changing concentrated feed blends has a marginal effect on CO₂e emissions due to tight nutritional and cost constraints. For the pigs feed studied, the maximum possible decrease in GHG emissions is 27.5%; ensuring nutritional integrity, the maximum possible reduction in GHG emissions is 7.5%. In rabbits feeds emissions could be decreased by 71%, but at a cost that would exceed the opportunity cost for farmers to reduce emissions elsewhere.

Changing feeds to mitigate GHG emissions is at best mildly cost-effective, but it cannot be discarded since any improvements will affect 825 million tons of feeds produced each year (Feed International, 2014).

Acknowledgements

This work was partially supported by the European Commission's 7th Framework Programme through Marie Curie Intra-European Fellowship for Career Development number 331896 for Project "Bio-LCA: Introducing biodiversity in Life Cycle Assessment (LCA)", and by grant SFRH/BPD/111730/2015 from Fundação para a Ciência e Tecnologia. The author thanks Sara Pax for kindly granting access to the Carbonistics database and two anonymous referees who provided important comments on earlier versions of this article.

References

Altun A.A., Sahman M.A., (2013), Cost optimization of mixed feeds with the particle swarm optimization method, *Neural Computing and Applications*, **22**, 383-390.

Babic Z., Peric T., (2011), Optimization of livestock feed blend by use of goal programming, *International Journal of Production Economics*, **130**, 218-223.

Caballero R., Gómez T., Ruiz F., (2009), Goal programming: Realistic targets for the near future, *Journal of Multi-Criteria Decision Analysis*, **16**, 79-110.

Castrodeza C., Lara P., Peña T., (2005), Multicriteria fractional model for feed formulation: economic, nutritional and environmental criteria, *Agricultural Systems*, **86**, 76-96.

Cederberg C., Mattson B., (2000), Life cycle assessment of milk production – a comparison of conventional and organic farming, *Journal of Cleaner Production*, **8**, 49-60.

Coello C.A., Pulido G.T., Lechuga M.S., (2004), Handling multiple objectives with particle swarm optimization, *Evolutionary Computation*, **8**, 256-279.

Dubeau F., Julien P.O., Pomar C., (2011), Formulating diets for growing pigs: economic and environmental considerations, *Annals of Operations Research*, **190**, 239-269.

Feed International, (2014), *World Feed Panorama April/May 2014*, WATT, Rockford, Illinois, On line at: <http://www.fi-digital.com/201404/>.

Finneran E., Crosson P., O'Kiely P., Shalloo L., Forristal D., Wallace M., (2010), Simulation modeling of the cost of producing and utilizing feeds for ruminants on Irish farms, *Journal of Farm Management*, **14**, 95-116.

Goodland R., Anhang J., (2010), *Livestock and Climate Change - What if the key actors in climate change are cows, pigs, and chickens?* WorldWatch November/December Report, WorldWatch Institute, Washington DC, On line at: <https://www.worldwatch.org/files/pdf/Livestock%20and%20Climate%20Change.pdf>.

Herrero M., Gerber P., Vellinga T., Garnett T., Leip A., Opio C., Westhoek H.J., Thornton P.K., Olesen J., Hutchings N., Montgomery H., Soussana J.-F., Steinfeld H., McAllister T.A., (2011), Livestock and greenhouse gas emissions: The importance of getting the numbers right, *Animal Feed Science and Technology*, **166-167**, 779-782.

Lewandowski I., Härdtlein M., Kaltschmitt M., (1999), Sustainable crop production: Definition and methodological approach for assessing and implementing sustainability, *Crop Science*, **39**, 84-193.

Moraes L.E., Wilen J.E., Robinson P.H., Fadel J.G., (2012), A linear programming model to optimize diets in environmental policy scenarios, *Journal of Dairy Science*, **95**, 1267-1282.

Moran D., MacLeod M., Wall E., Eory V., McVittie A., Barnes A., Rees R.M., Topp C.F.E., Pajot G., Matthews R., Smith P., Moxey A., (2011), Developing carbon budgets for UK agriculture, land-use, land-use change and forestry out to 2022, *Climatic Change*, **105**, 529-553.

Mostaghim S., Trautmann H., Mersmann O., (2010), *Preference-based Multi-Objective Particle Swarm Optimization using Desirabilities*, In: *Parallel Problem Solving from Nature, PPSN XI*, Schaefer R., Cotta C., Kolodziej J., Rudolph G. (Eds.), Proc. 11th International Conference, Krakov, Part II, 102-110.

Oishi K., Kumagai H., Hirooka H., (2011), Application of the modified feed formulation to optimize economic and environmental criteria in beef cattle fattening systems with food by-products, *Animal Feed Science and Technology*, **165**, 38-50.

Pellerin S., Bamiere L., Angers D., Beline F., Benoit M., Butault J.P., Chenu C., Colnenne-David C., De Cara S., Delame N., Dureau M., Dupraz P., Faverdin P., Garcia-Launay F., Hassouna M., Henault C., Jeuffroy M.H., Klumpp K., Metay A., Moran D., Recous S., Samson E., Savini I., (2013), *How can French agriculture contribute to reducing greenhouse gas emissions? Abatement potential and cost of ten technical measures - Summary of the study report*, INRA, Paris, On line at: <http://www.ademe.fr/en/how-can-french-agriculture-contribute-to-reducing-greenhouse-gas-emissions>.

- Peng Y., Li Q., (2011), *The Decision-Making for Feed Formula in Animal Husbandry Breeding Based on the Revised Simplex Method*, Proc. Artificial Intelligence, Management Science and Electronic Commerce (AIMSEC), Deng Leng.
- Peric T., Babic Z., (2009), *Optimization of Industrial Production of Feed Blends as a Multiple Criteria Programming Problem*, In: *Recent Advances in Technologies*, Strangio M.A. (Ed.), Intech, 147-168.
- Pomar C., Dubeau F., Létourneau-Montminy M.P., Boucher C., Julien P.O., (2007), Reducing phosphorus concentration in pig diets by adding an environmental objective to the traditional feed formulation algorithm, *Livestock Science*, **111**, 16-27.
- Sahman M.A., Cunkas M., Inal F., Inal S., Coskun B., Taskiran U., (2009), Cost optimization of feed mixes by genetic algorithms, *Advances in Engineering Software*, **40**, 965-974.
- Saxena P., Kumar V., Kumar J., (2016), *Optimization for Animal Diet Formulation: Programming Technique*, Proc. of 2016 3rd International Conference on Computing for Sustainable Global Development (INDIACom).
- Schulte R.P., Crosson P., Donnellan T., Farrelly N., Finnan J., Lalor S.T., Lanigan G., O'Brien D., Shalloo L., Thorne F., (2012), *A Marginal Abatement Cost Curve for Irish Agriculture*, Schulte R.P., Donnellan T. (Eds.), Teagasc, Oak Park, Carlow.
- Steinfeld H., Gerber P., Wassenaar T., Castel V., Rosales M., de Haan C., (2006), *Livestock's Long Shadow – Environmental Issues and Options*, Food and Agriculture Organization of the United Nations, Rome.
- Teixeira R.F.M., (2014), Critical appraisal of Life Cycle Impact Assessment databases for agri-food materials, *Journal of Industrial Ecology*, **19**, 38-50.
- Tukker A., Huppes G., Guinée J., Heijungs R., de Koning A., van Oers L., Suh S., Geerken T., Van Holderbeke M., Jansen B., Nielsen P., (2006), *Environmental Impact of Products (EIPRO) – Analysis of the Life-Cycle Environmental Impacts Related to the Final Consumption of the EU-25*, Institute for Prospective Technological Studies (IPTS) and the European Science and Technology Observatory (ESTO), Brussels, On line at: http://ec.europa.eu/environment/ipp/pdf/eipro_report.pdf.
- van der Werf H.M.G., Petit J., Sanders J., (2005), The environmental impacts of the production of concentrated feed: the case of pig feed in Bretagne, *Agricultural Systems*, **83**, 153-157.
- Weidema B.P., Wesnæs M., Hermansen J., Kristensen T., Halberg N., (2008), *Environmental Improvement Potentials of Meat and Dairy Products*, Eder P., Delgado L. (Eds.), Institute for Prospective Technological Studies, JRC Scientific and Technological Reports, On line at: <http://ftp.jrc.es/EURdoc/JRC46650.pdf>.
- Žgajnar J., Kavčič S., (2009), Multi-goal pig ration formulation: mathematical optimization approach, *Agronomy Research*, **7**, 775-782.
- Zhang J., Wang G., (2010), *Feed Formula Optimization Method Based on Multi-Objective Particle Swarm Optimization Algorithm*, Proc. Intelligent Systems and Applications (ISA), Wuhan, DOI: 10.1109/IWISA.2010.5473663.

Web sites:

www.carbonostics.com



“Gheorghe Asachi” Technical University of Iasi, Romania



AN ENHANCED ENVIRONMENTAL MULTIMEDIA MODELLING SYSTEM (FEMMS): PART II – USER INTERFACE AND FIELD VALIDATION

Zhi Chen^{1*}, Rong-Rong Zhang¹, Zong-Ping Wang²

¹Department of Building Civil and Environmental Engineering, Concordia University, 1455 De Maisonneuve Blvd. W., Montreal, Quebec, Canada H3G 1M8

²School of Environmental Science and Engineering, Huazhong University of Science and Technology (HUST), 1037 Luoyu Road, Wuhan, China 430074

Abstract

Environmental quantitative risk assessment requires the development of multimedia modeling tools to address dynamic site conditions at field scale. This work is the second part in a two-part series. A new fuzzy-set enhanced environmental multimedia modeling system (FEMMS) has been presented in Part I. Environmental multimedia modeling often involves a sizeable amount of parameters and data. The challenges have been the difficulties to quantify the uncertainties and to manage the data and main modules. Besides the efforts of developing a new EMMS for useful functionality and engineering applicability, a user-friendly graphical user interface (GUI) has been developed in this research for the FEMMS to provide support for the processing of model input and output as well as to facilitate technology transfer. To assess the developed FEMMS and its user interface system with real case application, a larger scale application with field data is conducted to examine the performance of FEMMS in this study. The field-scale validation presented in this paper indicates that the developed FEMMS is able to (1) predict the time and space varying chemical concentrations in a multimedia environment involving air, soil, and groundwater; (2) characterize the potential risk to human health presented by contaminants released from a contaminated site; and (3) quantify the uncertainties associated with modelling systems and subsequently providing robustness and flexibility for the remediation-related decision making. It also shows that, with the aid of fuzzy-set approach and the developed GUI, FEMMS is a reliable decision making tool to address complex environmental multimedia pollution problems and to provide technical support to strategy makers in managing the contaminated environmental sites.

Key words: fuzzy-set, landfill, multimedia modeling, risk assessment, user interface, validation

Received: March, 2013; *Revised final:* July, 2014; *Accepted:* July, 2014; *Published in final edited form:* April 2018

1. Introduction

Environmental quantitative risk assessment (EQRA) substantially depends on the information on chemical distribution in multiple environmental media and the chemical fluxes across their boundaries (Cohen and Cooter, 2002). One of the fundamental challenges of environmental risk assessment is to understand and characterize levels of chemical pollutants in air, water, soil, and vegetation, and to

estimate chemical mass flows between these different media, and between geographical regions (Chen et al., 2017; MacLeod et al., 2010). Multimedia models provide a solution for this challenge by quantifying cumulative, multipathway exposure to pollutants that originate from contaminated air, water, and soil (McKone and MacLeod, 2003).

Over the past few decades, multimedia models have been developed at different scales with different levels of complexity (Babendreier and Castleton,

* Author to whom all correspondence should be addressed: e-mail: zhi.chen@concordia.ca; Phone: +1 514 848 2424 ext.8775; Fax: +1514 697 4813

2005; Cohen and Cooter, 2002; Hsieh and Ouimette, 1994; Lin et al., 2009; MacLeod et al., 2010; Srivastava and Singh, 2005). Such multimedia models have been applied to environmental assessment, screening of environmental problems, and creating remedial strategy for a contaminated site (Droppo et al., 1993; Hsieh and Ouimette, 1994; León et al., 2007; Mustajoki et al., 2004; Saini et al., 2009; USEPA, 1996; Voigt et al., 2010).

The linked spatial single-media model (LSSMM) is an alternative to multimedia models (Cohen and Cooter, 2002; Hsieh and Ouimette, 1994). LSSMM depicts the environment as a system of uniform media and analyses the chemical behavior in multimedia system and the inter-media transfers under the dynamic conditions (Chen et al., 2014). It can therefore provide fine spatial and temporal resolutions to evaluate risk levels of exposure to hazardous contaminants. A fuzzy-set enhanced environmental multimedia modeling system (FEMMS) has been developed to extend the previously conceptualized LSSMM in Chen et al. (2014). It includes four modules: a pollution source module, an unsaturated zone module, a saturated zone module, and an air quality dispersion module. The pollution source module is to examine the contaminant's behavior within the polluted zone (e.g., landfill) based on the advective, diffusive and degradation processes in one dimension. This chamber-type source module, through intermedia mass fluxes, links the air module from the above and to the unsaturated zone module as well as the saturated zone module below. The modules for unsaturated zone and saturated zone are introduced based on pollutant's three-dimensional (3-D) description of fate and transport in porous media. The air quality dispersion module takes volatile components emission flux and input to a modified Gaussian equation to predict the spatial and temporal profiles of chemical concentration at a receptor of interest. Dynamic intermedia mass transfers are quantified to technically link the connected multimedia environmental system for a complex contamination site. Additionally, the developed FEMMS is embedded with a fuzzy-set approach to quantify the inherent uncertainties of modeling method and the contamination site. Overall, the developed FEMMS enables quantitative analyses to obtain the temporal and spatial contaminant distributions in each environmental medium as well as the flux rates across the environmental phase boundaries (Chen et al., 2014).

Few researches have been reported on the field application of the environmental multimedia models with uncertainties being quantified (Chau, 2007). One of the major challenges is that EMMs often involves a sizeable amount of parameters and data, which are further associated with a number of uncertainties (Chen et al., 2010; MacLeod et al., 2010). For example, environmental issues of a sanitary landfill include leachate waste from the bottom of the landfill going into the surround soil and groundwater media, and the landfill gases releasing into the atmosphere.

Investigation of these issues involve the installation of monitoring well, collection of site geo-hydrological data, and use of soil groundwater as well as air quality models to examine environmental impacts (Zhao and Cheng, 2006). Compared to single-medium environmental quality model, it appears that effective application of the developed FEMMS will lead to cost-effective management alternatives. Geng et al. (2001) showed that a user-friendly graphical user interface (GUI) could help to add intelligent data processing, model execution and results reporting functions, and facilitate technology transfer.

The objectives of the second part of this two-part series are: first to focus on object-oriented programming efforts needed to efficiently aggregate the developed FEMMS and its main functional modules through the development of an graphical user interface (GUI); and second to apply the developed GUI system to a field scale case study to further examine the performance and applicability of the developed FEMMS.

2. Development of a User-Friendly Engineer Interface (GUI)

The developed modeling approach FEMMS contains four modules to address one contamination site releasing pollutants to the surrounding soil, groundwater, and atmosphere media. Three out of the four modules, i.e., a three-dimensional (3D) unsaturated zone advection-dispersion module, a 3D saturated zone advection-dispersion module, and a simplified 1D Gaussian plume module, are linked to the fourth module (i.e., the dynamic module addressing contaminants releasing from the landfill waste chamber) through contaminants mass fluxes from the landfill chamber upward to the atmosphere, and downward to soil and groundwater (Chen et al., 2014). The governing system emphasizes the transition of initial and boundary conditions for the four modules, which will be integrated by a user interface system.

The field-scale multimedia impacts resulting from a dynamic contaminants release involves a number of atmospheric and hydrogeological site and pollutants fate and transport model parameters, which are all associated with different layers of uncertainties. In addition to the best available deterministic information or data, the developed FEMMS includes the option of using a fuzzy-set approach to quantify field scale site and model uncertainties. Management of the data structure and input output dataset is the essential component of the GUI system.

For easy implementation of the modeling approach, a GUI has been designed using Matlab program code. The user interacts with the GUI by communicating input data into FEMMS and executing the four functional modules to obtain the expected results (Zhang, 2006). Fig. 1 presents an overview of the GUI system design for FEMMS.

The concentrations in the groundwater and the ambient air in Fig. 2 are obtained by running the

FEMMS based on the supplied input data. Alternatively, the user can enter the required input parameters through the main user interface as shown in Fig. 2 for a specific case study and the corresponding results are automatically presented in the “output window” of the GUI. The results can be also saved to ASCII format or analyzed through the chart or visualization function built in Matlab. The graphical representation of results is displayed in a series of figures after pressing the “plot now” button with an example shown in Fig. 2.

The simulation results are presented in three different ways (Zhang, 2006): [1] pollutant concentrations in the groundwater and the ambient receptors presented in the GUI “output window”, i.e., the lower two sections of the main interface in Fig. 2; [2] the concentration distribution, the inter-media flux for consecutive years in text files (i.e., landfill file, unsaturated file, groundwater file, and ambient air quality file); and [3] a display of results in [1] and [2] in the form of a Matlab figure in the order of the evaluated year after pushing the “plot now” button on the GUI as shown in Fig. 2. The data managed by the developed GUI can be drawn up into six groups: chemical property; landfill module data; unsaturated

zone data; saturated zone data; and other inputs. These data are related to the site layout, the environmental conditions, the meteorological conditions, and the chemical properties. The data can be input through the interface as shown in Fig. 2 to save to an input data file and or to run the model, a prepared Access or Excel data file can be also read and input into the FEMMS. Sample data for the undermentioned case study is included for illustrating the key model parameters and data structure in Table 1.

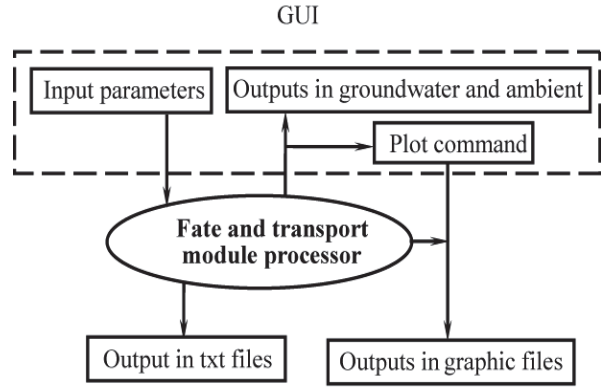


Fig. 1. The system schematic design (taken from Zhang, 2006)

Table 1. Physical properties and environmental conditions in the landfill site

Modules	Parameters	Symbols	Inputs	Modules	Parameters	Symbols	Inputs
Landfill module	length orthogonal to groundwater flow	A_y (m)	500	Landfill module	length parallel to groundwater flow	A_x (m)	800
	volumetric air content of the soil	a	0.2		volumetric water content at field capacity	θ	0.3
	organic carbon fraction	f_{oc}	0.0105		bulk density	ρ_b (kg/m ³)	600
	thickness of landfill cover	d (m)	1		landfill depth	L (m)	14
	gaseous velocity	v_G (m/d)	2.6 E-3		leachate velocity	v_L (m/d)	3.23 E-3
Un-saturated zone module	coefficient of longitudinal dispersion	D_L (m ² /d)	0.24		Saturated zone module	Darcy velocity	V_d (m/d)
	coefficient of transverse dispersion	D_T (m ² /d)	0.024	bulk density		ρ_{sat}	1350
	average velocity of fluid	v (m/d)	3.23 E-3	porosity		ϕ_s	0.3
	porosity	ϕ_{un}	0.365	organic carbon fraction		f_{ocsat}	0.0105
	bulk density of unsaturated zone	ρ_{unsat} (kg/m ³)	1350	half-life		τ_{sat} (d)	-
	half-life in unsaturated zone	τ_{unsat} (d)	-	dispersion coefficient in x direction		D_x (m ² /d)	1.728
	water table depth	z_{wt} (m)	10	dispersion coefficient in y direction		D_y (m ² /d)	.576
	organic carbon fraction	f_{ocun}	0.0105	dispersion coefficient in z direction		D_z (m ² /d)	0.968
Air module	annual wind speed frequency	$f(\varphi)$	0.13				
	wind speed	w (m/s)	4.3				

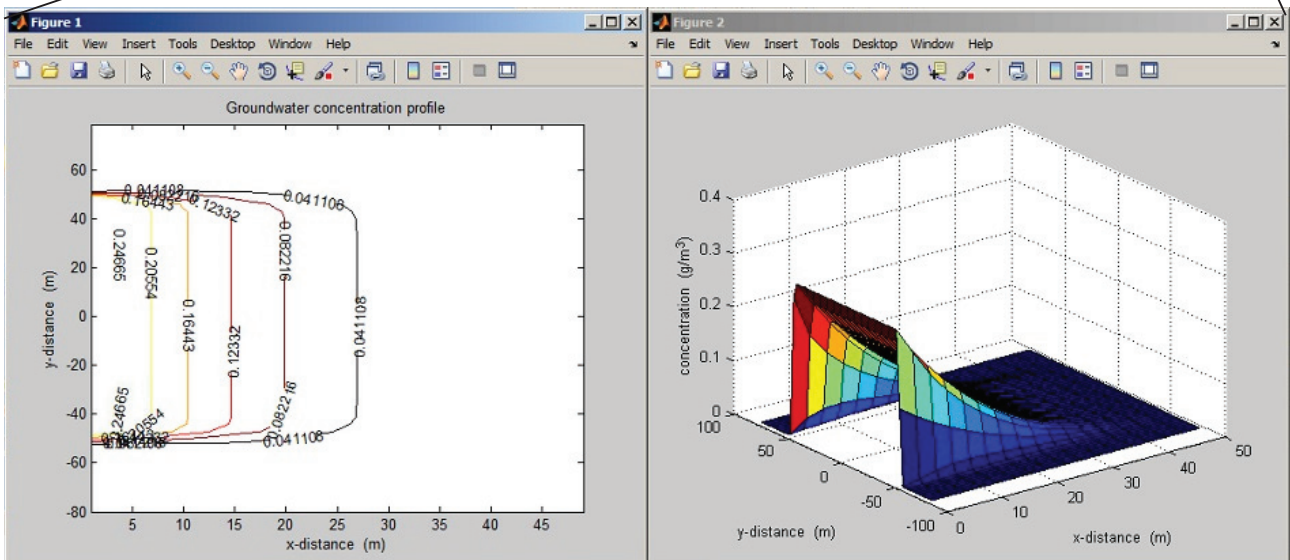
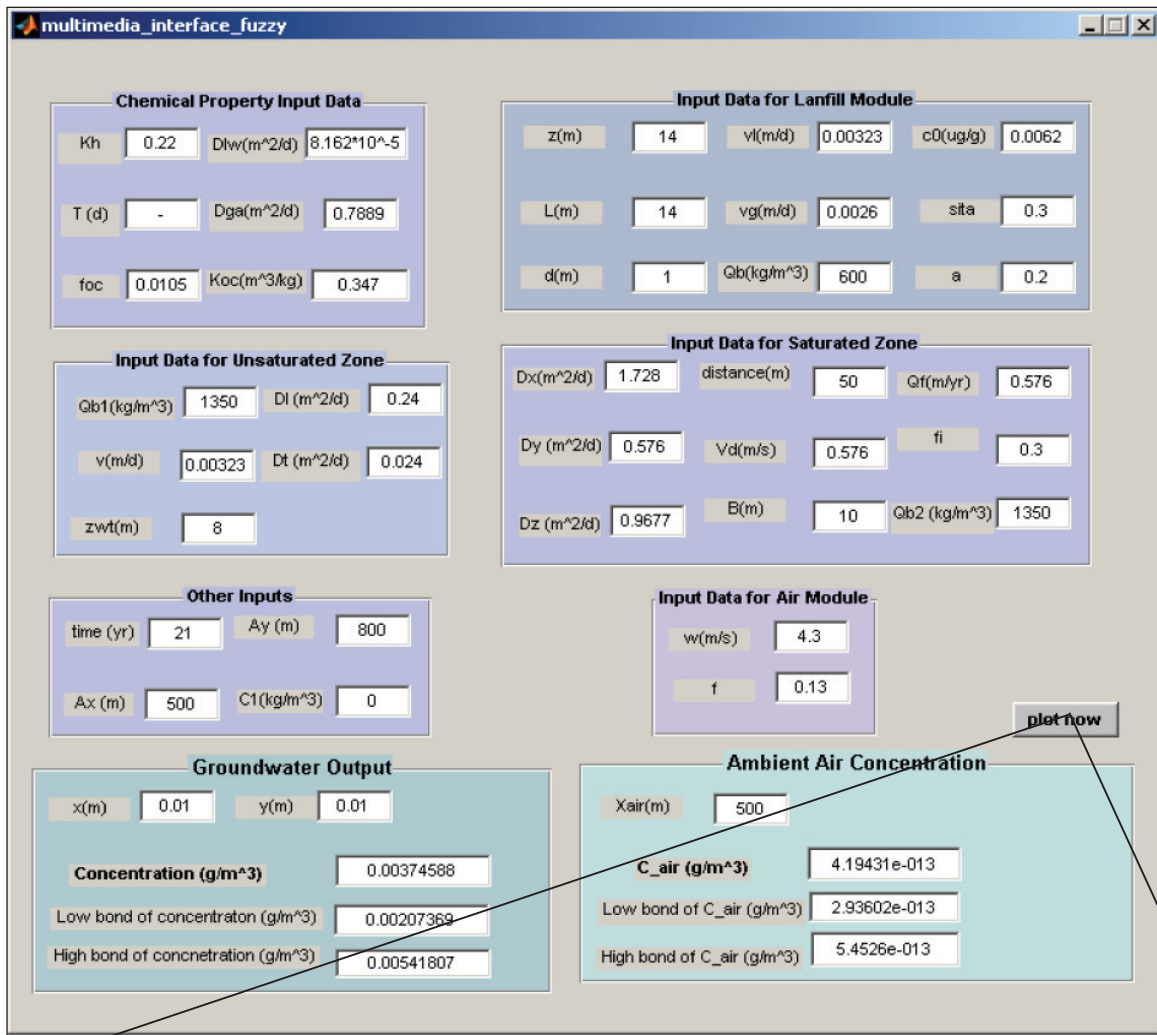


Fig. 2. An illustration of the main user interface (Adapted upon Zhang, 2006)

3. Field validation of FEMMS

The FEMMS was developed and evaluated in the part I of this series (Chen et al., 2014). However, the effectiveness of applying the FEMMS to a large

scale field contamination site is yet to be examined. A large amount of landfill site information are obtained from the Trail Road Sanitary Landfill in the Region of Ottawa-Carleton to conduct a field validation of the developed FEMMS in this study (TRNL, 1995, 2002).

3.1. Overview of the landfill site

The Trail Road Sanitary Landfill site is in the Region of Ottawa-Carleton, Canada (Abbey et al., 1998; Dillon Consulting Limited, 2008; Ziad, 2007). The site of approximately 2.023 km² (Shaker and Yan, 2010). The closest residence is 0.85 km from the landfill site boundary. The closest residential subdivision is Barrhaven, which is about 2 km away (Fig. 3). Approximately 500 meters from the northern boundary of the Trail Road Landfill is a large de-watering pond used for storing the local groundwater discharge. Jock River is located approximately 1 km from the north of the pond, water of which eventually discharges into it. Southwest of the Trail Road Landfill is the Nepean Landfill.

The Trail Road Sanitary Landfill site including the Nepean and Trail Road landfills has been operated in stages. The Nepean Landfill began operation in the early 1960s and received waste until the early 1980s when it was considered nearly full. The Nepean Landfill was capped with a polyethylene liner and soil in 1993 (Dillon Consulting Limited, 2008). After the Nepean Landfill closing, the Trail Road Landfill was opened in 1980.

It is difficult to obtain the detailed annual disposal rate of Nepean Landfill and Trail Landfill for the year 1960 to the year 1992 due to the lack of historical operation information. Therefore, based on the data from the Trail Road and Nepean Landfill (TRNL) (1995, 2002), the rate of refuse annually disposed in the landfill is estimated at 287,000 t/yr.

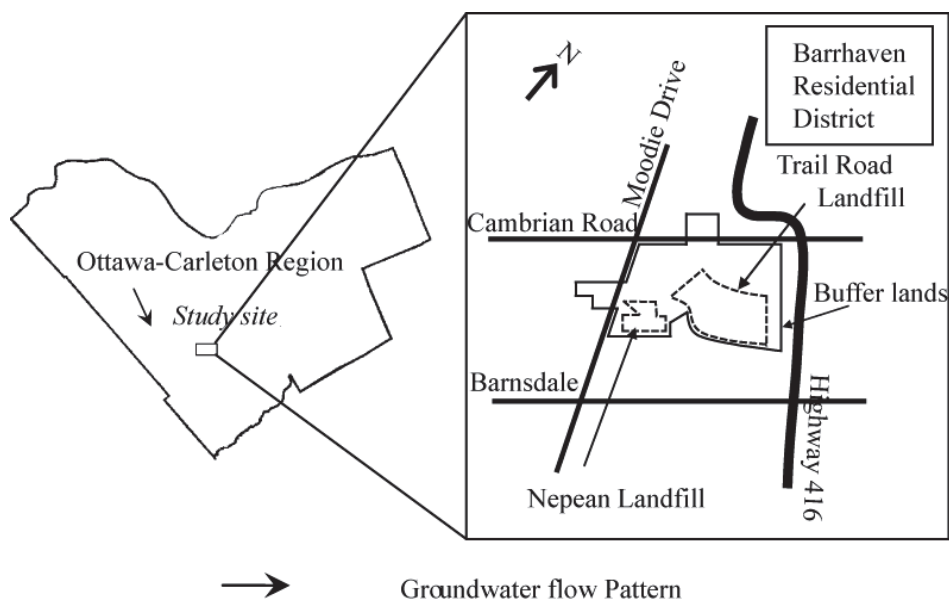


Fig. 3. Trail Road Sanitary Landfill (TRNL, 2002)

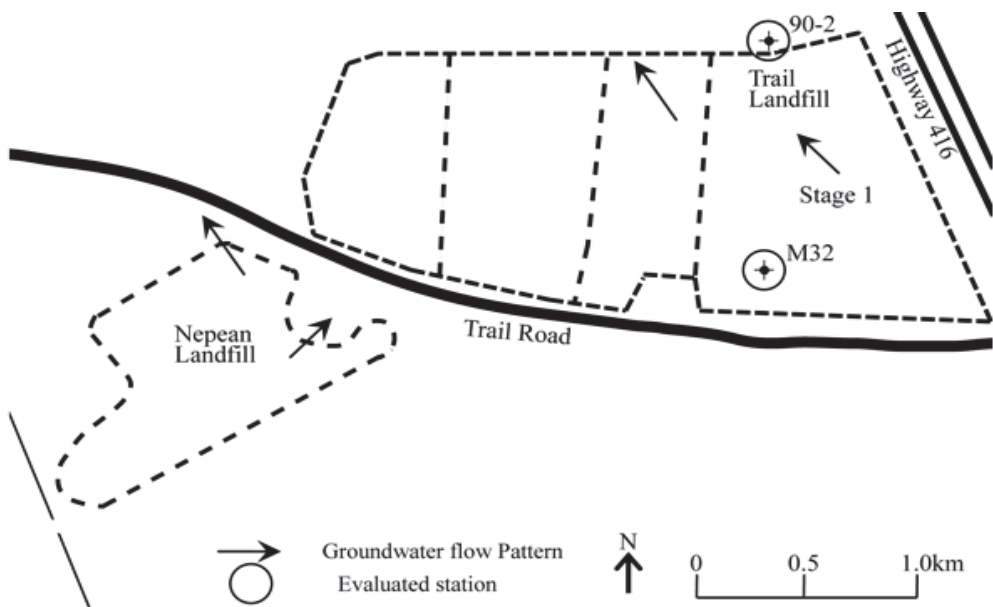


Fig. 4. Location of monitoring station (TRNL, 2002)

Table 2. Input parameters related to chemical properties

Parameters	Symbols	Benzene	Ethylbenzene	Toluene
Gaseous diffusion coefficient in air	D_g^a (m ² /d)	0.756	0.635	0.706
Liquid diffusion coefficient in water	D_l^w (m ² /d)	8.81×10^{-5}	6.7×10^{-5}	7.33×10^{-5}
Organic carbon partition coefficient	K_{oc} (m ³ /kg)	0.347	0.305	0.25
Henry's law constant, dimensionless	K_H	0.225	0.322	0.25
Half-life in landfill	τ (d)	-	-	-

3.2. Collection and preparation of model data

Following the approach outlined by the International Atomic Energy Agency (IAEA) (1989), important parameters that have relatively great potential influences on the modeling outputs are selected or estimated. The input parameters associated with environmental conditions and the physical properties of the site are summarized in Table 1 (Zhang, 2006). Other parameters related to chemical properties are given in Table 2.

Although a large amount of site information is obtained, data collected from the monitoring stations M32 and M90 of which locations are shown in Fig. 4 can be used for all the functions of FEMMS. All the input parameters are entered into the multimedia modeling system, and then they are utilized by the modules in accordance with the internal order of the model execution.

Imprecise and inaccurate input parameters are the primary source of modeling error for the environmental risk assessment. Some observed data can also be flawed due to sampling and analysis errors (Howard et al., 1991). For example, so far as the half-life of a chemical is concerned, there may be significant discrepancy between its value measured in the laboratory and the actual value on a site (Hazardous Substances Data Bank (HSDB), 2005). On the other hand, determination of a parameter value itself carries inherent uncertainty since the processes simulated by the model have a large natural variability in time and space.

Moreover, such values are often derived from the experimental data that refer to only a few discrete points in time and space (USEPA, 1996). In this

context, a fuzzy-set approach as described in Part I of this two-part series is employed to quantify various uncertain information associated with input parameters and the subsequent results besides the maximum effort on data collection. Therefore, there will be high and low bounds of modeling results in comparison with the observed data for the study contaminant.

3.3. Simulation results and comparison with field observation data

Detailed modeling results for the contaminants of ethylbenzene at M32 in the Trail Road landfill are given in Table 3. The simulated concentration of ethylbenzene in the groundwater at $x = 0$ gradually decreased from 29.5 mg/m³ in 1999 to 27.2 mg/m³ in 2002 due to spreading via dispersion in soil and groundwater, and a little loss via volatilization from the landfill cover; the low bound concentration decreased correspondingly from 16.2 mg/m³ to 15.0 mg/m³; and the high bound concentrations show the same trend from 42.8 mg/m³ to 39.4 mg/m³. Decrease in the concentration is achieved partly due to the infiltration into the landfill cover and the chemical properties. Ethylbenzene is not a highly volatile compound, implying that volatilization is not a significant loss pathway for this compound; instead, it migrates downward with infiltration and enters into the groundwater. Compared with the observed concentration in the groundwater beneath the Trail Road Landfill, the first two calculated mean concentrations agree with the field monitoring data, which get 0.88 and 0.87 of grade of membership in the fuzzy set outputs.

Table 3. Comparison of modeling results and observed ethylbenzene concentrations at the monitoring well M32

Year	Low bound of concentration (mg/m ³)	Modeled concentration at M32 (mg/m ³)	High bound of concentrations (mg/m ³)	Observed concentration (mg/m ³)	Fuzzy possibility grade
1999	16.2	29.5	42.8	31.1	0.88
2000	15.9	28.8	41.8	30.5	0.87
2001	15.4	28.1	40.7	1.8	-
2002	15.0	27.2	39.4	15.6	0.05

Table 4. Comparison of modeling results and observed toluene concentrations at the monitoring well M32

Year	Low bound of concentration (mg/m ³)	Modeled concentration at M32 (mg/m ³)	High bound of concentration (mg/m ³)	Observed concentration at M32 (mg/m ³)	Possibility
1999	58.3	106	153.7	92	0.71
2000	56.9	103.4	149.9	108	0.90
2001	55.2	100.3	145.4	21.6	-
2002	53.2	96.8	140.3	54.5	0.03

The monitoring data in 2001 it sharply decreased to 1.8 mg/m^3 and then rose to 15.6 mg/m^3 and is out of the range of the fuzzy set output. The reason includes that the precipitation rate in 2001 was smaller than that in 1999 and 2000 (e.g., the total precipitation in the Ottawa region was 987.4 mm in 2000, remarkably dropped to 753.6 mm in 2001, and increased again to 867.9 mm in 2002. Precipitation data are from the Historical Climate Database of the Government of Canada); more contaminants thus remained in the soil in that year than in the previous two years. After the infiltration rate rose again, the retarded contaminant was solved, and then along with the newly arriving pollutant leachate from the landfill was carried to the groundwater. As a result, the concentration at this location went up from 1.8 mg/m^3 to 15.6 mg/m^3 . Errors in sampling and chemical analysis and complexities in the site conditions could also have contributed to the noted discrepancies.

The simulated toluene concentration in the groundwater at M32 is shown in Table 4. Table 5 shows the predicted concentration in the groundwater for benzene at M90. The concentration of benzene decreased slowly from 6.1 mg/m^3 in 1999 to 5.7 mg/m^3 in 2002; the low bound was 3.4 mg/m^3 in 1999 and 3.1 mg/m^3 in 2002; and the high bound was from 8.8 mg/m^3 to 8.3 mg/m^3 during these 4 years. Dispersion could explain the main pathway loss, while volatilization of the benzene is limited due to its modest Henry's law constant and the protection of the landfill cover. The modeling results are very close to the observed concentration at the monitoring station in 1999 and 2000. However, the monitoring data oscillates in the following years and shows a trend that is different from those of the toluene and ethylbenzene at station M32. The big change in the monitoring data from 2000 to 2001 reflects the significant change of climate condition, e.g., change of precipitation as discussed earlier.

The discrepancy between that modeling results and monitoring data is also due to the diverse geological conditions under the landfill site. A greater amount of pollutant was carried to this point but could not be swept away due to the low groundwater flow and the retardation of the soil. Various errors in collecting and analyzing leachate samples and complexities of the landfill site mainly lead to the disagreement in the validation of FEMMS using the field-scale data. However, the validation results still demonstrates that FEMMS is capable of providing reasonable prediction of time and space varying pollutant concentration in media.

4. Prediction and assessment of the landfill contamination using the user-friendly FEMMS with uncertainty analysis

Following the validation of FEMMS using 1999 to 2002 field-scale data, the user-friendly FEMMS is applied to the Trail Road Landfill for an extended evaluation period. The evaluation locations for the groundwater are M32 and M90 unchanged,

while it is assumed that there is a receptor positioned 500 meters away from the landfill site boundary in a southwest direction. The modelling input parameters in Table 1 and Table 2 are used. The simulation results contain the contaminant concentration distribution in the environmental media and the inter-media fluxes, and the concentrations at the receptors in the groundwater and atmosphere for each contaminant: benzene, ethylbenzene and toluene (BET). However, for the comparison of variation of the contaminants in the groundwater or the ambient air, the outputs are discussed as two groups: the outputs for ambient groundwater and air quality.

4.1. Evolution of groundwater contaminant in the Tail Road Landfill site for 2003-2011

For assessing benzene contamination in the site, the fuzzy set approach is used (Chen et al., 2014). The fuzzy approach outputs of benzene concentrations at M90 are presented in Fig. 5. The high bound of concentration decreases from 8.0 mg/m^3 to 5.6 mg/m^3 , and the low bound decreases from 3.0 mg/m^3 to 2.1 mg/m^3 during the 9-year prediction period. This difference between high and low bounds indicates that the benzene concentration at the end of the evaluation period will fall into the range of 2.1 mg/m^3 to 5.6 mg/m^3 given that there are fluctuations in the environmental conditions or modeling errors. The ethylbenzene concentration predictions are presented in Fig. 6.

The high bound of concentration decreases from 38.1 mg/m^3 to 25.2 mg/m^3 , while the low bound decreases from 14.4 mg/m^3 to 9.6 mg/m^3 . At the end point of the evaluation period, the ethylbenzene concentration is between the range of 9.6 mg/m^3 and 25.2 mg/m^3 . It is interpreted as the fluctuation of environmental conditions and the discrepancy in the estimates of parameters. According to the predictions, the low bound of predicted concentration is much greater than the Ontario Drinking Water Standards (ODWS) at 2.4 mg/m^3 indicating that the M90 location under study will still be contaminated in 9 years.

Fig. 7 shows the outputs of uncertainty analysis for the toluene concentrations beneath the Trail Road Landfill site. The high bound of toluene concentration decreases from 134.5 mg/m^3 to 81.2 mg/m^3 , while the low bound decreases from 51 mg/m^3 to 30.8 mg/m^3 during the evaluation period. Since the toluene is present in high initial concentration compared to the other two contaminants, it still ranges between 30.8 mg/m^3 and 81.2 mg/m^3 after 9 years. The low bound of computed concentration is slightly over the ODWS at 24 mg/m^3 ; thus an action should be taken to protect the downstream groundwater.

4.2. Evolution of ambient air quality in the Trail Road Landfill site for 2003-2011

The computed yearly variance of the benzene concentration at the receptor is given in the form of a defuzzified output in Fig. 8.

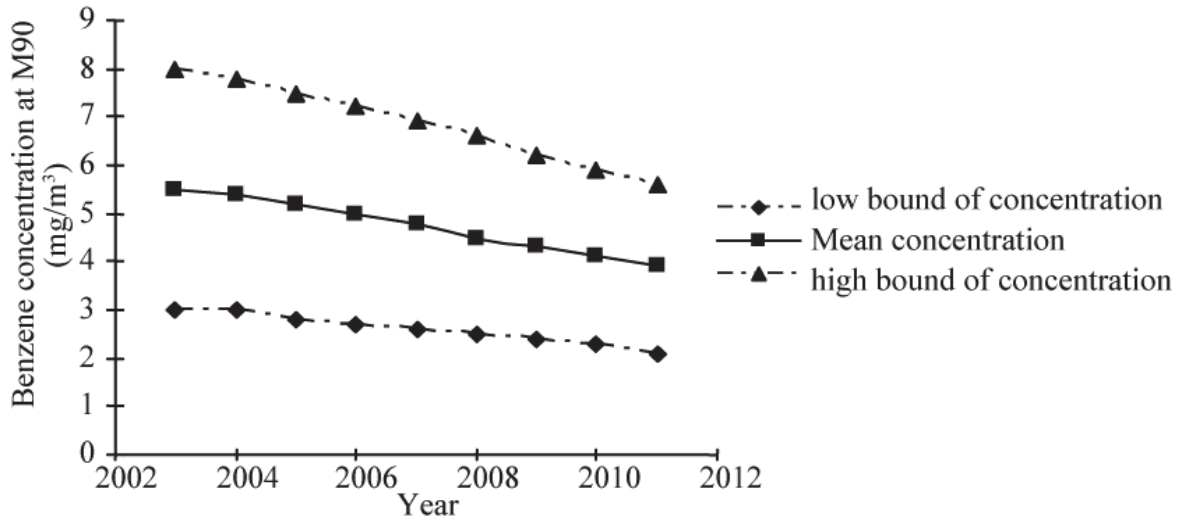


Fig. 5. Benzene concentrations at the monitoring well M90 for 2003-2011

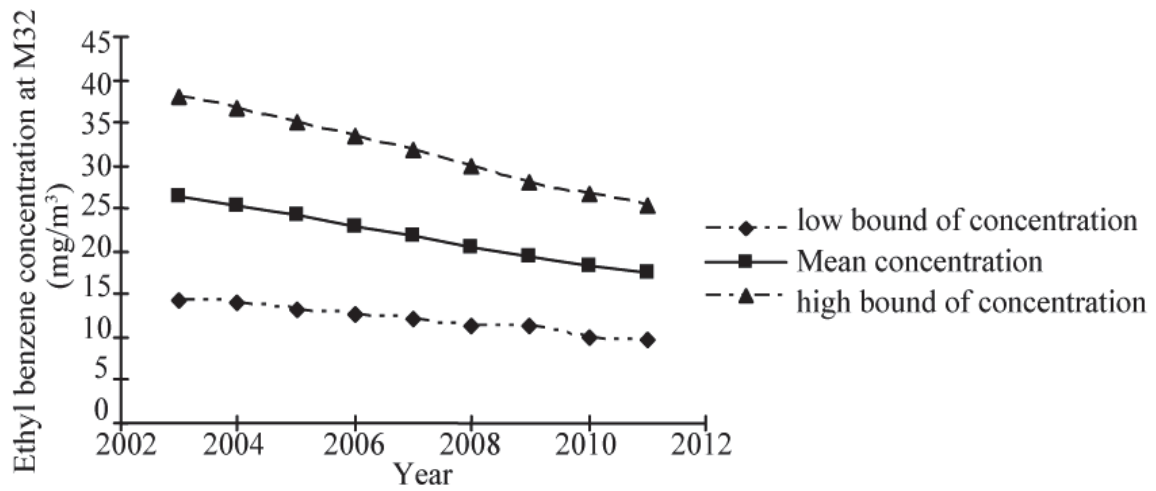


Fig. 6. Ethylbenzene concentrations at the monitoring well M32 for 2003-2011

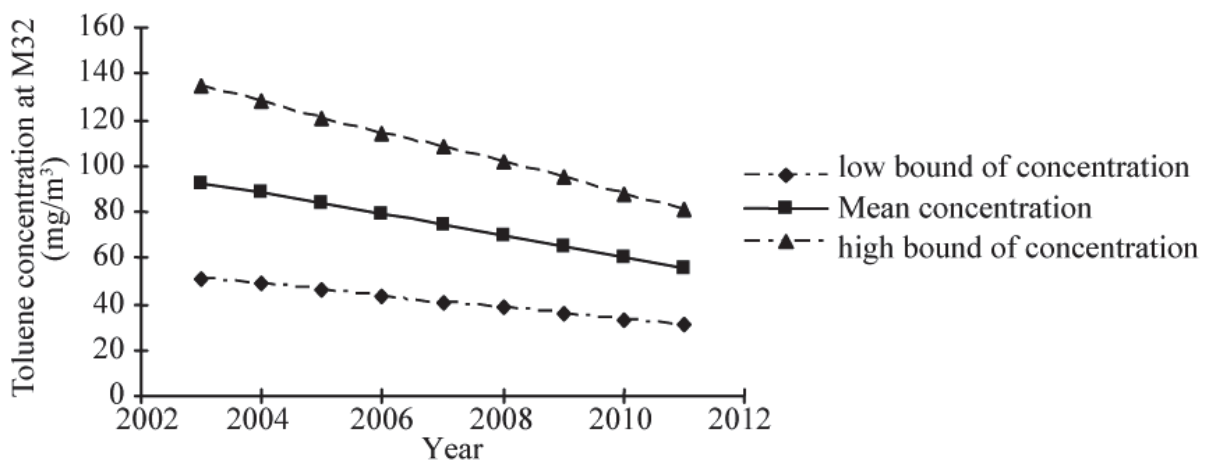


Fig. 7. Toluene concentrations at the monitoring well M32 for 2003-2011

Table 5. Comparison of modeling results and observed benzene concentrations at the monitoring well M90

Year	Low bound of concentration (mg/m ³)	Modeled concentration at M90 (mg/m ³)	High bound of concentration (mg/m ³)	Observed concentration at M90 (mg/m ³)	The possibility
1999	3.4	6.1	8.8	6.3	0.93
2000	3.3	6.0	8.7	6.2	0.93
2001	3.2	5.8	8.5	9.8	-
2002	3.1	5.7	8.3	3.5	0.15

The high bound decreases from 3.889 E-11 mg/m³ to 1.07 E-11 mg/m³, and also the low bound decreases from 2.049 E-11 mg/m³ to 5.76 E-12 mg/m³ for 2003-2011. Even the high bound of simulated benzene concentration for every evaluated year at the exposure site is far less than the 8.0 E-2 mg/m³ of the risk assessment reference concentration (USEPA, 1999, 2002). Thus it can be concluded that the risk resulting from the inhalation of benzene for human beings at the exposure site can be neglected.

The modeling results of yearly ethylbenzene concentration are shown in Fig. 9. The defuzzified outputs in 2003 are 2.036E-10 mg/m³ and 3.872E-10 mg/m³, and those in 2011 are 6.37E-11 mg/m³ and 1.183E-10 mg/m³ for low and high bounds,

respectively. According to the 1.0 mg/m³ of the reference concentration (USEPA, 1999), the ethylbenzene concentration has no adverse impact on human health at the exposure site.

The toluene concentrations for each evaluated year are shown in Fig. 10. They indicate that the low bound of estimated concentration decreases considerably from 2.641 E-10 mg/m³ to 6.11 E-11 mg/m³ and the upper limit decreases from 4.905 E-10 mg/m³ to 1.135 E-10 mg/m³ during the evaluation period. The toluene concentrations at the assessment receptor are much lower than 5 mg/m³ of the reference concentration (USEPA, 2005). Hence, the risk impact of toluene on human health is negligible.

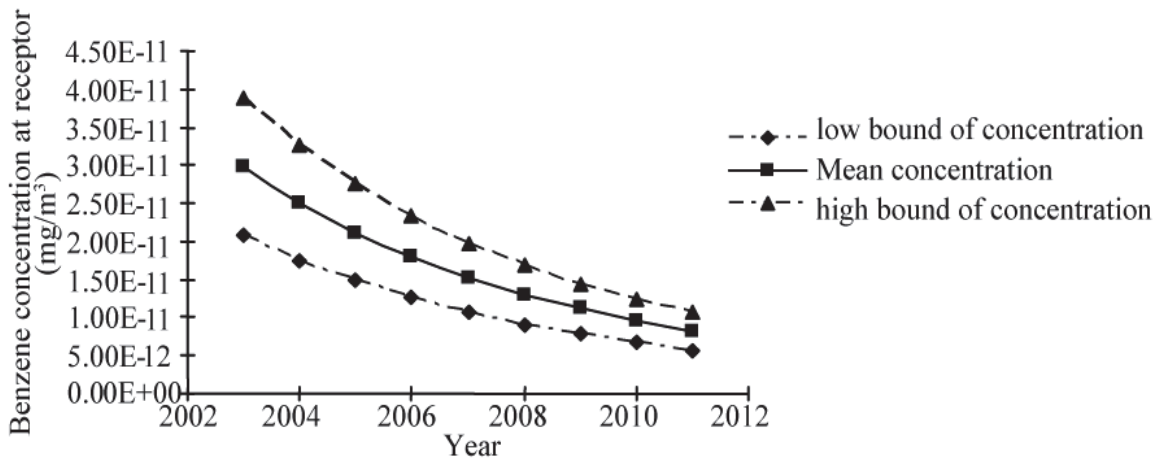


Fig. 8. Yearly benzene concentration profile at ground surface receptor for 2003-2011

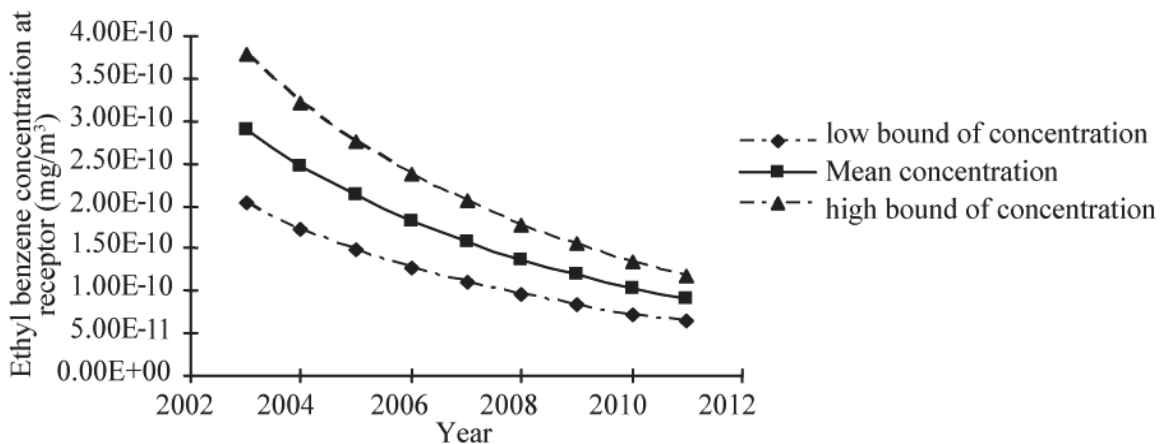


Fig. 9. Yearly ethylbenzene profile at ground surface receptor for 2003-2011

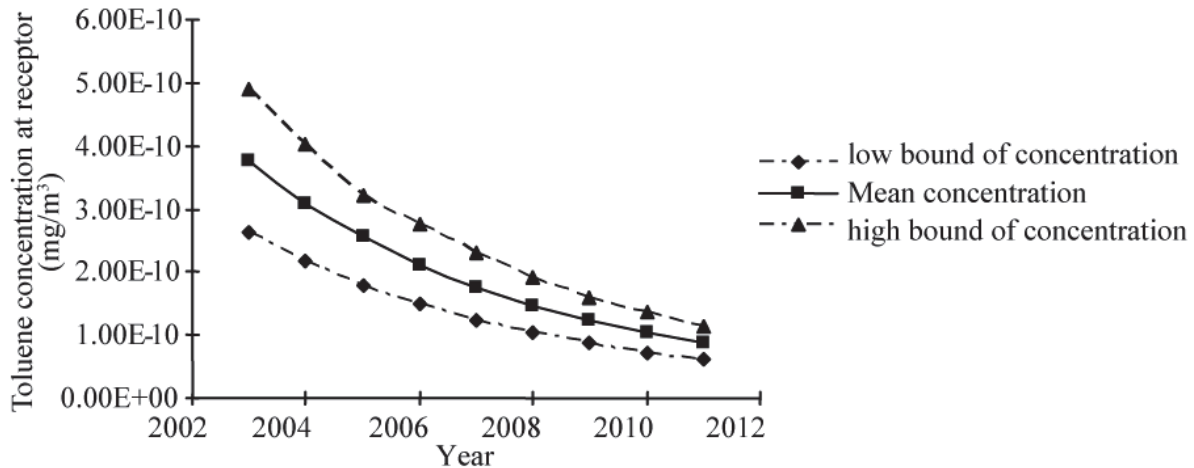


Fig. 10. Yearly toluene profiles at ground surface receptor for 2003-2011

5. Discussion

The model validation and application using field scale data show that FEMMS, enhanced with the aid of quantified uncertainties, can be applied to investigate large-scale site contamination with multimedia characteristics. Landfill is selected in this study as it involves a typical complex environmental multimedia, i.e., a landfill waste zone, the surrounding unsaturated zone, the atmosphere above the landfill, and the groundwater below the landfill. In such case, landfill waste zone evolves in releasing different contaminants at different rate into the regional three media, soil, ground water, and air.

The developed FEMMS is capable of simulating an unsteady state pollutants fate and transport within the landfill waste chamber, which result in dynamic emission sources into the connected atmosphere, soil, and groundwater. Subsequently, the dynamic emission sources are taken by three different modules to quantify multi-dimensional concentration profile in the unsaturated zone, saturated zone, and atmosphere zone above the landfill. This improves the spatial and temporal resolution of previous environmental multimedia models (e.g., McKone and MacLeod, 2003). Particularly, the developed FEMMS has been enhanced by a fuzzy-set approach to quantify different uncertainties associated with the modeling process and the complex site multimedia environmental conditions; this provides more quantitative details to support for the related site management decision making (e.g., Chen et al., 2010).

Like other models, the developed model is based on several assumptions such as initial uniform contaminant concentration in the landfill chamber and moderate climate change, which could be improved with more sampling analyses when possible. Such assumptions may limit the applicability of the model. Hence, engineer and decision-makers should be fully aware the assumptions to apply the model. Discrepancy in the model validation based on the

obtained deterministic data information could be traced to the combined effect of several contributing factors. Choosing proper input parameters to represent the site condition is important, since the parameters are site dependent. The input data for the model from the collected and analyzed samples may have errors, and they can also influence the outcome of model significantly. Consideration must be taken to reduce the combined effect of such factors to improve the accuracy of model prediction. The developed GUI effectively manages the major modeling processes including data analysis, communicating input data to functional modules, and results presentation.

In parallel to using a fuzzy-set approach to quantify model and site uncertainties and to overcome the possible field data availability issue during the simulation process, future work can further extend the developed FEMMS by: (1) considering numerical solution with irregular computational mesh for the governing equations in the FEMMS at higher computational cost; (2) improving modeling accuracy by improving numerical analysis algorithm for better addressing the site anisotropic and heterogenous conditions; and (3) including hydrological and climate change inputs into the modeling system to examine the effects of changing climatic conditions such as precipitation and temperature on the site contamination.

6. Conclusions

The developed user-friendly environmental multimedia modeling system (FEMMS) includes extended LSSMM-type fate and transport modules, a system GUI, a system input processing unit, and a system output processing function. The application of FEMMS to a complex landfill site in Canada demonstrate that it is functional, computational efficient, and user-friendly. FEMMS also quantify system uncertainties associated with modeling processes and site dynamics providing reliable risk or

impact assessment to support remediation decision making.

Data are obtained for the Trail Road Landfill in the years of 1999 to 2002, which have been applied to the field validation of the developed FEMMS in this study. The field validation and predication indicate that the soil and groundwater in the landfill area are under risks. Several major programs have been implemented by the City of Ottawa in recent years to manage the landfill site including waste to energy, composting, and facility optimization projects.

Full numerical analysis or computational fluid dynamics (CFD) can be employed in the next to generate numerical results of the FEMMS to examine non-equilibrium unsteady state environmental flow conditions and the anisotropic heterogenetic characteristics of the environmental media. It is also becoming more important to consider climate change and its effects on the dynamics of site contamination. Lastly, latest computer technology can help to build model based software interface.

References

- Abbey D.G., Mwenifumbo C.J., Killeen P.G., (1998), *The Application of Borehole Geophysics to the Delineation of Leachate Contamination at the Trail Road landfill Site: Nepean, Ontario*, Proc. of the Symposium on the Application of Geophysics to Engineering and Environmental Problems (SAGEEP).
- Babendreier J.E., Castleton K.J., (2005), Investigating uncertainty and sensitivity in integrated, multimedia environmental models: tools for FRAMES-3MRA, *Environmental Modelling & Software*, **20**, 1043-1055.
- Chau K.W., (2007), Integrated water quality management in Tolo Harbour, Hong Kong: a case study, *Journal of Cleaner Production*, **15**, 1563-1572.
- Chen Z., Zhang R.R., Han S.S., (2014), An integrated fuzzy set enhanced environmental multimedia modelling system (FEMMS): Part I – development, *Environmental Engineering and Management Journal*, **16**, 317-328.
- Chen Z., Zhao L., Lee K., (2010), Environmental risk assessment of offshore produced water discharges using a hybrid fuzzy-stochastic modeling approach, *Environmental Modelling & Software*, **25**, 782-792.
- Chen Z., Zhang R.R., Han S.S., (2017), An enhanced environmental multimedia modelling system (FEMMS): part i - development and model verification, *Environmental Engineering and Management Journal*, **16**,
- Cohen Y., Cooter E., (2002), Multimedia environmental distribution of Toxics (Mend-Tox) I: Hybrid compartment-spatial modelling framework, *Practice Periodical of Hazardous, Toxic, and Radioactive Waste Management*, **6**, 70-84.
- Dillon Consulting Limited, (2008), *Trail Road landfill Site 2007 Monitoring and Operating Report*, City of Ottawa, Canada, On line at: <http://citeseerx.ist.psu.edu/viewdoc/download?rep=rep1&type=pdf&doi=10.1.1.222.1881>.
- Droppo J.G., Buck J.W., Strenge D.L., Hoopes B.L., (1993), Risk computation for environmental restoration activities, *Journal of Hazardous Materials*, **35**, 341-356.
- Geng L.Q., Chen Z., Chan C.W., Huang G.H., (2001), An intelligent decision support system for management of petroleum-contaminated sites, *Expert Systems with Applications*, **20**, 251-260.
- Howard P.H., Boethling R.S., Jarvis W.F., Meylan W.M., Michalenko E.M., (1991), *Handbook of Environmental Degradation Rates*, Chelsea, MI: Lewis Publishers, Inc.
- HSDB, (2005), Benzene, Hazardous Substances Data Bank. United States National Library of Medicine, On line at: <http://toxnet.nlm.nih.gov>.
- Hsieh C.R., Ouimette J.R., (1994), Comparative study of multimedia modelling for dynamic partitioning of fossil fuels-related pollutants, *Journal of Hazardous Materials*, **37**, 489-502.
- IAEA, (1989), Measurement of radionuclides in food and the environment, International Atomic Energy Agency (IAEA), Vienna: Technical Report No. 295, On line at: https://www-pub.iaea.org/MTCD/publications/PDF/trs295_web.pdf
- León L.F., Lam D.C.L., Schertzer W.M., Swayne D.A., Imberger J., (2007), Towards coupling a 3D hydrodynamic lake model with the Canadian Regional Climate Model: Simulation on Great Slave Lake, *Environmental Modelling & Software*, **22**, 787-796.
- Lin C.E., Kao C.M., Lai Y.C., Shan W.L., Wu C.Y., (2009), Application of integrated GIS and multimedia modelling on NPS pollution evaluation, *Environmental Monitoring and Assessment*, **158**, 319-331.
- MacLeod M., Scheringer M., McKone T.E., Hungerbuhler K., (2010), The state of multimedia mass-balance modeling in environmental science and decision-making, *Environmental Science & Technology*, **44**, 8360-8364.
- McKone T.E., MacLeod M., (2003), Tracking multiple pathways of human exposure to persistent multimedia pollutants: Regional, continental and global-scale models, *Annual Review of Environmental Resources*, **28**, 463-492.
- Mustajoki J., Hämäläinen R.P., Marttunen M., (2004), Participatory multicriteria decision analysis with Web-HIPRE: a case of lake regulation policy, *Environmental Modelling & Software*, **19**, 537-547.
- Saini M., Natraj Y., Kankanhalli M., (2009), *Performance Modeling of Multimedia Surveillance Systems*, 11th IEEE International Symposium on Multimedia, 179-186.
- Shaker A., Yan W.Y., (2010), *Trail Road Landfill Site Monitoring Using Multi-Temporal Landsat Satellite Data*, Canadian Geomatics Conference 2010 and ISPRS COM I Symposium, Calgary, Canada.
- Srivastava A., Singh R.N., (2005), Use of multimedia mass balance model to predict concentrations of benzene in microenvironment in air, *Environmental Modelling & Software*, **20**, 1-5.
- TRNL, (1995), Trail Road and Nepean Landfill sites final report for the 1995 Monitoring and Operation Program, M.M. Dillon Limited and Gartner Lee Limited, Environment and Transportation Department Solid Waste Division, Ontario, Canada.
- TRNL, (2002), Trail Road and Nepean Landfill sites final report for the 2002 Monitoring and Operation Program. M.M. Dillon Limited and Gartner Lee Limited. Environment and Transportation Department Solid Waste Division, Ontario, Canada.
- Tuomi M., Rasinma J., Repo A., Vanhala P., Liski J., (2011), Soil carbon model Yasso07 graphical user interface, *Environmental Modelling & Software*, **26**, 1358-62.

- USEPA, (1996), Three multimedia models used at hazardous and radioactive waste sites, Washington, DC: U.S. Environmental Protection Agency, On line at: <https://www.epa.gov/sites/production/files/2015-05/documents/540-r-96-004.pdf>.
- USEPA, (1999), Integrated Risk Information System (IRIS) on Ethylbenzene, Washington, DC: National Center for Environmental Assessment, Office of Research and Development.
- USEPA, (2002), Toxicological review of benzene (noncancer effects), In Support of Summary Information on the Integrated Risk Information System (IRIS), Washington, DC: U.S. Environmental Protection Agency.
- USEPA, (2005), Toxicological review of Toluene, In Support of Summary Information on the Integrated Risk Information System (IRIS), Washington, DC: U.S. Environmental Protection Agency, On line at: https://www.epa.gov/sites/production/files/2014-03/documents/toluene_toxicology_review_0118tr_3v.pdf.
- Voigt K., Brueggemann R., Scherb H., Shen H., Schramm K.W., (2010), Evaluating the relationship between chemical exposure and cryptorchidism, *Environmental Modelling & Software*, **25**, 1801-1812.
- Zhao M.Y., Cheng C.T., (2006), Multiple criteria data envelopment analysis for full ranking units associated to environment impact assessment, *International Journal of Environment and Pollution*, **28**, 448-464.
- Zhang R.R., (2006), *Development of a Fuzzy-Set Enhanced Environmental Multimedia Modelling System*, MSc. Thesis, Concordia University, Montreal, Canada.
- Ziad B., (2007), *Investigation of leachate quality from the Trail Road landfill*, MSc Thesis, Ryerson University, Canada.

Environmental Engineering and Management Journal

"Gheorghe Asachi" Technical University of Iasi, Romania



73 Mangeron Blvd., 700050, Iasi, Romania
Tel./Fax: +40-232-271759, PO 10, BOX 2111,
URL: <http://omicron.ch.tuiasi.ro/EEMJ/>
e-mail: eemjournal@yahoo.com, eemj.office@gmail.com



INSTRUCTIONS FOR AUTHORS

1. Introduction

Environmental Engineering and Management Journal (EEMJ) is an international medium for publication of Original Papers, Reviews, Case Studies, Book Reviews on the fundamentals, applications in environmental engineering and technologies, applied environmental sciences, environmental health, management, sustainable development, education for sustainability. Advertising is also accepted with contractual payment forms.

Submission of a manuscript implies that the work described has not been published before (except in the form of an abstract or as part of a published lecture, or thesis); that it is not under consideration for publication elsewhere; that its publication has been approved by all coauthors, if any, as well.

Papers, books for review, offers to review, suggestions and commercials (advertising) should be submitted to the *Editor-in-Chief*. All papers will be published in English. Non-English speaking authors should seek the advice of a professional language expert or an English speaker to help translate the paper.

2. Legal requirements

The author(s) guarantee(s) that the manuscript is/will not be published elsewhere in any language without the consent of the copyright holders, that the rights of third parties will not be violated, and that the publisher will not be held legally responsible should there be any claims for compensation.

Authors wishing to include figures or text passages that have already been published elsewhere are required to obtain permission from the copyright holder(s) and to include evidence that such permission has been granted when submitting their papers. Any material received without such evidence will be assumed to originate from the authors.

The author(s) are encouraged to transfer the copyright of the article to the publisher upon acceptance of an article by the journal, using the Authors' Warranty and Assignment of Copyright agreement. This transfer enables the Editor to protect the copyrighted material for the authors, but does not relinquish the author's proprietary rights. The publication of an article is conditioned by the signature of the author to whom correspondence should be addressed on this Authors'

Warranty and Assignment of Copyright that is provided by the Editor.

Ethics in Publishing

For information on ethics in publishing for journal publication see <http://omicron.ch.tuiasi.ro/EEMJ/plagiarism.htm>

Conflict of interest

All authors are requested to disclose any actual or potential conflict of interest such as any financial, personal or other relationships with other people or organizations concerning the submitted work that could inappropriately influence, or be perceived to influence, their work.

3. Editorial procedure

For original papers, an upper limit of 7000 words is recommended (including Abstract, Keywords, References, Figures and Tables), processed with MS editing facilities.

For review papers (critical evaluation of existing data, defined topics or emerging fields of investigation, critical issues of public concern), an upper limit of 15000 words is recommended (including Abstract, Keywords, References, Figures and Tables).

Manuscripts should be written in English (American or British usage is accepted, but not a mixture of these) and submitted **electronically**, in .doc format (please do not use .docx) to the *Editor-in-Chief*, at **one (and only one)** of the following e-mail addresses: **eemjournal at yahoo dot com; eem_journal at yahoo dot com; eemjeditor at yahoo dot com; eemj_editor at yahoo dot com; eemjournal at gmail dot com; eemjeditor at gmail dot com; eemjoffice at gmail dot com.**

Please be sure to include your full affiliation and e-mail address (see Sample manuscript).

When submitting the manuscript, it is mandatory to include a cover letter to the editor. The cover letter must state:

- that all authors mutually agree that the manuscript can be submitted to EEMJ;
- that the manuscript contains the original work of the authors;

- the novelty in results/findings, or significance of results;
- that the manuscript has not already been published, or is not under consideration for publication elsewhere.

Manuscripts are evaluated first in the Editorial Office (as a preliminary condition for acceptance) in terms of meeting the requirements of the journal, including attempts of plagiarism. The authors are responsible for the accuracy of the whole paper and references. Authors will be notified about the registration of their contribution. Only those contributions, which conform to the following instructions, can be considered for the peer-review process. Otherwise, the manuscripts are returned to the authors, with observations, comments and annotations. The peer review process is decisive for paper acceptance. It could be done in several stages, depending on the revision quality of the manuscript in accordance with the requirements of paper evaluators. Please do not transmit electronic data or requirements to the publisher until your manuscript has been reviewed and accepted for publication. Please follow the instructions below.

A minimum of four suitable *potential reviewers* should be provided by the authors. Please provide their name, email addresses, and institutional affiliation. When compiling this list of potential reviewers please consider the following important criteria: they must be knowledgeable about the manuscript subject area of the manuscript; they must not be from the authors' own institution or country; they should not have recent (less than five years) joint publications with any of the authors. However, the final choice of reviewers is at the editors' discretion.

4. Manuscript preparation

General:

Authors must follow the Instructions for authors strictly, failing which the manuscripts would be rejected without review. Editors reserve the right to adjust the formatting style to conform to the standards of the journal.

Manuscripts should be concise, in 1.5 line spacing, and should have 2 cm all over margins. The font should be Times New Roman of size 12 points. The numbering of chapters should be in decimal form. Ensure that each new paragraph is clearly indicated, using TAB at 1.25 pts.

The text layout should be in single-column format.

Keep the layout of the text as simple as possible. Most formatting codes will be removed and replaced on processing the manuscript. However, do use bold face, italics, subscripts, superscripts etc. Add line numbering and page numbers. To avoid unnecessary errors it is strongly advised to use the 'spell-check' and 'grammar-check' functions of your word processor.

Title page will contain:

- A concise and informative title (Times New Roman bold, all caps of size 14 points); the maximum length of the title should be maximum 100 letters and spaces; The full name(s) of the author(s) (first name, then last

name, with Times New Roman bold 12 points) should be written below the title. The affiliation(s) and complete postal address(es) of the author(s) will be provided immediately after the full name of the authors and will be written with Times New Roman 12 points. When the paper has more than one author, their name will be followed by a mark (Arabic numeral) as superscript; for the corresponding author, an asterisk will be added using *Word_Insert_Reference_Footnote_Symbol* sequence. Also, the full and e-mail addresses, telephone and fax numbers of the corresponding author will be provided in the footer of the first page, as: Author to whom all correspondence should be addressed: email....., Phone....., Fax.....

- **Abstract:** each paper must be preceded by an abstract presenting the most important results and conclusions in no more than 250 words. Do not include citations in the Abstract.
- **Keywords:** three to five keywords should be supplied after the Abstract for indexing purposes, separated by comma, **ordered alphabetically**, using American spelling and avoiding general and plural terms and multiple concepts (avoid, for example, "and", "of"). Be sparing with abbreviations: only abbreviations firmly established in the field may be eligible.
- The text of the paper should be divided into **Introduction, Materials and methods (or Experimental), Results and discussion, Conclusions, References** (for papers dealing with environmental management, policy, education etc., the Experimental part can be replaced by case-studies presentation).

1. Introduction

State the objectives of the work and provide an adequate background, avoiding a detailed literature survey or a summary of the results.

2. Material and methods (or 2. Experimental)

Provide sufficient detail to allow the work to be reproduced. Methods already published should be indicated by a reference: only relevant modifications should be described.

3. Results and discussion

Results should be clear and concise. Discussion should explore the significance of the results of the work, not repeat them. Avoid extensive citations and discussion of published literature.

4. Conclusions

The main conclusions drawn from results should be presented in a short Conclusions section. Do not include citations in this section.

Formulae, symbols and abbreviations:

Formulae will be typeset in Italics (preferable with the Equation Editor of Microsoft Office 2003) and should be written or marked as such in the manuscript, unless they require a different styling. The formulae should be numbered on the right side, between brackets:

$$a^3 = 3M / 4N \quad (1)$$

Always refer in the text to Equations as (Eq. 1), Eqs. (1-4) etc.

The more complex Chemical Formulae should be presented as Figures.

Abbreviations should be defined when first mentioned in the abstract and again in the main body of the text and used consistently thereafter.

SI units must be used throughout.

Footnotes should be avoided.

References:

The list of References should only include works that are cited in the text and that have been published. References should be cited in the text in brackets (**Harvard style**) as in the following examples:

(Chisti, 1989), (Gavrilescu and Roman, 1996), (Moo-Young et al., 1999).

References should be alphabetically listed at the end of paper, with complete details, as follows:

Books: Names and initials of authors, year (between brackets), chapter title, title of the book (italic), editors, edition, volume number, publisher, place, page number:
Mauch K., Vaseghi S., Reuss M., (2000), *Quantitative Analysis of Metabolic and Signaling Pathways in Saccharomyces cerevisiae*, In: *Bioreaction Engineering*, Schügerl K., Bellgardt K.H. (Eds.), Springer, Berlin Heidelberg New York, 435-477.

Faber K., (2000), *Biotransformations in Organic Chemistry – A Textbook*, vol. VIII, 4th Edition, Springer, Berlin-Heidelberg-New York.

Handbook, (1951), *Handbook of Chemical Engineer*, vol. II, (in Romanian), Technical Press, Bucharest, Romania.

Symposia volumes: Names and initials of authors, year (between brackets), paper title, symposium name, volume number, place, date, page numbers:

Clark T.A., Steward D., (1991), *Wood and Environment*, Proc. 6th Int. Symp. on Wood and Pulping Chemistry, Melbourne, vol. 1, 493-498.

Journal papers: Names and initials of authors, year (between brackets), full title of the paper, full name of the journal (italic), volume number (bold), first and last page numbers:

Tanabe S., Iwata H., Tatsukawa R., (1994), Global contamination by persistent organochlorines and their ecotoxicological impact on marine mammals, *Science of the Total Environment*, **154**, 163-177.

Patents: Names and initials of authors, year (between brackets), patent title, country, patent number (italic):

Grant P., (1989), *Device for Elementary Analyses*. USA Patent, No. 123456.

Dissertations: Names and initials of authors, year (between brackets), title, specification (PhD Thesis, MSc Thesis), institution, place:

Aelenei N., (1982), *Thermodynamic study of polymer solutions*, PhD Thesis, Institute of Macromolecular Chemistry Petru Poni, Iasi, Romania.

Star K., (2008), *Environmental risk assessment generated by natural hazards*, MSc Thesis, Institute of Hazard Research, Town, Country.

Legal regulations and laws, organizations:

Abbreviated name, year (between brackets), full name of the referred text, document type, author, URL address:

ESC, (2007), Improving access to modern energy services for all fundamental challenge, Economic and Social Council, ENV/DEV/927, On line at: <http://www.un.org/News/Press/docs/2007/envdev927.doc.htm>.

EPA, (2007), Biomass Conversion: Emerging Technologies, Feedstocks, and Products, Sustainability Program, Office of Research and Development, EPA/600/R-07/144, U.S. Environmental Protection Agency, Washington, D.C., On line at: <http://www.epa.gov/Sustainability/pdfs/Biomass%20Conversion.pdf>.

EC Directive, (2000), Directive 2000/76/EC of the European Parliament and of the Council of 4 December 2000, on the incineration of waste, Annex V, *Official Journal of the European Communities*, L 332/91, 28.12.2000, Brussels.

GD, (2004), Governmental Decision No. 1076/2004 surnamed SEA Governmental Decision, regarding the procedure for strategic environmental impact assessment for plans or programs, *Romanian Official Monitor*, Part I, No. 707 from 5th of August, 2004.

Web references

The full URL should be given in text as a citation, if no other data are known. If the authors, year, title of the documents are known and the reference is taken from a website, the URL address has to be mentioned after these data:

Burja C., Burja V., (2008), Adapting the Romanian rural economy to the European agricultural policy from the perspective of sustainable development, MPRA, Munich Personal RePEc Archive, On line at: http://mpra.ub.uni-muenchen.de/7989/1/MPRA_paper_7989.pdf

Web references must not be listed separately, after the reference list.

All references must be provided in English with a specification of original language in round brackets.

Citation in text

Please ensure that every reference cited in the text is also present in the reference list (and vice versa). Do not cite references in the abstract and conclusions.

Unpublished results, personal communications as well as URL addresses are not recommended in the references list.

Citation of a reference as "in press" implies that the item has been accepted for publication.

Papers which have been accepted for publication should be included in the list of references with the name of the journal and the specification "in press".

References style

Text: All citations in the text may be made directly (or parenthetically) and should refer to:

- *single author:* the author's name (without initials, unless there is ambiguity) and the year of publication: "as previously demonstrated (Smith, 2007)"; "as Smith (2007) demonstrated"

- *two authors:* both authors' names and the year of publication: (Arnold and Sebastian, 2008; Smith and Hansel, 2006; Stern and Lars, 2009)

- *three or more authors:* first author's name followed by "et al." and the year of publication: "As has recently been shown (Werner et al., 2005)...", "Kramer et al. (2000) have recently shown"

Citations of groups of references should be listed first alphabetically, then chronologically.

Examples: "...as demonstrated (Aden, 1996a, 1996b, 1999; Allan and Jones, 1995; Han et al., 2007; Weiss and Schmidt, 1988)".

Abbreviations

Define all abbreviations at their first mention in the text. Ensure consistency of abbreviations throughout the article.

Acknowledgements

Include acknowledgements in a separate section at the end of the article before the references and do not, therefore, include them on the title page, as a footnote to the title or otherwise. List here those individuals who provided help during the research (e.g., providing language help, writing assistance or proof reading the article, funding supports etc.).

Footnotes

Footnotes must be avoided. Do not include footnotes in the Reference list.

Table footnotes

Indicate each footnote in a table with a superscript lowercase letter.

Tables

Draw the Tables in grid format using a basic, solid line style without shadows.

Ensure that the data presented in Tables do not duplicate results described in Figures or elsewhere in the paper.

Figures

Number Figures consecutively in accordance with their appearance in the text. All illustrations should be provided in camera-ready form, suitable for reproduction, which may include reduction without retouching. Photographs, charts and diagrams are all to be referred to as Figure(s) and should be numbered consecutively, in the order to which they are referred.

Figures may be inserted preferably as black line drawings. They should be pasted on, rather than taped,

since the latter results in unclear edges upon reproduction.

Ensure that each illustration has a caption, placed below the Figure. Supply also captions separately, not attached to the figure. A maximum limit of 8 Figures are allowed per manuscript.

A caption should comprise a brief title (**not** on the Figure itself) and a description of the illustration. Keep text in the illustrations themselves to a minimum but explain all symbols and abbreviations used. Multiple Figures can be expressed as one Figure (for e.g. 1a, 1b, 1c etc...), while retaining the maximum limit of 6.

ALL Figures must be submitted in either .jpg or .tiff format with a very good resolution (but do not submit graphics that are disproportionately large for the content).

Figures and Tables must be embedded in the text.

Proofs

Proofs will be sent to the corresponding author (by e-mail) and should be returned within 72 hours of receipt. Corrections should be restricted to typesetting errors; any other changes may be charged to the authors.

Paper in Electronic Format:

Authors are asked to submit their final and accepted manuscript as an attachment to one of the above-mentioned e-mail addresses. Use the **.doc** format (not .docx !).

5. Page charge

There is no charge per printed page for regular papers.

6. Reprints

The corresponding author will be provided with a .pdf file of the paper via e-mail, free of charge. A hard copy Of the issue containing the paper can be provided on request, for a fee. This request will be formulated when the final form of the manuscript (the electronic one) is provided.

7. Additional procedures for the editorial management of *Environmental Engineering and Management Journal*

Starting with volume 13/2014, the members of the Scientific Advisory Board and the Corresponding authors will receive each issue of the journal in electronic .pdf format. Printed copies can be delivered on request.

An author cannot appear on more than two papers per regular issue. An author cannot appear on more than three papers in a Guest Editor/ Conference issue.

The evaluation/peer-review process of manuscripts submitted for Guest Editor / Conference issues published according to journal *Editorial Procedure and Policy* will be handled and evaluated as with regular manuscripts, so that only consistent papers will be published. The manuscripts must be sent at least six months before the presumed data of publication. Those manuscripts which do not fulfill the journal requirements

will be rejected. This is to discourage superficiality in the development of the manuscript, from formal and scientific points of view. No amount of money will be refunded following the rejection of manuscripts.

No more than 160 pages and no more than 20 papers are acceptable for regular issues. No more than 180 pages and no more than 25 papers are opportune for special issues. The number of pages is based on the published version of an article, not on the submitted version (for instance, when page breaks are changed and when images are enlarged for easier viewing).

An issue can include, as an exception, a number of 25-30 papers as a maximum. This situation could appear when the authors of an already accepted paper need and ask for early publication, from the position in the list of accepted papers. In this circumstance, a yearly submission to our journal (500 Euro) will be asked for each already accepted paper, for its publication in advance.

A newly-received manuscript can be evaluated by priority, when a deposit of 200 Euro shall be paid by authors in advance. If the manuscript is deemed unsuitable for publication, the authors will not be eligible for a refund.

Failure to pay mandatory charges may result in the paper being withheld from early publication.

In all cases, the corresponding author will sign an agreement with the *Editor-in-Chief*, and the *Director* of the *EcoZone* Publishing House according to journal *Editorial Procedure and Policy*.

Automated software is used for checking against plagiarism. In order to avoid false results, the generated reports are cautiously checked and confirmed by journal staff. We do not send plagiarism reports to authors. Any manuscripts which do not prove to be at least 90% original will be rejected. The rejection for plagiarism may arise at any phase of the editorial / review process, even if the manuscript was accepted for publication. The authors are solely responsible for the originality of their submission. Therefore, any manuscript should be carefully checked for such inconsistencies before submitting to EEMJ.

The authors are required to follow academic publishing rules, to adhere to the principles of scientific ethics and to sign the Authors' warranty and Copyright transfer.

Detailed information concerning these issues may be found of the EEMJ website, under *Editorial Procedure and Policy*.

Environmental Engineering and Management Journal is edited by the
Publishing House **ECOZONE** of the
Academic Organization for Environmental Engineering and Sustainable Development (OAIMDD)
within the **Department of Environmental Engineering and Management – Faculty of Chemical Engineering and
Environmental Protection under the aegis of "Gheorghe Asachi" Technical University of Iasi**
73 Prof.Dr.docent Dimitrie Mangeron Street, 700050-Iasi, Romania



"Gheorghe Asachi" Technical University of Iasi